3rd Hull Performance & Insight Conference

HullPIC'18

Redworth, 12-14 March 2018

Edited by Volker Bertram

Sponsored by

www.jotun.com

www.dnvgl.com

K Y M A

www.kyma.no

www.ecosubsea.com

www.vaf.nl

www.bureauveritas.com

www.miros.no

www.hempel.com

www.ascenz.com

www.akzonobel.com

www.bmtsmart.com

coach-solutions.dk

www.stratumfive.com

www.insatech.com

www.hasytec.com

Index

Experience with Robotic Underwater Hull Cleaning in Dutch Ports

Alex Noordstrand, Fleet Cleaner, Delft/The Netherlands, a.noordstrand@fleetcleaner.com

Abstract

Fleet Cleaner has developed and implemented a robotic cleaning approach for ships. The remotely controlled robot removes fouling below and above the waterline in port while the ship is loaded and unloaded. The paper describes the general approach and milestones of implementation since first in-water trials in 2015.

1. Robotic cleaning approach

Robotic cleaning has been increasingly discussed in the maritime industries, with assorted solutions of varying maturity emerging, e.g. *Tribou (2008), Ishii et al. (2014), Curran et al. (2016), Odetti et al. (2016).* There are various factors driving this development, aiming at replacing the traditional in-water cleaning approach using divers by robotic solutions, Fig.1:

- The general progress in robotics allows mature and cost efficient industry applications now.
- The concern about invasive species at IMO level focusses concern hull cleaning.
- The discussion on performance monitoring has led to re-thinking current coating and cleaning strategies.

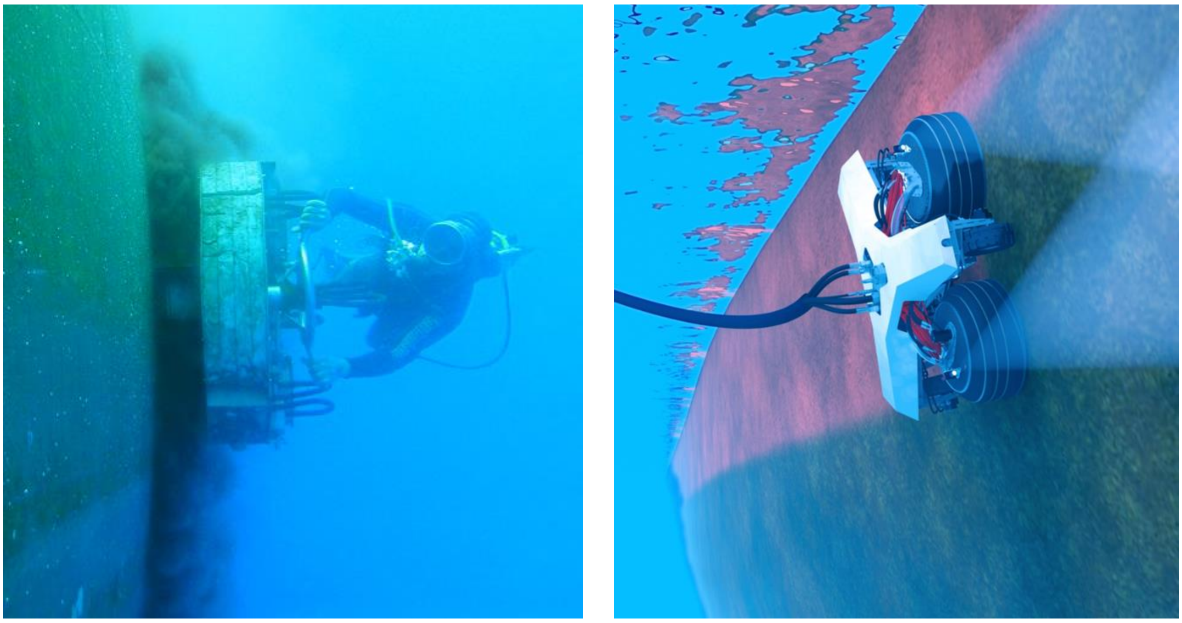

Fig.1: Current practice (left) and Fleet Cleaner robotic solution (right)

We present here our Fleet Cleaner robot, developed and deployed in the Netherlands, Fig.2. The robot uses magnets for attachment, allowing operation in water and in air, Fig.3. The cleaning is based on three cleaning heads with high-pressure waterjets, where the water pressure can be adapted to the coating and fouling as appropriate. At present, the robot is remotely controlled from a support ship, Fig.4 and Fig.5. However, the robot has autopilot and tracking functions to allow cleaning also in zero visibility. The robot is able to capture all removed fouling. The waste water is filtered and clean water released. All waste is collected, weighed and disposed properly in port. Consequently, the robot has been certified to clean in all Dutch ports despite their strict environmental (biofouling) regulations. The cleaning speed is such that usual loading/unloading times suffice to perform the cleaning, avoiding any extra downtime. The robot is designed to clean strongly curved ship surfaces, Fig.6, as especially smaller vessels have significant (up to 60%) percentage of the hull in curved areas.

Fig.2: Fleet Cleaner robot (L × B × H = 2.0 m × 1.8 m × 0.6 m)

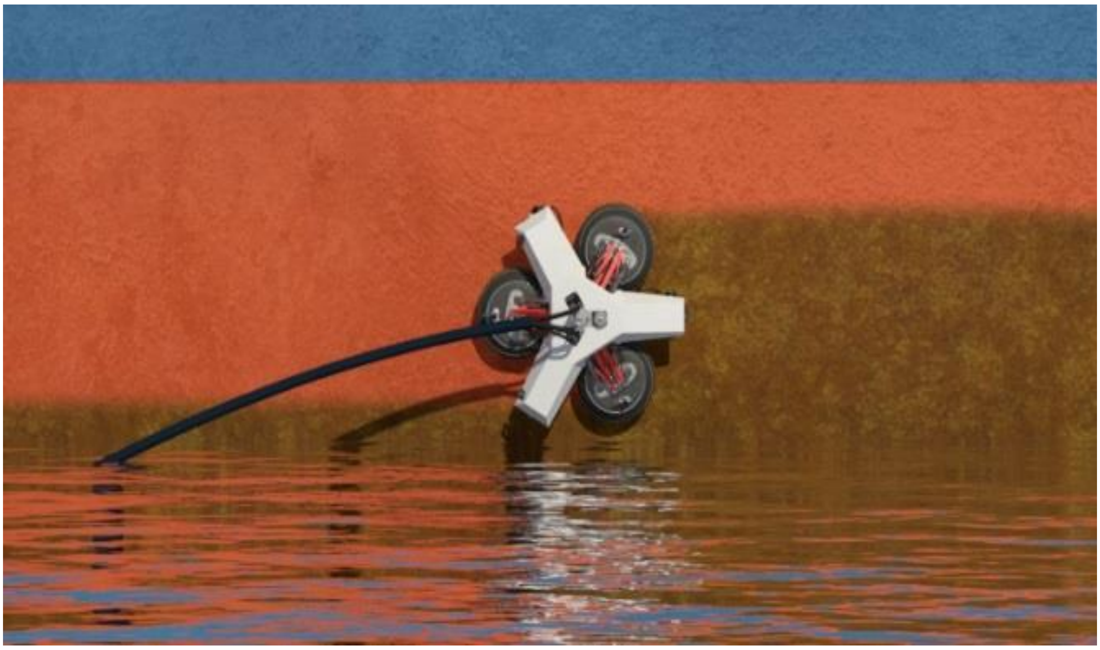

Fig.3: The robot can clean also above the waterline

Table I summarizes current cleaning practice using divers with our robotic solution.

Table I: Current practice vs Fleet Cleaner solutions

Current practice with divers	Fleet Cleaner solution
Cleaning outside ports	Cleaning during port time
Cleaning only underwater	Cleaning under water and above water
Ship coating possibly damaged (brushes)	Ship coating not damaged (waterjets)
Fouling released in water	Fouling captured

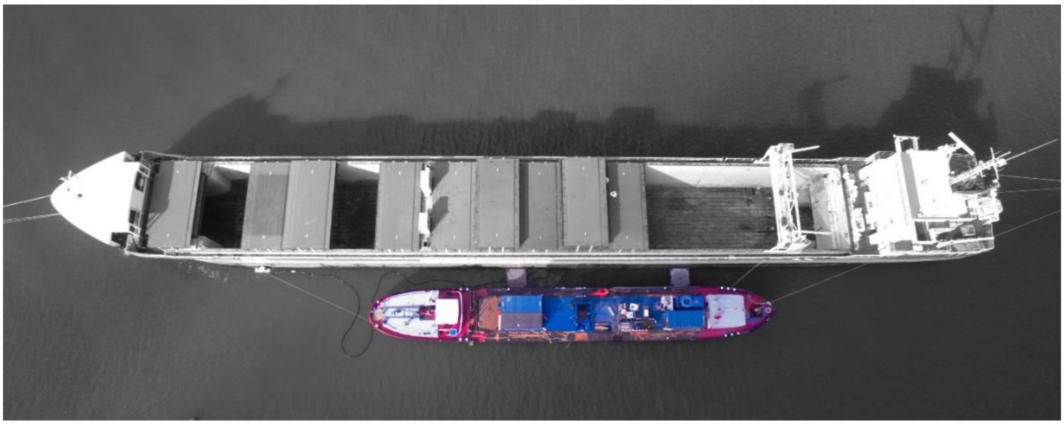
Fig.4: Workboat (bottom) alongside cleaned ship (top)

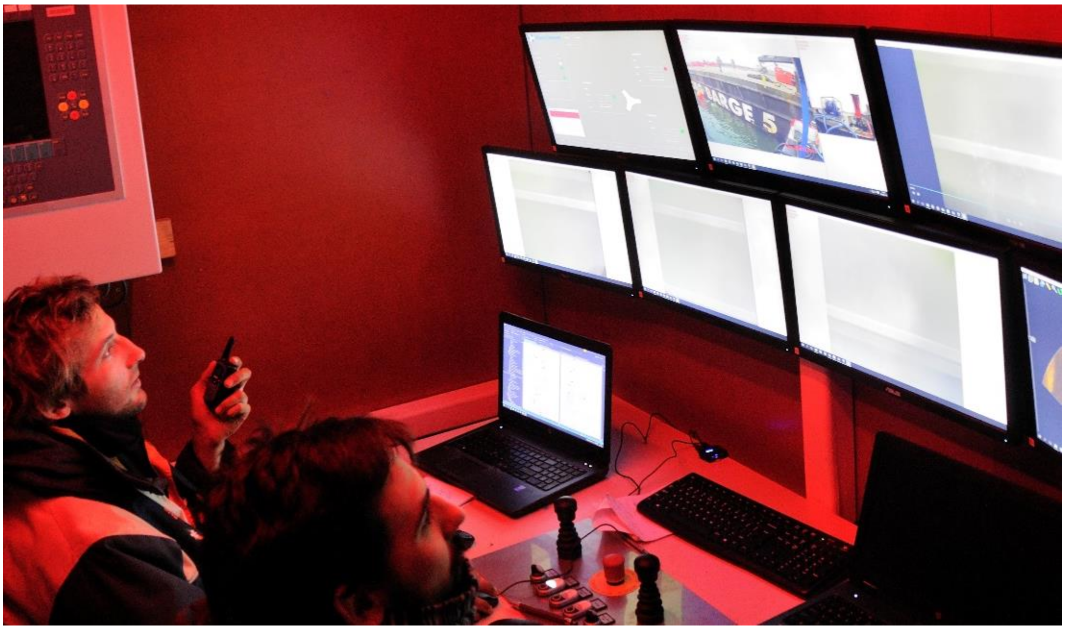
Fig.5: Remote control of cleaning robot from workboat

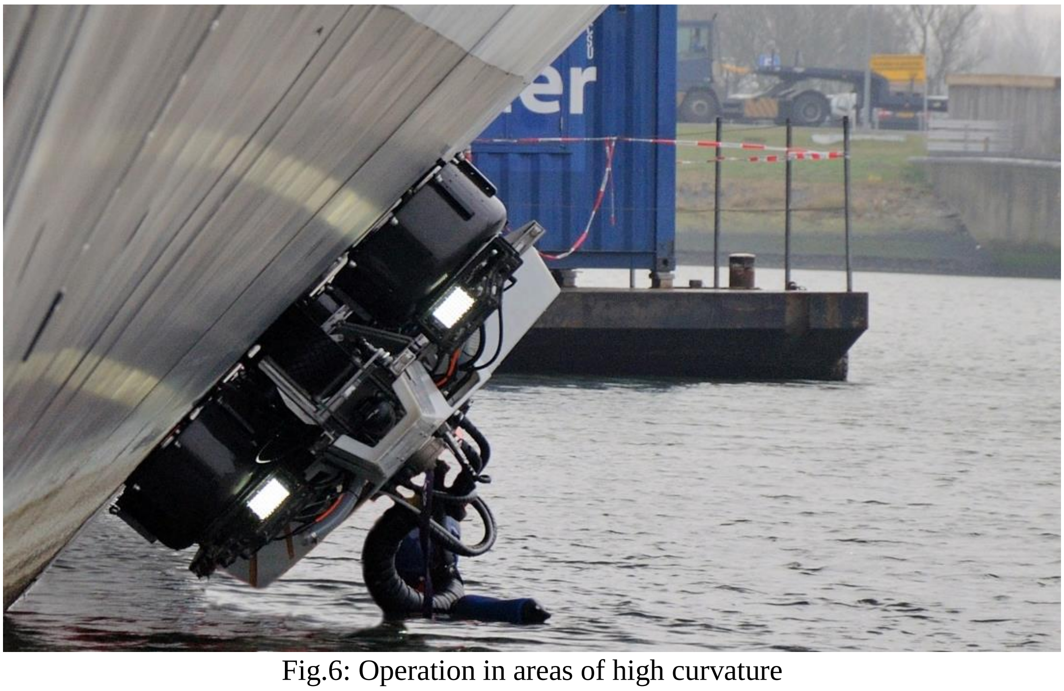
Fig.6: Operation in areas of high curvature

2. Implementation milestones and experience so far

- Development work started in 2011.

- Lab testing in August 2015, Fig.7
  Fleet Cleaner completed first test trials in laboratory conditions on land, using a representative welded steel surface. The tests proved that the robot performs as expected capturing all removed fouling during the cleaning process and is able to clean above water.

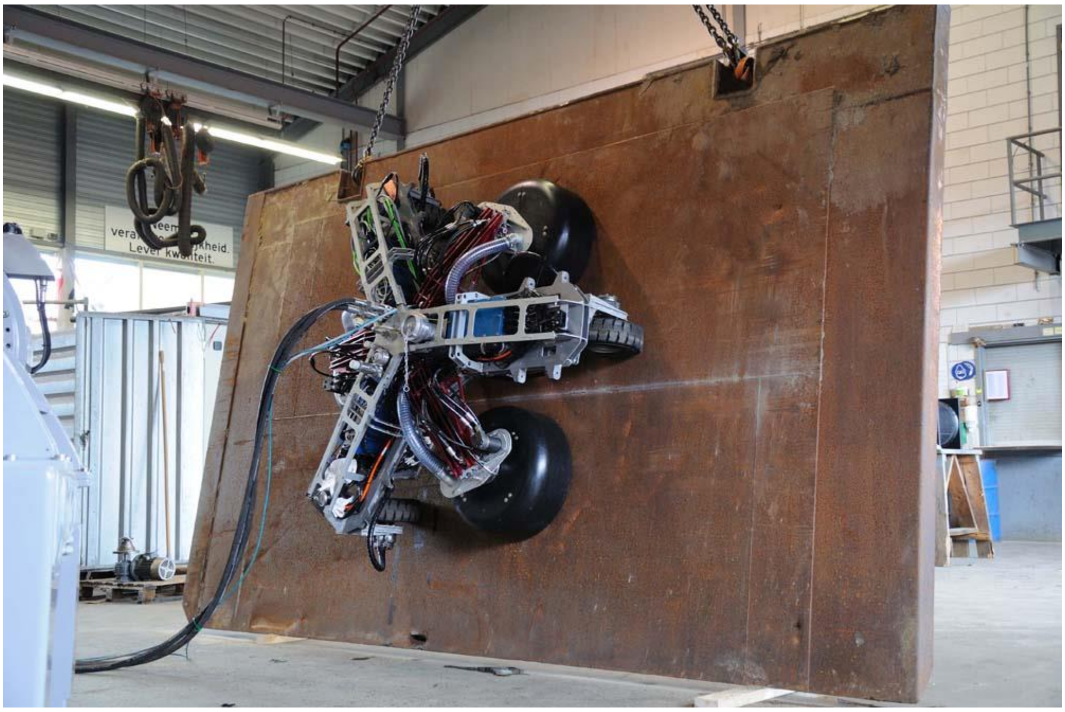

Fig.7: Fleet Cleaner robot and representative steel surface in laboratory workshop

- First system trial on barge in April 2016, Fig.8
  Tests on in-water cleaning were performed successfully in Groningen Seaports, applying the technology to barges of Royal Wagenborg. The tests were supervised by Rijkswaterstaat and Groningen Seaports, to validate that the system captures indeed the removed fouling.

Fig.8: First system trial on barge

- First ship hull cleaning trial in December 2016, Fig.9
  Fleet Cleaner completed its first ship hull cleaning on the HNLMS Karel Doorman, the largest vessel of the Royal Netherlands Navy. Both underwater and above-water cleaning were performed by the robot. External coating experts confirmed with several coating measurements that the high-pressure waterjet cleaning did not damage the coating.

Fig.9: First ship cleaned by Fleet Cleaner robot: HNLMS Karel Doorman

- Roll-out to all Dutch ports in 2017
  In 2017, the Fleet Cleaner service was approved and available in all Dutch ports: Port of Rotterdam, Port of Amsterdam. Port of Den Helder, Zeeland Seaports, Groningen Seaports and the Port of Flushing (Vlissingen). The regular industry service keeps adding experience and references. For example, very large containerships (> 350 m), Fig.10, were cleaned without causing any downtime for the shipping companies, even when combined with bunkering activities.


Fig.10: Large containership cleaned in Port of Rotterdam

Acknowledgement

We thank Volker Bertram (DNV GL) for his encouragement and support in writing this paper.

References

CURRAN, A.; O'CONNOR, B.; LOWE, C.; KING, E. (2016), *Analyzing the Current Market of Hull Cleaning Robots*, Worcester Polytechnic Institute, https://web.wpi.edu/Pubs/E-project/Available/E-project-121416-161958/unrestricted/USCG_Final_2016.pdf

ISHII, K.; NASSIRAEI, A.A.F.; SONODA, T. (2014), *Design concept of an underwater robot for ship hull cleaning*, 13th Conf. Computer and IT Applications in the Maritime Industries, Redworth, pp.540-545, http://data.hiper-conf.info/compit2014_redworth.pdf

ODETTI, A.; BIBULI, M.; BRUZZONE, G.; CACCIA, M.; RANIERI, A.; ZEREIK, E. (2016), *Co-operative robotics – Technology for future underwater cleaning*, 1st HullPIC, Castello di Pavone, pp.163-177, http://data.hullpic.info/hullpic2017_ulrichshusen.pdf

TRIBOU, M.E. (2006), *Underwater hull grooming for in-water ship hull coating maintenance*, Florida Institute of Technology, Melbourne

Reflecting Commercial Considerations in Vessel Performance Analysis

Nicolas Bialystocki, Antares Shipping, Haifa/Israel, nicolas@antares.co.il

Abstract

This paper describes an approach to generate speed-power curves (baselines). These curves play a vital role in charters. The semi-empirical approach combines commonly accepted theories on ship hydrodynamics and in-service data. Reflecting business realities, the approach expresses speed versus fuel consumption and is intended to be accepted by both parties in charter contracts throughout the charter party period. The approach reflects ship performance dependence of the speed, looking for performance at 5 different speeds representing the range from lowest eco-speed to maximum speed. However, corrections for different wind scales resulted in scatter (= uncertainties) where commercial risk considerations drive the more-or-less conservative choice of possible baselines. The approach is illustrated for a fleet of PCTC vessels. These were evaluated based on Noon Report data and benchmarked against similar (competing) ships.

1. Introduction

Vessel's performance within ISO 19030 is standardized in order to indicate the need for hull and propeller maintenance, repair and retrofit. Nevertheless, from the commercial point of stand, the performance of a chartered vessel is normally described as her speed and consumption. An example of such a charter party is Bimco's BALTIME 1939 (amended in 2001) where the speed capability on consumption is to be found in box number 12.

The performance as stated in a charter party was meant for the Maximum Speed, however, in recent years it was found that various vessels are slow steaming and as a consequence ship owners and charterers are required to agree upon a set of performances to the chartered vessel, i.e. fuel consumption at different speeds.

Nevertheless, as the focus of shipyards remains on technical specification of a new building, and such specification are for the Maximum Speed and not for a range of speeds, it became a ship owner task to propose a chartered vessel's performance for a set of speeds.

The performance of a vessel in various speeds can be estimated with different analytical approaches. In this paper, a semi-empirical statistical approach was selected combined with commercial considerations which are natural in the business of chartering and cannot be set aside.

The aim is therefore to propose a method for a ship owner to analyze his vessel's performance data in order to come up with a range of speed and fuel consumptions that are both technically and commercially viable and could be accepted by both parties and mandate throughout the charter party period.

2. Methodology

The principal condition for the selected approach is that the ship owner has time to carry out analysis based on operational data. In that case, data acquisition is carried out on daily basis by the crew and sent in a form of a Noon Report for further analysis. The Noon Reports are to be totally objective and this is achieved due to the fact that at the time of collecting the data, vessel's performance is yet to be agreed between the parties.

On the other hand, in the case that the ship owner doesn't have the time for analyzing the performance of the running vessel, the proposed methodology is not practicable and another approach will be needed. The methodology is described in Fig.1.

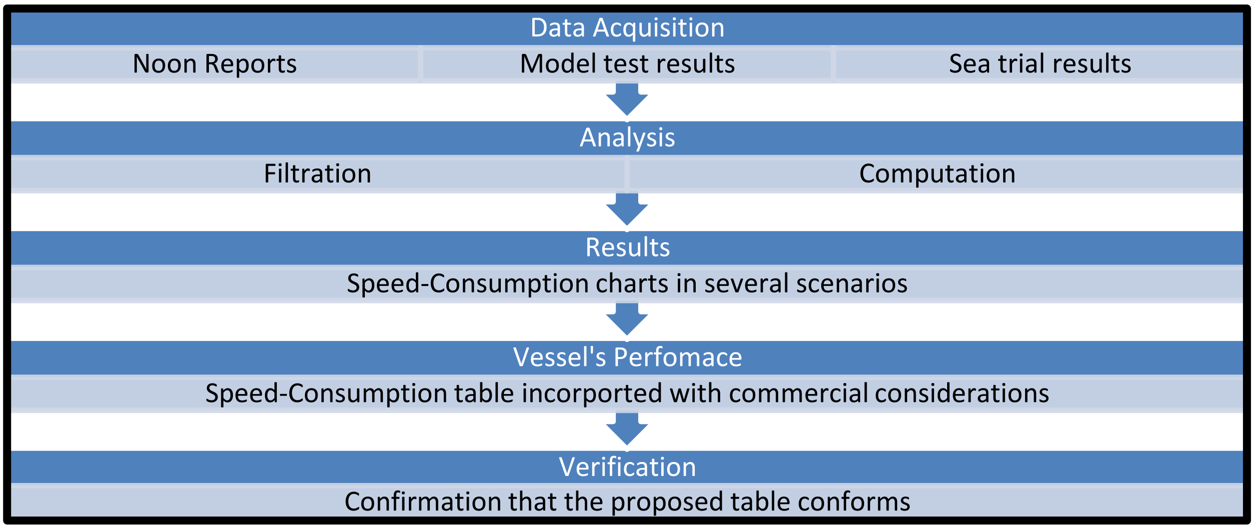

Fig.1: Process to speed consumption table

The data acquired from Model Test and from Sea Trial include the shipyard's estimated speed - power and speed - fuel consumption curves. Fuel consumption is calculated with the following formula:

$$Fuel\ Cons. = SFOC \cdot P \cdot 24 \cdot 10^{-6}$$

Where *SFOC*, measured in g/kWh, is Specific Fuel Oil Consumption as given by the main engine manufacturer and *P*, measured in kW, is the NCR (Normal Continues Rating) Power as measured both in Model Test and in Sea Trial.

While the Model Test is carried out usually at both ballast and designed drafts, the Sea Trial is carried out only at ballast draft and therefore forces the shipyard to estimate the vessel's performance at design draft based on the performance at ballast draft.

In both Model Test and Sea Trial it is normal to include allowance for sea margin, however at the same time results are normally corrected to weather force BF-0.

Data acquisition from the operating vessel includes following information, for every day while the vessel is under voyage:

- Vessel's name
- Distance travelled [nautical miles]
- Time of run [h]
- Average speed [kn]
- Main Engine output [kW]
- Main Engine fuel oil consumption [t]
- Draft (fwd + aft) [m]
- Wind scale [BF]

The Noon Reports analysis incorporated at its preliminary stage, filtration of reports that are considered to introduce error and without any significant contribution to the computations. The filtration process is subjective from its nature.

Reports which are filtered out are such that for instance provide unreasonable information due to typos or other human mistakes. Other reports which were filtered are such that reflect short operating time implying that the vessel was at manoeuvring in/out of port. More so, Noon Reports which reflect sea passage in harsh weather condition i.e. BF-7 and above, were filtered.

Calculation is carried out based on data acquired from each report, of the following parameters:

- Main Engine daily fuel oil consumption [t/day]
- Draft mean [m]
- Trim [m]
- Displacement [t]
- Power at design draft [kW]
- M/E DFOC - daily fuel oil consumption, at design draft [t/day]
- Power corrected to BF-0 and to BF-4 of wind scale [kW]
- M/E DFOC at design draft corrected to BF-0 and to BF-4 of wind scale [t/day]

Correction of M/E power and DFOC was done to BF-0 in order to be able to compare the actual vessel's performance to the results from Model test and Sea Trials. On the other hand, correction to BF-4 was elected since this weather force is considered from commercial point of view (as well as in ISO 19030) as an acceptable limit for measurement of vessel's performance as agreed in common charter parties.

The power correction to design draft was calculated using the Admiralty Coefficient which for a specific speed, $P \propto \Delta^{2/3}$. The power correction to BF-0 and to BF-4 of wind scale was carried out in accordance with the NSMB trial allowance chart (NSMB publication no.524a).

The output results of this analysis are various speed-consumption curves based on different conditions. Except of curves extracted from Model test and Sea trial, the semi-empirical statistical approach provides with curves based on different weather forces the vessel encounters. All of these curves were considered thereafter, from commercial point of view, before concluding with a vessel performance table.

Any voyage completed after that the performance table had been produced, was examined from the perspective of the agreed speed-fuel oil consumption rate in order to verify the conformity of the performance table.

3. Case study

The case study is a 7,700 CEU PCTC (Pure Car and Truck Carrier) vessel built in Hyundai Mipo Dockyard and her 3 sister ships all built between the years 2013-2015, Fig.2, Table I.

Table I: Vessels' main particulars

Cargo capacity	7700 units
LOA	199.95 m
Breadth	35.4 m
Draft (design)	9.0 m
Main Engine	B&W 7G60ME-C
MCR Power	12927 kW
Speed (design)	19.5 kn

Fig.2: Case study vessel

The data is based on 433 ship's Noon Reports from 72 voyages of all 4 sister vessels. The date of the first analyzed voyage and Noon Report is 22/11/2014, whereas the date of the last analyzed voyage and Noon Report is 16/04/2016.

Acquisition of data is carried out by the ship's captain and officers using various instruments:

- Distance travelled from the DGPS
- Time of run from the Ship's Clock
- Main Engine output from Horse Power meter.
- Main Engine fuel oil consumption from Flow meters which form integral part of the F.O. supply unit and can be read from vessel's IMACS (Integrated Monitoring Alarm and Control System).
- Draft (fwd + aft) at departure and arrival from Draft gauges.
- Wind scale from the Anemometer.

Ballast operation during voyage is not a common practice for the case study vessel thus it was assumed that draft during voyage is an interpolation between departure and arrival drafts.

4. Results

4.1 Effect of Weather

Vessel's Speed-Consumption charts in several scenarios were plotted in Fig.3, in accordance with the methodology suggested. For reasons of confidentiality the daily fuel oil consumption figures cannot be presented here; nevertheless, the curves and their trends are shown.

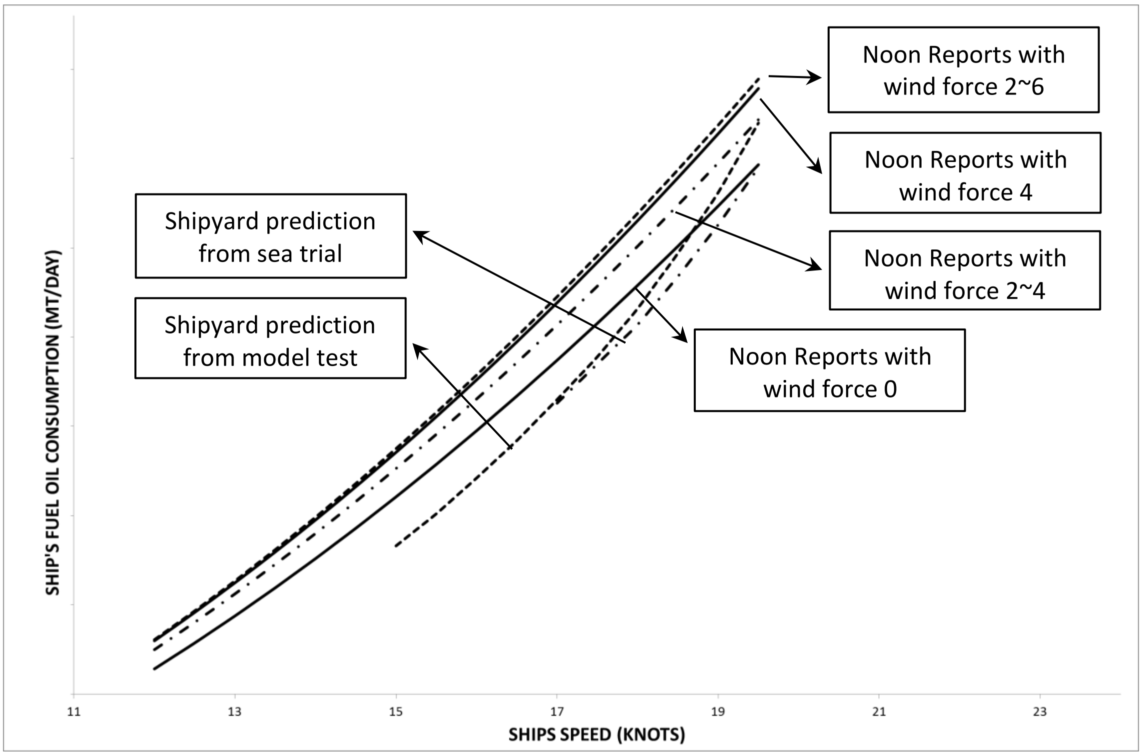

Fig.3: Case study vessels' performance in various scenarios

Different results were obtained depending on the correction due to wind force, and these were compared to the sea trial results and to the model test results from the towing tank at design stage. It was found that the performance of the vessels in all unfiltered weather forces i.e. BF-2 to BF-6, reflecting 97.0% of all Noon Reports (as shown in Figure No.4) is very similar the performance when corrected to BF-4. Furthermore, the performance improves when the vessel faced BF-2 to BF-4, as expected, and further improvement when the vessel performance was corrected to BF-0.

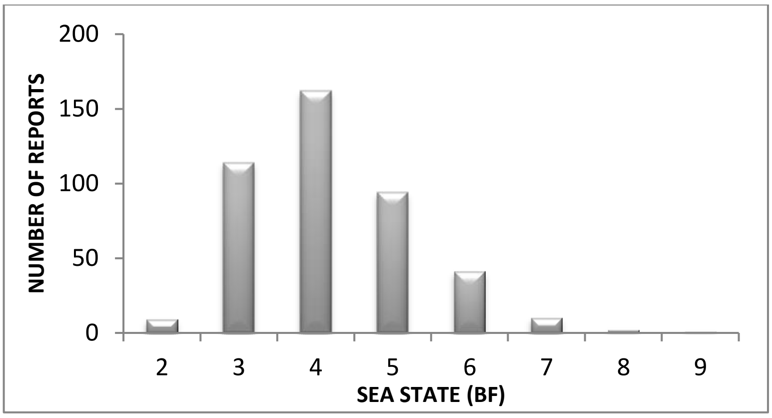

Fig.4: Distribution of Noon Reports per weather state

Range of speeds is more extensive when taking data from the vessel' compared to the data taken from Model Test and from Sea Trial. The reason for that is that shipyards still focus on Maximum designed Speed and do not take into consideration the current trends of vessels slow steaming. Fig.3 reflects also that consumption obtained from Model Test and from Noon Reports at BF-0 is very similar at the designed speed only. On the other hand, the less speed the vessel is running, the more difference was found between the two scenarios, which can be as much as 10%. Shipyard's prediction based on Sea Trials reflects the best performance at design speed and also at slow steaming. Compared to Noon Reports at BF-0 there is again similarity of the performance at design speed only.

4.2 Effect of Trim and Draft

Vessels' trim distribution, Fig.5, was not considered in this analysis because it was found that trim for the case study vessel does not normally form part of the vessel's performance clause in a time charter party.

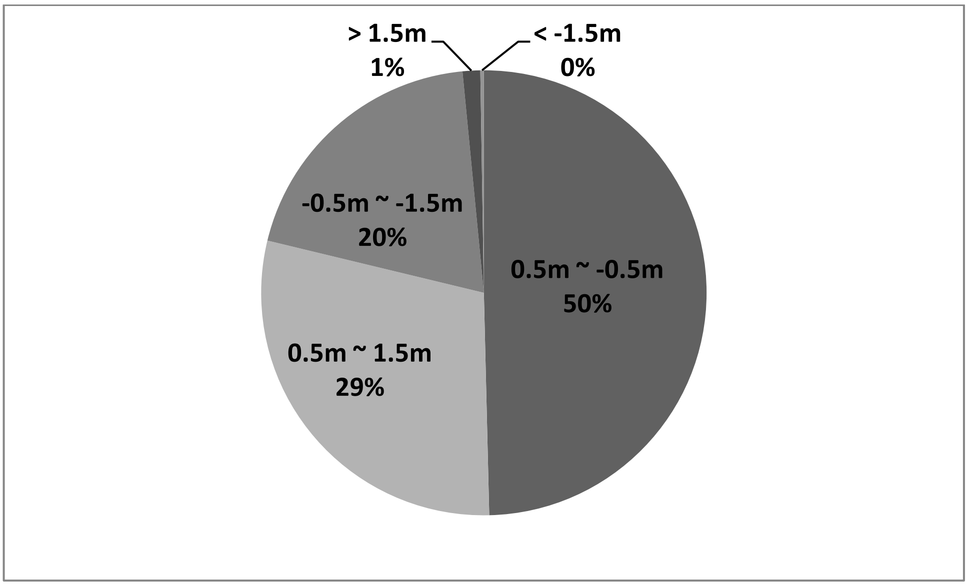

Fig.5: Trim distribution in the collected Noon Report

On the other hand, draft is standardly a condition in a performance clause of a charter party, therefore sensitivity analysis was carried out in order to evaluate the influence of the Admiralty Coefficient, which was the method selected to correct the power due to different draft. Noting that only 3 records are exactly at the design draft (Ts) of the case study vessel (=9.0 m), it was decided to consider 9.00±0.25m as a benchmark for design draft.

Therefore, the number of recorded/calculated drafts for each range is as follows:

- Drafts between and including 8.75m – 9.25m : 29 records.
- Drafts between and including 8.50m – 9.50m : 63 records.
- Drafts between and including 8.25m – 9.75m : 165 records.
- Drafts between and including 8.00m – 10.00m : 354 records.
- All Drafts : 391 records.

It was found that the Admiralty Coefficient as a method for draft correction is more effective for performance prediction the closer the draft is to the design draft, as shown in Table II. However, and at the same time ,it was found that using the Admiralty Coefficient for all range of drafts and displacements provided more conservative results, i.e. extra margin (5.5~5.7%) to the ship-owner.

Table II: Draft correction sensitivity results

Vessel's speed	Difference between Ts±0.50m to Ts±0.25m	Difference between Ts±0.75m to Ts±0.25m	Difference between Ts±1.00m to Ts±0.25m	Difference between All Recorded Drafts to Ts±0.25m
14 kn	1.4%	4.1%	7.1%	5.7%
15 kn	0.5%	3.4%	6.7%	5.6%
16 kn	-0.2%	2.7%	6.3%	5.6%
17 kn	-0.9%	2.1%	6.0%	5.5%
18 kn	-1.5%	1.6%	5.7%	5.5%
19 kn	-2.0%	1.2%	5.4%	5.5%
20 kn	-2.5%	0.8%	5.2%	5.5%

It was also found that at slow speeds of PCTC i.e. 14-17 knots, using the Admiralty Coefficient as a correction mean to the draft reflects marginal difference between Ts ±0.25m to Ts ±0.50m. However, at high speeds i.e. 18-20 knots, the Admiralty Coefficient correction reflects marginal difference between Ts ±0.25m to Ts ±0.75m. This can be explained by the design of the vessel being optimized for the Maximum Speed, which means that at higher speeds, the vessel performance can cope with wider range of drafts.

For the case study vessels, correction of drafts up to ±1.00m gives very similar results as for the full range of drafts. The reason for that is that for the case study PCTC vessel this variation of draft is equivalent to 90.5% of all measured drafts, which means the vast majority.

4.3 Specific Fuel Oil Consumption

Performance was also evaluated in terms of SFOC (Specific Fuel Oil Consumption) and results are shown in Fig.6. It was found that the actual measured SFOC is about 10% above the theoretical and designed SFOC as per manual, and this is in accordance with the Main Engine supplier (MAN) re-commendations, which is based on ISO 3046-3, Reciprocating internal combustion engines – Performance, Part 3 – Test Measurements.

Uncertainties of SFOC based on MAN include:

- Torque (±1%)
- Speed (±1%)

- Fuel Volume (±2%)
- Density of Fuel (±1%)
- Lower Calorific Heat Value (±1.5%)
- Time (±0.1%)

On top of the above, 5% standard tolerance is considered and thus the overall 10% is considered by MAN as a recommendation for evaluating SFOC measurements during Sea Trial or Sea Voyage.

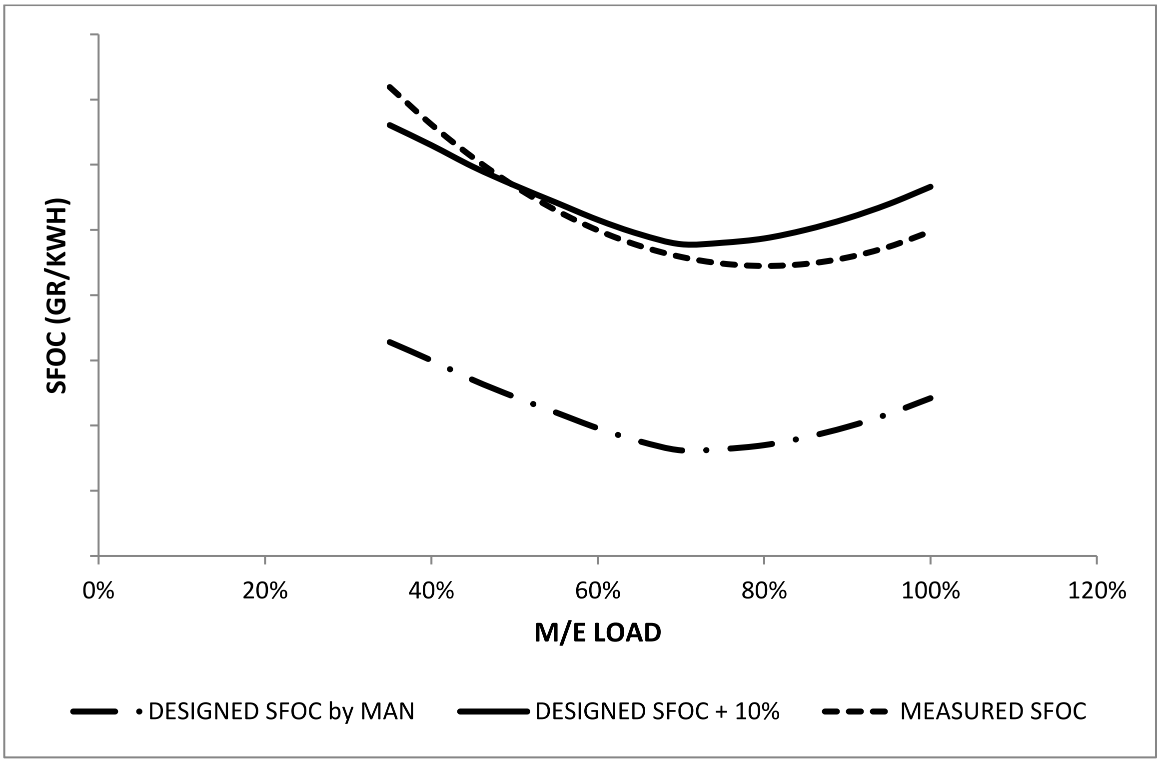

Fig.6: Designed and measured SFOC per M/E Load

5. Commercial Considerations

The produced curves, Fig.3, were not sufficient for determining an acceptable vessel's performance intended to be used in a charter party. The reasons are that:

1. A single proposal is needed.
2. Commercial considerations should be taken into account.

For a matter of practicability for being contractual part of a charter party, a table was preferred rather than a chart for description of the consumption at stepped speeds. Providing a curve without an equation seems to be irrelevant for commercial applications. As such, it was agreed between partied to provide a table of speed-consumption of the case study vessels with a total of five selected speeds, the lowest one being the most Economic Speed and the highest being the Maximum Speed, with three Intermediate Speeds.

In contrast with ISO 19310, Ships and marine technology – Measurement of changes in hull and propeller performance, which give standard for calculating performance indicator based on fixed power and respective percentage of speed loss over time, in this case study, power and fuel oil consumption could not be considered as fixed, but speed dependent. Moreover, the proposed vessel performance was to be agreed for the entire time of charter, and thus time dependent analysis was of lesser relevance in this case.

A voyage dependent PI (Performance Indicator) analysis was carried out based on ISO 19310 for each of the case study vessels, which have resulted, Fig.7, that speed loss from reference voyage being voyage number 1 of each vessel is scattered. This can be explained for a PCTC vessel being most of the time sailing with short port time and thus the effectiveness of anti-fouling can be considered to be almost steady.

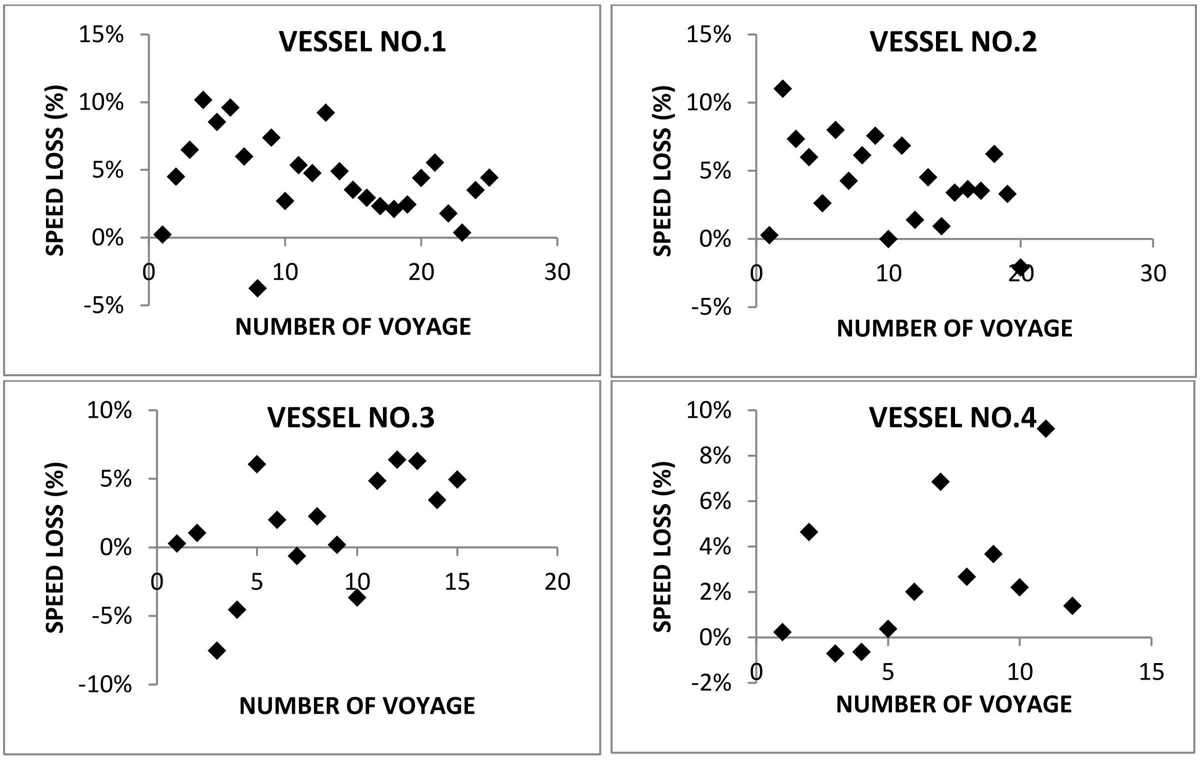

Fig.7: PI of vessels 1 to 4

A performance proposal could be either conservative which means taking into account the lowest performing obtained curve of the vessel, could be on the other hand radical which is taking into account the best performing scenario, or could be an average. On top of these alternatives, any other performance could be selected as long as it is in the range between the best and the least performing curves.

Normal charter party tolerances of 0.5 kn and 5% for fuel oil consumption were also taken into consideration, as well as considerations such as competitiveness of the vessel's performance compared to other known designs of similar size. Moreover, consideration in the final performance curve was given to the fact that the vessel should maintain her performance along the charter party period. The latter means that margin due to deteriorating hull roughness was taken into account.

The Maximum Speed with corresponding consumption was benchmarked by the New Building technical specification which was confirmed on CFD calculations and at the Model Test. This Maximum Performance was agreed between the ship-owner and the shipyard and transferred vis a vis to the charter party between the ship-owner and the charterer with slight modification due to the fact that both Sea Trial and Noon Reports resulted in better performance. There was therefore high fidelity with the Maximum Speed performance of the vessel, being verified at various stages from Initial Design to verification during voyages after delivery of the vessels. Intermediate Speeds and the most Economic Speed were out of focus during the design; therefore, the corresponding performance was mostly based on real-life voyages analyzed as detailed in this paper.

Two groups were formed to propose the vessel's performance which was intended to be used in the charter party. First group is the analytical and used the methodology described within this paper to propose the speed-consumption table. The second group is the experience-driven and consisted of the technical and operation managers of the vessels, which are in a daily contact with the vessel and were able to receive additional feedback regarding the performance.

The results of both working groups was discussed and taken into consideration before deciding on a single performance table and by taking all of the above into account. As a result, after benchmarking of the Maximum Speed and corresponding Fuel Oil Consumption, the other four performance steps in way of Fuel Oil Consumptions at particular Speed were determined plotting a curve with similar trend to the trends obtained from the Noon Report analysis, whilst intersecting with the selected Maximum Performance.

6. Summary and Conclusions

A challenge was brought to the ship-owner, to propose vessel's performance in way of speed-consumption which can be set in a charter party. A methodology which includes an analysis based on known theories was carried out based on data acquired from the case study vessels' Noon Reports and several speed-consumption plots were drawn at different wind force scenarios, and at the design draft.

The effect of Trim was considered negligible due to practically not being considered in a charter party of the Case Study vessels. On the other hand, the effect of draft correction was considered in a sensibility analysis and the Admiralty Coefficient was found to be conservative way for correcting power due to different draft and displacement.

SFOC analysis was carried out and obtained results were as expected with the normal tolerances. However, the design SFOC used in Model Test was found to be theoretical and therefore it suggested to be taken into account when basis for charter party performance is a Model Test. Applicability of ISO 19030 for establishing a vessel performance acceptable in charters was critically discussed and found to be lacking.

The ship’s Maximum Speed was selected based on the analysis and incorporating also commercial considerations such as long time charter, competitiveness of the design, acceptable margins for speed and for fuel oil consumption, and also charterer's expectations were to be taken into account. Having this benchmark and the analysis with trends of curves, was the ground to establish vessel's performance at lower speeds.

The procedure of ship design performance analysis took about 18 months of data acquisition from the vessels, filtration, analyses, and taking all relevant considerations in order to propose a speed and fuel oil consumption table that can be accepted by the charterers and incorporated in a charter party.

Model Test and Sea Trial for new building were also considered in the analysis, however for high speeds only due to the limited range of speed provided by the shipyard. It is suggested that shipyard adapt to market trends in way of slow steaming and carry out such tests in low speeds.

The methodology is such that it can be updated on one hand, and on the other hand it can be verified that the proposed curve is reliable for future voyages of the case study vessels.

References

BIALYSTOCKI, N.; KONOVESSIS, D. (2015), *On the estimation of ship's fuel consumption and speed curve: A statistical approach,* 12th IMDC, Tokyo

BIMCO BALTIME (2001), *Bimco Uniform Time Charter*, BIMCO, Copenhagen

ISO 3046-3 (2006), *Reciprocating internal combustion engines – Performance, Part 3 – Test Measurements*, ISO, London

ISO 19030 (2016), *Ships and marine technology – Measurement of changes in hull and propeller performance*, ISO, London

JONG, H. J. DE; FRANSEN, H.P. (1977), *Netherlands Ship Model Basin Trial Allowances 1976*, Int. Shipbuilding Progress 24/279

KRAPP, A.; BERTRAM, V. (2016), *Hull Performance Analysis – Aspects of Speed-Power Reference Curves*, HullPIC'16, Pavone

Hull and Propeller Fouling Decomposition and Its Prediction based on Machine Learning Approach

Jinmo Park, Boram Kim, Hunseob Shim, Kyoungsoo Ahn, Jin Hyoun Park, Donghoon Jeong, Seyong Jeong, Hyundai Heavy Industries, Seoul/Korea, jinmo.park@hhi.co.kr

Abstract

Hull and propeller fouling is a very important issue in maritime industries since it is directly related to the operation cost of shipping companies. However, many studies focused on total fouling effect (i.e.., hull and propeller) and there are difficulties to decide which part to be cleaned. In this study, a new approach for investigating the decomposition of hull and propeller fouling effect with machine learning and naval engineering view is proposed. To analyze the performance of the vessel, two estimators were created using a machine learning approach to derive the relationship between rpm - power and rpm - speed. Using the relationship between rpm - power and rpm - speed, the effect of the hull fouling and propeller fouling were theoretically decomposed. Based on analysis results of several ships, the database of the fouling effect is built and the future predictor is created by using a machine learning approach. The fouling estimation of predictor shows the accurate result with larger than 0.93 level of determination coefficient (R squared) comparing with the actual fouling level.

1. Introduction

In recent days, many efforts such as optimal weather routing, *Park and Kim (2015)*, ESD (Energy Saving Device) development, *Kim et al. (2015)*, EMS (Energy Management System) development, *Jeong et al. (2018)*, and hull form optimization, *Zhang et al. (2009)* have been conducted to save fuel consumption of ship. However, to evaluate the cost saving effect of such products in the actual seaway, it is essential to have a proper hull and propeller performance analysis method including fouling level analysis. Therefore, research on evaluating ship hull and propeller performance, *ISO 19030 (2016)* came into a spotlight with the requirement above. In actual voyage, bunker fuel cost represents 60~70 percentage of whole operational cost and hull and propeller fouling can cause increase up to 40% of fuel consumption, *Lauri (2012)*. Therefore, analyzing the fouling level of their vessels means knowing the actual vessel performance and cost-saving point to the shipping company. However, many recent studies related to fouling analysis focused on total fouling level analysis *ISO 19030 (2016)* or roughness investigation of hull surface as fouling develops, *Townsin (2003)*. Previous studies have limitations for ship managers to make decision what part (hull or propeller) they should clean or polish and how much fouling will be developed in the future.

Therefore, the goal of this paper present a novel method to decompose the fouling effect of propeller and hull and build a future predictor for fouling level of the vessel to have a high level of accuracy. This paper is organized as follows. The first section presents a brief review and example of machine learning approach to evaluate ship's speed-power performance in the calm water. The second section explains assumptions and procedures for the decomposition of hull and propeller fouling effects and the example of that analysis. The third section briefly explains a procedure for building fouling level predictor and the example of that prediction. Finally, the fourth section presents a summary of this research and the conclusions drawn from the results.

2. Evaluation of hull and propeller performance (Baseline)

The object of fouling effect analysis is finding the deterioration trend of hull and propeller performance excluding the effect of environment factors such as wind, waves, etc. Therefore, the first step for evaluating fouling level should be to reveal ship's speed-power performance in calm water. This data-driven approach with machine learning method is based on the study by *Park et al. (2016)*. To evaluate ship performance, two estimators are considered. The first one is for estimating the speed of ship along the voyage condition and the second one is for estimating the propulsion power of ship according to voyage condition. The concept of evaluation of performance is shown in Fig.1. The combination of two estimators draws the baseline which tells speed-power performance of vessel. Fig.2 shows the example of baseline. Through these estimators, the corrected speed and power can be obtained and it can be mapped into the speed-power plane. Baselines of each draft are shown in Fig.3. As the figure shows, the speed-power performance in calm water is obtained and the fouling level can be evaluated based on these lines.

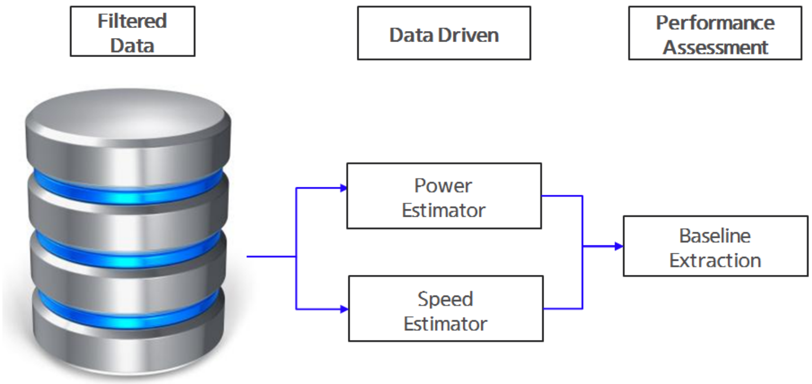

Fig.1: Concept of Performance Evaluation by Using Machine Learning

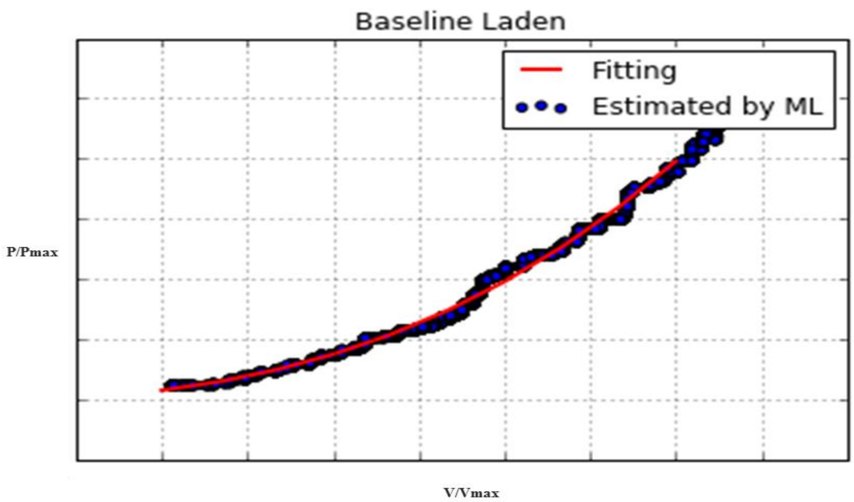

Fig.2: Example of Baseline without the effect of environment factors

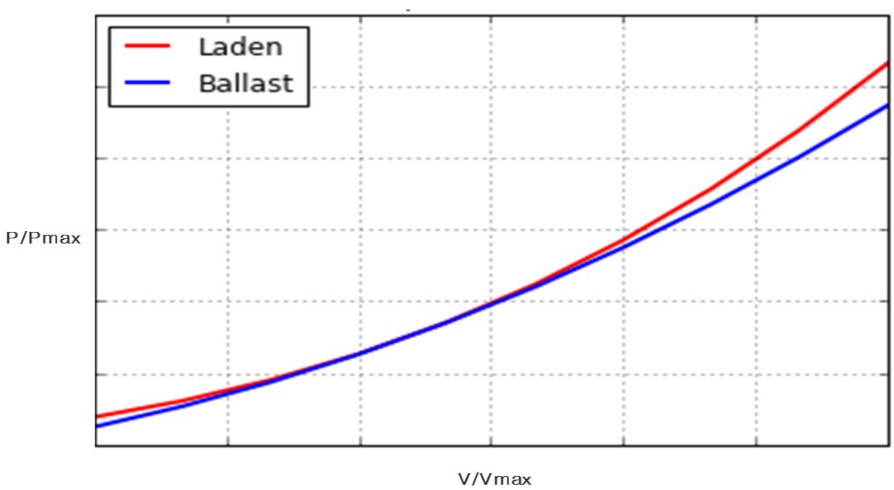

Fig.3: Example of Baselines according to the draft condition

3. Decomposition of hull and propeller fouling

In this chapter, the procedure for the decomposition of hull and propeller is explained. Fouling decomposition of hull and propeller is based on assumptions as below.

Assumption:

- The fouling only affects propeller and hull.
- There is no change of propeller shape according to propeller fouling, i.e. propeller makes the same thrust at same rpm regardless of propeller fouling.
- Therefore, the speed reduction of the ship at the same rpm is caused by hull friction increase (hull fouling).

The first step to decompose fouling effect is obtaining the rpm-speed curve. To compare status of ship, the sea trial result or model test result converted to full scale ship is adopted as reference curve. Fig.4 shows an example of rpm-speed curve of fouled ship comparing with new built ship. From these curves, designed propeller rpm (R_d) and actual rpm (R_a) are obtained at the reference speed V_{ref} .

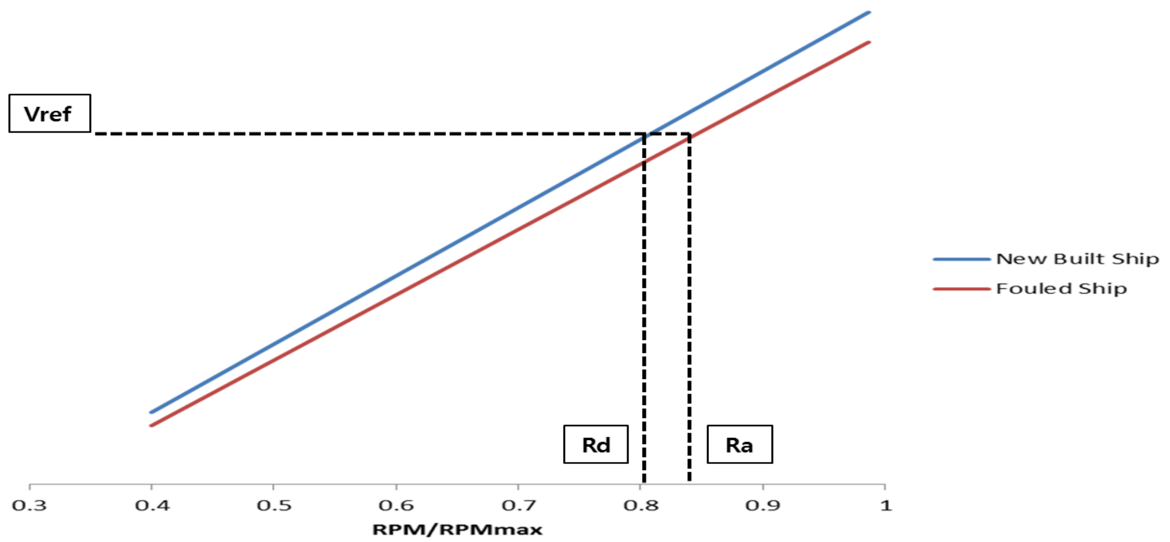

Fig.4: Concept of Hull Propeller Fouling Decomposition: RPM-Speed Curve

With obtained rpm, let's move on to rpm-power curves to decompose hull and propeller fouling effects. Fig.5 shows rpm-power curves of new built ship and actual fouled ship. If the rpms of R_a and R_d are matched to propulsion powers as shown in Fig.6, three power points of A, B and C can be found. The point A can be interpreted as rpm and power at the reference speed V_{ref} in new built ship and the point B means required rpm and power in the case only hull is fouled. Since we assumed that the rpm-power curve cannot be changed according to the propeller fouling and therefore the power difference between A and B can be seen due to the hull fouling. However, the actual rpm and power in the fouled ship is C, which includes hull and propeller fouling effects. Hence, the power difference B and C can be interpreted as the propeller fouling effect and the power difference A and C is the total fouling effect.

By the procedures above, the fouling effect of hull and propeller can be decomposed. Fig.7 to Fig.9 shows the example of fouling effect decomposition along the time. Here, the fouling effects means the ratio of increased power to the required power of new built by fouling. Since the propeller is always submerged to water, the propeller fouling effect comprises almost same portion regardless of draft.

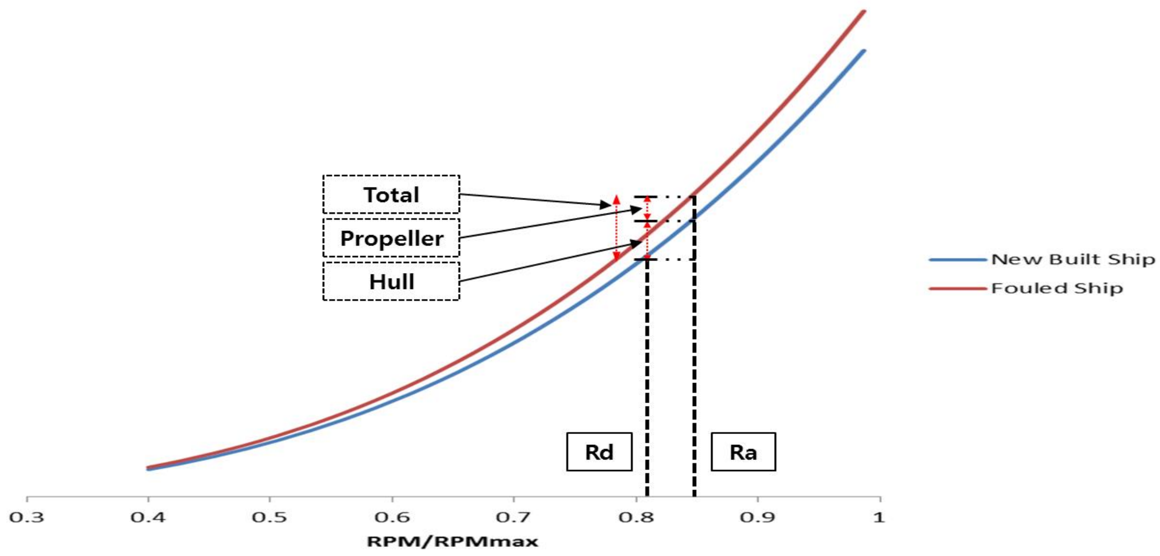

Fig.5: Concept of Hull Propeller Fouling Decomposition: RPM-Power Curve

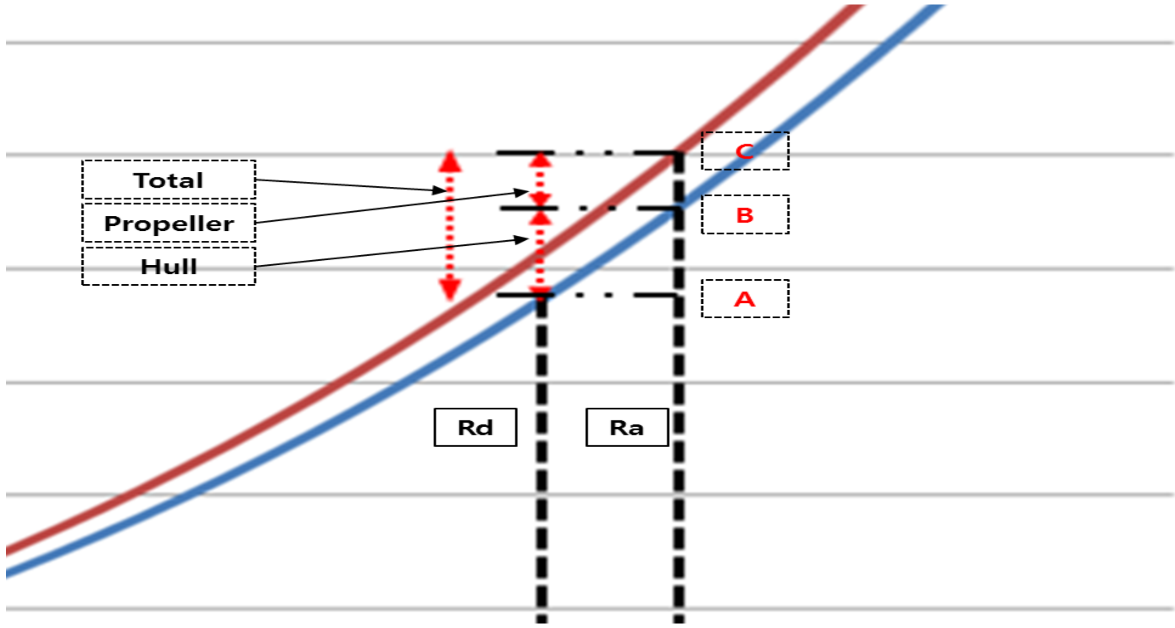

Fig.6: Concept of Hull Propeller Fouling Decomposition: Zoom in

However, the hull fouling effects in laden condition shows upward shifted tendency with certain amount of portion compared to ballast voyage condition. This upward shifted portion is exactly corresponding to the difference portion of friction resistance to total resistance of two voyage condition. According to *ITTC1978 (1978)*, the total resistance coefficient is obtained by Eq.(1), where C_{AA} is air resistance coefficient, C_R is residual resistance coefficient, C_{FS} is frictional resistance coefficient calculated from the *ITTC1957 (1957)* model-ship correlation, S_B is wetted surface area of bare hull, S_{BK} is wetted surface area of bilge keels, ΔC_F is roughness allowance coefficient and k is form factor based on *ITTC1957 (1957)* model-ship correlation. The viscous resistance C_F is described as $(S_B + S_{BK})[(1+k)C_{FS} + \Delta C_F]/S_B$ in Eq.(1). Table I shows the example of the portion of viscous resistance to total resistance of ship at the reference speed. The difference in ballast/laden draft voyage condition is almost same as the hull fouling effect gap in Fig.8. This means that the assumption for fouling decomposition is properly established and the result shows physically reasonable.

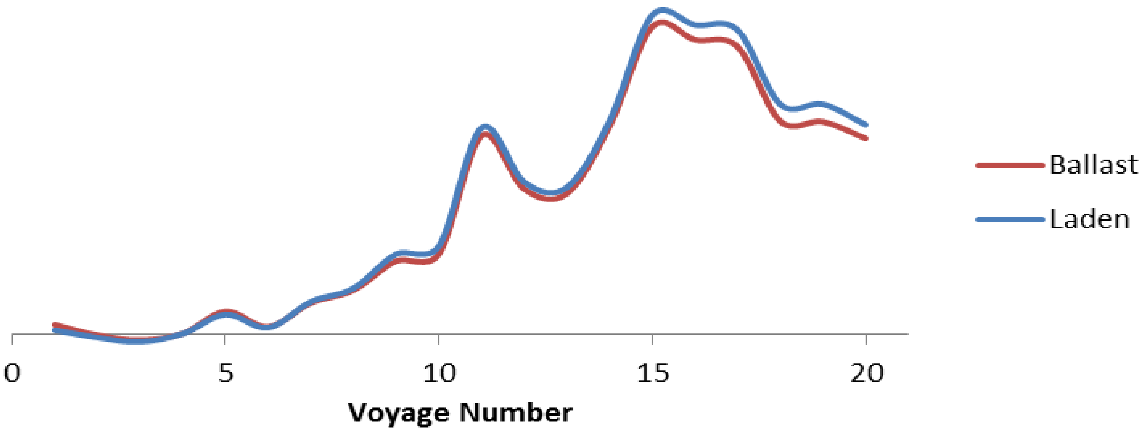

Fig.7: Example of Propeller Fouling Effect

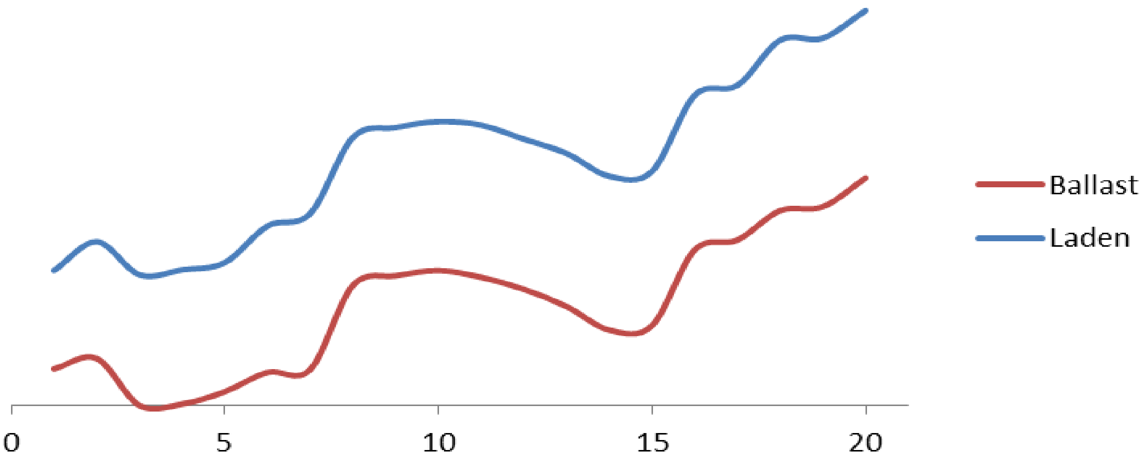

Fig.8: Example of Hull Fouling Effect

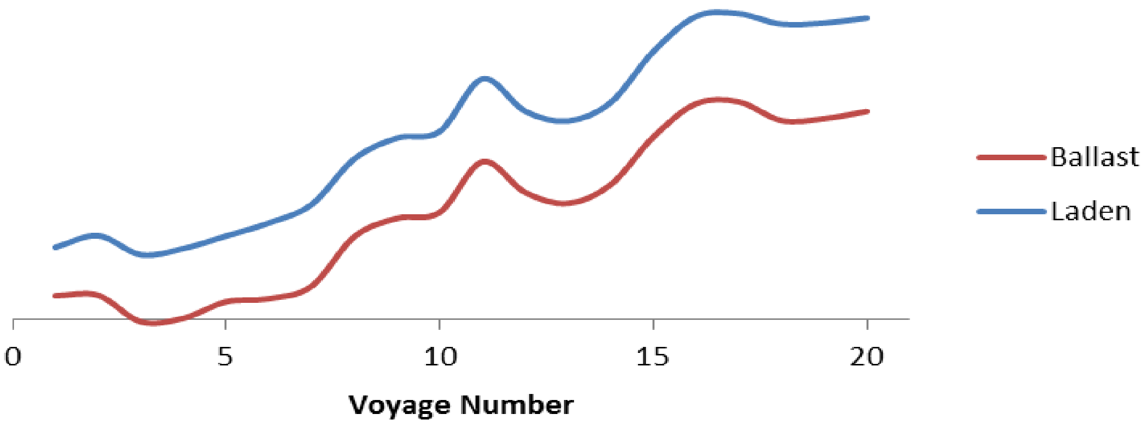

Fig.9: Example of Total Fouling Effect

$$C_{TS} = C_F + C_R + C_{AA} = \frac{S_B + S_{BK}}{S_B}[(1+k)C_{FS} + \Delta C_F] + C_R + C_{AA} \tag{1}$$

Table I: Example of Resistance Coefficient Decomposition

	Ballast	Laden
C_F / C_T	0.88	0.92
C_R / C_T	0.07	0.04
C_{AA} / C_T	0.05	0.04

4. Future prediction of fouling effect

The future predictor is based on the fouling analysis results of the previous chapter and seawater temperature forecasting is applied as an environmental factor. For prediction of fouling level, the analysis results go through a preprocessing step such as normalization. 90% of vessel voyage records out of all data are used as training data for predictor and fouling level of one vessel for one-year is predicted. Fig.11 and Fig.12 shows the actual fouling level and predicted fouling level. The prediction shows accuracy with greater than 0.93 level of determination coefficient (R squared) comparing with the actual fouling level. And the prediction result could be more improved with the increase of data.

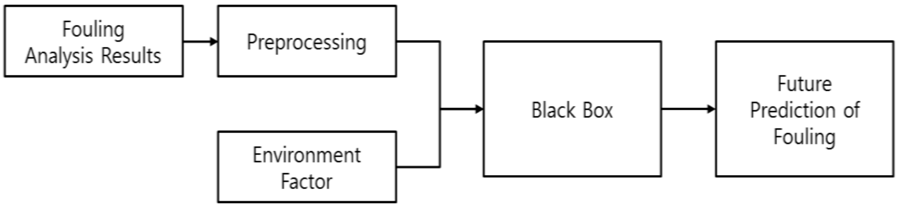

Fig.10: Concept of Future Prediction of Fouling Effect

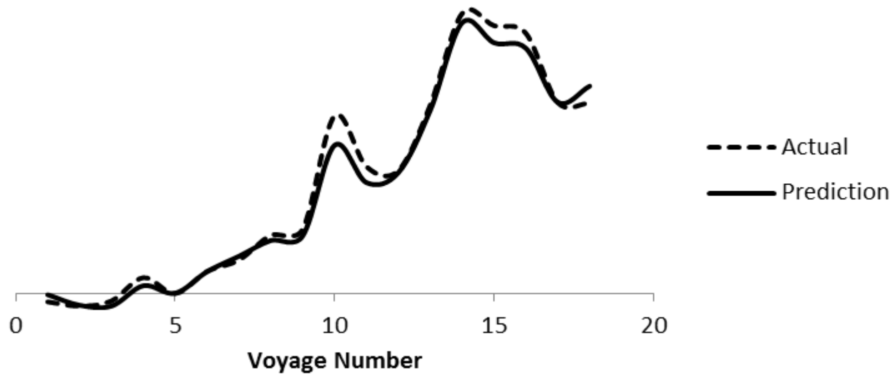

Fig.11: Prediction of Propeller Fouling

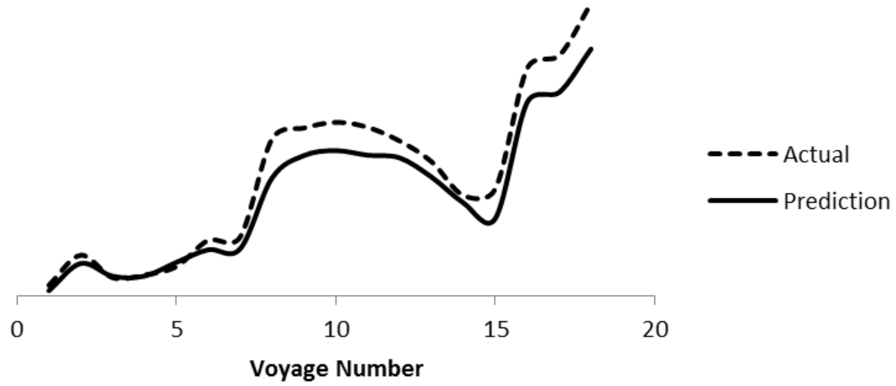

Fig.12: Prediction of Hull Fouling

5. Summary and conclusion

This paper presented a new methodology for fouling effect decomposition of hull and propeller from the viewpoint of the naval architect and the future prediction of fouling effect. To evaluate the speed-power performance in the calm water, a machine learning based approach was adopted and it could draw the performance baseline of the ship according to the draft condition. Assumptions and procedures for fouling effect decomposition were established and the analysis results showed that it is physically reasonable. Based on the fouling analysis results and environmental factors of the voyages, the estimator for future prediction of vessel fouling level was built. This prediction showed degree of accuracy with greater than 0.93 of determination coefficient (R squared) comparing with the actual fouling level.

References

BERTRAM, V. (2012), *Practical Ship Hydrodynamics*, Butterworth & Heinemann, Oxford

ISO (2016), *ISO19030 - Measurement of changes in hull and propeller performance*, ISO, Geneva

ITTC (1957), *Resistance and propulsion test and performance prediction*, ITTC

ITTC (1978), *Resistance and propulsion test and performance prediction*, ITTC

JEONG, S.; JEONG, D.; PARK, J.; PARK, J.; KIM, B.; AHN, K. (2018), *Maritime energy management system: from automatic data logging and diagnostics to operations support tool*, RINA, London

KIM, J.H.; CHOI, J.E.; CHOI, B.J.; CHUNG, S.H.; SEO, H.W. (2015), *Development of energy-saving devices for a full slow-speed ship through improving propulsion performance*, Int. J. Naval Architecture & Ocean Engineering 7(2), pp.390-398

LAURI, K. (2012), *Hull fouling: Study of hull fouling on cruise vessels across various seas*, ENIRAM

PARK, J.; AHN, K.; BYUN, S., (2016), *Machine learning approach to ship performance analysis by using gradient tree boost method*, The Society of Naval Architects of Korea, Chang-Won

PARK, J.; KIM, N. (2015), *Two-phase approach to optimal weather routing using geometric programming*, J. Marine Science and Technology 20(4), pp.679-688

TOWNSIN, RL. (2003), *The ship hull fouling penalty*, Biofouling 20, pp.9-15

ZHANG, B.J.; KUN, M.; JI, Z.S. (2009), *The optimization of the hull form with the minimum wave making resistance based on Rankine source method*, J. Hydrodynamics Ser. B 21(2), pp. 277-284

Extensive Full-Scale Measurement on Propeller Performance of 14000 TEU Container Ship

Yasuhiko Inukai, **Yasuhiko Sudo**, **Hakuya Osaki**, Japan Marine United Corporation, Tokyo/Japan
{inukai-yasuhiko, sudo-yasuhiro, osaki-hakuya}@jmuc.co.jp
Tetsuo Yanagida, MTI, Tokyo/Japan, tetsuo_yanagida @monohakobi.com
Masahiko Mushiake, **Satoshi Kawanami**, Furuno Electric, Nishinomiya/Japan,
{masahiko.mushiake,satoshi.kawanami} @furuno.co.jp

Abstract

Nippon Yusen Kaisha (NYK), MTI Co, Ltd. (MTI) and Japan Marine United Corporation (JMU) started a joint research project on extensive measurement of full scale propeller performance for 14,000 TEU container ships. In this project, we will perform the extensive works, such as thrust measurement and cavitation observation. The most challenging work among them is a direct measurement of full scale flow field around the propeller by new instrument; Multi-Layered Doppler Sonar (MLDS) collaborated with Furuno Electric Co. Ltd. (FURUNO). As a first step of the project, one MLDS was installed to a vessel in the series of 14,000 TEU container ships and the flow filed measurement was carried out in order to investigate its capability and the propeller cavitation pattern was observed at the same time. In this report, we show the flow field measurement results and the observed cavitation.

1. Introduction

In order to minimize fuel oil consumption of ships, great efforts have been made all over the world on a development of hull, propeller and energy saving device in design phase and on an improvement of operational efficiency in service. Whichever before or after a delivery of a ship, a grasp of ship performance in full scale is essential to attain an energy efficient ship for all designers, owners and operators. The accurate performance monitoring in service yields an efficient operation, *NN (2016),* and an adequate judgement of a maintenance timing for such as cleaning of hull and propeller *Ballegooijen (2016*). The information on ship performance in full scale is also treasurable for a designer. Ship design is usually based on model tests and/or theoretical calculations. One of difficulties in the design is a scaling of flow field from model to ship. Although an optimal design in model scale is accomplished, full scale optimization could not be evidenced due to the lack of the correlation data concerning Reynold's scaling effect. Further, direct calculation in full scale is becoming available with development of computation fluid dynamics (CFD), but optimization in full scale purely based on CFD is still questionable because there is few reliable data for the verification and validation. For substantial improvement of the ship performance, we need to collect full scale data and deepen understanding on the scaling effect.

With the above background, Nippon Yusen Kaisha (NYK), MTI Co, Ltd. (MTI) and Japan Marine United Corporation (JMU) started a joint research project on full scale measurement for 14,000 TEU container ships. Especially a propeller performance was focused on because it has great impact on the whole ship performance. The purpose of this project is to grasp the precise working condition of propeller during voyage and feedback to the design.

In this project, we will perform the extensive works, such as thrust measurement and cavitation observation, in addition to the usual performance monitoring (speed, power etc.). Fig.1 shows an illustration of the measurement system.

Direct measurement of full scale flow field around the propeller is most challenging. Inflow velocity to the propeller influences hull and propeller performance and thus is important information for a ship designer. However, the measurements of flow velocity, e.g. by LDV, *Tanibayashi (1990)* or PIV, *Kleinwachter (2015),* were confined by their complexity with heavy prices in measurement system.

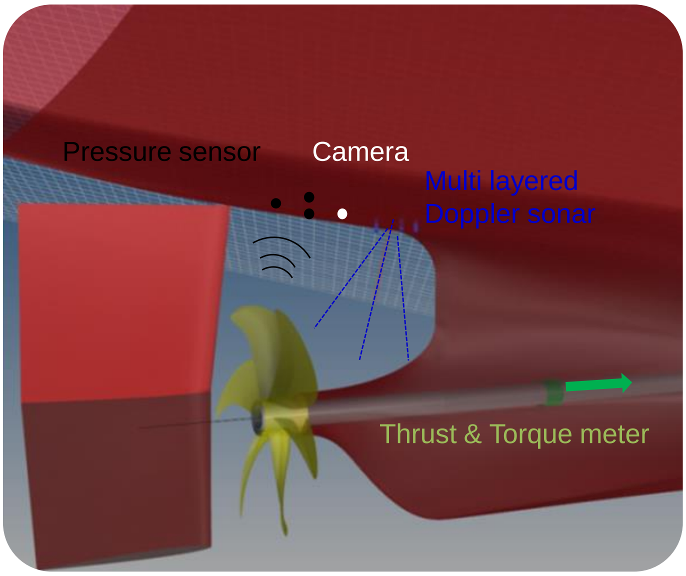

Fig.1: Illustration of the measurement system

To break through this situation, we applied the world's first new measurement system; Multi-Layered Doppler Sonar (MLDS) collaborated with Furuno Electric Co. Ltd. (FURUNO). MLDS is an acoustic Doppler sonar capable of measuring relative water velocity at multiple arbitrary depths along ultra-sonic beams. NYK, MTI and FURUNO has already applied this MLDS to a pure car carrier in service and reported that the measured flow velocity distribution at stem bottom agreed well with the CFD calculation, *Sudo (2017)*. The flow measurement at the stern, however, was thought to be more difficult compared with that at the stem because of the following reasons.

- The flow field at the stern lay in a complicated thick boundary layer.
- The sonar should be located on the hull surface near the water surface where rich bubbly flow might occur.
- There are obstacles like hull and propeller on the ultra-sonic beams.
- The propeller emits acoustic noise.

Thus, we divided the project into two stages. At the 1st stage, one MLDS was installed at the stern to investigate whichever it could measure the velocity within reasonable accuracy overcoming possible error causes. Furthermore, the propeller cavitation, which is influenced strongly by the inflow velocity distribution to the propeller disk, was observed using a borescope. In case that we could confirm the capability of MLDS at the 1st stage, we will proceed to the 2nd stage and carry out more advanced measurement as shown in Fig.1. In this paper, results of full scale measurement at the 1st stage are presented.

2. 14000 TEU container ship

The measurement was performed for 14,000 TEU container series built by JMU and operated by NYK, Table I. The measurement at the 1st stage was performed in August 2017 on the way from Suez Canal to Rotterdam. During the measurement, the weather was generally good, with absolute wind velocity up to 13 m/s and significant wave height up to 2.5 m.

Table I: Particulars of 14000 TEU container ship

Length overall	364 m
Breadth	50.6 m
Depth	29.5 m
Summer load draft	15.8 m
Trade route	Far east – Europe

Fig.2: NYK 14,000 TEU series container ship

3. Multi-Layered Doppler Sonar (MLDS)

Multi-Layered Doppler Sonar (MLDS) was developed by Furuno Electric Co. Ltd. (FURUNO) based on their product model DS-60 with revised signal processing algorism. Table II shows specifications of "DS-60". Three ultrasonic beams are transmitted from the transducer and the flow velocity in the beam direction is measured using acoustic Doppler effects. Fig.3 shows an illustration of the principal of Doppler sonar and direction of the transmitted beams, *Sudo (2017)*. MLDS can measure the flow velocities simultaneously at the depth of nine points designated arbitrarily. The beam direction can change by 180° so that you can measure the flow velocity in six directions at every 60°. It is easier to install and less expensive compared to other measurement system such as LDV or PIV because MLDS has same hardware as "DS-60" which are widely used as a speed and distance measurement equipment (SDME). In fact, a "DS-60" as a SDME was installed to the subject vessel at the stem. Fig.4 shows the MLDS equipped on the subject vessel at the stern. The transducer was attached to the bottom at the port side and measured data was transferred to the PC via the transceiver in the steering gear room. Neither the distributor nor the indicator, which is a standard component of "DS-60", was installed.

Table II Specifications of DS-60, http://www.furuno.com/en/merchant/dopplersonar/

Water tracking inaccuracy	±1.0% or ±0.1 kn, whichever is greater
Depth range	0.5-25 m
Transducer diameter	112 mm
Gate Valve diameter	125 mm
Gate Valve weight	120 kg

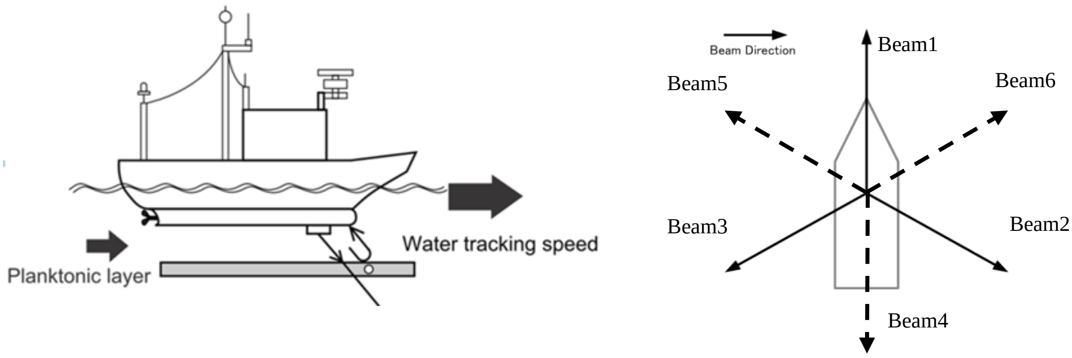

Fig.3: Principle of Doppler sonar and ultrasonic beams transmitted from the transducer, *Sudo (2017)*

Fig.4: MLDS equipped (Left: the gate valve for the transducer of the MLDS at the bottom, Right: the transceiver of the MLDS and PC for analysis in the steering gear room)

4. Flow field measurement

Fig.5 shows the velocity distribution in the beam direction against the distance from the transducer to measured points. The velocity is normalized by the ship speed measured by a “DS-60” equipped at the stem. Each mark represents a mean velocity which was measured at several times a day for about 10 minutes when not maneuvering. The numbering of the beam in the figure corresponds to those in Fig.3. The estimated velocity by calculation is also shown as the lines in Fig.5. The calculation was done using CFD code “SURF”, *Hino (1997)*, which is an incompressible Reynolds averaged Navier Stokes solver, developed by National Maritime Research Institute. Further, the standard deviation of measured velocity normalized by the ship speed is shown in Fig.6.

The following findings can be derived:

- In the range of within about 6 m from the transducer, the measured mean velocity in the beam direction fairly agrees with the estimation by the CFD. When the distribution was drawn as a contour on a surface of hexagonal pyramid composed of the six beams as shown in Fig.7, we can see more easily that the measurement agreed well with the CFD calculation.
- Generally good reproducibility was seen in the range of within about 6m from the transducer. The only data measured on 29th July (marks of asterisk) were scattered, but the reason of the discrepancy is not obvious. Since the sea condition was not so different from the other days, the water quality might affect the measurement result. More investigation on the reason is required.
- The standard deviations of velocity in the beam direction were reasonable within 5% of the ship speed in the range of about 3 m from the transducer, while they increased gradually as the distance from the transducer got larger.
- In the area far from about 6 m from the transducer, beam 2 hits the propeller and the beam 6 hits the hull as shown in Fig.7, which influenced on the measured velocity in the direction of the other beams. Accordingly, the standard deviation in the direction of all other beams got larger by mutual interaction and reasonable measurement became impossible.

In conclusion, it was confirmed that the MLDS worked very well over our expectation although we need some modification especially to measure the velocity in the far region.

Fig.8 compares the velocity distribution in the beam direction between the calculation in model scale and the onboard measurement. The calculated distribution in full scale agrees well with the measurement as shown Fig.5, whereas lee accurate in model scale. From view point of the verification of CFD in full scale, it can be concluded that full scale measurement is essential.

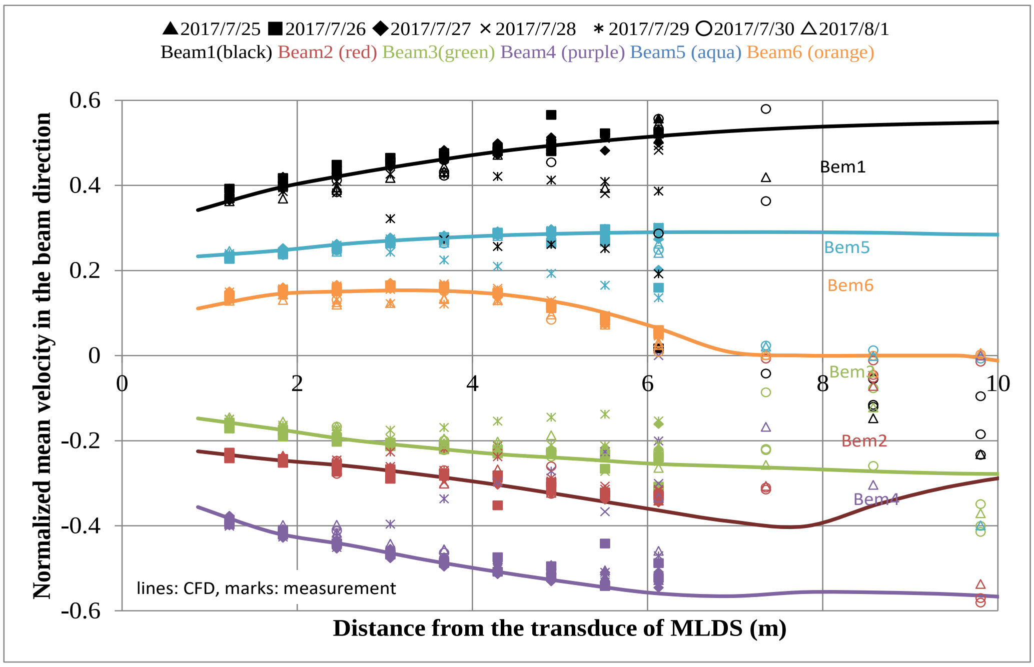

Fig.5: Measurement and calculation in full scale on normalized mean velocity in the beam direction (lines: CFD, marks: Measurement)

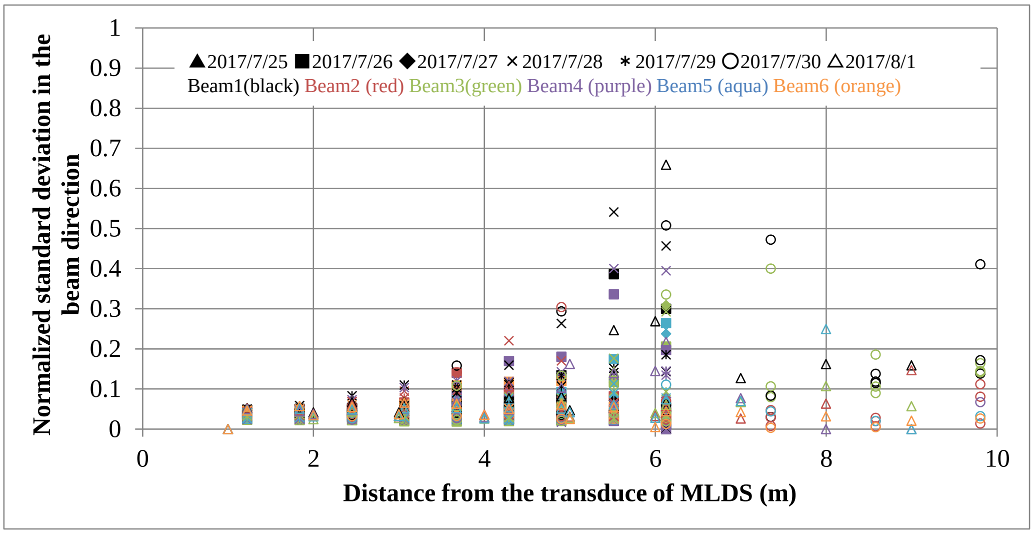

Fig.6: Normalized standard deviation of velocity in the beam direction

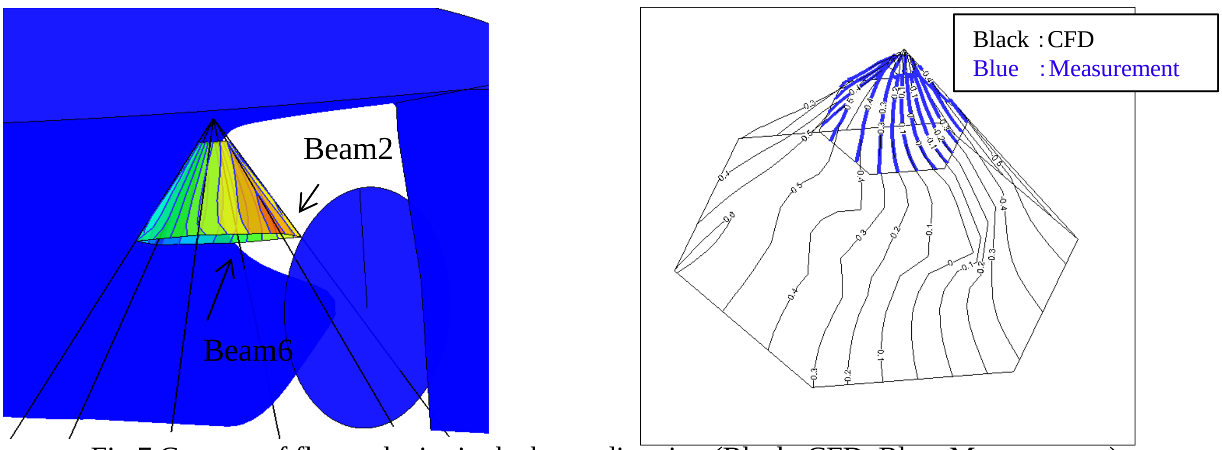

Fig.7 Contour of flow velocity in the beam direction (Black: CFD, Blue: Measurement)

From this fruitful result, we decided to proceed to the 2nd stage of the project. We are now studying a countermeasure against the problem that the beam hitting the propeller or the hull affected the measurement on the other beams. At the 2nd stage, we plan to revise the MLDS and will enlarge the range of the measurement.

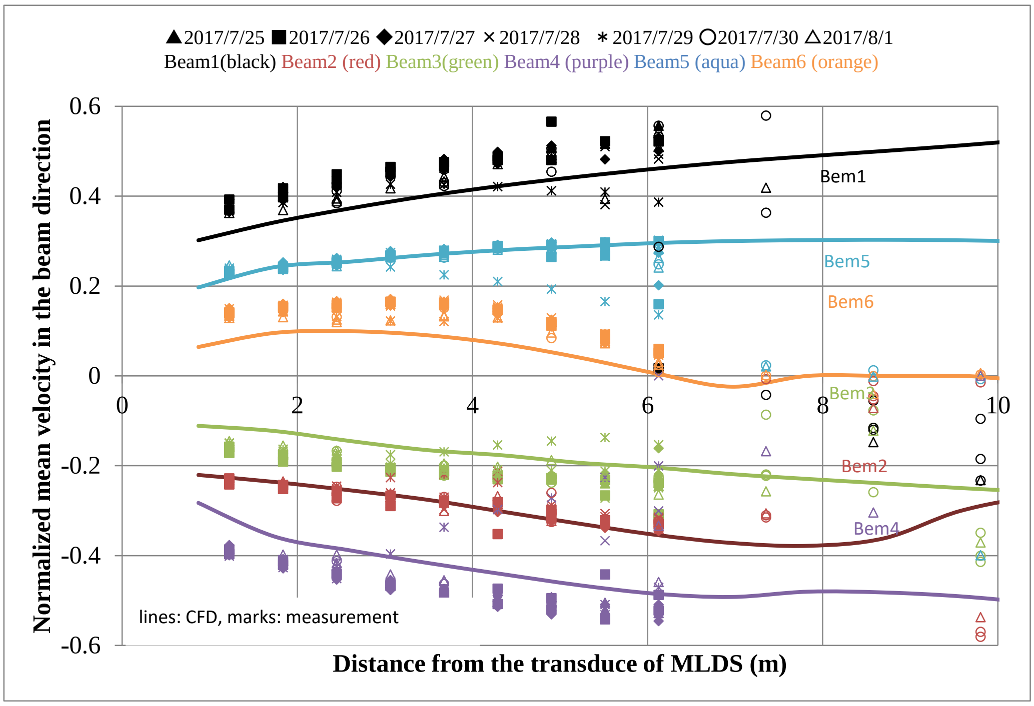

Fig.8: Measurement and calculation in model scale on normalized mean velocity in the beam direction (lines: CFD, marks: Measurement)

5. Cavitation observation

Propeller efficiency shall be maximized in parallel with moderate cavitation since excessive cavitation causes harmful phenomena such as vibration on hull and/or erosion on propeller and rudder.

The cavitation performance and the efficiency are generally in conflicting relationships and thus how to control cavitation is most important issue in propeller design. One of the reasons why the flow measurement is so important is that cavitation behavior is influenced strongly by the flow field in which the propeller works, i.e. wake field, *ITTC (2011)*. We observed cavitation during the same voyage as the flow measurement and investigated how different the cavitation pattern was from that in a model test, which gave us hints to consider the flow field in full scale.

The model test was conducted in JMU cavitation tunnel with a square test section of 0.6m x 0.6m. The wake field was generated by wire mesh screen placed upstream of the propeller. The wake distribution was simulated by extrapolating the measured model scale wake with Sasajima-Tanaka method, *Sasajima and Tanaka (1966)*, which is well known wake scaling method. The cavitation was observed using high speed camera. On the other hand, the full scale observation was taken with a borescope and two kinds of camera, high speed camera and ultra-high sensitivity camera. Fig.9 shows a setup of the full scale observation system.

Thanks to a good water quality of Mediterranean Sea we could capture very clear pictures by both high-speed cameras. Figs.10 and 11 compare observed cavitation patterns between model and full scale. The cavitation pattern in full scale was widely similar to that in model scale. As we say that 0° is the position when a key blade of the propeller is at the top, sheet cavitation appeared at around 5° position, developed into maximum extent at around 35° position and disappeared at around 70° position. The largest sheet cavitation covered over the non-dimensional propeller radius of r/R=0.85.

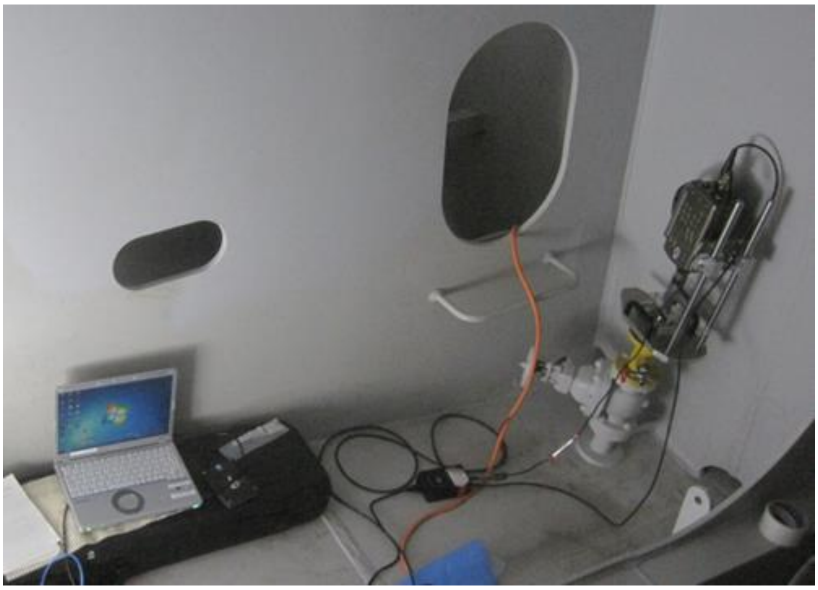

Fig.9: Setup of full scale observation system

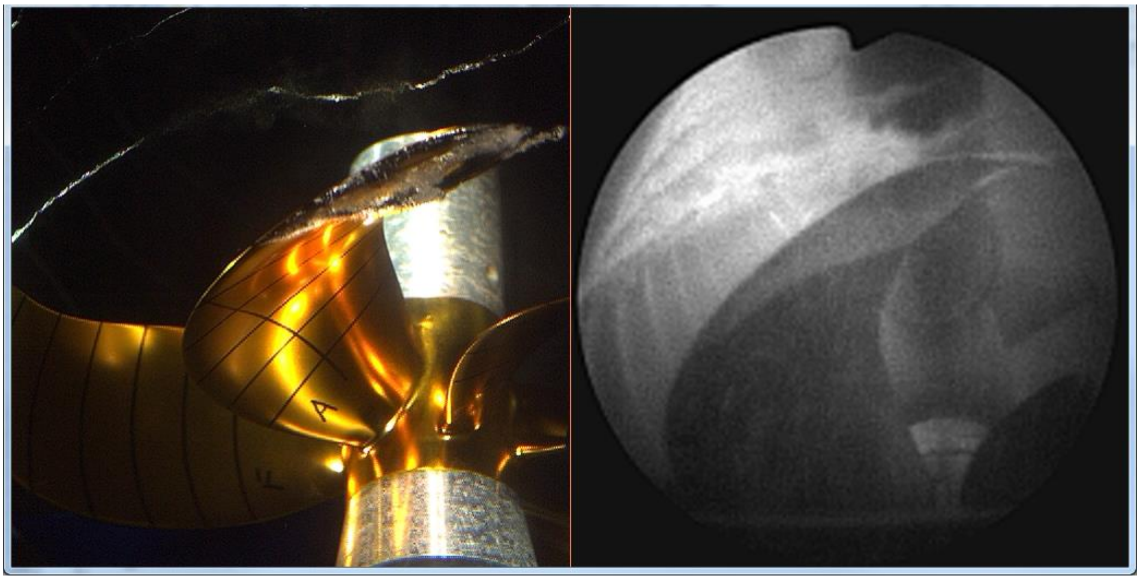

Fig.10: Cavitation pattern at the 35º position in model test (left) and in full scale (right)

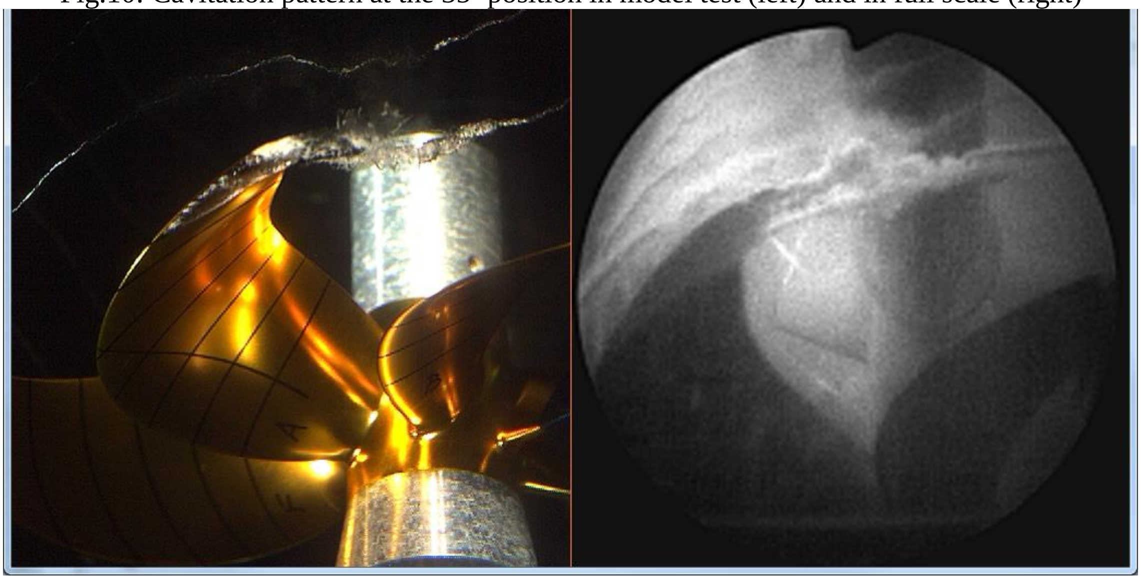

Fig.11: Cavitation pattern at the 55º position in model test (left) and in full scale (right)

These implied that the prediction by Sasajima-Tanaka Method gave a good approximation for the full-scale wake field. However, an extent of the sheet cavitation in full scale was a little bit larger than that observed in the model test when the blade going downward and passing at around 55° position as shown in Fig.11. Since cavitation occurs more in the region where the inflow velocity into the blade is slower, it was presumed that the flow velocity at around 55° position was slower than the assumed flow in the model test. This kind of observation would greatly contribute the further development of the present wake scaling method.

6. Conclusion and future work

We have confirmed the capability of the MLDS for the measurement of full scale flow field at the 1st stage of the project. Further, the cavitation behavior has been observed, which gave us hints to consider the flow field in full scale. It has become a big step toward further sophisticated propeller design.

Following the fruitful result, we proceed to the 2nd stage and will carry out more advanced measurement this spring for the sister vessel. Fig.12 shows a picture of sensors equipped with the subject vessel. During this measurement, wider range of flow field measurement with multiple MLDSs, direct measurement of propeller thrust and pressure fluctuation, and cavitation observation will be executed.

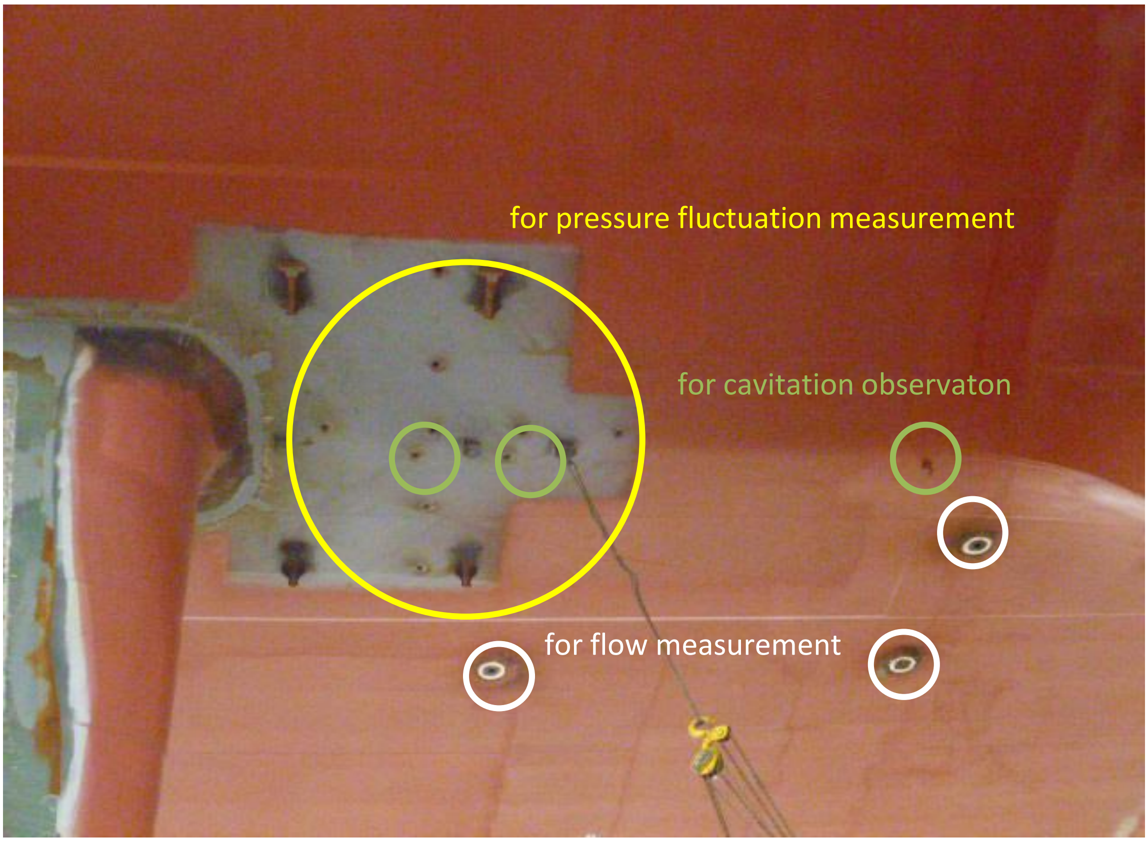

Fig.12: Sensors equipped with the vessel

References

BALLEGOOIJEN, E. (2016), *Fuel saving potentials via measuring propeller thrust and hull resistance at full scale*, 1st Hull Performance & Insight Conference, Pavone

HINO, T. (1997), *A 3D unstructured grid method for incompressible viscous flows*, J. Society of Naval Architect of Japan 182, pp.9-15

ITTC REPORT (2011), *The Specialist Committee on Scaling of Wake field*, Proc. 26th ITTC, pp.379-417

KLEINWACHTER, A.; et al. (2015), *PIV as a novel full-scale measurement technique in cavitation research*, 4th Int. Symp. Marine Propulsors

NN (2016), *Big Data and IoT in shipping*, The Naval Architect, pp.43-47

SASAJIMA, H.; TANAKA, I. (1966), *On the estimation of wakes of ships*, Proc. 11th ITTC

SUDO, Y.; et al. (2017), *Study on improvement of measuring accuracy of ship's speed through water*, J. Japan Society of Naval Architects and Ocean Engineers 24, pp.31-38

TANIBAYASHI, T. (1990), *Full-Scale LDV measurement of ship stern flow*, Group Discussion at the 19th ITTC, pp.506-509

Experience with Full-Scale Thrust Measurements in Dynamic Trim Optimisation

Erik van Ballegooijen, VAF Instruments, Dordrecht/Netherlands, evballegooijen@vaf.nl
Torben Helsloot, VAF Instruments, Dordrecht/Netherlands, thelsloot@vaf.nl
Marc Timmer, VAF Instruments, Dordrecht/Netherlands, mtimmer@vaf.nl

Abstract

This paper presents an explorative study on the role that thrust measurements can play in trim optimisation. Currently data-driven trim optimisation solutions rely on a shaft power meter, but it will be demonstrated that also thrust measurements are a valuable input. A better understanding of the subject is gained by discussing the effects of trim and assessing different approaches to trim optimisation. Possible improvements that thrust measurements can bring to the data-driven method are suggested and investigated with the help of a case study. In this case study, continuously monitored data of a ship that was equipped with a thrust sensor and power meter is presented. With the help of the thrust measurements insight is given in how the hull and propeller separately respond to changes in trim. Through further analysis of the full-scale data it is shown that there is a promising potential for improving data-driven trim optimisation by incorporating thrust measurements in addition to power measurements.

1. Introduction

The trim of a ship is the difference between its forward and aft draught. Trim can be influenced relatively easily. Before the start of a voyage it can be altered by carefully choosing the weight distribution of cargo, and during the voyage by changing the levels in the ballast tanks. Fuel savings can be achieved by choosing the right trim in the right circumstances, and therefore the subject of trim optimisation is of high interest to the maritime community.

Changing the trim changes a ship's resistance, even when all other variables are kept the same. As such there is an optimal trim value, at which fuel consumption is lowest. The optimal trim value is different in different operating conditions because it is dependent on other variables, most importantly speed through water and draught, see e.g. *Bertram (2014)*.

To be able to sail as efficiently as possible the optimal trim must be known at all times. Sailing at any draught and at any speed, the ship's crew must be able to select the amount of trim for which the required power is minimal. This means that the power must be determined for many different combinations of trim, speed and draught. Determining this has traditionally been done with full-scale trials and/or model tests, *SSPA (2009)*. More recently the capabilities of computational fluid dynamics (CFD) have progressed far enough so that it is economically viable to compute the influence of trim for a large array of speeds and draughts, *Hansen and Freund (2010)*. Even more recently the maritime industry has become increasingly data driven, enabling the advent of data-driven trim optimisation, in which machine learning algorithms deduce the relation between trim and power by learning from data measured when a ship is in service, *Ignatius et al. (2013)*.

Technological progress has thus increased the options and potentially improved the accuracy of trim optimisation. In this paper the role that another innovation, thrust measurements, can play in further improving trim optimisation is discussed. VAF Instruments has developed the TT-Sense®; a device that in addition to being a torque and power meter, measures the thrust provided by the ship's propellers. Information regarding thrust adds much value because it is measured at the shaft, in between the propeller and the thrust bearing, Fig.1, allowing the hull and propeller to be analysed separately.

It is therefore expected that thrust data can be a valuable input for data-driven trim optimisation. The application of the TT-Sense® with regard to trim optimisation had already been envisioned by its designers. Now that the sensor has been on the market for several years the first steps to making this a reality are presented.

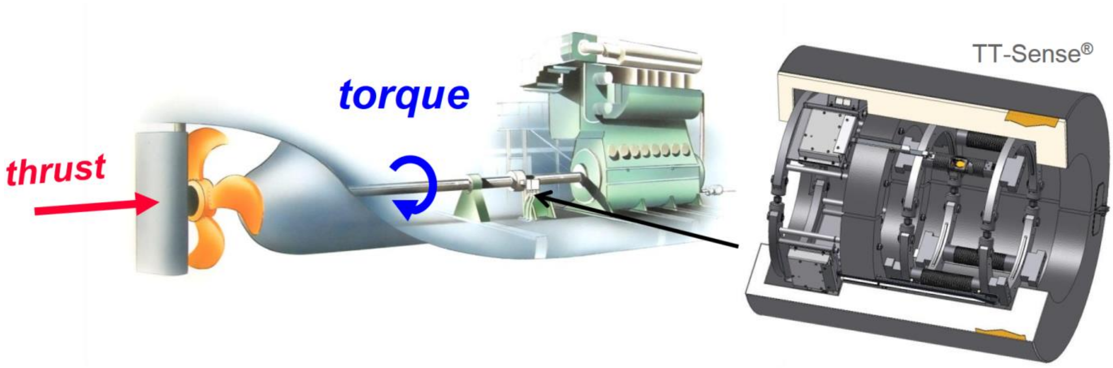

Fig.1: Measuring hull and propeller performance with the TT-Sense®

2. The effects of trim

Trimming changes the shape of the submerged part of the hull and because of this different hull shape almost every resistance and propulsion related aspect is affected by trim. As discussed by *Reichel et al. (2014)*, the most important influences on the required propulsive power are the change in residual resistance of the ship and the change in propulsive efficiency.

The residual resistance changes primarily due to a change in the wave pattern that is generated by the ship. Especially when a bulbous bow is present the effect of trim on the wave pattern can be large. A favourable trim will result in a favourable wave pattern in which less energy is dissipated.

The propulsive efficiency is affected because the flow around the hull changes with trim. This causes the thrust deduction factor and wake fraction to change resulting in a changed hull efficiency η_h. Moreover, the propeller starts to operate in a different wake and therefore the propeller efficiency η_o changes. These two effects result in a changed propulsive efficiency. A favourable trim will result in a favourable flow pattern around the hull so that less power is lost by the propeller and by hull-propeller interaction.

An important distinction must be made between static and dynamic trim. The trim before the start of the voyage is referred to as static trim. *Gourlay and Klaka (2007)* discuss that when underway, the flow around the hull and the influence of the active propeller change the pressure distribution beneath the hull which, amongst other factors, causes the actual trim to change with respect to the static value. The trim as measured during a voyage is referred to as dynamic trim. When the operating conditions of a voyage are known in advance, it is possible to predict the dynamic trim based on the static trim, and vice versa. Trim optimisation software can both give a static trim advice before the voyage commences, and a dynamic trim advice while sailing. Whenever trim is mentioned in this paper it should be understood as dynamic trim.

3. Predicting the effects of trim

To predict the effects of trim it is most important that the change in (residual) ship resistance and the change in propulsive efficiency are correctly determined. The resistance has to do with the hull, whereas propulsive efficiency is the domain of the propeller (forgetting for a moment about interaction effects). Therefore, to have a good prediction of the effects of trim, both the hull and propeller need to be correctly captured. In the next few paragraphs three methods of modelling that were mentioned in the introduction will be briefly discussed, addressing the uncertainties involved with them. The three methods are; the model test approach, the CFD approach and the data-driven approach.

3.1. Model tests

In the model test approach, self-propulsion tests will need to be performed to take into account both the hull and the propeller. To account for viscous scale effects corrections will have to be made, translating the model results to full scale. Because the hull and propeller adhere to different scaling laws they will have to be treated separately. The full-scale corrections are the biggest source of uncertainty with model scale tests. Another contribution to the uncertainty of model tests results from imprecision and bias in sensors, but because of the controlled laboratory environment of a towing tank this uncertainty can be kept to a minimum. It has been observed that different experimental approaches can lead to differences in the predicted optimal trim, *Reichel et al. (2014).*

3.2. Computational Fluid Dynamics

CFD computations can be done at full-scale, which eliminates the influence of scale effects. However different CFD models use different approximations to model viscous effects, which means that there are modelling uncertainties involved. Moreover, the use of numerical methods introduces a numerical uncertainty. The propeller is often separately modelled from the hull, and the models are coupled e.g. in the approach taken by *Hansen and Freund (2010)*. Just as in the model test approach the hull and propeller are thus treated separately.

3.3. Data-driven approach

The focus of this paper lies on the data-driven approach, which uses full-scale data measured during regular ship service. This alleviates the problems of scale-effects and numerical uncertainty. However, the conditions in which these measurements are made are quite the opposite of a laboratory environment, and hence the data is more scattered than model test data. The sensors operate in harsh conditions and the data is dependent on a lot of changing external factors (wind, waves, temperature etc.) that are not present during a model test. This introduces uncertainty. The trim optimisation that is done based on the full-scale measured data relies on machine-learning algorithms that are able to cope with noisy and uncertain data that depends on many variables. There are many choices to make in the selection of the machine learning model and the relevant parameters it takes into account (feature selection). Those choices may influence the optimal trim predicted from the same data, which means there is also an uncertainty involved in the model selection for the data-driven approach, *Pétursson (2009).*

3.4. Pros and Cons

When using CFD computations and model tests the influence of trim on the hull and the propeller can be separated. This is not the case for the data-driven approach when it relies on the power meter only. Even though the optimal trim can be predicted based on power only, it does take away the additional insight that the other two methods can give.

Another weakness that the data-driven approach arguably has, is the problem of data scarcity. When conducting experiments or computations a predetermined matrix of draught, speed and trim can be accounted for such that there is a knowledge base covering all operational conditions of a ship, even those it rarely encounters. A trim optimisation model that learns ‘on the job’ from data obtained in service may not accurately predict in newly encountered conditions simply because it does not yet have the data to do so. These considerations are more elaborately discussed by *Bertram (2014).*

To cope with data scarcity it is also important to mitigate what is known as the ‘curse of dimensionality’. This is a problem that occurs with high-dimensional data because with an increase in dimensions the volume spanned by those dimensions rapidly becomes larger, effectively making the data scarcer. If the dimensionality of data (i.e. the number of relevant variables) can be reduced, this can improve the optimal trim prediction of the machine-learning model, *Pétursson (2009).*

Each of the methods to predict the relationship between trim and fuel consumption has its own strengths and weaknesses. Which method is most accurate or most cost-effective is an interesting question that will not be discussed in this paper. Instead it will be investigated if some of the challenges in the data-driven method can be addressed by incorporating additional information in the form of thrust measurements.

4. Advantages of using thrust measurements in trim optimisation

In the previous sections, it was discussed that trimming can be used to optimise the resistance of the hull as well as the performance of the propeller. It was also addressed that when using a power meter, the data-driven trim optimisation methodology only optimises the system as a whole (i.e. total propulsive power) without giving any insight into the contribution of the separate components. In addition, it was mentioned that it is favourable to reduce the number of relevant variables that are used as an input for machine-learning models. Taking this into account, it will be discussed in this section how the measurement of thrust can be used to the advantage of data-driven trim optimisation.

4.1. Separating hull and propeller

Suppose that a ship is continuously sailing at exactly the same speed. When the hull resistance increases because of the adoption of a sub-optimal trim, the power required to propel the ship will increase. The thrust delivered by the propeller will also have to increase to match the increased resistance.

Now suppose that only the efficiency of the propeller decreases due to a sub-optimal trim. The required power will increase as well, but because the hull resistance does not increase the propeller will not have to deliver a larger amount of thrust. In both cases the power demand increases, but only if the hull resistance increases does the thrust increase. This is why thrust measurements are needed to make a distinction between the performance of the propeller and the hull. (In reality there are interaction effects between propeller and hull that make matters more complicated, and one would need to measure flow speeds in the ship's wake to resolve this. As this is not practical the pragmatic approach is chosen to apportion the increase in required power that can be linked to an increase in thrust to the hull, and the remainder to the propeller.)

When thrust measurements are available the effect that trim has on hull resistance can thus be separately analysed from the effect that trim has on propeller efficiency. In Section 5 this will be demonstrated with real in-service data.

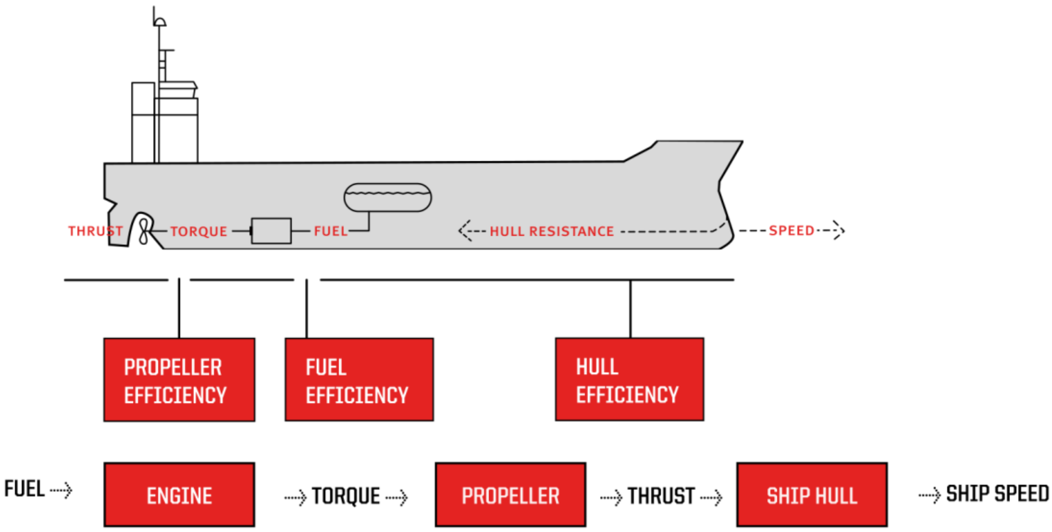

Fig.2: Only by measuring thrust can propeller efficiency be separated from hull resistance

4.2. Reducing relevant parameters

The ability to separate hull resistance and propeller efficiency can be beneficial when there are influences aside from trim that influence the one but do not affect the other. An example will be given in the following paragraphs.

Some ships are equipped with a propeller of which the blade angles (pitch) can be adjusted during sailing. This type of propeller is called a controllable pitch propeller (CPP). In contrast to a conventional propeller, a CPP can deliver the same amount of thrust at different rotation rates by using a different pitch. The efficiency of the propeller will depend on the chosen pitch and will therefore affect the power needed to propel the ship, Fig.3.

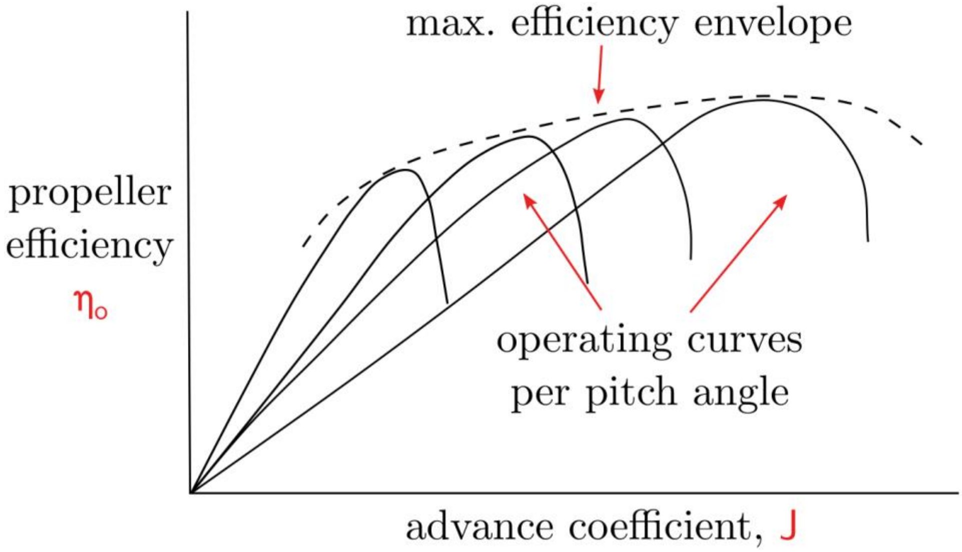

Fig.3: Schematic graph of propeller efficiency and pitch (CPP)

To illustrate how this can affect trim optimisation suppose the following scenario takes place: A ship sails with a speed of 14 knots and a draught of 6 m. It does so with a low value of trim and consumes a relatively low power. This data point is provided to the trim optimisation software which learns from the experience. Two weeks later the ship sails again with 14 knots at a draught of 6 m. It now has a high value of trim and consumes a relatively high power. However, its CPP now has a different pitch and efficiency than it did a week before. Now the increase in power cannot be ascribed to the high value of trim, because it may have been caused by the difference in propeller pitch. Therefore, when power measurements are used to optimise trim the change in propeller pitch (efficiency) must be taken into account.

Suppose now that this same ship had used thrust measurements to optimise trim. At a low value of trim it turns out a relatively low thrust was needed to overcome the resistance of the ship. Two weeks later when it sailed at a higher trim it turns out that an even lower amount of thrust was needed to propel this hypothetical ship, in other words, its hull resistance had decreased. When thrust measurements are used to optimise trim, the CPP efficiency is no longer relevant and there are less variables to take into account.

A sensibly designed ship will have an optimised hull shape equipped with a propeller that has been optimised to operate behind that same hull. In general one can expect the propeller to operate most efficiently in those cases where the hull resistance is lowest (taking into account some limiting factors such as propeller submergence). The optimal trim value can thus be found relying on thrust measurements. Some evidence for this will be presented in Section 5.

4.3 Increasing reliability

The assumption that the trim value that minimises the required thrust and the trim value that minimises the required power are approximately equal, leads to the possibility of consolidating those two values. In doing so a greater reliability can be achieved by the trim optimisation software.

Ideally the machine learning model is able to learn realistic relationships between speed, draught, trim and thrust or power, while taking into account the relevant external conditions. If it has successfully done so the model can predict the optimal trim even when the ship sails in new, unseen conditions. Conditions for which no data is available yet.

However, there is a risk that the model predicts wrong, and overfits certain parameters in such a way that the model output corresponds to observations within the current set of available data, but makes bad predictions when the results are extrapolated to predict certain conditions that are void of data, *Pétursson (2009)*. Overfitting can be detected when two models are trained to find the optimal trim, one based on thrust, the other based on power. If the two models predict roughly the same optimal value it is safe to say that it is close to the truly optimum trim. If the two models predict entirely different values it may be an indication that overfitting has taken place.

5. Case study

The previous sections introduced the concept of data-driven trim optimisation, and discussed the possibility of using thrust measurements instead of or in addition to power meter readings. To demonstrate that thrust measurements are indeed a useful input, some full-scale TT-Sense® data is presented within this case study.

In this section data is shown in order to compare the effect of trim on power with the effect that trim has on thrust. The case study encompasses a month of continuously monitored data that, to protect the interests of our clients, is completely anonymised. The vessel in question has a length between 200 and 300 m and is equipped with a fixed pitch propeller. No machine-learning algorithms will be used in the case study, instead a more perspicuous approach is chosen so that the results can be more clearly understood.

5.1 Relevant variables

The variables that are used in the case study are:

- Thrust
- Power
- Trim
- Speed through water
- Draught
- Wind speed
- Water depth

Thrust and power were measured by the thrust and torque sensor developed by VAF Instruments called the TT-Sense®. As discussed by *Ballegooijen and Muntean (2016)*, the working principle of the TT-Sense® is based on measuring shaft compression and torsion. Optical sensors detect the small displacements over the shaft length, in both axial and tangential directions, corresponding to the compression (thrust) and torsion (torque) of the propeller shaft. The used optical measurement principle allows for an independent measurement of both the thrust and the torque. Torque, combined with the measured rotation rate, is used to compute power, Fig.4.

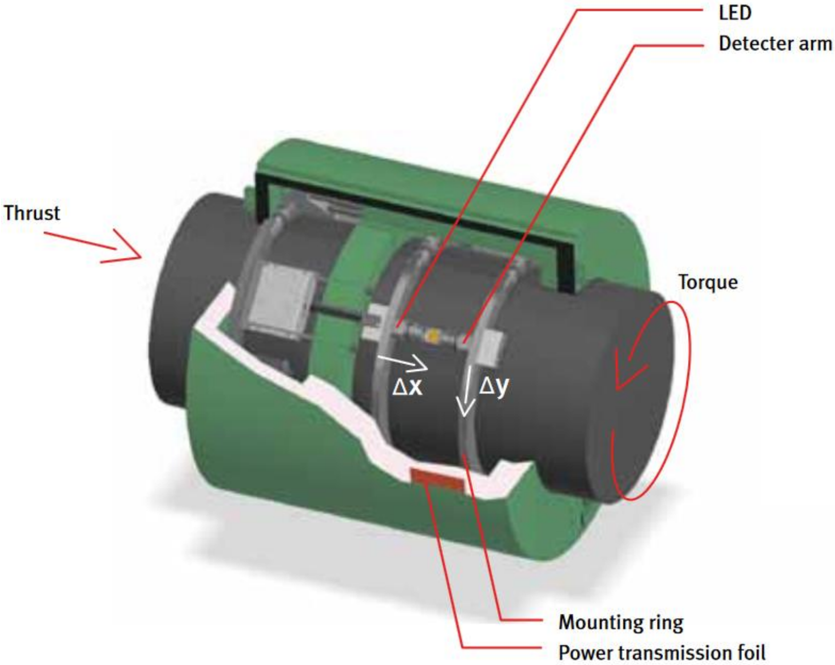

Fig.4: TT-Sense®, Thrust and Torque Sensor

Trim is measured by two draught sensors near the bow and the stern of the ship. Unfortunately, this is not the most accurate way of measuring trim, since the sensors are sensitive to variations in speed. In the ensuing analysis, the results will be presented in very narrow ranges of ship speed, which will mitigate this problem. However, for future studies it is preferable to use a dedicated instrument to measure trim, such as an inclinometer or real time kinematic (RTK) GPS technology.

Speed through water is measured by the speed log. It is a known problem that the speed log is not always a reliable instrument. Fortunately, the speed log data used did not show any obvious signs of faultiness.

Draught sensors located near midship are used to measure the draught of the ship. Wind speed is measured with an anemometer and water depth with a depth gauge.

The values of these variables have been logged on board of the vessel with a sampling interval of one second. The average value of each minute was stored and sent to shore. The minute averaged values are used in the ensuing analysis.

5.2 Data preparation

In order to isolate the effect of trim on power and thrust, the effects of external influences should be minimal. To ensure this is the case the data is filtered. Firstly, data is only used from those periods in time during which the ship was sailing at a near constant speed. In other words, data from periods of time during which the ship was accelerating and not in physical equilibrium are removed from the data set. Moreover, the data set is filtered for deep water and low wind speeds so that the influences of shallow water effects, waves and wind are small. For the sake of clarity and transparency no corrections or alterations have been applied to the data.

From the filtered set of data of which external influences have been mitigated, three subsets are selected of narrow ranges in draught and speed. For each of these subsets both the draught and speed are only allowed to vary within ±2% of their mean value. This ensures that the influence of draught and speed variations is small in those subsets, so that only the relation between trim and thrust and power remains.

Even with the narrow speed range a noticeable dependency of power on speed was observed. This is to be expected, considering power relates roughly to the cube of speed. In order to further remove the influence of speed, the power was therefore made adimensional with the cube of speed. Analogously the thrust was made adimensional using speed squared. In order to compare the influence of trim on both power and thrust in the same graph they need to share the same axis. This has been achieved by dividing the adimensional power and thrust of each individual data point in a subset, by the average of the adimensional power and thrust of all data points within that subset. The resulting variables are:

$$P^* = \frac{\frac{P}{v^3}}{\langle \frac{P}{v^3} \rangle} \qquad T^* = \frac{\frac{T}{v^2}}{\langle \frac{T}{v^2} \rangle}$$

P* indicates a relative power, T* indicates a relative thrust. A data point having a P* of 1 needed the expected, average amount of power. A data point with a P* of 1.05 needed 5% more power than the average, and with a P* of 0.95, 5% less. The same goes for thrust. When it is approximated that effective towing power is linearly related to thrust, a 5% increase in T* equates to a 5% increase in towing power. If both P* and T* increase with 5%, that means the propeller efficiency stayed equal, and the increase in power can be ascribed to an increase in hull resistance entirely. If for a certain trim the increase in P* is larger than the increase in T*, that means the propeller has also become less efficient.

5.3 Results

In this section measured thrust and power data from the TT-Sense® will be shown as a function of trim. This will be done for three operating conditions. For all three operating conditions the draught is the same, but they have different speeds; 14, 14.5 and 18 knots.

The figures show the measured values of thrust and power, converted to the adimensional values T* and P* respectively. All values were sampled while the ship sailed in very similar conditions, calm weather, deep water, and with only ±2% variation both in ship speed and draught. With the influence of all other parameters mitigated, the thrust and power are only dependent on trim. The figures can be used to estimate the dependency for the applicable operating condition.

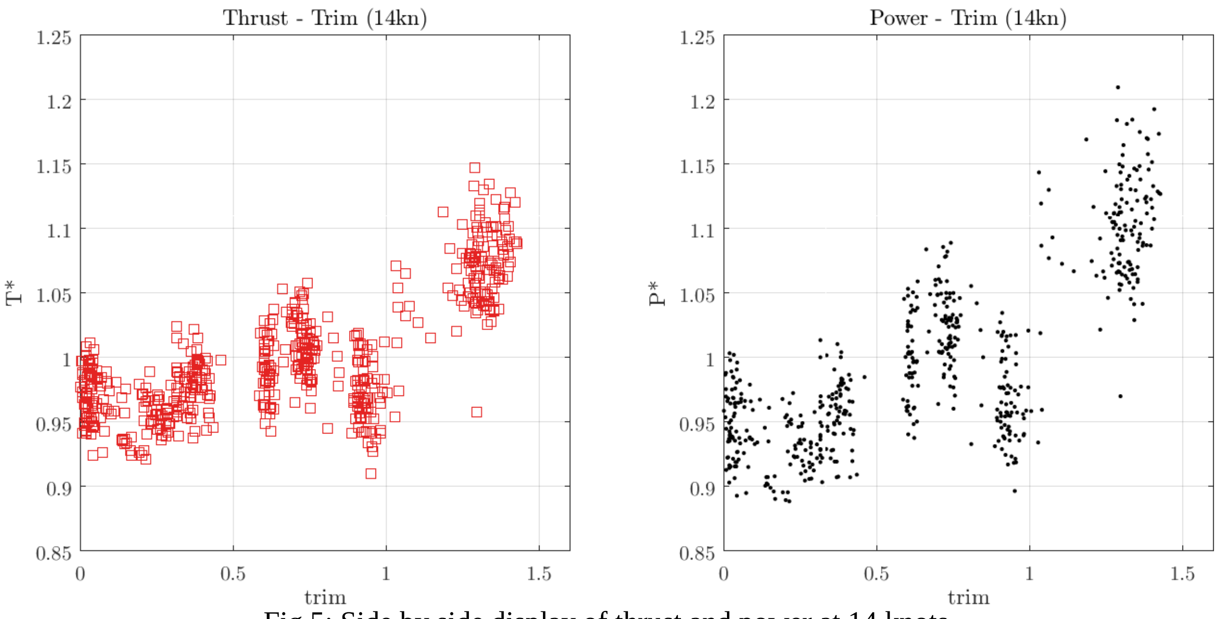

Fig.5: Side by side display of thrust and power at 14 knots

In Figs.5, 7 and 9, the thrust and power values are shown side by side. In Figs.6, 8 and 10, the exact same data points are shown again within the same graph. For the latter set of figures a polynomial fit has been drawn through the data points in order to highlight the differences between them. The polynomial fits are purely indicative; they are meant to show the general trend that is followed by the data points.

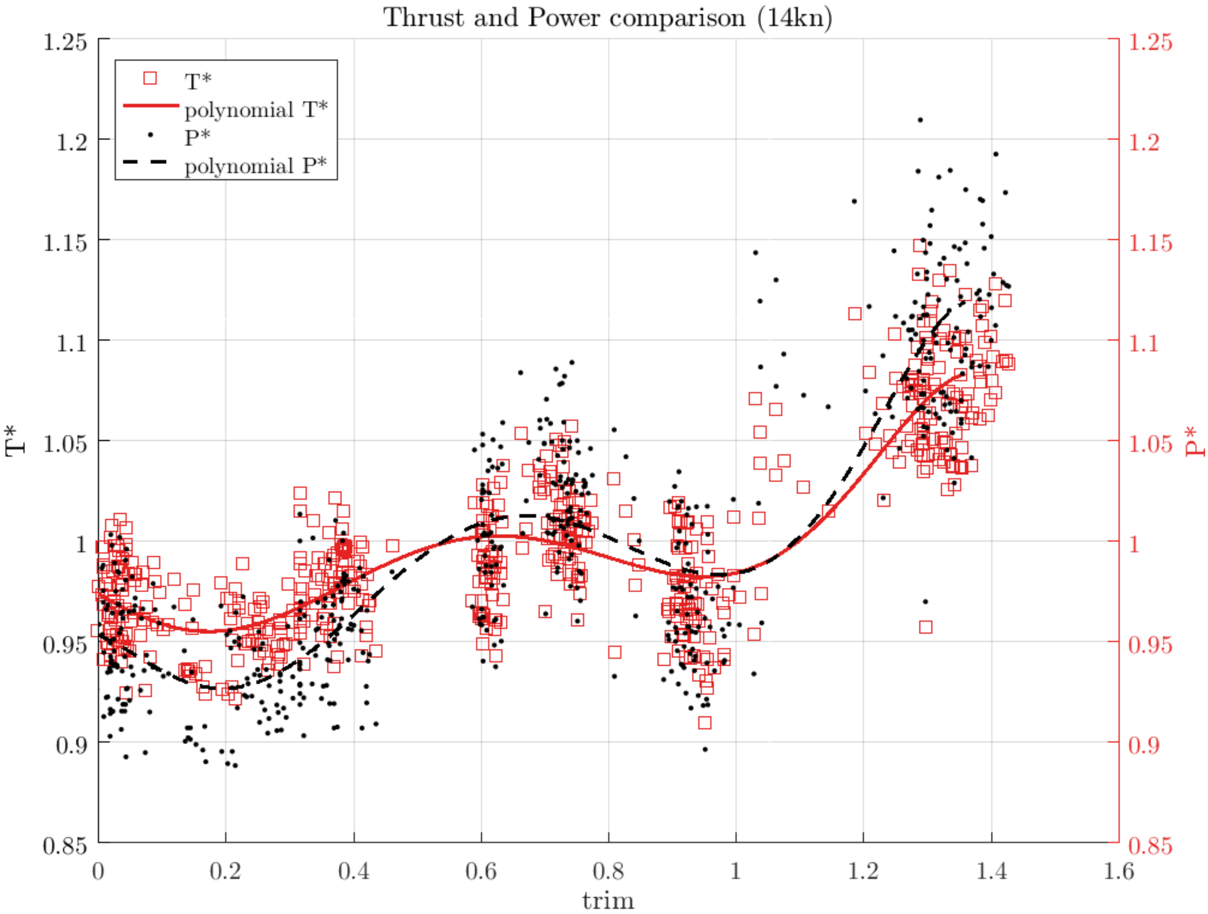

Fig.6: Direct comparison of thrust and power at 14 knots

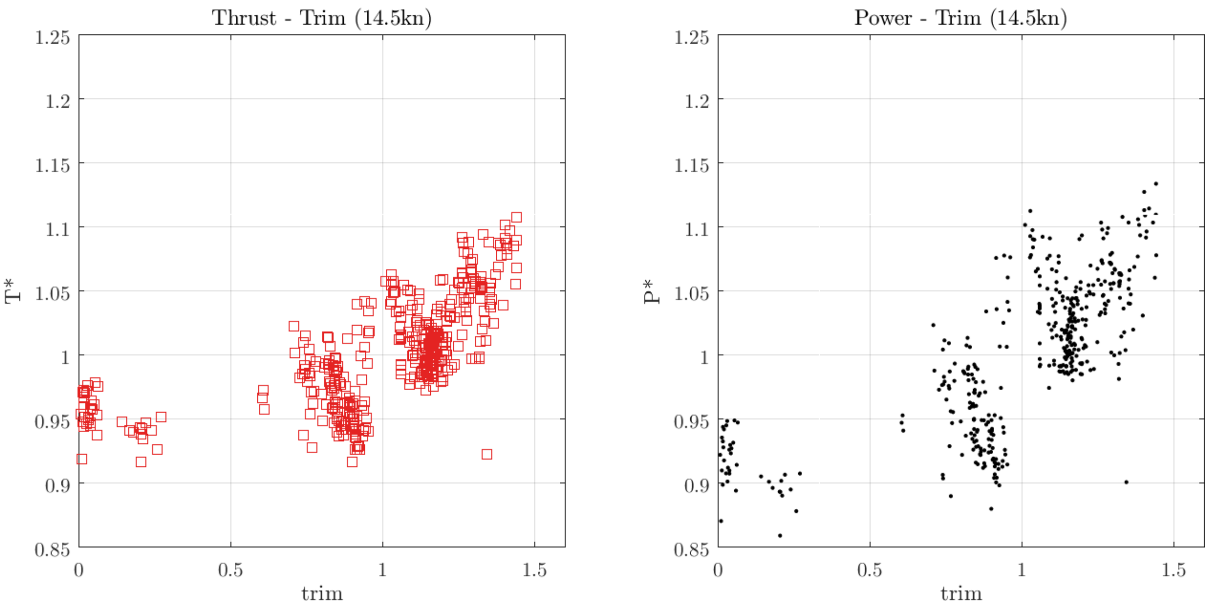

Fig.7: Side by side display of thrust and power at 14.5 knots

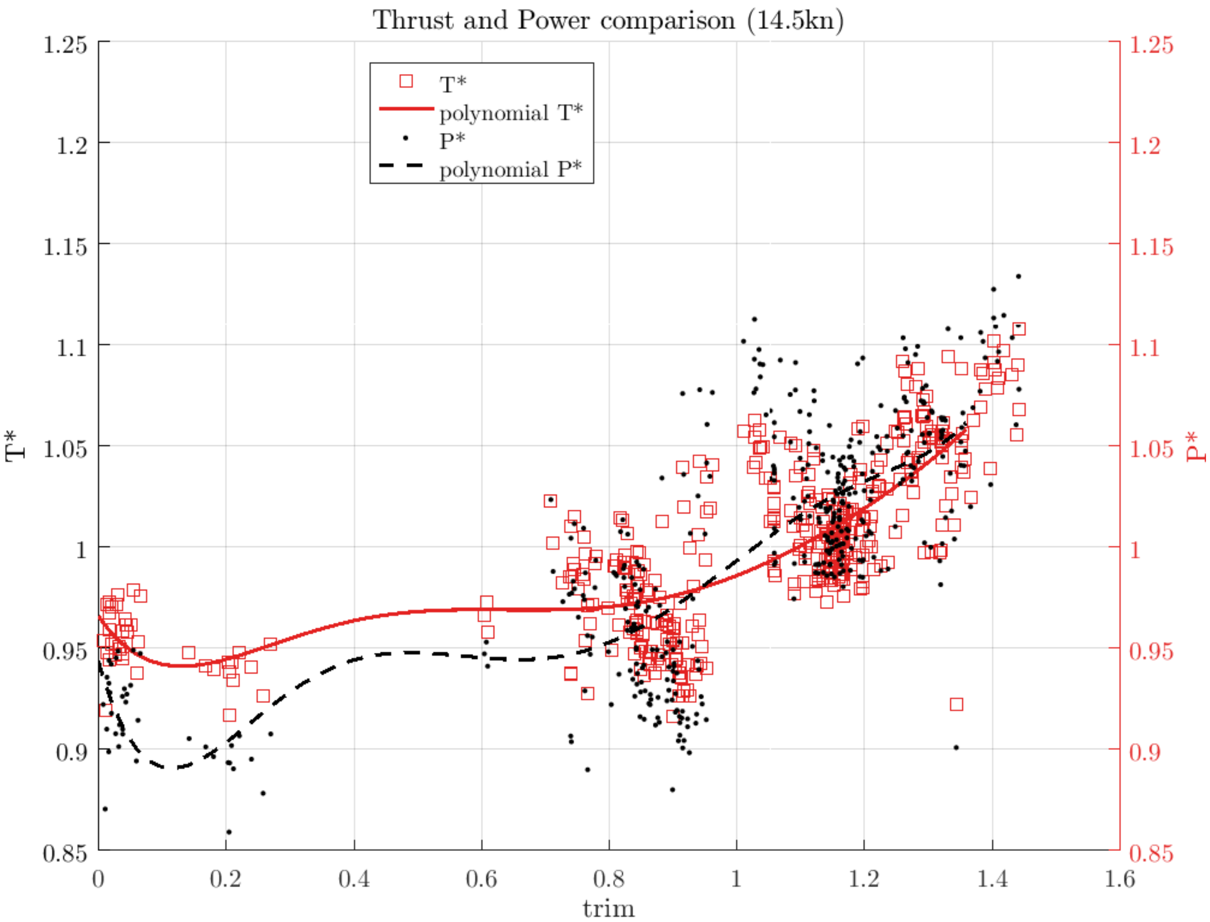

Fig.8: Direct comparison of thrust and power at 14.5 knots

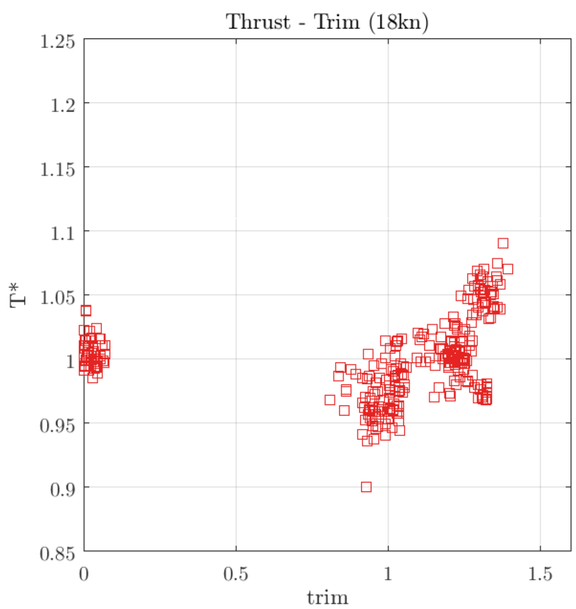

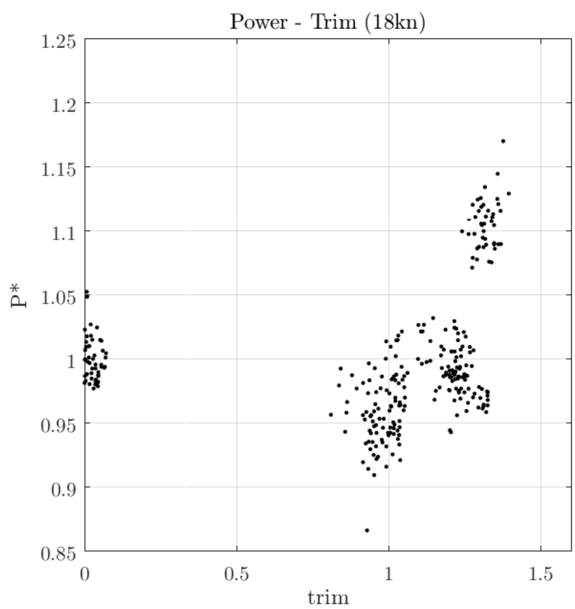

Fig.9: Side by side display of thrust and power at 18 knots

5.4. Discussion

The quality of the measurements in this case study is found to be sufficient for data-driven trim optimisation. The measurements of power and thrust show a very similar relationship to trim in the three investigated cases. Moreover, the derived relationships between trim, thrust and power are plausible, demonstrating the capabilities of the TT-Sense® as a measuring device.

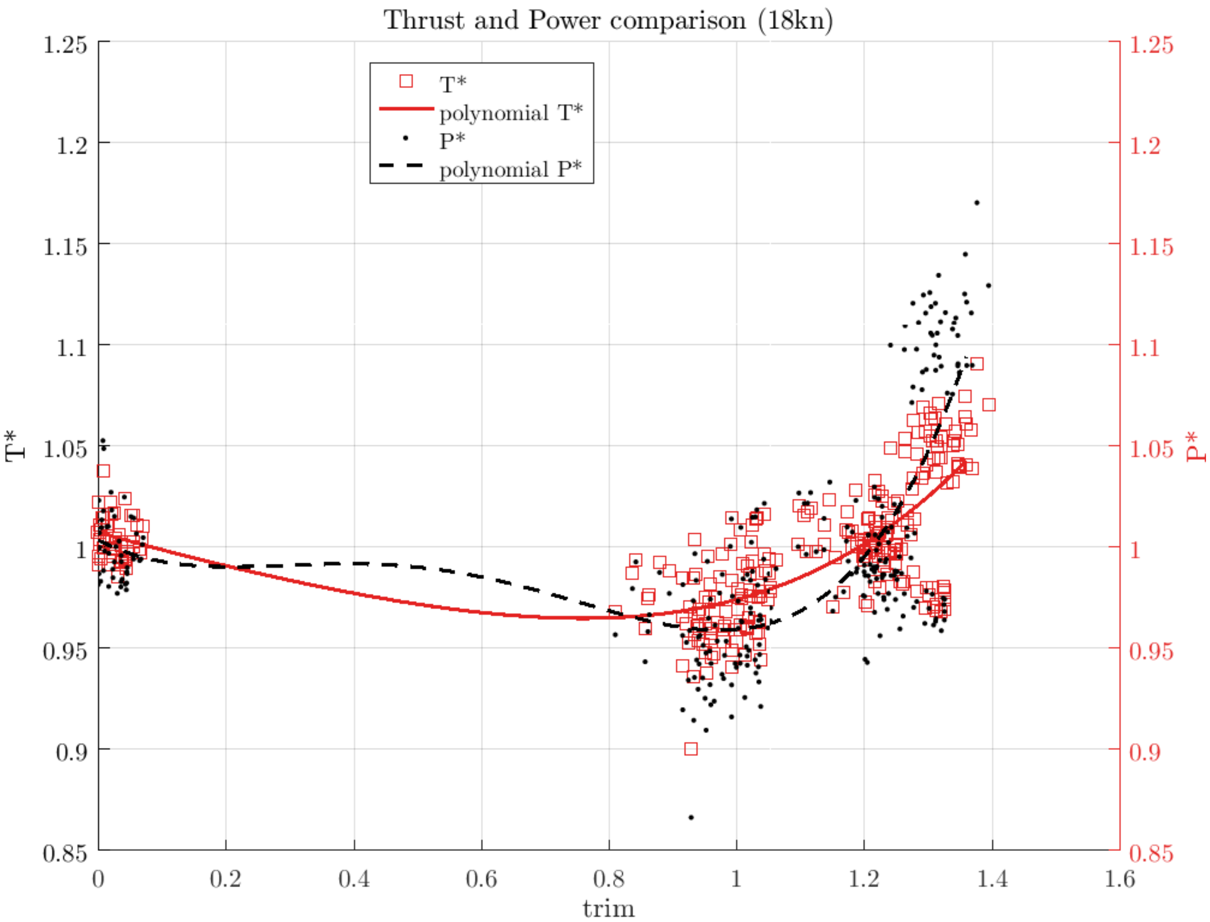

Fig.10: Direct comparison of thrust and power at 18 knots

The trim value where thrust is smallest is almost the same as the trim where required power is smallest. However, where T* has a low value, P* has an even lower value. This means that the decrease in required power cannot be explained only by the decrease in hull resistance, but that the propeller is more efficient in those cases as well. As was hypothesised in Section 4.2 the propeller appears to be most efficient when the hull resistance is smallest. At least for the investigated draught. The reverse also applies, when T* is large P* is even larger, indicating that the propeller experiences an unfavourable wake when hull resistance is largest.

Even though the polynomial estimation suggests even lower values, the lion's share of the data indicates a most optimal P* of about 0.95. This means that by always sailing at the most favourable trim the ship under investigation can save about 5% in propulsive power consumption compared to how it is currently trimming. This seems to roughly agree with values reported by commercial parties (see *SSPA (2009)*, *Ignatius et al. (2013)*, *Hansen and Freund (2010)* and the overview given in *McMillan and Jarabo (2013)*). It must be taken into account that it is not always possible to adopt the optimal trim in practice.

For the operating condition at 14 knots there is a good amount of data spanning the entire range of trim. For the other two operating conditions however, there is data missing for certain values of trim. This is simply because the ship never sailed in such a condition. In Fig.10 between 0.1 and 0.8 meter trim the polynomials for thrust and power predict opposing trends, without there being any data to justify this. It nicely exemplifies the problem of data scarcity. Even though trim optimisation software will make a much more sophisticated estimate than a simple polynomial, a generalisation will inevitably be made without there being data to validate it.

6. Conclusion

There is a promising potential for improving data-driven trim optimisation by incorporating thrust measurements in addition to power measurements. In a case study, it was shown that the TT-Sense® provided thrust data of a good quality. The information on thrust allowed for a separate measurement of trim effects on the hull and the propeller. This separation can especially be helpful when dealing with controllable pitch propellers.

The conventional propeller investigated in the case study seems to perform best when the hull resistance is low and worse when hull resistance is high. As a consequence, the trim value that minimises hull resistance is very close to the trim value that minimises total power.

During the period of continuous monitoring, the ship did not sail at every possible combination of trim and speed. This caused gaps in the data. When trim optimisation software tries to predict what happens in these data gaps there is a risk of overfitting. This was demonstrated with simple polynomial fits. When such fits are based both on thrust and power measurements, it can be checked whether they do not deviate too much. By incorporating thrust measurements into data-driven trim optimisation software, its reliability can thus be improved.

An interesting next step would be to build a proof of concept of trim optimisation using thrust data. Additional research with more data of ships (with CPPs) would be supportive in this.

References

BALLEGOOIJEN, E.v.; MUNTEAN, T.V. (2016), *Fuel saving potentials via measuring propeller thrust and hull resistance at full scale. Experience with ships in service*, 1st HullPIC, Pavone

BERTRAM, V. (2014), *Trim optimization – Don't blind me with science*, The Naval Architect, July/August, pp.66-68

GOURLAY, T.P.; KLAKA, K. (2007), *Full-scale measurements of containership sinkage, trim and roll*, Australian Naval Architect 11.2, pp.30-36

HANSEN, H.; FREUND, M. (2010), *Assistance tools for operational fuel efficiency*, 9th Conf. Computer and IT Applications in the Maritime Industries (COMPIT), Gubbio

IGNATIUS, J.; RÄSÄNEN, J.; TERVO, K.; ELLIS, T. (2013), *A comprehensive Performance Management Solution*, 12th Conf. Computer and IT Applications in the Maritime Industries (COMPIT), Cortona

McMILLAN, C.; JARABO, A. (2013), *Ship Efficiency: The Guide*, 2nd Ed., Fathom, pp.15-24

PÉTURSSON, S. (2009), *Predicting optimal trim configuration of marine vessels with respect to fuel usage*, Master Thesis, University of Iceland

REICHEL, M.; MINCHEV, A.; LARSEN, N.L. (2014), *Trim Optimisation - Theory and Practice*, TransNav: Int. J. Marine Navigation and Safety of Sea Transportation 8.3, pp.387-392

SSPA (2009), *Trim Optimisation – Sustainable Savings*, SSPA Highlights 47, pp.2-3

Enhanced Performance Analysis and Benchmarking with CFD Baselines

André Kauffeldt, DNV GL, Potsdam/Germany, Andre.Kauffeldt@dnvgl.com
Heikki Hansen, DNV GL, Potsdam/Germany, Heikki.Hansen@dnvgl.com

Abstract

This paper shows how speed-power baselines can be generated using CFD (Computational Fluid Dynamics) simulations. Examples of performance analyses based on measurements combined with comprehensive CFD baselines and reduced data sets are presented, which show that the result quality is significantly improved when using comprehensive baselines and that these differences can change decision making. The paper also shows how vessel benchmarking can be performed with CFD baselines, comparing the expected performance of different vessels for the specific operating profile. New approaches such as Virtual Trial allow generating CFD baselines in a consistent, transparent and efficient way without expert knowledge and in-house computing resources.

1. Introduction

Energy efficiency is an important factor in the life cycle costs of a ship. With rising fuel oil prices and an increasingly competitive market improving energy efficiency is vital. The maritime sector is known for sometimes being reluctant to embrace change and tends to stick with proven concepts and best practices, which have been developed and applied for a long time. However, times change and today many shipping companies invest in performance analysis as the 4th wave of energy efficiency improvement. They realize that a holistic view on the vessel performance is important to continuously lift the remaining potential of performance improvement. The low hanging fruits were already harvested through different stages of energy efficiency improvement measures in the last years, Fig.1:

- 1st wave: slow steaming
- 2nd wave: trim optimization and other tools
- 3rd wave: retrofits now the monitoring and controlling gains importance.
- 4th wave: Managing operations and performance management

During the first stages, specific energy efficiency topics were addressed, while now the focus shifts to ensuring that vessels operate efficiently all the time by addressing the whole spectrum of measures effecting the vessel performance. To achieve this a good and detailed understand of the vessel is important. This is where performance management is important.

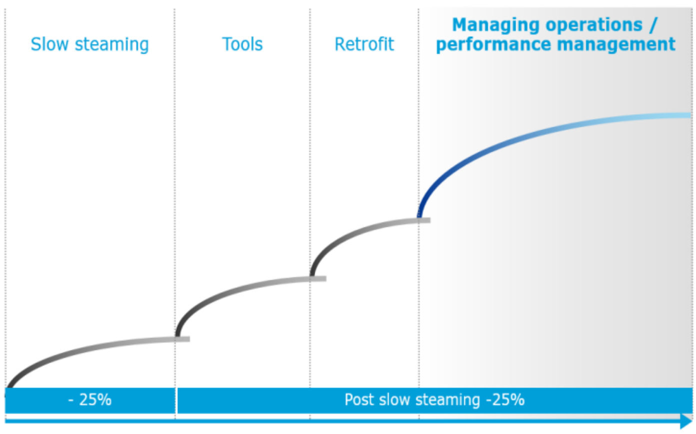

Fig.1: Steps of energy efficiency improvement measures

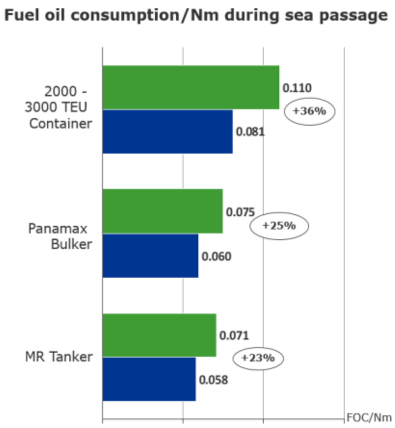

Fig.2: Remaining potential of performance improving measures:
- green: class average
- blue: best performer in class

Monitoring and controlling of individual vessels gains importance, as these measures support the shipping companies to identify, evaluate and correct performance issues in a timely manner. Fig.2 visualizes that currently still large potentials for improvement are available, which can be released through performance management.

From the operators point of view, performance management covers a wide range of aspects and considers the ship as a holistic system. This approach can become very complex and involve monitoring a wide range of parameters. It can be extended almost indefinitely depending on the operator's approach. However, most performance analyses consider the following main aspects:

- Efficient main engine operation (power, fuel oil consumption (FOC), RPM, etc.)
- Efficient management of auxiliary engines (combination, power, FOC, etc.)
- Controlling of other auxiliaries (boilers, separators, etc.)
- Hull and propeller performance considering:
    - Resistance
    - Weather
    - Propulsion
    - Trim
    - Hull degradation
- Voyage management (Optimized routing, consumptions, weather, speed, legs)
- Bunker statistics
- Port/supplier rating
- Emissions and disposals
- Maintenance and survey interval optimization

This list is not exhaustive and shall only demonstrate the complexity of the topic. The paper focuses on hydrodynamic performance, considering resistance, propulsion, hull degradation and propeller effects.

Experience has shown that it is not sufficient to simply plot the measured power demand during operation over time to draw conclusions on the performance. The scatter observed in such plots is dominated by speed and draft variations in operation, which have a much bigger impact on the power demand than the rather small effect of hull degradation. Hence, to identify trends in hull degradation, it is necessary to normalize the power measurements to eliminate the effects of different operating conditions regarding speed, draft and trim. Basis of such a normalization could be the ideal power demand determined for the same condition. It can be used as a reference, representing the theoretical power demand for the vessel at this condition. Measured power and reference power demand together allow conclusions about the hull performance and, therefore, the hull degradation.

Simply put, looking at the impact of the hull, a performance analysis compares a measured power demand for a certain operating condition to a reference value valid for that condition. Here, the relevant condition is mainly defined by the following parameters:

- Operating conditions:
    - Draft
    - Trim
    - Vessel speed
- Environmental conditions:
    - Wind (force and direction)
    - Sea state (height and direction)
    - Swell (height and direction)
    - Temperature (air and water)
    - Current (speed and direction)
    - Water depth

By comparing the measured with a reference power of a comparable condition, a performance index can be deduced, which enables operators to easily infer conclusions about the vessel performance.

Many factors influencing performance make it difficult to distinguish effects and hence understand the parameters that drive performance. Therefore, for a meaningful and accurate performance analysis it is crucial to have a matching reference condition for all measured operating conditions. Hence, comprehensive baselines covering the entire operating range regarding draft, trim and speed are prerequisite to get the most out of the performance analysis. Or the other way around, the further an existing reference condition must be extrapolated to meet a measured operating condition, the worse is the result of the performance analysis.

For assessing ship performance, speed-power curves of the individual vessels serve as a reference. They reflect the calm water power demand of the corresponding vessels under ideal conditions:

- Clean hull
- Deep water
- No wind
- No waves

2. Generating speed-power curves

There are several well-known ways to determine speed-power curves for a vessel, which can serve as reference in a performance analysis. As summarized in Fig.3, each approach has its own advantages and disadvantages:

- **Empirics**:
  Based on generalized equations this approach is not intended to fit a specific vessel. Neglecting the individual characteristics of a vessel, this approach delivers a general idea of the magnitude of the power demand only.
  - *Pro:* Very quick and therefore cheap
  - *Contra:* Inaccurate and not suited for ship specific comparison due to neglecting of individual vessel characteristics

- **Model scale measurements**:
  A well-established approach, which is based on measurements in model scale. Since these measurements are conducted under laboratory conditions, the accuracy of the model scale results is generally high.
  - *Pro:* The widely accepted approach with its accurate results is well suited for the comparison of different hull shapes.
  - *Contra:* Building of a scale model, preparation and execution of each test is time consuming and expensive. Due to uncertainties when extrapolating to full-scale, the results are not fully consistent across different test facilities. Possible scaling effects are not considered.

- **Full-scale measurements**:
  General accepted approach to validate the performance predictions for a newly delivered ship. With additionally installed measuring equipment the power results are very accurate. However, the measurement quality strongly depends from the environmental conditions. It is not the first choice for comparative measurements.
  - *Pro:* Accurate power results without scale effects.
  - *Contra:* Often only conducted at ballast draft and under non-ideal conditions. The correction of the environmental conditions as well as the extrapolation to the design draft lead to uncertainties. Depending on the used correction and extrapolation methods the results are not fully consistent across different test facilities or yards.

- **CFD simulations**:
  CFD has become a well-established tool for relative comparison of different designs, configurations and operating conditions. The absolute accuracy still depends on the CFD setup and available resources.
    - *Pro:* A fast and effective approach to conduct full-scale simulations and, thus, become independent of scaling effects. Well suited tool for comparative studies.
    - *Contra:* There are still substantial computing capacities required to conduct large-scale studies efficiently. The absolute accuracy depends on the CFD setup and the experience of the user.

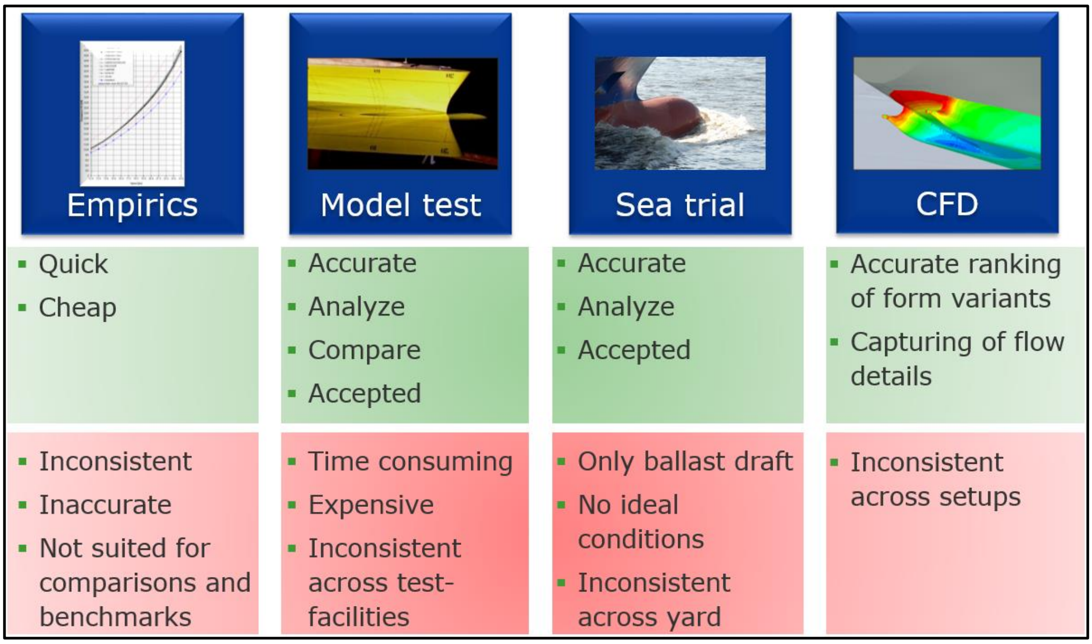

Fig.3: Methods of power demand analysis for ships

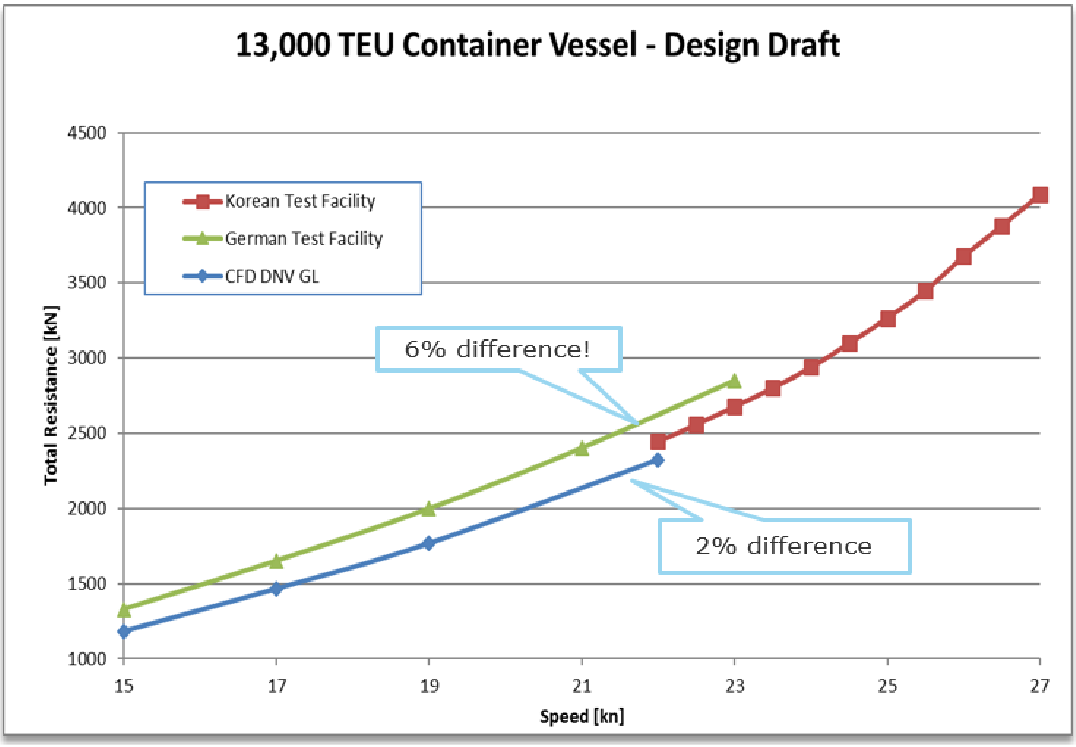

Fig.4: Difference in power prediction

Probably none of the common methods is perfectly suited to meet all requirements of the maritime industry. Fig.4 visualizes the mentioned inconsistencies of absolute power predictions, that not only vary between model test and CFD but also between different model test facilities. In some cases, differences of up to 10% are reported between different model test facilities using the same model.

3. Why CFD for computing baselines?

CFD capabilities have improved significantly in recent years, Fig.5. Not only the availability of large computer resources has improved. CFD methods have also been developed much further. Today, standardized setups ensure high comparability. The application of state-of-the-art fully viscous, free surface CFD approaches using Volume of Fluid (VoF) and Reynolds averaged Navier Stokes equations (RANSE) in combination with standardized prediction methods as well as full-scale computations (no scale effects), provide reliable results.

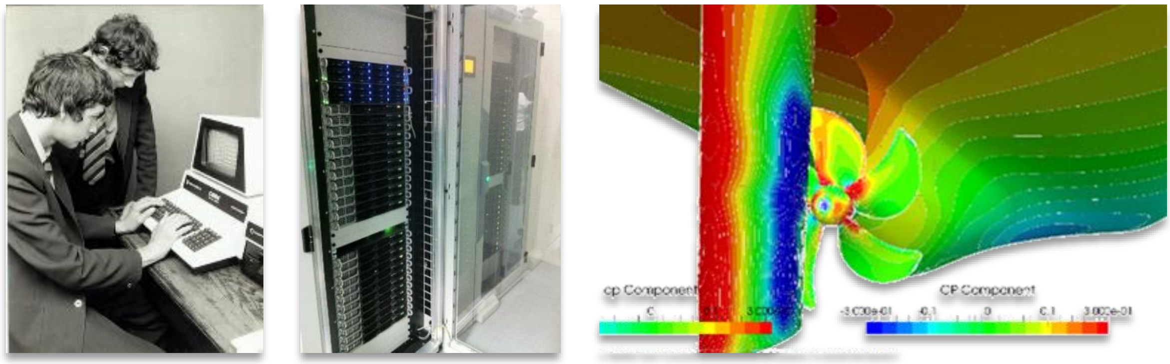

Fig.5: CFD - then and now

Beside the significant technical enhancement, the constantly growing computing power and the resulting reduction in lead time and cost means that large numbers of simulations can be conducted efficiently – a crucial factor when developing comprehensive baselines for performance analysis.

When generating baselines, it is indispensable to cover all relevant operating conditions of a vessel regarding draft, speed and trim to get reliable performance information. More precisely, the operational profile must be closely covered by the reference simulations to minimize the uncertainties due to extrapolation from the available reference to the recorded operating condition. This means that a large amount of reference conditions is required to produce accurate power baselines.

It is very costly and time consuming to use model tests to generate this amount of reference data. One model test run, including waiting time until the basins surface is calm again, takes typically around 15 minutes. Therefore, model tests are not the first choice to generate hundreds of reference points covering the entire operating range, as the time required in the towing tank facility is extensive and hence costly. The use of CFD approaches, on the other hand, allows us to process hundreds of simulations efficiently. If large computing capacities are available, the simulations can also be carried out in parallel saving additional time.

4. Comparison of comprehensive CFD baselines with reduced data base

This chapter substantiates and illustrates on a real-world example the difference between using comprehensive CFD baselines and a reduced data base. Figs.6 and 7 show a typical operating condition of a large container vessel (red cross) relative to the reference points based on different data sets. Fig.6 presents an example with a dense grid of reference points based on comprehensive CFD simulations. A matrix of 7 trims, 11 speeds and 8 drafts results in 616 reference points covering the operational profile of the vessel. Fig.7, on the other hand, shows a reduced data set based on a standard model test of the same vessel. Here, the matrix contains only 3 drafts (scantling, design and ballast), 1 trim and 6 speeds resulting in 18 reference points inhomogeneously distributed over part of the operating range. The example with the reduced data set shows impressively the distance between the measured operating condition and reference points. To make matters worse, the speed must be extrapolated significantly below the minimum speed of the reference points.

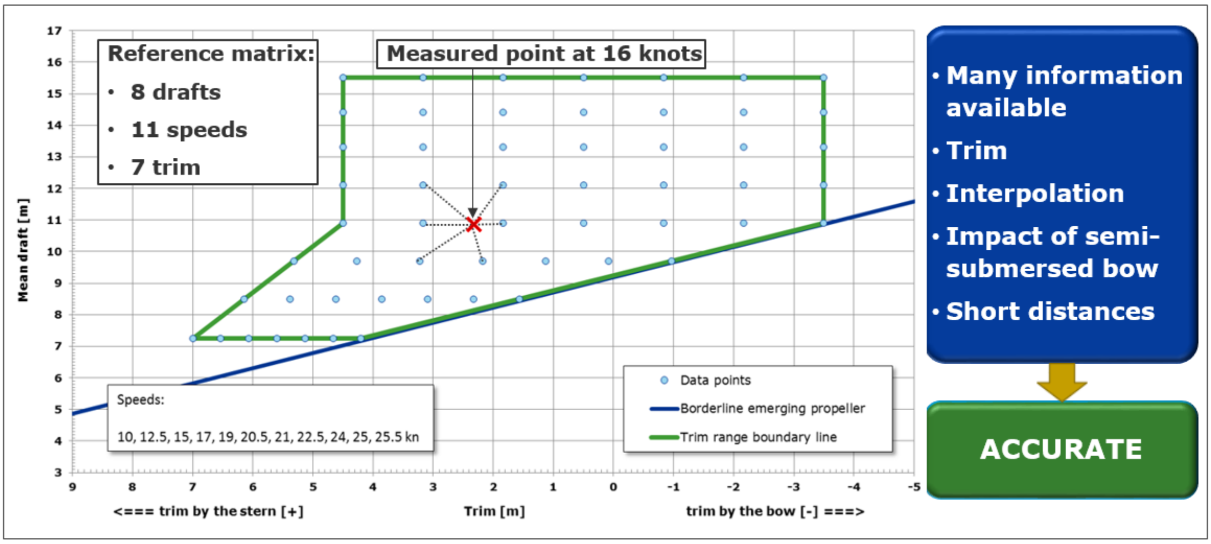

Fig.6: Interpolation of a measured conditions using a dense grid of reference points based on CFD simulations

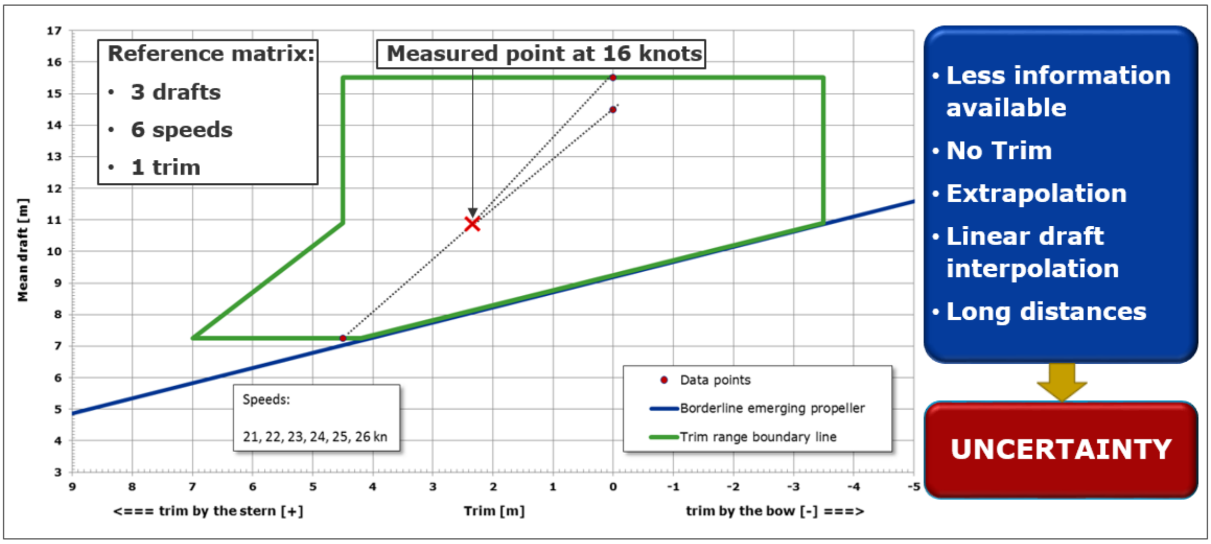

Fig.7: Extrapolation to a measured condition using a reduced data base referring to a standard model test with ballast, design and scantling draft available

The operating profile of this container vessel, Fig.8, is typical for many container vessels. It demonstrates, that the vessel practically never sails at design condition, which in this case is at 24.3 knots and 14.5 m draft. Instead the draft ranges from 10 m to 15 m and the speed varies between 12 knots and 21 knots. So, it is very likely that the vessel operates far from the speed range contained in model tests for a large percentage of the time and extrapolated reference values are used for the performance prediction.

The missing trim information of the reduced data set increases the uncertainties further since container vessels are very trim sensitive. This alone can lead to deviations of several percent in the performance predictions.

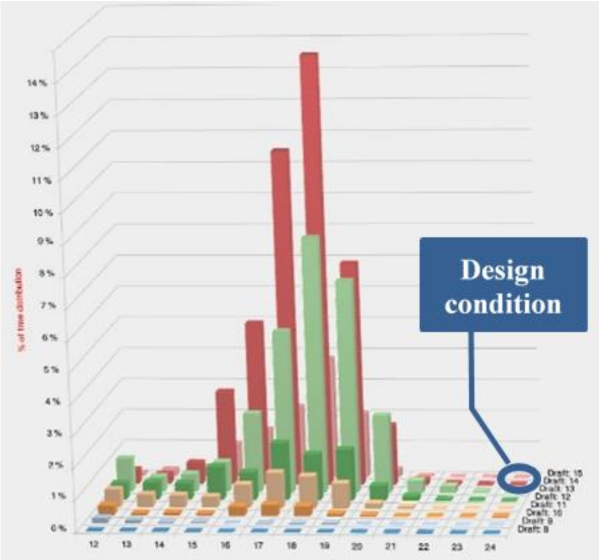

Fig.8: Operating profile of the sample vessel

Fig.9 illustrates possible complications, which can occur when interpolating between far distant drafts. At design draft as well as at ballast draft, the flow field around the bow looks nice and smooth. If there are no other information available an intermediate draft can only be interpolated by using mathematic approaches. In this case the real flow field at the intermediate draft is neglected. The CFD results, however, reveal a very unfavourable flow field with large breaking bow waves and deep troughs behind the bulbous bow. The nasty flow field significantly affects the wake making resistance of the vessel, which has a direct impact on the power demand. Hence, the results based on the interpolation of ballast and design draft underestimate the power demand significantly.

The same applies to the speed extrapolation. Since off-design conditions are often not fully considered in ship design, slow steaming generally can worsen the flow in the bow region of vessels with a bulbous bow. Mathematical methods cannot account for this deterioration of the flow field without additional reference points. How far these deviations can go is exemplarily shown in Fig.10. It presents the speed-power curves of the sample vessel for ballast and design draft based on:

- Model tests
- CFD simulations
- Mathematical extrapolation.

As shown, the available model test results (solid line) cover only a limited speed range around the design speed, which is not sufficient to cover the real operating speed range of the vessel. The CFD based simulations, however, extend over the entire operating speed range. The presented diagram clearly shows that both curves fit well in the area where both curves exist. Large deviations occur where the model test results end. The trend of the mathematically extrapolated model test results (square dots) differs significantly from the CFD based power curve. As a result, at slow steaming the predicted power can vary by up to 50% depending on the method. This, of course, has a distinct impact on performance evaluation. It is therefore advisable to account for the changing flow field by using a sufficient number of reference points in performance analysis.

Together, the draft interpolation, the speed extrapolation and the missing trim information cause a large scatter in the performance index, which makes a meaningful interpretation difficult. The impact of the available data base on performance evaluation is presented in Fig.11. The upper diagram shows the performance over time based on comprehensive CFD data, whereas in the lower diagram only a reduced data set is used to generate the performance plot for the same vessel.

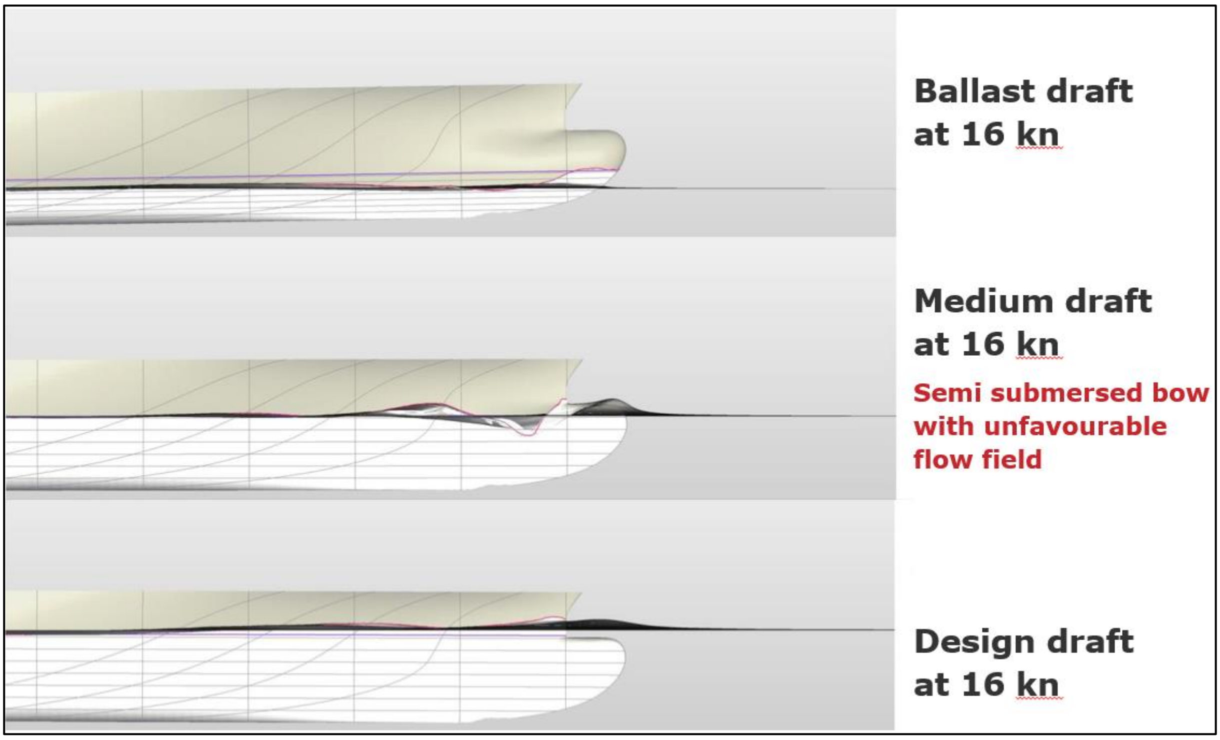

Fig.9: Unfavorable flow fields of a semi submersed bulbous bow at medium draft complicate the interpolation between drafts

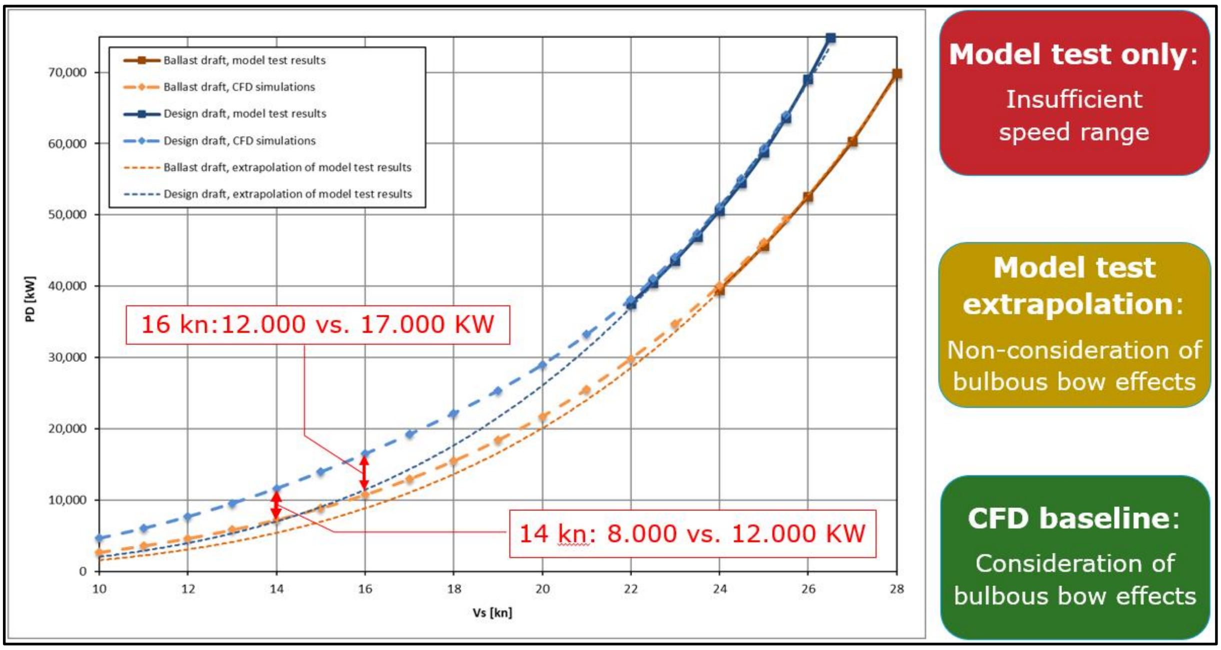

Fig.10: Comparison of different approaches of power prediction

The plotted performance index is based on the following equation:

$$Performance\ index = \frac{reference\ power}{corrected\ measured\ power} \tag{1}$$

The reference power reflects the reference power demand under ideal conditions, whereas the corrected measured power is based on the measured power corrected for the influence of the weather.

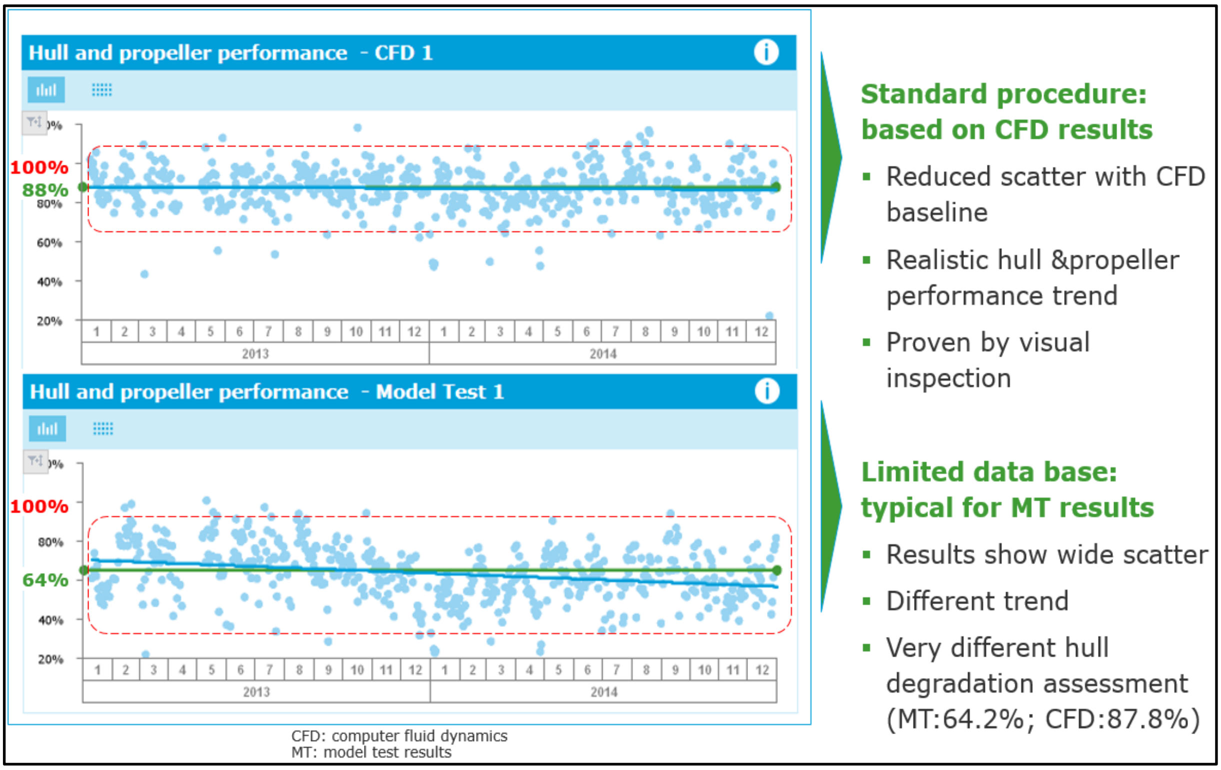

Fig.11: Impact of different data bases on performance evaluation

The weather correction is mostly based on empirics and often includes the following corrections:

- wind
- sea state
- swell
- water temperature
- current

Using Eq.(1) to determine performance means, that the vessel performs at 100%, if the corrected measured power is equal to the reference power. If the corrected measured power is twice as large as the reference power, the vessel only performs at 50%. Hence, using this performance index it is expected that the performance is ideally close to 100%. Fig.11 shows that the performance index based on the comprehensive CFD baselines shows less scatter. In addition, the magnitude of the performance index seems to be more realistic and the deduced hull degradation trend is more plausible when using the comprehensive baselines.

The hull degradation trend is the key parameter for deciding whether the next hull cleaning is advised. It may also provide insight on the performance of various hull coatings and may support the decision process for the best suited product depending on the characteristics of the operating area and profile. Depending on that, the corresponding decisions can vary significantly.

Besides the data base quality, the existing scatter also results from uncertainties with respect to long-term measurements during normal operation. If the measuring equipment is not calibrated on a regular basis, the accuracy of the reported measurements decreases with time. In addition, reporting environmental conditions is obviously still a challenge for many crews causing uncertainties in the weather correction. Finally, there are just too many variables to consider to completely avoid scatter.

Besides performance evaluation, the quality of the reference data is also decisive for other applications. Trim optimization for example also depends on a comprehensive data base, since local flow phenomena strongly affect the prediction results. Fig.12 presents response surfaces based on two different data sets for another sample ship. It is obvious, that there are shape variations depending on the data sets. These differences directly affect the trim trend prediction as presented in Fig.13. Based on the reduced data set the trim tool recommends a bow down trim. At -1 m bow down trim for example a power saving of 2% is predicted, which equals to 1.7 t/day fuel oil savings. Based on the comprehensive CFD data, however, an increased power demand of about 1% is predicted. Here, the fuel oil consumption will increase by 0.8 t/day. So, if the captain follows the predictions based on an insufficient data base, the vessel performance may even decline. Although this is an extreme example, it clearly emphasizes the importance of good baselines.

Fig.13 also emphasizes that trim strongly effects the power demand, especially for container vessels. Therefore, it is crucial to consider the impact of trim when conducting performance analysis.

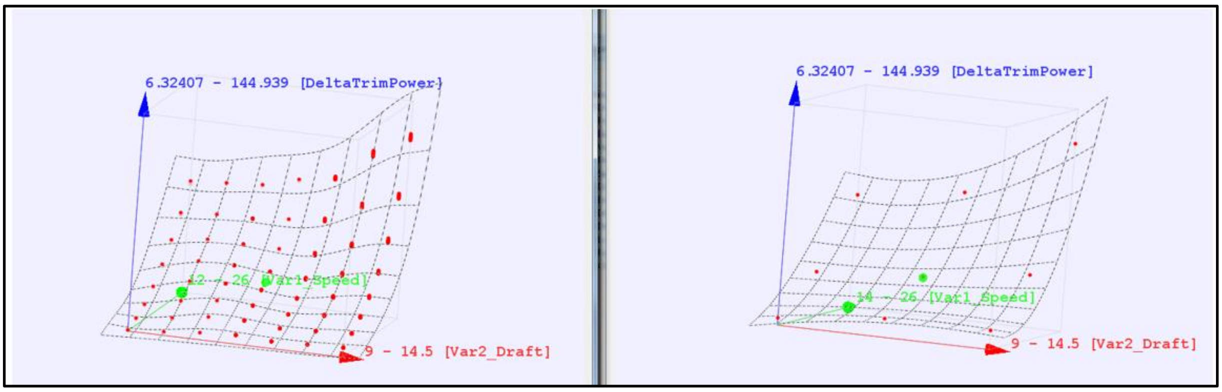

Fig.12: Comparison of response surfaces based on different data sets, comprehensive CFD baselines on the left and a reduced 3x3x3 matrix on the right

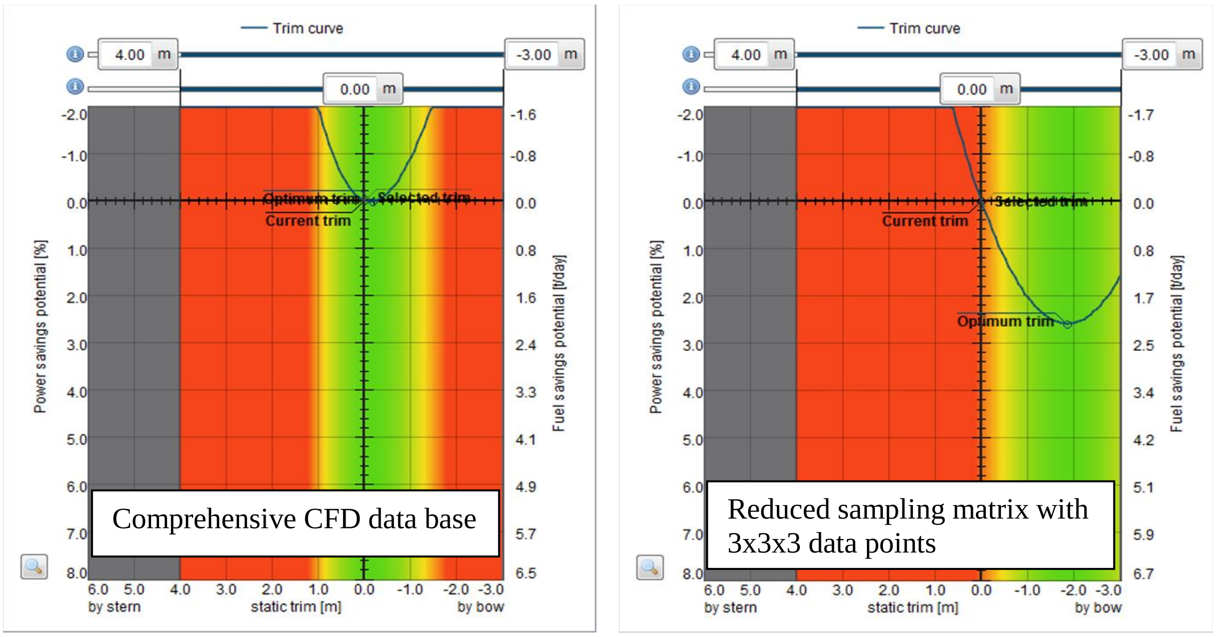

Fig.13: Comparison of predicted trim trends depending on data base quality

5. CFD baselines and the ISO 19030 performance standard

CFD baselines are also best suited to fulfill the high requirements of the new ISO 19030 performance standard. In ISO 19030 Part II Annex F, CFD approaches are explicitly allowed to “obtain ship specific power-speed-draught-trim databases”. The norm defines high standards for the installed measuring equipment and tight environmental filters to ensure the best possible measurement quality. Among others the environmental filters aim at the following parameters to reduce scatter due to extreme conditions:

- Wind (≤ 7.9 m/s)
- Water temperature (≥ 2°C)
- Water depth (defined by equations)
- Sea state, swell and viscosity is not yet considered by ISO 19030

The norm also introduces strict standards defining the applicable reference condition. Regarding the performance analysis with reduced data base (e.g. model tests) the ISO 19030 norm defines strict limits which must not be exceeded if this standard is to apply. These rules affect the following three reference parameters:

- **No Speed extrapolation allowed**:
  Delivered power must stay within the range of provided power values covered by the available speed-power reference curves.
- **Introduction of displacement bands**:
  The actual displacement is not allowed to differ more than ±5% from a reference displacement for which a speed-power reference curve is provided.
- **Introduction of trim bands**:
  The actual trim is not allowed to differ more than ±0.2 % of the length between perpendiculars from a reference trim for which a speed power curve is provided.

As shown in Figs. 14 and 15 these rules dramatically limit the range of allowed measurements when applying ISO 19030. Together with the tight environmental filters the extrapolation limits mean that much of the measured data cannot be used for an ISO-compliant performance analysis. Prohibiting the extrapolation of the reference speed means that most of the slow steaming data is not usable for performance analysis. Therefore, a reduced data base has almost no practical benefit with respect to ISO 19030 performance analysis, since it only covers a very small part of the operating range regarding draft, trim and speed.

In contrast, CFD baselines can fulfil the requirements of ISO 19030 regarding the allowable draft and trim spacing as well as the speed range.

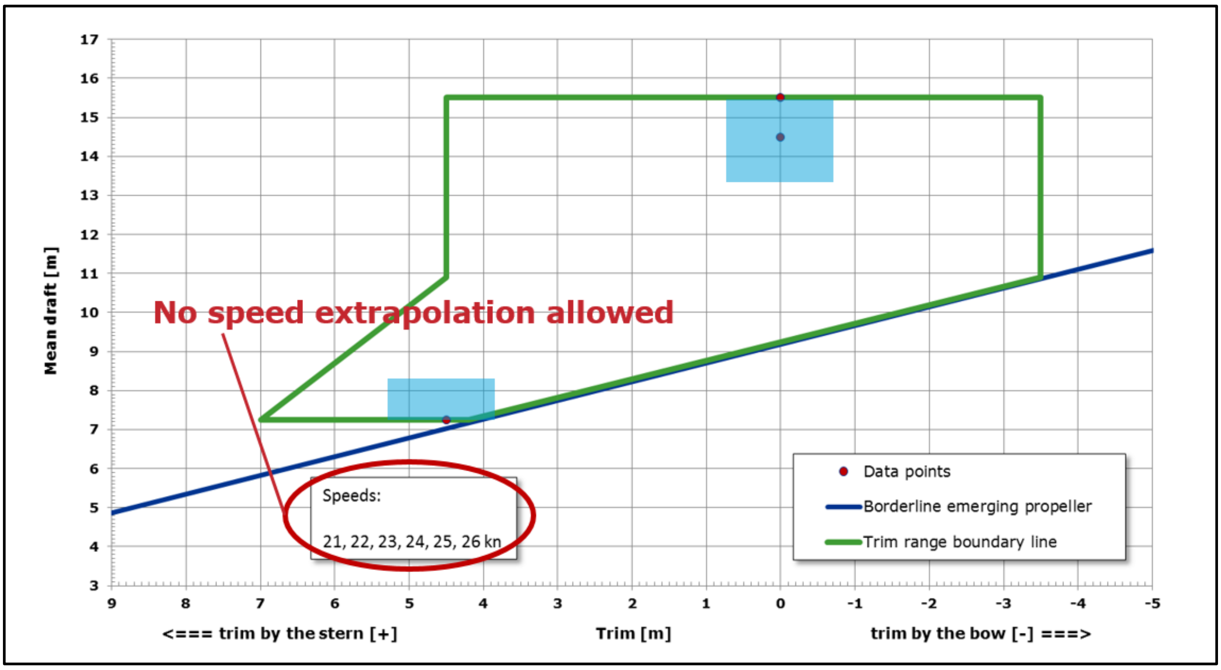

Fig.14: Covered area (blue) for ISO 19030 compliant performance analysis for reduced data base

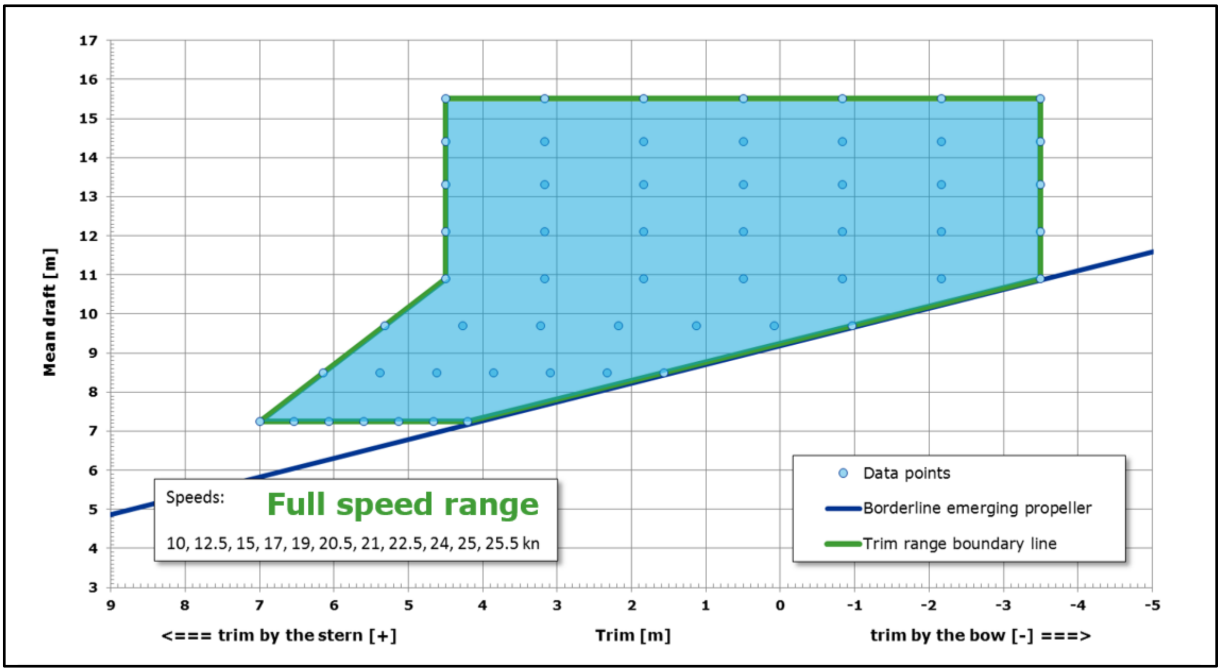

Fig.15: Covered area (blue) for ISO 19030 compliant performance analysis for comprehensive CFD simulations

6. Benchmarking with CFD

CFD baselines also have advantages when directly comparing, analysing and benchmarking designs during the design and build process. Compared to model tests, lead time and cost are reduced, and the designs can be analysed in full-scale. However, the computer resources and expert know-how to design and carry out CFD tests is still not widespread. At the same time, the varying assumptions and simulation parameters used by different suppliers, yards and design offices make reliable comparison and benchmarking nearly impossible.

To change this the Virtual Trial application has been developed. It removes the need for expert support by streamlining and automating the CFD simulation process. Users can upload individual vessel hull forms and, without the need for any CFD-specific input, can conduct fully automated, full-scale RANSE (Reynolds-averaged Navier-Stokes equations) VoF (Volume of Fluid) CFD simulations on the propulsion of their vessel.

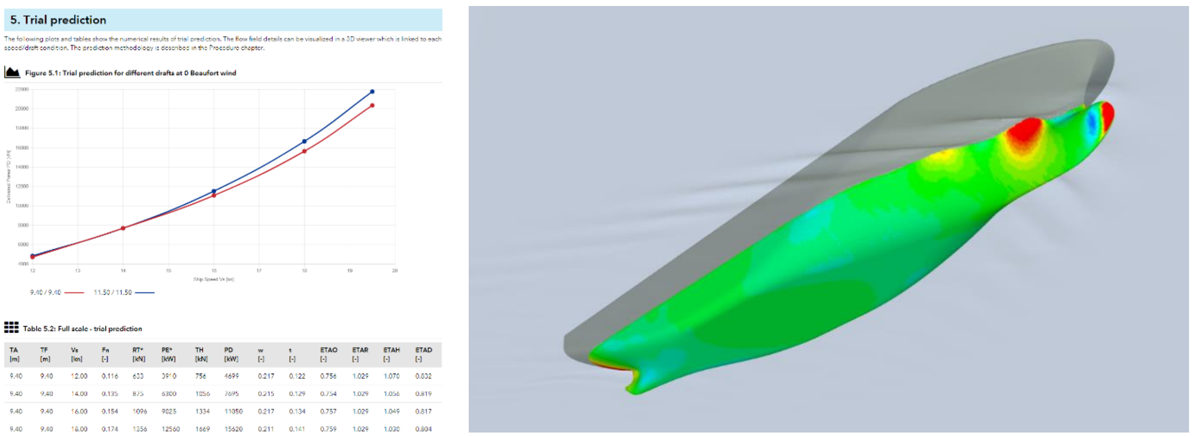

Fig.16: Speed power curves (a) and 3D viewer (b) to investigate flow details in web-based report

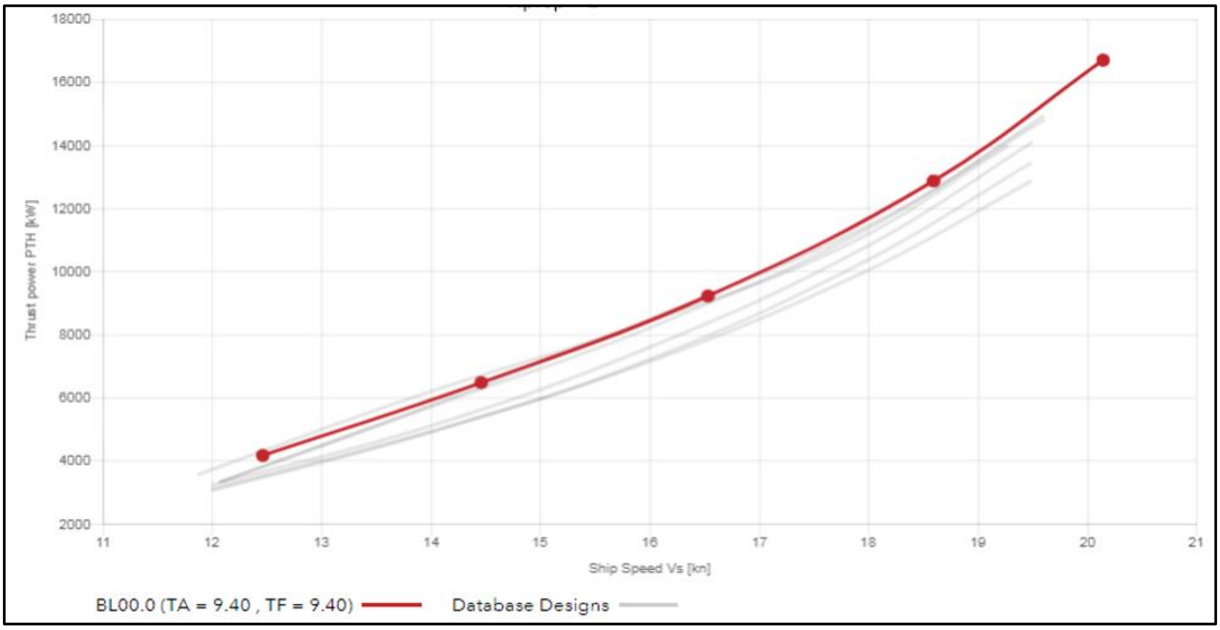

Fig.17: Benchmarking of simulation results with comparable vessels

The results are available within one week in a Web-based report combining tabular data with graphical information to support the understanding of the flow characteristics, Fig.16a. Fig.16b shows the embedded 3D viewer to visualize flow details to better understand the results. Fig.17 shows the simulation results benchmarking against database designs.

A typical use case of Virtual Trial might be design offices and shipyards wanting to analyze and benchmark different hull options during the conceptual design phase. During the later design phase, they could track the influence of design changes on the vessel's hydrodynamic performance, ensuring that contractual requirements are still achievable.

The standardized CFD setup also lets shipyards and designers see where they could improve their designs by comparing them against anonymized state-of-the-art designs from a database.

Ship owners can compare design proposals from different yards or design offices during the bidding process. Competing designs can be uploaded by the designers themselves, to ensure that the hull lines stay confidential. The ship owner can then be granted access to the results, providing him or her with a consistent and impartial assessment of the designs at a fraction of the cost and lead time of model tests.

For vessels in service, the results could act as a performance certificate to show potential charterers that the vessel has undergone a transparent efficiency assessment. Even with advanced performance monitoring solutions, it can be difficult to predict the performance or the fuel consumption for a different operating profile. But with the Virtual Trial app, the owner could simulate the intended operating parameters and provide a tailored performance assessment to the potential charterer within a week.

Virtual Trial's standardized report format could also become an industry-accepted reference for comparison and benchmarking. Ship designs can be compared against each other within a set frame of reference, even if the projects are submitted from different parties, making performance predictions more transparent and reliable. Virtual Trial lets customers take control of their data, benefit from industry-wide benchmarking capabilities, and enhance their market competitiveness.

7. Summary

Today, efficient operation of commercial vessels is crucial to survive in an increasingly competitive market. After harvesting the low hanging fruits by adopting slow steaming and trim optimization first, many operators now focus on performance analysis to further increase their fleet performance by monitoring and benchmarking their vessels individually. One important aspect to increase operational efficiency through performance analysis is to assess the hydrodynamic performance of the vessel to determine the effects of hull and propeller fouling, speed loitering, etc. A promising approach is to utilize power baselines for the different operating conditions as a reference to calculate the performance deviation for the expected value

CFD methods with their standardized setups and significantly increased computer capacities can determine the absolute power demand for a large number of reference conditions serving, which serve as the basis of performance analysis. Using a real-word example, this paper reveals the benefits of comprehensive power baselines based on CFD simulations compared to baselines with a reduced data set. The dense grid of reference conditions allows physical effects in the wave field to be resolved adequately. This improves the quality of the predicted reference power and hence of the performance assessment. In addition, it is illustrated that comprehensive CFD baselines also fulfil the requirements of the strict ISO 19030 performance standard.

Furthermore, a new CFD based approach to benchmark individual vessels is introduced in the paper. This approach called Virtual Trial reduces the barriers to use full-scale CFD simulation testing and comparative benchmarking and therefore provides a competitive advantage during the conceptual design and bidding phase of a newbuilding project, or during the purchasing process and charter party negotiations for vessels in service. Virtual trials can be launched in complete anonymity, from anywhere, at any time, by simply uploading the hull geometry file and defining the operating profile. The results are available within one week, in a Web-based report showing the CFD results and hull lines in 3D to enable users to gain more insight into the flow details.

Global Hull Performance:
Propulsion Power Optimization and Operational Diagnosis Tool

Panos Deligiannis, Pavlos Zouridis, Neda Maritime Agency, Piraeus/Greece,
technical@nedamaritime.gr

Abstract

Environmental awareness and current market of low revenue, call for an even more focused and optimized management of the fossil fuel global consumption and in effect more efficient power utilization. An online, real-time monitoring system is proposed, which is comprised of a thermo/ hydrodynamic, single global efficiency coefficient model and a fully automated data transfer and screening system, effectively coping with the handling of vast amount of available data. The system is utilized to provide a unique value, which in turn is analyzed for the purpose of differentiating between combustion, hull and propeller related energy loss and is primarily used for vessels' performance assessment and energy efficiency indexation.

Nomenclature

foc:	Fuel oil consumption rate, Kg/day
NCV:	Net calorific value, MJ/kg
U:	Vessel speed
N:	Main engine revolution rate
C_f:	skin friction coefficient
S:	Slip
T:	Propeller thrust force, N
P:	Main Engine power
B:	Vessel breath, m
D:	Vessel depth, m
PDno:	propulsion diagnosis number
α:	propeller load
LOA:	length overall
wf:	wake coefficient
VDC:	Vast Data Collection

Indices

mx	MCR power and revolution rate
act	actual
s	speed through water
g	speed over ground

1. Introduction to shipping digitalization

Digital era in shipping is materialized with the great percentage of the shipping companies internationally, to have already turned to some type of data gathering from numerous sensors onboard the fleet and its transmission to the office, *Logan (2011)*. Many (especially elderly in shipping business) may wonder whether this was needed, however traditional shipping has been all about better controlling and digitalization brings asset closer to home and for this reason it becomes important. Having said that, radical strategic shift to digitalization is a long way from the minds of many in shipping today, who are focused on practical measures to remain competitive in today's difficult market. Digitalization for shipping requires new faculties such as vast data analysts and cyber security experts, topics that traditional ship owners never have thought of before and therefore it is proving a challenge for every company of today. Current and future technical potential may offer "*star trek*" resembling evolution, but certainly cannot guarantee the survival of a shipping company through harsh market times. Balancing between vision and realism requires careful consideration since the data transmission of a continuously increasing number of different lines of parameterization provides a natural blind to the problem that becomes increasingly important and crucial. The question then becomes: Is all this data really telling something?

Arguably, merchant shipping remains the largest carrier of freight throughout the recorded history due to the financial advantages involved. Optimum management of the global propulsion power may result in a large cut down on marine fuel consumption, which in turn will benefit environment and the economics of the shipping community. The most important OPEX cost factor is the marine fuel, Journee and Meijers (1980). Its price affects world trading pattern and mode.

From the above, it can be safely concluded that performance and efficiency parametrization becomes easier and possible with today's technical developments. Therefore, tools that meticulously monitor, screen and validate the on-line/real-time data flow are more than ever required. In future, added value, will be strongly related to the data rather than the asset itself.

Present study focuses on the transformation of a well-performing KPI to utilize the digitalization facilities of today's shipping and improve accuracy of fuel oil consumption prediction in an effort to facilitate charter party requirements and ship-owners' overwhelming anxiety especially in times of overcoming recession periods.

1 Theory

ISO 19030-2 defines the changes in hull and propeller performance as "*the changes in delivered power/fuel consumption required to move the ship through water at a given speed or equivalently changes in speed through water at a given delivered power/fuel consumption, given unchanged transmission and main engine efficiency and the same environmental, conditional and operational profile", ISO (2015). Deligiannis (2017)* proposed a key performance indicator (KPI) that compares the chemical energy of the consumed fuel with the produced propulsion effect. Based on hydro-dynamic fundamentals, a group of parameters, extracted from a daily "sailing" report, are utilized to provide a unique value for the ***PDno***,

$$PDno = \frac{foc \times NCV \times (1 - \%s)}{w_f \times N^2 \times V_s} \quad (1)$$

The above relationship obeys main Key Performance Indicator characteristics, such as:

1. Dimensionless number
2. Unique value for an individual vessel
3. Target value easy and accurately determined, utilizing common speed trial data
4. Inclusive of the hull resistance effects (wave, wind, swell, current)
5. Statistically constant between characteristic periods of time (dry-docking, major main engine overhauling, hull & propeller cleaning)
6. Capable of providing diagnosis on the
    a. efficient operation of the main engine (inferior quality bunkers, poor combustibility) and
    b. power transmission system (shafting-bearing arrangement)
    c. hull coating and propeller deficiencies
7. Specific for crew to grasp
8. Measurable, achievable, realistic and timely available

PDno value is defined during sea trials or an initial benchmarking period and is compared to the actual figure for the purpose of identifying hull and main engine defects.

1.1 Revised approach

The publication aims to the improvement of the accuracy of fuel consumption prediction and in turn performance monitoring, as this is based on the individual value of the ***PDno***. Analysis of a large set of data collected from a fleet of 20 vessels, comprised of large tankers and bulk carriers, has shown that the extremes of theory application may noticeably deviate due to the variation of the main engine specific consumption of [***sfoc - power*** relationship] and the effect of the wake coefficient

[$w_f = \frac{U_s - U_a}{U}$] deterioration when hull experiences variable degree of turbulence.

In Eq.(1), the original assumption utilized the constant wake coefficient hypothesis, which was represented with a wake coefficient function given as: $w_f = f(N, p)$. However, real data analysis has shown that under extreme weather and hull fouling conditions, the calculated propeller load deviates significantly from reality, resulting in an increased value of ***PDno*** and consequently underestimation of ***foc***.

The wake coefficient function $\mathbf{w_f}$ is related to the quantity of seawater flow upstream of the propeller and in turn dictates the degree of propeller loading. For the usual hydrodynamic conditions ($Re \approx 1E9$), $\mathbf{w_f}$ depends on $\mathbf{U_s}$, $\mathbf{u_*}$ and the geometrical characteristics of the hull. The geometry refers to the shape and roughness of the hull and relates to the parallel body, hull lines and draught. The initial $\mathbf{w_f}$ also includes improvements due to the energy saving devices (ESDs) installed in the vicinity of the propeller for the sole purpose of restoring rotational in-flow through the propeller disc to parallel streamlines ($\frac{\partial \overline{\overline{uv}}}{\partial y} \to 0$).

1.1.1. Hull wake

The propeller always operates in a wake and for any given condition its effect on performance varies with speed, wetted hull lines, roughness and sea conditions. Reynold's number and therefore flow instability increases with vessel's speed. Hull roughness increases friction coefficient, which in turn increases wake coefficient function. Vessel's wetted surface influences flow disorder and consequently wake. With this in mind, an attempt is made to define the wake coefficient function based on a simplified analogy of stream-wise momentum equation maintaining only the significant parts of the mean longitudinal hull flow to the cross-flow turbulence transportation given as:

$$w_f = C_T \times (\frac{u_*}{U_s})^2 \times \left(\frac{L_c}{\delta}\right)^z \quad (2)$$

$\boldsymbol{\delta}$ is the boundary layer thickness and $\mathbf{u_*}$ is the friction velocity that characterizes the severity of turbulence, given as, *Schlichting (1979)*:

$$\delta = \frac{LOA \times 0.37}{Re^{0.2}} \quad (3)$$

$$u_* = c_T \times U_s \times \sqrt{\frac{C_f}{2}} \quad (4)$$

C_T and z are turbulence intensity constants that can be benchmarked depending on actual hull lines and energy saving devices (ESDs).

1.1.2. Hull friction coefficient

Within the operational pattern of the fleet, the existence of a fully "rough" hull boundary layer can be safely assumed, for which the friction coefficient depends on $\boldsymbol{\delta}$ and a mean hull roughness size, [r_h] and can be given as, *Schlichting (1979)*:

$$C_f = \left[1.89 - 1.62 \times log\left(\frac{r_h}{\delta}\right)\right]^{-2.5} (5)$$

1.1.3. Characteristic lengths L_c and r_h

Several hull characteristic lengths were evaluated, including vessel's draught, overall length and others that were calculated based on combinations of the 'block', 'prismatic' and 'midship' coefficients. The analysis of actual data showed that the most accurate representation for the current momentum deficit model is the "distance between propeller and aft end of the parallel body". The value of $\mathbf{L_c}$ characterizes the size of the area of vessel's wake and therefore, brings in the calculation the macro-geometrical effect, whereas, $\mathbf{r_h}$ represents the micro-geometrical dependency on the friction coefficient.

1.1.4. Propeller Load: engine & power transmission

The propeller load ($\boldsymbol{\alpha}$) and the charter party speed order impose the engine power and the rate of revolution. The propeller load accounts for the non-uniform flow distribution in the vicinity of the propeller and the degree and extent of cavitation as well as the more macroscopic hull resistance. Based on the above the engine power is given as:

$$P = M_T \times N = \frac{P_{mx}}{N_{mx}^{\alpha}} \times N^{\alpha} \quad (6)$$

and the shaft torque, M_T, becomes:

$$M_T = \frac{P_{mx}}{N_{mx}^{\alpha}} \times N^{\alpha-1} \quad (7)$$

P_{mx} and N_{mx} is the maximum continuous power and attained revolution rate respectively.

Fig.1 shows the constant engine load $\boldsymbol{\alpha}$ curves on the M_T – N plane for a given engine.

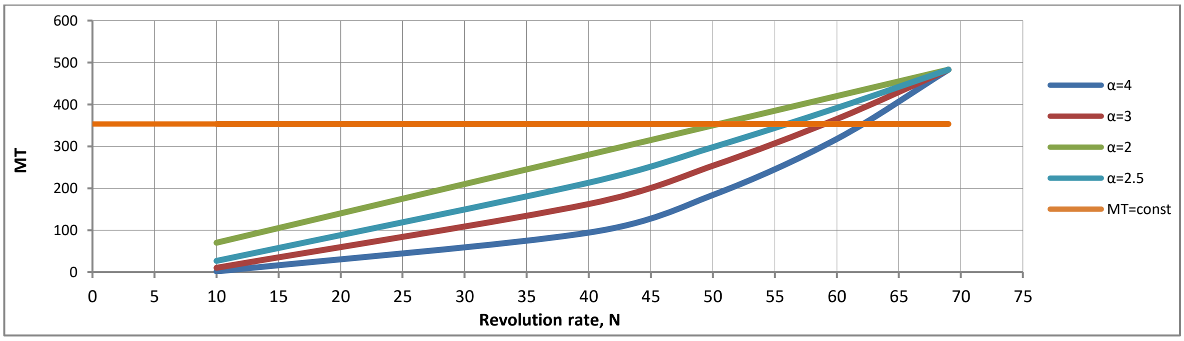

Fig.1: Propeller load (torque/rpm)

Assuming that ***sfoc-N*** relationship is known from the shop testing of the engine, then it can be shown that:

$$\alpha = \frac{\ln\left(\dfrac{foc}{sfoc \times P_{mx}}\right)}{\ln\left[\dfrac{N}{N_{mx}}\right]} \quad (8)$$

Thus, following process is valid:

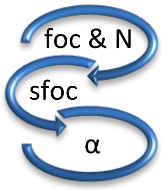

Fig.2: RPM, sfoc and propeller load relationship

The propeller load ($\boldsymbol{\alpha}$) is related to the thermal load of the engine and it is directly affected by the hydrodynamic defects, considering constant transmission efficiency. Latest fact is supported by relevant VDC analysis for a VLCC as per Fig.3. Minimum value of "α" is 2, which signifies upper limit of shafting system structural integrity.

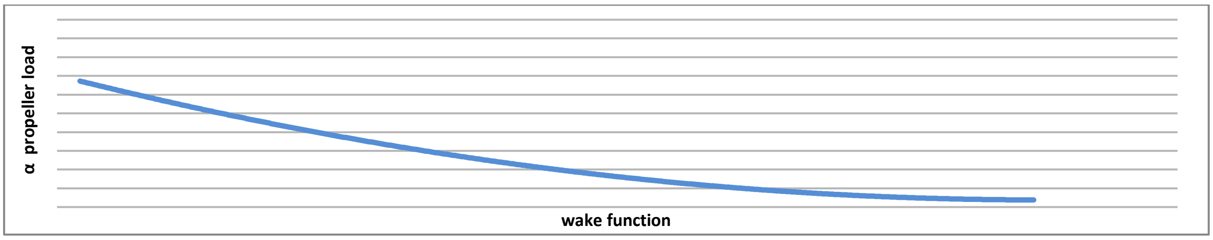

Fig.3: 309k DWT - propeller load (α) vs wake function

1.1.5. Propeller load: wake & jet flow

For a given set of speed orders, the propeller thrust is determined by the flow velocity (specific mass flow rate) and the flow acceleration (jet flow velocity, ΔU_j) through the propeller disc area (A_{pp}) as, *NN (2009)*:

$$T = \rho \times A_{pp} \times U_p \times [U_j - U_a] \qquad (9)$$

$\mathbf{U_a}$ and $\mathbf{U_j}$ are the upstream and downstream propeller flow velocities and $\mathbf{U_p}$ defines the flow through the propeller, Fig.4. By defining the propeller jet flow coefficient as $C_j = \frac{U_j}{U_s}$, the power transfer to the seawater flow from the propeller-shafting system can be given as:

$$P = \rho \times A_{pp} \times \frac{U_s^3}{4} \times [C_j - (1 - w_f)] \times [C_j + (1 - w_f)]^2 \quad (10)$$

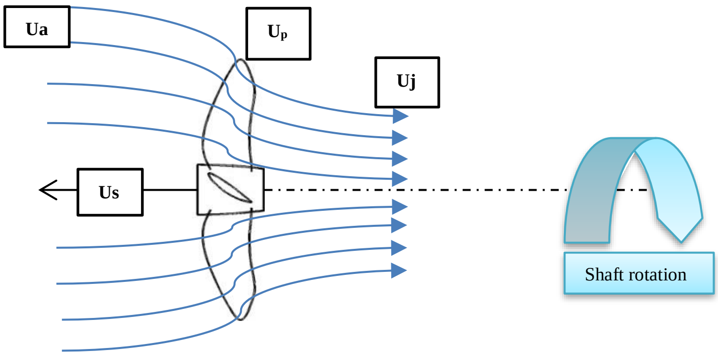

Fig.4: Water flow through the propeller

Based on Eq.(10), the hydro-efficiency loss coefficient C_h is defined as:

$$C_h = \frac{4 \times P}{\rho \times A_{pp} \times U_s^3} = [C_j - (1 - w_f)] \times [C_j + (1 - w_f)]^2 \quad (11)$$

From Eq.(11), $\mathbf{C_j}$ can be evaluated, based on iterating process that incorporates the estimation of $\mathbf{w_f}$ (the initial value can be estimated from VDC on the assumption of original hull roughness) and the measured value of $\mathbf{C_h}$.

As $\mathbf{w_f}$ increases, $\mathbf{U_a}$ reduces, resulting in the propeller flow acceleration, ΔU_j $(= U_s \times [C_j - (1 - w_f)]$, increase. By applying Bernoulli principal, any flow acceleration increase will lead to propeller pressure load increase (ΔP_{pp}). The propeller overloads (rotating faster) in order to overcome inlet flow deficiency, easier to grasp by the below schematic presentation, Fig.5. However, for a fixed charter party ***foc*** [i.e. fixed combustion indicated pressure and in turn shaft torque], any external resistance will result in reduction to shaft revolution rate and eventually reduction of vessel's speed.

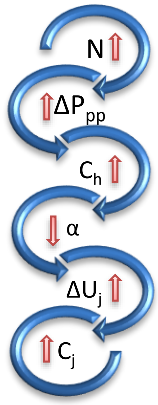

Fig.5: Disturbed flow relationship

2. Methodology

Ship digitalization progress has made it easier for improved form of equation(s) to be materialised and complex modelling to be incorporated into the performance evaluation. To this extent, Data Acquisition system [**DAQ**], which is designed and constructed by Vector Marine is utilized for the real-time/on-line **VDC** transferring and handling (filtering, verification, archiving). Readings from a number of sensors and systems, including bridge equipment for navigation, engine control room data related to the main and auxiliary engines, steering, auxiliary boilers, fuel consumption and *the cargo control room* systems for the cargo tank area and loading condition comprise the **VDC** population.

DAQ system collects data from fleet via satellite for the purpose of assessing the performance measures and continuously monitor machinery operation, efficiency and vessel's location, following ISO 19030-2 guidelines.

The navigation, combustion and in general sailing information is assembled and stored in a complex structured string parameter that is processed, utilizing correlation and autocorrelation process for the sole purpose of filtration and phenomena evaluation such as the weather, current and fouling on the one side and engine, power transmission on the other. The vast number of received parameter values, are used to compute the corrected ***PDno*** (Eq.1), as per Fig.6.

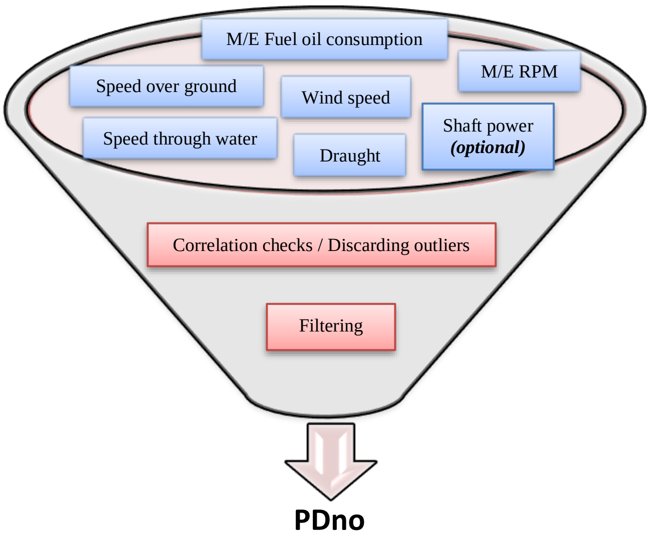

Fig.6: Data analysis

PDno is used to calculate the expected fuel oil consumption and its deviation from the measured value signifies the ***total efficiency loss*** (**L_T**). The comparison between the shop test ***sfoc*** and the measured one provides an accurate indication of the ***machinery efficiency loss*** (**L_{MACH}**). The effect of the main engine ***sfoc*** on the performance measurements is assessed with the use of the detailed shop test engine data. Experience has shown that shop test data is the most accurate source for the production of ***sfoc–power*** curve. For vessels not equipped with a shaft torque meter or in cases where power measurements experience frequent irregularities with respect to accuracy, the ***sfoc–N*** curve is utilized instead.

The ***hydro efficiency loss*** (**L_{HYDRO}**), being arguably the most difficult to identify, is calculated on the basis of the correlation of the propeller load **α** deviation and the **[L_T,L_{MACH}]** differential. For confident assessment of the hull fouling, the correlation coefficient must be greater than 98%.

Deviation from the benchmarked value of the propeller jet coefficient defines the ***propeller efficiency loss*** (**L_{PROP}**), which in turn determines the ***hull loss*** (**L_{HULL}**) that through the wake model, an equivalent average roughness value is calculated, Fig.7.

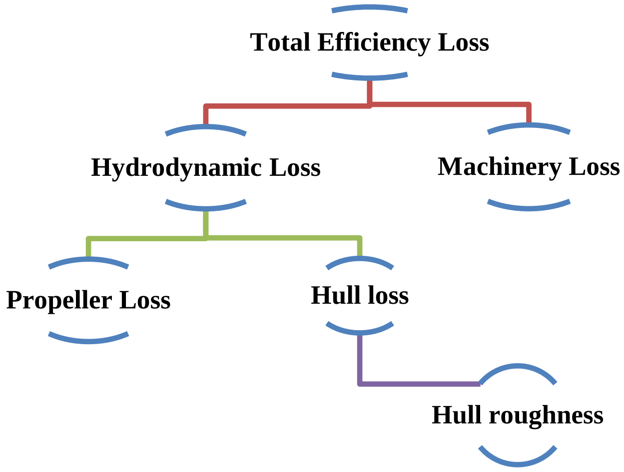

Fig.7: Schematic process representation

In the present work the momentum deficit of the flow around the hull is related to the propeller load increase and in turn the increase of power and thrust in order for the charter party speed to be achieved. As external hull resistance increases, so does the slip thus there is a monotonic relationship between the propeller load and the slip as real data collected from fleet VLCC indicates Fig.8.

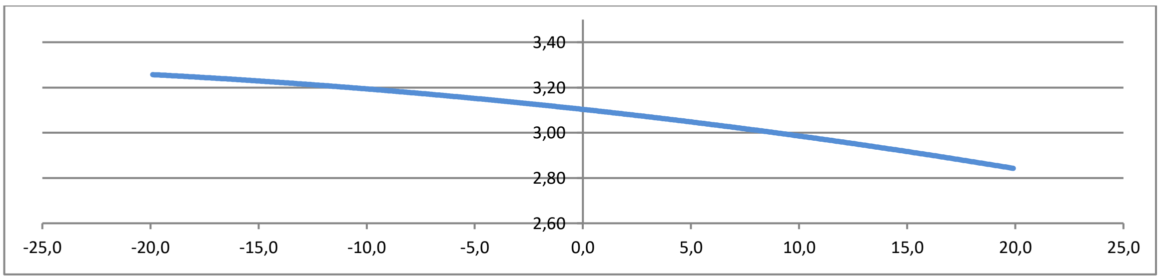

Fig.8: 320k DWT - propeller load (α) vs slip through water

3. Discussion

Vast-data-collection handling process model is proposed for the purpose of distinguishing between the engine and hull energy deficiency. The hydrodynamic effect that reflects the hull and propeller roughness deterioration is evaluated and rated.

Fig.9 shows the similarity of the ***sfoc*** and PDno curves. The applied correction with respect to ***sfoc*** improves fuel oil consumption prediction; however, remaining part of deviation is covered through the involvement of the wake coefficient function model.

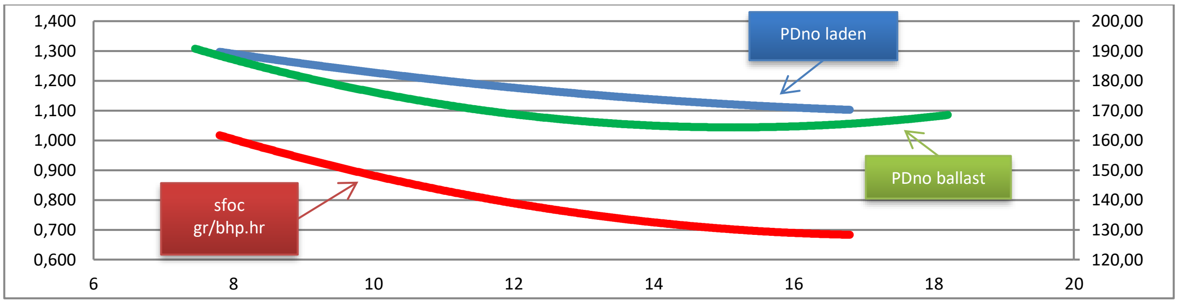

Fig.9: 320k DWT PDno & SFOC speed dependency

Fig.10 illustrates the dependency of the wake function coefficient of a VLCC in ballast and laden condition and the vessel's speed (through water).

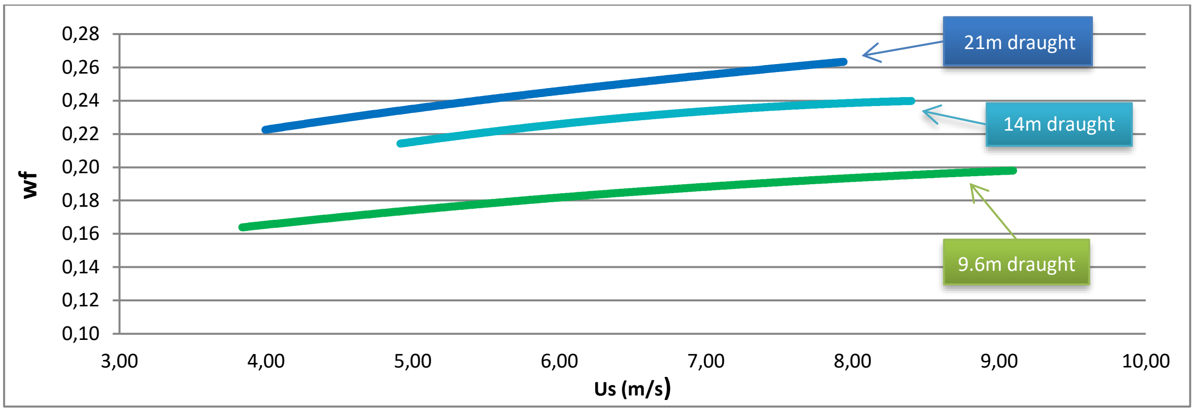

Fig.10: 300k DWT wake coefficient function vs speed through water

Fig.11 shows the calculated equivalent hull roughness for a VLCC, which is estimated through wake coefficient function deterioration with the initial average hull roughness measured at 90 microns in dry dock.

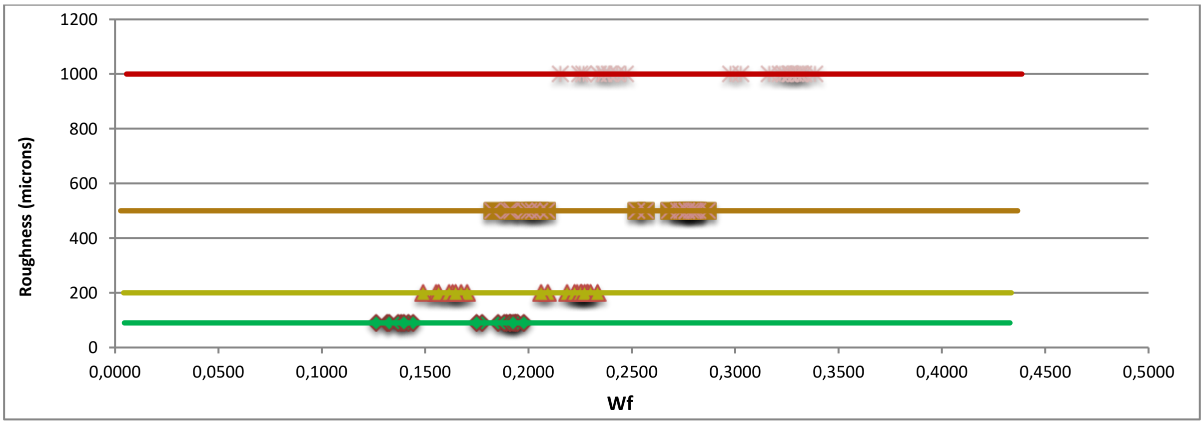

Fig.11: Wake function dependency on roughness

From the analysis, it is shown that for a clean hull & propeller and calm seas, propeller load follows a known relationship which is a function of vessel's wetted surface and in turn the draught and remains almost constant throughout the power range of the individual hull – engine – propeller system.

Table I: Propeller load (**α**)Table I shows the characteristic values for ballast and laden conditions of individual vessels. To all intents and purposes of the proposed flow modelling, it is assumed that the relationship between ***α*** and the wetted surface is linear.

Table I: Propeller load (**α**)

Vessel - dwt	Ballast condition	Laden condition
VLCC 319k	3.15	3.09
VLCC 319k	3.07 / 3.20 (silicon)	3.01 / 3.15 (silicon)
VLCC 300k	3.10	2.90
VLCC 309k	3.00	2.89
VLCC 318k	3.04	2.90
Aframax 115k	3.06	2.81
Aframax 120k	2.80	2.7
Bulker 180k	3.17	3.10

A noticeable observation is with respect to the first two sister vessels, which experience a varying degree of ***α*** attributed to the power meter deviation and the hull coating finish. During their first dry docking in 2017, both vessels underwent identical hull treatment with respect to blasting; however, the coating system of the 2nd one was upgraded from high performance antifouling to silicone (verticals only). The post-drydock VDC analysis suggests 4.5% improvement to the wake and in turn the propeller load for both the ballast and laden conditions and 2% to ***PDno***.

Hull efficiency loss, Fig.12, shows the clear improvement between the pre- (10 months) and post- (7 months) dry docking periods.

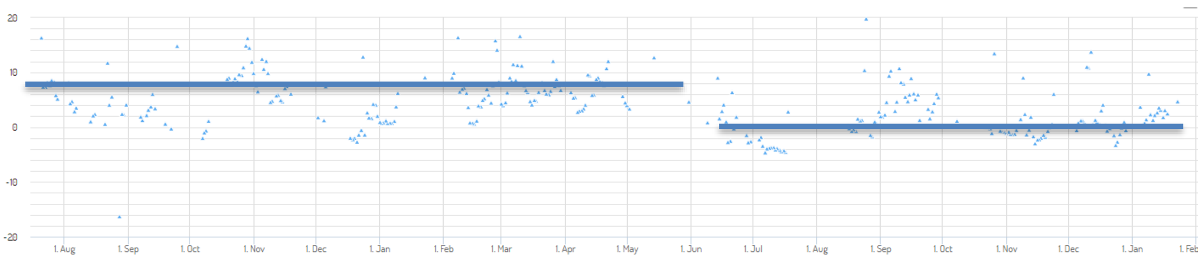

Fig.12: VLCC 319k DWT, before and after dry-docking with improved hull coating

3.1. Correlation - autocorrelation

Correlation process is an integral part of the proposed scheme and is defined as the degree of association of two variables or one variable at different time windows. With this process defined, a filtration procedure is attempted through which unreliable data is excluded in a rather simple and effective manner. VDC screening becomes effective, leaving only meaningful data for further filtering and analysis. In Fig.13, for the regions where difference is in excess of 2% (red arrows), an error on measurement has been traced back.

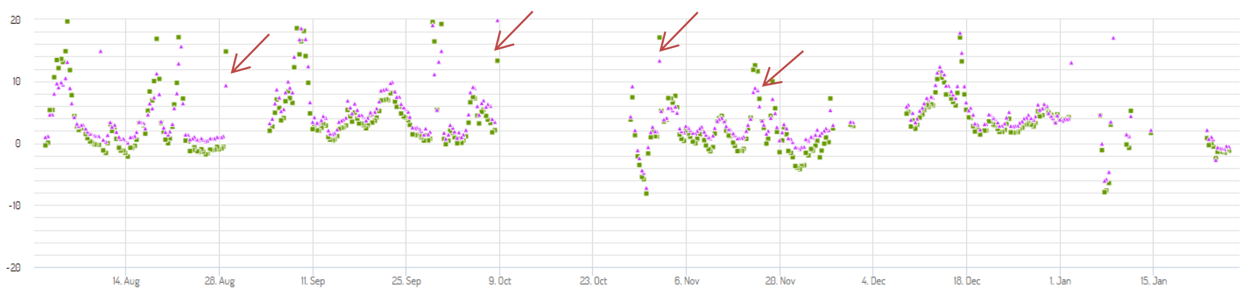

Fig.13: Hydrodynamic efficiency loss correlation

For the purpose of present work, the correlation coefficient C_c of two variables a and b is defined as:

$$C_c = \frac{\overline{a \times b}}{\sqrt{\overline{a^2} x \overline{b^2}}}$$

If C_c=1, the correlation is said to be perfect.

With this definition in mind, a year old VLCC experiences the correlated effects in Table II. Note that the correlations involving %S somewhat deteriorate with respect to propeller load and hull friction.

Table II: VLCC 300K, correlation coefficient

Correlation Coefficient	Value
α,C_j	0.995
w_f,C_j	0.989
α,w_f	0.997
α,C_h	0.959
α,%S	0.707
w_f,%S	0.682
C_j,%S	0.869

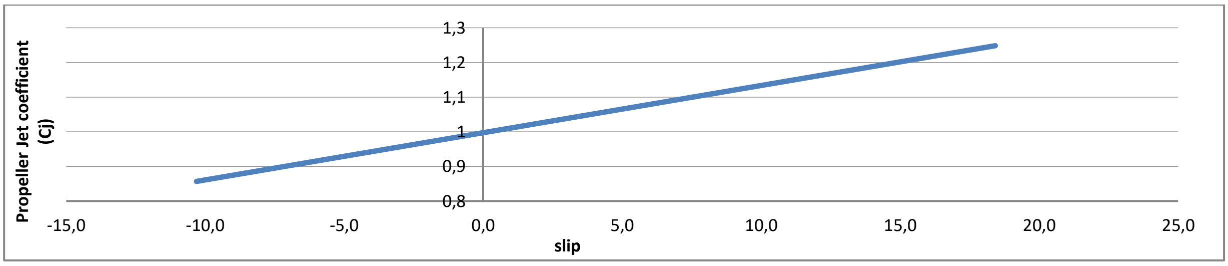

Fig.14: Propeller jet coefficient vs slip through water

3.2. Applied corrections accuracy

Fig.15 shows the calculated hydrodynamic defect, inclusive of weather condition effect. Green dot graph corrects PDno with the benchmarked value of $\boldsymbol{\alpha}$, while yellow dot graph with the actual value of $\boldsymbol{\alpha}$. Comparison of resulted values shows that when the actual $\boldsymbol{\alpha}$ correction is applied, $\mathbf{L_{HYDRO}}$ is as per initial benchmarking; meaning that any hydro-flaw is excluded (weather, fouling). For this reason it is safely concluded that applied correction of benchmarked $\boldsymbol{\alpha}$ to the PDno, correctly signifies the wake deterioration and therefore the overall model degree of applicability.

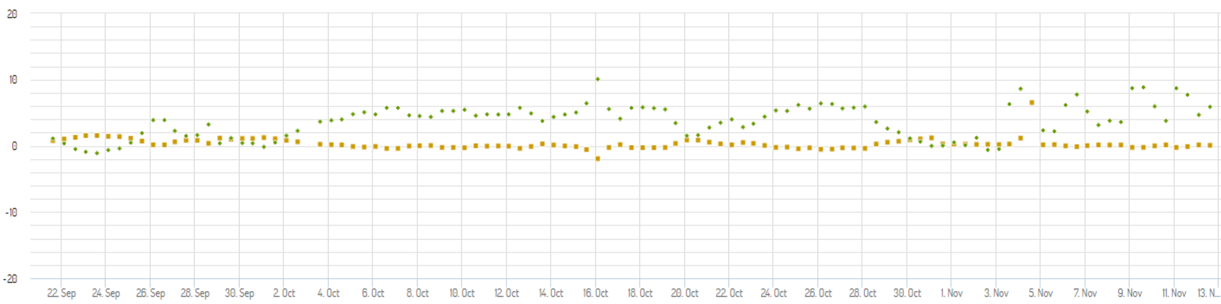

Figure 15: Hydrodynamic efficiency loss, corrected for actual propeller load ($\boldsymbol{\alpha}$)

3.3. The effect of current

Fig.16 shows the ***unfiltered*** performance of a new-build VLCC in mixed ballast/laden conditions as well as varying speed and power for the selected time window. The second half of both May and

November show reduced propeller efficiency, due to favorable currents that increase back pressure on the propeller plane thus deteriorating propeller performance due to flow acceleration. Also, the second half of September shows an increasing trend for machinery loss; this coincides with the 3,000 running hours of the fuel injector replacement interval as well as super-slow-steaming voyage; the increased consumption was adversely affected due to the deteriorated fuel valves. Following relevant overhauling works, L_M seems to have reduced, however not quite close to a satisfactory level. Further investigation confirmed an increasing fuel oil leakage from the high-pressure pipes, thus validating this way the accuracy of the methodology. Total hydrodynamic efficiency loss is seen to oscillate around the benchmark value; hull was confirmed clean by underwater inspection.

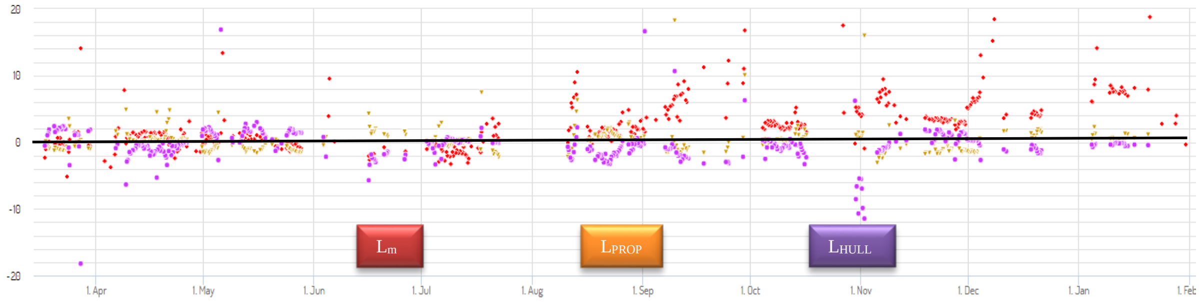

Fig.16: New build 300k DWT, 11-month trend of machinery, propeller and hull efficiency loss

3.4. The simplified C_j-w_f regime

As $U_{pp} \looparrowright U_{s},\ C_j \looparrowright 1$ and equation (10) becomes:

$$P = \rho \times A_{pp} \times \frac{U_s^3}{4} \times w_f \times [2 - w_f]^2$$

For C_j=1, the maximum wake coefficient $\mathbf{w_{fx}}$ is 0.667. $\mathbf{C_j}$ being a function of propeller load accounts also for the flow non-uniformity in the vicinity of the propeller disc as well as the extent and degree of cavitation and blade spatial load difference, NN (2009), pp.244-245.

For the generic case of $C_j = \frac{U_j}{U_s}$, it can be shown that for a specified propeller power and vessel speed, the loci of maximum propeller jet coefficient, C_{jx}, values can be estimated as:

$$C_{jx} = \sqrt[3]{\frac{P}{\rho \times A_{pp} \times U_s^3 \times 0.296}} \quad \text{and} \quad 1 - w_{fx} = \frac{C_{jx}}{3}$$

Cj can be benchmarked and monitored for possible deviation, indicating propeller induced hydrodynamic loss. Benchmarking can be characterized as accurate and reliable for correlation coefficient **Cc[α,C$_j$]** of 0.98.

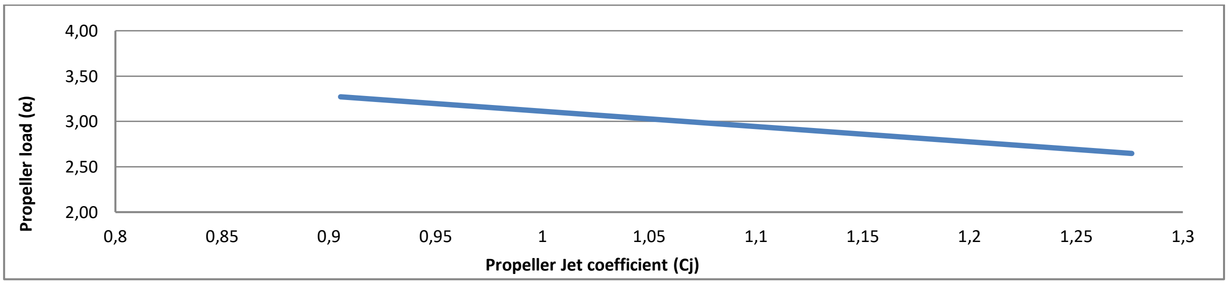

Fig.17: Propeller Load vs Propeller jet coefficient

3.5. Effect of Drydocking, hull and propeller cleaning

Fig.18 shows the period before and after drydocking of a 5 year old VLCC. The hull treatment included full SA2 blasting at verticals and full SA1 at flatbottom and boottop; the applied coating was the same as per original specification (high performance silyl methacrylate). The hydrodynamic efficiency loss returned to initial resistance, which coincides with new-building benchmarking; minor deviation from zero line is due to weather and current effects (not excluded in below graph).

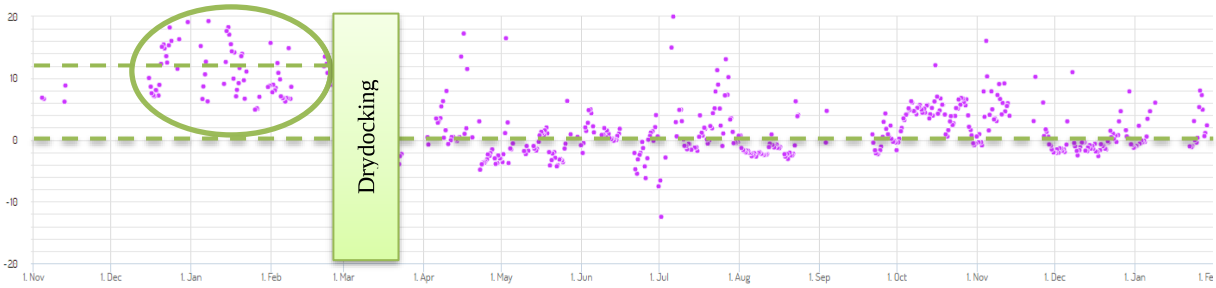

Fig.18: 319k DWT Hydrodynamic efficiency loss before/after dry-docking

Fig.19 shows the 22 months (April 2016 to February 2018) trend of hull and propeller loss of a silicon coated VLCC. Captioned vessel was dry-docked in February 2015 and the performance was mostly stable until December 2016. Since then both jet coefficient and wake coefficient function, reflecting the propeller and hull performance respectively, started increasing. Operational restrictions, however, allowed only for propeller polishing in February 2017 and August 2017, when improvement was noted even though not to the benchmarked level. In January 2018 propeller and hull (verticals) were cleaned by paint makers' approved subcontractor and performance returned to the benchmarked level for both hull and propeller. February and August 2017, propeller polishing jobs did not allow for the energy loss to return to zero due to hull fouling and therefore deteriorated wake which effectively reduces water velocity upstream of propeller disk.

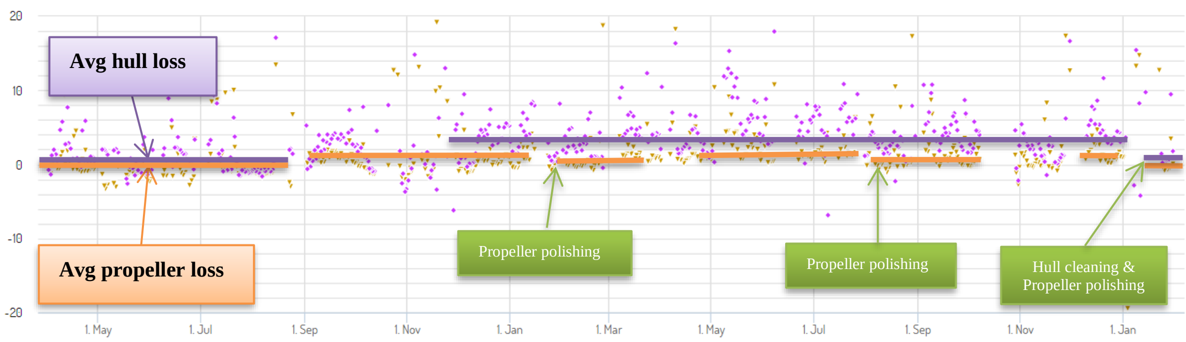

Fig.19: 318k DWT Hull and propeller loss before/after cleaning

Fig.20 refers to a recently dry-docked VLCC, where machinery loss (red dot) increases throughout, despite main engine key component dry-dock overhauling. Accuracy of data was confirmed and reason for increased fuel consumption was attributed to the leakage of the service tank return valve, which allowed unnecessary recirculation of the fuel. The correct operation of the flowmeter provided accurate record of the extra consumption with hydrodynamic loss being stable at benchmarking level (green dot).

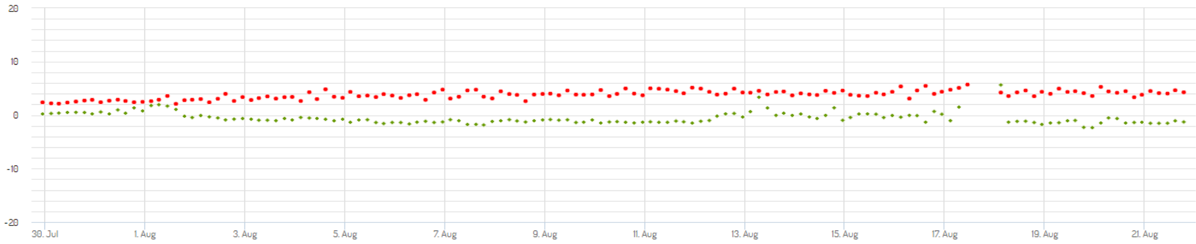

Fig.20: 320K DWT machinery/hydrodynamic efficiency graph

In Fig.21, no screening procedure is applied in order to show the effect of weather, on the hydro-dynamic efficiency loss (green dot) and the machinery efficiency loss (red dot). There is, no thermodynamic deficit noted, however, reduction in engine performance during adverse weather is expected and confirmed.

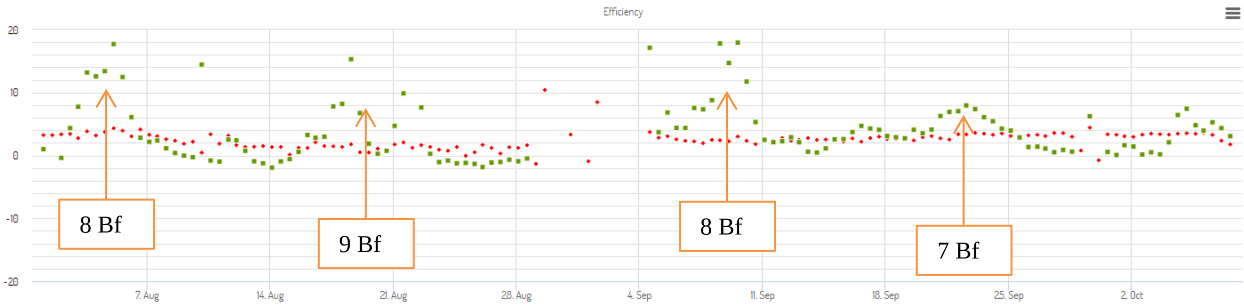

Fig.21: 318K DWT, voyage analysis, machinery/hydro loss

4. Conclusions

a. Proposed methodology accurately predicts fuel oil consumption and differentiates effectively between thermo- and hydro-dynamic loss
b. Propeller self- and hull- induced energy deficit can be distinguished
c. Hull roughness is an important parameter responsible for the energy deficit and fuel overconsumption
d. Hull treatment either in dry dock or afloat benefits ship owners by reducing OPEX
e. Timely diagnosis of hull, propeller, engine and power transmission allows for the prompt re-instating of vessel/system condition and benefits prudent ship owners
f. ***sfoc***, can be used for the engine efficiency benchmarking and the screening of extreme ambient conditions
g. Distance between propeller and aft parallel body was proven to be the characteristic length for optimising wake upstream of the propeller disk
h. Differentiating between hull and propeller momentum defects, is possible through the accurate correlation of C_j and w_f and the time-based autocorrelation of w_f
i. Adverse sea current improves propeller load ($\boldsymbol{\alpha}$), by reducing jet coefficient

Acknowledgment

The authors gratefully acknowledge the support of the Neda Maritime Agency Management for allowing the reproduction of the fleet data in the preparation of this paper.

References

DELIGIANNIS, P. (2017), *Ship performance indicator*, J. Marine Policy, pp.204-209

ISO (2015), *ISO 19030-2. Ships and marine technology – Measurements of changes in hull and propeller performance*, ISO, Geneva

JONAS, P.; MAZUR, O.; URUBA, V. (2009), *Determination of skin friction on a rough surface*, Colloquium Fluid Dynamics, Prague, pp.1-8

JOURNEE, J.; MEIJERS, J. (1980), *Ship routeing for optimum performance*, Delft University of Technology

LOGAN, K.P. (2011), *Using a ship's propeller for hull condition monitoring*, ASNE Intelligent Ships Symp. IX, Philadelphia, pp.1-20

NN (2009), *Compendium Marine Engineering*, Seehafen Verlag

SCHLICHTING, H. (1979), *Boundary-Layer Theory*, McGraw-Hill

TENNEKES, H.; LUMLEY, J. (1972), *A First Course in Turbulence,* MIT, Cambridge

TOWNSIN, R. L. (2002), *The Ship Hull Fouling Penalty*, Biofouling 19

Practical Experience with ISO 19030 at Chevron Shipping - Part 3

Jørgen Abrahamsen, Jotun, Sandefjord/Norway, jorgen@abrahamsen@jotun.no

Abstract

This part focus on the practical experience of utilizing extensive data exchange for verification and calibration of an operators' hull performance strategy based on analysis. Finally, we will describe areas of improvement for the ISO 19030 methodology based on findings from the ongoing optimization program with Chevron Shipping.

1. Methodology

In order to benchmark and compare the different vessels within the fleet, we needed sufficient data quality throughout the fleet for the parameters we were going to base our analysis upon. First step was then to screen and analyse the data visually, Fig.1, to sort out the range (histograms) and consistency (time series). When accessing the Chevron data platform, we found 221 data tags to choose from where we picked out 21 for the analysis. In accordance with ISO 19030 we tried to look at the speed-power relationship, but found out that the power values are reported differently. There might be that other power data is available and that different vessel classes report on different tags, but this have not been tested further and will be a discussion before the next review.

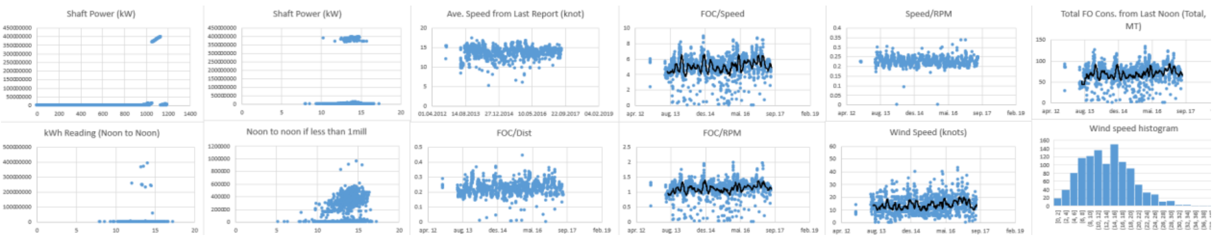

Fig.1: Visual screening of the data range and consistency

Figs.2 and 3 show examples from 6 of the vessels from the analysis. The blue data points on top is power readings. The periods with upward trends is probably cumulative reporting while the lower values represent the reported steaming hours. There is no consistency in the reporting meaning that the cumulative vs daily value reporting appears at different time for the different vessels. Blue dots below with black moving average line shows the noon-to-noon power – neither consistent reporting as they report on different scale at different times. At the same time the grey points are RPM showing normal operation. If we were doing single vessel analysis, we could try to convert the different periods to comparable scale and calculate the daily values for the power, but when looking at multiple vessels at the same time in the same report, that would be too time consuming and too many ifs and buts.

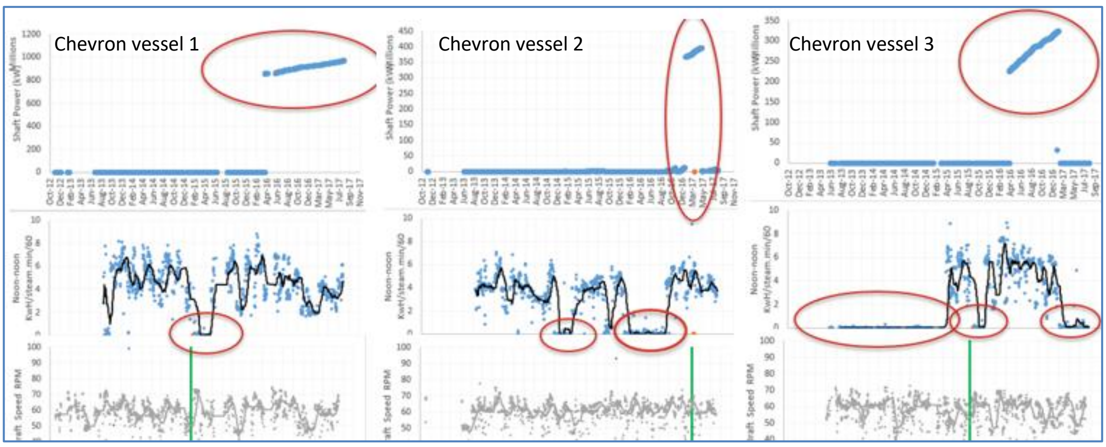

Fig.2: Inconsistent Shaft power and Noon-to-noon power and steady RPM

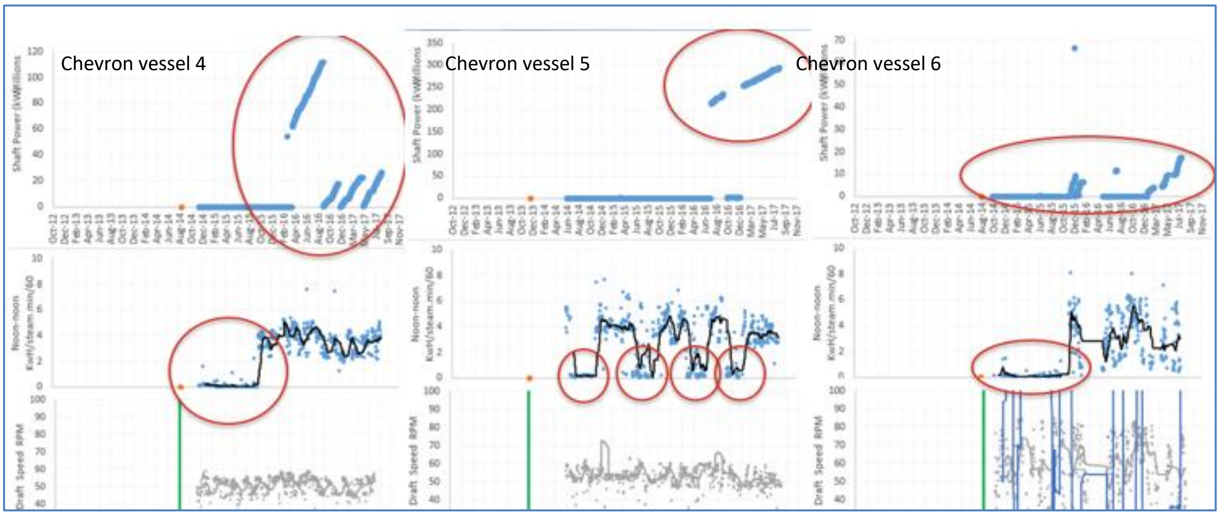

Fig.3: More examples; inconsistent reporting from most vessels

With inconsistency in the power reporting and with limited knowledge of the other parameters, we calculated several alternative Key Performance Indicators (KPIs). We then created a "dashboard", Fig.4, with filters to maneuver through the fleet and to be able to look at all the KPIs in parallel**.** By fixing the scales we could benchmark "normal" levels for each vessel group and more important; to see if the alternative KPIs showed the same patterns and indicated the events. The result of this evaluation was that we ended up using speed-fuel as main KPI with back-up from slip, speed-distance and speed-rpm.

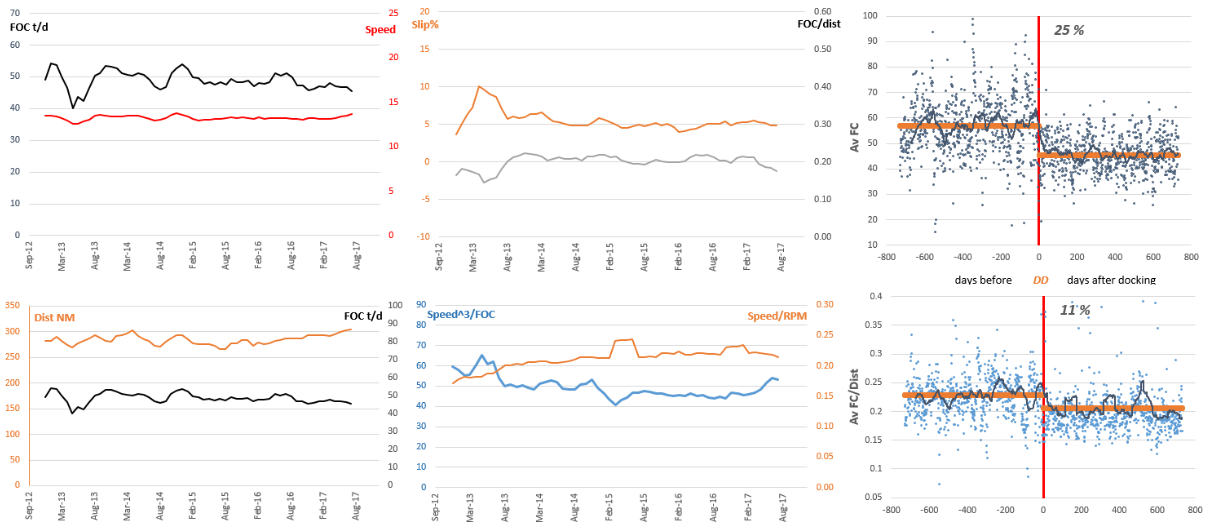

Fig.4: Chevron data – KPIs from all vessels combined in a dynamic "dashboard"

When filter for single vessels, the dry-dock appear as a green vertical line and we can now evaluate the quality of the alternative KPIs, Fig.5. Do we see the dry-dock effect? How is the fuel development vs speed? Is the calculated slip backing up the other KPIs? Do we get more nautical miles per fuel? In general, there was consistency and good dry-dock effects.

This Excel report was then used as input to a PowerPoint presentation where we coupled the graph with information from dive/cleaning reports, Fig.6. Main KPI was obtained speed per tons of fuel (mid bottom graph, blue line from Fig.5; speed^3/FOC. Note a lag and smoothening effect from moving average.

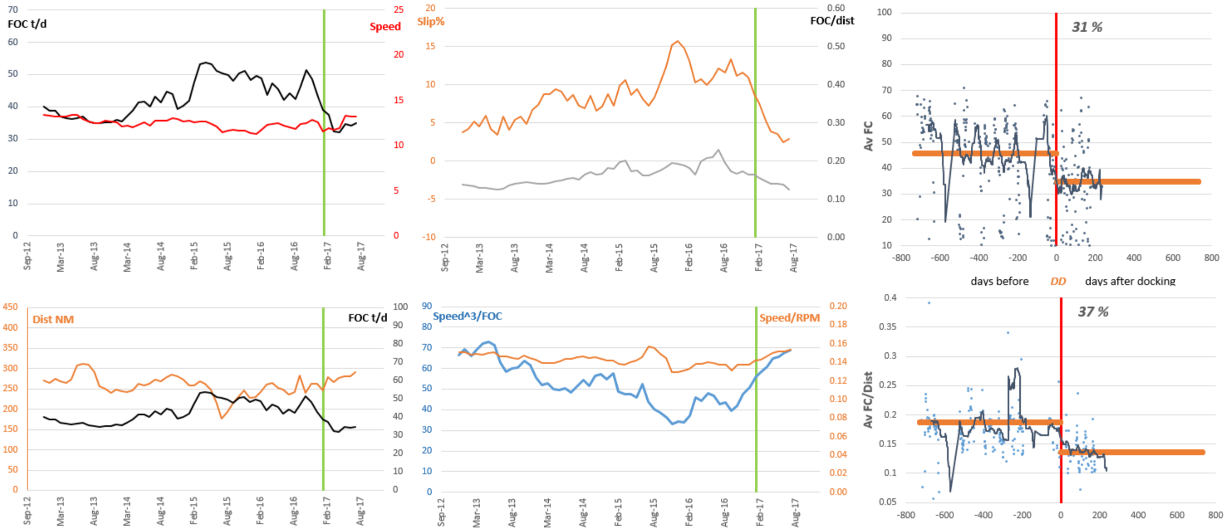

Fig.5: With single vessel filter. Top left; fuel and speed. Top mid; slip and fuel/distance. Top right; fuel consumption, pre/post dry-dock. Bottom left; distance and fuel. Bottom mid; Speed/fuel and speed/RPM. Bottom right; fuel per distance, pre/post dry-dock.

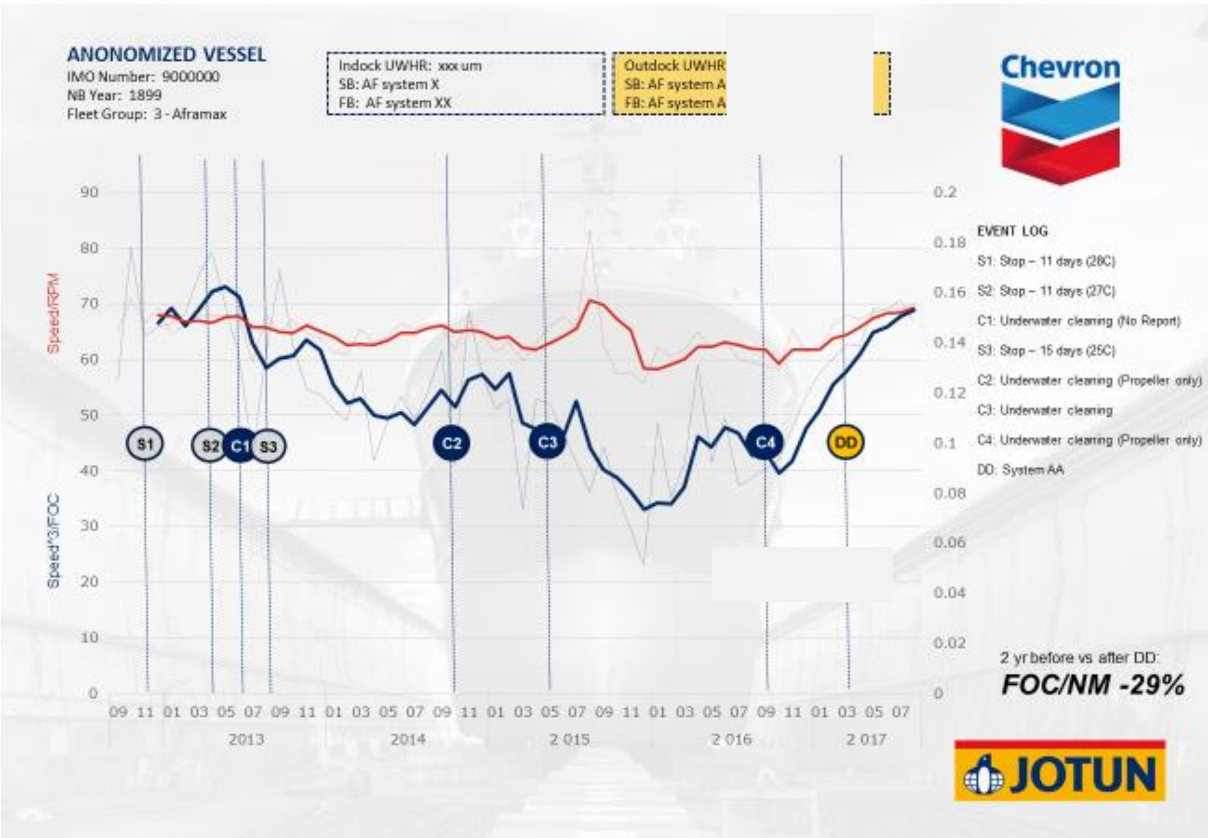

Fig.6: PowerPoint slide example for “vessel-by-vessel go-through” when meeting Chevron

2. Results and conclusion

The data set contained data from 26 vessels from the last 5 years with even distributions of dry-dockings throughout the period. In other words, we had very few vessels with data for the whole sailing periods between two dry-dockings to look at the in-service performance. Therefore, we created a dashboard where we could look at the overall performance development of the fleet, group wise, and for single vessels. For dry-docking effects, we added a day count for all the dockings where day 0 was the dry-dock, minus days before, - and plus days after the docking.

The dashboard was also good for data quality check (fixed scales in charts/graphs) and comparisons within the same vessel groups.

Inconsistent power readings made it difficult to use speed/power relationship. Speed to fuel ratio were used instead as main performance indicator with back-up from speed/RPM, slip and distance. Several data parameters (KPIs) in parallel gave us a valuable verification of the main KPI.

The use of visual inspections/dive reports was very useful for understanding and back-up of the data.

3. Possible Improvements

1. Should noon reports and raw data be treated differently? Should we look at other parameters and filter less for noon reports when operation and conditions are evenly time distributed? We might lower the absolute speed loss level with less weather filter, but if there is consistency throughout the period, this approach could be more accurate since the weighting of the few points left, combined with noon report inaccuracy, give too much impact when applying standard filters. Is it better to filter more dynamically to ensure enough data and capture the overall trend?
2. Ensure correct baselines – plot actual speed-power relation vs design curves and construct new baseline curves if trading outside of the design curves (both shape and range).
3. Hypothesis; some data easier to report correctly than others? E.g. RPM, distance (slip) and fuel where the crew have better understanding of the values? These should at least be considered if the power values are unreliable. Note: this is not an issue for raw data/auto-reporting – only noon reports.
4. "Best practice noon reporting" as a part of ISO 19030? It is important with detailed instructions for noon reporting throughout the fleet. All values should represent the steaming hours, with standardized tags and on the same scale. Best practice reporting methodology for the tags related to the hull and propeller performance could be described in the ISO 19030, alternatively as an appendix.
5. Another improvement could be to increase the reporting frequency to every change in operation or weather condition throughout the 24 hours – e.g. day/night speed vs average values if that is how the vessel operates. This is a cost-benefit discussion of needed detail level of the reports. However, if not only the hull condition, but also the operational impact on fuel consumption should be analysed, this should be considered.
6. A step further would be to utilize AIS data to a greater extent. From the AIS source, we have access to high resolution data for the world fleet of speed, draft and positions which again could be linked up to external weather data. All we then need from the vessel is accurate power and fuel data - hence more focus on correct reporting on these tags. This will give the operational and weather insight throughout the 24 hours that we miss in a standard noon reports.

Finally, this project has been a great learning for us and we discovered many improvement possibilities on the way forward. By capturing the right data, improve and standardize the reporting further, there is a great potential for very good analysis. Main message is that it is difficult to generalize – we should look at data quality case-by-case and use the data that gives the most accurate analysis. Further, overall trends are obvious while detailed short-term effects could be difficult to spot with the data given.

Performance Values vs. Speed – A Declaration of Independence?

Dinis Oliveira, Lena Granhag, Lars Larsson, Chalmers University of Technology, Gothenburg/Sweden, dinis@chalmers.se

Abstract

Percentage speed loss due to a deteriorated condition of hull and propeller is used as performance value in ISO 19030:2016. However, for a number of reasons, this performance value is speed-dependent. In this paper, equivalent sand roughness height is proposed as an alternative performance value, being calculated from increased shaft power due to hull-and-propeller condition. Results for a Panamax tanker (noon reports) are analysed and discussed. It is argued that uncertainties for final performance indicators can, in principle, be similar or even lower than using percentage speed loss, while removing some of the speed dependency detected in the percentage speed loss.

1. Background

In the maritime transport sector, the current high dependency on fossil energy brings about both environmental and economic issues. Detailed quantification of energy consumption on board (sub-metering) is therefore of utmost importance for rationally deciding on energy-saving measures, *Poulsen and Johnson (2016).*

Marine growth (biofouling) and mechanical damage generally lead to progressively rougher surfaces of the ship's hull and propeller, where roughness increases with time since last out-docking or since last underwater maintenance. Rough hull and propellers lead to increased hull resistance and decreased propulsion efficiency, respectively, meaning higher propulsion power required for reaching a given speed, *WHOI (1952), Schultz (2007),* and consequently a higher fuel consumption for the same transport work (tonnes fuel / tonne-mile). Methods for quantifying this effect range from diving inspections or simple speed criteria, *NSTM (2006), Schultz et al. (2011)*, to more advanced performance monitoring approaches, *Andersen et al. (2005), Munk et al. (2009), Pedersen (2015), ISO (2016).*

In a performance monitoring approach, the International Standard ISO 19030:2016 provides the first attempt at raising the transparency and quality of performance monitoring regarding changes in hull and propeller roughness condition. The methods described in the standard enable to compare the performance of a given vessel to itself at different periods in time (ISO 2016).

In ISO 19030:2016, the hull and propeller performance at any given point in time is termed 'performance value', corresponding to percentage speed loss V_{diff} between the measured speed V_m (rough hull) and the expected speed V_e (smooth hull):

$$V_{diff} = 100\frac{V_m - V_e}{V_e} \tag{1}$$

Speed V_e is obtained from reading a reference power-speed curve, as exemplified in Fig.1, corresponding to the expected speed at the *measured* delivered power, P_m. Finally, the difference between time-averages of performance values V_{diff}, i.e. between an evaluation period and a reference period, is termed a 'performance indicator', which can be calculated when evaluating dry-docking maintenance (comparison between two out-docking conditions), in-service performance, underwater maintenance effect, or even as a maintenance trigger, *ISO (2016).*

Alternatively to the speed-loss perspective, one can think of deteriorated performance in terms of power increase (in Fig.1, $P_m - P_e$). Thus, the delivered power required for reaching a given speed V_m will be higher for the rough hull/propeller P_m compared to the smooth hull P_e, since a rough hull is associated with a higher towing resistance R_T, and a rough propeller leads to decreased propulsive efficiency η_D

compared to the smooth hull/propeller reference, where the delivered power is given by *ISO (2016)*:

$$P = \frac{R_T V}{\eta_D} \tag{2}$$

For a smooth hull, the towing resistance R_T (calm water resistance) can be further decomposed into viscous resistance $(1+K)R_F$, residuary resistance R_R, and air resistance R_A, *ITTC (2014):*

$$R_T = (1+K)R_F + R_R + R_A \tag{3}$$

R_F is the flat-plate frictional resistance and K is a form factor accounting for hydrodynamic differences between a flat plate and the hull. The residuary resistance R_R is mostly composed of wave-making resistance, as determined from model-scale resistance tests, *ITTC (2014)*. Each resistance component is a function of speed, where it is well-known that wave-making resistance eventually overcomes the viscous component at higher speeds, *WHOI (1952), Larsson and Raven (2010)*. Now, since hull roughness is usually assumed to only affect the viscous component of resistance - in contradiction with this traditional view, recent viscous simulations by *Demirel et al. (2017)* suggest a negative effect of hull roughness on wave-making resistance - *WHOI (1952), Schultz (2007)*), which is predominant at lower speeds, a given hull roughness should result in a higher percentage penalty at lower speeds compared to higher speeds, as already pointed out earlier by *Bertram (2017)*. This can potentially create scatter in the performance data, in case of a vessel with varying speed operational profile.

In addition to the above reasoning for a speed-dependency in percentage penalties, there is a still more obvious reason for such dependency, which however makes it difficult in practice to clearly identify which mechanism contributes most to speed-dependency. In fact, V_{diff} is, by definition (Eq.(1)), a linear function of the measured speed V_m. By rearranging Eq.(1), one finds the slope and intercept for this linear relation:

$$V_{diff} = \left(\frac{100}{V_e}\right) V_m - 100 \tag{4}$$

Thus, according to Eq.(4), once $V_m \neq V_e$ (this should be true for most cases, allowing however for measurement errors in the rough-hull speed V_m and uncertainties in the smooth-hull speed V_e), all data points obtained for approximately the same delivered power and loading conditions (draft and trim) should fall on the same line, with slope $100/V_e$ and intercept $V_{diff}(V_m = 0) = -100$, meaning a perfect correlation between V_{diff} and V_m would be obtained for constant loading and powering conditions. However, since loading and powering conditions do change, and consequently V_e does change, a perfect correlation between V_{diff} and V_m is not expected, due to changes in the slope $100/V_e$, in Eq.(4).

From the above, it becomes clear that hull and propeller performance for a vessel that operates within a given range of speeds will present speed-dependency when using a performance value such as the percentage speed loss V_{diff} (Eq.(1)), as used in ISO 19030:2016. The current paper thus proposes an alternative performance value, which is based on the Granville method, *Schultz (2007),* and the concept of equivalent sand roughness height k_s, *Bradshaw (2000),* as described in more detail in the next section.

In short, the equivalent sand roughness height, k_s is a hydraulic roughness parameter that serves as "common currency" in translating the hydrodynamic effects caused by disparate roughness types (different roughness geometries) in the fully-rough regime, *Bradshaw (2000)*. More specifically, it corresponds to the equivalent sand grain size that collapses the roughness function ΔU^+ to the fully-rough regime data obtained by *Nikuradse (1933)* for uniform sand grains, *Bradshaw (2000)*. In boundary layer flow over a flat plate, ΔU^+ corresponds to the downward shift in the logarithmic region of the velocity profile, as caused by wall roughness. The equivalent roughness height k_s can only be determined for any given random roughness geometry by means of experimental measurements that quantify roughness effects on the flow or, in some cases, by relying on scaling correlations for known types of roughness (e.g. *Schultz (2004)* for barnacles). The roughness parameter k_s is extensively used in CFD (Computational Fluid Dynamics) in different engineering applications, and it is also used as an input to the Granville scaling method, the later enabling to scale-up friction results to the full-scale ship, using Granville's similarity law scaling, which assumes that hull roughness only affects the flat-plate frictional component of resistance, *Schultz (2007)*. Thus, using the concept of equivalent sand roughness height and the Granville method (faster than CFD), it is possible to translate a certain hull-and-propeller penalty $\Delta P(V_m) = P_m - P_e$, Fig.1, into an average roughness height, the equivalent sand grain size. This approach is similar to what Bertram referred to as the "hydrodynamic model to end all hydrodynamic models", *Bertram (2017)*. Finally, even though such roughness height does not correspond to a physical height on either hull or propeller, it can be shown to be theoretically independent from speed. Also, it enables setting up calculations on operational scenarios different from those in which the measurements originally took place.

In this paper, the newly proposed performance value k_s is compared to the ISO-standard performance value V_{diff}, by applying both performance values to voyage data from a Panamax tanker (noon reports).

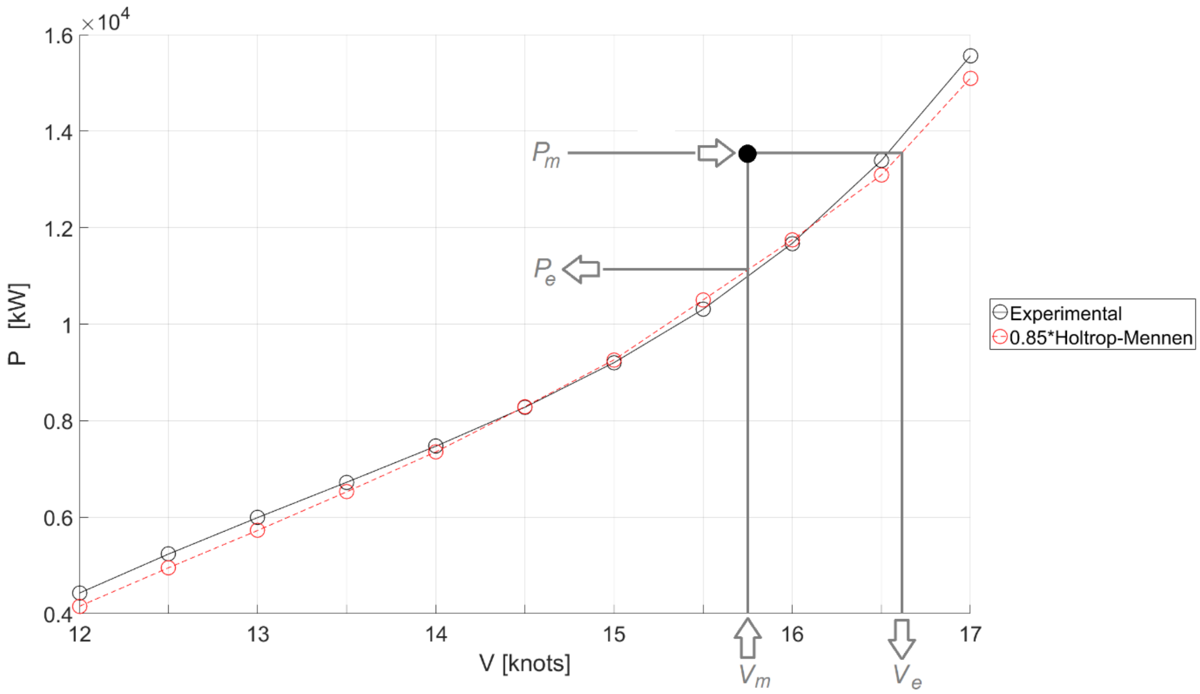

Fig.1: Reference power-speed curve for Panamax tanker from towing tank results (Brodarski Institut, Zagreb) and from Holtrop-Mennen method, *Holtrop and Mennen (1982)*, multiplied by factor of 0.85, with definitions of measured speed V_m, measured delivered power P_m, expected speed V_e and expected delivered power P_e for an arbitrary rough-hull operation point (filled circle). Direction of the arrows indicates which results are extracted or serve as input to the power-speed curve. Conditions: L_{WL} = 222.96 m, $T_F = T_A$ = 12.20 m (zero trim), ρ = 1027 kg/m^3, ν = 1.3604×10^{-6} m^2/s.

2. Materials and Methods

2.1. Data set and external data

Noon reports were kindly provided by a collaborating shipping company for a Panamax tanker (L_{PP} = 220.00 m, B = 32.25 m, C_B = 0.85, year built 2008), spanning more than 3.5 years, from Jan 1 2014 to Sept 6 2017. The noon reports had been compiled in Excel format, containing the following fields:

voyage number, port of departure, port of arrival, laden/ballast, cargo amount [mt], voyage orders (speed, main engine consumption and auxiliary engine consumption), date, draft (fore and aft), sea state (International scale 1-9), wave direction (8 quadrants), wind direction (8 quadrants), wind force (Beaufort scale), steaming time, logged distance, ground distance, average rotations per minute (RPM), average propeller pitch, average shaft power, fuel consumption [mt/d] (main engine, auxiliary engine and boiler, separately), vessel remarks, and in/out-of-performance codes for charterers. A Self-Polishing Copolymer (SPC) anti-fouling paint had been applied in the last dry-docking.

Additionally, external data was provided by the shipping company, in form of hydrostatic tables (displacement as a function of draft and trim) and towing-tank experimental results from resistance, open-water and self-propulsion tests, for the same Panamax tanker (Brodarski Institut, Zagreb). From the later experimental results, full-scale power P and propulsive efficiency η_D were used, for a range of speed 12 – 17 knots, at steps of 0.5 knots (Fig.1). It should be noted that only a single power-speed curve is currently available, corresponding to draft T_F = T_A = 12.20 m (zero trim). Since a single reference curve does not provide sufficient accuracy for comparison with operational conditions (e.g. in the dataset, average draft varied in the range 7 – 14 m), power-speed curves for other draft conditions were obtained using the Holtrop-Mennen approximate power prediction method, relying on the following procedure:

(1) full-scale conditions corresponding to the towing-tank tests were used as input to the Holtrop-Mennen method,
(2) towing resistance R_T obtained from step 1 was converted to P using Eq.(2) and assuming the same η_D values obtained from towing tank results,
(3) a factor of 0.85 was found to be appropriate for matching the results from step 2 to the experimental power-speed curve, Fig.1, and
(4) the Holtrop-Mennen method was finally used in obtaining power-speed curves for the same loading conditions as in voyage data. This procedure was deemed sufficiently accurate for the current demonstrative purpose.

2.2. Diving inspection reports

In addition to noon reports and external data, information on underwater maintenance was available for the same tanker during the sampled period, totalling seven cleaning events (hull brushing and propeller polishing). Underwater photographs, before and after the cleanings, as well as written reports from the diving companies, were also available for the last five cleaning events. From the divers' reports, it was possible to obtain an approximate estimation of the power penalty due to biofouling, using the diver's visual evaluation of type of fouling, estimated height and percentage cover. These results were used for comparison with performance values calculated from voyage data, as further detailed in the subchapter 2.5.

2.3. Performance Value I – Percentage speed loss, V_{diff}

For determining percentage speed loss, a procedure based on ISO 19030:2016 – Part 3 (alternative methods) was adopted, with the following relevant remarks. As referred above, the frequency of the data is daily (noon reports), and primary parameters of speed and shaft power therefore correspond to average values over the corresponding period of 24 hours. Manual logging probably introduces human error and reduces the amount of available data, especially considering that filtering for strong wind conditions is applied (data points with relative wind > Bft 4 were excluded from the dataset). Also, due to low frequency of the data, it was not possible to create 10-min blocks for validation purposes, *ISO (2016)* – Part 2. Finally, other variables were not available from the noon reports: rudder angle, water depth (only available as a remark from the watch officer for shallow waters, defined as depth <20 m), seawater temperature (assumed as 10°C), ambient air temperature, and atmospheric pressure, neither were available. Thus, the dataset was simply filtered for low wind conditions, no corrections for wind resistance were introduced at the current stage (wind resistance coefficients were not available at the time of writing), and the difference between measured speed V_m (logged miles divided by steaming time) and expected speed V_e (derived from average shaft power and power-speed curve corrected for operational conditions) were finally used in calculating V_{diff}, according to Eq.(1).

2.4. Performance Value II – Percentage power increase, P_{diff}

Referring to Fig.1, an equivalent alternative to determining a change in speed for a constant delivered power, P_m, corresponds to determining the increase in delivered power for measured speed, V_m. The formula used for calculating the increase in delivered power was then:

$$P_{diff} = 100\frac{P_m - P_e}{P_e} = 100\frac{\Delta P}{P_e} \tag{5}$$

2.5. Performance Value III – Equivalent sand roughness height, k_s

For determining the performance value proposed in this paper, i.e. the equivalent sand roughness height k_s, an iterative procedure was adopted, as illustrated in Fig.2.

The first part of the procedure is similar to the one described above for P_{diff}, where the increase in delivered power ΔP is determined from the comparison between measured P_m and expected P_e (Fig.1) for any given point in time (data point). Further steps are then required in order to find a k_s value through an iterative routine, as explained next.

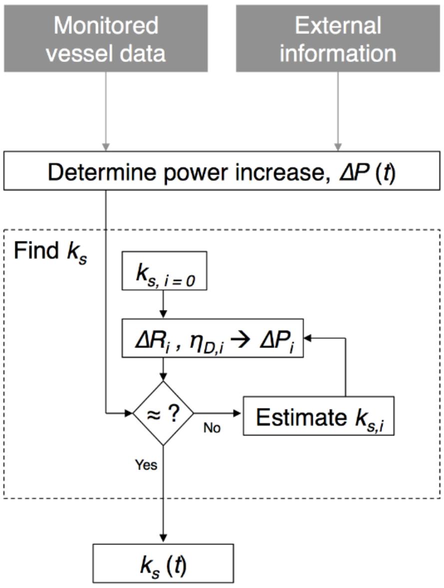

Fig.2: Iterative procedure used for determining the equivalent sand roughness height, k_s

The iterative routine schematized in Fig.2 was implemented in Matlab. For each data point in the dataset, the "Find k_s" routine starts with a reasonable first guess $k_{s,i=0}$, which serves as input to the Granville method (Schultz 2007), enabling to determine the change in towing resistance ΔR_i associated with that value of $k_{s,i}$, taking also into account all available operational conditions for the vessel at that point in time (speed, draft, etc.). In short, the Granville method predicts the increase in resistance for a flat plate with same length and wetted surface area as the hull, used here as a model for the increase in ship resistance due to hull roughness; details on this method can be found in *Schultz (2007)*. This step introduces model uncertainties, as also discussed below in this paper. Then, ΔR_i is converted to increased delivered power ΔP_i by taking into account the propulsive efficiency η_D. Presently, the propulsive efficiency was assumed as independent from hull roughness, see *Svensen (1983)*, pp.49-61, and therefore the same η_D experimental values were used, as obtained from the towing tank. Also, the propeller roughness is implicitly included in the final performance value, as in ISO 19030:2016 (in order to separate hull from propeller performance, accurate thrust measurements would be required). By the end of the first iteration, the obtained ΔP_i is compared to the power increase determined from the comparison between measured and expected P (from power-speed curves). A new estimate for k_s is then obtained ("Estimate $k_{s,i}$") and the routine is repeated until a certain stopping criterion is satisfied. In the current paper, a stopping criterion of <1% difference between ΔP_i and the ΔP obtained from the power-speed curve was deemed reasonable for the current demonstrative purpose. A lower tolerance would introduce lower numerical uncertainty, but would require a higher computation time (at the current tolerance level, computation takes ~0.1 s / data-point on a laptop computer).

Finally, performance values k_s obtained using the above method could be compared to values reported in the literature for different degrees of biofouling on ship hulls, Schultz (2007), Table I, and also to values of k_s determined from estimates of height and percentage cover of hard fouling (barnacles, tubeworms, etc.) reported by divers immediately before each of five underwater cleaning events performed on the current Panamax tanker. Physical height (k_t) and percentage cover reported by the divers (visual inspections) were scaled to equivalent sand roughness height k_s using the formula from *Schultz (2004)*:

$$k_s = 0.059\, k_t\, (\%\text{ Barnacle Fouling})^{1/2} \tag{6}$$

3. Results and Discussion

Results for percentage speed loss V_{diff}, based on ISO 19030:2016 – Part 3, are presented in Fig.3a for the Panamax tanker. The timeline starts at the last dry-docking and it should be noted that no data was available for the first 8.5 months after the dry-docking. Underwater maintenance (cleaning events), in the form of combined hull brushing and propeller polishing, are marked with vertical blue lines.

Despite of some scatter in the performance value, some trends can already be identified in Fig.3 (top): A generally better performance (V_{diff} closer to zero) towards the last dry-docking (t = 0) and towards the beginning of each underwater maintenance interval; an apparent increase in performance at some cleaning events (maintenance effect); and deterioration in performance when data points immediately after each cleaning event are compared, possibly indicating mechanical damage to the SPC paint.

However, when speed loss V_{diff}, in Fig.3a, is compared to the velocity profile of the vessel, Fig.3 (bottom), similar trends are observed, where V_{diff} is more negative for lower measured speed V_m. This speed-dependency, which is confirmed by plotting V_{diff} against V_m (Fig.6a, coefficient of determination R^2 = 0.721), can both be due to the linear dependency on V_m (Eq.(4), for $V_m \neq V_e$) and can also be due to the fact pointed out by *Bertram (2017)* that a higher percentage of viscous resistance occurs at lower speeds, compared to higher percentage of wave-making at higher speeds (unaffected by hull roughness), thus resulting in a higher percentage penalty at lower speeds. The same occurs for P_{diff} plotted against V_m, Fig.6c, where the same correlation between these variables is observed (R^2 = 0.721) as for V_{diff} against V_m.

If one decides to do something about the above speed-dependency of the performance value, and would avoid additional filtering of the dataset for speed, further calculation steps are required, e.g. using a procedure similar to that schematized in Fig.2, where hull roughness effects on equivalent-flat-plate friction are modelled. This leads us to the currently proposed performance value, the equivalent sand roughness height k_s, represented in Fig.4 for the same data (Panamax tanker). Qualitatively, trends in the k_s results, Fig.4, are apparently similar to those of V_{diff} , Fig.3a), though a logarithmic scale is now used for k_s (y axis) for sake of readability. Quantitatively, one should first consider whether the obtained k_s values are physically sound, which can be done by comparing these k_s values to those obtained experimentally for different types of fouling, *Schultz (2007),* Table I, and also comparing these results to the divers' reports available for the last five cleaning events.

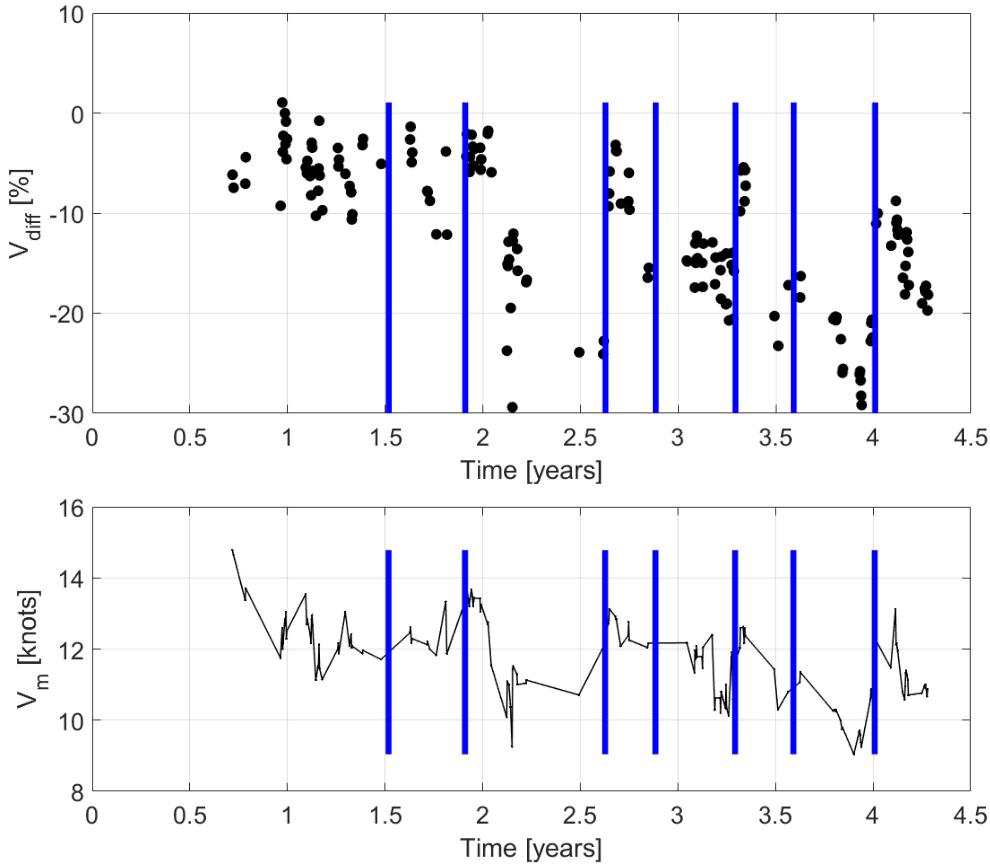

Fig.3: Percentage speed loss (V_{diff}) and measured speed (V_m) for the Panamax tanker. Vertical blue lines = cleaning events.

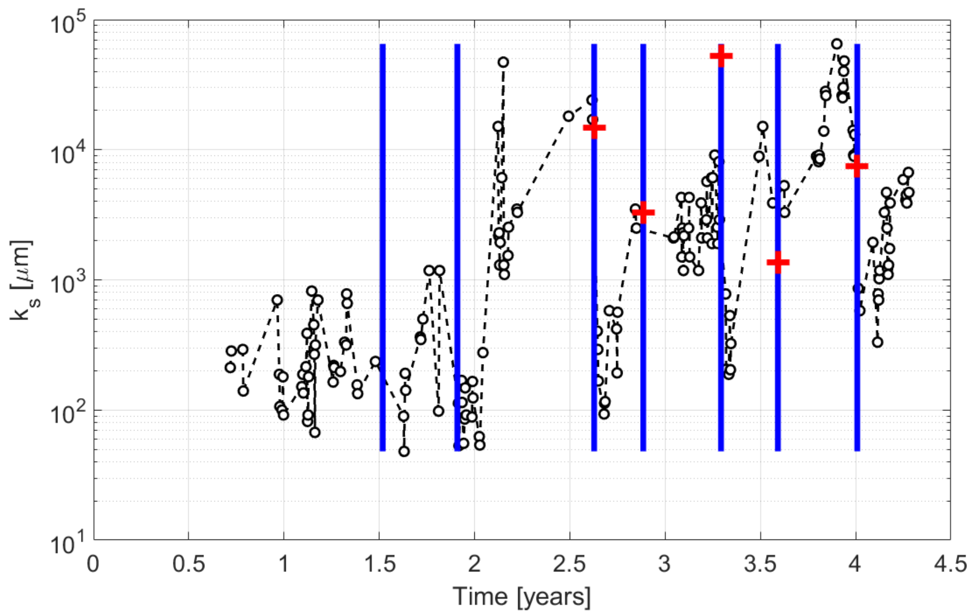

Fig.4: Equivalent sand roughness height (k_s) for the Panamax tanker. Vertical blue lines = cleaning events, Plus signs = performance values estimated from diver's reports, using Eq.(6).

Before the first cleaning event, at t ~ 1.5 years from the last dry-docking, k_s is ~60 to ~1000 µm, Fig.4. According to *Schultz (2007)*, Table I, this would correspond to a hull condition somewhere between a deteriorated coating or light slime (k_s = 100 µm) and small calcareous fouling or weed (k_s = 1,000 µm).

Cleaning event	Before cleaning	After cleaning
3rd		
4th		
5th	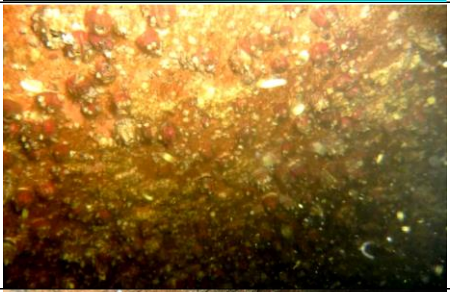	
6th		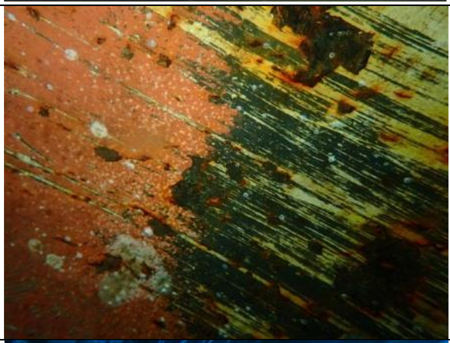
7th		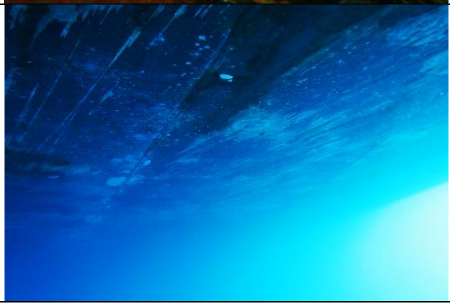

Fig.5: Representative underwater photographs of the flat bottom of the Panamax tanker, before and after each cleaning event. No scaling available, besides size of hard fouling (left), which corresponded approx. to 30 mm, 12.5 mm, 100 mm, 6.5 mm and 13 mm, for cleaning events 3rd through 7th, respectively.

Similar values are also observed between t = 1.5 and 2 years. Unfortunately no diving reports were available for this period. Later, in the maintenance interval after the second cleaning event (t ~ 1.9 years), k_s increases dramatically to >10,000 µm. Closer inspection of the voyage data revealed that the tanker had been idle for a period of ~3 months, between t = 2.18 and 2.42 years, which probably exacerbated marine growth. As a result, a hull condition of heavy calcareous fouling seems to have settled in at t ~ 2.5 years (according to *Schultz (2007),* Table I, k_s = 10,000 µm). From the second cleaning event on, i.e. t > 1.9 years, k_s resembles a saw-wave function, Fig.4, with peaks generally coinciding with data points preceding a cleaning event, which is typical of a failing/depleted SPC anti-fouling coating. Closer inspection of underwater photographs taken immediately after these cleaning events confirms that the self-polishing anti-fouling paint was depleted at some locations on the hull, since the underlying anti-corrosive paint layers, and even bare metal, can be identified, Fig.5 (right). Finally, the occurrence of heavy calcareous fouling before each cleaning is confirmed from divers' reports available for the last five cleaning events, as well as photographs taken immediately *before* cleaning events, Fig.5 (left).

The divers' reports were also used quantitatively, by translating the estimated height and percentage cover of hard fouling into equivalent sand roughness height (Eq.(6)). These k_s results are also plotted in Fig.4 (plus signs), for comparison with performance values from voyage data. Even though two out of five performance values seem to be under- and overestimated, at t = 3.3 and t = 3.6 years respectively, the performance values match quite satisfactorily with those estimated from divers' reports. It should be noted that propeller roughness was not taken into account, which would further increase the values associated with divers' reports, Fig.4 (plus signs).

The above observations seem to indicate that the obtained performance value k_s makes physical sense and correlates with observations done by divers. However, it should be noted that the current Panamax tanker was heavily fouled, making it easier to detect changes in performance. In fact, it is still a matter of debate whether an absolute performance value is achievable, considering the many uncertainties involved, *Paraeli and Krapp (2017).*

Besides the uncertainties already identified in ISO 19030:2016, such as model errors, sample size and sensor precisions (ISO 2016), the newly proposed performance value k_s comes with two additional uncertainty sources, introduced by the numerical tolerance associated with a stopping criterion in the iterative algorithm, Fig.2, and model uncertainties associated with the Granville method (roughness modelling). Of these two uncertainty sources, only the first one, associated with the numerical tolerance, can be easily quantified and minimized, although here the computation time represents a barrier: already with 1% tolerance, computation takes ~0.1 s/data-point on a laptop computer, which would mean 4.8 hours for computing one month of voyage data at an acquisition frequency of 0.07 Hz (following the default method in ISO 2016, Part 2). However, with the new performance value k_s, it is argued that precision could also increase by reducing speed-dependency, as analysed next.

Using the above results for the Panamax tanker, the ISO 19030:2016's performance value V_{diff} and the newly proposed k_s are plotted as function of measured speed, V_m, in Fig.6a and Fig.6d, respectively. As expected, a linear speed dependency is observed for V_{diff} (and P_{diff}), for which data points are fairly scattered around a linear trend, Fig.6a and Fig.6c, compared to k_s, for which a linear trend is not obvious, Fig.6d. Accordingly, V_{diff} (or P_{diff}) against V_m is associated with a higher coefficient of determination, R^2 = 0.721, for linear regression, Fig.6a and Fig.6c, compared to k_s against V_m, which scores only R^2 = 0.418, Fig.6d. The remaining speed-dependency in k_s at the lower speed range (9 – 11 knots) is probably due to speed reduction at the end of each cleaning interval, Fig.3b, either as instructed by the charterer, or due to excessive drag caused by fouling.

Looking more carefully at the speed-dependency of V_{diff}, one observes in Fig.6b that by plotting Eq.(4) with slope 100/V, where V varies from the minimum expected speed V_e (high-slope thin solid line) to the minimum V_e (low-slope thin solid line), where the dashed thick line was obtained using the average V_e value for calculating the slope 100/V, a pattern in the data stands out: groups of data points seem to lay on straight lines with intercept at the origin V_{diff} (V_m = 0) = -100. This confirms the expected linear dependency on measured speed by definition (Eq.(4)). Still, this effect cannot be separated from an eventual speed-dependency caused by a different impact of roughness at different speeds due to an increase in wave-making for higher speeds, *Bertram (2017)*.

Thus, by using k_s , and depending on the speed profile of the vessel, an improvement in precision can be expected by lowering the speed dependency, potentially compensating for introduced roughness modelling and numerical tolerance in k_s and leading to a lower overall uncertainty in the performance value k_s compared to the currently used V_{diff}. Additionally, it should be noted that the newly proposed k_s can also be used in setting up calculations on operational scenarios different from those in which the measurements took place. For example, an operator may wish to determine the required delivered power and fuel consumption for a planned voyage, under the current hull-and-propeller condition, before deciding on underwater maintenance prior to that voyage. This feature is not currently available using V_{diff} as defined in ISO 19030:2016. Future work should focus on applying the newly suggested performance value to other types of vessels, such as containerships/Ro-Ro's that operate with shorter idle periods, to evaluate to what degree the operation mode affects speed dependency.

4. Conclusions

A new hull-and-propeller performance value is proposed, which is based on applying roughness modelling (Granville method) in an iterative algorithm. This new performance value is tested with real data from a Panamax tanker (noon reports) and compared with the percentage speed loss as defined in the ISO 19030:2016 standard. Results using the new parameter show good correspondence with visual inspections by divers and show less speed-dependency compared to the standard method. Although uncertainties have not been quantified, precision can potentially increase compared to the standard. The new performance value can additionally be used for predicting fuel performance in planned voyages, enabling rational decisions on underwater maintenance.

Nomenclature

B	breadth
C_B	block coefficient
i	iteration number
k_s	equivalent sand roughness height, *Nikuradse (1933)*
k_t	height of the largest barnacles, *Schultz (2004)*
K	form factor
L_{WL}	waterline length
L_{PP}	length between perpendiculars
P	delivered power to the propeller (proxy: shaft power)
P_{diff}	percentage change in delivered power, $P_{diff} = 100\frac{P_m - P_e}{P_e}$
ΔP	change in delivered power
R_A	air resistance
R_F	flat plate frictional resistance
R_R	residuary resistance
R_T	total towing resistance
ΔR	change in towing resistance
t	time since last dry-docking
T	draft
ΔU^+	roughness function
V	ship speed
V_{diff}	percentage change in ship speed, $V_{diff} = 100\frac{V_m - V_e}{V_e}$
η_D	propulsive efficiency
ν	kinematic viscosity
ρ	density

Subscript

A	aft
e	expected
F	forward
m	measured

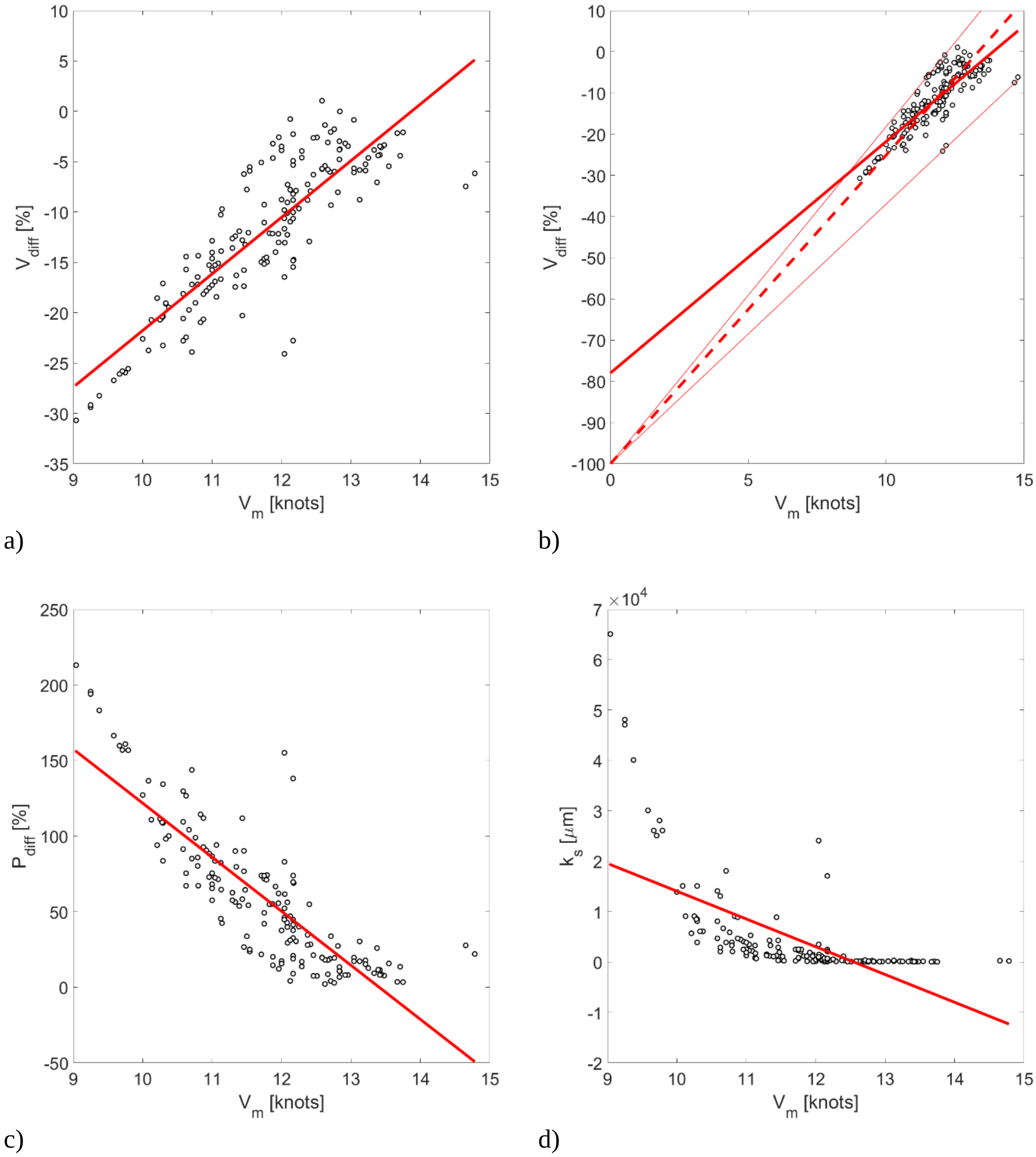

Fig.6: Performance values *versus* measured speed V_m: (a-b) percentage speed loss V_{diff}, coefficient of determination $R^2 = 0.721$, (c) percentage delivered power increase P_{diff}, $R^2 = 0.721$, (d) equivalent sand roughness height k_s, $R^2 = 0.418$. Solid thick line – linear regression; dashed thick line and solid thin lines in (b) represent Equation 4 with slope $100/V$, where V is the minimum (high-slope thin line), average (dashed thick line) or maximum expected speed V_e (low-slope thin line).

References

ANDERSEN, P.; BORROD, A.-S.; BLANCHOT, H. (2005), *Evaluation of the Service Performance of Ships*, Marine Technology 42(4), pp.177-183

BERTRAM, V. (2017), *Some Heretic Thoughts on ISO 19030*, 2nd Hull Performance & Insight Conf. (HullPIC), Ulrichshusen, pp. 4-11

BRADSHAW, P. (2000), *A note on "critical roughness height" and "transitional roughness"*, Physics of Fluids 12(6), p.1611

DEMIREL, Y.K.; TURAN, O.; INCECIK, A. (2017), *Predicting the effect of biofouling on ship resistance using CFD*, Applied Ocean Research 62, pp.100-118

HOLTROP, J.; MENNEN, G.G.J. (1982), *An approximate power prediction method*, Int. Shipbuilding Progress, 29, pp.166-170

ISO (2016), *ISO/DIS 19030: Measurement of changes in hull and propeller performance*, TC 8 Ships and marine technology

ITTC, 2014. *Recommended Procedures and Guidelines - 1978 ITTC performance prediction method*, 7.5-02-03-01.4 (Revision 03)

LARSSON, L.; RAVEN, H.C. (2010), *Decomposition of Resistance*, In: The Principles of Naval Architecture Series - Ship Resistance and Flow, SNAME

MUNK, T.; KANE, D.; YEBRA, D.M. (2009), *The effects of corrosion and fouling on the performance of ocean-going vessels: a naval architectural perspective*, In: Advances in Marine Antifouling Coatings and Technologies, Woodhead Publ.

NIKURADSE, J. (1933), *Strömungsgesetze in rauhen Rohren* [*Laws of Flow in Rough Pipes*], Forschungsheft 361 [translated as National Advisory Committee for Aeronautics, 1950, Technical Memorandum 1292], VDI Verlag

NSTM (2006), *Chapter 081 – Water-borne underwater hull cleaning of Navy ships*, Washington DC

PAERELI, S.; KRAPP, A. (2017), *Hull and Propeller Performance… On an Absolute Scale?*, 2nd Hull Performance & Insight Conference (HullPIC), Ulrichshusen, pp.282-292

PEDERSEN, B.P. (2015), *Data-driven Vessel Performance Monitoring of Ships*, PhD thesis, Technical University of Denmark

POULSEN, R.T.; JOHNSON, H., (2016). *The logic of business vs. the logic of energy management practice: Understanding the choices and effects of energy consumption monitoring systems in shipping companies*, J. Cleaner Production, 112, pp. 3785-3797

SCHULTZ, M.P. (2004), *Frictional Resistance of Antifouling Coating Systems*, J. Fluids Eng. 126(6), p.1039

SCHULTZ, M.P. (2007), *Effects of coating roughness and biofouling on ship resistance and powering*, Biofouling 23(5–6), pp. 331-341

SCHULTZ, M.P. et al. (2011), *Economic impact of biofouling on a naval surface ship*, Biofouling 27(1), pp. 87-98

SVENSEN, T.E. (1983), *A techno-economic model of ship operation with special reference to hull and propeller maintenance in the face of uncertainty* (Volume 1), PhD thesis, University of Newcastle

WHOI (1952), *Marine fouling and its prevention*, Woods Hole Oceanographic Institute, George Banta Publ.

Trim Optimization in an Operational Environment using Existing Sensor Installations

Jorinna Gunkel, Maersk Line, Copenhagen/Denmark, jorinna.gunkel@maersk.com
Jesper Dietz, Maersk Line, Copenhagen/Denmark, jesper.dietz@maersk.com
Nikolaj Purup, Maersk Line, Copenhagen/Denmark, nikolaj.purup@maersk.com

Abstract

Maersk Line is working on a fleet wide fully automated performance system using high frequency data to plan and optimize the performance of the vessels during sea and port operations. To enable new functionalities, sensor measurements need to be analyzed in detail to understand their potentials and limitations. This paper shares experiences with connecting to onboard systems by focusing on draught sensors and common problems are being illustrated. In addition, well-known concerns regarding the estimation of dynamic trim from draught sensors are discussed from Maersk Line's perspective.

1. Introduction

Digitization has found its way into the maritime industry and, as several other shipping companies, Maersk Line makes a large effort to use the new opportunities. The transformation from a manual to a data-driven performance world requires continuous sharing of learnings, the development of new competencies and procedures, and the adjustment of existing tools and mindsets. This paper aims to illustrate parts of this process by addressing one of the first steps made towards improved trim optimization on fleet level which is of special relevance for operators due to its direct link to fuel savings.

In particular, the focus is on draught sensor data from which trim can be estimated. Coming from manual data, the first step for a shipping company is to use sensors and data that are easily available. As draught sensors are installed on many Maersk Line vessels, it is natural that their capabilities are explored extensively to ensure a satisfactory trim recommendation to crew and onshore staff. The major findings of these exploratory studies are presented in this paper. The first part illustrates very practical problems that have been experienced when first connecting to vessels' onboard systems by using the example of draught sensors. It is furthermore outlined what processes are required inside the organization to obtain data of sufficient quality from sensors and considerations on corresponding output uncertainties. The second part addresses the concerns regarding the capabilities of draught sensors to capture dynamic trim correctly.

2. Status Quo: Draught and trim in the world of manual data collection

As is well known in the industry, understanding the link between trim and fuel consumption is key to unlock large savings for most ship operators. The following subsections give a high-level description of Maersk Line's current approach for trim optimization based on crew reports and the details of manual data collection to illustrate the need for new solutions.

2.1. Trim optimization in Maersk Line and operational challenges

The vessel's draft and trim condition during sea passage plays an important role on performance. Changing the trim – just by e.g. 0.5 m, while keeping the displacement of the vessel constant can change the required propulsion power significantly. i.e. from an operator's point of view, you can easily gain or waste fuel. Maersk Line is working extensively with the trim of the vessel through storage planning, voyage planning and by adjusting the trim during operation. Trim evaluation is being done based on a detailed propulsion model holding results of e.g. towing tank tests, calibrated with operational data. Fig.1 shows an example of a trim table used in operation.

Draft/Trim [m]	4.0	3.5	3.0	2.5	2.0	1.5	1.0	0.5	0.0	-0.5	-1.0	-1.5	-2.0	-2.5
14.0					15%	13%	10%	10%	9%	8%	8%	7%	5%	4%
13.5					13%	10%	7%	6%	6%	5%	4%	3%	2%	1%
13.0					11%	7%	4%	3%	3%	1%	0%	-1%	-2%	-2%
12.5					9%	5%	1%	0%	0%	-2%	-4%	-5%	-5%	-5%
12.0					6%	2%	-2%	-3%	-3%	-5%	-8%	-9%	-8%	-8%
11.5					7%	4%	0%	-1%	-2%	-3%	-5%	-6%	-7%	-7%
11.0					7%	5%	3%	2%	0%	-1%	-2%	-4%	-5%	-7%
10.5					8%	7%	6%	3%	1%	1%	0%	-2%	-4%	-6%
10.0	-1%	1%	3%	6%	8%	8%	8%	5%	3%	2%	2%	0%	-3%	-6%
9.5	4%	4%	4%	4%	4%	5%	5%	3%	1%	2%	2%	1%	-2%	-5%
9.0					1%	2%	3%	1%	-1%					
8.5					-3%	-1%	1%	-1%	-3%					
8.0									-6%					
7.5									-9%					

Fig.1: Example of trim table used in operation

The table holds the results of a towing tank test in calm water at a given vessel speed for different combinations of draft and trim. I.e. if the vessel is at even keel, mean draft of 11.0 m, a reduction of 4% on the propulsion power requirement should be expected by changing to a trim of -1.5m while keeping the same displacement. Going the other way, I.e. towards a positive trim, an increased propulsion power requirement is expected to keep the same vessel speed.

Normally, the tables are made to cover the entire operational profile of the vessel. This allows the crew onboard the vessel as well as shore personnel to get an indication of the optimal trim. However; as not all effects have been accounted for in the empirical trim table, the true optimal trim condition of the vessel could likely be different. Some effects that might lead to unreliability in a traditional empirical trim table are:

a) Uncertainties in the empirical model including, but not limited to:
    a. Extrapolations / interpolations to fill entire operational range
    b. Scaling issues.
    c. Idealization of model (hull degradation, etc.)
b) Uncertainties in data points used for calibration of the empirical model
c) Dynamic effects such as weather and currents, hull bending, squat effects, etc.

Since trim tables are calibrated based on operational data, the data quality plays an important role to optimize trim recommendations during planning and in operation.

2.2. The collection of draught and trim through manual reporting

For many ship owners, the current "State of the art" in collecting draught and trim data is manual reporting where the information is submitted to a performance system by the crew. This reporting occurs regularly during sea passage, maneuvering and in port and reflects the crew's best guess of the draught of the vessel based on different sources of draught readings.

In port, the draughts at arrival and departure are of particular importance to verify that the calculated loading condition represents the true condition of the vessel. Therefore, the officer on duty reads draught marks from the quay side before the first and after the last container movement. At this point, the ship is usually at even keel and with minimum heel, which is important as the draught readings can only be done on one side of the ship. In addition, the officer takes a sample of water to measure the water density. Due to its impact on vessel safety, this piece of information is required in the loading computer where the visual observation of the departure draught is used to verify the calculated departure condition. In addition, the information is entered in Maersk Line's performance system and into the

Captain's logbook to e.g. fulfil legal requirements. Even though human error is always a risk, this visual observation is considered a reliable measurement with an expected error of ±10 cm.

During operation at sea, the vessel draught must be reported every four hours into the Captain's logbook as well as once per day to the Maersk Line performance system. Visual observations of draught marks are usually impossible at sea, the draught can either be read from the onboard loading computer (calculation of static draught) or, if available, the draught sensors (measurement of dynamic draught). The latter is especially problematic, as crew members repeatedly state their lack of trust in draught sensor readings and their preference of loading computer calculations. In addition, the reported drafts during a voyage are more uncertain due to e.g. the dynamic nature of the vessel, bending of the hull girder and squat effects.

3. Auto-logged draught and trim from draught sensors

Draught sensors have been installed on a significant part of the Maersk Line vessels for many years which allows for measurement and transfer of high-frequent draught data. The frequency problem inherent to manual reporting is thereby solved by integrating to already available onboard systems. However, to give correct trim advice to onboard crew and staff involved in voyage planning, the behavior of the sensor must be well understood. The different learnings and experiences made within Maersk Line are outlined focusing on practical problems with draught sensors and potential shortcomings of pressure sensors in this field of application.

3.1 An introduction to draught sensors

Understanding how draught sensors work, provides essential insights into inherent sources of uncertainties, as well as sources for operational problems. The draught measuring devices onboard Maersk Line ships are different kinds of pressure sensors. Most ships use sensors following the piezo-resistive measuring principle, while some newer ships have been equipped with capacitive sensors. Depending on the specific ship and practical feasibility, these sensors are installed at some height above the baseline and measure the water column between the sensor and the water surface.

The Piezo-resistive sensors use materials that react with a change of electric resistance when being subjected to pressure. Capacitive sensors use capacitors that indicate pressure changes due to changes in electric capacity. Common for both types is that the electric signals obtained needs to be translated to a draught reading in meters. To do this correctly, the sensors and displaying software need to be calibrated before first use to define a zero-point at the specific depth of installation. In addition, this calibration is done at a certain temperature and water density. Though the impact of temperature changes on piezo-resistive materials is known and sea water temperature can generally be measured and corrected for, draught sensors encountered on Maersk Line vessels rarely have the required technology built in. Similarly, density is rarely adjusted and is in most cases assumed to be 1025 kg/m^3. These two assumptions naturally introduce some uncertainty to the measurement, as both temperature and density may vary from voyage to voyage as well as during a single voyage.

During operation, it is highly likely that the draught sensors at some point drift and that the derived draught no longer are representative for the actual draught. Three specific types of calibration problems are typically observed:

1. Due to sudden impacts of either over-pressure or under-pressure, the sensor loses its zero-calibration called zero-point drifting and all values will from that point onwards be measured with an offset.
2. Especially piezo-resistive sensors suffer from a calibration error, where the piezo-resistive material wears out over time. It usually starts giving larger electrical signals which are consequently translated to larger draughts.
3. Due to either lack of or due to faulty maintenance build-up of material on the sensor membrane causes the pressure to be measured with an offset.

From this it can be concluded that there are different sources for data quality issues on draught sensors. One source of uncertainty is caused by the measurement principles i.e. static pressure measurement and the lack of correction for temperature and density changes. Another source of uncertainty is that the sensors are exposed to a harsh environment and need to be properly maintained and calibrated by the crew.

3.2. Working with draught sensors on Maersk Line vessels

In order to use draught sensor data for optimization purposes, it is important to ensure that they are functioning properly. Their exposure to sea water indicates that certain maintenance activities are required to maintain their good shape. In the previous years, feedback from the crew regarding draught sensors has been mixed. While some crew members use them actively during operation, others report failures and data quality issues. Because high frequent data from a large number of Maersk Line vessels was made available during 2017 for onshore analysis, a study has been conducted analysing the 2017 status of draught sensors in the fleet to deduce, mainly, two kinds of learnings:

- A log of common errors and issues derived from an overview of the number of working and broken sensors respectively.
- A set of measures to improve or maintain the quality of the sensors catering for the demands of digitised performance analyses.

The findings are presented in the following subsections.

3.2.1. Status of draught sensors on Maersk Line vessels

Digitization of the fleet means that sensors that were previously less important are now suddenly being monitored closely. This means that when connecting to the vessel's data for the first time, a lot of issues surface. For the draught sensors, some of the issued identified were missing data, frozen signals and sensors that had reached the end of their lifetime. In addition to these errors, several sensors showed erratic behavior or were only able to report draught in a limited range though not frozen. Typical errors can be described as:

- **Temporarily missing data:** Instead of a draught value "NaN"/" Not available" is received as the result of a connection loss. Root cause could be a communication error between onboard system and sensor, a connection loss between ship and shore or internal errors in the onboard system.
- **Frozen signals:** The received draught information is constant, even though tiny fluctuations would be normal even in stable draught conditions.
- **Limited range signal:** The draught value is not constant but the value does not change significantly, even during on- and offloading or during trimming. This error is usually seen in comparison to the other draught sensors which show a different behaviour (see Fig.2).
- **Dead sensor:** The sensor transmits either a frozen signal or a signal with tiny deviations from the sensors minimum value. This minimum value corresponds to the height above baseline at which the sensor is installed and is usually between 6-8m.
- **Erratic behavior:** The sensor measurement is extremely unsteady and does not represent the vessel's behavior anymore

Calibration errors as mentioned in section 3.1 are to some extent seen as limited range of frozen signals. The deviation from the zero-point or a general offset due to wear-out are more difficult to capture, as they develop over time and are only visible via a comparison of all available sensors.

Fig.2 further illustrates some of these issues by a time series of draught sensor data collected between April and May 2017.

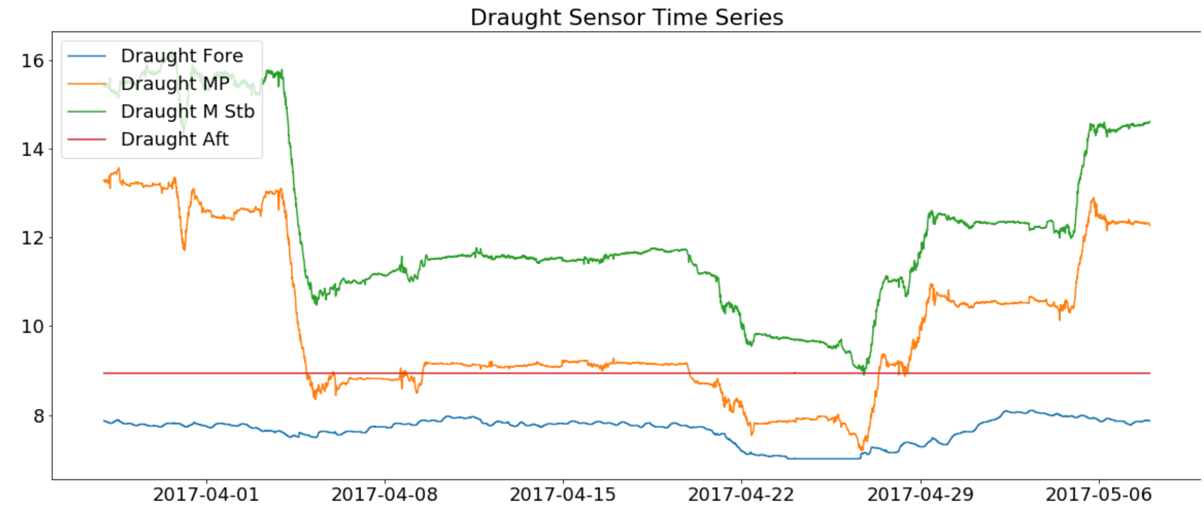

Fig.2: A typical draught sensor time series for a newly connected vessel

As Fig.2 shows, the aft draught signal is clearly frozen. The forward draught sensor does not provide accurate draught indication either, as the range of draught values is extremely limited. This assumption is supported when comparing to the reported draughts for the time period which support the general behaviour of the midship sensors instead of the forward sensor. Even though the two midship sensors seem to work normally indicating changing loading conditions, it is likely that at least one of them lost calibration, as the implied heel is often around 2 m. The manual reports for the investigation period usually lie somewhere in between the two sensor measurements which underlines this assumption. Some of these errors like frozen signals are easy to pick up and therefore, a fleet-wide investigation has been created providing a first overview of the sensor status just after connecting to the sensors. Table I presents the findings for a sample of 50 vessels between January 1st and November 1st, 2017. It should be noted that not all ships sent data during the full period but all errors below have been present for at least one day and usually significantly longer, from two days up to several months.

Table I: Overview of the number of draught sensor errors in Jan-Nov 2017 per vessel class

Type of draught sensor error	Class 1	Class 2	Class 3	Class 4	Class 5	Class 6	Class 7	Class 8	Class 9	Class 10	Class 11
Temporary missing data [%]	14	20	0	8	25	0	0	0	0	0	0
Frozen [%]	11	53	0	2	31	0	0	0	0	0	0
Limited range [%]	11	8	0	0	0	0	0	0	12.5	0	12.5
Erratic [%]	4	0	0	4	0	0	0	0	12.5	0	12.5

It is evident from Table I that there are noticeable differences between the classes. Class 2 struggles with issues on the majority of their sensors which is in line with crew reports. Other classes, such as class 4, face very few problems and on e.g. classes 3 or 6 none of the known issues are observed in the investigated period. In addition, vessel-specific analysis shows that more issues are seen on aft draught sensors than on fore draught sensors. To use draught sensor data for new trim optimization approaches, some efforts are necessary to secure a high level of data quality in the fleet.

3.2.2. Handling of draught sensor errors and failures

Resulting from the findings on the fleet-wide draught sensor state, new ways of handling the equipment and their errors need to be defined. This requires awareness of the occurrence of errors and failures and a defined set of actions to correct them.

Early detection of sensor errors and failures is therefore an essential step towards maintaining a continuous flow of high quality data. This can be achieved by a multi-layer validation chain that includes rules identifying sensor-specific errors. An example is shown in Fig.3.

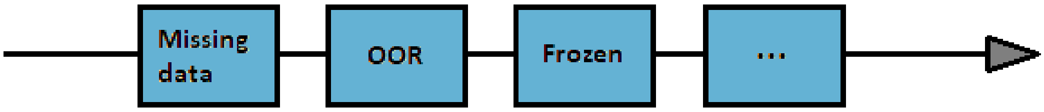

Fig.3: Schematic view of draught sensor validation flow

Detection of missing data is already available in onboard systems, as it follows from connection loss. The causes differ and include e.g. software updates or damaged cabling. In addition, an out of range check detects unrealistic measurements comparing to the vessels dimensions. For draught sensors, algorithms to detect frozen signals or erratic behaviour represent further vital validation layers.

The validation should lead to an alert that both onboard crew and shore staff can react to as required. Moreover, the system can transfer an error message to ensure that bad data is not used to deliver optimization advice.

Improving the general data quality will require improved focus from all staff and relevant procedures need to be in place which have not been necessary so far. The raised importance of sensor quality and uncertainties need to be understood, sensors need to be monitored and communication lines must be in place to enable quick reactions. Draught sensors are only few of many sensors that will have to be attended to, so the procedural perspective has a large impact on the data quality and data-driven initiatives.

3.3. Draught sensors in a dynamic environment

It is no secret that dynamic effects occurring at sea are a huge challenge for draught sensors and might entirely rule out the possibility of using the draught sensors for optimization purposes. Section 3.1 supports this concern, as the measurement principle requires a static environment. From an operator's point of view, it is important that this theoretic knowledge is reflected in the data from own vessels. Hence, Maersk Line has conducted a pilot study with the aim to better understand how draught sensors react when a vessel is sailing.

3.3.1. Introduction to Maersk Line study on static and dynamic draught sensor performance

To get an impression of the dynamic environment's impact on draught sensor measurements, the performance in the static environment needs to be known. In order to describe this baseline draught sensor performance, the measurements have to be compared to another measurement. As the study is supposed to happen on fleet level, only manually reported draughts can be used for a comparison. These are the only alternative draught measurements that are readily available. In consequence, the study presented in the following is based on two datasets, the auto-logged data that has already been used in section 3.2 and the manual reports of the same ships in the same time period.

Based on above considerations, the study can be split in two parts:

1. A comparison at departure condition sets the level of data quality that the draught sensors can achieve.

2. Based on a successful departure draught comparison, the study is extended to a comparison at sea where the vessels sail at significant forward speed.

As manually reported draughts are deemed very reliable at departure, it is natural to use this condition to define the baseline for draught sensors. The essential aspect is that the comparison has to be done at the correct timestamp. From the reports, the timestamps are known at which departure draughts have been measured, so that the corresponding auto-logged draughts can be identified. It is expected that auto-logged and manual draughts match fairly well at departure condition.

If the draught sensors perform equally well at open sea, the comparison to manual data should ideally look like the comparison at departure condition. However, the comparison between auto-logged and manual draughts at open sea is more uncertain. Apart from the investigated uncertainty in draught sensor data resulting from the vessels dynamic behaviour, the manual draughts are less reliable as they are based on static calculations. In addition, the crew does not follow one method of reporting draughts at sea and might either report an average over a couple of hours or even an instantaneous value.

Furthermore, it should be noted that the longitudinal location at which the draught sensors are installed can play a role in the comparison. Fig.4 illustrates the locations of draught marks, draught sensors and perpendiculars for one of the bigger vessels.

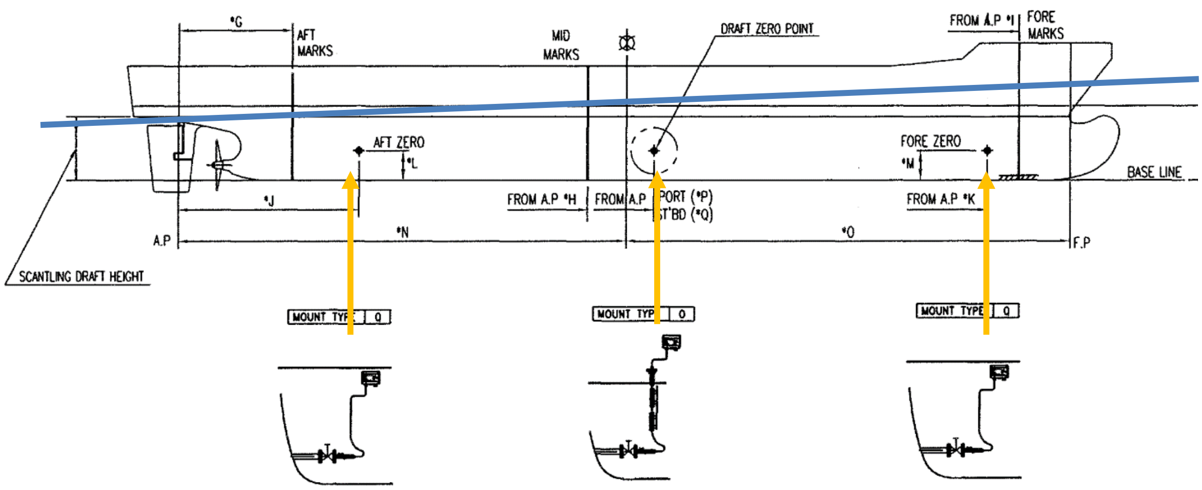

Fig.4: Example of positioning of draught sensors (yellow) and draught marks on the ship’s hull for large vessel types

The draught sensors are usually installed at relative proximity to the marks. So, even though they seem far away from each other on the sketch, they are located within a meter from each other. However, both are relatively far from the fore and aft perpendiculars. At departure condition, comparing sensor to draught mark readings is therefore relatively safe. At sea, where draught is usually reported based on loading computer information, the comparison contains noticeable differences for big ships. Most loading computers are set to calculate draught in the perpendiculars while sensors are located up to 30m away from them. In a trimmed condition (blue line), the reported and auto-logged draught cannot be identical for large ships with below installations. As most ships usually aim for negative trim (see Fig.1), the tendencies for an “at sea” comparison should be as follows: The majority of reported fore draughts should be (slightly) larger than auto-logged fore draughts. Similarly, reported aft draughts should be (slightly) smaller than auto-logged aft draughts.

Due to described limitations, the study does not aim to quantify the uncertainty within draught sensor measurements while sailing. The main goal is to get an impression whether the effects are clearly seen or not.

3.3.2. Findings of the study

The fleet level findings of the study are described by correlation plots showing the auto-logged draughts over the manual draughts for the forward and aft draught sensors which are most important in basic trim estimation. As the study considers departure and open sea condition, the results are described independently.

Fig.5 shows the correlation plots at departure condition giving an indication of how well auto-logged and manual draughts match at relatively calm and steady sea in port. It is evident seen that some of the sensors are frozen due to the horizontal lines in both plots. However, the general impression is very positive because most of the data points are grouped tightly around the diagonal. The diagonal is the indicator of perfect match between draught sensors and manual reports. Other points are indeed widely scattered around the diagonal and further analysis of these points mostly reveals that they can be linked to wrong reporting. The time at which departure draughts are reported does not match with the operational mode of the ship which has sometimes already been sailing for two or three hours. These points therefore need to be neglected. All in all, the draughts sensors operate well in port though it should be noted that the aft draught seems to perform slightly worse than the forward sensors. In addition, there is a tendency of the draught sensors to provide higher values than the manual draughts which could also be a sign for calibration problems.

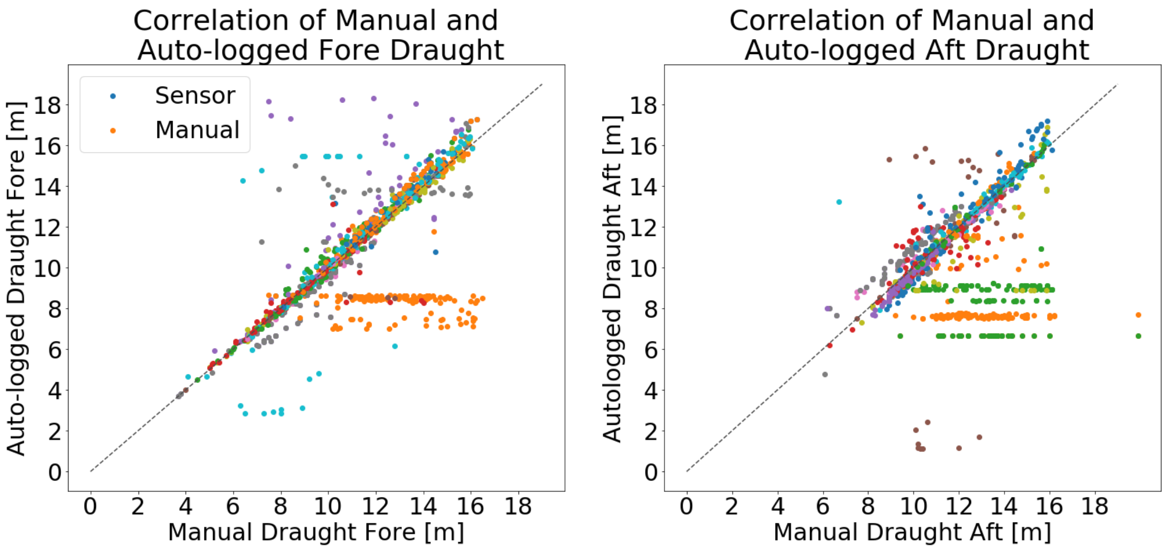

Fig.5: Departure Comparison: Correlations between manual draught (x-axis) and auto-logged draught (y-axis) for the aft draught (left) and the fore draught (right)

A similar set of plots is shown in Fig.6 representing the draught comparison while sailing. It is apparent that the data points are not as close to the diagonal as in Fig.5. In addition, the tendency of the forward draught sensors to provide high values at high draughts is even more explicit. However, it is difficult to conclude whether this wider grouping around the "perfect match" is a result of the draught sensors' incapability of capturing draught in a dynamic environment, as the manual draught is not fully reliable either. However, remembering Fig.4 and the draught sensor locations compared to draught marks and the perpendiculars, it is remarkable that the sensor measurements show such a clear tendency to increase. For the more common negative trim, the manual forward draughts should be larger than the sensor measurement, as their reference points are positioned in front of the sensors.

The comparisons shown in Fig.5 and Fig.6 have one shortcoming: They miss the link to the vessels' speed through water. The ship speed is known to have a huge influence on the pressure field around the hull, so the ability of draught sensors to capture dynamic trim must be closely linked to the speed through water (STW).

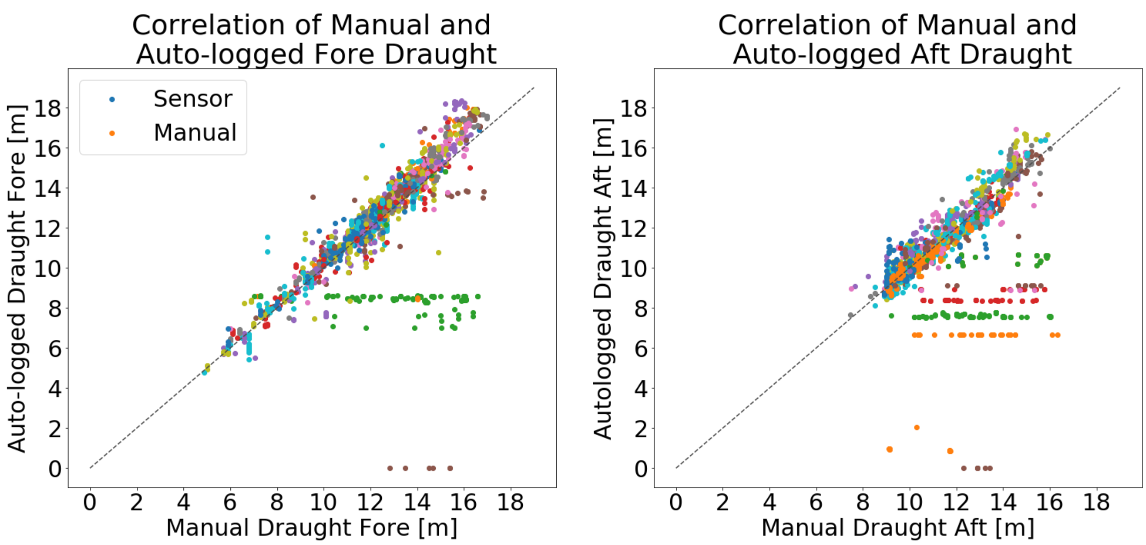

Fig.6: At Sea Comparison: Correlations between manual draught (x-axis) and auto-logged draught (y-axis) for the aft draught (left) and the fore draught (right)

Therefore, Fig.7 shows manual and auto-logged draughts over STW for class 4 (see Table I). Manually collected draughts to speed log values are seen in red while auto-logged draughts to STW are shown in blue. As sensor data is transferred every 10 minutes while manual reports are sent once a day, the number of sensor data points is significantly larger. Class 4 has been selected because it includes several ships and the integration to their onboard systems happened early in the Maersk Line's digitization process. Consequently, relatively large datasets are available for these vessels. However, few ships struggled to transfer speed information in the past which slightly reduces the number of data points used in this comparison.

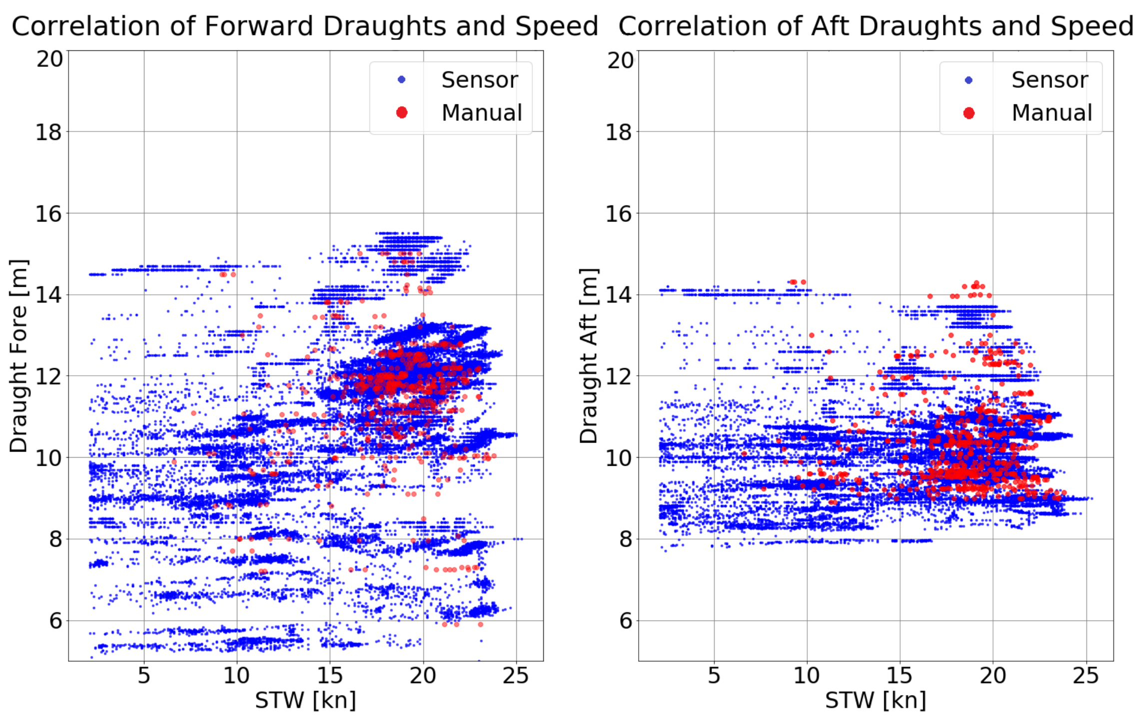

Fig.7: Auto-logged (blue) and manual (red) draughts over speed through water for one particular class 4 and their aft (left) and fore (right) draught sensors

At first sight, a slight tendency of the forward draught sensor to increase value with speed is seen by several clouds of data points moving upwards. In turn, the aft draughts show a small downward trend.

More insight is achieved by looking at individual vessels. An example for this comparison is shown in Fig.8. Again, the aft draught decreases slightly with increasing speed, though a similar tendency can be identified in manually reported draughts.

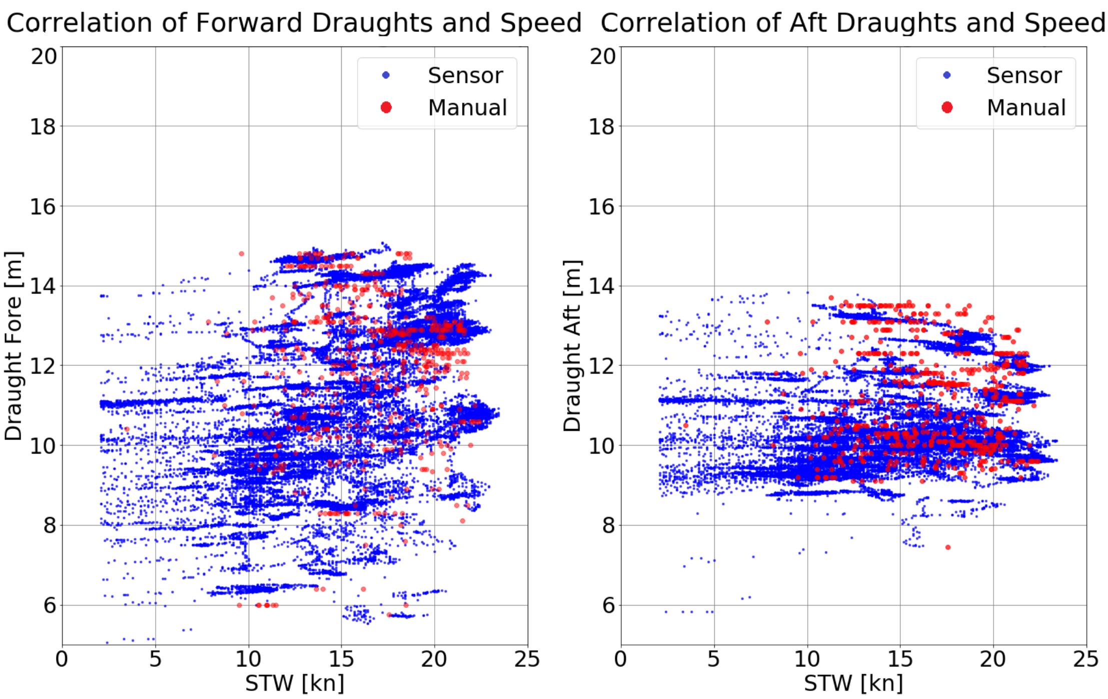

Fig.8: Auto-logged (blue) and manual (red) draughts over speed through water for one particular vessel from class 4 and her aft (left) and fore (right) draught sensors

However, it is difficult to draw definite conclusions from these investigations or yet to quantify the impact of speed and resulting dynamics on draught sensors. The upward trend may be biased by the fact that speed increase and trim increase are not separated in this plot. If the speed slightly changes speed a little while still trimming, the increase in draught sensor trim would reflect actual operations rather than the impact of STW. Consequently, much more insight could be gained by considering individual voyages to see whether draught sensor measurements rise mainly during actual trimming or also when trim is constant but STW increases. To draw meaningful conclusions from a breakdown to voyage level, manual draughts and trim are not sufficient due to their low frequency. An alternative high-frequent measure of draught and trim would be required. Inclinometers provide this alternative but they are rarely available on container vessels.

This study illustrates one of the biggest challenges for operators who can mainly rely on manually reported data to conduct analysis. For both the study on draught sensors in dynamic condition as well as the trim advice during operation, manual data can point to a direction but an accurate quantification is not possible. Above studies show that draught sensors generally perform well in static conditions e.g. at port or at low speeds. The picture is not clear when the ship speeds up and to get to accurate trim recommendation for planning and operation, the accuracy of the sensors needs to be verified and if necessary, actions must be taken to get more precise draught and trim data.

4. Discussion of draught sensors use for automated trim optimization

When the digitization process was initiated in Maersk Line, draught sensor data was the first available input to new trim optimization initiatives. A significant problem of manual draught and trim data is the low frequency, which is solved by these sensors because data can now be transferred to shore every 10 minutes. Another advantage is the ability to get readings at sea. As previous sections show, the sensors contain several sources of uncertainty, which raises new questions:

- How can reduced data quality and data loss be compensated for?
- Is it possible for the static draught sensors to give a reliable estimate of dynamic trim?

Different solutions for dynamic trim optimization are already available on the market, but most do not use the draught sensors, but data from either inclinometers, draught radars, GPS or other sources. For a large fleet of vessels, the requirement of installing additional technology can be a challenge. Several aspects must match when new technologies or systems are installed, which can mainly be categorized as technical, operational and financial aspects.

While it may pay off from a financial point of view to invest into different hardware for Maersk Line ships, a few practical problems remain unsolved. New hardware would only be installed on owned vessels which additionally need to have a certain lifetime lying ahead of them. For old or chartered ships, these investments do usually not pay off due to the short service time and due to additional costs for installation and crew training. The development and communication of new procedures and the time to create acceptance of new equipment usually take time. Maersk Line therefore prefers a solution based on sensors already available that might even be accessible on parts of the chartered fleet.

From a technical perspective, it is not yet clarified that the challenges which static draught sensors face in a dynamic environment cannot be overcome by using the available data science methods e.g. machine learning or sensor fusion. With a larger set of data points describing the environment of the vessels, a solution might be found that does not only provide a sufficiently reliable draught and trim estimate but that also creates analytical redundancy in case of sensor failure.

From an operational point of view, any solution needs to provide a stable trim estimate that represents the environment as closely as possible. Within the current setup, a certain deviation from the (unknown) true value can be accepted. The power of a data-driven trim estimate should be the capability to help the crew find and reproduce the most efficient trimmed condition in any situation to save fuel. The current approach based on manual data tries to give this advice to the crew but operational experience has shown that the available information is not sufficient to always guide the crew to the best condition.

From above study, we believe that solutions can be found to utilize the existing static draught sensors to do trim optimization without further installation of draught radars, GPS antennas, etc. The exact technical solution remains unsolved though. Maersk Line would like to invite to an open discussion about potential approaches to find a solution that is feasible from operational, technical and financial perspectives.

5. Conclusions

From Maersk Line’s perspective, draught sensors are the first choice for determining trim and giving trimming recommendation during voyage planning and execution. This paper shows that certain practical problems and general concerns affect the estimation of trim from draught sensor data. After first connecting to vessels’ onboard systems, different draught sensor problems have been identified, which need to be addressed by new procedures including data validation and increased maintenance to ensure satisfactory data quality. In general, issues as seen on draught sensors have been found on many other sensors, as the new focus on data quality changes the way sensors are handled onboard. It is therefore natural that connecting to onboard systems is only the first out of many steps to make data available for further use.

In the case of draught sensors, there are additional factors that question their usability in the intended field, the estimation of dynamic trim. As they are made for static environments, they are naturally deficient in measuring dynamic draughts. It is therefore questioned if this issue can be addressed by using data science methods or if use of different hardware is the only option. This question would best be answered by honest discussions of the different members of the industry.

Case Study: Ship Performance Evaluation by Application of Big Data

Carlos Gonzalez, Kyma, Bergen/Norway, cg@kyma.no
Bjarte Lund, Kyma, Bergen/Norway, bl@kyma.no
Erik Hagestuen, Kyma, Bergen/Norway, eh@kyma.no

Abstract

The maritime industry, in common with many other fields, is currently undergoing a rapid process of digitalization. For some companies, the addition of the required measurement, telemetry and evaluation systems to their fleet requires a level of investment and upheaval for which the tangible benefits are not immediately apparent. This paper aims to illustrate, by reference to a real-world case study, the potential benefits of implementing a big data system with a high sampling resolution (15 s, in line with ISO 19030 recommendations) on the ship performance evaluation of LNG vessels.

1. Introduction

The technological evolution is constant and cannot be stopped, the progress is inevitable, this revolution is the result of our own desire to lead a better life, as it is pointed by R.S. Amblee. Concepts like automation, machine learning, mobile computing or artificial intelligence are not utopia, they are the reality.

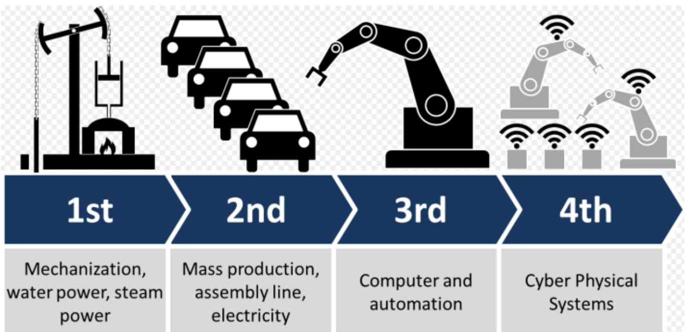

Fig.1: The technological revolution phases, http://globalblog.posco.com

Big Data is a trending term since some years ago. The industries are evolving their whole business's structures into more digitalized models. From Big Data, managers can measure, and hence know, radically more about their businesses, and directly translate that knowledge into improved decision making and performance, *McAfee and Brynjolfsson (2015)*. Big Data seeks to glean intelligence from data and translate that into business advantage. In the words of Lord Kelvin "To measure is to know. If you cannot measure it, you cannot improve it". Big Data is based on the below keywords, *Lund et al. (2017)*:

- *Volume:* The quantity of generated and stored data. The size of the data sets determines the value and potential insight- and whether it can be considered as Big Data or not.
- *Variety:* The type and nature of the data. This helps people who analyse the data sets to effectively use the resulting insights.
- *Velocity:* In this context, it is the speed at which the data is generated and processed (frequency) to meet the demands and challenges that lie in the path of growth and development.
- *Variability:* Inconsistency of the data sets can hamper the processes to handle and manage it.
- *Veracity:* The quality of captured data can vary greatly, affecting the possibility to accurate analysis

It is straightforward to see that the term "Big Data" is worldwide spread and a very attractive topic to talk about. However, for businesses, implementing something like a big data strategy must be more than attractive: it must be practical, https://www.forbes.com/sites/bernardmarr/2016/08/25/the-most-practical-big-data-use-cases-of-2016/#340a6bd43162.

Usually the main goal for most organizations is to enhance customer experience, cost reduction, better targeted marketing and improvement of the operational performance.

Most of the business fields are investing resources (financial and human) to restructure their companies to be in line with the digital revolution of our age. There are several examples showing the benefits and potential advantages of using Big Data within diverse businesses and for different applications. For example, Big Data is being used for Preventive Maintenance and Support being able of getting benefits to improve equipment maintenance. As the Industrial Internet of Things (IoT) begins to become a reality, factories and other facilities that use expensive equipment are deploying sensors that can monitor that equipment and transmit relevant data over the Internet. They then use big data solutions to analyse that information — often in real time — to detect when a problem is about to occur. They can then perform preventive maintenance that may help prevent accidents or costly line shutdowns, https://www.datamation.com/big-data/big-data-use-cases.html. Another quite popular usage and one of the most well-known application of Big Data is the recommendation engine. When you are watching a movie at *Netflix* or shopping for products from Amazon, you probably now take it for granted that the website will suggest similar items that you might enjoy. Of course, the ability to offer those recommendations arises from the use of Big Data analytics to analyse historical data. These recommendation engines have become so commonplace on the Web that many customers now expect them when they are shopping online. And organizations that haven't taken advantage of their big data in this way may lose customers to competitors or may lose out on upsell or cross-sell opportunities, https://www.datamation.com/big-data/big-data-use-cases.html.

The shipping industry is not different than the other industries, while it is true that the shipping industry is more conservative than other industries, so the digital revolution and Big Data concept is being adopted more slowly.

In recent years, several studies have been carried out within the maritime industry about the benefits and challenges of the digitalization and high-frequency data generation for shipping companies and other players of the maritime industry. See e.g. *Aldous et al. (2015)* or *Mak et al. (2014)* where they show their research work about the benefits and challenges of using continuous ship performance monitoring systems.

Modern vessels incorporate sensors to measure and capture an extensive set of data including navigation, cargo, machinery and auxiliary systems. The sensor's quality and accuracy are continuously improved giving very high level of precision in the measurements and data transmission.

Moreover, the ship-to-shore communication and internet availability on board has been significantly improved, making it easier to transfer data from ship to shore. Before 2025, many ships, systems, and components will be linked to the Internet, making them accessible from almost any location in the world. Maritime connectivity will advance significantly, and will dramatically affect how the industry manages information, https://to2025.dnvgl.com/shipping/digitalization/.

This paper aims to illustrate, by reference to an actual case study, the potential benefits of implementing a Big Data system with a high sampling resolution (15 s, in line with ISO 19030 recommendations) on the ship performance evaluation of LNG ships, without being incompatible with any other ship type. To get sensible results on this study, Big Data have been converted into Smart data to get sensible results that can be actually used for decision-making.

2. LNG Carriers - Brief introduction to the LNG industry within the shipping

The LNG global trade is constantly increasing. For the third consecutive year, the global LNG trade set a new record reaching 258 million tons (MT) in 2016, *IGU (2017)*.

Traditionally, the LNG market has been dominated by long term charter contracts, however, since 2011, the short and medium-term LNG market has acquired more importance within the global market. In 2016, 28% of the global LNG trade was covered by short or medium-term charter contracts, *IGU (2017)*.

Moreover, the LNG spot trading - trades where cargoes are delivered within three months of the transaction date - made up 18% of total imported LNG volumes in 2016, an increase from 15% the year before. All these signs are indicating that the LNG market is experiencing an evolution to greater flexibility in the LNG trade, *GIIGNL (2017)*.

The expansion and diversification of the LNG market worldwide has introduced a higher competition level between the charters and ship owners. The number of new LNG carriers delivered over the years to cover the LNG global demand has increased significantly from the beginning of this century as it is shown in the Fig.2, http://maritime.ihs.com/.

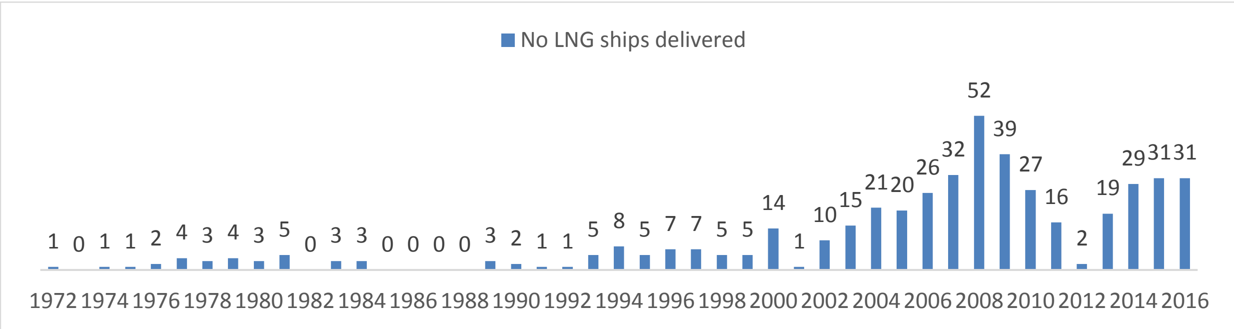

Fig.2: LNG carriers delivered, based on delivered year

Global production of LNG is forecasted to reach 292 MT in 2017, marking an increase of 34 MT from 2016, *Gas strategies (2017)*. Traditionally, the charters have signed a contract with the ship owners under the form of a Time Charter Party (TCP). The TCP specifies the guaranteed vessels maximum fuel consumption versus the transit speed under specific weather conditions (usually looking at the Beaufort scale). Even so, the greater flexibility in the LNG trade is making new strategies by some LNG tanker owners, which have joined forces and operate their ships within the sport market making a LNG carrier pool. This aims to cut the operating costs, trying to optimize the ship's operation through improved scheduled ability, cost efficiencies and common marketing, www.reuters.com/article/lng-shipping-pool/lng-ship-owners-launch-vessel-pool-to-cut-costs-in-depressed-market-idUSL5N10T1OM20150818. It is not daring to say that facing this situation, the LNG charterers will try to choose those shipping companies with higher ship efficiency, reporting in the most transparent way and with the most truthful data.

3. Data collection: Low-frequency vs High- frequency data

There is an old and recurrent dilemma for the shipping companies: Ship performance analysis based on noon to noon report (manual readings/entries by the crew) or based on SPM collecting high frequency data (automatically or semi-automatically).

The answer is not straightforward because it closely related to the individual company ethos: Some companies are very open to innovation and at the forefront of technological evolution whilst others are much more traditional and conservative in terms of adopting new technological solutions.

The major component of the operational costs for the ships is the amount of fuel oil consumed (70-80% of the operational costs). Therefore, one of the main parameters to be reported is the fuel consumption on board. This study tries to enlighten the differences between low-frequency or high-frequency data collection. In this regard, there are mainly two methods used by the shipping companies to record the fuel consumption on board:

A. Bunker Delivery notes + Tank Soundings (checking the Remaining Fuel On-Board, ROB)
B. By flow meters

Tank sounding (by gauges or manually) is common practice in the sector. Sounding frequencies on a ship, however, differ from company to company and depend on company policies and the nature of operations on board. According to Marine Insight, www.marineinsight.com/guidelines/understanding-sounding-ullage-and-frequency-of-sounding/, all fuel oil tanks lube oil tanks and diesel oil tanks must be sounded twice a day, once in the morning and once in the evening, and recorded in the event of a leak or any other emergency related to the oil content of tanks.

The accuracy of tank sounding, estimated at 2-5% (Saniship), is very sensitive and depends on the means by and conditions under which the sounding is carried out. Furthermore, larger ships have several fuel tanks, with different quantities, temperatures and fuel qualities. The accuracy of tank readings may be limited by the ship's motions, trim, etc. Manual sounding may be very inaccurate at sea, due to the ship´s movements, *IMarEST (2012).*

Another way in which inaccuracy may occur is because the tank monitoring devices, such as gauges, that need to be regularly calibrated to ensure accuracy and this may currently not always be done as there are no regulations for this, *CE Delft (2009).*

Lastly, discrepancies may exist between the tank volume determined and the actual volume consumed. Differences may exist e.g. due to sludge and water removed from the fuel (fuel treatment on-board). This may lead to a tendency to over-estimate fuel usage, *IMO (2012).*

The tank monitoring approach could be undermined in different ways:

a) Not all relevant tanks are monitored.
b) The tanks could be monitored with insufficient frequency.
c) The maintenance of the monitoring device could be insufficient.
d) The monitored data could be documented falsely.
e) The monitored data could be reported falsely.

The other approach to monitor the fuel consumption of a ship can be by means of flow meters. These meters allow for determining the amount of fuel that is flowing through the respective pipes and represent the actual fuel usage. The fuel flow is often measured directly (by volume, velocity or mass) or indirectly (inferential) by pressure. In order to monitor all the fuel oil used on-board, all input flows of to all consumers on-board would actually need to be monitored.

A wide variety of flow meters is available, such as electronic, mechanical, optical and pressure based. Electronic fuel flow meters provide an accurate and reliable method of measuring fuel consumption in marine diesel engines. Their accuracy is ±0.2%, *CE Delft (2009)*. Coriolis flow measurement technology measures the mass flow directly, eliminates the need for any mathematical conversions, and is very accurate (between 0.05 and 2%), https://www.emerson.com/documents/automation/-direct-approach-to-mass-flow-measurement-en-64236.pdf. In general, the accuracy of flow meters may vary depending on the installation, maintenance and calibration requirements of the system and on-board operator competence, *IMO (2012), IMarEST (2012).*

Another advantage of using the flow meters for continuous monitoring of fuel consumption is that that fuel flow measure is actual the real fuel consumed because the water and sludge is already removed before the flow pass through the flow meters, increasing the accuracy of the fuel readings.

Compared to the tank sounding method, fuel flow monitoring could potentially be more accurate since it measures the actual fuel consumed in the fuel combustion system. This better accuracy is favored because the flow meters send the fuel flow values constantly to the data collector system making possible the analysis of the fuel oil consumption at any time and instantly.

The flow meter monitoring approach could be undermined in different ways:

a) Not all relevant flows are monitored.
b) The flow meter could not continuously register the fuel flows.
c) The monitored data could be documented falsely.
d) The monitored data could be reported falsely
e) The flow meters could not be calibrated properly

This is indicating that in case of having the lowest accuracy, the automatic and continuous recording (flow meter) would provide a higher accuracy than the manual recording (tank sounding, human measurement), 2% error against 5% error by tank sounding, according with the mentioned above.

Human error can happen at any measurements and at any time if the report completion is not automated. Other issue that may occur when the data collection and reporting is not made automatically is the difficulty of doing the data entries at same time every day, this may cause inaccurate information, for example for distance sailed daily, total revolution per day, etc.

The shipping companies are using the fuel oil consumption records for optimize their fleet and in commercial discussions with different stakeholders (mainly the charters). Hence, the fuel consumption shall be corrected based on the environmental conditions which are affecting the ship performance, it can also be intuitive that the ambient data is of vital importance in the ship efficiency analysis.

However, within the shipping industry, the noon reports are still the predominant way of tracking the ship performance. The noon reports may include weather data, such as wind direction, wind force, sea and swell condition. They are general values, taken at the time of report preparation. As we all know, weather can change significantly during a day. An instant value of the wind speed at noontime might vary significantly from the actual wind speed experienced during the rest of 24 hours, indicating that the average values from noon reports might be useless, www.linkedin.com/pulse/why-noon-reports-do-work-assessment-fuel-efficiency-dan-veen/?trackingId=NXlXekbts6T0LJT0ApQD7A%3D%3D.

The environmental conditions are associated with great uncertainty if they are not collected from sensors, i.e. the Beaufort number, are associated with a large degree of aleatory error which is exacerbated by the low resolution of the Beaufort scale itself and therefore rounding errors when converting from wind speed, *Aldous et al. (2013*)

Therefore, low data frequency used on the noon reports may lead to incorrect daily average values being recorded, particularly for environmental parameters and ship speed where effect on fuel consumption of accelerations/decelerations and ship maneuverings cannot be captured or even reported, *Aldous et al. (2013).*

4. Method and data used on this study

The goal of this paper is to show the benefits of using Big Data, with high frequency data collection, on the ship performance analysis, the following examples are taken from LNG carriers. The data have been recorded by a SPM system on board the ships, which is interfaced with several sensors and data systems.

The data is received in the SPM system, and then every 15 seconds the SPM software is making a new entrance in the “Big Data database”. This database is collecting the raw data, without any filtering. This database is the one used on this study for showing the potential analysis and results that Big Data can offer for Ship Performance analysis. The data used on this study is the averaged data in periods of 15 minutes.

The ship performance evaluation is done analysing the relevant parameters for the hull performance, fuel efficiency and operational performance. The parameters considered on this case are:

- MCR profile for ballast and laden leg
- Speed Profile for ballast and laden leg
- Time spent at sea, manoeuvring and at port
- Fuel consumptions and CO_2 emissions associated
- Weather conditions
- Hotel Load and energy used for auxiliary systems
- Steam dump – waste of energy
- Comparison with Time Charter reference (Fuel vs Speed)

The ship performance analysis is done by comparing the performance of two sister ships for the same voyage, including one leg in ballast and another in laden condition.

5. Case study

As it has been mentioned, this study is focused on the ship performance analysis on LNG carriers by applying the high frequency data collected on board. The LNG Carriers are one of the ship types more advanced within the maritime industry due to the sophisticate and numerous telemetry available on board, which is making easier the possibility of generating big data on board with high levels of precision for further analysis. It has been adopted some assumptions for the time spent at sea, manoeuvring and at port, it has been considered one assumption for "manoeuvring mode", which is when the ship changes her speed profile just before the ship is berthed as shown in Fig.3.

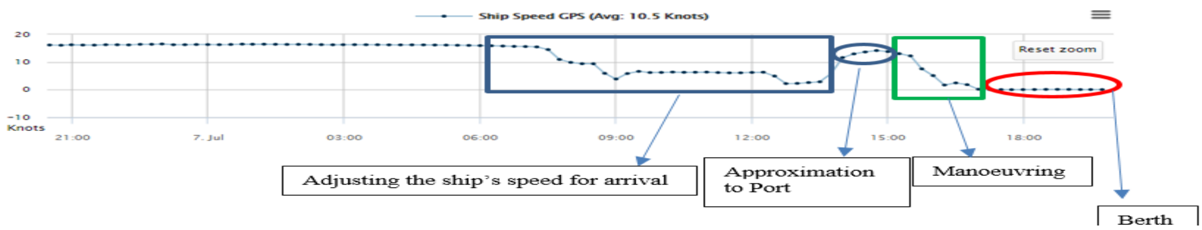

Fig.3: Phases pre-post ship's manoeuvring

The voyage concept is considered as a round trip (2 legs, one in laden and one in ballast). Therefore, the voyage's events considered are:

Sailing (laden) ⟶ Manoeuvring ⟶ Berth ⟶ Manoeuvring ⟶ Sailing (ballast)

The time spent at "anchorage" has been considered as sailing time on this study.

5.1. Vessel's particulars

The ships selected for this study are described in Table I. These two LNG carriers are using two types of fuel on board, HFO and the Boil-Off Gas (BOG) from cargo tanks. The fuels are consumed by the main boilers, where is generated the superheated steam which is led to the main turbine (and other systems). The main turbine is connected to the propeller shaft through a gearbox.

Table I: Vessel's particulars

Vessel No.	Propulsion System	Power delivered at MCR (kW)	RPM at MCR (rev)	DWT (Tons)	Cargo capacity (m^3)
#1	ST	24161	86	83068	142988
#2	ST	24161	86	83160	142988

ST: Steam Turbine

5.2. Ship Performance Analysis

The first of this analysis is referring to the comparison between sister ships (vessel number 1 and 2) which are doing the same voyage. The voyage analysed for the two sister ships have the below details:

Table II: Voyage details

Departure Port	Arrival Port	Cargo condition	Distance
Bonny	Bahia Blanca	Laden	4645 nm
Bahia Blanca	Bonny	Ballast	4645 nm

The two sister ships did the same voyage within the second and third quarter of 2017. The Maximum Continuous Rate (MCR) operated by the vessel has a great impact on the fuel consumption and of course, in the speed profile. All the propulsions system has an optimum operational point where the amount of fuel needed to develop a kilowatt is the minimum, therefore, that is the area where the ships should be operated to keep the fuel efficiency as high as possible. The vessels did the same voyage with the below operational profiles (MCR level) shown on Fig.4.

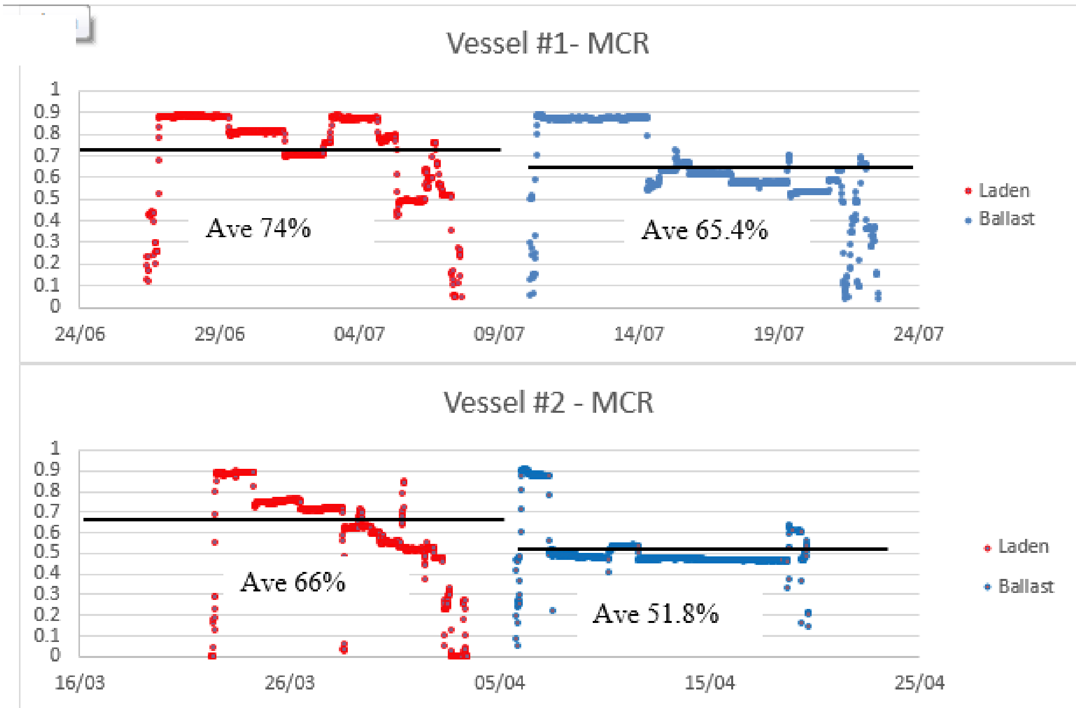

Fig.4: Operational profile for the ships during the whole voyage

Vessel #1 is operated with MCR levels steady for short periods; she kept the same behaviour on both legs despite different average MCR for each leg (it is normal to sail one leg laden and one leg on ballast). However, vessel #2 has different behaviour for the laden leg, having declining trend in the MCR selected, starting on 90% and finishing the voyage around 40% of MCR, which doesn´t seem to be the most efficient operation. The most optimal fuel consumption is commonly reached between 70-85% MCR. Having said that, vessel #1 sailed at average MCR of 74% for the laden leg and 65.4% for the ballast leg. While vessel #2 sailed at average MCR of 66% and 51.8% for laden and ballast, respectively.

Table III: Comparison of the operational profile of these two ships at sea and during manoeuvring

Vessel	Average MCR Sailing Laden	Average MCR Sailing Ballast	Average MCR Manoeuvring Laden	Average MCR Manoeuvring Ballast
#1	74%	65.4%	7.14 %	6.13%
#2	66%	51.8%	6.93%	11.2%

The ship´s MCR will impact the ship's speed, because the Speed-Power relation. Both ships are being operated on Time Charter by the same charter, and they are being analysed for the same voyage. Therefore, it would be normal to think that both ships should receive the same voyage instructions regarding the speed profiles**.** However, as it is shown in the Fig.4 and it is corroborated in the Fig.5, the ships are being operated with very different profiles.

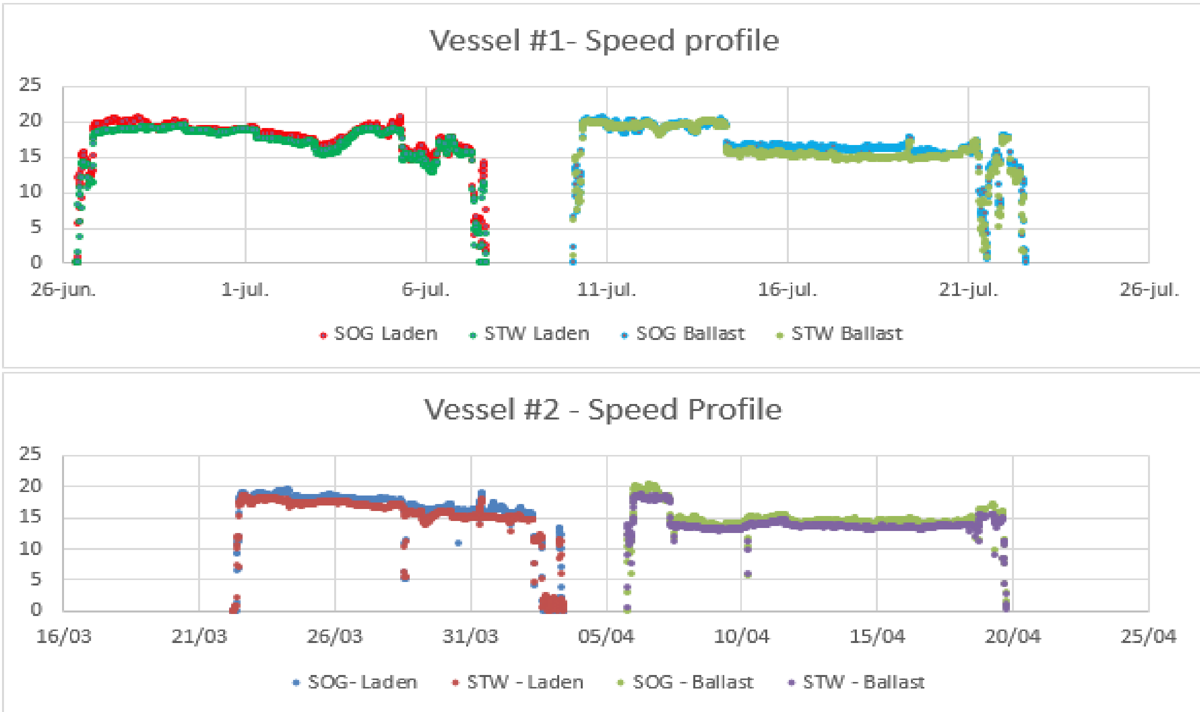

Fig.5: Speed Profile

There are some differences between the ship through the water and the speed over ground as it is shown in Table IV. The difference between both speeds is an indicator of the sea current effect, guessing that the Speed Log instrument and the GPS are well calibrated. The difference between the SOG and STW is constant for both ships, being higher the SOG than the STW for both legs. So the effect on the ship performance evaluation for this two ships is omitted.

Table IV: Comparison of averaged speed through the water and over ground for both ships

Vessel	Average SOG-Laden (knots)	Average STW-Laden (knots)	Average SOG-Ballast (knots)	Average STW-Ballast (knots)
#1	17.65	17.00	16.70	16.09
#2	15.88	15.15	14.80	13.98

The speed profile will impact on the voyage time, as it is expected because the sailing distance is the same, but the speed profile is different. Vessel #1 does the trip in less time than vessel#2. There is a difference on the voyage time spent by these two ships, mainly because the different speed profiles developed. The time spent by the ships during the different voyage events is shown in the Fig.6.

Vessel #2 spent two extra days than vessel #1 for the same voyage. It means that in the hypothetical situation that these two ships were only sailing on this route, vessel #1 could do 14 voyages per year and vessel #2 13 voyages per year.

Based on the data collected from the mass flow meters installed on board the two ships, the ships consumed the amount of fuel and gas described in Table VI.

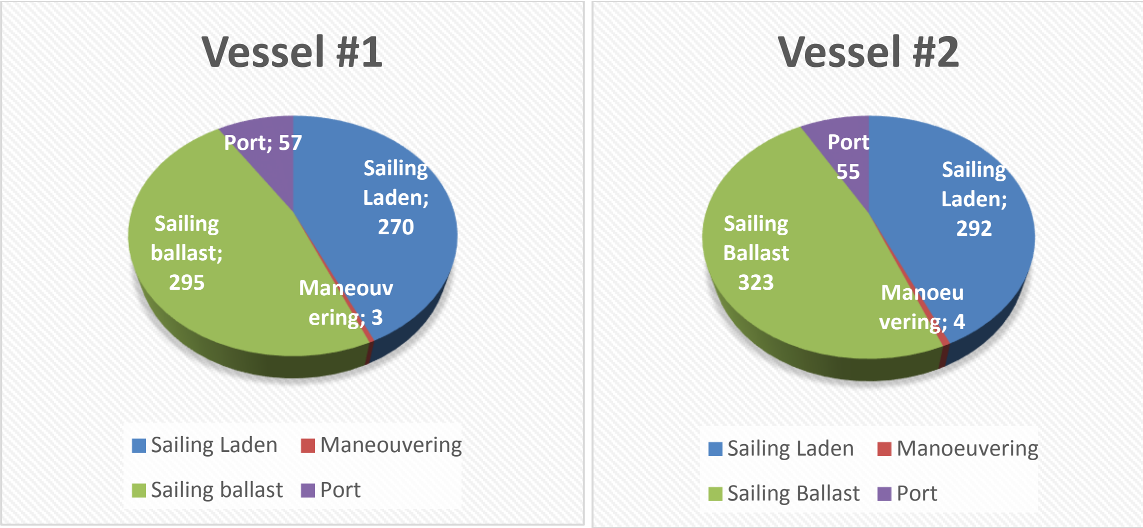

Fig.6: Voyage Time distribution (hours)

Table V: Voyage time comparison

Vessel	Time at sea (h)	Time Manoeuvring (h)	Time at Port (h)	Total Voyage time (h)	Voyage days
#1	565.25	2.75	56.75	624.75	26.03
#2	615.25	4.25	55.25	674.75	28.11

Table VI: Fuel consumption (MT) and CO_2 emissions

Vessel	HFO (MT)	BOG (MT)	FOE (MT)	CO2 emissions (MT)	TCO2/nautical mile*
#1	294.9	2687.3	3532.9	8308.4	0.894
#2	105.2	2722.1	3619.8	7813.9	0.841

*Using the distance according the Table II

The main fuel consumer on LNG Carriers with steam plant as propulsion system are the main boilers, which are the steam generators to feed the steam plant. This superheated steam goes to the Main turbine, Feed pumps, Turbo generators and also, the excess of steam is dumped to the main condenser. The turbo generators are the equipment in charge of generate the energy demanded for the hotel load and auxiliary system, so the energy demand on board, will have impact on the overall ship fuel consumption.

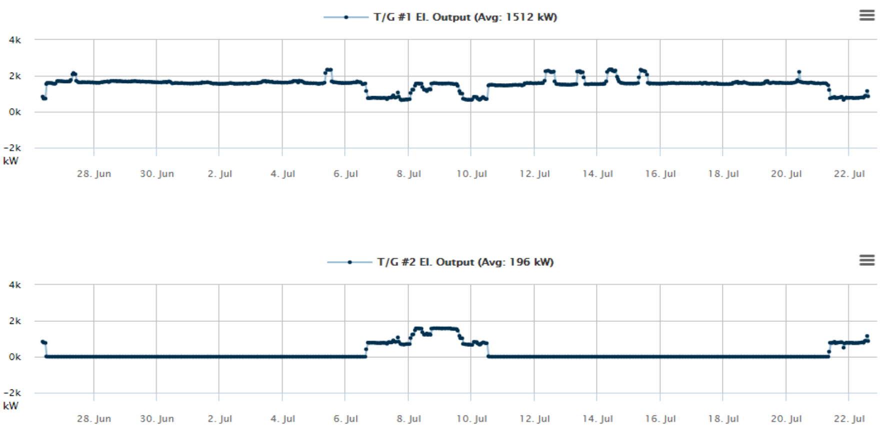

Fig.7: Turbo Generators profile for vessel #1

Vessel #1 uses one Turbo Generator (TG) to supply the required energy when the ship is sailing, and she uses two TG at port. For the whole voyage vessel #1 used 1078.1 MWh for hotel load and auxiliary systems.

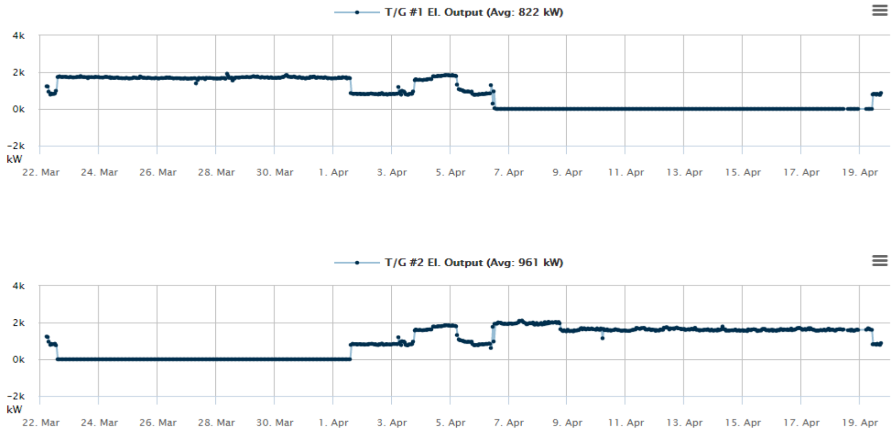

Fig.7: Turbo Generators profile for vessel #2

For the whole voyage vessel #2 used 1207 MWh for hotel load and auxiliary systems. It means that for the same voyage, vessel #2 spent 128.9 MWh more than vessel#1. This additional energy used by vessel #2 caused also an additional fuel consumption because more steam was required to produce that extra consumption.

Vessel #1 used both TG at same time for 129 hours, which means 20.6% of the voyage time. While vessel #2 used two TG simultaneously for 136 hours, being the 20.15% of the voyage time.

Other special consideration that shall be evaluated on LNG carriers is the availability and generation of Boil-Off Gas (BOG) from the cargo tanks. The LNG contained on the cargo tanks, will be naturally evaporated due to the cargo tanks get warmed during the voyage, it causes that the liquefied natural gas evaporates a certain amount of it due to the raise of the tank temperature, generating the BOG. For safety reasons, is critical to keep the tank pressure within limits, so when the BOG occurs, the tank pressure increase, so it must be relief to keep the safe conditions. On LNG carriers with steam plant as propulsion system, the BOG is burnt in the Main Boilers, where is generating the steam used in the steam plant. When there is an excess on BOG, it is still burnt in the main boilers, generating more steam than the required by the steam plant, then this excess of steam is wasted through the dump valves, which led the excess of steam to the Main condenser without doing any work on the steam plant.

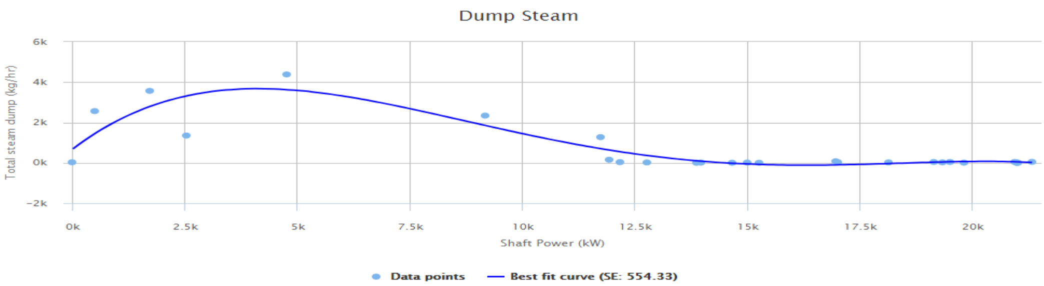

Fig.8: Steam dump flow (kg/h) compared with the shaft power (kW), vessel #1

Vessel #1 wasted 23.9 t of steam during the whole voyage. Estimating that to generate one ton of superheated steam is required 0.075 tons of fuel, vessel #1 wasted 1.79 t of fuel due to the steam dumped. While vessel #2 wasted 17 t of steam during the whole voyage, it is 1.275 t of fuel wasted for the voyage.

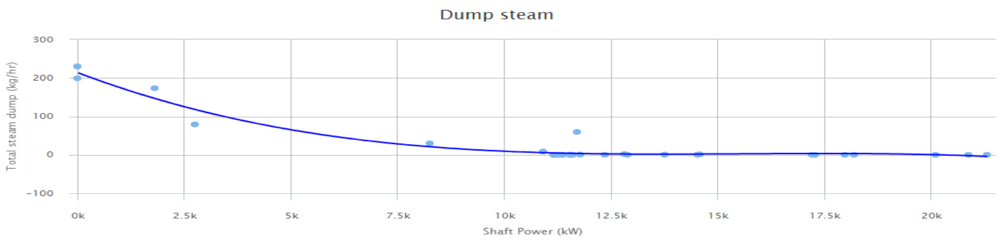

Fig.9: Steam dump flow (kg/h) compared with the shaft power (kW), vessel #2

The ship performance is highly influenced by the environment conditions. The wind and the waves might increase the ship´s resistance which will cause a consequent increasing on the fuel consumption due to extra power required. Due to the availability every 15 s of the wind true speed, it is possible to analyse only the ship performance for good weather condition, discarding the bad weather conditions. We set up the wind limit at 21 knots (same as the TC contract defines), so data above this limit is removed for the corrected fuel consumption analysis in contrast with the data shown in Table VI, which is including all the data without filtering out the data collected during bad weather.

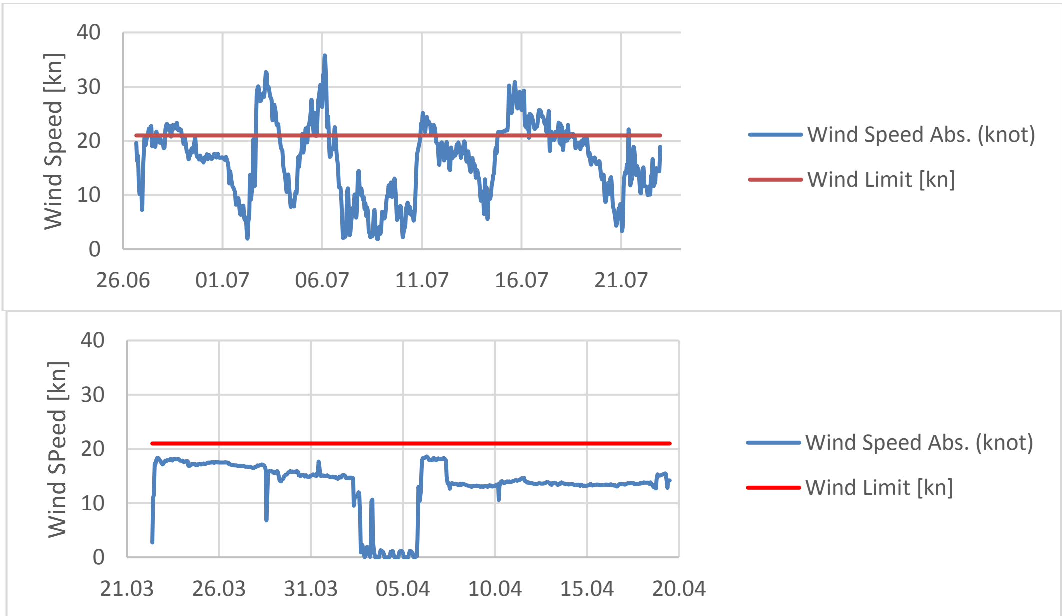

Fig.10: Wind profile for both vessels for the voyage

Vessel #1 overpassed the wind limits several times during the voyage. However, vessel #2 sailed under good weather conditions the whole voyage. It has impact on the fuel oil consumption for vessel #1 from the commercial point of view (comparison with the TC contract).

The total time within the whole voyage where vessel #1 was sailing above the wind limits, was 177.75 hours (7.4 days), which means the 28.45 % of the total voyage time. For the ship performance analysis from a commercial point of view, the Time Charter (TC) contract specifies an allowed equivalent fuel consumption reference curve (relation of the ship speed and allowed fuel oil equivalent consumption in MT per day). For such purpose, it has been used a dedicated software called “Charter Party module” (*Kyma*). Both ships are compared with the same TC curves (one for ballast and one for laden). Table VII details the TC reference curves defined by the charter of these two LNG carriers.

Table VII: Time Charter reference curves used on this study

	Ballast	Laden
STW (Knots)	**FOE (ton/day)**	**FOE (ton/day)**
20	193	-
19	172	179
18	155	157
17	141	143
16	129	132
15	117	120
14	113	115

STW: Speed Through the water, FOE: Fuel Oil Equivalent

The comparison against the TC contract requires the application of some filters, those filters are defined in the TC contract. In this case, the example filters are:

- Exclude data above Beaufort Scale 5 (21 knots)
- Only consider ship's speed above 13.5 knots

Figs.11 to 14 compare the actual ship status (blue dots) with the TC reference curve (red line).

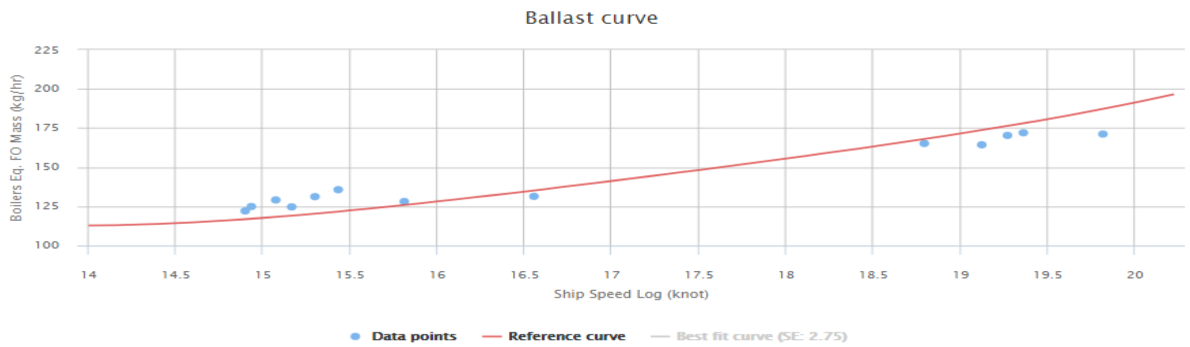

Fig.11: Vessel #1 graphical comparison with TC reference curves for ballast leg

Table VIII: TC evaluation for the Ballast voyage, Vessel #1

From date	To date	Actual FOE (MT)	Allowed FOE (MT)	Difference (MT)	Distance (nm)
09. Jul, 2017	10. Jul, 2017	31.54	32.90	-1.36	86.14
10. Jul, 2017	11. Jul, 2017	83.91	91.93	-8.02	233.26
11. Jul, 2017	12. Jul, 2017	131.12	136.14	-5.02	354.42
12. Jul, 2017	13. Jul, 2017	148.64	154.31	-5.67	403.76
13. Jul, 2017	14. Jul, 2017	164.30	176.94	-12.64	459.03
14. Jul, 2017	15. Jul, 2017	36.08	32.41	3.67	98.52
15. Jul, 2017	16. Jul, 2017	10.75	9.87	0.88	30.10
16. Jul, 2017	17. Jul, 2017	10.21	9.79	0.43	29.83
17. Jul, 2017	18. Jul, 2017	57.91	55.49	2.42	169.64
18. Jul, 2017	19. Jul, 2017	99.52	91.69	7.83	279.00
19. Jul, 2017	20. Jul, 2017	119.77	112.45	7.32	343.75
20. Jul, 2017	21. Jul, 2017	107.37	106.05	1.32	318.17
21. Jul, 2017	22. Jul, 2017	39.23	41.20	-1.96	118.66
Summary		1040.37	1051.18	**-10.81**	2924.28

The comparison of the ship performance for vessel #1 against the allowed consumption by the charter, gives the result of *10.81 MT* less than the FOE allowed for the ballast leg.

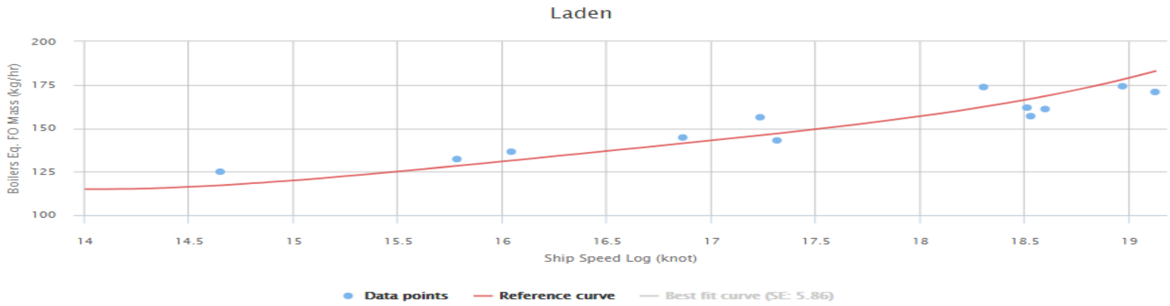

Fig.12: Vessel #1 graphical comparison with TC reference curves for laden leg

Table IX: TC evaluation for the Laden voyage, Vessel #1

From date	To date	Actual FOE (MT)	Allowed FOE (MT)	Difference (MT)	Distance (nm)
26. Jun, 2017	27. Jun, 2017	95.34	92.93	2.41	252.18
27. Jun, 2017	28. Jun, 2017	93.27	95.51	-2.23	243.77
28. Jun, 2017	29. Jun, 2017	87.72	94.36	-6.64	235.56
29. Jun, 2017	30. Jun, 2017	156.84	161.77	-4.93	430.44
30. Jun, 2017	01. Jul, 2017	157.00	168.05	-11.05	444.69
01. Jul, 2017	02. Jul, 2017	143.03	147.16	-4.13	415.63
02. Jul, 2017	03. Jul, 2017	25.93	25.33	0.59	72.52
03. Jul, 2017	04. Jul, 2017	117.87	111.78	6.09	298.04
04. Jul, 2017	05. Jul, 2017	117.01	123.01	-6.00	324.22
05. Jul, 2017	06. Jul, 2017	33.35	32.62	0.72	95.50
06. Jul, 2017	07. Jul, 2017	101.09	97.52	3.57	285.01
09. Jul, 2017	10. Jul, 2017	2.60	2.46	0.14	7.33
Summary		1131.06	1152.51	**-21.46**	3104.88

The comparison of the ship performance for vessel #1 against the allowed consumption by the charter, gives the result of *21.46 MT* less the FOE allowed for the laden leg. For the whole voyage, vessel #1 consumed *32.27 MT* less than the FOE allowed consumption by the charter. The using the same filters, vessel #2 performed the voyage as it is shown in following as below

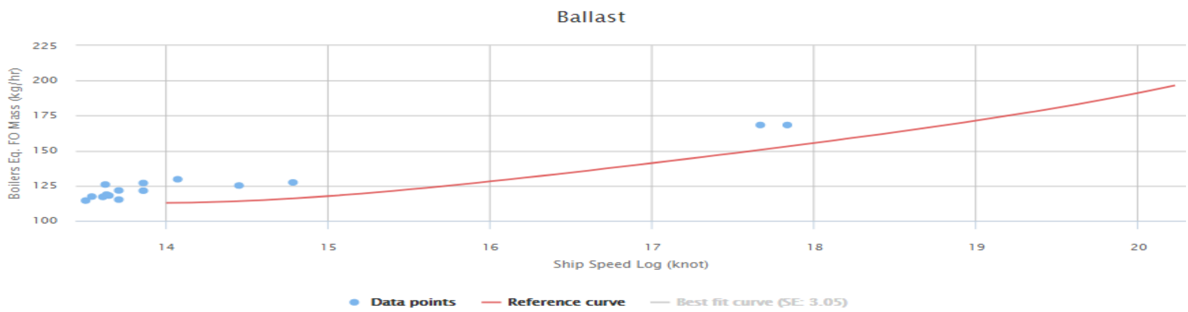

Fig.13: Vessel #2 graphical comparison with TC reference curves for ballast leg

Table X: TC evaluation for the Ballast voyage, Vessel #2

From date	To date	Actual FOE (MT)	Allowed FOE (MT)	Difference (MT)	Distance (nm)
05. Apr, 2017	06. Apr, 2017	87.43	80.36	7.07	222.36
06. Apr, 2017	07. Apr, 2017	165.63	150.27	15.37	417.22
07. Apr, 2017	08. Apr, 2017	58.58	52.81	5.77	152.17
08. Apr, 2017	09. Apr, 2017	0.08	0.08	0.00	0.23
09. Apr, 2017	10. Apr, 2017	33.24	29.59	3.64	87.09
10. Apr, 2017	11. Apr, 2017	123.98	108.23	15.75	323.08
11. Apr, 2017	12. Apr, 2017	107.41	100.31	7.10	294.07
12. Apr, 2017	13. Apr, 2017	98.27	91.47	6.80	265.79
13. Apr, 2017	14. Apr, 2017	61.50	58.78	2.71	169.59
14. Apr, 2017	15. Apr, 2017	8.54	8.28	0.26	23.83
15. Apr, 2017	16. Apr, 2017	11.89	11.54	0.36	32.97
16. Apr, 2017	17. Apr, 2017	60.24	57.89	2.35	167.19
17. Apr, 2017	18. Apr, 2017	94.19	92.64	1.55	269.19
18. Apr, 2017	19. Apr, 2017	59.26	54.56	4.70	165.11
19. Apr, 2017	19. Apr, 2017	22.17	20.25	1.91	61.43
Summary		992.40	917.06	**75.35**	2651.30

The comparison of the ship performance for vessel #2 against the allowed consumption by the charter, gives the result of 75.35 MT exceeding the FOE allowed for the ballast leg.

Table XI: TC evaluation for the Laden voyage, Vessel #2

From date	To date	Actual FOE (MT)	Allowed FOE (MT)	Difference (MT)	Distance (nm)
22. Mar, 2017	22. Mar, 2017	1.77	1.37	0.40	4.04
22. Mar, 2017	23. Mar, 2017	176.30	154.14	22.16	426.95
23. Mar, 2017	24. Mar, 2017	173.33	153.37	19.96	425.72
24. Mar, 2017	25. Mar, 2017	152.44	145.94	6.50	413.43
25. Mar, 2017	26. Mar, 2017	153.05	149.62	3.44	420.11
26. Mar, 2017	27. Mar, 2017	145.93	142.50	3.43	406.89
27. Mar, 2017	28. Mar, 2017	147.00	140.44	6.56	402.89
28. Mar, 2017	29. Mar, 2017	130.67	117.92	12.74	347.78
29. Mar, 2017	30. Mar, 2017	136.18	125.35	10.83	371.84
30. Mar, 2017	31. Mar, 2017	136.06	122.54	13.52	364.36
31. Mar, 2017	01. Apr, 2017	127.33	119.01	8.33	356.74
01. Apr, 2017	02. Apr, 2017	104.32	99.42	4.89	297.92
Summary		1584.87	1472.05	**112.82**	4239.85

The comparison of the ship performance for vessel #2 against the allowed consumption by the charter, gives the result of 112.82 MT exceeding the allowed FOE for the laden leg. For the whole voyage, vessel #2 consumed *188.17 MT* more than the FOE allowed consumption by the charter.

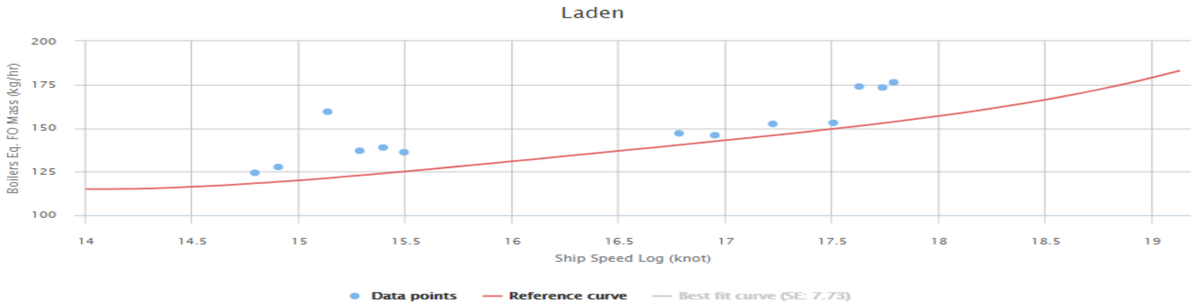

Fig.14: Vessel #2 graphical comparison with TC reference curves for laden leg

The application of the high-frequency data collected by SPM system gives the chance of a better and more accurate results due to the possibility of using actual measured data with selected filters for any conditions (wind, ship´s speed, etc.). This is not possible with low-frequency data available on noon reports to reach this high level of accuracy. In addition, the possibility of keeping the historical data stored and apply powerful data-management tools, it permits the companies to make ship´s models and predict the vessel's behaviour to take better decisions and possibly get greater savings. As an example, it is possible to analyse the historic data for the ship's fuel and speed data for the last 6-12 months to get valuable information (by applying filters on high-frequency database to avoid wrong readings, un-steady data which could invalidate the analysis). We take as example vessel #1, and we try to see the benefits of planning a voyage with a steady speed (we use the averaged speed through the water for the trip Bonny – Bahia Blanca, for ballast and laden condition). The reason why we have chosen vessel #1 is to show that even seeing that this ship was performing better than the TC requirements, she can perform better by means of using more steady speed during the voyage.

The filters considered in this example are: slip, steam dump flow, wind speed absolute, SFOC and ship speed). After processing the historical data stored in the high-frequency database, we get the below information that might be used by the operators to predict the fuel consumption at the desired speed, giving the chance to plan better the voyage.

Table XII: Fuel consumption Vessel #1- actual vs predicted

Voyage	**Actual FOE (MT)**	**Average STW (knots)**	**Included hours (hours)**	**Predicted FOE (kg/hr)**	**Predicted Acc. FOC (MT)**
Ballast	1040.37	16.09	187.33	5241.36	1020.8
Laden	1131.06	17.00	179.88	5993.36	1078.1
Summary	2171.43				2098.9

Based on the prediction of the FOE required to sail at steady speed, we see that vessel #1 could have consumed less fuel during the voyage if she had sailed with steady speed, having a potential maximum fuel savings up to 72.53 MT for the whole voyage (2717.43 – 2098.9 = 72.53 MT).

6. Conclusions

The application of the high frequency data on the analysis of the ship performance of these two sister ships sailing on the same route gives the following conclusions:

- Vessel #1 did the voyage more efficiently, looking at the FOE consumption, voyage time and operational profile (MCR)
- Vessel #2 emitted during the voyage Bahia Blanca – Bonny less CO_2 emissions, mainly because vessel#2 used more LNG than HFO.
- Vessel #2 consumed less HFO during the voyage than vessel #1. It means that vessel #1 is emitting more SOx to the atmosphere due to the consumption of more residual fuels.

- Vessel #2 performed the trip exceeding the FOE consumption compared with the TC reference curves. However, vessel #1 has a better performance and she used less FOE than the specified in the TC contract with the specific filters applied.
- Vessels with high levels of telemetry installed on board, allows the analysis of any parameters and operational conditions that might have effect on the ship performance, giving to the users a powerful tool which can help them in taking decisions.
- High-frequency data increases the reliability of the averaged data compared with the low-frequency data, especially on the analysis of parameters which have high uncertainty inherent (environmental data, shorter events, etc.)
- High-frequency data collected allows more detailed and precise analysis due to the reduction of the human error by minimizing the manual inputs
- The availability of high-frequency data allows better analysis and more accurate for events in shorter periods, such as manoeuvring, operation in ECAs, etc.
- The generation and storage of high-frequency data permits a better and more accurate post-analysis of the data, helping to the companies to develop models for more accurate ship´s performance predictions.

References

ALDOUS, L.; SMITH, T.; BUCKNALL, R. (2013), *Noon report Data Uncertainty*, Low Carbon Shipping Conf., London

ALDOUS, L.; SMITH, T.; BUCKNALL, R.; THOMPSON, P. (2015), *Uncertainty analysis in ship performance monitoring*, Ocean Engineering 110, Part B, pp.29-38

CE DELFT, (2009), Technical support for European action to reduce Greenhouse Gas Emissions from international maritime transport, https://www.cedelft.eu/en/publications/download/825

GAS STRATEGIES (2017), *LNG Outlook 2017: Surplus or balance?*, http://www.gasstrategies.com/sites/default/files/download/lng_outlook_2017_-_final_edition.pdf

GIIGNL (2017), *GIIGNL Annual Report*, Int. Group of Liquefied Natural Gas Importers, www.giignl.org

IGU (2017), *IGU World LNG report*, International Gas Union

IMarEST (2012), *Global-based approach to fuel and CO2 emissions monitoring and reporting*, MEPC 65/INF. 3, Institute of Marine Engineering, Science and Technology, London

IMO (2012), Report of the Marine Environment Protection Committee on its sixty-third session, MEPC 63/23, Int. Maritime Organization

LUND, B.; GONZALEZ, C. (2017), Big Data Concept in a Performance Monitoring Perspective, 2nd HullPIC, Ulrichshusen

MAK, L.; KUCZORA, A.; SULLIVAN, M.; MILLAN, J. (2014), *Ship Performance Monitoring and Analysis to Improve Fuel Efficiency*, OCEANS Conf., St. John's

McAFEE, A.; BRYNJOLFSSON, E. (2015), *Big Data: The Management Revolution, Harvard Business Review*, https://hbr.org/2012/10/big-data-the-management-revolution

Practical experience with ISO 19030 at Chevron Shipping – Part 1

Johnny Eliasson, Chevron Shipping Company, San Ramon/USA, Johnny.eliasson@chevron.com

Abstract

This presentation outlines the start and interim results of a multi-year collaborative project between Chevron Shipping and two of the major suppliers of fouling control coating products to the maritime industry. The main objective of the project was to optimize the hull and propeller performance on Chevron ships. The two coatings companies involved are JOTUN MARINE PAINT and AkzoNobel. The project started in early 2014 while ISO 19030 was still under development. The project applied the principles of the evolving standard from the start. The interim results summarized in mid-year 2017 were obtained using the published ISO 19030 standard with some modifications. In total, 15 out of 26 ships analyzed were dry docked during the project period. This hull performance optimization project will continue. The process of the collaborative hull performance optimization was validated by the interim results. Also, several aspects were identified using noon reports as the primary data source. This presentation will highlight the hull performance optimization process at Chevron Shipping. Both JOTUN and AkzoNobel will present their own findings on their experience from this collaborative project with a focus on the use of ISO 19030 and their constructive criticism geared towards improving it.

1. Hull Performance Optimization

It is clear from reviewing the dry-docking data collected from some 26,000 dry docks world-wide during the course of 2 years from 2016 to 2017, that the vessel owners and operators only selected to coat around 35% of the ships with a so-called higher quality fouling control coatings product. The definition of "higher quality" is not based on the author's opinion, but rather on all of the various paint manufacturers' published information.

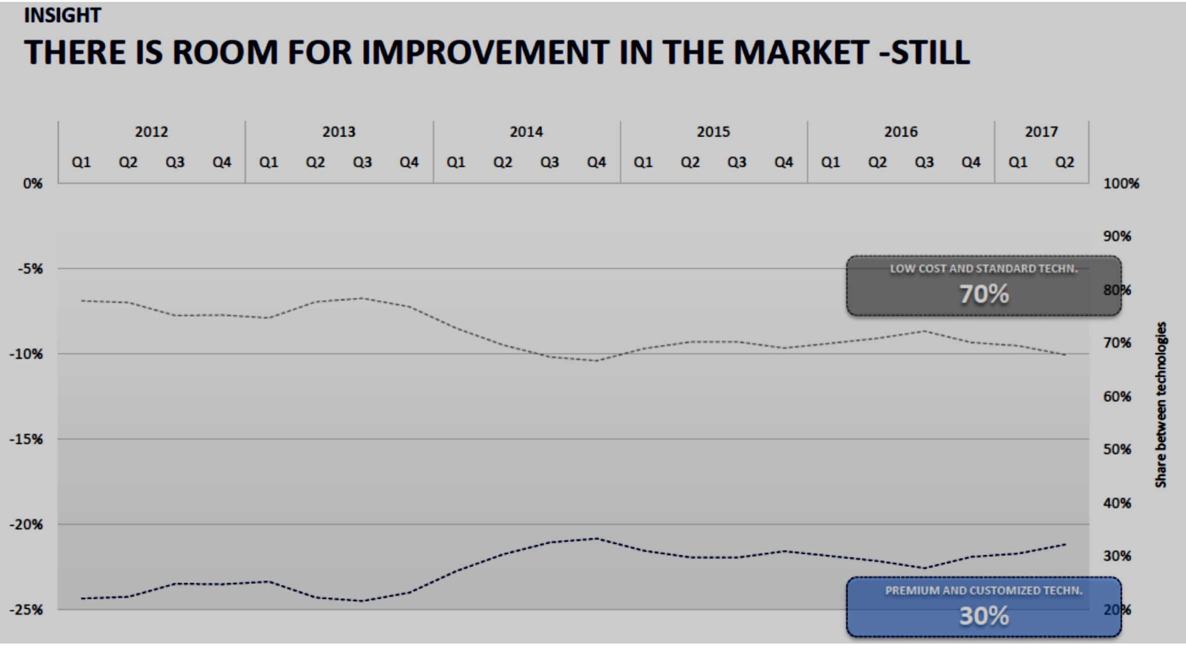

Fig.1: Market distribution if low-cost and high-end coatings in shipping

The above is essentially supported by IMO MEPC 63/4/8 (2011) which identified a potential for improvement of 20% in efficiency across the world fleet by improved dry docking processes and the use of optimized fouling control coating products. This is much in line with Chevron Shipping's interim results.

Chevron Shipping initiated a hull performance optimization program in 2014 to improve on hull efficiency to in turn reduce fuel consumption, air emissions and the risk of spreading invasive aquatic species arising from hull fouling.

The shipyard planning process at Chevron Shipping is well defined and standardized. It starts 18 months before the planned dry-docking date. The hull treatment and fouling control coatings product optimization steps are implemented early in the planning process and include:

Before dry dock:

- Monitor hull and propeller performance as per ISO 19030
- Past hull performance review – extending three dockings back when available
- Analysis of diver reports
- Establish the past trading pattern using IHS data and confer with fleet and operation departments about planned future ship deployment
- Have the ship measure and advise on its opinion as to ship's performance (typically miles travelled/ton fuel)
- Draft the detailed hull treatment specification
- Ask the involved paint manufacturer for an optimized fouling control system specification based on the ship's expected future operative profile
- Communicate with the paint manufacturer on the fouling control coating product selected and the specification required for the expected future operative profile, including the proper thickness for the entire dry docking cycle.
- Finalize the hull antifouling system specification

During dry docking:

- Inspect the hull fouling condition at each location of the hull
- Take in-docking under water hull roughness measurements after thorough hull cleaning
- Inspect and define all areas to be grit blasted
- Carefully supervise yard surface preparation and paint application activities
- After painting is complete, take final under water hull roughness measurements
- Estimate the expected hull performance

After dry docking:

- Have the ship validate expected hull performance when back in service
- Continue monitoring as per ISO 19030
- Perform scheduled propeller polishing with hull fouling surveys
- Perform hull cleaning as required based on a review of the vessel/fleet KPI expectations and/or as determined by observations of the fouling condition via dive inspection reports?

Looking at the results in 2017 after 3 ½ years with 15 ships dry docked out of 26 ships analyzed, the overall improvement in hull efficiency was 12% (as miles travelled / ton fuel) with the 15 dry docked ships contributing 17% in as a group. This can be interpreted as the hull optimization process contributing 11.9% to the efficiency gain and other efficiency measures contributing the remaining 5.1%.

We looked at the 15 ships that dry docked on a normalized time line. These ships showed a steady overall performance for 2 years prior to the docking event. On monitoring the ships for a period of two years following dry dock, a steady line could be drawn representing their performance after the optimization process had been concluded. Naturally, not all ships had been in operation for a full two-year period post dry dock and not all ships were optimized to the same degree. We analyzed the data as accurately as possible and considered other factors which may have influenced the results.

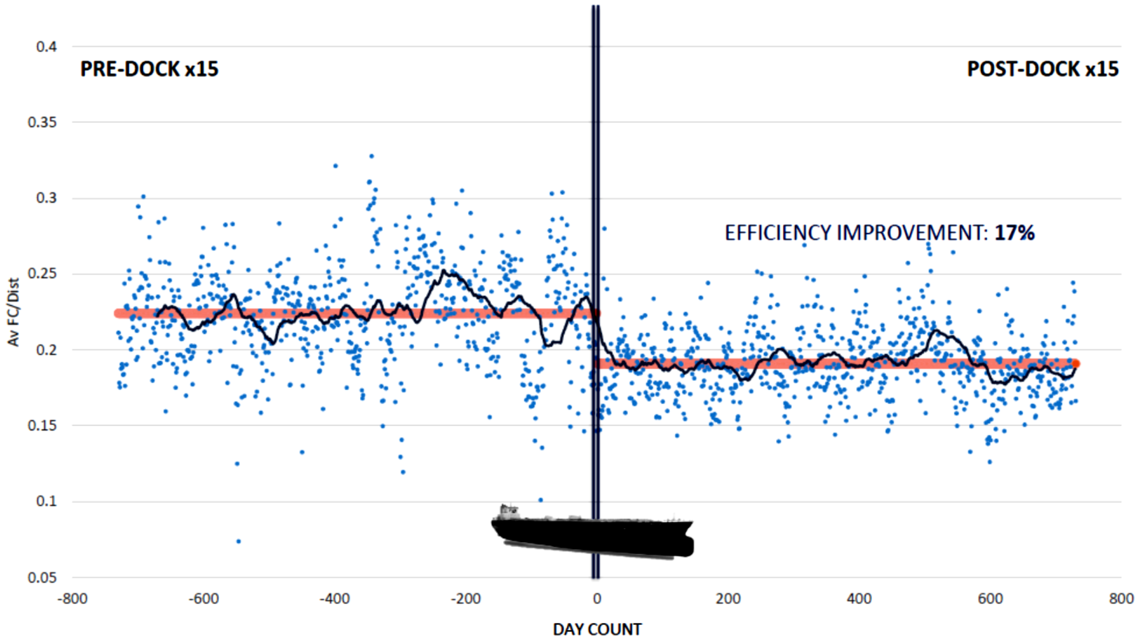

Fig.2: Performance monitoring results

The ISO 19030 analysis was based primarily on noon reports. These were found to provide data that was ideal for analyzing ships in groups. The noon reports were found to be less accurate in analyzing individual ships. They contained a less than ideal amount of data points after normalizing, although some conclusions could still be drawn. It is also clear that improvements in the noon report data quality would greatly improve the quality of the analysis results.

The other efficiency measures employed included increased adherence to company policy regarding propeller polishing, hull cleaning and power train efficiency improvements. We found that to evaluate each specific ship, all these measures had to be put on the time line to make good sense of the data.

This project is continuing and further updates are planned.

2. ISO 19030 KPIs

Chevron's Performance Manager analyzed the noon data and reached the conclusion that there was a significant efficiency gain between 2015 to that collected in 2016. In addition, AkzoNobel and Jotun Marine Paint independently performed analysis work based on ISO 18930 from early 2014 to mid-2017. All three parties came to essentially the same conclusion, namely the aforementioned significant efficiency gain.

Part of the scope of this work was also to evaluate ISO 19030 as a tool for ship hull and propeller performance monitoring. The general consensus was that it is a good tool. However, the maintenance trigger and maintenance effect KPIs were not found to be sufficiently accurate based only on noon reports.

The two paint manufacturers were provided copies of all diver reports and had access to our noon report database.

AkzoNobel and Jotun Marine Paint will provide more in-depth information on the analysis process and offer suggested improvements to ISO 19030.

On the Effect of Navigation Support System
– From Collecting Data to Operational Support

Toshiyuki Kano, National Maritime Research Institute, Tokyo/Japan, kano@nmri.go.jp

Abstract

The National Maritime Research Institute of Japan has conducted the "Eco-Shipping Project" for Japanese coastal vessels to provide energy saving navigation plan, supported by Ministry of Environment from 2013 to 2015 fiscal year. The project has shown 14% energy saving potential and demonstrated 4% fuel consumption reduction effect using the navigation support system. Then, it has been put into practical use for 17 cement tankers since April of 2016, and as a result, it had exceeded 4% energy saving. The indicators EENI (Energy Efficiency of Navigational Indicator) and Kn (Energy Efficiency of Propulsion Indicator), fuel consumption reduction amount and operation performance were evaluated on the individual ship using ship monitoring data. The author describes the above evaluated results and compare the performance of the vessels with each other using these indicators for 2016 fiscal year.

1. Introduction

In recent years, regulations on CO_2 and other GHG emissions have been strengthened, coupled with high interest in environmental issues. Under such circumstances, the demand for energy saving in the maritime sector is increasing from the viewpoint of economy. For energy saving, countermeasures on the hardware side such as hull form optimization and improvement of engine efficiency are effective, but measures on the software side such as optimize of route and ship's speed plan by Weather Routing Service are also effective. Recently, the importance of the latter has been recognized widely, and various efforts related to improving operational efficiency have been implemented. It is easy to put them to existing ships and has a potential of wide applicability.

The National Maritime Research Institute of Japan (NMRI) has been conducted in research and development of environmentally friendly ship navigation support system in collaboration with shippers, shipping companies, NPO Marine Technologist (MTL) and others. This support system improves operational efficiency by utilizing ICT technology to achieve economic, environmental and punctual operations. In response to the Fourth Industrial Revolution, ICT innovation has begun. It is now an opportunity to revitalize the shipping industry using these technologies.

The NMRI has conducted the "Eco-Shipping Project: Verification Project for CO_2 Emission Reduction with Ship-Scheduling/Voyage-Planning System " for Japanese coastal vessels to provide energy saving navigation plan, supported by Low Carbon Technology Research and Development Program, Ministry of Environment from 2013 to 2015 fiscal year, Fig.1. This project has verified 14% energy saving potential based on the simulation study of the actual operation situation, and demonstrated 4% fuel consumption reduction effect in the operating actual vessels, using the navigational support system.

As a result of this achievement, the navigation support service (eE-NaviPlan) has been put into practical use for 17 Japanese coastal cement tankers since April of 2016, and saved fuel consumption exceeding 800kl (about 5% energy saving) of 2016 fiscal year. In addition, due to weather and oceanic forecast information, the keep schedule and safety operation have improved. eE-NaviPlan service adopted energy efficiency navigational indicator (EENI), energy efficiency propulsion indicator (Kn), etc. as indicators of ship operational status. EENI and Kn were proposed to evaluate energy efficiency of both loaded and unloaded conditions in difference size and speed of ships. These indicators were derived using readily available monitoring data such as fuel consumption, displacement, and navigation distance, etc.

The author introduces outline of the navigation support system, and describes the above evaluated results and compare the performance of the vessels with each other using these indicators for 2016 fiscal year.

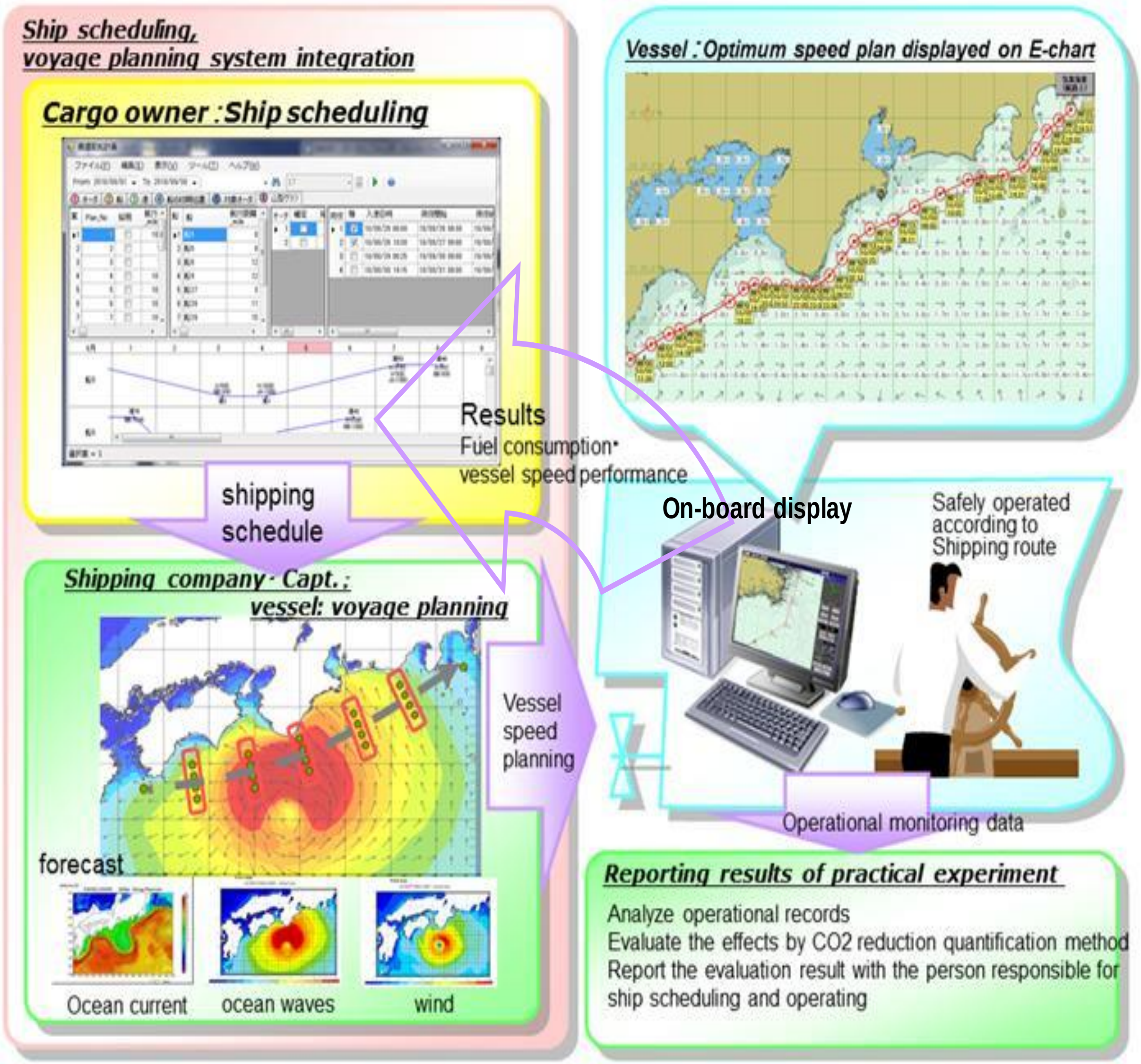

Fig.1: Concept of “Eco-Shipping Project”

2. Navigation Support System

2.1 Outline of the System

The navigation support system shall provide the optimal navigation plan based on weather routing technology (PLAN), speed plan of the system provides to reduce a vessel’s speed on voyage to meet on arrival time at the destination port. Then reduction speed will result in reduce fuel consumption, thereby reduce GHG and other exhaust emissions. Captain navigates with reference to the plan provided (DO). And the system reports evaluation of fuel consumption reduction effect, and operating status of the ship by monitoring data (CHECK & ACTION), supports the efficient PDCA for fleet operation management conducted by ship operators.

2.2 Optimum Voyage Plan

2.2.1 Just-in-time Optimal Navigation Plan（Plan）

The system provides the vessels with the minimum necessary optimum output plan arriving at the destination port just in time. The plan is calculated using mathematical programming method with highly accurate weather and oceanic forecast information and estimated vessel propulsive performance at sea.

2.2.2 Evaluate propulsion performance at sea

In order to formulate an optimal voyage plan that minimizes fuel oil consumption under the ship's schedule and loading condition etc., it is required weather and oceanic forecast information and to estimate the specific propulsion performance of the ship at sea.

In a ship operation, the propulsion power generated by the main engine is transmitted to the propeller becomes the thrust and ship's speed is determined so that the propulsion power and work (product of resistance force acting on the hull (R) and ship's speed) are balanced. Resistance acting on the hull is expressed as a component separation model which separates the resistance (R) into the still-water resistance (R_{base})and added resistances due to wind (R_{wind}) and due to wave (R_{wave}). Ship' speed is expressed as follows.

$$V = \frac{P\eta}{R} \tag{1}$$

$$= \frac{P\eta}{(Rbase + Rwind + Rwave)} \tag{2}$$

P is main engine power, (kw); η is quasi-propulsive efficiency, (-);R is total in service resistance, (N); V is ship speed through water, (m/s)

It was estimated accurate additional resistances caused by wind and wave using the VESTA (Vessel performance Evaluation Tool in Actual Sea of NMRI, *Tsujimoto et al. (2013)*.

2.2.3. Regression by monitoring data

Vessel performance data measured automatically and collect sequential data every 10 minutes by on board PC. And collect data is emailed to the shore-based server. The coefficients expressing the model are determined by regressing the measurement data and wave forecast data. Estimate the ship's speed loss by external force such as wind and waves with the model, *Kano et al. (2015)*. For just-in-time optimum ship speed planning, it is important to evaluate the influence of the waves, which are greatly affecting the decrease in ship speed. Therefore, the resistances caused by wave evaluated with every 30° wave direction in detail, Fig.2.

In order to evaluate the performance accurately, it is sometimes required to take into account the usage of the shaft generator, but in many cases, it is not monitored. *Murata et al. (2017)*, even in this case, developed a clustering method to classify the data into used and unused data of shaft generator, and confirmed that it can be separated with about 90% accuracy, Fig.3.

By continuously analyzing the operation monitoring data and evaluating the current ship's performance, it is possible to improve the accuracy of the propulsive performance estimation at sea.

In addition, analysis of sea margin, energy saving equipment, confirmation of painting effect, fouling condition can be estimated. Monitoring data can also contribute to improving accuracy of ocean current forecast, *Miyazawa et al. (2015)*.

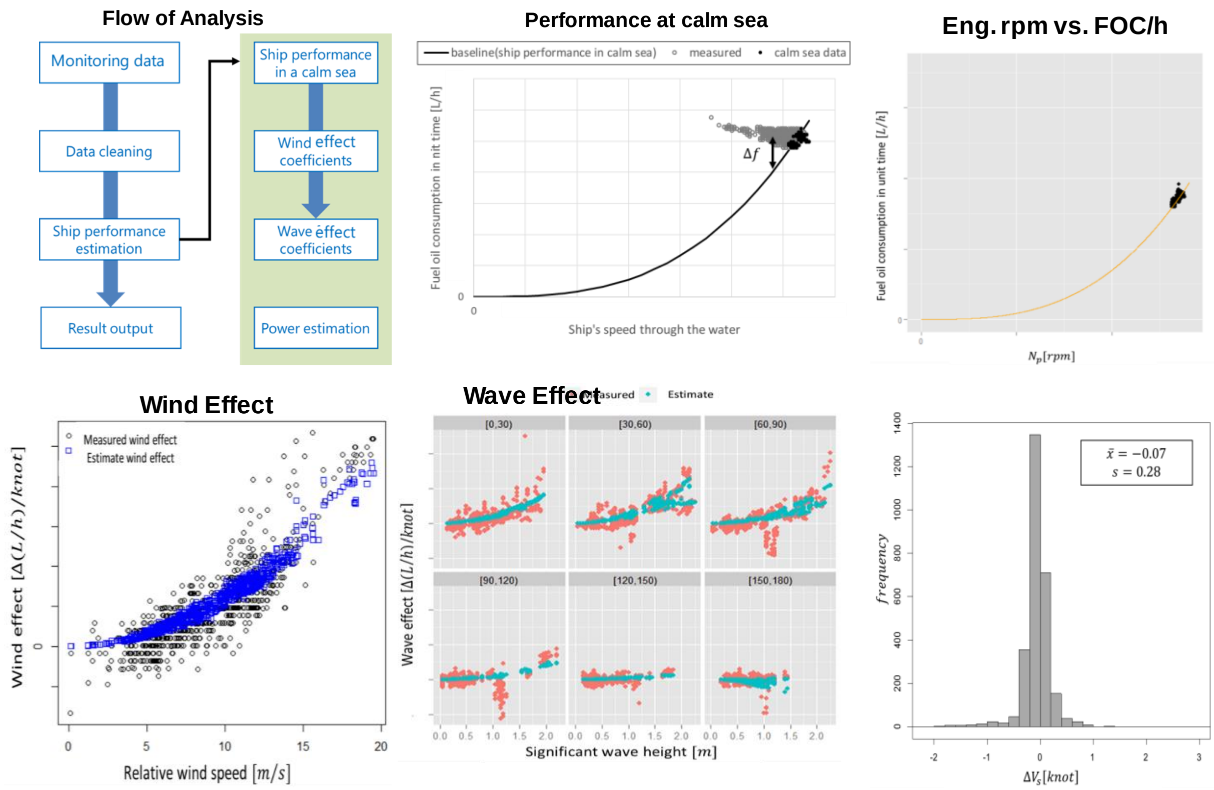

Fig.2: Evaluation of ship's performance at sea

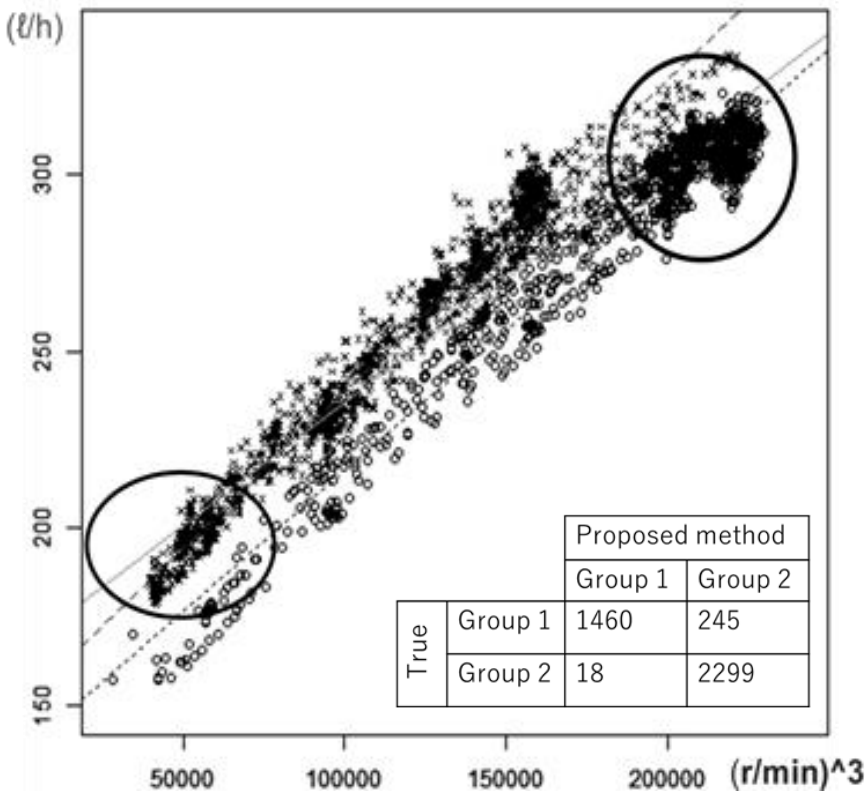

Fig.3: Separated data and linear regression lines of a ship and validation of proposed methodology

2.2.4. Weather& Ocean current forecast information

Weather and ocean currents have a major impact on shipping routes, navigation plan and economic operation, so highly accurate forecast information is required. This system uses 3 km meshed forecast information of weather and ocean current up to 3 days ahead for coastal areas in Japan. Regarding wind direction / wind speed, wave height, wave period, wave direction, updated every 3 hours, it is the most available and most precise information in Japan. This forecast information is also provided to the ship.

2.2.5. Ocean current information

In the coastal region of Japan, a very strong ocean current called "Kuroshio", which is important information for planning the optimum navigation plan for the Japanese coastal ships. The Japan Agency for Marine-Earth Science and Technology (JAMSTEC) conducted the Japan Coastal Ocean Predictability Experiment (JCOPE, http://www.jamstec.go.jp/jcope/), provides as detailed ocean current forecast information updated daily with 3 km mesh. Fig.4 shows how the Kuroshio big meander occurred for the first time in 12 years, and shows the ocean current prediction information around Ohshima off the IZU Peninsula. It is found the information is high resolution, this system uses this information updated daily.

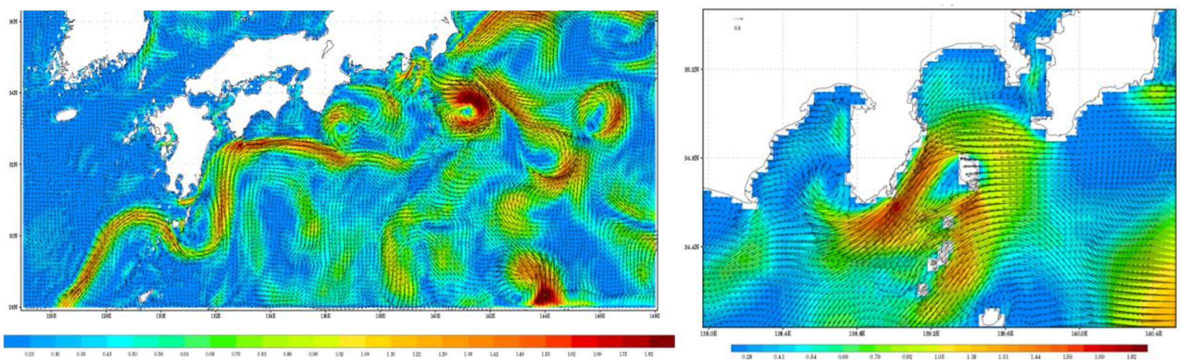

Fig.4: Kuroshio big meander and predicted ocean current around Ohshima off the IZU Peninsula

2.2.6. Voyage plan (PLAN)

The system calculates and provides a just-in-time voyage plan by using mathematical programing method. By inputting the latest weather and ocean current forecast information into the ship's specific propulsion performance model with the route and required arrival time as the constraint condition, the navigation time and the fuel consumption are accurately calculated, and optimum ship's speed (or revolution of the propeller shaft) plan was formulated. On the electronic chart of the on-board display (GUI), the optimum revolution of the shaft / blade angle (in the case of Controllable Pitch Propeller) is displayed for each waypoint (WP) on the route.

At the same time, it also displayed forecast weather, oceanic and tidal current conditions, Fig.5, as navigational reference. By referring proposed voyage plan, the captain is able to navigate with energy saving operation by maximizing the energy saving performance of the ship.

2.2.7. Ship's operational status (CHECK & ACTION)

Monitoring data related to navigation and engine conditions are collected from the AIS, engine data logger, etc. to the PC of on-board display while the ship is sailing, and these data send to the server of the office by ship-to-shore communication. By analyzing the collected data in the server, the following information can be confirmed with the web browser by the information infrastructure system, Fig.6:

- Current and planned ship position and passing time at waypoint,
- Ship's route pass
- Time history of engine output for each voyage,
- Forecast of weather and sea conditions

- Fuel consumption saving amount by adopting this system
- EENI, Kn, etc.

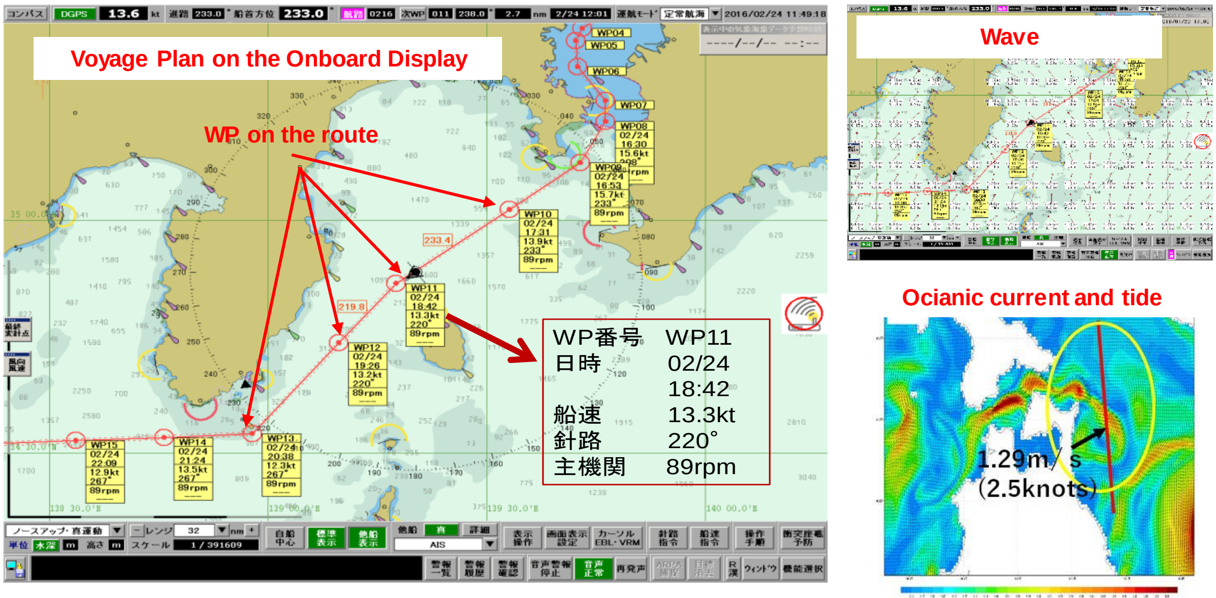

Fig.5: Displayed optimum voyage plan

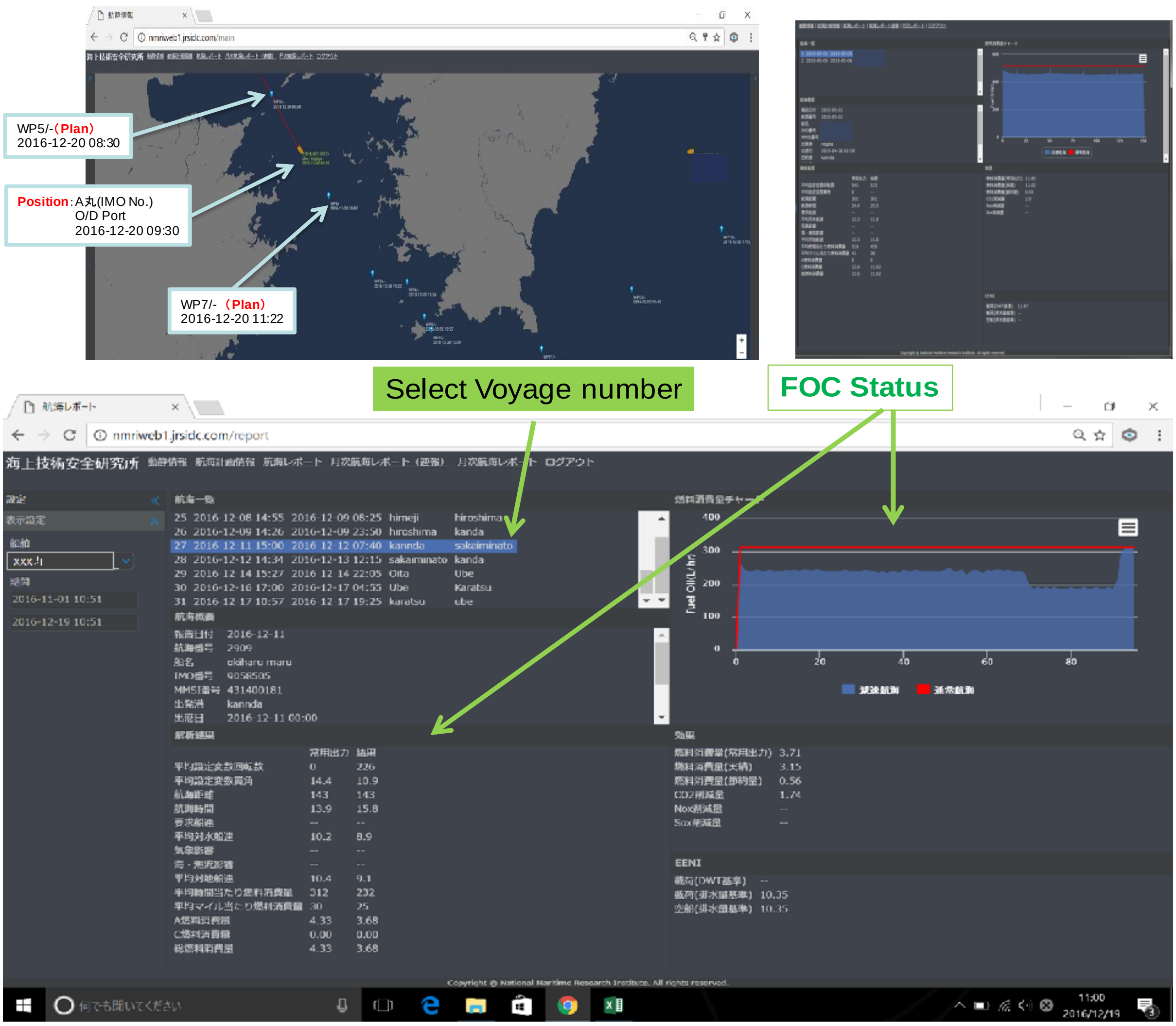

Fig.6: Web browser views of the information infrastructure system

In this way, the operating status is “visualized”, and sharing it with operators, related persons will make the awareness of energy saving operation and safety deepened. By deepening awareness of economic and safety, it can contribute to operation improvement activities.

2.2.8. Evaluation of energy saving effect (VERIFICATION)

The energy saving effect is evaluated by comparing the case not using the navigation support system (Business as Usual) and the case used (Project), *Kano et al. (2014a).* The fuel consumption is accurately evaluated in consideration of the propulsion performance of the ship and operating conditions and weather/oceanic conditions. And the energy saving effect is calculated by the methodology which was developed by NMRI, Kano et al. (2011) and has confirmed validity by a third party reviewing agency. Fig.7 shows a monthly report on the amount of fuel saving per voyage.

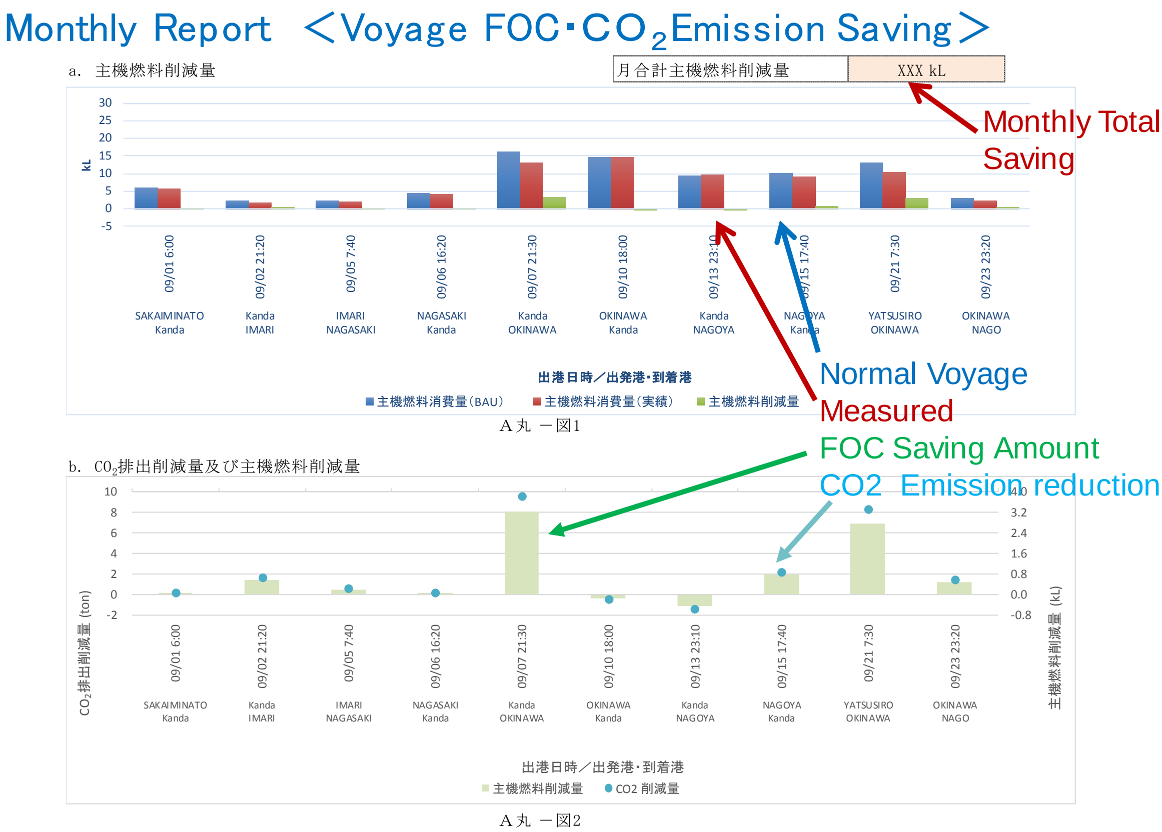

Fig.7: Monthly report on the amount of fuel saving per voyage

Fig.8 shows the monthly trend of the fuel saving amount of the fleet in 2016 fiscal year by the optimal navigation plan support (eE-NaviPLan) service. 17 cement fleets saved fuel consumption of over 800 KL and CO_2 emissions of about 2,400 tons were suppressed. In the busy season of cement transportation, there are many opportunities for voyages at high speeds, and the amount of reduction becomes small. So, monthly reductions vary from 40 KL to 80 KL.

3. Mutual Comparison

Energy Efficiency Design Index (EEDI) is adopted as an index of CO_2 emissions from ships by IMO. This index regards the product of the DWT corresponding to the summer full load water lines and the navigation distance as the work performed by the ship. This index based on weight of cargo is not able to evaluate at unloaded voyage.

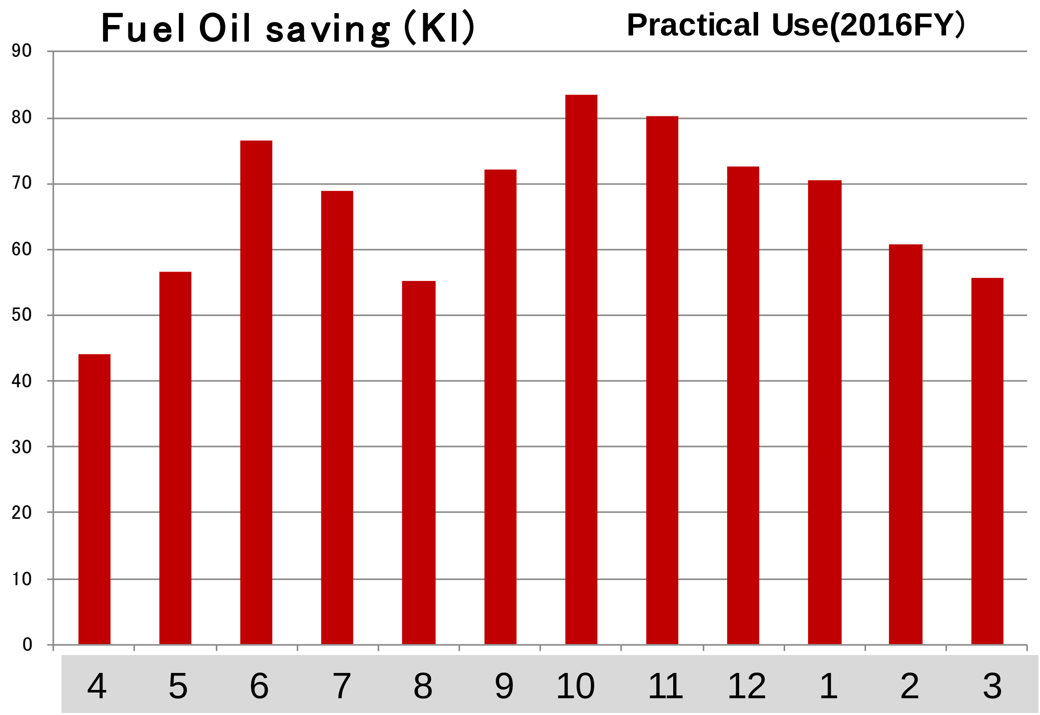

Fig.8: Monthly trend of the fuel saving amount of the fleet in 2016 fiscal year

Hence, EENI was proposed to evaluate energy efficiency of both loaded and unloaded conditions in different size and speed of ships. The indicator is based on the navigational work done by the ship on the product of displacement and sailing distance. This is obtained as follows, based on the ratio of the CO_2 emission converted from the fuel consumption FC and the navigational work. Therefore, EENI is the indicator for energy efficiency of navigation.

$$\mathrm{EENI} = \frac{\sum_j \mathrm{FCj} \times \mathrm{C_{Fj}}}{\mathrm{W} \times \mathrm{D}}$$

$$EENI = \frac{\sum FCj \times CFj}{W \times D} \qquad (3)$$

By dividing the numerator and denominator by time, it can be transformed as follows.

$$= \frac{\sum SFCj \times Pj \times CFj}{W \times V} \qquad (4)$$

J is fuid type; *FCj* is fuel consumption for fuel *j*; *CFj* is fuel mass to CO_2 mass conversion factor; *W* is diplacement (tonnes); *D* is the sailing distance in nautical miles *j*; *SFCj* is specific fuel cinsimption(g-fuel/kw/hour); *P* is Main Engine power (kw).

By clarifying the physical meaning of EENI, it shows that it is proportional to the square of ship's speed and inversely with the third root of displacement (KANO et al. 2014b). Then EENI expressed as follows.

$$EENI = \frac{\sum_j (SFC \times C_{T\nabla} \times v^2)_j \times C_{Fj}}{\rho \times g \times \eta \times \nabla^{\frac{1}{3}}} \qquad (5)$$

$C_{T\nabla}$ is total resistance coefficient; ρ is density of sea water; *R* is total resistance in the sea conditions; *P* is brake power; η is propulsion efficiency. It may be considered to be Froude number that uses third root of displacement as a measure.

$$Fn'^2 = \frac{V^2}{g \times \nabla^{\frac{1}{3}}} \qquad (6)$$

Since the indicator is a non-dimension paramter and has a physical meaning,it is easy to undeastand the data and also posible to investigate voyage performance well. EENI is influenced of the by external forces such as wind and waves, varying with each voyage, but it can be expected to converge if avereage over a certain number of voyage.

$$\text{Average EENI} = \frac{\sum_i \sum_j SFCij \times Pj \times CFj}{\sum_i Wi \times Vi} \qquad (7)$$

According to the Eq.(5), Kn was introduced to exclude ship speed effect as follows. Therefore, EENI is the indicator for energy efficiency of navigation.

$$Kn = \frac{EENI}{V^2} \qquad (8)$$

As the fuel-based indicator is requested from the operator side rather than the CO_2 equivalent value,. the eE-naviPlan service reports EENI 'and Kn' on a fuel (liter-fuel) base to shipping companies, etc. and check the navigation status for each voyage. This report helps to check the ship's state of operation accurately and specific performance, and also, is effective in taking the consideration of energy saving navigation by operators and promoting fuel consumption saving activities.

By evaluating values of these indicators for a certain period, it is also possible to compare mutual operational performance of ship. Fig.9 and Fig.10 shows the one year from April of 2016 to March of 2017 average values of EENI 'and Kn' of Japanese middle/large-sized coastal cement tankers in the case of loaded and unloaded conditions are shown on displacement basis, respectively. These data are well organized on displacement basis.

It shows that the EENI is greatly influenced by the ship's size and is arranged as a function of the displacement. Improve the energy efficiency greatly by upsizing the ship. In addition, it can be seen that the effect of enlarging a smaller ship is great. Since the influence of the speed is excluded, the variation of the Kn is relatively smaller than EENI.

Characteristic curves of EEDI' and Kn' were obtained in the same expression of EEDI's reference line of the cement tankers and it is expressed as follows.

$$EENI' = 2679.701 \times W^{0.714} \qquad (9)$$

$$Kn' = 37606.14 \times W^{0.790} \qquad (10)$$

It is thought that the characteristic curve of EEDI' and Kn' quantitatively represents the operational and propulsion performance in the actual sea of the cement fleet in 2016 fiscal year, respectively. These indicators are applicable to many type of ships, because those derived using readily available data such as fuel consumption, displacement, and sailing distance etc. And characteristic curves corresponding to each ship type of fleet can be proposed.

4. Conclusions

In order to contribute to energy saving ship's operation of Japanese coastal vesels, NMRI has developed navigation support system, which tales into acount the PDCA operation cycle.

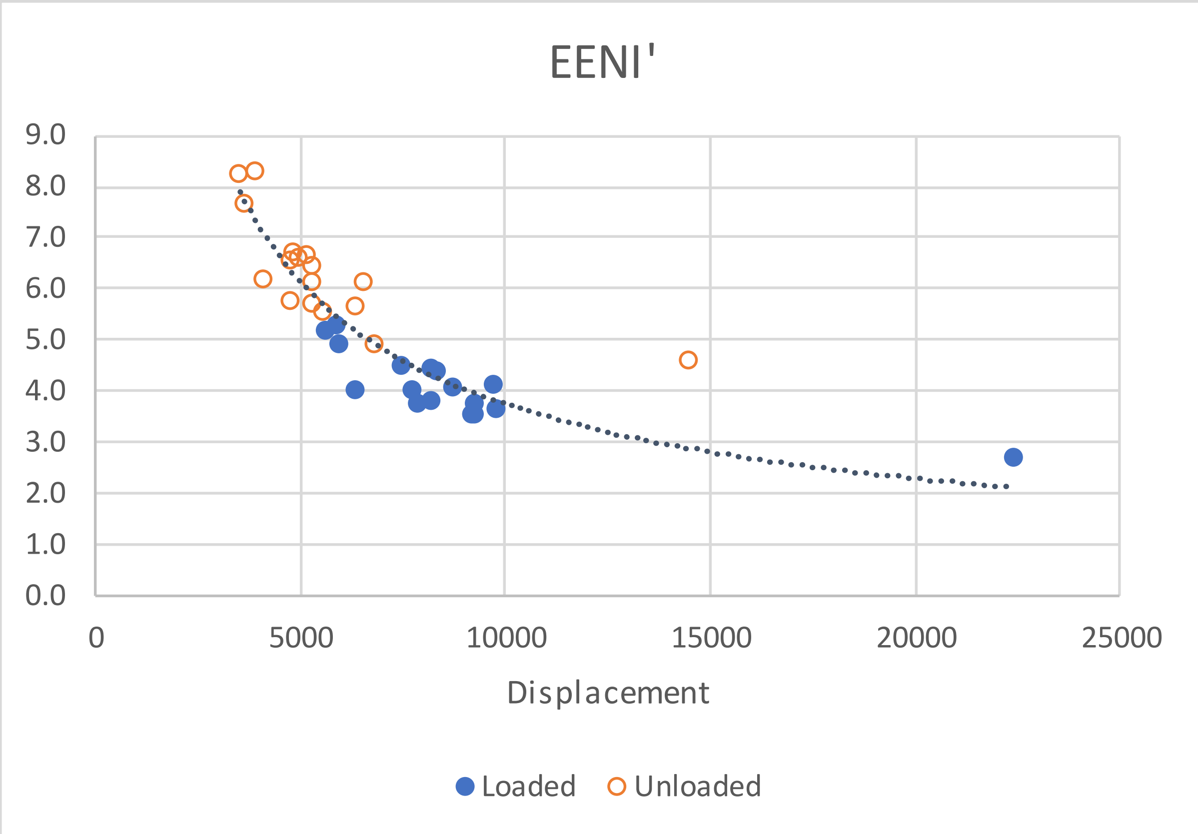

Fig.9: EENI’ distributions and characteristic curve on displacement basis (Coastal Cement Tankers)

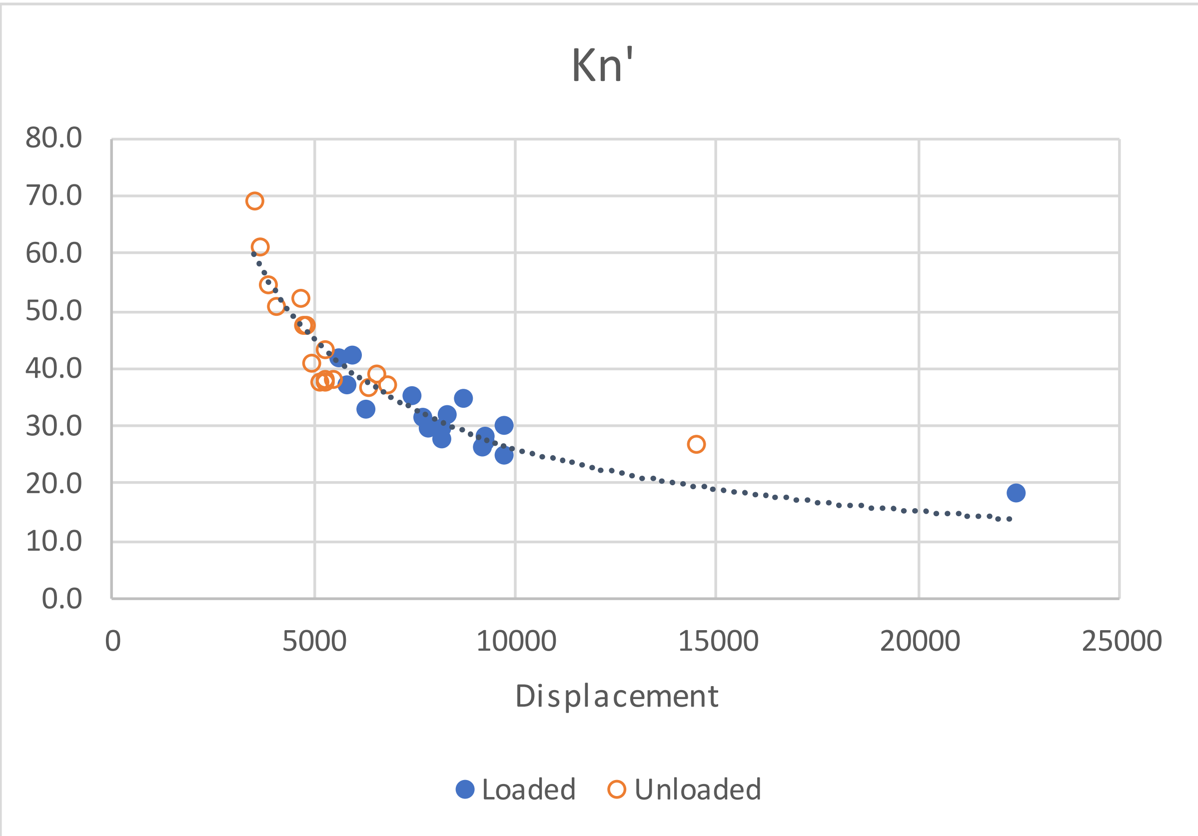

Fig.10: Kn’ distributions and characteristic curve on on displacement basis (Coastal Cement Tankers)

This system was practically operated as eE-NaviPLan service in 17 cement fleets, and as a result, in fiscal year 2016, energy saving effect has exceeded 4% (exceed 800 kl in fuel oil).

Regarding the evaluation of operational performance using monitoring data, indicators EENI' and Kn' were applyed to the cement tankers, evaluated ship's energy efficiency of both loaded and unloaded conditions in difference size and speed of ships, compared each other, and derived the characteristic curves on the fleet of Japanese coastal cement tankers.

These indicators expected to be applicable to many types of ship, because those derived using readily available data such as fuel consumption, displacement, and sailing distance etc.

It was thought that the characteristic curve of EEDI' and Kn' represents the operational and propulsion performance quantitatively in the actual ship's operation.

In addition, these indicators had a physical meaning and there is also a merit that it was easy to understand the result. These were valuable and useful indicators for operators in practical use.

Through such services, the author hope to revive vitality in the domestic shipping industry, and eventually lead to the reduction of global environmental impact and sustainable development for children.

Acknowledgment

The navigation support system was derived from the results of consignment projects by NEDO and the Ministry of the Environment, which were implemented with the cooperation of shippers, shipping companies, and NPO Marine Technology. The author would like to express sincere appreciation to Ube-Mitsubishi Cement Co., Ltd for their kind and invaluable cooperation in collectiong data. The author also indebted to the NEDO, MOE, Ms.Kon, Ms Yamazaki(MTL) are gratefully acknowleged for there valuable suggestions and persevring job.

Reference

IMO (2009), *Guidelines for Voluntary Use of the Ship Energy Efficiency Operational Indicator (EEOI)*, MEPC 1/ Circ. 684, IMO, London

IMO (2011), *Amendments to the Annex of the Protocol of 1997 to Amend the International Convention for the Prevention of Pollution from Ships,1973, As Modified by the Protocol of 1978 Relating Thereto, Annex 19*, Resolution MEPC 203(62), IMO, London

IMO (2012), *Guidelines for the Development of A Ship Energy Efficiency Management Plan (SEEMP), Annex 9*, Resolution MEPC 213(63), IMO, London

KANO, T.; NAMIE, S. (2014a), *A Study on Estimation of GHG Emission for Speed Planning Operation Using Energy Efficiency Index and Time-Series Monitoring Data*, COMPIT, Redworth, pp.167-180

KANO, T.; NAMIE, S.; SHIMURA, Y. (2015), *On the Evaluation Methodology Applying Ship-Scheduling /Voyage-Planning System for CO_2 Emission Reductions*, Proc. Japan Society of Naval Architect and Ocean Engineers 21, pp.77-82

KANO, T.; SETA, T.; SATO, K. (2015), *Eco-Shipping Project for Japanese coastal vessels - Verification Project for CO_2 Emission Reduction with Ship-Scheduling/Voyage-Planning System,* 16th Int. Congress of the Int. Maritime Association of the Mediterranean (IMAMM 2015), pp.175-182

MURATA, A.; KANO, T. (2017), *Applies the clustering method using navigational monitoring data into ship's fundamental propulsion performance*, Asia Navigation Conference (ANC 2017)

MIYAZAWA, Y.; GUO, X.Y.; VARLAMOV, S.M.; MIYAMA, T.; YODA, K.; SATO, K.; KANO, T. (2015), *Assimilation of the seabird and ship drift data in the north-eastern sea of Japan into an operational ocean nowcast/forecast system*, Scientific Reports, http://dx.doi.org/10.1038/srep17672

KANO, T; NAMIE, S. (2014b), *A Study on Estimation methodology of GHG Emission by using energy efficiency index and time series monitoring data*, *Proceedings of Conference on Maritime-Port Technology* (MTEC 2014),2014, pp.35-41

TSUJIMOTO, M.; KURODA, M.; SOGIHARA, N. (2013), *Development of a calculation method for fuel consumption of ships in actual seas with performance evaluation*, 32nd OMAE, Nantes, OMAE2013-11297, pp.1-10

Hull Performance Prediction beyond ISO 19030

Daniel Schmode, DNV GL, Hamburg/Germany, daniel.schmode@dnvgl.com
Ole Hympendahl, DNV GL, Hamburg/Germany, ole.hympendahl@dnvgl.com
Ditte Gundermann, Hempel, Copenhagen/Denmark, DIGU@hempel.com

Abstract

This paper discusses experience with ISO 19030 and proposals to deviate from the default method to improve accuracy and practicability. These comprise filtering and correcting for environmental conditions as well as statistical corrections based on our 1000+ vessel database.

1. Focus of ISO 19030

The aim of ISO 19030 is to provide a method for measuring changes in hull (and propeller) performance. ISO 19030 is organized in three parts, where Part 2 describes the default method. The default method stipulates high-frequency data capturing. Changes in hull and propeller performance are quantified in terms of four KPIs, which are designed to evaluate the effect on performance over time of different maintenance, repair and retrofit activities. As stated in the documents, the method is not intended for determining "absolute" levels of performance (as opposed to ISO 15016 on sea trials for newbuildings) in order to, for instance, compare different ship types, but only to compare performance changes over time for a given ship. The weather corrections in ISO 19030 are relatively simple:

- Wind
  The ISO 19030 weather correction is based on generic wind corrections with wind force coefficients taken from open literature. The coefficients published in ISO 19030 are ship-type specific, e.g. "containership, laden". They do not consider details like ratios of main dimensions, deck geometry, etc. *Bertram (2017)* reports differences between ISO 19030 ship-type specific coefficients and wind-tunnel measured ship-specific coefficients of 40%. ISO 19030 addresses the accuracy issue by imposing strict limits on wind speed, recommending to filter above Beaufort 4.
- Wind sea and swell
  Corrections for added power (or speed loss) in waves are notoriously difficult and inaccurate, *Bertram (2016)*. ISO 19030 has no explicit correction for added power or speed loss in waves. Instead the default filter recommendations limit wind speed. For mature wind sea, there is a direct correlation between wind speed and significant wave height of wind sea. For swell, the implicit assumption of ISO 19030 is "hope for the best".

The simplistic correction for ambient conditions in ISO 19030 motivated relatively strict filtering recommendations. In practice, this means that typically more than 85% of the recorded datasets are filtered out. Even with high-frequency recording, this may lead to unreasonably long periods of time before reliable trends are seen. For monitoring schemes based on low-frequency recording (once per day in noon reports or three times per day at best), this strict filtering often makes performance monitoring completely unfeasible.

In principle, better correction schemes can compensate for lower frequency in data capturing. But also, more intelligent filtering schemes may lead to more surviving data sets without loss of reliability or accuracy. The basic idea in both cases is to consider more parameters rather than a constant "one size fits them all" approach.

2. Practical experience with ISO 19030

As described earlier, the ISO 19030 is only intended for evaluating changes in the performance of ships, rather than for comparing absolute performance levels between ships. When evaluating coatings and other maintenance and retrofit activities however, one would often wish to compare the absolute performance of ships, and it is our experience, that the ISO analysis results are often used for this purpose, contrary to what is intended. This can lead to misinterpretations and calls for an alternative measure for absolute performance which is more directly related to the condition of the hull.

It is important to have enough data to average out statistical errors, but operational data should also cover a representative set of operational conditions. By applying strict filtering, it might occur that over a winter season there are thousands of valid 15 second intervals, but that these data sets cover only some hours of operation and a very specific operational condition which is no representative of the overall operational profile.

One of the basic guidelines of ISO 19030 has been to be practical. However, requiring high-frequency data logging contradicts current industry practice, where an estimated 85% of the world fleet does not have automatic data loggers. While automatic data logging is de facto standard on newbuildings, for years to come manual data logging will be a practical constraint in performance monitoring. The challenge is then to preserve as many usable data sets as possible, and more intelligent filtering, better data quality and better correction methods are keys to achieve this.

3. ECO Insight hull performance prediction

ECO Insight, http://performance.dnvgl.com, follows the default method in ISO 19030 Part 2 in some elements, but deviates in other elements using the leeway given in Part 3. The main differences between our approach and the default method are:

a) **We do not require a certain data frequency**
The method works with manual reported data as well as with high-frequency data logging. Based on our experience, for typical time periods one measurement per day is sufficient to eliminate errors introduced by typical reading inaccuracies. Using noon reporting has many drawbacks: Typically, weather data is reported as noon weather, while performance data is averaged over 24h. To overcome this, we recommend "snapshot" reporting. Here performance and weather data is averaged over a 15 min period. The period is chosen so that vessel, engine and rudder operate in steady state.

b) **We correct for sea water temperature**
Frictional resistance depends on sea water viscosity, which varies with temperature. Thus, we record the temperature and correct the measured power to an equivalent power at 15°. We compute viscosity by:

$$nu = 10^{-6}\,(0.0014 * S + (0.000645 * T - 0.0503) * \mathrm{T} + 1.75)$$

Where S is the salinity [$^{0}/_{00}$] and T the sea water temperature [°C]

c) **We apply vessel group specific weather corrections**
The ISO 19030 wind correction – as the ISO 15016 sea trial wind correction – is based on lateral area and a ship-type specific, but otherwise generic wind force coefficient. In our experience, the coefficients tend to overestimate the wind resistance significantly, sometimes by up to 40%. An excessive overestimation of wind forces leads to the paradoxical situation that due to over-correction the performance index may become better in harsh weather than in calm weather. By correlating the hull performance against wind conditions, we derive vessel group specific corrections. These cluster ship types and sizes into more coherent groups, thus reducing the scatter for actual wind force coefficients. This grey-box approach makes performance index less weather dependent. Smaller scatter equates better accuracy.

d) **We apply smarter wind filters**
Filtering for higher wind force (Bft) shall reduce the uncertainty in the performance index, which in turn is due to the uncertainty in the (direct and indirect) added resistance due to wind. The effect of the error in this added resistance depends on the portion it has in the total resistance. E.g. for low ship speed and strong headwind, the wind resistance can be 25% of the total resistance. Overestimating it by 40% would make the performance index ~10% too good. On the other hand, for high ship speed and wind from astern, the wind resistance may account for only 2% of the total resistance and overestimating by 40% would cause less than 1% error in the index. ISO 19030 recommends filtering only depending on wind speed, not considering wind direction or the ship speed for the filter threshold. We apply a filter considering also ship speed and wind direction. This leads to many more surviving data sets without global loss of accuracy. See Fig 4 for illustration.

e) **We reduce the speed dependency in the performance indicator**
Calm-water ship resistance can be decomposed into wave resistance, viscous pressure resistance and frictional resistance. Hull fouling dominantly affects the frictional resistance, to a lesser extent the viscous pressure resistance. For simplicity, viscous pressure resistance and frictional resistance are grouped together in the viscous resistance.

At high speed, and partial draft, wave-generating and viscous resistance components are about 50:50 distributed for a containership. Thus, we have e.g. P_w=10 MW wave-generating power and P_v=10 MW viscous power demand. Now, let hull fouling increase the viscous resistance by 20%, leading to a viscous power of $P_{v,fouled}$=12 MW. We can then express the ratio between the ideal (unfouled) condition and the present (fouled) conditions as the hull performance index HPI = (10 MW+10 MW)/(10 MW+12 MW) = 91%.

At very slow speed, the ratio between wave resistance and viscous resistance may be 10:90, say P_w=0.1 MW and P_v=0.9 MW. 20% increase in viscous resistance due to fouling then leads to $P_{v,fouled}$=1.08 MW, and hence HPI = (0.1 MW+0.9 MW)/(0.1 MW+1.08 MW) = 85%.

This simple example demonstrates that the Index based on total power depends on the ratio of wave and viscous resistance. This ratio varies with vessel speed. From many CFD calculations, we know the resistance components and can calculate the index on the viscous part only which gives a more realistic and less speed dependent value. Our index is $HPI_v = P_{v,ideal}/(P_{meas}-P_{w,ideal})$.

f) **We apply a machine learning (ML) correction to account for effects not modelled**
Even after applying all mentioned measures, we still see systematic biases in data. E.g. at design speed the performance index is very realistic, but at slow steaming the index is too small. These effects come from complex hydrodynamic effects (e.g. drifting and flow separation in front of the propeller). These effects are not present in sea trials. The effects depend on speed, draft, drift angle, trim and propeller RPM. To cover all relevant combinations of these parameters for the range of operating conditions, more than 4000 CFD simulations including complex propeller modelling would be required. A cheaper approach is used here. We compute these effects based on the data we have in our database, employing also data from similar ships.

4. Results

In the following, we compare results obtained by the ISO default method with results obtained by the DNV GL method. We apply the ISO default method also to manually recorded data and present the results in terms of the hull performance index:

$$\text{HPI} = \frac{\boldsymbol{Ideal\ Power}}{\boldsymbol{Corr.\ meas.\ Power}}$$

The hull performance index translates into the ISO 19030 Power Performance Value (PPV):

$$\text{PPV} = \frac{Corr.meas.Power - Ideal\ Power}{Ideal\ Power} = \frac{1}{HPI} - 1$$

The DNV GL method is based on an index derived from the viscous components only:

$$\text{HPI}_v = \frac{\boldsymbol{Ideal\ Power - wave\ Power}}{\boldsymbol{Corr.\ meas.\ Power - wave\ Power}}$$

Fig.1 shows HPI following ISO 19030 and the DNV GL method for a tanker. In the middle of the monitoring period, a new paint coating was applied. For the ISO 19030 default method, the data shows an increasing hull performance in the first period and a level of ~85% after the application of new paint. For the DNV GL method, there are more data points left after filtering. The trend in the first period is more realistic and the level after application of new paint is ~97% which is also more realistic. Fig.2 compares the two methods for a containership with snapshot reporting. Data is relatively sparse and the level of HPI is lower than expected for the ISO 19030 default method. For the DNV GL method, more data points are left after filtering and the level of the index is more realistic.

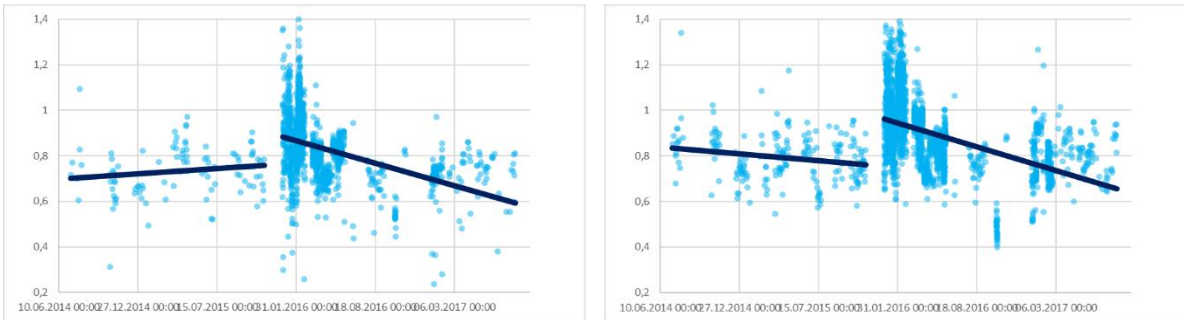

Fig.1: Hull Performance Index following ISO 19030 (left) and DNV GL method (right) for a tanker

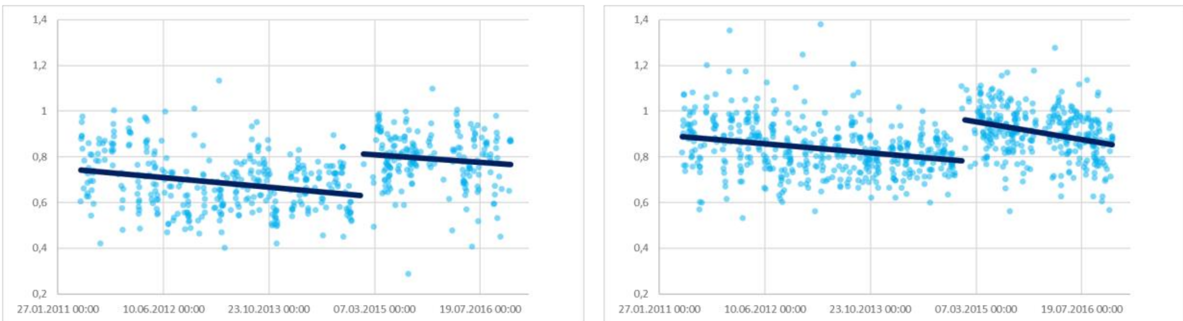

Fig.2: As Fig.1, but for a containership

Fig.5. shows the performance index over the speed. For data processed according to ISO 19030 the performance index is speed dependent. For the same data processed with the DNVGL method the data is not speed depended.

5. Conclusions

ISO 19030 provides a solid basis for performing hull performance prediction. The proposed default method can quantify changes in hull performance. However, the dependence of the ISO 19030 default method on high-frequency data logging limits its practical value for ships with manual logging. Data processed by the default method shows a speed dependency, e.g. giving a higher hull performance index at high speed and lower index at low speed for same ship and fouling condition. Using the viscous Hull Performance Index for performance evaluation has at least two advantages compared to the normal Hull Performance Index and the ISO 19030 PPV:

1. It is a direct measure for the increase in the frictional resistance alone (assuming limited propeller degradation) rather than the increase in the total resistance. This makes it more suited for comparing different ships and different coating technologies, since it eliminates the ship specific element.
2. It eliminates (most of) the speed dependence of the index arising from the difference at varying speeds in the relative magnitudes of wave and frictional resistances.

On the other hand, while the pure ISO 19030 method is relatively straight forward to adopt, the HPIv method requires a more complex ship model which requires more know-how and access to a lot of ship model or CFD data.

In the above, we have proposed simple extensions to the ISO 19030 default method addressing these shortcomings. The proposed changes are in line with Part 3. The changes implemented in our DNV GL method yield more realistic hull performance values, both for the relative change over time and the absolute performance levels, for manually reported low-frequency data logging.

References

BERTRAM, V. (2016*), Added Power in Waves – Time to Stop Lying (to Ourselves)*, 1st HullPIC Conf., Pavone, pp.5-13

BERTRAM, V. (2016*), Some Heretic Thoughts on ISO 19030*, 2nd HullPIC Conf., Ulrichshusen, pp.4.11

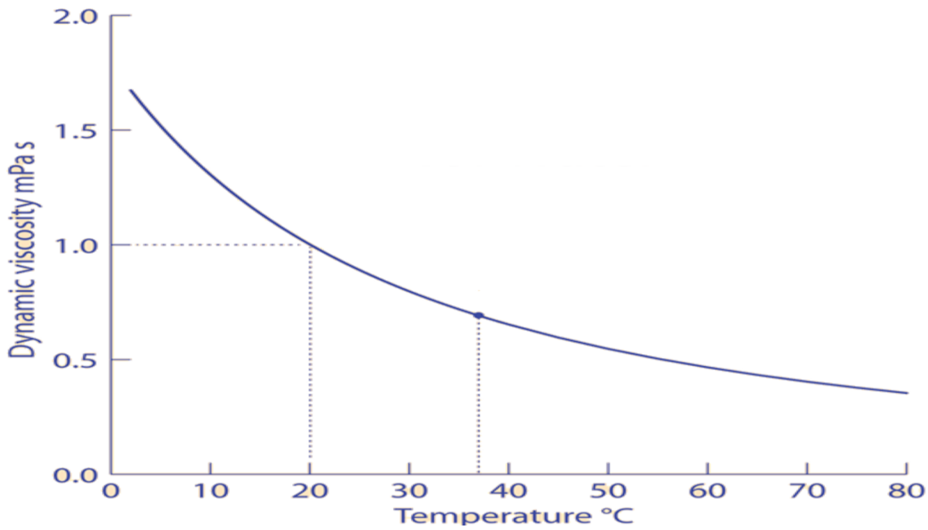

Fig.3: Water viscosity depending on temperature

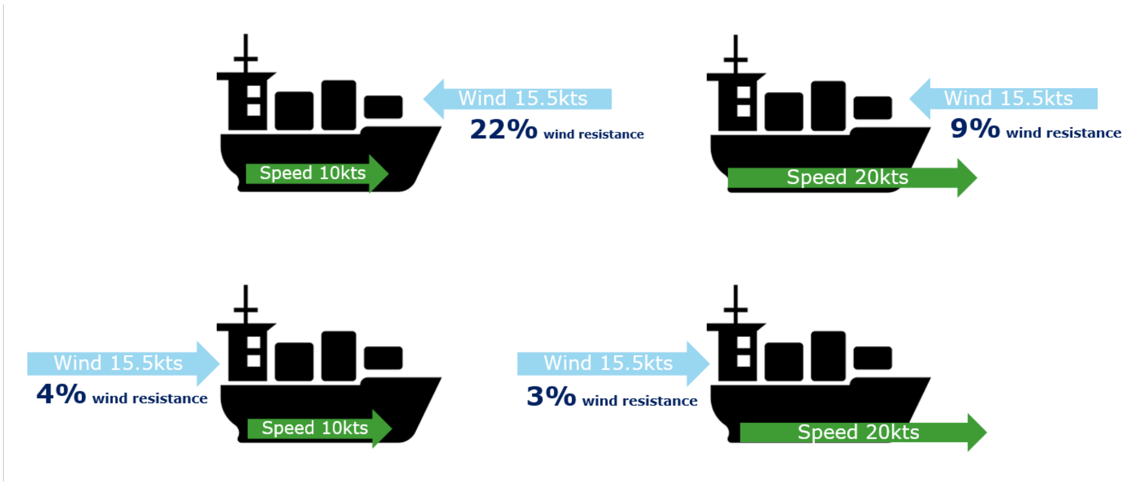

Fig.4: Added resistance depending on wind direction and vessels speed

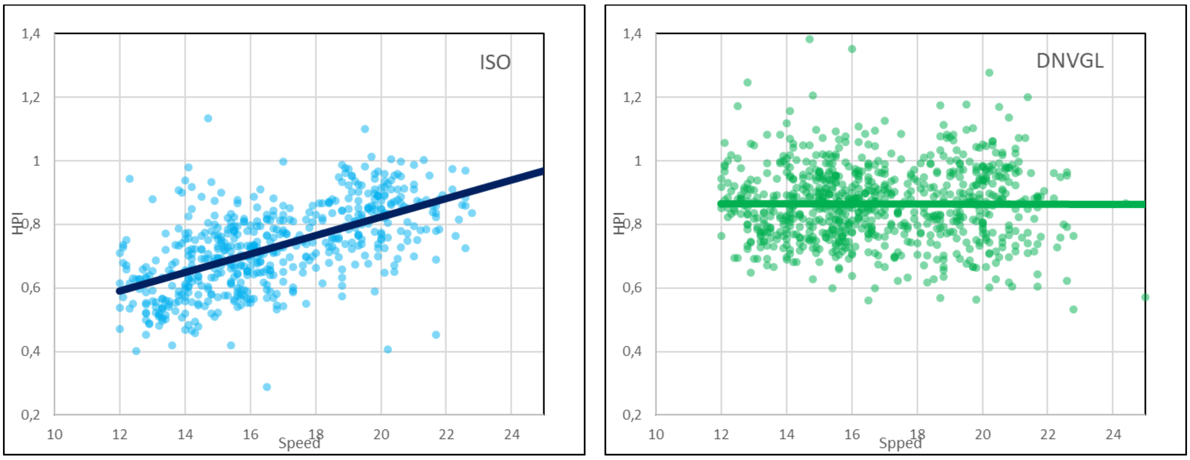

Fig.5: Hull Performance Index HPI over vessel speed for ISO 19030 default method (left) and DNV GL method (right)

Thrust Measurements during Sea Trials – Opportunities, Challenges and Restrictions

JanWienke, DNV GL, Hamburg/Germany, jan.wienke@dnvgl.com

Abstract

This paper gives two examples of thrust measurements during speed trials and during a series of speed trials with trim variation. Besides, time series of a gale passage are presented. The thrust meter is strain gauge based; amplification and calibration, disturbance by torque and the zero setting stability are critical parameters which have to be controlled.

1. Introduction

For non-permanent shaft power measurements, the application of strain gauges is the common measuring principle. This standard method for torque measurements was extended to measure the thrust on the propeller shaft as well. Basically, this can simply be realized by turning the alignment of the strain gauges by 45°.

The first challenge of the thrust measurement results from the fact that the thrust signals are lower by a factor of ten compared to the torque measurement. Accurate amplifiers and sophisticated calibration procedures are required. Additionally, the torque superposes the thrust when the measuring device is not properly installed, already resulting in large measuring faults for a small angle deviation of the strain gauges. Special strain gauge arrangements and the combination of three different strain gauge applications allow compensating this effect. The third challenge is the zero setting. The zero-point must be adjusted for a turning shaft.

These three challenges affect the trueness (absolute accuracy) of the thrust measurement. For shaft power meter the accuracy is commonly around 1.5%, but for the thrust measurement the uncertainty is up to 10%.

The next challenge is the long-term stability of the thrust measurement. Zero drifting occurs which is partly related to temperature changes of the shaft. Temperature monitoring and the combination of different strain gauge arrangements allow identifying time intervals of stable thrust measurements.

The zero drifting reduces the precision (relative accuracy) of the thrust measurement. For permanent thrust meter to monitor hull performance this precision is the restricting characteristic, but for the non-permanent installation proper time intervals can usually be chosen.

During newbuilding sea trials the model test performance prediction is verified in full scale. Speed tests are performed to check the speed – power curve. A reliable measurement of the thrust at the same time allows verifying the predicted propulsive efficiency. But an uncertainty of 10% is too large to perform a reliable verification of model test values.

A more promising application of the non-permanent thrust measurement is to compare different conditions during sea trials. This includes different operational conditions like different shaft speeds and propeller pitch settings, but also different drafts or trim settings. Examples of thrust measurements for different conditions are given in the following.

Besides, the influence of the weather conditions can be evaluated. The measured propeller shaft thrust of a large container vessel during a gale passage with up to 12 Bft within an interval of 36 hours is presented.

2. The strain gauge arrangement

For thrust measurements a combination of three different strain gauge arrangements is installed on the shaft, *Uto (1998)*: A torque measuring full-bridge arrangement with strain gauges in an angle of 45° referred to the shaft axis, a conventional thrust measuring full-bridge arrangement with strain gauges along and rectangular to the shaft axis and a so-called Hylaridis arrangement, *Hylaridis (1974)*.

For the Hylaridis arrangement two strain gauges which are arranged in an angle of 90° are combined for two parts of the full-bridge, the other two parts of the bridge contain passive resistances. This arrangement compensates any influence of torque and is applied to correct the thrust measured with the conventional measuring set-up with regard to the measured torque.

The three combined strain gauge arrangements are sketched in Fig.1 and a photo of an installation is shown. For the combination of the three strain gauge arrangements a common 4-channel telemetry is applied. The telemetry is powered by batteries. The fourth channel is used for a temperature measurement on the shaft with a resistance temperature detector of type PT-100.

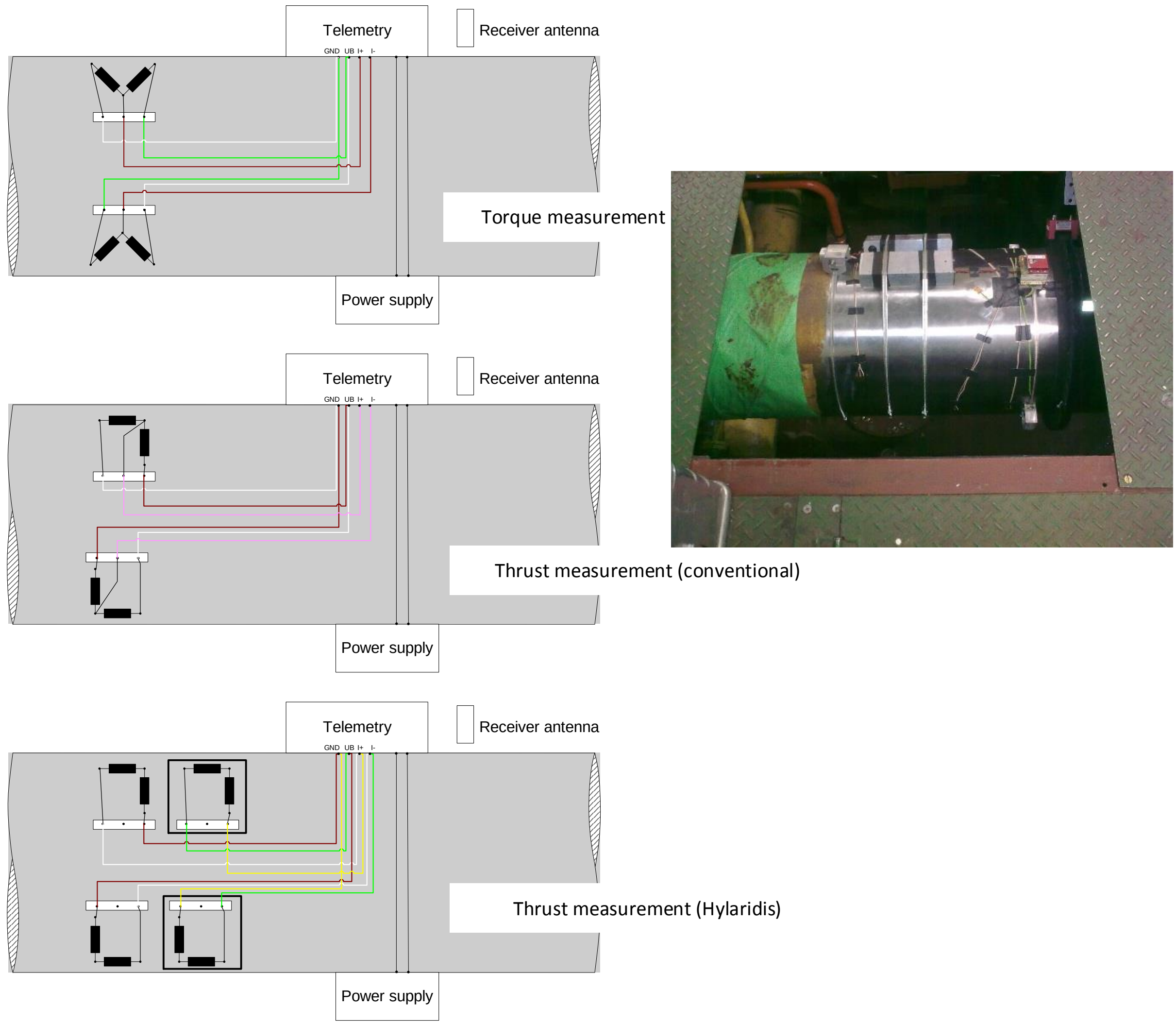

Fig.1: Combination of 3 different strain gauge arrangements

3. Mile runs

During sea trials the ship performance is identified by speed trials according to ISO 15016. Double runs with reciprocal heading are performed for different engine settings. For each engine setting the shaft speed is kept constant for both runs. The heading is chosen to get wind and waves directly from ahead or from astern respectively.

In Fig.2 the measured thrust and torque are presented for a series of six mile runs with three different engine settings. The duration of each mile run is 10 minutes, measuring frequency is 1 Hz, so that each cloud contains 600 measuring points. The blue (63 rpm), red/orange (72 rpm) and green (80 rpm) dots represent one engine setting. In each case the lower cloud represents the run with wind and waves from astern, whereas the upper cloud is the run against wind and waves. It is obvious that the clouds of the runs with wind and waves from astern are on a common regression line, but the regression lines of the runs headed into wind and waves have a lower slope and are in parallel to each other.

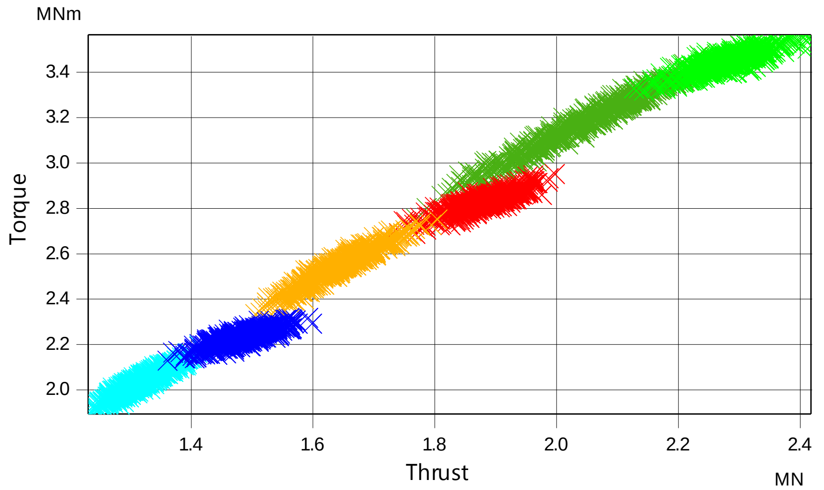

Fig.2: Thrust and torque during six mile runs

To understand the orientation of the clouds in Fig.2 the according time series of the propeller speed are plotted in Fig.3. The colour of the lines is in agreement with the colour of the dots in Fig.2. For the runs with wind and waves from astern the shaft speed is varying slowly with larger amplitudes, for the reciprocal heading the variation of shaft speed is faster with lower amplitudes.

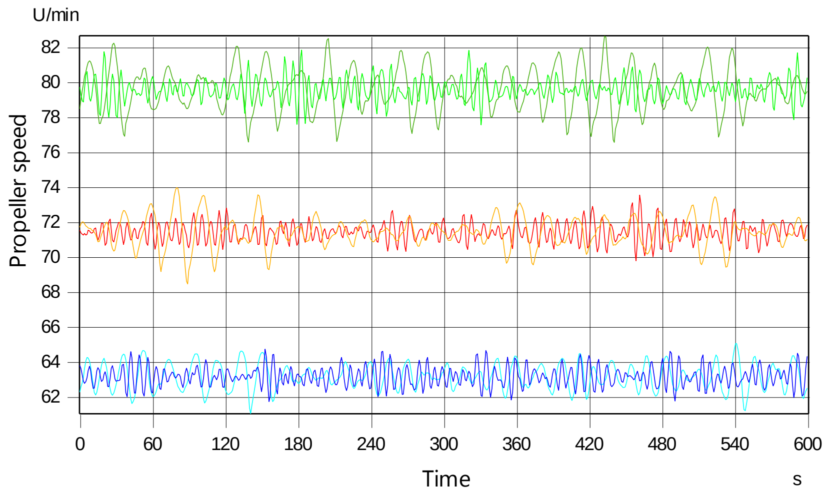

Fig.3: Propeller speed variation during mile runs

When running with wind and waves from astern, the propeller is operating on the same propeller curve with constant light/heavy running margin (constant relation between torque and thrust); thrust and torque vary in agreement with the slow shaft speed variation. The regression line through the three clouds represents the thrust torque relation for this propeller curve.

It is different for the runs against wind and waves. The variation in thrust and torque is not following the shaft speed variation; the regression through these curves represents the load variation with a heavier running propeller. The regression lines through the three clouds are in parallel to each other, meaning that the load variation factors are about the same for the different engine settings.

For further analysis, the thrust and torque coefficients are determined for each measuring point and plotted in Fig.4.

$$K_T = \frac{T}{\rho \cdot n^2 \cdot D^4}$$

$$K_Q = \frac{Q}{\rho \cdot n^2 \cdot D^5}$$

The calculated points of all 6 mile runs are in agreement with a single regression line. The runs with wind and waves from astern are in the lower part of this regression curve and the runs against wind and waves are combined at the top of the curve. This presentation is in agreement with the propeller characteristics and allows a reliability check of the measured data.

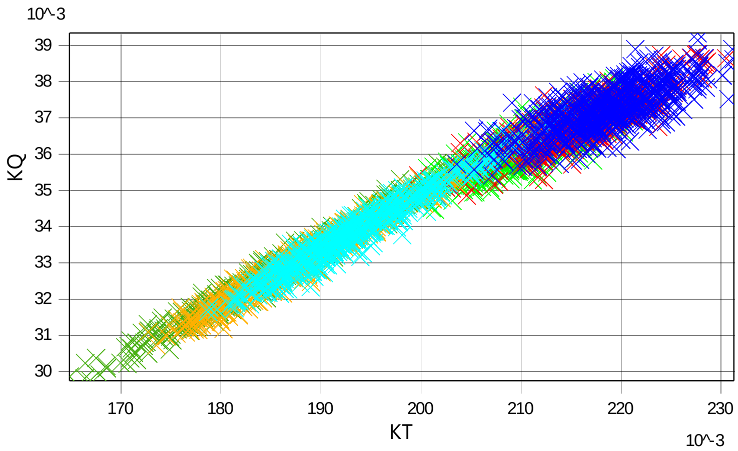

Fig.4: Thrust and torque coefficient during mile runs

4. Trim variation

Sea trials with a vessel in service were performed to evaluate the ship performance for trim variation. The vessel is a large container vessel with a length of 350 m. The mean draft during the measurements was 14.5 m. Three different trim settings were investigated: A trim by 1 m to the aft, the even keel condition and a trim of 1 m to the fore.

The weather conditions during all mile runs were fine and similar; each with low wind of 2-3 Bft and smooth sea with sea state 2. For each trim setting a series of 6 mile runs was performed; each time double runs with 70 rpm, 77 rpm and 86 rpm were carried out. The measuring frequency was 1 Hz, measuring time was 10 minutes for each run, meaning 600 measuring points were registered each time.

The thrust and torque values are combined in Fig.5 for the 18 mile runs. The clouds for the even keel condition and the fore trim are in good agreement, only the cloud of the aft trim is above the other clouds.

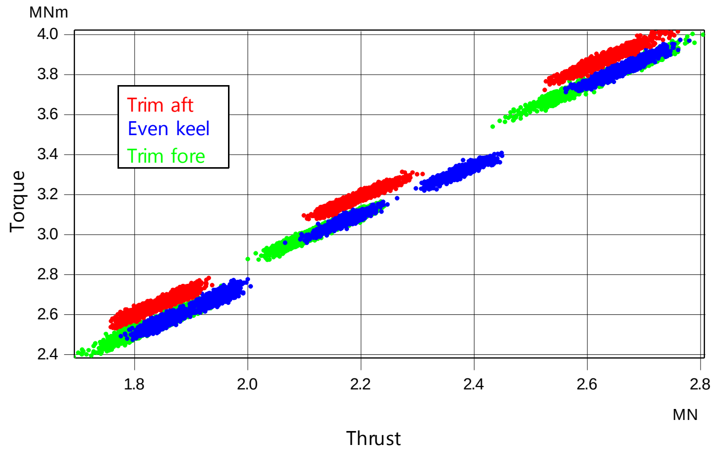

Fig.5: Series of mile runs for different trim settings

The reduction of data to the mean values of each double run is shown in Fig.6. The lines of the even keel condition and the fore trim are close to each other, only the line for the aft trim differs. The comparison of the even keel condition and the fore trim shows that the points of constant shaft speed are shifted to lower values for the fore trim setting. This means that the resistance is reduced for the fore trim.

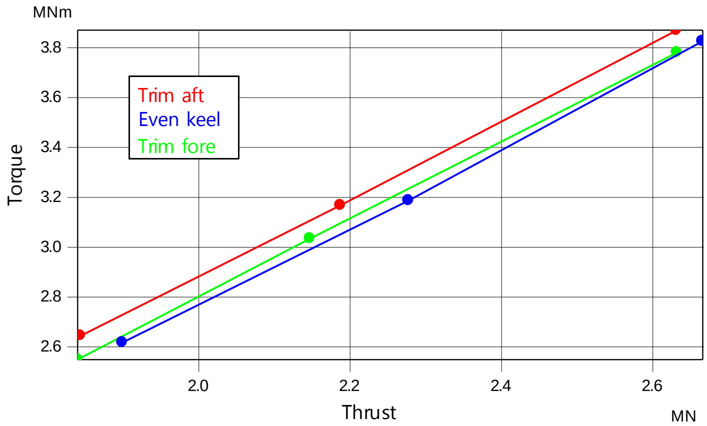

Fig.6: Mean values of each double run

The corresponding thrust and torque coefficients of each measuring point are calculated and are presented in Fig.7.

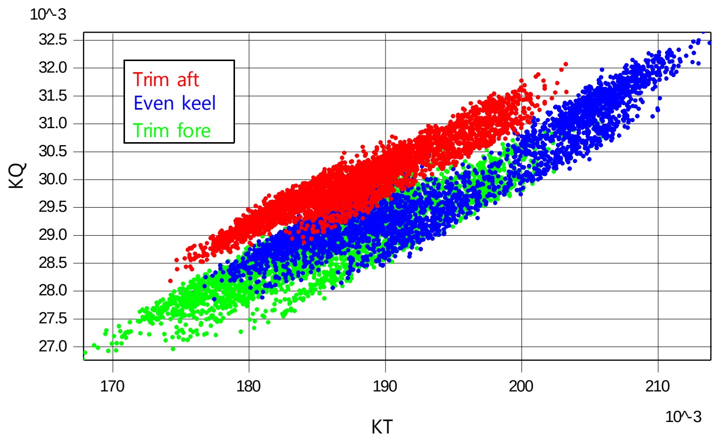

Fig.7: Thrust and torque coefficient for different draft settings

Again, even keel and fore trim condition show good agreement but the aft trim condition differs. It is expected that the curve of the thrust and torque coefficients agree for all measurements. Therefore, this is an indication that the measurement for the aft trim condition is not fully reliable. It must be noted that the aft trim measurement was performed two days prior the investigation of the other two trim settings. For the even keel and aft trim condition the mile runs were performed at the same day with only a break of 1 hour for the trim change. Therefore, it is supposed that a slight zero drifting of the thrust measurement occurred in the period between the aft trim mile runs and the other mile runs.

A dynamic correction of the zero setting of the thrust measurement with regard to the thrust and torque coefficient curve might help to get a stable thrust measurement. The zero setting is influenced by a lot of parameter as temperature and shaft position between the bearings which are not fully observed. The correction according to the thrust and torque coefficients compensates the unknown effects. Nevertheless, it is doubtful whether this correction is sufficient to get a zero stable, strain gauge based thrust measurement for a longer period.

5. Gale passage

During a loading voyage a vessel with an installed torque and thrustmeter passed a heavy storm with wind speeds up to 12 Bft. In Fig.8 time series of selected measured values are shown for this passage. The interval is 36 hours and the measuring frequency is 1 Hz. The measured power, shaft speed, torque and thrust are plotted, as well as the ship speed through water, the relative wind speed and angle and the dynamic trim.

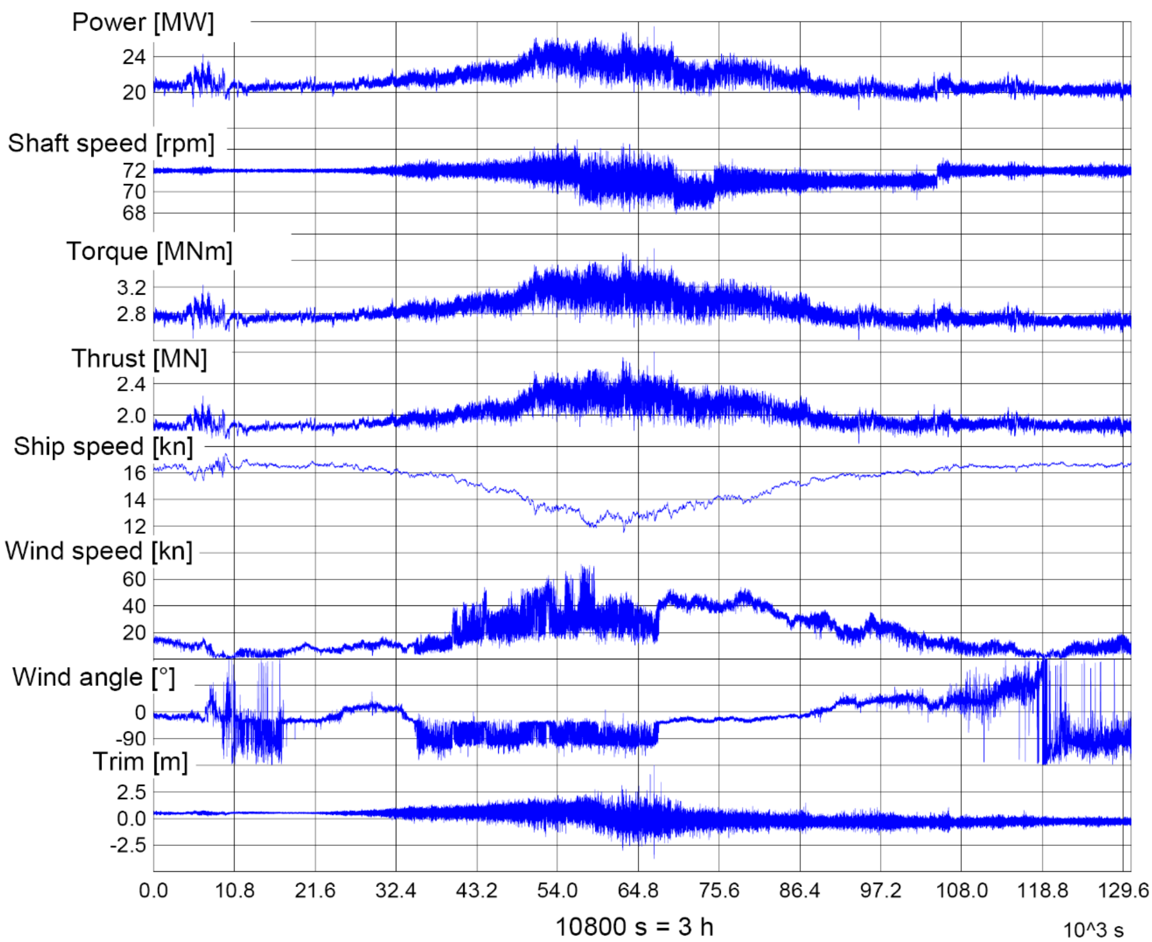

Fig.8: Time series for an interval of 36 hours

It can be seen that power, torque and thrust were increasing when the wind speed rose. At the same time the speed through water was decreasing. Besides, the vessel started pitching and a fluctuation of the shaft speed occurred. After 16 hours according to the time axis of the presentation in Fig.8 the shaft speed was reduced by the crew. Approximately 3 hours later the crew changed the course of the vessel by 10°. The shaft speed was reduced once more and the pitching was decreasing. After another 1.5 hours the shaft speed was slightly increased and 2 hours later the wind speed started to go down. 29 hours after beginning of the time series the shaft speed was set to the same value as at the beginning. The wind speed was down and power, torque and thrust were on the original level again.

During the gale passage the thrust was increasing by 32% due to the wind. Regarding the oscillation of the thrust due to waves, a total increase of even 48% was observed while the shaft speed was reduced by 1 rpm at the same time.

The measured torque and thrust values for the 36 hours during the gale passage are combined plotted in a thrust - torque diagram which is shown in Fig.9.

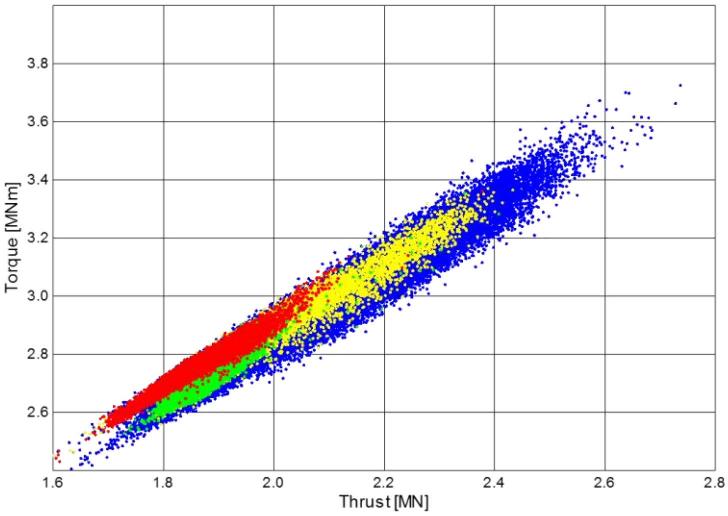

Fig.9: Thrust - torque diagram for the gale passage

For an analysis of the thrust - torque diagram only the points for the constant approach shaft speed of 72 rpm with a range of ±0.1 rpm are considered. These are all points of the diagram without the blue ones. For the constant shaft speed the breadth of the cloud is almost the same, only the part of the cloud for high torque / thrust values is separated.

During the storm the autopilot had to apply large rudder angles up to 18° to keep course. In the next step of the analysis all points with rudder angles larger than 3° are dropped off. The remaining green and red dots are in the area of lower torque / thrust values, but the cloud almost keeps its breadth. Again, only the part of the cloud for high torque / thrust values is separated. This is of course an obvious fact that the larger rudder angles will give an additional resistance.

For the last subdivision the trim is considered. All points with a trim of 0.5 m aft within a tolerance of ±0.3 m have a red colour. Points with a different trim are green. This time the separation is different than the two times before where the high torque / thrust part was cut off. In this case the separation is along a line of the torque – thrust relation, meaning that points with less loaded propeller (red dots) were separated. The trim of 0.5 m aft was the approach trim. The time series of the trim in Fig.8 show that the trim of the vessel was changed during the storm and the trim was -0.4 m fore at the end of the time series.

6. Conclusions

The experience with the strain gauge based thrust meter shows that extensive effort is required to realize precise (long-term stable) thrust measurements based on strain gauge applications. Other measuring principles like optical or magnetostrictive methods might be superior. But for these methods the zero setting and potential drifting are a challenge as well. It is not only the sensor characteristic that reduces the long-term stability of the thrust measurement but also the condition of the shaft which might change due to temperature or different position in the bearings.

References

HYLARIDIS (1974), *Thrust measurement by strain gauge without the influence of torque*, Shipping World & Shipbuilder

UTO, S.; NARITA, S. (1998), *Experimental study on the propulsive performance of icebreaker PLH "Soya"*, The Japan Society of Naval Architects and Ocean Engineers 229, pp.45-50

Different Approaches in Vessel Performance Monitoring, Balancing Accuracy, Effectiveness & Investment Aspects, from the Operator's Point of View

Antonios Tzamaloukas, Stefanos Glaros, Kerasia Bikli, Eastern Mediterranean Maritime, Glyfada/Greece, antontz@eastmed.gr

Abstract

Eastern Mediterranean Maritime Ltd. (EMM) uses an in-house methodology based on traditional Noon Reports, including data pre-processing, filtering, corrections to good weather conditions and evaluation. Despite inevitable errors by Noon Reports, this method has been proven to fit the intended purpose, which is mainly to identify trends. As a measure to overcome inherent drawbacks and limitations, the concept of 'Additional Technical Performance Reporting' has been conceived and applied in parallel with the traditional Noon reports. This concept, familiar in shipping industry from the sea trials, involves recording of performance parameters for a specified time period with relatively constant operating and weather conditions. In order to evaluate the concept and effectiveness of the 'in house methodology' and also to have a feedback from Big Data Methods for possible future adaptation, an 'Automatic Data Collection System' including performance evaluation features, of well-known maker, was installed and tested onboard four sister Aframax Tankers. The obtained figures and records were compared, concluding that 'Additional Technical Performance Reporting' measurements' accuracy approaches 'Automatic Data Collection System' accuracy, avoiding Noon Reports disadvantages and providing an alternative to the 'Automatic Data Collection Systems'.

1. Introduction

In the last few years, considerable attention has been raised towards the reduction of the Green House Gas (GHG) emissions in order to control levels anticipated within the next decades and the resulting impact on climate change. There has been a growing interest in the shipping industry, the International Maritime Organization (IMO) and governments globally to operate ships more efficiently, *MEPC (2012,2016a,b), MRV (2015)*.

In the quest of efficient ship operations, the monitoring of fuel consumption has been compulsory through Ship Energy Efficiency Management Plan (SEEMP), *MEPC (2016a)*, EU Monitoring Reporting and Verification Regulation (MRV), *MRV (2015)*, and the forthcoming IMO Data Collection System (DCS), *MEPC (2016b)*, and the performance evaluation systems have been gaining increased importance.

There is a variety of performance evaluation methodologies based on noon reports data, e.g. *Glaros et al. (2015), Bialystocki and Konovessis (2016),* DNV GL's Navigator Insight, automatically logged data, e.g. ISO 19030, *Lund and Gonzalez (2017),* and alternative methods of combining noon reports with high-frequency data, e.g. *Antola et al. (2017)*. However, several practical questions arise when dealing with a practical, feasible, economic and accurate performance evaluation system.

Eastern Mediterranean Maritime Ltd. (EMM) has been developed, applied and tested a systematic performance evaluation methodology using Noon Reports as data source, *Glaros et al. (2015)*. In addition, the concept of 'Additional Technical Performance Reporting' has been evolved and applied in parallel with the traditional Noon reports. In parallel, in order to evaluate the effectiveness of the 'in house methodology', to estimate accuracy improvement with the introduction of the new reporting scheme, and finally to have a feedback from Big Data Methods, an 'Automatic Data Collection System' of well-known maker, was installed and tested onboard four sister Aframax Tankers.

The purpose of this paper is to share the results of the in- house comparison of the different approaches in vessels' performance evaluation.

2. Applied EMM Methodology

EMM has developed a methodology for systematic fleet performance monitoring and evaluation based on performance data collected through traditional daily Noon Reports. The methodology's main concept involves the correction of actual/measured data to some equivalents that correspond to ideal conditions, i.e. clear weather, no current and at specific design or ballast draft, *Glaros et al. (2015)*. The implementation takes place in four main stages, namely data preprocessing/setup, data filtering, corrections and calculation of equivalent data and analysis, Fig.1, *Glaros et al. (2015)*.

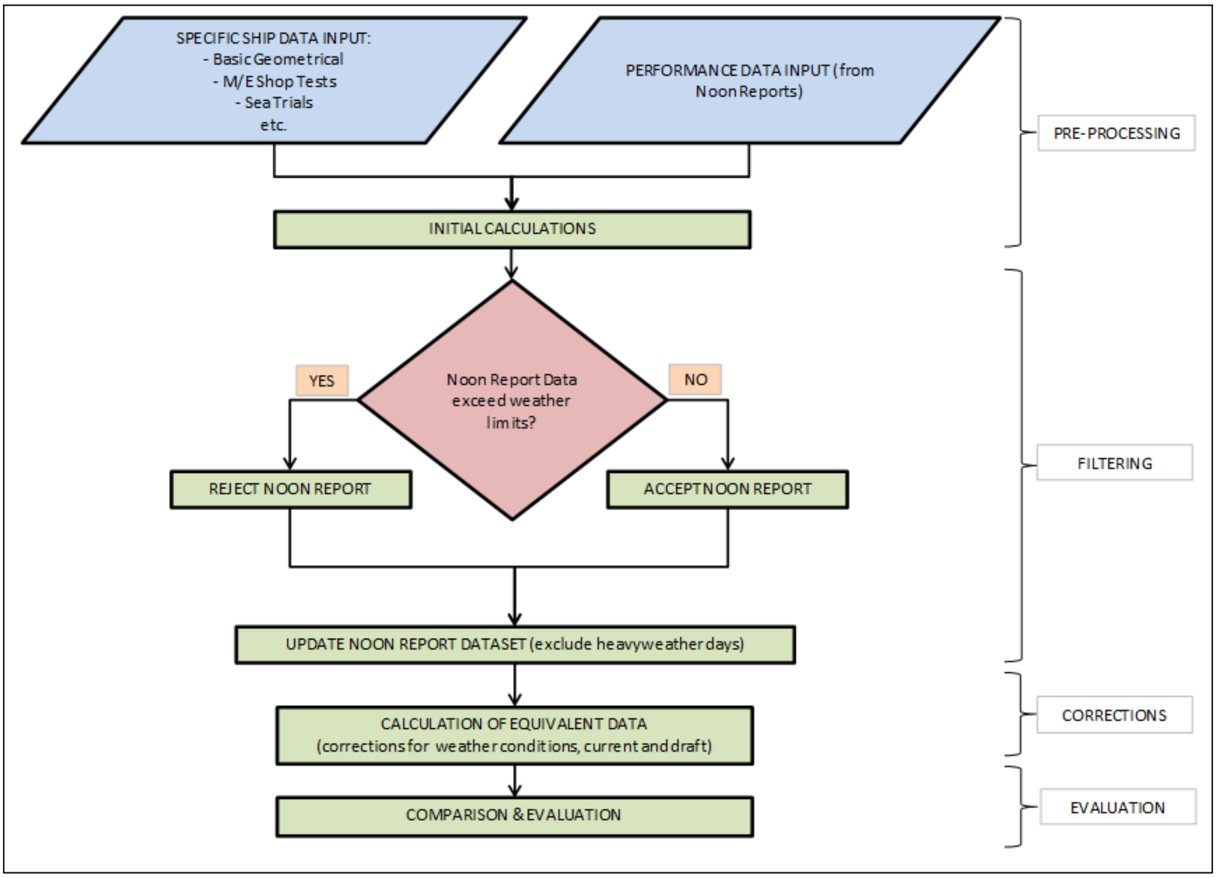

Fig.1: Method flowchart

Data preprocessing includes a set of preliminary calculations, prerequisite to the analysis for each vessel. The required dataset contains parameters related to specific vessel main dimensions, sea trials, model tests and main engine and auxiliary engines power and consumption curves. Performance data are drawn from Noon Reports prepared by the vessel at daily intervals.

Data filtering refers to evident erroneous reporting and to checking if weather conditions exceed some pre-defined thresholds that represent relatively good weather conditions, *Glaros et al. (2015), ISO 15016 (2015), Ainsworth (2006).*

Corrections stage is related to calculation of equivalent data, i.e. the conditional vessel performance at no weather conditions, applying the empirical relations of *Kwon (2008)*, along with corrections for current and draft.

Evaluation is applied through the comparison of corrections results to reference curves, as drawn at data preprocessing stage.

The methodology has been implemented for a three years' period for the entire company's fleet acting as the main tool for the compilation of the weekly performance evaluation report which is circulated internally in order to raise attention of the concerned parties if any issue such as erroneous reporting, under-performance or overconsumption is observed. The methodology application has also revealed weaknesses, mainly related to Noon Reports data inaccuracy that influences significantly the obtained results quality. Recognizing this weakness, alternatives were evaluated for the data source.

3. Problems with Noon Reports

The Noon reports were, and still are, the common reporting scheme worldwide from vessels to Operators and Charterers. For this reason, Noon Reports are used traditionally as the basis for any performance analysis, since no changes in the reporting is required. The most common disadvantage of utilizing Noon Reports as data source for vessels performance analysis is the inaccuracy involved which is mainly attributed to:

I. Problems associated with variations and average values

- Average values for RPM and Speed
  Although one average value is reported for RPM and speed, it does not mean that these two operational parameters remain constant during the 24-hour period covered by the report. Depending on the operational instruction for constant RPM or constant speed, one or both parameters may vary, to an extend that reduce significantly reporting accuracy.

- Average values for M/E load indications
  Although M/E load indications (i.e.: M/E Power, Pump Mark, Load Indicator and M/E load) are strongly related to consumption analysis, vary during the reporting period, but are reported as an average.

- Average weather and sea conditions
  Although the wind, waves, swell and currents normally fluctuate significantly during the reported period, representative average indications supposed to be reported. In addition, this dubious task is also performed by deck officers onboard without specialization in weather reporting. In Fig.2, a typical example of difference between ‘average’ weather conditions of Noon Report and actual weather conditions as obtained from a weather company is demonstrated.

- Fuel consumption
  The only parameter that is not averaged is the total fuel consumption, which is correlated with other parameters’ averages.

II. Unintentional errors

- Weather and sea conditions
  The wind, waves, swell and currents are usually entries of each Bridge swift in the log book. From these entries, only the wind speed and current can be obtained from instruments outputs, while the waves and swell height figures based on visual observations, which is highly questionable.

- Mixing the required reports
  Two or more ‘performance reports’ are required to be sent to different recipients, i.e. the operator and the involved charterers. These reports may have different formats and this complexity often leads to wrong reporting of different parameters to different reports.

- Human errors
  As the reporting is based on manual entries, the unintentional mistakes are unavoidable.

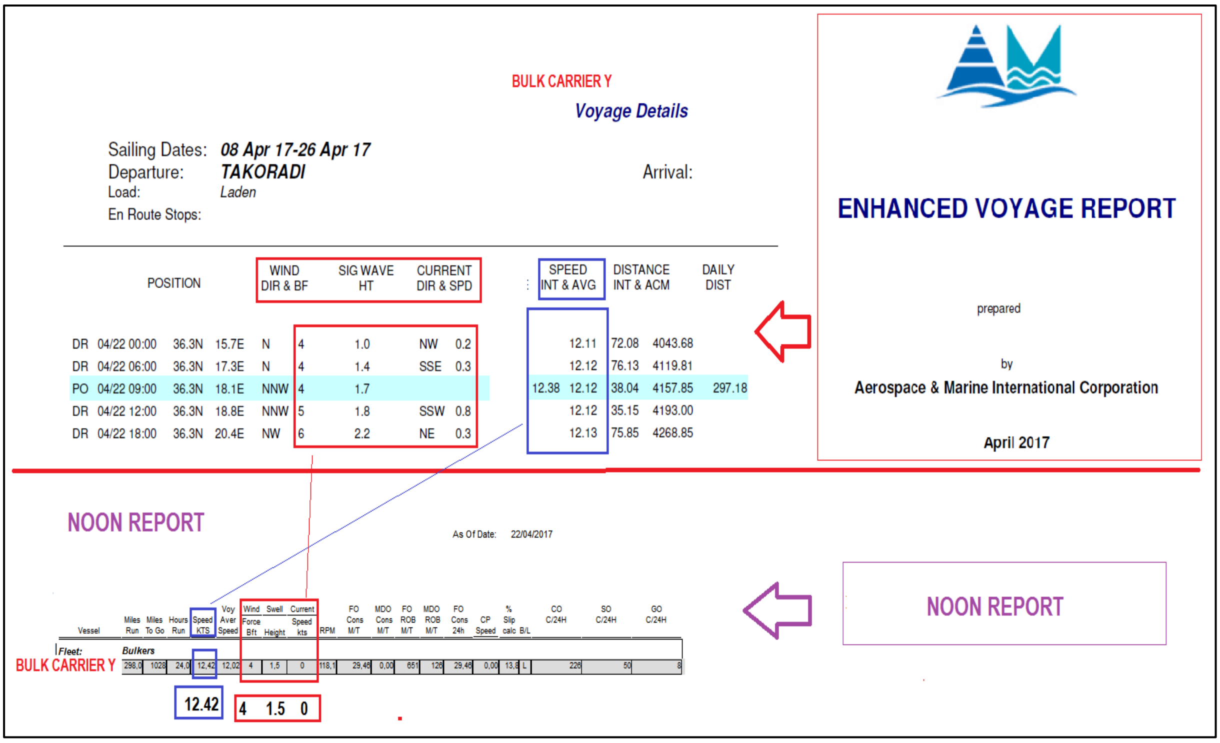

Fig.2: Differences in weather reporting

III. Intentional false reporting

Provided the fact that Noon Reports are compiled manually, it can be falsified to serve intended purposes.

- Speed reporting
  In cases where the operational advice is ‘constant speed’ and ordered speed maintenance becomes automatically a Key Performance Index, the ordered speed is often reported instead of actual. As shown in Fig.3, referring to a Bulk Carrier, constant speed was reported for a range of Fuel Oil Consumption (FOC) and constant FOC was reported for a range of vessel speeds, which are both obviously wrong. In this case, the reported slip is also wrong. Same can occur due to mixing of reports where the time Charter Speed is also reported in the Noon Report.

- Deviations from fuel economy measures and SEEMP best practices
  Sometimes the unjustifiable fuel consumption of various consumers is attributed to the M/E so that undesirable practices are not reported. A wrong cargo heating strategy, a bad discharging planning for a tanker vessel or the necessity for water production utilizing steam due to wrong water management, can easily result in the attribution of the consequent consumptions to the M/E consumption during a long voyage. In this way, crew members, who may not advocate the appropriate energy saving and environmental practices, may avoid time consuming feedback and explanations, to the involved departments of the operating company.

- Shortages in bunkering
  Shortages in bunkered fuel quantities is a common scenario for shipping. Such shortages can be either intentional or accidental from vessel crew or supplier. Irrespective of the reason, many times it leads to intentionally wrong fuel consumption reporting in order to cover the actual difference of the bunkers quantity onboard.

For all the above reasons, it is evident that Noon reports are essentially introducing high uncertainty, if used as input data for analysis. This fact reflects also EMM experience in performance monitoring based on Noon Reports, and is irrelevant to any attempt to introduce more reported data/parameters in the Noon Reports for better cross checking and verification. The uncertainty level can be such may lead to inclusive results of performance evaluation, even after careful filtering and conditional corrections.

After this realization the necessity for some countermeasures towards better accuracy became evident. In this direction, it was decided to proceed in two directions as a pilot study for future fleet level adaptation in EMM, differing significantly in terms of cost. The two alternatives examined are the 'Automatic Data Collection System' and 'Additional Technical Performance Reporting'.

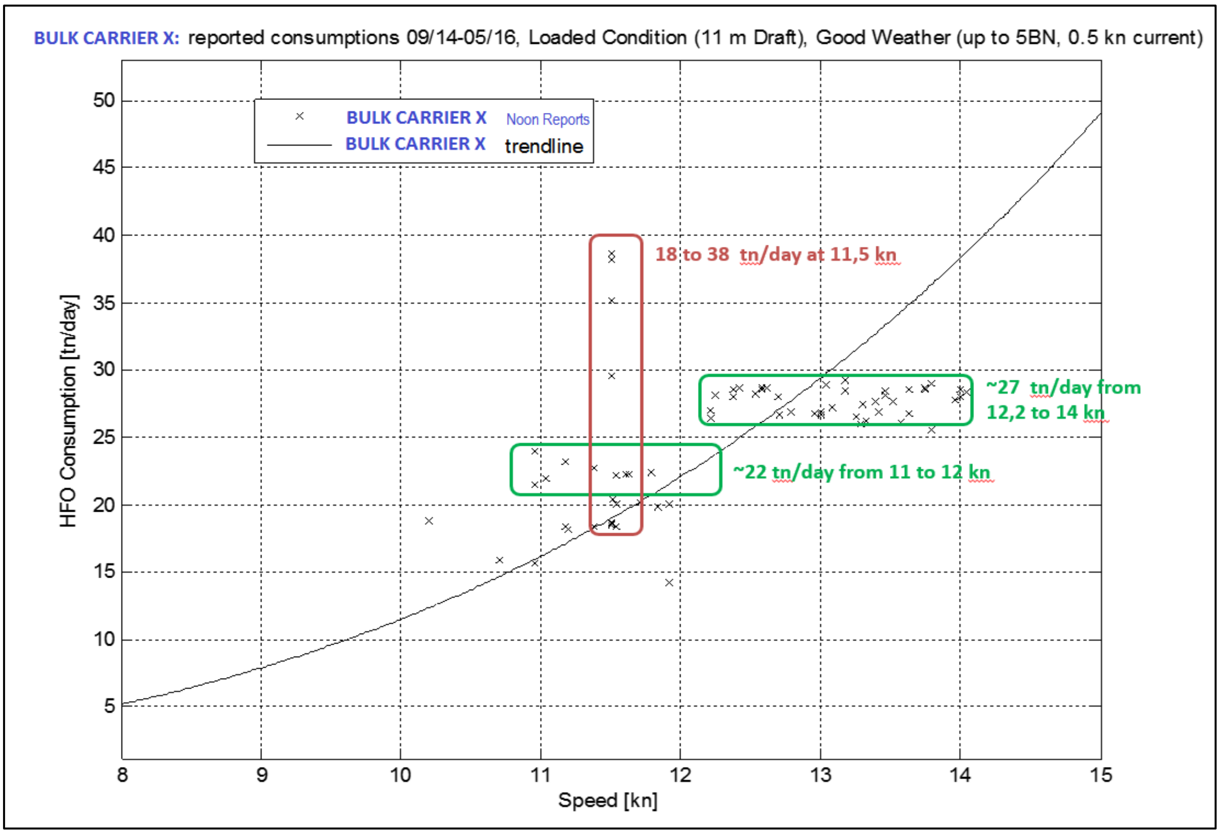

Fig.3: Typical Example of erroneous speed/FOC reporting

4. 'Automatic Data Collection System'

The increasing trend towards installation of 'Automatic Data Collection System's is supported by the recently published ISO 19030 standard and also by *OCIMF (2017)*, Charterers and other commercial entities. The benefits of such a method are undoubtable (i.e. accuracy, continuous monitoring, elimination of human factor errors) but still the problem for an operator is that the different solutions vary significantly in terms of initial and maintenance costs, complexity of installation and claimed accuracy.

EMM decision was to install a well-established system with a good reference list and support, in order to obtain an objective evaluation of this methodology for two reasons:

- To evaluate the possible application to the entire fleet in near future. Thus, it was not desirable to be biased by any problems that could be encountered from low standards systems with minor support.
- To utilize this system in order to compare results from the other alternative and also to further calibrate EMM methodology for performance monitoring. For this reason, the accuracy expectation was higher than an entry level system.

In order to overcome the possible problems of the complexity of installation and to ease the calibration of the system, the ''Automatic Data Collection System'' was installed on newly constructed vessels in the building stage four Aframax Tankers identical sister vessels, instead of existing vessels with unknown performance history. The main system's characteristics are the following:

- Automatic data collection of 91 parameters for analysis with ten minutes acquisition interval, resulting in 144 reports for a 24-hours period.
- Automatic reporting for weather by a weather provider, including waves and swell data and reporting from sensors for wind and current speed (vectors).
- Logging of all reported data to a cloud-based application with no intervene or limitations in terms of storage and evaluation from the operator side.
- Capability for real time diagnostics on system status and sensors condition.
- Capability for data comparison of any chosen period from installation of the system and onwards.
- Expert reports from the maker of the platform for the vessels performance.

5. Additional Technical Performance Reporting

As discussed above, an alternative method was sought in order to enable more accurate and meaningful performance analysis but without any additional cost. The formulation of this method was relied on EMM acquired experience in performance monitoring and also in well proven methodologies in shipping industry for sea trials, *ISO 15016 (2015)*. Essentially, the following aspects were applied and utilized:

- The inherent problems of the Noon Reports, as already identified, had to be overcome as far as practicable.
- The decoupling of the commercial reporting (to operators and charterers) from the technical reporting.
- The complexity and extra load to crew for this additional report had to be considered.
- The format had to be such that could be easily combined and cross-referenced with the Noon reports analysis.
- The only well proven concept of manual reporting for performance monitoring, i.e. the sea trials, was mainly utilized.

After review of all the above aspects the result was essentially the introduction of an 'Additional Technical Performance Reporting', similar to Noon report but with following features:

- The additional reports are completely independent of the Noon Reports of the same day.
- The report covers a one-hour period.
- Stable M/E load and RPM are maintained during the reporting period.
- The reported period is chosen by crew in order to satisfy the following criteria; open sea condition with minimum steering requirements and stable weather (i.e. weather force not more than 5 BN, swell: less than 2 m, wave: less than 2 m).
- The weather conditions as reported by the weather company for the reported period are also included in the report for cross reference.
- No calculations or averaging is involved by crew.
- The requested frequency for the report was three reports per week in an attempt to mitigate the extra crew workload.

The 'Additional Technical Performance Reporting' data are processed by EMM performance evaluation methodology, compared to the Noon reports analysis. This new concept has been applied and evaluated in a fleet level for more than two years' period. Despite the benefits of this concept which are described in detail in paragraph 6, some weaknesses have been identified and are listed below:

- Due to crew mentality, or wrong understanding of instructions the reporting is sometimes linked with the Noon reports.
- The frequency of reporting can be biased from crew workload.
- The trading pattern of the vessels (i.e. short voyages, etc) could not provide the required conditions for the report.
- Extended bad weather periods inhibit reporting.
- The short time of the period reported makes even small-time deviations in the procedures important, i.e. obtaining consumption with 5 minutes difference has a significant impact in the accuracy, it is reflected in the analysis as a 2-hour period in daily consumption.

6. Comparison of 3 methods – Results

In order to investigate and verify the potential accuracy improvement with the implementation of 'Additional Technical Performance Reporting' data, same was compared to 'Automatic Collection System data' of four sister Aframax Tankers for a considerable time period, along with the traditional daily Noon reports. This section summarizes the findings of performance evaluation analysis based on obtained records from all three data sources (i.e. 'Additional Technical Performance Reporting' and 'Automatic Data Collection System', Noon Reports).

No additional statistical analysis was performed in the data obtained by the 'Automatic Data Collection System' and only the averages as calculated by the expert platform of the system were utilized.

The comparison of three data sources is implemented in two stages; direct comparison of good weather data and comparison of EMM performance evaluation methodology resulting utilizing three data sources as input.

6.1. 1st stage - Direct comparison of good weather data from the three sources

The comparison refers to good weather conditions data (not exceeding 5 Bft, 0.5 kn current speed and 2 m significant wave height). A typical example referring to data of Aframax Tanker I is demonstrated in Fig.4, where the good coincidence between Automatic Collection System data and 'Additional Technical Performance Reporting' is remarkable. On the other hand, it is observed that the Noon Reports data differs from the other two data sources.

The good correlation between the 'Additional Technical Performance Reporting' and Automatic Collection System data, along with the low quality of Noon Reports Data and vessels speed (kn) frequent erroneous reporting is also verified in the field of FOC vs. speed, Fig.4d. Meantime, it has to be stated that similar findings were obtained by direct comparison applied on Aframax Tankers II, III and IV.

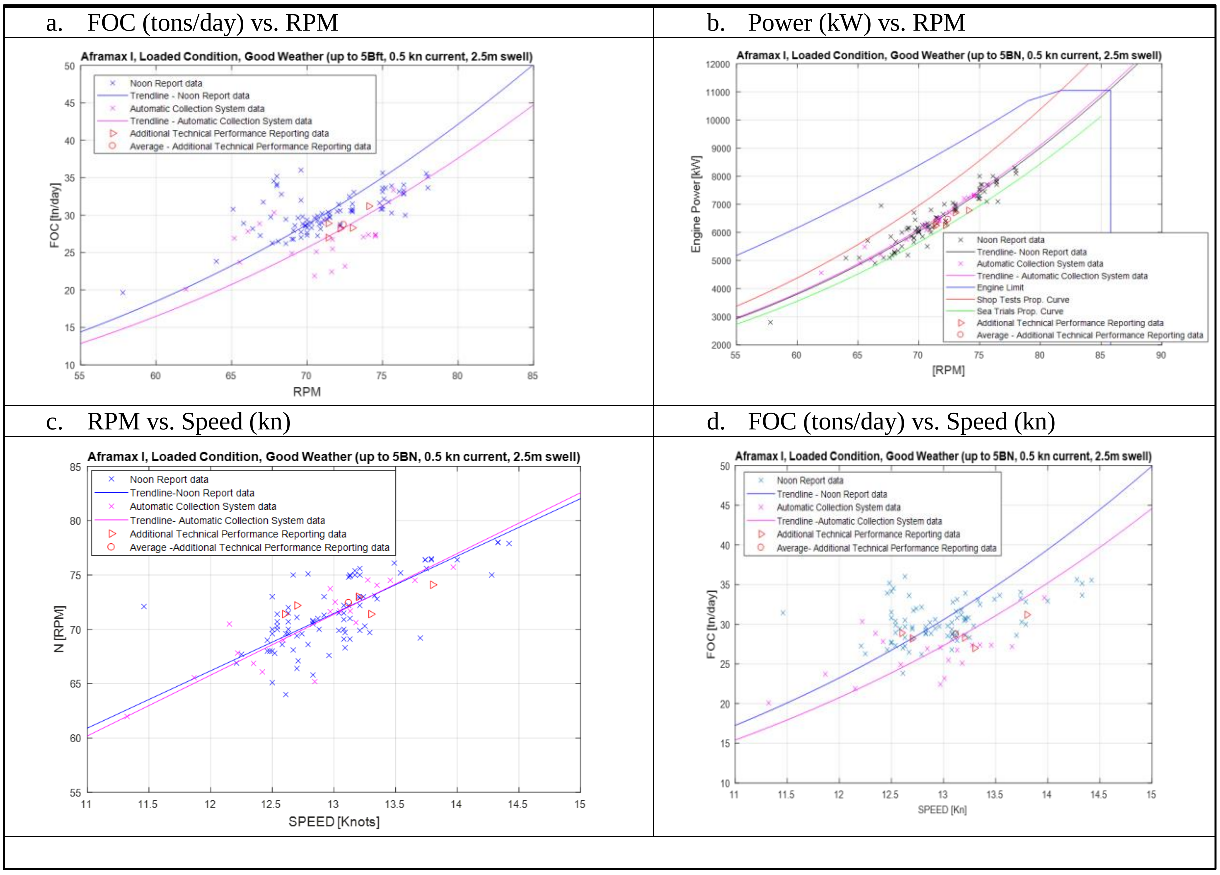

Fig.4: Comparison of Noon Reports, ‘Additional Technical Performance Reporting’ and ‘Automatic Data Collection System’, Aframax Tanker I

6.2. 2nd stage - Results of EMM performance evaluation methodology using data from the three sources

For further evaluation and comparison of the three data sources the EMM performance evaluation methodology was utilized. The results provided additional input for the evaluation of the two alternatives for fleet application. Data from the three data sources (i.e. Automatic Collection System, ‘Additional Technical Performance Reporting’, Noon Reports Data) were introduced to EMM Performance Evaluation methodology and the obtained results were compare. The comparison refers to figures of M/E load vs. RPM and to the difference between FOC equivalent and FOC expected. FOC equivalent corresponds to the FOC that the vessel should have in good weather condition as calculated applying weather/draft corrections, while FOC expected represents the reference consumption of the vessel at given speed as defined by model test curves, *Glaros et al. (2015)*. Data from the four sister vessels were subjected to the above described analysis, indicating sufficient agreement between Automatic Collection System and ‘Additional Technical Performance Reporting’.

The impact of underwater hull cleaning and propeller polishing, in performance improvement of Aframax Tanker II was determined through the application of EMM performance evaluation methodology by using data of all three data sources for the periods before and after the maintenance. The performance evaluation methodology outcomes before and after underwater works are presented in Figs.5 and 6, respectively.

Aframax Tanker II - Noon Reports Data – Before Underwater maintenance

Power (kW) vs. RPM

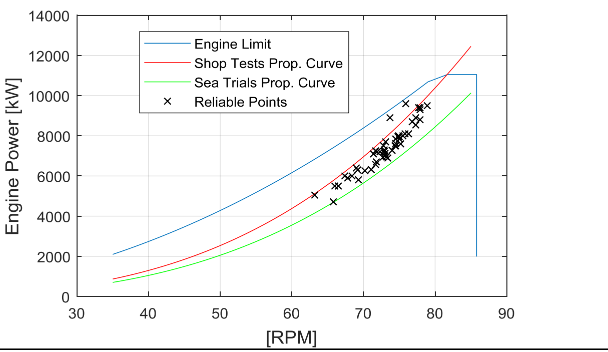

FOC Difference : Equivalent- Expected (mt)

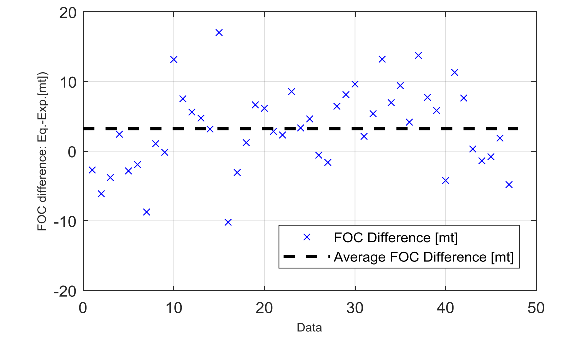

Aframax Tanker II – Automatic Collection System Data – Before Underwater maintenance

Power (kW) vs. RPM

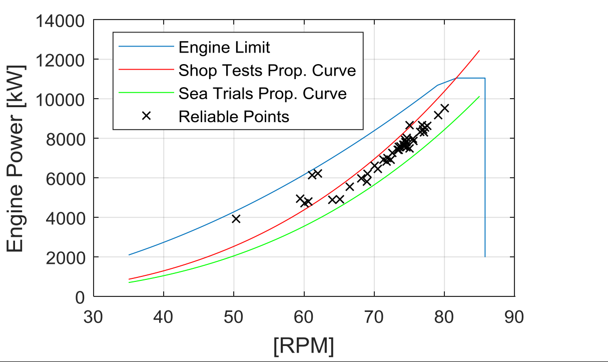

FOC Difference : Equivalent- Expected (mt)

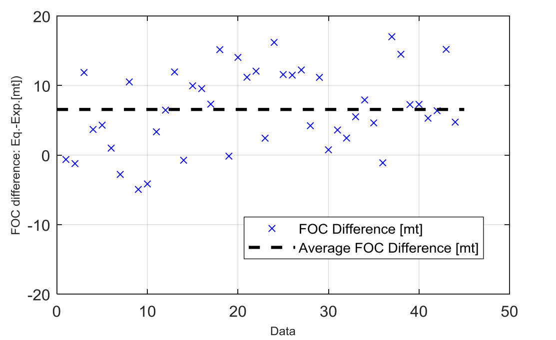

Aframax Tanker II – Additional Technical Performance Reporting – Before Underwater maintenance

Power (kW) vs. RPM

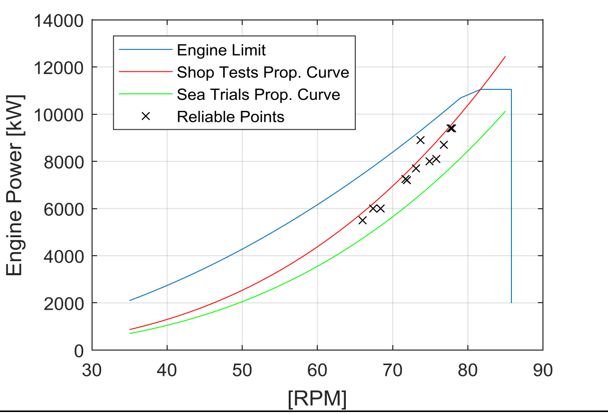

FOC Difference: Equivalent- Expected (mt)

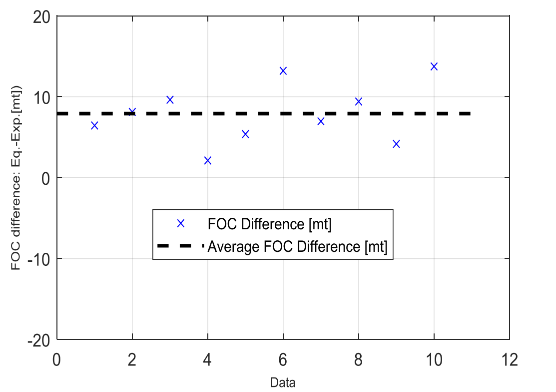

Fig.5: Comparison of Noon Reports and ‘Automatic Data Collection System’, Aframax Tanker II, before underwater maintenance

As shown in Fig.5, remarkable difference between FOC equivalent and FOC expected was observed indicating hull and propeller fouling; the correlation between Automatic Collection System and ‘Additional Technical Performance Reporting’ data is notable. Based on this finding, underwater works were carried out. The performance improvement after underwater works was confirmed for the Aframax Tanker II, with satisfactory agreement between ‘Additional Technical Performance Reporting’ and Automatic Collection System Data. The positive impact of hull cleaning and propeller polishing on both M/E Power and FOC is clearly identified.

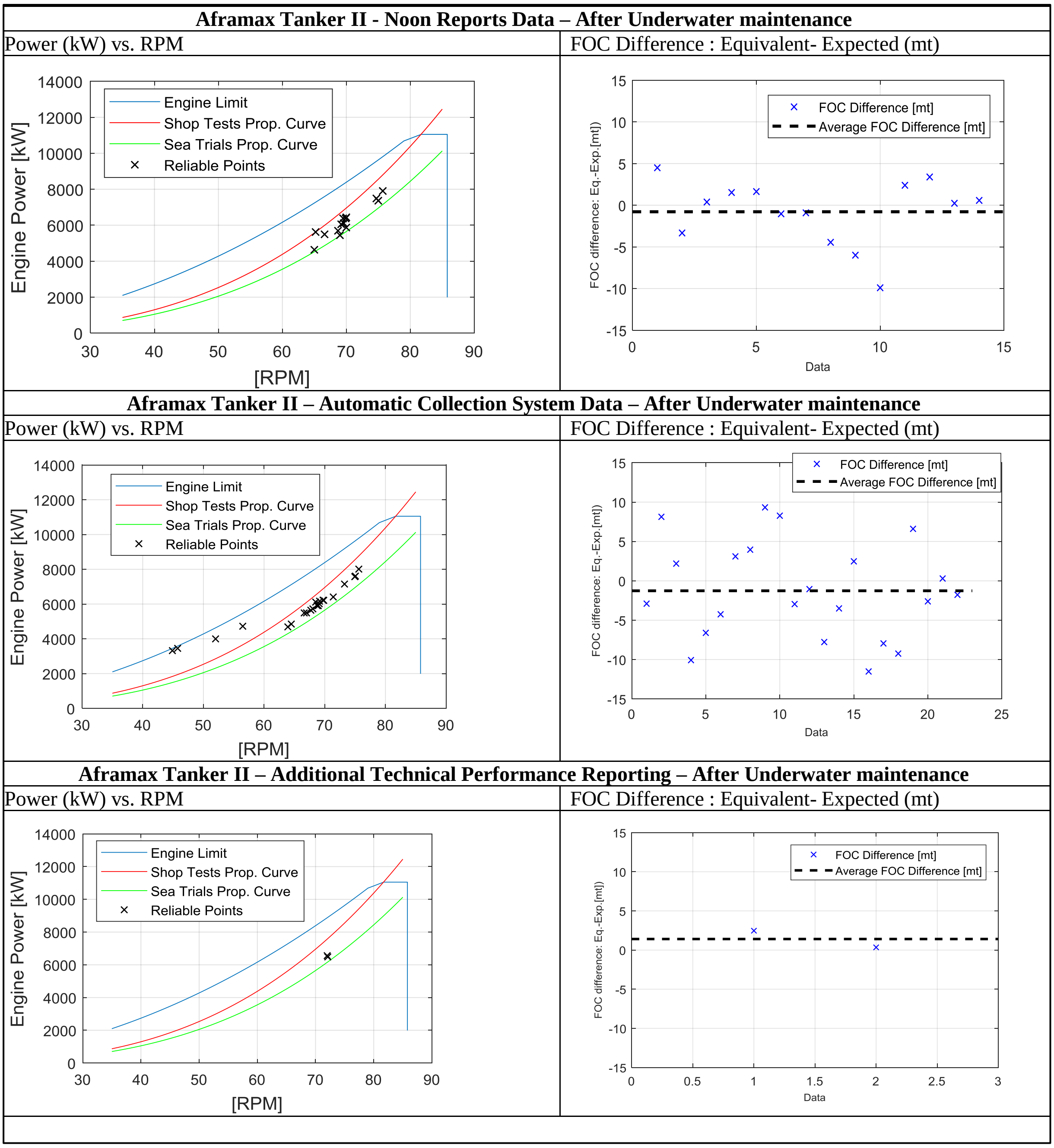

Fig.6: Comparison of Noon Reports, ‘Additional Technical Performance Reporting’ and ‘Automatic Data Collection System’, Aframax Tanker II, after underwater maintenance.

7. Other findings

As shown in Fig.7, a significant scattering of the 10-minute reports within a day from the ‘Automatic Data Collection System’ was observed. The daily averaging of these scattered values for performance evaluations, led to following observations:

- It is rather difficult to reach a conclusion for a vessel performance with few days’ data. This fact is not an implication for long term performance evaluation but is a constraint if a decision has to be taken during a short voyage after a standstill anchorage waiting period for a possible expensive underwater hull maintenance and possibly required ‘off-hire’ period.
- Scattering of the fractional report data is an indication that even when the overall performance of a day is considered as acceptable period, individual datasets may be non-optimum.

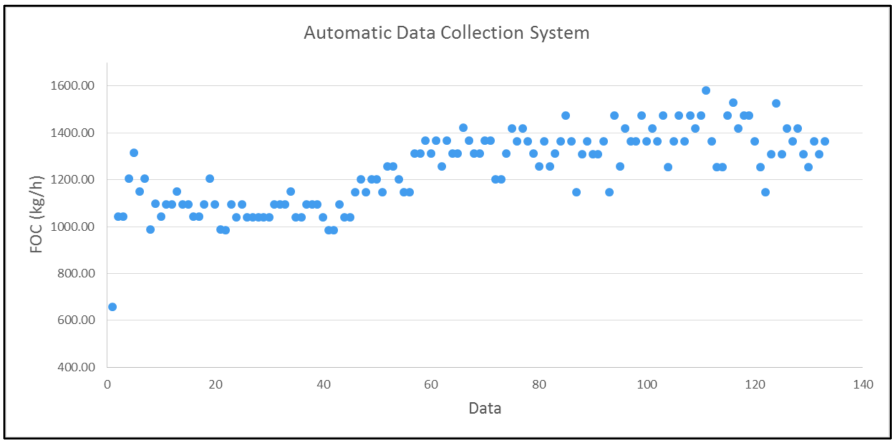

Fig.7: FOC (kg/h) reported values, ‘Automatic Data Collection System’, Aframax Tanker

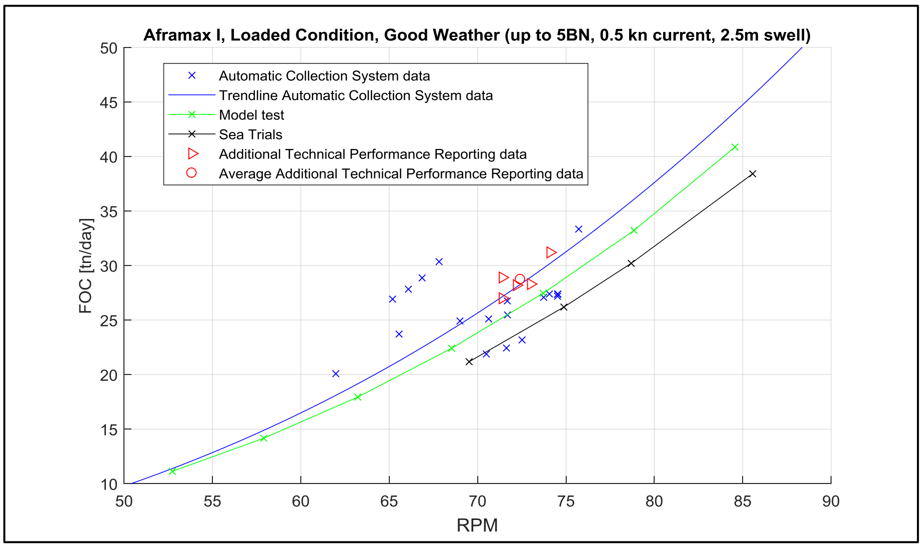

Fig.8: FOC (tons/day) vs RPM, comparison of Noon Reports, ‘Additional Technical Performance Reporting’ and ‘Automatic Data Collection System’, Aframax Tanker

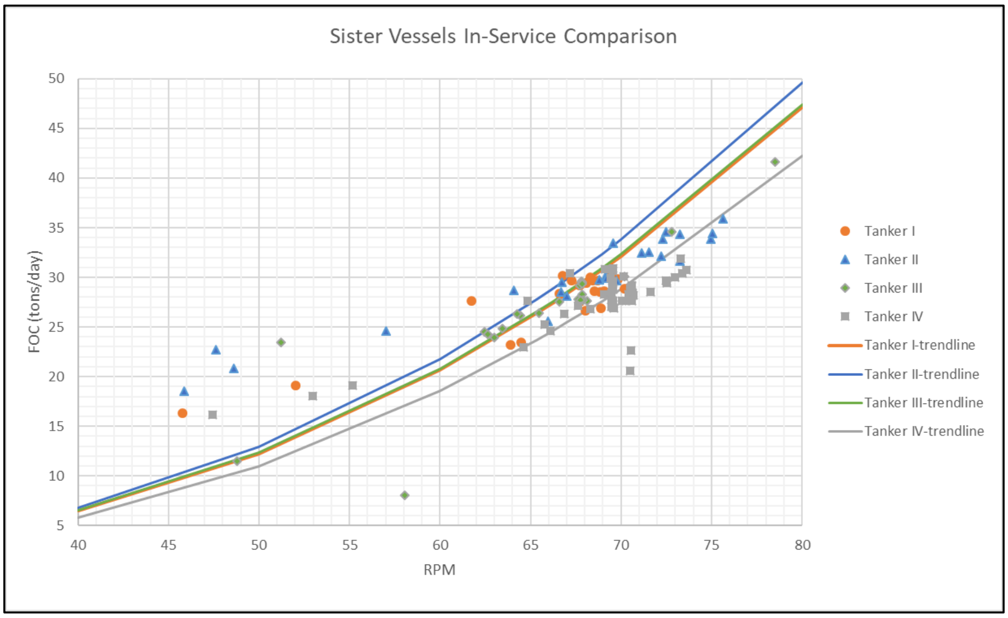

Fig.9: Sister vessels in-service comparison

Moreover, Fig.8 presents a noticeable deviation between expected full scale in service consumption figures based on model tests, the respective sea trial results and the actual in service performance. This finding is rather important since the model test in service predictions and the sea trials results are used as performance benchmark and considered accurate for this purpose.

Finally, the utilization of advanced performance reporting schemes, such as ‘Automatic Data Collection System’ or ‘Additional Technical Performance Reporting’ scheme contributes also to quantification of inherent performance differences between sister vessels. Sister vessels although identical, appear to have often non-negligible differences in terms of performance, as shown in Fig.9. Same was observed from the initial Energy Efficiency Design Indexes (EEDI) calculations.

8. Future Work

The results of the first stage of evaluation of the two alternatives for the improvement of the performance analysis accuracy highlighted the following:

- The inaccuracy of the Noon reports and the necessity to decouple commercial (to operators and charterers) and technical reporting.
- The usefulness of ‘Additional Technical Performance Reporting’ as an alternative method to identify vessels performance trends, given the agreement with the ‘Automatic Data Collection System’.

On that basis, the next steps in evaluation are already set, in order to take a final decision for the application in fleet level.

- Establish a procedure introducing the ‘Additional Technical Performance Reporting’ scheme, since its necessity is well proven.
- Further improvement of EMM methodology with more frequent ‘Additional Technical Performance Reporting’ and utilization of weather data from weather providers for accuracy improvement.
- Specify and set up of custom ‘Automatic Data Collection System’ with minimum required parameters for acquired results towards minimization of cost for fleet level application.

9. Conclusions

The conclusions reached can be summarized as follows:

- It is evident that Noon reports do not provide sufficient accuracy and an alternative for a meaningful performance evaluation has to be applied.
- The introduction of the ‘Additional Technical Performance Reporting’ was proven to increase substantially the performance evaluation accuracy and to have very good agreement with the ‘Automatic Data Collection System’, which has a proven accuracy.
- The fact that for the adaptation of the ‘Additional Technical Performance Reporting’ no capital investment and annual maintenance cost is required, makes this alternative attractive in terms of a cost.
- Intense effort, time and persistence are required for the correct adaptation and implementation of the ‘Additional Technical Performance Reporting’ onboard.
- Even with an advanced ‘Automatic Data Collection System’ a number of problems were faced, primarily related to data transmission and secondarily with sensors failures, which resulted in periods with data gaps. These problems have been finally attributed to many factors, including company IT security protocols, satellite coverage etc.
- Significant scattering of the 10-minute reports data was observed within 24 hours period from the ‘Automatic Data Collection System’.

- It is proven that identification of trends is the only certainty. Given that the absolute values vary significant within a day, the accuracy of hardware system and 'Automatic Data Collection System' data logging frequency and analysis complexity are overvalued.
- A considerable deviation is observed between expected full scale in-service performance based on model tests, the sea trial results and the actual in-service performance.
- Even if an advanced 'Automatic Data Collection System' is used, in-house interpretation of results and adaption to internal procedures are still required. Therefore, human resources should be allocated accordingly.

Acknowledgements

The contribution of Mr. A. Martinos, EMM Managing Director and Mr. S. Tsonakis, EMM Technical Manager by their trust in this project and allocation of resources is gratefully acknowledged.

References

AINSWORTH, T. (2006), 'Significant Wave Height, a closer look at wave forecasts', National Weather Service, Juneau

ANTOLA, M.; SOLONEN, A.; STABOULIS, S. (2017), *The Art of Scarcity: Combining High-Frequency Data with Noon Reports in Ship Modeling*, 2nd HullPIC, Ulrichshusen

BIALYSTOCKI, N.; KONOVESSIS, D. (2016), *On the estimation of ship's fuel consumption and speed curve: A statistical approach*, J. Ocean Eng. and Science 1, pp.157-166

GLAROS, S.; TZAMALOUKAS, A.; BIKLI, K. (2015); *A Methodology for Systematic Fleet Performance Evaluation*, Energy Efficient Ships Conf., Rotterdam

ISO 15016 (2015), *Ships and marine technology – Guidelines for the assessment of speed and power performance by analysis of speed trial data*, Int. Standard Org., Geneva

KWON, Y.J. (2008), *Speed loss due to added resistance in wind and waves*, The Naval Architect, March, pp.14-16

LUND, B.; GONZALEZ, C. (2017), *The Big Data concept in a performance monitoring perspective*, 2nd HullPIC, Ulrichshusen

MEPC (2012), *Resolution MEPC.215(63) - Guidelines for Calculation of Reference Lines for Use with the Energy Efficiency Design Index (EEDI)*, Marine Environment Protection Committee,

MEPC (2016a), *Resolution MEPC.282(70) - 2016 Guidelines for the Development of a Ship Energy Efficiency Management Plan (SEEMP)*, Marine Environment Protection Committee

MEPC (2016b), *Resolution MEPC.278(70) - Amendments to the Annex of the Protocol of 1997 to Amend the International Convention for the Prevention of Pollution from Ships, 1973, as modified by the protocol of 1978 relating thereto (Data collection system for fuel consumption of ships)*, Marine Environment Protection Committee

MRV (2015), *Regulation (EU) 2015/757 of the European Parliament and of the Council of 29 April 2015 on the monitoring, reporting and verification of carbon dioxide emissions from maritime transport, and amending Directive 2009/16/EC*, European Union

OCIMF (2017), *Tanker Management and Self-Assessment, A Best Practice Guide*, 3rd Ed., OCIMF, London

Practical Approaches of Systematically Analyzing KPIs Before and After Maintenance Events with Alternative Methods

Bastian Gehnke, Navis, Flensburg/Germany, bastian.gehnke@navis.com

Abstract

This paper describes an approach to visualize and standardize the process of tracking the vessels hull performance and automatically generate KPI alerts when exceeding the set limits. The paper is focusing on the change in hull and propeller performance measured before and after a maintenance event highlights the first results generated with data collected from manual reports. The idea is to make use out of the existing data within a shipping company and automatically detect implausibility's to filter out data sets, which should not be used for hull performance analysis. This is done by crosschecking the relevant information against each other and against different data sources. The proposed approach is supposed to be used with minimum available information such as reported data and limited hull reference models, but to be ready to work with high quality source information as well. The aim is to standardize the process of filtering and correction according to ISO 19030 or derivate company rules fleet wide and generate KPI alerts in case of conflicts automatically.

1. Introduction

The ISO 19030 is still highly controversial and may be far away from being perfect, *Bertram (2012)*. However, it is a standard, which allows for the first time to develop products with clear standards on corrections, filters and KPIs. As feedback, various owners and technical managers clearly state that most vessels with today's equipment are not able to follow the default method of ISO 19030. The reality is that most vessels are equipped either with insufficient or with inhomogeneous equipment over the fleet. Older vessels are often even not equipped with sensor data collection systems and only manual reported information are available ashore. Based on the present situation, it should be the aim to develop a solution, which is able to handle fully compliant ISO 19030 analysis but also allow customers with reduced availability of information to get insights of the vessels hull performance based on existing data as accurate as possible.

2. Data Source

Because vessels are more or less isolated environments sailing around the world and equipped with various, inhomogeneous systems, an application for whatever purpose would need to be very flexible in handling data from different sources. Since the available sources and systems vary on vessels within a fleet, performance systems shall have an API (Application Programming Interface) for integration purposes of third-party companies.

A preferred approach is to develop the API first and then build applications on top of that, *Levin (2016)*. If you use your own API in the same way as third-party providers do, you are safe to be always able to use the full scope of the application in the same way independent from the data source, *N.N. (2017)*.

Since most of the sailing fleets are only partly or even not at all equipped with an automated data collection system it should be possible to take measured data as well as manual reported data sets into the system and combine them in a sense that the advantages of both data sets can be fully applied. The next three sub-chapters will highlight a practical approach regarding different data sources.

2.1 Reference models

According to the default method, data correlating vessel speed, draft, trim and power must be available for the vessel in question, which may originate from the following estimation approaches, *ISO* (*2016*):

- Full scale speed trials according to ISO 15016
- Towing tank tests compliant with the international standards of quality
- Computational fluid dynamics (CFD) simulations

Limitations are frequently detected when the operational profile of the vessel is compared with the parameters of available reference curves. CFD simulations or towing tank tests are made during the ship design phase, for an operational range around the design speed and draft. Later it is sailing within different profiles, where slow steaming is very common, *Bertram* (*2012*).

This leads to the effect, that whenever the vessels operational data is analyzed, a significant amount of data sets cannot be used to calculate a speed loss or power increase. Therefore, it should be possible to use a standardized hull monitoring module based on available references, which are in the ideal case the above mentioned, but may also be a reduced subset of available parameters or reference models generated differently, compared to the classical approaches. E.g. the reference models can generated from measured data using system identification or machine learning approaches.

The system should be able to fall back to lower quality models if the best options are not available to ensure a speed loss indication at the best available level. However, every “compromise” should be detected and available as an indication of the result quality.

2.2 Automatic data

Measured sample data sets have a few very clear advantages compared to manual data, mainly:

- Much higher data density
- Comparable low error rate (sensor drift, sensor inaccuracy)
- Wide range of sample points

Apart from draft sensors, which are even not part of the default method, measured data are taken as best available source for hull performance monitoring.

However, in practice there are reasons why not all vessels are fitted with all required sensors:

- Relatively high investment costs.
- High requirements on communication equipment, if data is transferred in real time.
- Older ships are often not suitable for retrofits due to high investment costs.

Even vessels, which are equipped with automated data collection systems, are facing sensor break downs, inaccurate values due to low quality sensors and communication losses due to satellite coverage. As a conclusion, the best case for hull performance monitoring is available on a small percentage of a customer’s fleet. A fallback mechanism should allow using the proxy values according Part 3 of ISO 19030, which includes alternative data acquisition by low frequency methods such as noon report data, *ISO* (*2016*)

2.3 Manual data

Whenever data analysis is performed from manually gathered data, the complications are similar: the data is often incomplete, faulty and inconsistent. A lot of work is required to identify and then correct the errors, even if it is possible in the first place. This is especially the case if a lot of time has passed between the gathering of the data and the analysis, which is mostly the case in terms of hull performance analysis. The reasons for the quality problems are numerous:

- Reporting tools on board not adequately formalized (especially for use with Excel, etc.). In such cases, it can often be quite difficult to process the data mechanically.
- Fragmented templates, meaning that essential information is not recorded.
- Inadequate verification of the plausibility.
- Copy-Over of report data from the previous day in order to save time.
- Typing errors when entering data.
- Inadequate understanding of the exact data be recorded.
- Insufficient awareness of the importance of reporting.
- Lack of continuity in the onshore validation of the data.

Greater attention should therefore be paid in future to ensuring high quality data. The following measures are possible:

1. Use of reporting tools that formalize the input of data and thus support the crew. Certain actions, such as complete transfer of data from the last report, should not be possible.
2. Pre-validation of the data during input. Therefore, it should not be possible to make physically impossible or extremely implausible entries. Moreover, it must be ensured that critical data has to be entered.
3. Intensive, automatic validation of the data in real time when sent ashore. The data should be checked with respect to the properties of the respective ship, machine characteristics, consumption curves and hull models. In addition, the consistency of the reports should be checked in terms of chronological order and consistency to ensure that there are no time gaps or multiple entries.
4. Automatic notification of the crew with respect to the data quality and the existence of potential errors.
5. Aggregation of the data quality in corresponding KPIs and presentation in suitable dashboards in order to provide a quick overview of the data quality of the fleet for the responsible onshore personnel.
6. The automatic plausibility check should continue to generate comprehensible and transparent messages that can be used to quickly locate the source of the error.

Therefore, it requires special focus on the above-mentioned plausibility checking of the report data. Every report received has to be validated comprehensively. Moreover, a specific check tailored to the respective application scenario (in that particular case the hull performance monitoring) has to be performed automatically for each report, *Alfke* (2017).

That means for example, that any issue regarding the auxiliary engines will be detected as an overall plausibility issue, but not considered as a relevant error for hull monitoring since it is not affecting the hull performance and taking this data set out unnecessarily reduce the number of available data sets. Below picture shows an example of a plausibility dashboard which generates specific messages for each issue which has been detected.

An automatic plausibility check verifies the data against the properties of the respective ship, machine characteristics, consumption curves and hull models. It generates comprehensible and transparent messages that can be used to quickly locate the source of the error. Apart from the validation and plausibility checks to be performed on board, while the data is being entered in the corresponding reporting tool. A much more comprehensive plausibility check can be carried out onshore.

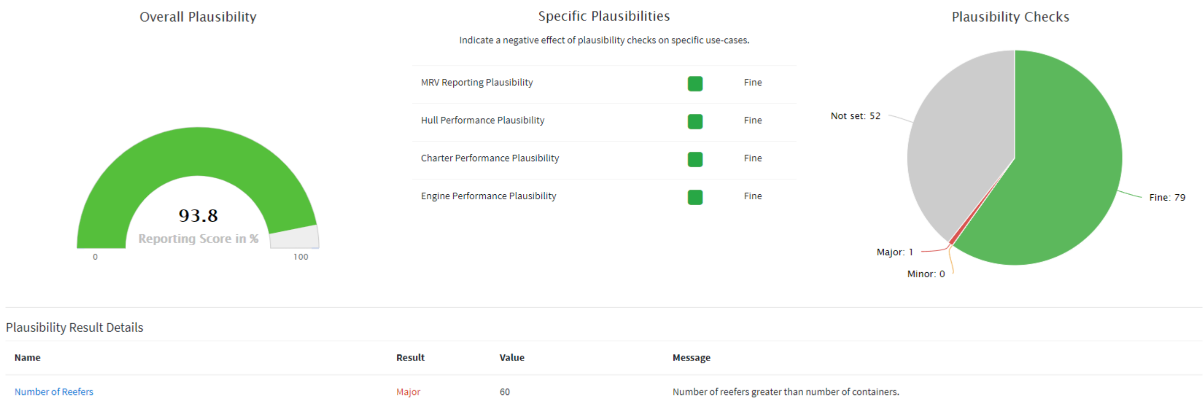

Fig.2: Plausibility check display

The verification rules can be divided into four categories:

1. Physical limits: It is checked, if the specified values are within physically meaningful limits. Raw input errors can be identified in this way.
2. Ship-dependent limits: It is checked, if the specified values are within meaningful limits for the ship in question. This includes, for example, cargo capacity, service speed, maximum speed of the main engine, performance limits, etc. Raw input errors are also identified in this case, but in a more specific way for the respective ship. The ship data required for this must be available.
3. Simple correlation check: It is checked if the values are logical in relation to one another. For example, it is checked whether fuel is being consumed when the main engine is operating. This allows identifying missing input, for example, which is then frequently reported as not available.
4. Characteristic check (extended correlation check): The coherence of the values is checked based on available reference data (consumption curves, sea-trial data, etc.). Correlating data can therefore be checked more precisely.

3. KPIs

All relevant KPIs defined in the ISO 19030 require data over longer periods up to more than one dry docking cycle. The first practical results can often be evaluated with the Performance Indicator of the “Maintenance Effect” whereby data sets 3 month before (reference period) and 3 month after (reference period) any maintenance event are required, *ISO* (*2016*).

The calculation of the average speed loss over the reference period shall be independent from the data sources and reference model and being calculated as:

$$\bar{V}_{d,ref} = \frac{1}{k}\sum_{j}^{k}\frac{1}{n}\sum_{i}^{n} V_{d,j,i}$$

where

k	number of reference periods
j	reference period counter
n	number of data points in the processed data set under reference conditions in the reference period j
i	counter of data points in reference period j
$\bar{V}_{d,ref}$	average percentage speed loss over the reference period(s)
$V_{d,j,i}$	percentage speed loss for data point I in reference period j

For the evaluation period, the average percentage speed loss shall be calculated as:

$$\bar{V}_{d,eval} = \frac{1}{n}\sum\nolimits_{i}^{n} V_{d,eval,i}$$

where

n	number of data points in the processed data set under reference conditions of the evaluation period
$V_{d,eval,i}$	percentage speed loss for data point I in a data set of the evaluation period
$\bar{V}_{d,eval}$	average percentage speed loss in data set of the evaluation period

The definition of the performance indicator is given as the change in the average speed loss in the reference period and the average speed loss in the evaluation period, *ISO* (*2016*). Following the practical approach to get a most useful result out of a hull performance-monitoring tool, the following additional KPIs can give a daily indication:

3.1. Absolute speed loss KPI

The absolute-speed-loss-KPI shows if the speed loss of a particular vessel based on the current value exceeds the defined absolute limits. Depending on the set limits the KPI state will change its color. If the actual speed loss is:

- below the lower limit (Limit minor), it will turn green.
- between lower and upper limits, it will turn orange.
- above the upper limit (Limit major), it will turn red.

The values for "Max wave height", "Max swell height" and "Max wind speed" define filter criteria which must be met to include a data set into consideration. All data exceeding the maximum values will be ignored. Data which significantly deviates due to plausibility issues can also be filtered out by setting handling of plausibility issues to "Exclude major issues" or to "Exclude major and minor issues". To avoid false indications due to variations in the available data, the significant speed-loss is calculated by averaging a number of data sets. The value Sample size controls how many data sets are used for averaging the significant speed-loss.

3.2. High degradation rate KPI

The high-degradation-rate-KPI indicates, if the speed-loss drops faster over time than expected. To calculate this KPI, maintenance events are required, which define the maximum allowed yearly speed-loss decrease per event, as well as the minor and major tolerance. The events can be defined in the module itself. Customers are able to decide which yearly degradation rate is allowed after a specific maintenance event such as hull painting or propeller polish. The values for "Max wave height", "Max swell height", "Max wind speed" and "Min plausibility" define filter criteria which must be met to include a data set into consideration. All other data sets will be ignored. To avoid false indications due to variations in the available data, the significant speed-loss is calculated by averaging a number of data sets. The value "Sample size" controls how many data sets are used for averaging the significant speed-loss. The value "Min number of samples for regression" disables the KPI if only a few data sets are available after a hull performance event.

3.3. Dashboard

A dashboard shall provide an overview of the current KPI situation. An overview of the hull performance of the whole fleet will be displayed and color-coded tiles shall show a summary of minor and major issues as well as fine KPIs.

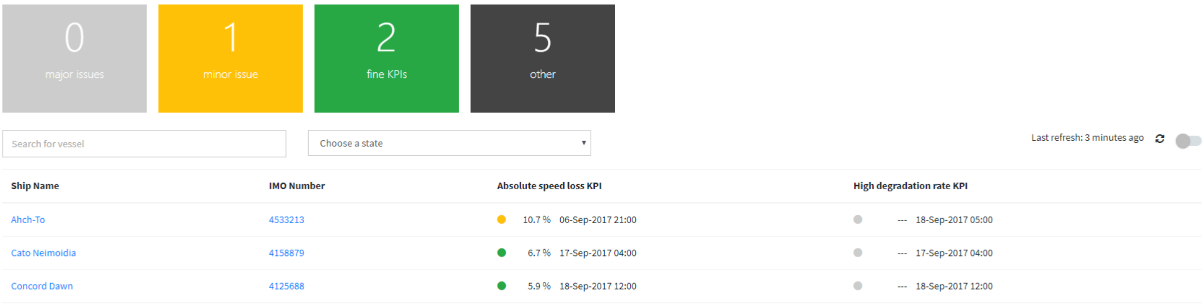

Fig.3: Dashboard

In the below example a KPI details page provide a time plot of the KPI along with a color indication of the KPI status. Next to the time plot, a pie chart indicates the distribution. The effective KPI settings provide an overview of the current effective settings of the setup section. On the left, the last significant KPI value is shown in a colored tile together with a clear message explaining whether the status is other than good.

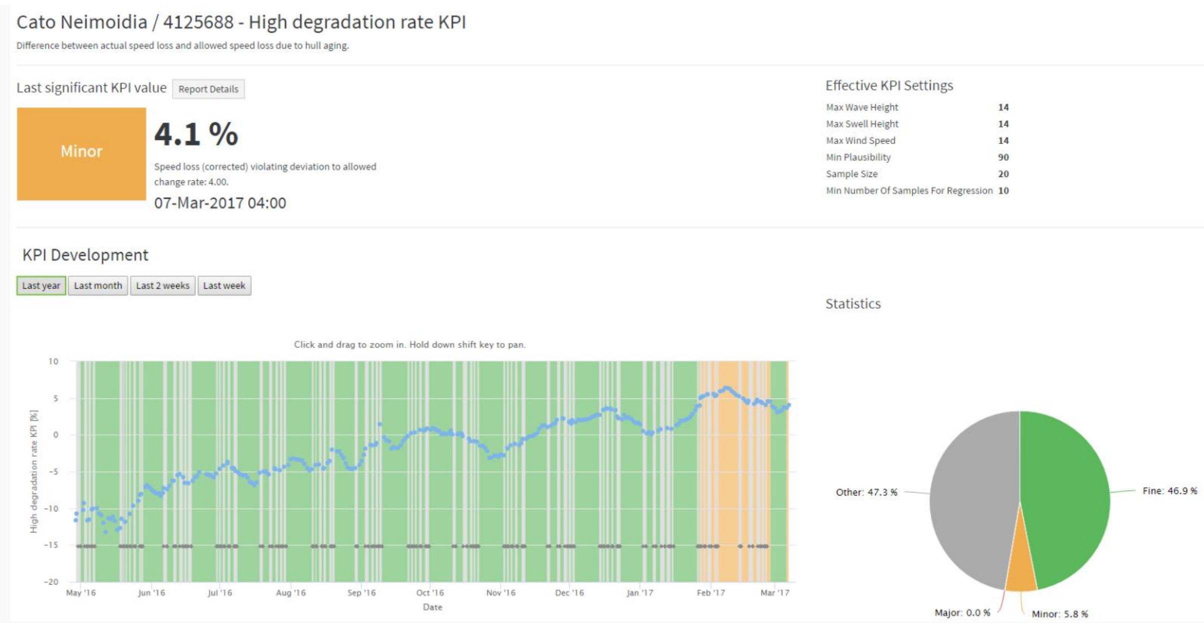

Fig.4: Example of KPI details

3.4. Hull Survey

The screenshot in Fig.5 shows a possibility to visualize a hull survey. In the shown example, the hull survey of a specific vessel can be accessed either by clicking on the vessel on the Dashboard. The hull survey will display the calculated speed loss over time. The tooltip will give some details of each value when hovering over the respective point. The section to the right provides statistics and settings for filters, regressions and corrections.

4. Summary

To get a daily overview of the hull performance over a whole fleet in a most specific manner it is crucial to be able to use data from any available source but ensure to get a clear indication and score if the data sets have a reduced quality from whatever reason. Clear displayed KPIs and email feedback can increase the data quality significant and a standardized system over the whole fleet is able to apply a hull performance analysis according to ISO 19030 standards. As more complete and accurate, the available data sets are as closer can the analysis be to the default method. Additional KPIs or even more extensive corrections apart from the ISO can be applied to a fully standardized process.

Fig.5: Display of hull survey

References

ALFKE, H. (2017), *MRV - Background Data Validation*, Interschalt Maritime Systems, Hamburg http://www.interschalt.com/software/bluetracker/blog/entry/news/mrv-background-data-validation-verification.html

BERTRAM, V. (2012), *Practical Ship Hydrodynamics*, Butterworth & Heinemann, Oxford

ISO (2016), *Measurement of changes in hull and propeller performance Part 2: Default Method* – ISO 19030-2, ISO, Geneva

ISO (2016), *Measurement of changes in hull and propeller performance Part 3: Alternative Methods* – ISO 19030-3, ISO, Geneva

LEVIN, G. (2016), *An API-First Development Approach*, DZone, https://dzone.com/articles/an-api-first-development-approach-1

N.N. (2017), *api (application programming interface)*, Retriever Media Informatie, https://www.retriever.nl/en/buzzword/api/

Experimental Quantification of Drag Change of Commercial Coatings Under the Effect of Surface Roughness and Soft Fouling

Irma Yeginbayeva, Chalmers University of Technology, Gothenburg/Sweden, irmay@chalmers.se
Lena Granhag, Chalmers University of Technology, Gothenburg/Sweden, lena.granhag@chalmers.se
Valery Chernoray, Chalmers University of Technology, Gothenburg/Sweden, valery.chernoray@chalmers.se

Abstract

The paper presents an experimental study of roughness and hydrodynamic characteristics for biocidal and non-biocidal antifouling coatings. In the study both smooth panels (Rt(50)≈40-90 μm) and panels with roughness commonly found on ship hulls (Rt(50)≈110-125 μm) were used. Measurements of drag were obtained from torque measurements in a rotating disc facility and the biocide content (Cu and Zn) of the paint were measured using X-Ray Fluorescence. Preliminary results show that Cu concentration in coatings is between 6700 mg/cm^2 and 9600 mg/cm^2, whereas Zn results are under 900 mg/cm^2.The results of torque measurements shows that typical antifouling biocidal coating with Rt(50) value of 116 μm demonstrated around 19% higher torque coefficient (C_m) at the highest Reynolds number (Re_r) when compared to the smoothest disk with Rt(50) value of 43 μm. In addition, the paper also describes future plans of including microalgal fouling to the tested disks.

1. Introduction

The drag performance data of newly-applied and clean coatings are not sufficient to fully reflect and estimate the drag and consequent fuel efficiency of marine coatings over a typical period between dry-docking, which incorporate the increase in surface roughness and development of different fouling stages.

A comprehensive review of studies on the ship roughness and fouling (available before 1952) is given in MFIP (1952). The review covers laboratory tests and full-scale ship tests on different rough surfaces and fouled surfaces under various conditions. From cited reviewed works, *Beery (1939), Benson et al. (1938), Snyder (1938), Graham (1940),* it follows that the average drag increase during the static submerging is about 0.1 per cent per day during the first 2 month for antifouling paints and about 0.5 per cent per day for a passive (anticorrosive) paint. A useful observation was made in *Hiraga (1934)* that the drag of samples measured directly after submerging was initially larger and the resistance was decreasing to abovementioned values when the top layer of the slime was removed during the towing. From study by *McEntee (1915)* it follows that after 3-4 months of submerging there is a sudden resistance increase with 50% a month and after this time the resistance grows about 30% a month.

In the full-scale tests on Lucy Ashton ship, *Denny (1951), Conn and Lackenby (1953),* the hull was allowed to foul for 40 days, on a coating of bituminous aluminium. Only slime was present after this time and the frictional resistance increased by 5% i.e. 0.125% per day. Similar drag increase rate was obtained by *Lewthwaite et al. (1985)* for 240-day and 600-day trials, where the increase of drag was by 25% and 80% correspondingly.

In *Munk et al. (2009)* drag curves over time for different vessels are analysed and an average resistance increase of 0.5-1% a month is reported. For a tanker, which sat for one month in a port, the drag has increased by 10%. Upon subsequent operation, the self-polishing copolymer coating was activated, and the fouling was reducing over the course of 6 month until the drag change has reached the value of 5%. After this period the drag started to increase as described in previous works with the rate of 1% a month.

The mechanical and physical properties of biofilms will impact the magnitude of the drag they generate, *Towler et al. (2003)*. On fouled flat plates the thickness and community structure of attached biofilm was seen to affect drag, *Schultz and Swain (1999,2000)*. In test on antifouling coatings the effect on increased drag could come either from differences in the properties of the biofilms attached on the various coatings, or to their adhesion to the coatings, due to properties of the coatings.

Marine biofilms contain different species of bacteria, cyanobacteria, diatoms, protozoans and other microorganisms, *Dobretsov (2010), Callow and Callow (2011)*. On a ship hull diatom species like *Amphora* and *Navicula* are present and in some studies these diatoms are found to be tolerant to copper in anti-fouling paint, *Zargiel et al. (2011), Callow (1986)*. Tolerance to copper is also find to differ between diatom species and cyanobacteria, *Barranguette et al. (2010)*. However, it was concluded in the study by *Barranguette et al. (2010)* that the main factor regulating the sensitivity of the biofilm to Cu toxicity during short-term exposures was the physical structure of the biofilm (package of cells and thickness) and not the species composition.

The roughness of the substrata will have impact on biofilm formation. At a fine-scale (e.g. 10 μm, 22 μm and 50 μm) roughness, total diatom density (cells per cm^2) were found to be higher on 10 μm while the total biomass did not differ between the three roughness tested, *Sweat and Johnson (2013)*. In the tests by *Sweat and Johnson (2013)* natural biofilms were used consisting of 58 different diatoms species with size (length) span from 14 to 552 μm. In lab tests bacterial biofilms (inoculum from Montana State University duck pond) grown directly on rheometer disks rotated in a chemostat for 12 days resulted in biofilms that were heterogeneous and ranged from 35 μm to 50 μm in thickness, *Towler et al. (2003)*. Natural biofilms including diatoms are much thicker and in riverine water in Netherlands a 1-2 mm thick biofilms were developed during a 3-week colonization period, *Barranguette et al. (2010)*.

The literature survey shows that there are rather many experimental studies on the fouling drag available. However, few of these studies are reporting on correlation of fouling surface characteristics with its drag. Based on the above need, this research aims to understand the fouling attachment mechanisms of ship microalgal species (diatoms and green algae) on commercial biocidal and non-biocidal coatings and resulting drag.

This paper presents the experimental results on surface roughness and drag characteristics of hull coatings with relatively smooth and coarse roughness finishes without the effect of fouling used as baseline measurements. The paper also reports on future plans for the project.

2. Detailed description of experimental work

2.1. Test surfaces

Test disks were of 300 mm diameter. Two smooth, uncoated PVC disks were used as reference surfaces. PVC disks coated with antifouling paints on one side were used as test surfaces and summarized in Table 1. In the table, biocidal and non-biocidal antifouling coatings were denoted as BAC and FR respectively. Disks coated with *BAC-A*, *BAC-B* types were typical antifouling polishing coatings with biocides and *FR-A, FR-B, FR-C, FR-D* types were typical non-biocidal foul-release coated disks. To investigate the effect of roughness ranges, disks with *BAC-A* type only have undergone smooth and realistic rough applications. Biocide containing disks were prepared in two replicates. All FR type coatings were applied on disks using smooth application procedures. FR coated disks were prepared in three replicates. Surface roughness of these mentioned disks were measured by industry type Hull Roughness Gauge.

Table I: The list of antifouling coatings

Application type	Biocidal types	Non-biocidal types
Smooth	BAC-A smooth 1	FR-A smooth 1
	BAC-A smooth 2	FR-A smooth 2
	BAC-B smooth 1	FR-A smooth 3
	BAC-B smooth 2	FR-B smooth 1
		FR-B smooth 2
		FR-B smooth 3
		FR-C smooth 1
		FR-C smooth 2
		FR-C smooth 3
		FR-D smooth 1
		FR-D smooth 2
		FR-D smooth 3
Rough	BAC-A rough 1	-----
	BAC-A rough 2	----

2.2. A campaign of rotary disk tests

A rotating disk facility was used to assess the hydrodynamic performance of coated disks in their clean (i.e. unexposed to fouling) conditions. A schematic of a custom built small-scale rotating disk facility is illustrated in Fig.1, *Atencio (2016)*. The facility capable of measuring a boundary layer over disks by using a micro-PIV (Particle Image Velocimetry) and drag via torque readings. The resisting moment (torque) of rotating disks is measured by a Kistler type 4503A torque meter which is installed on a shaft connecting an electric motor with the rotating disk. The torque sensor operates on a strain gauge principle. The torque meter output is monitored by an analogue-to-digital converter (ADC) controlled by a PC.

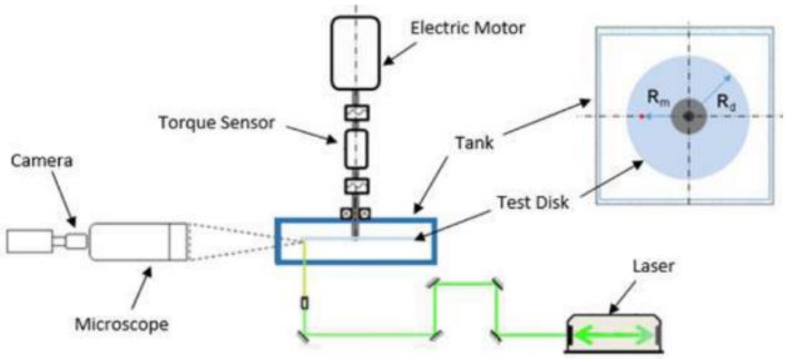

Fig.1:Rotating disk rig with torque and micro-PIV measurement capability, *Atencio (2016)*

Before the drag measurements, all the air from the tank was evacuated and the bearings were lubricated. The facility was warmed-up at 600 rpm together with the measurement electronics for at least 20 minutes. First, the torque from the shaft together with bearings and seals (but without a disk) was measured. These readings were later subtracted from the total measured torque to obtain the torque of the disks. Following, the torque contribution from the disk's cylindrical edge was also subtracted in order to estimate the drag of only coated part of disks. A water tank filled with tap water and torque data for coated disks as well as reference PVC disk were collected at different motor speeds as shown Fig.2. The water viscosity and density was evaluated analytically based on the temperature in the tank, which was logged during the tests.

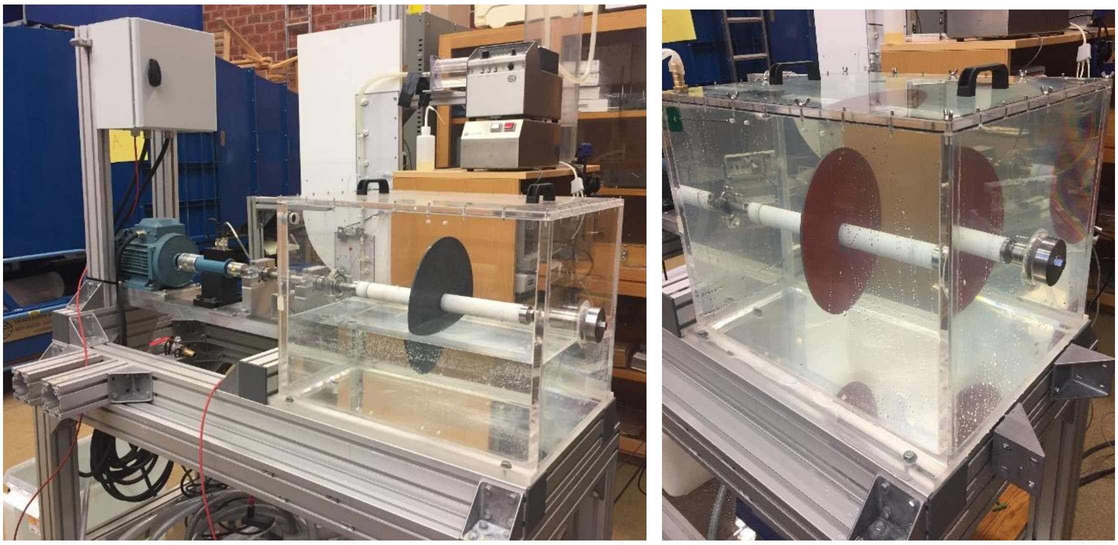

(a) (b)

Fig.2: Installation of the reference PVC disk (grey) on the shaft of the rotating rig for torque measurements (a). The photo of coated disk taken during experiments (b).

Torque data were collected at nominal rotational velocities of 450, 600, 900 and 1200 rpm. At 450, 600 and 900 rpm data were collected twice (during the increase and decrease of rotational velocity). Since current test disks were coated on one side, additional post-processing procedure was introduced to subtract the torque of the smooth side.

The moment coefficient is obtained from Eq.(1):

$$C_m = \frac{4M}{\rho r_0^5 (\phi\omega)^2} \tag{1}$$

M is the torque of one side of the disk, r_0 is the radius of the disk, ω is the angular velocity and ρ is the density of the fluid. For a disk rotating in a container a swirl may develop which reduces the effective angular velocity to $\phi\omega$ where ϕ is a swirl factor for enclosed rotating disk $\phi^2 = C_{m,en}/C_{m,\infty}$. The swirl factor in the tank is equal to 0.97. However, typically, the precise value of the swirl factor is not crucial for the roughness characterisation, since differences are considered.

The angular velocity is calculated using Eq.(2):

$$\omega = 2\pi \frac{RPM}{60} \tag{2}$$

The Reynolds number is defined as in Eq.(3):

$$Re_r = \frac{r_0^2 \omega\phi}{\nu} \tag{2}$$

The water density ρ and kinematic viscosity ν are evaluated at actual water temperature of the experiment.

2.3. Measurements of Cu and Zn concentrations in biocidal antifouling coatings

A method based on XRF spectrometry was used to determine the concentration of metals, namely copper (Cu) and zinc (Zn) in biocidal coatings applied on 300 mm diameter disks. XRF is an acronym for X-ray fluorescence, a process whereby electrons are displaced from their atomic orbital positions.

This process is accompanied with a release of burst of energy. Each element (e.g. metals) has its specific energy bursts, which is registered and identified by the detector in the XRF instrument, https://www.bruker.com/products/x-ray-diffraction-and-elemental-analysis/handheld-xrf/how-xrf-works.html. The method utilizing a handheld XRF analyser has recently been developed for the in-situ measurement of release of metallic biocides from antifouling paints, *Ytreberg et al. (2017).*

As shown in Fig.3, the handheld XRF (DELTA-50, InnovX) was directly positioned on the coated disk and a total of 6 points in 4 places per disk were analysed using 50 kV beam. Each measurement point which was a circular area was measured during a 30 s time. The concentration of metals such as Cu and Zn in the coatings are expressed in mg per square centimeter (mg/cm^2).

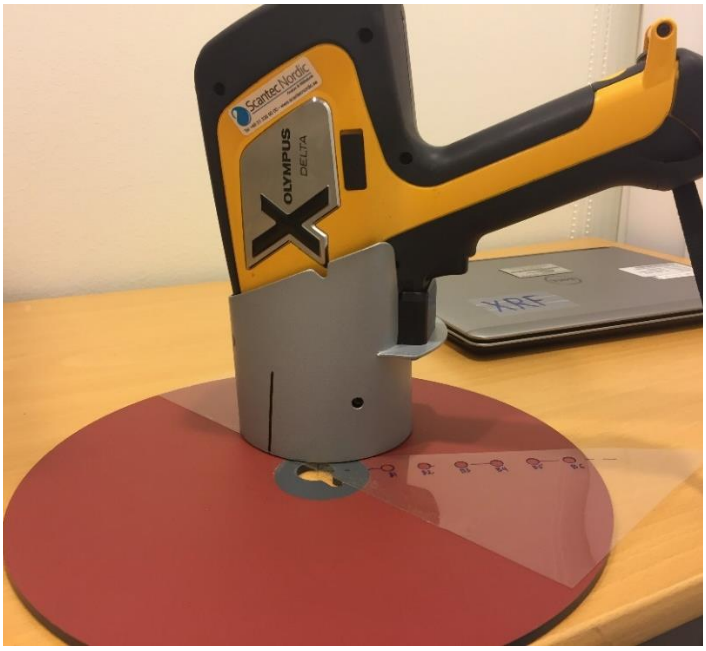

Fig.3: XRF measurements of Cu and Zn in *BAC-A* type applied on disks

For the XRF film analysis, it is important to define the film thickness beyond which the X-ray signal is absorbed by the sample and is not detected by the instrument. This thickness is also known as critical thickness, d_{thin}. *Ytreberg et al. (2017)* designed an experiment to determine this d_{thin} for Cu and Zn in antifouling coatings. Their study recommended that the dry film thickness of coating should be under 40 μm to avoid absorption effects and consequent underestimation of metal concentration in coatings.

In this study, the thickness of coatings applied on test disks exceeds the critical thickness d_{thin}, why we would have an uncertainty in XRF readings. But still results can be used as screening tests for relative comparisons of Cu and Zn concentration between different biocidal coatings.

2.4. Results and discussions

2.4.1. Roughness measurements

The maximum peak-to-valley height roughness values over a 50 mm sampling lengths (*Rt50*) was collected on test disks using an industry gauge hull roughness analyser, https://www.tqc.eu. In marine industry, this parameter has been adopted as a standard measure of hull roughness. In total 20 measurements were obtained by moving the sensor unit of TQC hull roughness gauge in straight lines around disks.

Figs.4 and 5 present boxplot diagrams for *Rt(50)* values collected on biocidal and non-biocidal coated disks respectively. In the boxes the median, which is a measure for the center of *Rt(50)* values, are represented by the mid-line. Observed mean and medium *Rt(50)* values for all coatings are very close except some disks. As it can be seen in Fig.4, mean values for *Rt(50)* for biocidal coatings ranged from 72 µm (*BAC-B smooth 1*) to 123 µm (*BAC-A rough 2*). Looking at the boxplot it is obvious that *BAC-A* type coating which had rough application finishes were the roughest amongst the biocidal group. Two way Analysis of Variance (ANOVA) was carried out to determine whether smooth and rough applications of the same *BAC-A* type coating were significantly different from each other. ANOVA test are run with an α level (or significance level) of 0.05 (5%). According to the result, the 0.05<*p*-value was found to be significantly smaller than specified α level meaning that differences in *BAC-A-smooth* and *BAC-A rough* applications were achieved.

Looking at the pattern of box plots, *BAC-B* coating replicates show wide range in data spread. This might be explained by trip of TQC' sensor tip that resulted in high variation of readings.

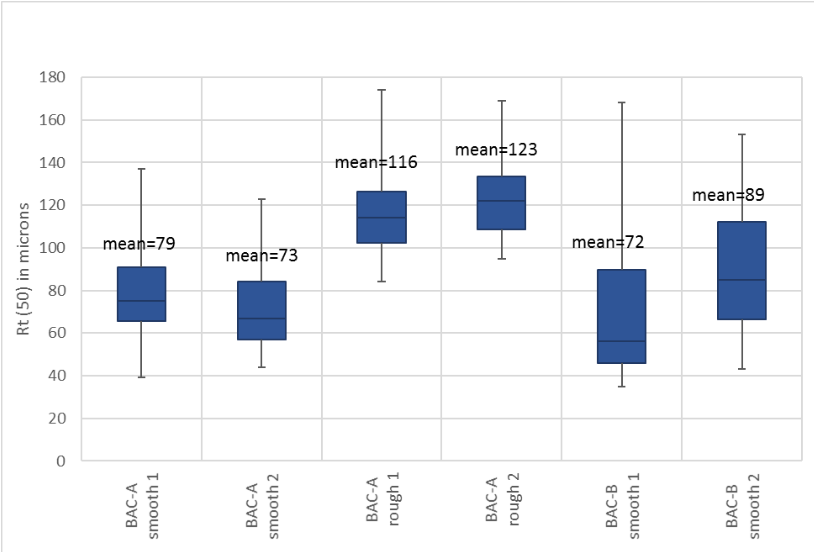

Fig.4: Boxplot diagrams of *Rt(50)* expressed in microns (µm) for biocidal coatings

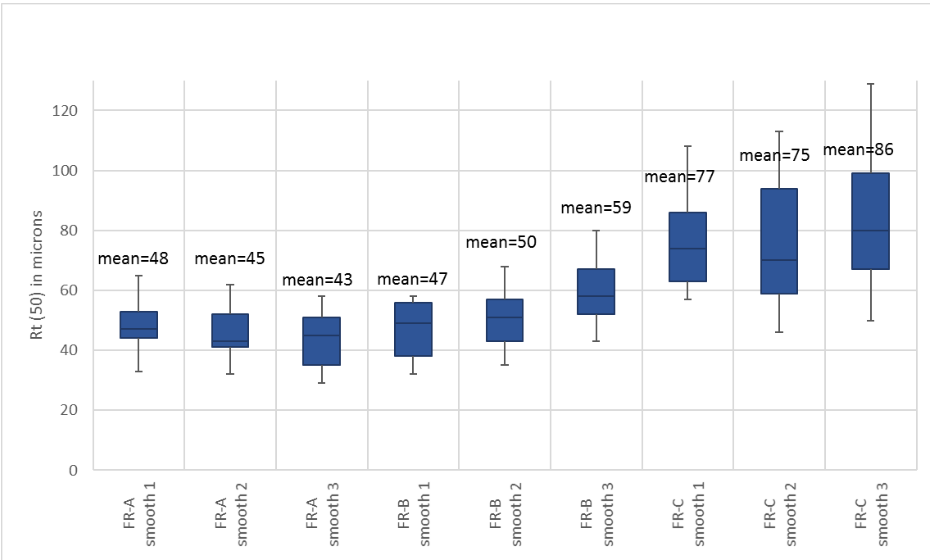

Fig.5: Boxplot diagrams of *Rt(50)* expressed in microns (µm) for non-biocidal coatings

Rt(50) values for non-biocidal coatings were small. A minimum of 43 µm and maximum of 86 µm was observed for *FR-A smooth 3* and *FR-C smooth 3* respectively. The *Rt(50)* values for *FR-B* type coatings were in the mid-range. Fig.5 does not show values for *FR-B* type since we could not take any measurements on this particular coating type due to its sticky nature not allowing the tip to move forward.

2.4.2. XRF results

In total 24 measurements points per disk were used to collect the XRF readings presented in Fig.6. This figure graphically demonstrates the mean values (also standard deviations in black vertical lines) for concentration of Cu and Zn for three biocidal type coatings.

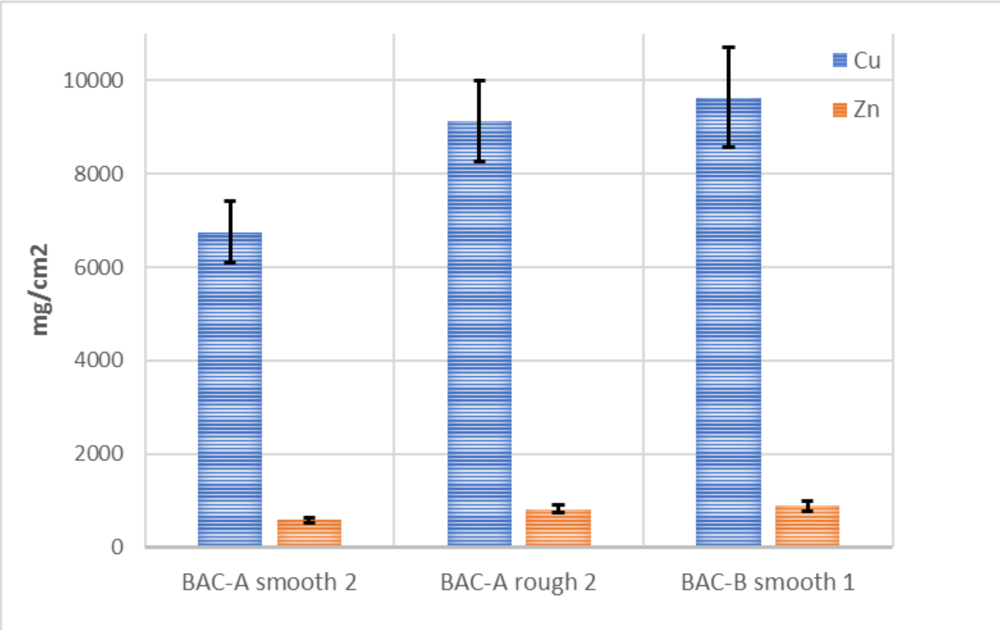

Fig.6: Concentration (expressed in mg/cm^2) of Cu and Zn in biocidal coatings applied on disks

Preliminary results show that *Cu* concentration in coatings is 6700 to 9600 mg/cm^2, whereas *Zn* results are under 900 mg/cm^2. As mentioned earlier in XRF section, the thicknesses for coatings were above critical thickness of 40 µm. Moreover, the coating thicknesses vary between *BAC* coatings types. Therefore, the current results were not compared with previous studies.

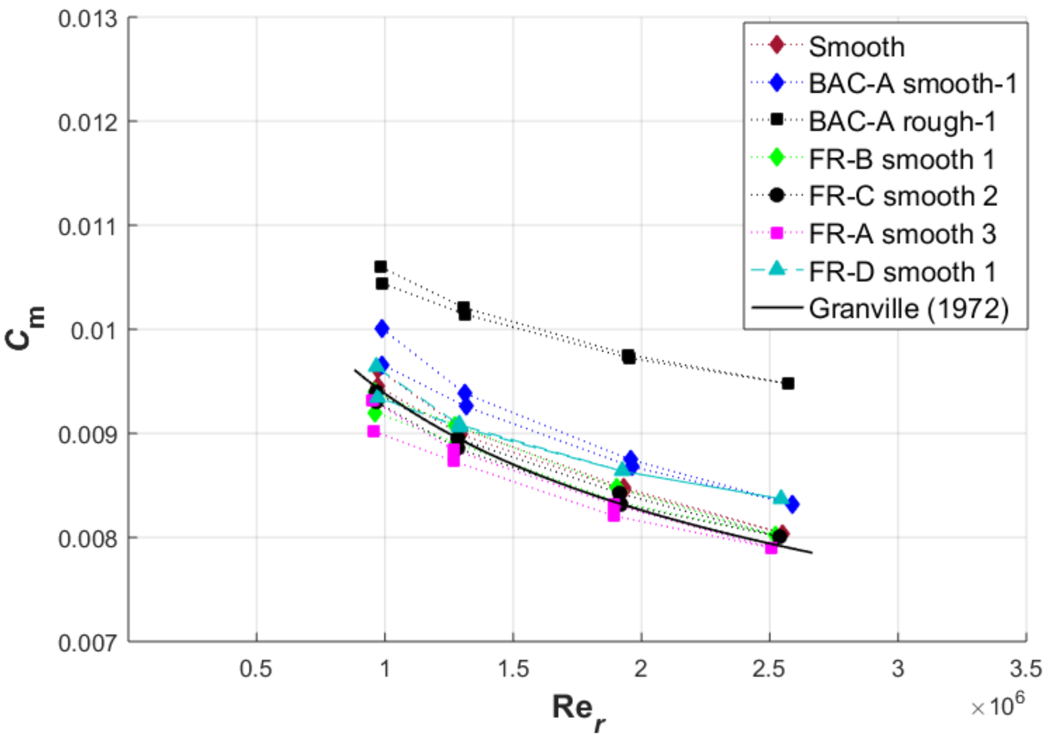

Fig.7: Change of non-dimensional torque coefficient for coated disks as function of Reynolds number

2.4.3. Torque measurements using the rotating disk rig

Fig.7 shows the torque coefficient (C_m) in non-dimensional variables plotted against Reynolds number, Re_r for all coated tested disks. In these results the torque of shaft, bearings, disk edge and uncoated side is subtracted, so that the drag effect of only coatings are present. As seen the results for smooth uncoated disk given in red-diamond curve agree well with the theoretical curve of *Granville (1972)*.

From these preliminary results, it can be inferred that drag effects of coatings are dictated by their surface heights. As an example, one replicate of *FR-A* type coated disk seems to perform better than the smooth PVC reference disk and the rest of the coated disks. When *Rt(50)* values were compared the same *FR-A* type replicates were found to be the smoothest amongst all coated disks. For other coated disks a gradual increase in drag was noticed according to their *Rt(50)*parameter. Overall, an increase of around 19% in C_m at the highest Reynolds number was noticed for the replicate of rough biocidal coating (*BAC-A rough 1*) as opposed to the smoothest disk coated with non-biocidal coating (*FR-A smooth 3*).

3. Future work

More drag data collection on different coatings with different roughness and fouling is planned using a flow channel facility based on flat plates, which is being manufactured during spring 2018.

In the planned experiment, we will work both with natural assemblages of microfouling from Port of Gothenburg and controlled lab-grown biofilms consisting of the diatoms *Amphora* and *Navicula* together with young stages of the green alga *Ulva.*

For the XRF measurements a calibration is planned which will enable measurement of metal concentration of films with the critical thickness d_{thin} >40 μm. This calibration will allow the accurate estimations of Cu and Zn in paints before and after they have been exposed to polishing.

This study has a potential to adding to knowledge on long term performances of hull coatings to guide in management strategy for ship operators.

Acknowledgements

We acknowledge the funding received from Chalmers Area of Advance Transport to support this work.

References

ATENCIO, B.N. (2016), *Measurement and Prediction of Friction Drag of Rough Surfaces*, Licentiate thesis, Chalmers University of Technology

BARRANGUETTE, C.; CHARANTONI, E.; PLANS, M.; ADMIRAAL, W. (2010), *Short-Term response of monospecific and natural algal biofilms to copper exposure*, Eur. J. Phycol 35, pp.397-406

BEERY, T.D. (1939), *Investigation In the N.A.S.A Tank of the Effect of Immersion in Salt Water On the Resistance of Plates Coated with Different Shipbottom Paints*, Supplementary Memorandum Report, National Advisory Committee for Aeronautics, C&R C-S19-1(3)

BENSON, J.M.; EBERT, J.W.; BEERY, T.D. (1938), *Investigation in the NACA Tank of the Effect of Immersion in Salt Water on the Resistance of Plates Coated with Different Shipbottom Paints*, NACA Memorandum Report C-S19-1(3), Washington (DC), National Advisory Committee on Aeronautics

CALLOW, J.A.; CALLOW, M.E. (2011), *Trends in the Development of Environmentally Friendly Fouling-Resistant Marine Coatings*, Nature Communication 2(244)

CALLOW, M.E. (1986), *Fouling Algae from 'In-Service' Ships*, Bot. Mar 29, pp.351-358

CONN, J.F.C.; LACKENBY, H. (1953), *B.S.R.A Resistance Experiments on the Lucy Ashton: Part 2- The Ship Model Correlation for the Naked Hull Conditions*, Trans INA 22

DENNY, M.E. (1951), *B.S.R.A resistance experiments on the Lucy Ashton: part 1- full-scale measurements*, Trans INA 93, pp.40-57

DOBRETSOV, S. (2010), *Marine Biofilms*, In Biofouling, Wiley-Blackwell, pp.123-136

GRAHAM, D.P. (1940), *Investigation of Frictional Resistance of Plates Painted with Three Shipbottom Systems*, Memorandum for File, Bureau of Construction and Repair

HIRAGA, Y. (1934), *Experimental investigations on the resistance of long planks and ships*, Zosen Kiokai 55, pp.159-199

LEWTHWAITE, J.C.; MOLLAND, A.F.; THOMAS, K.W. (1985), *An investigation into the variation of ship skin frictional resistance with fouling*, Trans. RINA 127, pp.269-284

MFIP (1952), *Marine Fouling and Its Prevention*, Contribution No.580 from the Woods Hole Oceanographic Institution, George Banta Publ.

MUNK, T.; KANE, D.; YEBRA, D.M. (2009), *The effects of corrosion and fouling on the performance of ocean-going vessels: A naval architectural perspective*, In Advances In Marine Antifouling Coatings and Technologies, pp.149-176

SCHULTZ, M.P.; SWAIN, G.W. (1999), *The effect of biofilms on turbulent boundary layers*, J. Fluid Mechanics 121, p.51

SCHULTZ, M.P.; SWAIN, G.W. (2000), The influence of biofilm on skin friction drag, Biofouling 15(1-3), pp.129-139

SNYDER, P.W. (1938), *Fouling Tests of Friction Plates*, Memorandum for File, Bureau Of Construction and Repair

SWEAT, L.H.; JOHNSON, K.B. (2013), *The effects of fine-scale substratum roughness on diatom community structure in estuarine biofilms*, Biofouling 29(8), pp.879-890

TOWLER, B.W.; RUPP, C.J.; CUNNINGHAM, A.L.B.; STOODLEY, P. (2003), *Viscoelastic properties of a mixed culture biofilm from rheometer creep analysis*, Biofouling 19(5), pp.279-285

YTREBERG, E.; LAGERSTROM, M.; HOLMQVIST, A.; EKLUND, B.; ELWING, H.; DAHLSTROM, M.; DAHL, P.; DAHLSTROM, M. (2017), *A novel XRF method to measure environmental release of copper and zinc from antifouling paints*, Environmental Pollution 225, pp.490-496

ZARGIEL, K.A.; COOGAN, J.S.; SWAIN, G.W. (2011), *Diatom community structure on commercially available ship hull coatings*, Biofouling 27(9), pp.955-965

Ideas on How to Improve ISO19030 based on the Results of Applying to Field Data

Beom Jin Park, KRISO, Daejeon/Republic of Korea, baracude@netopia.re.kr
Myung-Soo Shin, KRISO, Daejeon/Republic of Korea, msshin@netopia.re.kr
Min Suk Ki, KRISO, Daejeon/Republic of Korea, mski@kriso.re.kr
Gyeong Joong Lee, KRISO, Daejeon/Republic of Korea, gjlee@kriso.re.kr
Sang Bong Lee, Lab021, Busan/Republic of Korea, sblee@lab021.co.kr

Abstract

This paper describes possible alternatives to the current ISO19030 filtering scheme, which has the problem of removing too much data and thus has possibility of providing unreliable performance evaluations. Averaging and resistance-in-waves correction is proposed and are applied to the operational data obtained from a 176K bulk carrier. In case of averaging, it did not give any better results than the current filtering scheme. However, resistance-in-waves correction gave more reliable results since it is based on much more data and gives similar results in cases when the current filtering scheme removes relatively less amount data.

1. Introduction

In HullPIC 2017, we presented a paper discussing problems with applying ISO10930 to data collected during ship operation. In summary, availability of data necessary for ISO19030, too much data being filtered out, and inconsistency of performance analysis results were found as major areas for improvement.

This paper proposes averaging and a resistance-in-waves correction as an alternative to the current filtering scheme. In order to evaluate the feasibility of applying these alternatives, they are applied to a set of data obtained during the operation of a 176K bulk carrier. Average PVs are calculated using each alternative method, as well as the current ISO19030 filtering scheme. The results are compared for each voyage to analyse if any alternatives have the possibility of providing more reliable or accurate representation of the ship's performance.

2. Operational data

The operational data used in this paper is measured during the operation of a 176K bulk carrier carrying coal and ores, Table I. Since it is a bulk carrier, the ship usually travels in either ballast or laden condition and hardly ever in other load conditions.

Table I: Main dimensions of the bulk carrier

Length between perpendiculars	282.00 m
Breadth, moulded	45.00 m
Depth, moulded	24.75 m
Mean draught, Laden	18.25 m
Mean draught, Ballast	7.90 m

The operational data was measured from 22nd Feb, 2017 to 18th Nov, 2017 on 6 voyages, each with 2 or 3 legs of journey, Table II. All measurements were recorded with 10 s interval corresponding to a data frequency 0.1 Hz. Measured data items are shown in Table III.

Table II: Voyage details of the bulk carrier

Voyage	Leg	Departure	Arrival	Loading	Mean Draught
49	2	2017.02.22	2017.03.08	Ballast	8.91 m
	3	2017.03.13	2017.03.29	Laden	17.80 m
50	1	2017.04.03	2017.04.17	Ballast	7.72 m
	2	2017.04.26	2017.05.12	Laden	18.02 m
51	1	2017.05.16	2017.05.16	Ballast	7.51 m
	2	2017.05.16	2017.05.31	Ballast	7.63 m
	3	2017.06.08	2017.06.23	Laden	18.10 m
52	1	2017.06.28	2017.07.12	Ballast	7.55 m
	2	2017.07.18	2017.08.03	Laden	18.07 m
53	1	2017.08.08	2017.08.20	Ballast	7.48 m
	2	2017.09.07	2017.09.19	Laden	18.17 m
54	1	2017.09.23	2017.10.04	Ballast	7.38 m
	2	2017.11.05	2017.11.18	Laden	18.22 m

Table III: On-board Measured items

Category	Measured items
Speed	Speed through water, speed over ground
Location	Latitude, Longitude
Heading	Gyro heading, GPS heading
Propulsion	Shaft power, torque
Draught	Aft, fore, starboard and port side draught
Wind	Relative wind speed, direction
Temperature	Sea water temperature, air temperature
Depth	Sea depth

3. Data filtering in ISO19030

In ISO19030, the following data filtering criteria is used to only leave data with relative calm sea conditions and stable cruising period during a ship's operation.

- Outlier filtering (ISO19030-2 Annex I)
  - Use Chauvenet's criterion to a 10 min block to remove outliers
- Validation (ISO19030-2 Annex J)
  - Standard error of the mean of RPM for a 10 min block is less than 3 rpm
  - Standard error of the mean of speed through water for a 10 min block is less than 0.5 knots
  - Standard error of the mean of speed over ground for a 10 min block is less than 0.5 knots
  - Standard error of the mean of rudder angle for a 10 min block is less than 1°
- Reference condition (ISO19030-2 6.2.1)
  - Water temperature is above 2° C
  - True wind speed is between 0 – 7.9 m/s (BF 0 and BF 4)
  - No shallow water

Outlier filtering is intended to remove any outlying value due to sensor errors, etc. Validation criteria tries to remove the portion of data when a ship is increasing or decreasing speed or changing the direction. Reference condition selects the portion data with environmental conditions that environmental correction methods applied in ISO19030 can deal with.

Park et al. (2017) discussed that too few records are left when the above filters are applied and that such few records cannot represent the performance of a ship correctly.

ISO19030 uses validation based on standard error of means to discard data while a ship is increasing or decreasing speed. However, speed measurements in a ship is not stable enough for standard error of means value of 0.5 kn. Fig.1 shows an exemplary portion during the bulk carrier's operation. As you can see on overall trend, the bulk carrier is cruising at stable shaft speed of around 82 RPM. However, during this stable period, speed through water and speed over ground fluctuate by more than 1 kn frequently. Therefore, data in this stable period of cruising has high probability to be discarded according to the validation criteria of ISO19030 despite the intention of the standard.

This paper recognises possible area of shortcomings in the current ISO19030 standard and proposes possible alternatives to the current filtering scheme in ISO19030. The subsequent sections examine each possible alternative and compares analysis results with analysis results of current ISO19030.

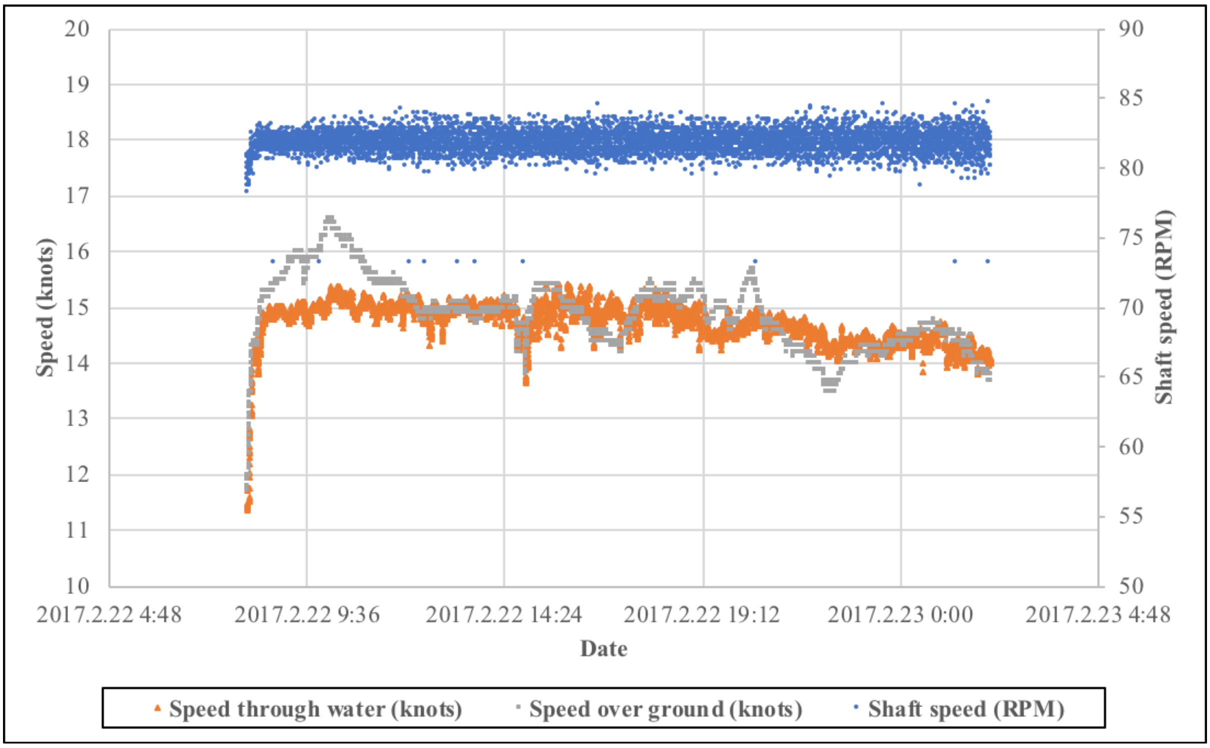

Fig.1: Comparison of shaft speed, speed through water and speed over ground

4. Averaging data

The first alternative filtering scheme is to simply average data. Averaging usually reduces fluctuations and increases the probability of getting stable results. ISO19030 also uses averaging for calculating performance indicator where each performance value is averaged over the reference and the evaluation period to obtain a single performance indicator value.

The operational data used in this paper has measuring interval of 10 s. From this data, averaged value of 2 min, approximately 12 records, was used instead of original data and no other filter, validation or reference condition in ISO19030 was applied.

Fig.2 shows analysis results with ISO19030 default filtering scheme and averaging. PV is the performance value as described in ISO19030, which is the percentage of difference between expected speed calculated from the model test or sea trial speed power curve and measured speed. PVs of a voyage is averaged to represent a point in Fig.2. As shown in the figure, averaging does not give much better results than default filtering scheme. It gives similar results at best and can give very different results (-22% instead of -7%) where it obviously gives wrong results. Therefore, averaging does not give any better performance analysis results.

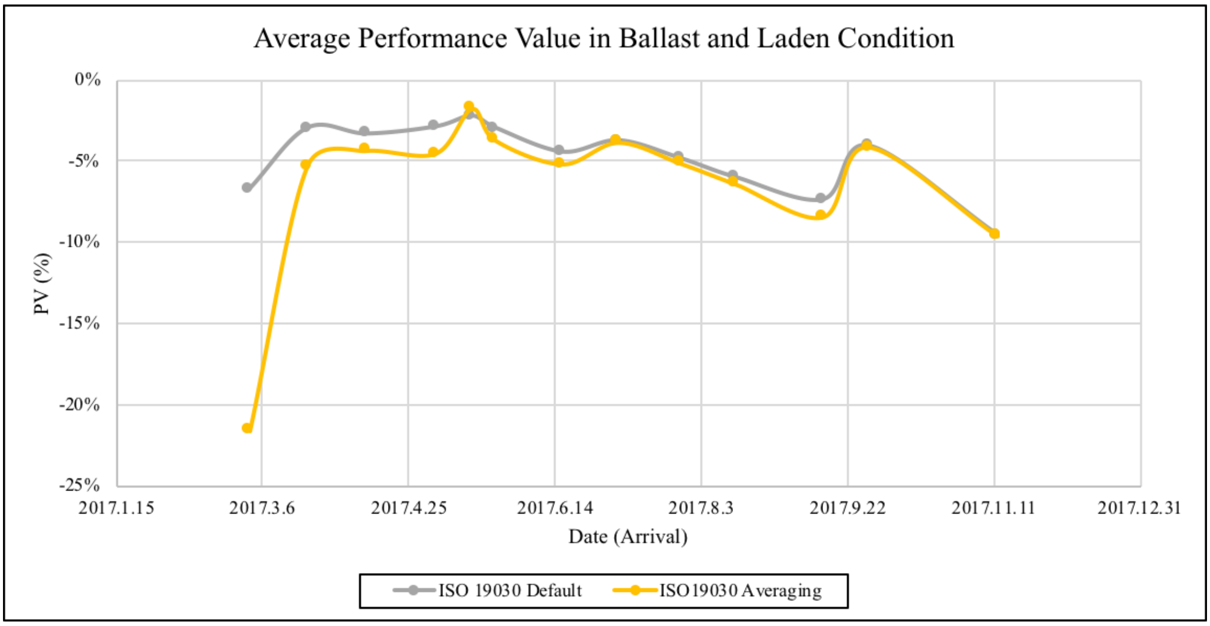

Fig.2: Comparison of average PV between ISO19080 default filtering results and averaging results

5. Environmental correction for added resistance due to waves

The next alternative is to complement what is the mission in ISO19030. In environment correction methods used in ISO19030, wave correction is not included since wave data (height, period, direction) is not easily measurable on-board a ship. It is also assumed, when a ship's operation profile is not changed, during long reference and evaluation period of performance indicators (typically 1 year) wave effect will be averaged out when calculating relative, not absolute performance difference.

However, for many shipping companies employing performance analysis methods such as ISO19030 to identify their fleet's performance, making comparison by years is too long. Shipping companies typically want to identify any possible degradation of their fleet's performance voyage by voyage or at least between several months. When comparing performance between such short period of time, assumptions in ISO19030 for not including wave correction no longer hold.

Also, wave measurement data can be obtained from the sources other than on-board measurements. There are publically available sources for weather data such as NOAA (National Oceanic and Atmospheric Administration) and shipping companies usually have contracts with weather data providers to receive weather forecast data for their optimal voyage planning. In this paper, NOAA wave data is used in the added resistance due to waves calculation.

There are two environmental correction methods used for added resistance due to waves in this paper; STAWAVE II and the theoretical method, both included in ISO15016:2015, the standard for analysing a ship's speed trial. STAWAVE II uses simpler formulae, requiring very small amount data on a ship's geometry and very fast to calculate. However, STAWAVE II can only calculate waves having incident angle within ±45° of a ship's heading. When applying STAWAVE II methods, all data with wave direction outside ±45° are considered as having 0 resistance. While ISO15016:2015 bestow the same restriction as STAWAVE II to only use the theoretical method in calculating waves within ±45° of a ship's heading, the original proposal of the theoretical method was to be able to calculate waves with direction all around a ship. However, the theoretical method requires much more data on the geometry of a ship and takes quite some time, typically 1 to 2 min for each data point to calculate added resistance due to waves. When considering the amount of data handled in a ship's operation, taking 1 to 2 min for each data point is nearly unusable. To solve this problem, the added resistance is pre-calculated for possible wave heights, periods, direction and the ship's speed through water for both ballast and laden condition. When calculating for each data point, wave resistance value is read from pre-calculated tables. In both cases, no other filtering scheme is used, but certain filtering is implicitly applied. As performance value of a data point with measured speed through water not within the range of model test or sea trial speed power curve cannot be calculated, and usually speed range of the speed power curve is near the normal cruising speed of a ship, most of data used for performance value calculation are during the stable cruising period of operation. Therefore, much of data during change of speed and direction is usually removed.

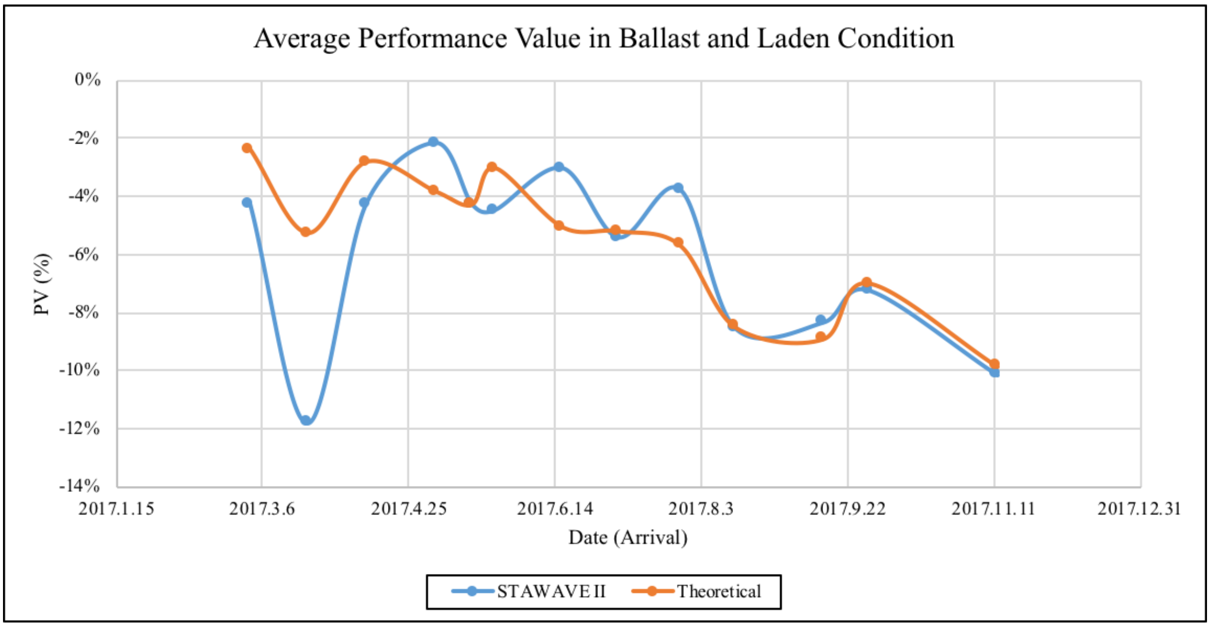

Fig.3: Comparison of average PV between STAWAVE II results and the theoretical method results

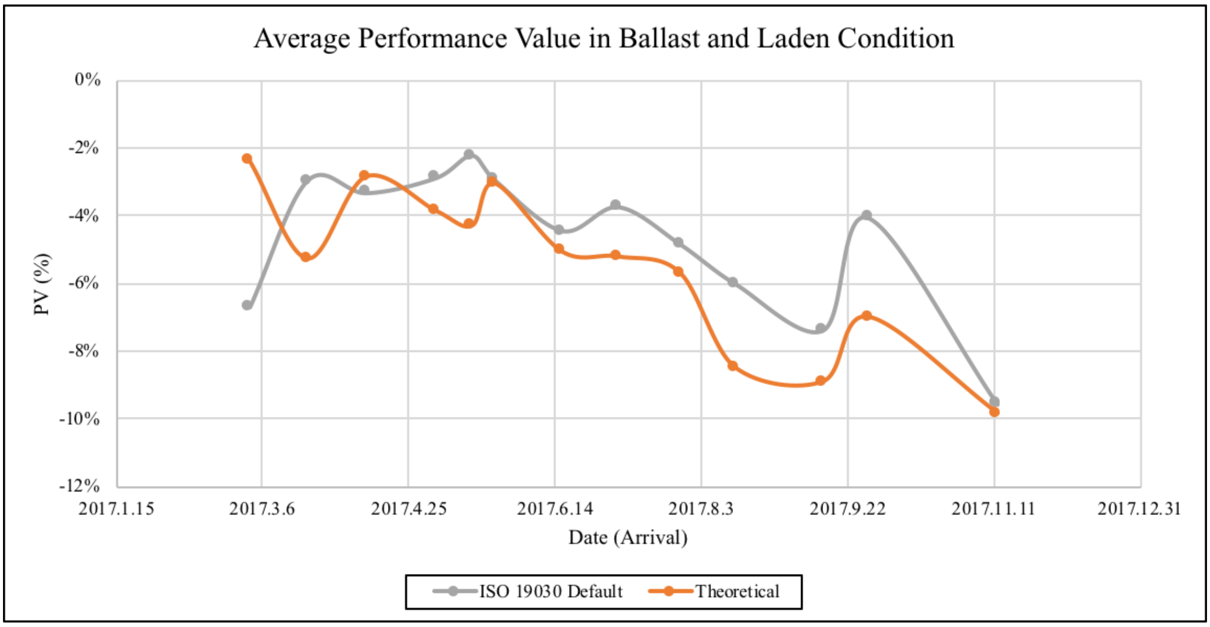

Fig.4: Comparison of average PV between ISO19080 results and the theoretical method results

Fig.3 compares the analysis results applying STAWAVE II and theoretical methods. The analysis results of both method show general decline in performance as expected, however, applying STAWAVE II method gives more fluctuating curve than applying theoretical method. As each voyage, represented as a point in Fig.3 are quite short, wave profile encountered in each voyage will not be the same with each other. Since STAWAVE II method only corrects a certain portion of wave data, difference in the encountered wave profile will have more effects when using STAWAVE II methods, while theoretical methods correcting all wave data give more stable curve. Therefore, where applicable, it will be better use the theoretical method than STAWAVE II method for environmental correction of added resistance due to waves.

Fig.4 compares the analysis results applying ISO19030 and the theoretical method. Generally, the performance values using ISO19030 is better than using the theoretical method. Since ISO19030 default filtering scheme removes much of data where environment condition is adverse, the performance analysis results using ISO19030 tends to be better than using the theoretical methods.

Table IV: Number of records filtered out using ISO19030 and the theoretical method

Voyage	Leg	No. Records				
		Original	ISO 19030		Theoretical	
49	2	122,028	4,720	4%	96,537	79%
	3	133,795	15,232	11%	119,546	89%
50	1	115,804	12,029	10%	83,817	72%
	2	133,964	12,644	9%	115,694	86%
51	1	1,950	731	37%	1,720	88%
	2	124,893	31,123	25%	120,080	96%
	3	129,428	31,497	24%	125,788	97%
52	1	117,116	54,058	46%	112,252	96%
	2	118,081	21,569	18%	113,809	96%
53	1	97,803	38,344	39%	91,135	93%
	2	103,607	48,168	46%	98,075	95%
54	1	90,229	50,315	56%	87,097	97%
	2	104,364	67,591	65%	99,769	96%

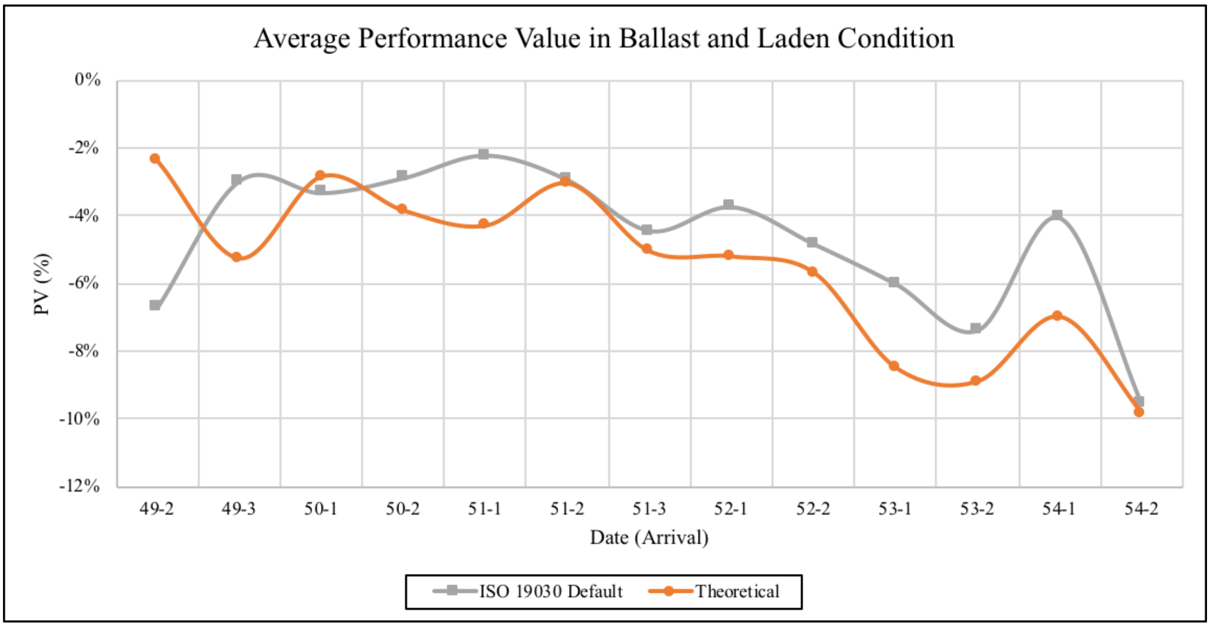

Fig.5: Comparison of average PV between ISO19030 and theoretical methods results by voyage

Table IV shows the number of records filtered out using ISO19030 and the theoretical method. The number of records filtered out using ISO19030 vary greatly from voyage to voyage, but the theoretical method uses consistently large percentage of data. Looking at Fig.5, which shows average PV by voyage, it is notable that voyages with only very small percentage of records remain for calculation in

ISO19030, such as voyage no. 49 and 50, average PV shows different trends than using theoretical method. However, when more than 30% of the original data remain for calculation using ISO19030 such as the case in voyage no. 51-1, 52-1 and 53, average PV shows very similar trends to using theoretical method while ISO19030 shows better average PVs.

6. Conclusions

In this paper, two possible alternatives to the current ISO19030 filtering scheme are proposed. The first alternative, averaging, does not give any better performance evaluation results than the current filtering scheme.

For the second alternative, resistance-in-waves correction, two correction methods included in ISO15016:2015, STAWAVE II and the theoretical method are applied. Comparing the two methods, the theoretical method gives more stable results, being less affected by the difference in the encountered wave profile. When comparing the current ISO19030 filtering scheme to the theoretical method, they both show similar trends for the cases when the current filtering scheme does not remove major portion of data but ISO19030 shows almost consistently better performance results. Therefore, wave resistance correction can be a possible alternative to improve the reliability and accuracy of ISO19030. However, more study with other datasets are necessary to draw general conclusions.

Acknowledgement

This research was supported by a grant from National R&D Project of "Development of advanced speed-power analysis technology to attain high energy efficiency and GHG reduction of operating ships under real sea condition (10048825)" funded by the Ministry of Trade, Industry & Energy, Republic of Korea.

References

ISO19030-1 (2016), *Ships and marine technology – Measurement of changes in hull and propeller performance – Part 1: General principles*, ISO, Geneva

ISO19030-2 (2016), *Ships and marine technology – Measurement of changes in hull and propeller performance – Part 2: Default method*, ISO, Geneva

ISO19030-3 (2016), *Ships and marine technology – Measurement of changes in hull and propeller performance – Part 3: Alternative methods*, ISO, Geneva

ISO15016 (2015), *Ships and marine technology – Guidelines for the assessment of speed and power performance by analysis of speed trial data*, ISO, Geneva

PARK, B.J.; SHIN, M.S.; KI, M.S.; LEE, G.J.; LEE, S.B. (2017), *Experience in applying ISO19030 to field data*, 2nd HullPIC, Ulrichshusen, pp.150-155

Practical Experience with ISO 19030 at Chevron Shipping - Part 2

Barry Kidd, AkzoNobel, Gateshead/UK, barry.kidd@akzonobel.com
Haoliang Chen, AkzoNobel, Singapore, haoliang.chen@akzonobel.com
Yuhuai Seah, AkzoNobel, Singapore, yuhuai.seah@akzonobel.com
Wen Xiang Chue, AkzoNobel, Singapore, wenxiang.chue@akzonobel.com
Alistair A. Finnie, AkzoNobel, Gateshead/UK, alistair.finnie@akzonobel.com

Abstract

This paper reviews AkzoNobel's practical experiences of applying ISO 19030 to vessel performance datasets provided by Chevron Shipping. It highlights benefits and limitations of noon report datasets and illustrates some of the challenges that are encountered when applying the ISO 19030 standard using data that does not meet the strict data-quality requirements of the standard. Consequently, data-analysts must use their judgement, make assumptions and apply ad hoc modifications to the methods prescribed by ISO 19030 in order to interpret these datasets and extract useful and meaningful vessel performance data to support decision making. Based on detailed discussions of practical adjustments to analysis method and the uncertainties in the results, it points out the need for sufficient data quality and quantity. The findings are valuable information and provide useful starting points for future improvements of ISO 19030.

1. Introduction

1.1. Background

This is the second in a short series of papers that will present the interim results of a multi-year technical project involving Chevron Shipping, AkzoNobel Marine and Protective Coatings and Jotun Paints relating to Chevron's experience of ISO 19030 on measurement of changes in hull and propeller performance, *ISO (2016a,b,c)*. *Eliasson (2018)* introduces the concept behind the collaborative project, its objectives and, in broad terms, some of the outcomes so far. This second paper of the series considers the practical aspects of applying the 3-part ISO 19030 standard to a series of vessel datasets provided by Chevron. *Abrahamsen (2018)* reviews the perceived limitations of ISO 19030 and discuss future potential changes to improve the practical applicability of the standard.

In common with many vessel operators, Chevron have a wealth of in-service performance data to-hand for the vessels in their fleet but may not always have the necessary in-house resource, expertise or available dedicated time to thoroughly interrogate and interpret the data. As a result, the impact of past investment decisions is often difficult to meaningfully assess, and the impact of potential future decisions difficult to reliably predict, especially when a range of vessel performance is seen across a fleet. Assembling a team of experts from various scientific disciplines may seem like an obvious solution, but historically individual fleet owners have often been very protective of their information on the operational efficiency of their vessels. In this project, Chevron have adopted a more collaborative approach to share data with two of its fouling control coatings suppliers in order to develop a better understanding of the connection between hull condition, fouling control coating selection and vessel operational efficiency.

The choice of fouling control coating is one of the key variables influencing the hull condition and ship efficiency for any particular vessel. ISO 19030 is intended to provide practical methods for measuring changes in ship-specific hull and propeller performance and defines a set of relevant performance indicators for hull and propeller maintenance, repair and retrofit activities. In principle, this enables vessel performance datasets to be reviewed in order to quantify the impact of past and future selections of energy saving solution options such as the choice of fouling control coating. This paper will review some of the practical experiences of AkzoNobel's vessel performance analysis team when applying ISO 19030 to vessel performance datasets provided by Chevron Shipping.

1.2 Project Overview

The overall aims of the project have been outlined in *Eliasson (2018)* and its general structure is schematically represented in Fig.1. It is acknowledged that the project objectives are ambitious and may not be fully realised in the short term and it is understood that it may take many years to generate and interrogate sufficient quantity and quality of data to fully deliver every aspect of the project.

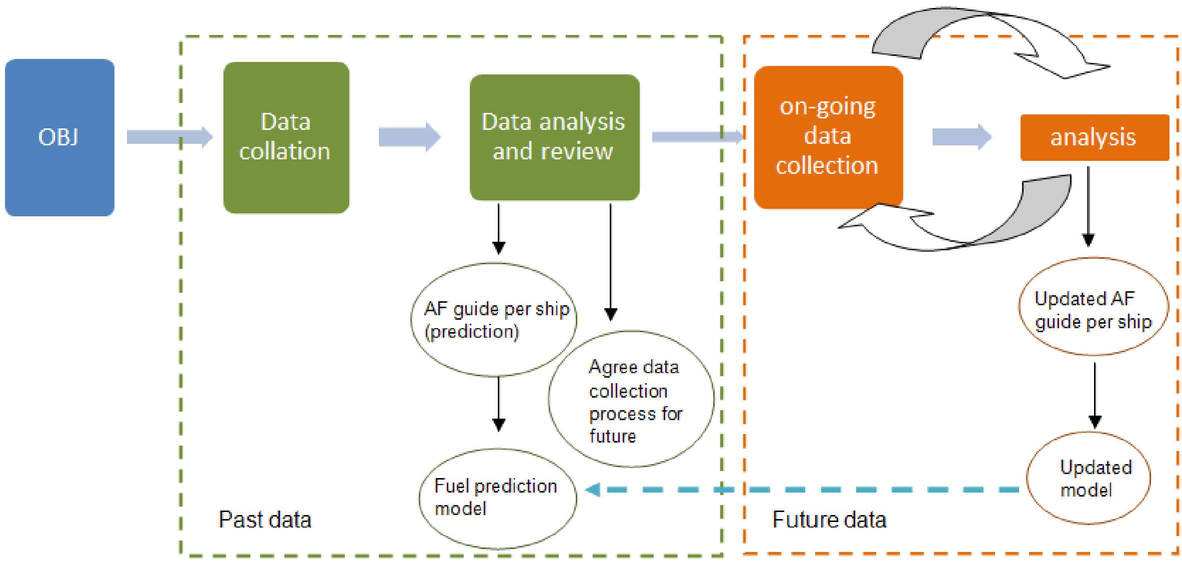

Fig.1: High-level project overview

2. Chevron Fleet In-Service Performance Datasets and Subsets

The applicability of ISO 19030 to the analysis of in-service performance datasets will be illustrated using a sub-set of data for 10 vessels from Chevron's tanker fleet. Table I gives summary information on the vessels and the relevant data-sets before and after a dry-docking (DD) event. Table II lists a selection of the parameters included within the noon reports for the sub-set of vessels from Chevron's fleet.

Table I: Summary information on the vessels reviewed in the project

Vessel Identifier	Vessel Type	DWT	Activity (%)[a]		Number of months in-service for the dataset		Data Points Available (before processing)		Data Points Available (after processing)	
			Before DD[b]	After DD	Before DD	After DD	Before DD	After DD	Before DD	After DD
A	VLCC	320,000	76	77	18	29	820	898	202	333
B	VLCC	321,000	70	76	28	22	840	736	202	285
C	VLCC	317,000	81	73	23	25	730	833	180	287
D	VLCC	321,000	80	84	36	17	1011	553	302	238
E	Shuttle	154,000	40	57	33	7	1046	393	153	59
F[c]	VLCC	319,000	-	76	-	32	-	1103	-	384
G[c]	VLCC	319,000	-	78	-	46	-	1741	-	468
H[d]	Aframax	105,000	-	39	-	48	-	1776	-	166
I[d]	Aframax	106,000	-	68	-	21	-	514	-	235
J[d]	Aframax	105,000	-	38	-	49	-	1789	-	210

[a] Activity (%) = total percentage of time the vessel operated with a speed over ground (SOG) > 3 knots during the relevant period; [b] DD = dry-docking event; [c] new-build vessels so there is no applicable pre-DD data; [d] no pre-DD data available.

Table II: List of selected parameters from Chevron's noon reports

Average speed through water from last report (knots)
Steaming distance from last report (NM)
Shaft power (kW)
Total fuel oil consumption (FOC) from last noon
Average RPM from last report
Wind speed (knots & Beaufort number) & direction
Wind sea height (m) & wind sea direction
Swell height (m) & direction
Loading conditions (ballast or laden)
Slip from last report (%)
Total hours reporting

The in-service vessel performance datasets from Chevron's fleet consist of noon reports that are derived from daily recordings of parameters such as the vessel speed and heading etc., as well as calculated averages of speed through water, fuel oil consumption (FOC) etc. since the previous noon report. The reported noon data is manually collected by the crew and inputted to an Excel spreadsheet which is then transferred to a central database. Typically, it takes the crew around 15 minutes per day to collect and transfer the noon report data.

3. Data Treatment

As the in-service vessel performance dataset from Chevron consisted of noon reports, it was not possible to analyse these datasets via the ISO 19030-Part 2 default method, *ISO (2016b)*, as the minimum data-quality requirements were not met. As such, the analysis was therefore conducted in a manner consistent with the general principles set out in ISO 19030-Part 3, *ISO (2016c)*, which outlines alternative methods. However, even here it should be noted that the Chevron in-service vessel performance noon report datasets are not fully consistent with the data-requirements of any of the four specific alternative methods that are outlined in Part 3. The method with the closest fit to the Chevron dataset is ISO 19030-Part 3 method 3-4, but without use of the water depth and speed over ground parameters as these data were not available.

The principle outputs from ISO 19030 are a series of performance indicators (PIs) in relation to the dry-docking performance, in-service performance, maintenance trigger and maintenance effect. To calculate these PIs, however, the data-analyst more or less always has to apply their own interpretation regarding how to best apply ISO 19030 to individual datasets. Specifically, in the case of the datasets provided by Chevron, four key aspects of the data-analysis are discussed below.

1) Vessel performance datasets almost invariably exhibit large variation in the raw data. As a result, the large variations are carried through from the raw data to the PIs. This is the case even after outlier data-points have been identified and removed using standard tools such as application of Chauvenet's criterion or multiple standard deviation filters. The dispersity of the data leads to larger uncertainties than would be otherwise desired.
2) Section 6.3.2 of Part 3 of the standard, *ISO (2016c)*, recommends that reference curves are either provided or determined for all relevant draught conditions within which only a small range of draught variance is permissible. In order to have sufficient data points to construct reliable reference curves, a commonly adopted approach is to simply split the dataset into ballast and laden draught conditions corresponding to the loading condition of the vessel. This approach was utilised for the analysis of Chevron's tanker fleet dataset.
3) Given that ISO 19030 primarily focusses on changes in the power / speed relationship of a vessel over time, assessing the reliability of these measured parameters is of considerable importance. Following a review of the reported shaft power data for all vessels, it is clear that there were serious inconsistencies in the dataset. As a result, the shaft power data was not considered in this project. Instead, the focus within this project shifted to the relationship between FOC / speed, which

is often assumed as to be a proxy for the power/speed relationship. It should be noted that this represents a marked deviation from the normal practice of ISO 19030.

4) The reference best-fit regression curves for both the power speed or FOC / speed relationship for the processed data is very often found to exhibit a low level of fitness to the data. ISO 19030 recommends that “coefficient of determination (R^2-value) for the generated speed-power curves must be above 0.8”. When the R^2-value is less than 0.8, as is the case for the example datasets illustrated in Fig.2, the cubic law was used to normalize the power or fuel to a specific speed.

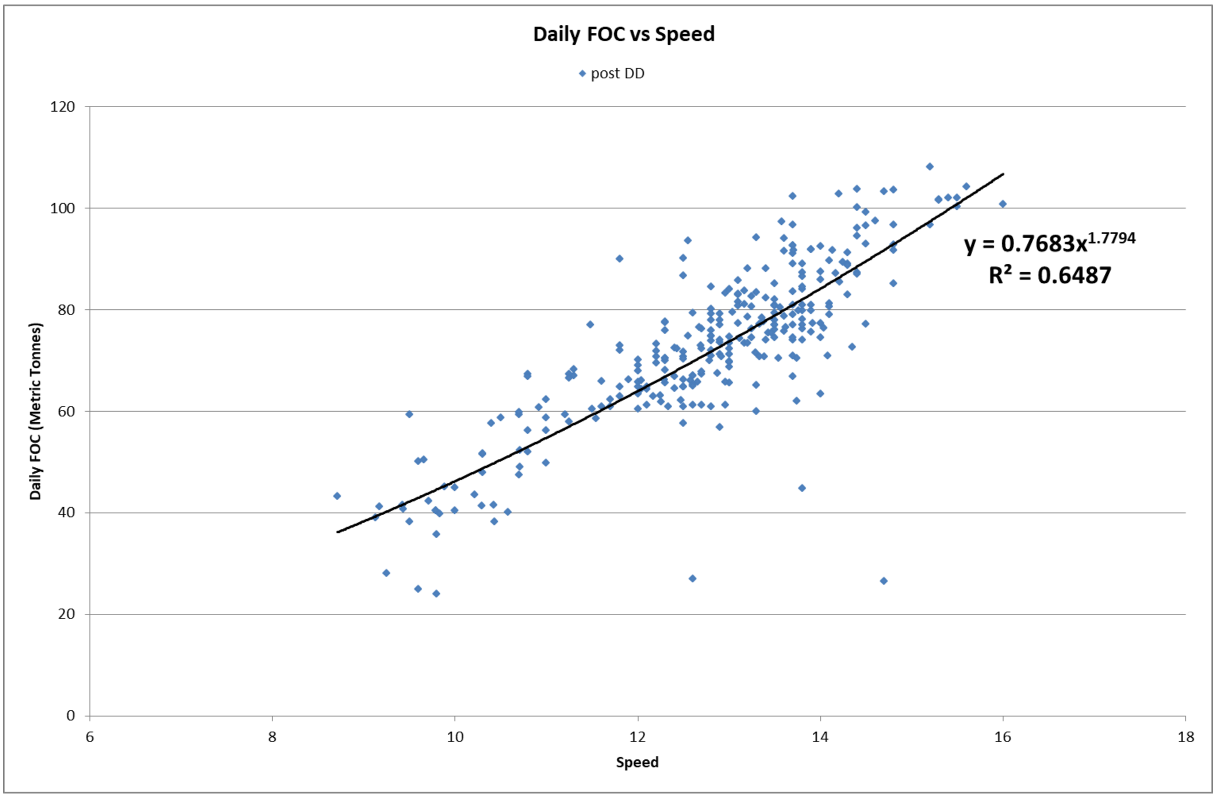

Fig.2: Example of a FOC / speed curves derived for vessel A in the laden condition post dry-docking

4. Results & Discussion

Using historical data and information regarding maintenance events such as dry-dockings, hull and propeller cleans, the ISO 19030 PIs associated with the dry-docking, in-service, and maintenance effect have been determined using the modifications to the ISO 19030-Part 3 procedure outlined above. As the purpose of this paper is to illustrate the process rather than to presents the detailed results, the majority of the examples provided below will focus on the PIs relevant to laden draught condition.

4.1. Dry-docking PI

ISO 19030-Part 2 stipulates that the reference and evaluation periods when calculating the dry-docking PI must be a minimum of 1 year. However, ISO 19030-Part 3 allows for shorter periods to be used where necessary or desirable. In this example, the dry-docking PI has been determined for reference and evaluation periods of 6-month pre- and post-dry-docking. Based on their experience, most ship owners would likely expect to observe an improvement in vessel performance as a result of a dry-docking, and as illustrated in Fig.3, this is the case here for the five vessels in the Chevron dataset with pre- and post-DD data.

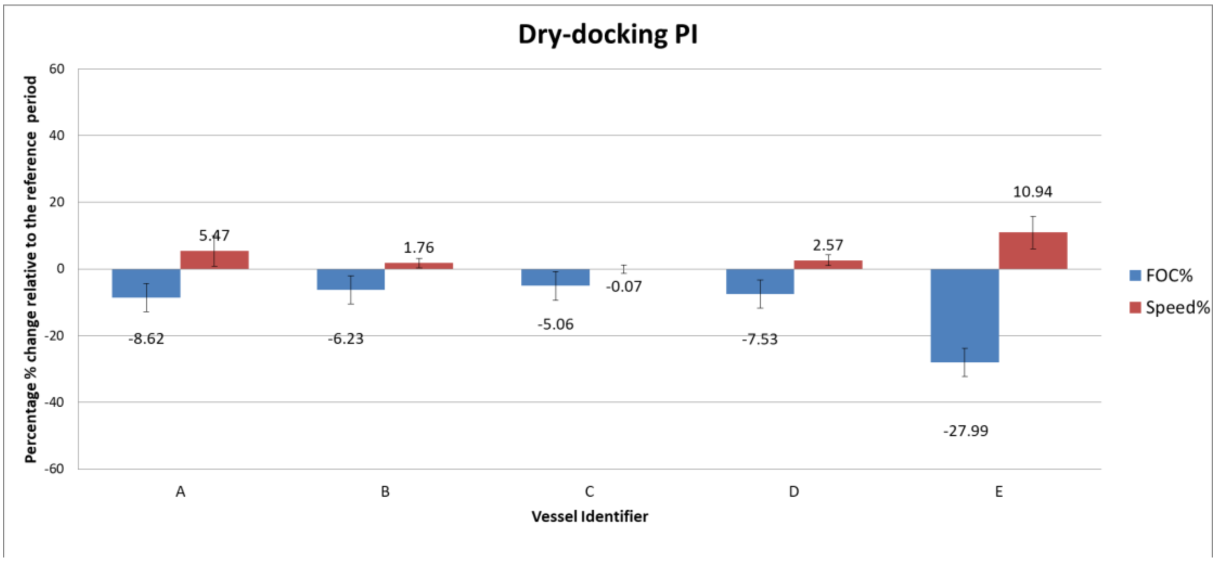

Fig.3: Examples of the dry-docking PI for selected vessels; error bands represent 95%CI. Note: FOC is being used as a proxy for the shaft power parameter specified by ISO 19030-Part 3.

If there are no major retrofit works during the dry-docking that may significantly impact on the FOC of each vessel, it may be possible to link the degree of change between the pre- and post-underwater hull and propeller condition with the dry-docking PI. The magnitude of the improvement in the DD PI may then be dependent on several factors associated with the underwater hull and propeller condition, such as the hull and propeller condition pre-DD, extent of damage and repair, extent and nature of substrate preparation, the application of new coatings schemes, propeller cleaning and maintenance etc. As can be seen in Fig.3, the dry-docking PI varies from vessel to vessel and without a full knowledge of each vessel's history and its hull/propeller condition it would be very difficult to make sense of where the improvements originate. Future work will consider a review of the likely contributory factors to the dry-docking PI.

The magnitude of the error bar (uncertainty band) for each vessel PI reflects the degree of scatter within the dataset. Not surprisingly, large uncertainties are associated with most of PI values. The large uncertainty bands indicate that the apparent differences in the PI for some vessels, for example for vessels A and B, may not be statistically significant. Future work using standard statistical methods (e.g. ANOVA) will be used to look into this more closely. Reducing the uncertainty associated with this PI would be useful as it would allow greater discrimination between datasets. *Abrahamson (2018)* reviews how this can be achieved, in particular for noon datasets.

In light of the large uncertainty within an individual vessel's dry-docking PI, one useful approach is to generate an aggregated view and determine an average value for a range of similar vessels in a fleet, as illustrated in Fig.4.

Fig.4 shows the average DD PI determined for the five-vessel Chevron fleet sub-set. The average DD PI determined for these vessels, i.e. the difference between the pooled average FOC for the 6 months pre-DD period and the pooled average FOC 6 month post-DD period, is approximately 17%. This indicates that for this sub-set of vessels, an efficiency improvement of around 17% in FOC and with a corresponding reduction in GHG emissions is achieved as a result of the maintenance and repair conducted whilst the vessels were in dry-dock. However, it is not possible to use this data to determine the relative contribution to the overall improvement that arose from any retrofitting/engineering works that were undertaken from the contribution that arose from the application of fresh coating schemes or other general hull and propeller maintenance operations.

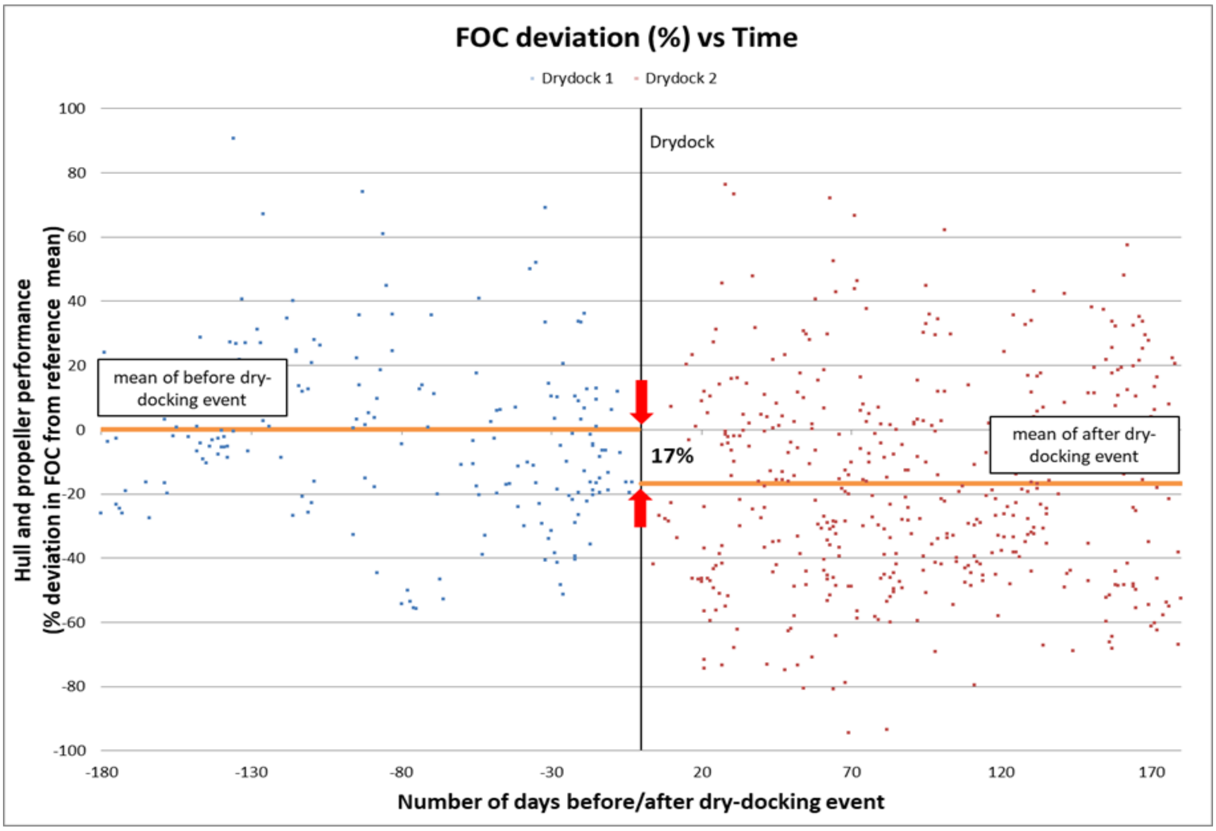

Fig.4: Overall average dry-docking PI for the Chevron fleet sub-set

4.2. In-service PI

As was the case for the dry-docking PI, ISO 19030-Part 3 allows for shorter post-DD reference and evaluation periods to be used for the in-service PI where necessary or desirable. In this example, the in-service PI has been determined for the nine vessels in the Chevron fleet which have suitable post-DD reference and evaluation periods of 6-months (vessel E is excluded as data is only available for 7 months in total). The in-service performance of each vessel will be dependent on many factors including but not limited to vessel type and size, its operational profile, effectiveness of the fouling control coatings etc. etc. That said, it might be expected that the accumulation of damage and wear and tear over time may lead to a slow but progressive loss of in-service performance. However, this does not appear to be true for most of the vessels within Chevron's sub-set of vessels illustrated in Fig.5. As before, it is not possible to use this data to determine the relative contribution of engineering factors from the contribution of the fouling control coating or other aspects of the hull and propeller condition.

Whether the indication of reduced FOC over time is valid or not is hard to determine without a more detailed inspection of the dataset. Again the degree of scatter or noisiness within the dataset and its impact on the statistical significance of each vessel's PI need to be carefully reviewed when attempting to compare the performance of vessels within a fleet.

As a further illustration of the in-service PI, Fig.6 provides an example where the in-service PI is calculated for an evaluation period ranging from the end of a 6-month reference period to the end of the 48-month overall dataset for vessel G in ballast and laden condition. The progression of the in-service PI over time can be clearly seen and there is a general trend of increasing FOC for the ballast condition, whereas there is a decreasing FOC trend for the laden condition.

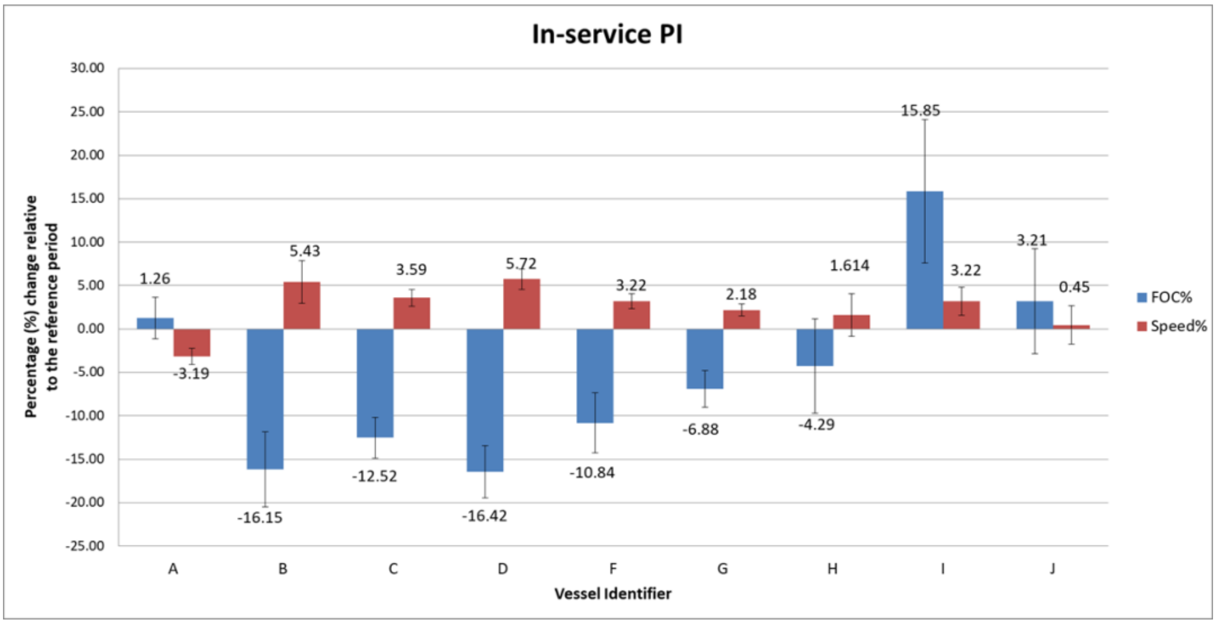

Fig.5: Examples of the in-service PI for selected vessels; error bands represent 95%CI.
Note: FOC is used as a proxy for the shaft power parameter specified by ISO 19030-Part 3.

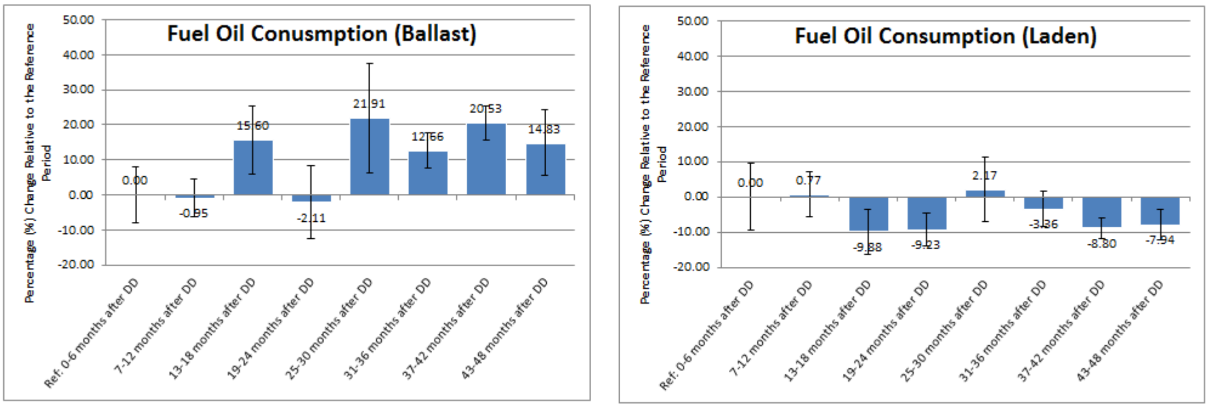

Fig.6: Time series evolution of in-service PIs for vessel G; error bands represent 95%CI. Note: FOC is being used as a proxy for the shaft power parameter specified by ISO 19030-Part 3.

The contrasting trends evident for the ballast and laden conditions are not uncommon and have been observed in noon datasets associated with vessels from different fleets. As the in-service PI is the measure used to indicate performance deviations and potentially trigger a maintenance event according to pre-defined maintenance trigger, the relative large uncertainty observed in the derived in-service PI suggests that other supporting information is required to validate and justify the need for a maintenance intervention. As such it is always recommended that a visual inspection be undertaken to validate the PI trends prior to commissioning hull and propeller cleaning.

4.3. Maintenance effect PI

For the purposes of ISO 19030 a maintenance event is a hull or propeller clean or other in-service maintenance activity that may impact on the performance of the vessel. ISO 19030-Parts 2 and 3 stipulate that the reference and evaluation periods in relation to the maintenance effect PI must be a minimum of 3 months. The maintenance PI is illustrated in Fig.7 for those vessels A, B, C, D, H and J that have been subject to a hull clean. Where vessels have been cleaned twice (i.e. vessels A and B) each clean is treated as a separate maintenance event.

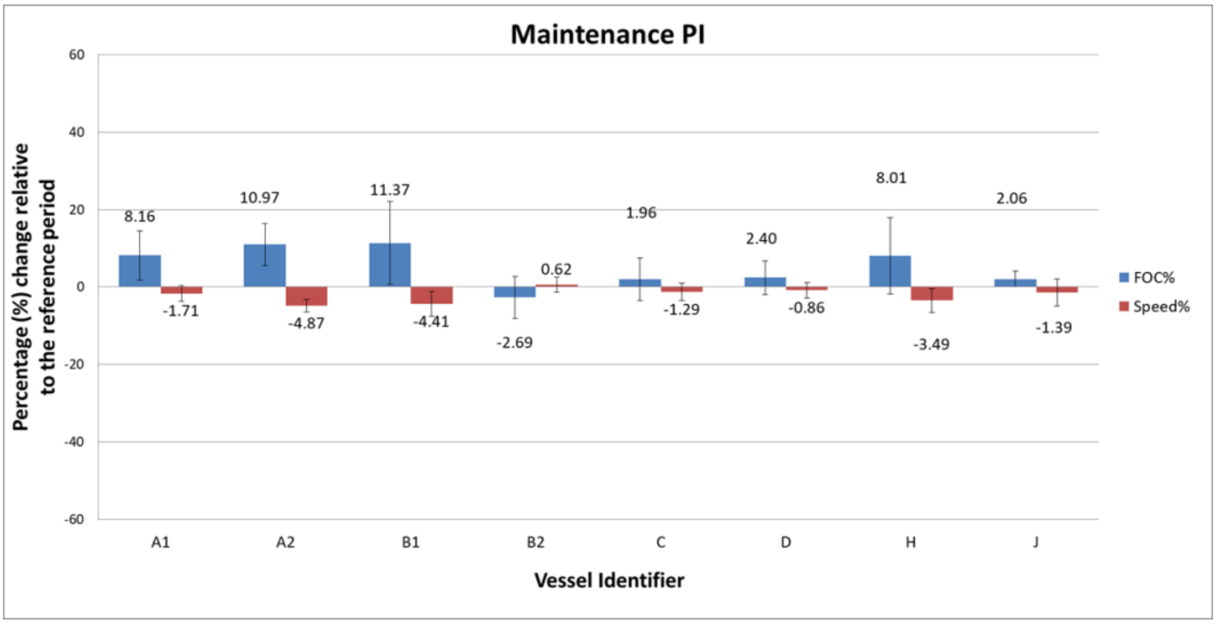

Fig.7: Examples of the maintenance effect PI for selected vessels; error bands represent 95%CI. Note: FOC is being used as a proxy for the shaft power parameter specified by ISO 19030-Part 3. 3-month periods are used before and after hull cleanings (HC) in the calculation, except A2 and B2 which use 3 months before HC and 1 month after HC due to the data availability.

As can be seen in Fig.7, the maintenance effect PI determined for these vessels suggests that the apparent differences in the impact of the hull cleaning event on the FOC change between different vessels again may not always be statistically significant. This may be in-part due to the relatively small size of the datasets available pre- and/or post- hull cleaning as well as the inherent high degree of scatter within such datasets.

A key missing element when reviewing the maintenance event PI when either a hull and/or propeller clean has taken place is often the absence of a visual record of the hull and propeller condition before and after the cleaning event. Such visual records would allow the apparent requirement for the clean to be undertaken in the first place, as well as aiding the understanding of the quality and extent of the cleaning work that was done.

Moreover, in the absence of suitable photographic and/or video records of each vessel's hull and propeller condition, it is not possible to validate any potential assumption that the apparent impact of the cleaning event as indicated by the maintenance effect PI is directly associated with a change in the hull and/or propeller condition.

5. Conclusion

The general applicability of the ISO 19030 standard for measuring changes in hull and propeller performance has been illustrated using noon report data for a sub-set of Chevron's tanker fleet. This has highlighted some of the challenges that are encountered when applying the ISO 19030 standard to such datasets. An overall aim of the standard is to provide a series of data requirements, analysis procedures and specified performance indicators that can be used by the industry in a consistent manner. However, it should be noted that in practice many noon report datasets, such as those collected by Chevron, do not meet the strict data-quality requirements of the ISO standard, including the four alternative methods set out in Part 3 of the standard. Particular issues include missing data parameters and the inability to generate appropriate reference curves. It is the authors' experience that very few noon report datasets from any ship owner fully align with the requirements of ISO 19030-Parts 2 or 3.

Consequently, the professional data-analyst must therefore use their judgement, make assumptions and apply ad hoc modifications to the methods prescribed by the ISO 19030 standard in order to interpret these datasets and extract useful and meaningful vessel performance data. In this way, as illustrated for example by the Chevron datasets, it is possible to understand the general trend of performance change for a particular vessel, although the resulting PIs are often associated with a degree of high statistical uncertainty, mainly due to the quality and quantity of data in the noon reports. To what extent the results are acceptable or considered valuable by an owner depends on their particular requirements and will likely vary case-by-case.

The technical project involving Chevron, AkzoNobel and Jotun is ongoing and will involve more comprehensive data-analysis as it progresses. This will lead to an enhanced understanding of ship performance in general but will specifically help identify the benefits and limitations in using ISO 19030 performance indicators to support future investment choices. Based on the learning, some possible improvements of ISO 19030 can be identified which should be addressed in the future development of the standard. This is discussed by *Abrahamsen (2018)* in more detail.

References

ABRAHAMSEN, J. (2018), *Practical experience with ISO 19030 at Chevron Shipping – Part 3,* 3rd HullPIC, Redworth

ELIASSON, J. (2018), *Practical experience with ISO 19030 at Chevron Shipping – Part 1*, 3rd HullPIC, Redworth

ISO (2016a), *ISO 19030-1:2016, Ships and marine technology — Measurement of changes in hull and propeller performance — Part 1: General principles*, ISO, Geneva

ISO, 2016b: *ISO 19030-2:2016, Ships and marine technology — Measurement of changes in hull and propeller performance — Part 2: Default method,* ISO, Geneva

ISO, 2016c: *ISO 19030-3:2016, Ships and marine technology — Measurement of changes in hull and propeller performance — Part 3: Alternative methods*, ISO, Geneva

ISO 19030 -The Good, the Bad and the Ugly

Vasileios Tsarsitalidis, Vector Marine Software, Athens/Greece, btsars@vector.gr
Spiros Rossopoulos, Vector Marine Software, Athens/Greece, sgr@vector.gr

Abstract

This paper attempts to start a discussion of constructive criticism on the ISO 19030 by using real life examples. Scope of this paper is to acknowledge the Good principles and draw attention to the Bad possible realizations of the standard, while acknowledging, evading (when possible) and making use of (when necessary) the Ugly reality, by handling the same raw data from real vessels in different (but compliant) ways, with focus on the early detection of problems and distinguishing hull from propeller contribution.

1. Introduction

The arrival of ISO 19030, signified the first serious attempt to contain the loosely defined problem of ship performance within some clear boundaries, an extra assurance to charterers that efforts are made in the direction of monitoring and improvement of efficiency, and a new tool for operators, but also an extra cost to the ship owners (especially for producing a reliable, high resolution speed-power-draught-trim database), and headaches to the implementers. What is clear to most propulsion experts, is that simple adherence to the standard, does not necessarily mean that performance is clearly monitored, especially for small changes, and for vessels that have a highly diverse operational profile (i.e. bulkers, spot market tankers) some results can even prove to be misleading and many would argue that it is not mature enough for them to switch hull and propeller cleaning from the scheduled to an "as needed" basis.

Despite the valid criticism on several aspects of the Standard, *Bertram (2017)*, it is a very Good starting point, that can provide very useful insight, if properly applied, and allows for expansion to a more real time monitoring system, with the employment of the same elements and it appears that distinguishing between the contribution of propeller and hull is feasible after some more filtering, *Paereli et al. (2016)*, or extra (event driven) calculations, *Grigoropoulos and Theodosiou (2012)*. On the other hand, faulty assumptions, improper filtering or too strict filtering, can lead to Bad data which in turn will give bad results, not carefully conducted CFD calculations for the construction of the reference model, might even miss trends, especially at off design conditions and big averages can be easily affected by unexpected noise and can reduce the capability of early detection of problems (i.e. rapid growth of fouling or improper cleaning). Last but not least, The Ugly reality of non-ideal ships, where communication can be lost, sensors can be damaged, faulty or miscalibrated, and proxies can induce more noise and/or inconsistent data, calls for the standardization of handling, evaluation, cross referencing and prioritizing, when multiple sources are available.

2. Background

For this study, data from three different vessels are collected and stored according to the methods of ISO 19030, (i.e. automated logging, 15 s sampling, Chauvenet's criterion, 10-minute block averaging, etc.) and analyzed as discussed in the sequel. A program, for automatically handling data from ships has been developed to compute the expected speed and expected power for the given conditions (according to baseline models), after applying the filters given by the standard. For the purpose of discussion, the filters and the setting values are user modifiable, in order to show the corresponding effects. Finally, yet importantly, regardless of the method the reference value databases were built, the end models were produced in analytical form via a high order (16 terms) multivariate regression, so that the end product can very quickly calculate the expected speed or power as a function of draft, trim, and power, or speed accordingly.

3. Part 1 – The Good

The Standard itself, as expressed in ISO Part 1, aims to prescribe practical and feasible methods for measuring changes in hull and propeller performance. These methods, if followed exactly, should produce results of the same accuracy and fidelity with a known level of confidence. Those alone, can assure a level field and a steady quality of the evaluation results for owner, operators and charterers.

- “Political” principles
  A unified system of condition evaluation, with same input, data manipulation methods and solid scientific background for calculations, ensures to the non-expert a trusty frame of reference and to the vessel (owner/operator) a layer of protection against performance related claims. If combined with SEEMP and MRV, it can provide a platform where the “good players” are confirmed and protected, while room for “foul play” is very limited, so long as auditors are strict and cautious on the application.

- Scientific Principles
  One of the biggest assets of the Standard is that of filtering. As shown in Figs.1 and 2, the noisy primitive data are cleared and showing steady conditions for further processing, just by applying Chauvenet’s Criterion, validation and wind/rudder filtering.

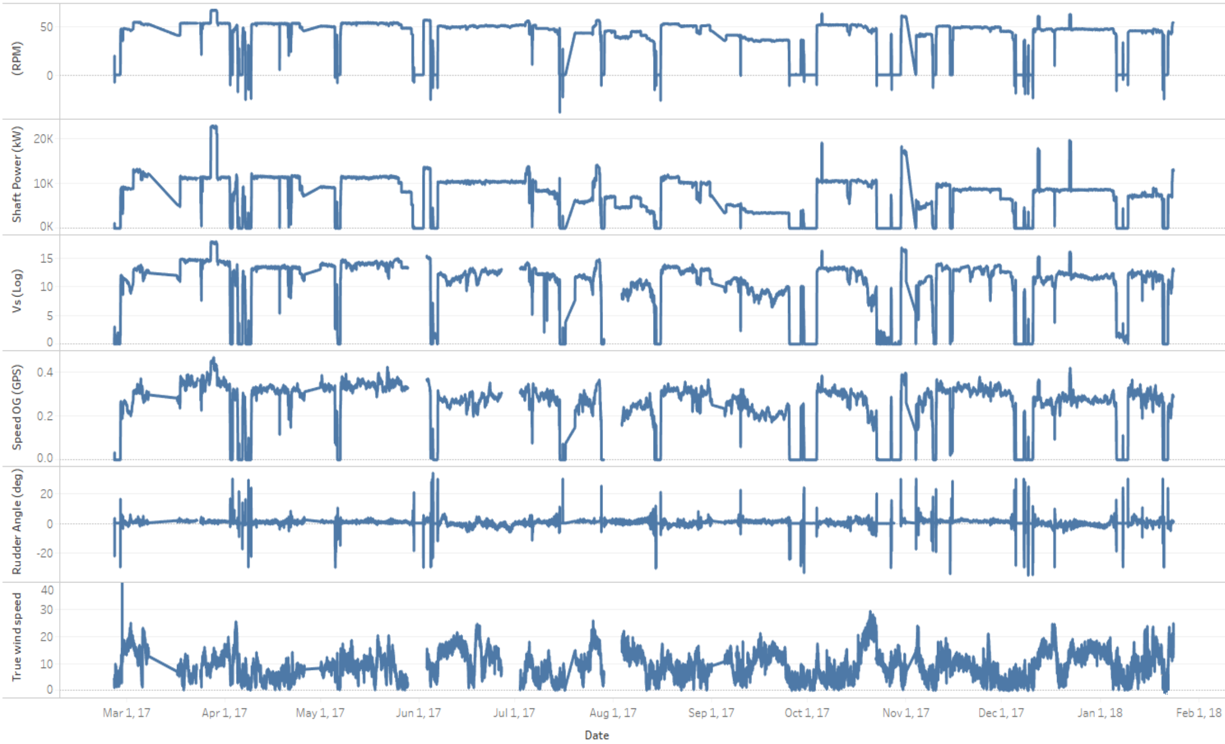

Fig.1: Unfiltered data for Vessel 1

The validation process (checking the standard error of the mean), also dismisses points from transient conditions, thus allowing for safer calculations. Along with the establishment of a system that collects, relays and stores all the data, a solid foundation for further investigations and attempts of different approaches is set, as also discussed further in Part 4.

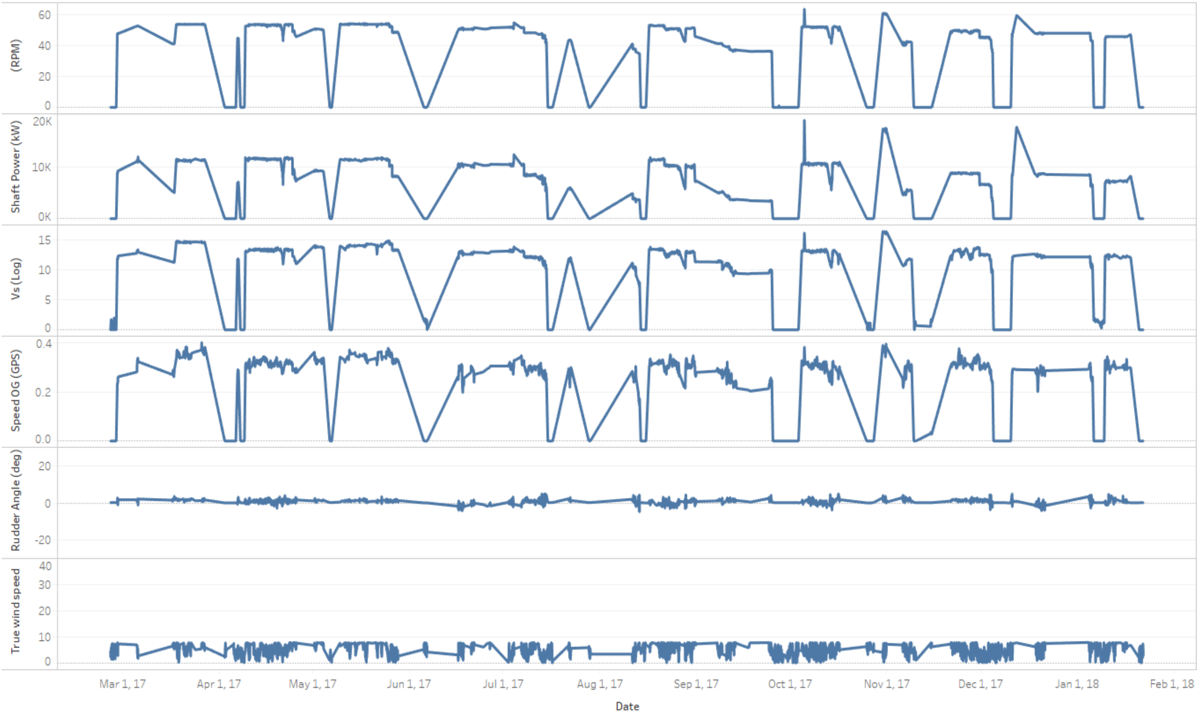

Fig.2: Data of Vessel 1 after outlier, weather and rudder filtering

4. Part 2 - The Bad

The ISO-19030 approach is quite simple and can be implemented with data that is generally available via different vessel performance monitoring solutions and data platforms. Simplicity, however, comes with a cost; the level of accuracy of the method appears to be good enough for tracking general long-term trends in changes of vessel performance, but detailed assessment of individual effects, especially of small impact (below 5%), can be difficult. In addition, since the standard measures relative performance (and not absolute), comparing vessels is difficult. But even for the long-term results, there are potential risks of making serious errors.

- Skewed Baseline Model
  Possibly the biggest risk for the operation of the Standard is having a faulty reference model, as all comparisons are made against it. Since the model is supposed to simulate physical values and almost definitely there are data from sea trials and some tank tests, the highest possibility of error is for off design conditions. Especially for bulk carriers and tankers, slow steaming and not fully loaded ships are the norm, thus chances are that the vessel will operate in off design conditions for the a very large part of its life.

- Concerns on CFD quality
  Fig.3 shows indicative results from the "2016 Workshop on Ship Scale Hydrodynamic Computer Simulation". An interesting point is that, even though there is quite a serious discrepancy in the results, for the highest speed, five out of eight participants achieved quite good accuracy (hint that potential effects are caught by everyone, but viscous effects are more complicated). The quick deduction someone could make is that even experience and good codes are not enough for the production of an accurate and reliable model. On the other hand, when the tests are not blind, the simulations can be finely tuned, to come to a better agreement with the reality. Note that the standard gives a minimum specification about the CFD calculations ("be able to capture breaking waves"). However, the requirement of capturing the breaking waves can be fulfilled by having a finer mesh in the vicinity of the free surface, while the rest of the mesh is not good enough.

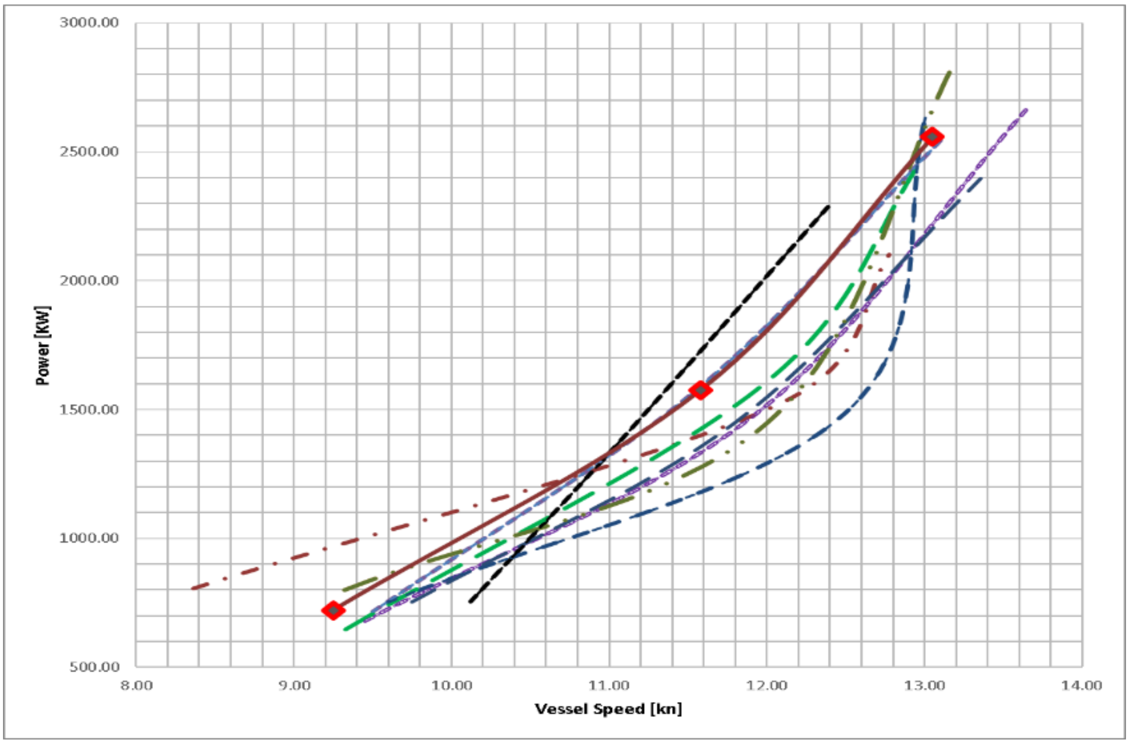

Fig.3: Comparative results from the "2016 Workshop on Ship Scale Hydrodynamic Computer Simulation". Each line shows the results from one participant. The curves are estimations of the total Power for the self-propelled vessel from different participants and the markers are the measured points form sea trial according to ISO 15016.

To show this, the following example is produced from the process of building the model for Vessel 1. Fig.4 shows the meshes for the 4 and 6 million cell simulations made, while producing the mesh independence test for the same vessel. Overall results of the test can be seen in Fig.5, where the average difference in resistance from the densest mesh (10M cells) is plotted. From an observation of the plot, it is understandable that a 6M cell mesh would be adequate for the simulations, but some could argue that even the 4M cell mesh is good as the difference is less than 3% and is expected to follow the trends well. To investigate this, the same set of simulations were conducted for the whole range of trim, draft and speed, for the both meshes in order to build two databases for the ISO. In order to distinguish only the effects of CFD for resistance, the bare hull simulations were varied, while self-propulsion characteristics (Kt,Kq/J curves, w, t, n_R as functions of speed and draft) were kept the same. The required shaft horsepower is calculated according to textbook methodologies (e.g. *Harvald (1983), Carlton (1994), Bose (2008)* etc.). For the sake of size, no further details are shown. Comparisons between the models using the two can be seen in the Figs.6-8. As it can be seen, the differences can be serious both in scale but also in trend. Especially at lower speeds, where the viscous effects are dominant, the differences are significant.

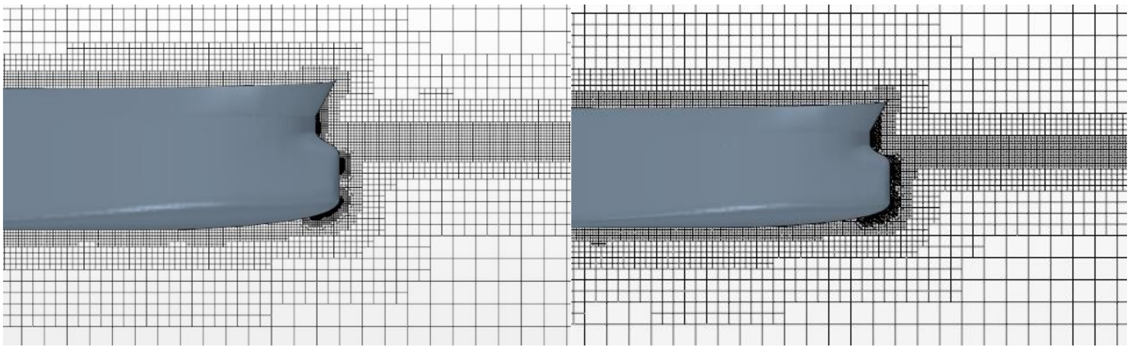

Fig.4: Mesh sections for the 4M cell (left) and the 6M cell (right) simulation

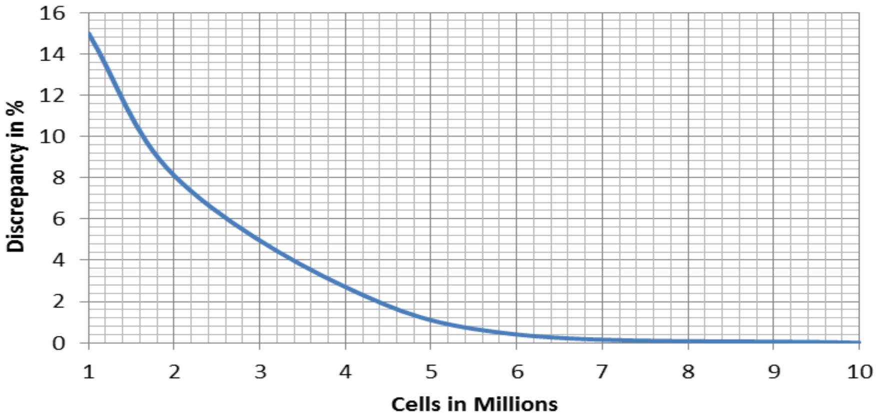

Fig.5: Mesh independence test for specific case

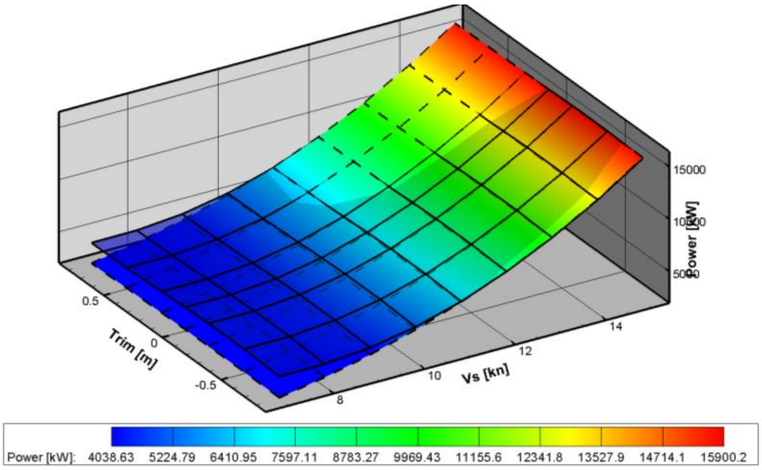

Fig.6: Two Different databases for the same draft T=21.6 m (design draft). Brighter colors and dashed lines for the coarser mesh simulation results and darker with solid line for the denser. The section lines of the two are also visible.

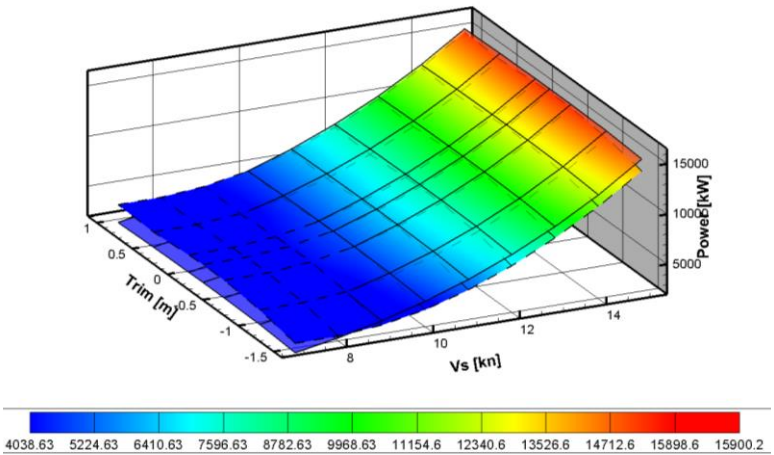

Fig.7: Two Different databases for the same draft T=15 m. Brighter colors and dashed lines for the coarser mesh simulation results and darker with solid line for the denser.

Even in Fig.6 (design draft), where the two models are very close, even for the design speed, a difference in the trend is observable, meaning that the model can give very misleading results. This is shown very clearly in Figs.9 and 10, where the expected values of power and speed are plotted against the actuals. The model of the coarser mesh overestimates power (and underestimates speed) at very slow speeds and at ballast conditions. A possible solution to such a problem, could be to exclude those conditions from the model, but this would also mean much fewer data points. Still, if the user would have to employ such a model, a good precaution would be to check a short period rolling average of speed loss or added power and when the difference is too big or erratic, the corresponding conditions should be signified for further investigation (correction or omission).

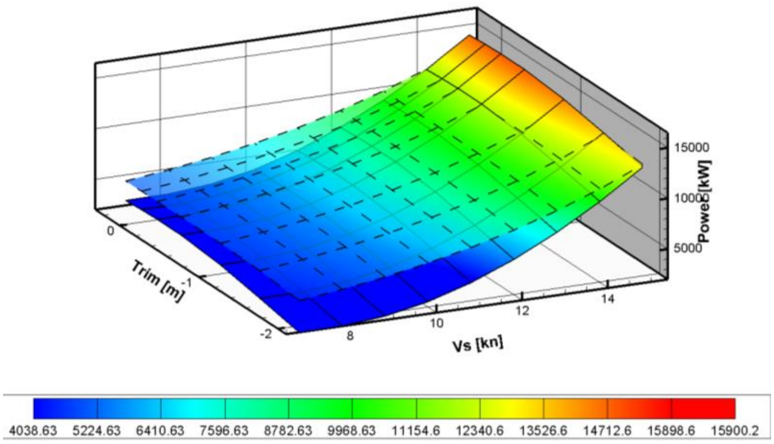

Fig.8: Two Different databases for the same draft T=10m (ballast draft). Brighter colors and dashed lines for the coarser mesh simulation results and darker with solid line for the denser.

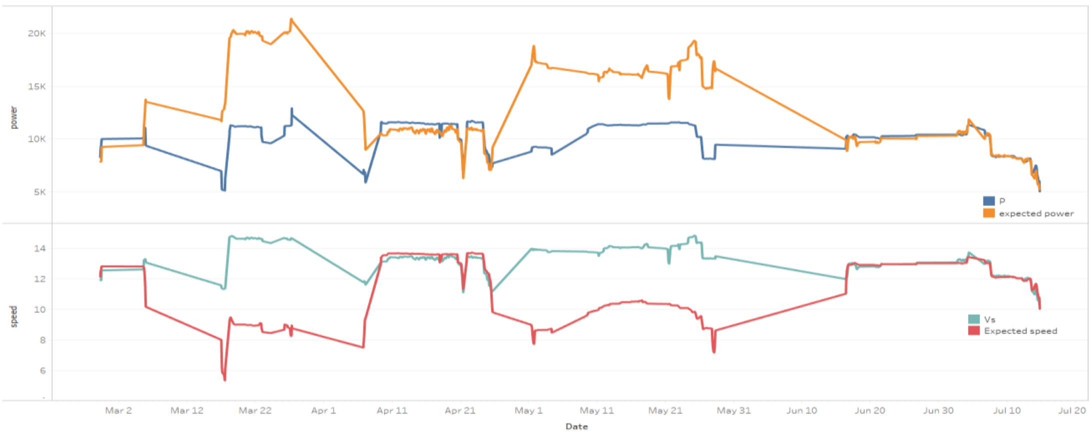

Fig.9: Expected Power for the given vessel speed and expected speed for the given power, using the model produced using CFD with the coarser mesh. The period shown is the reference period. All filters of the standard are applied.

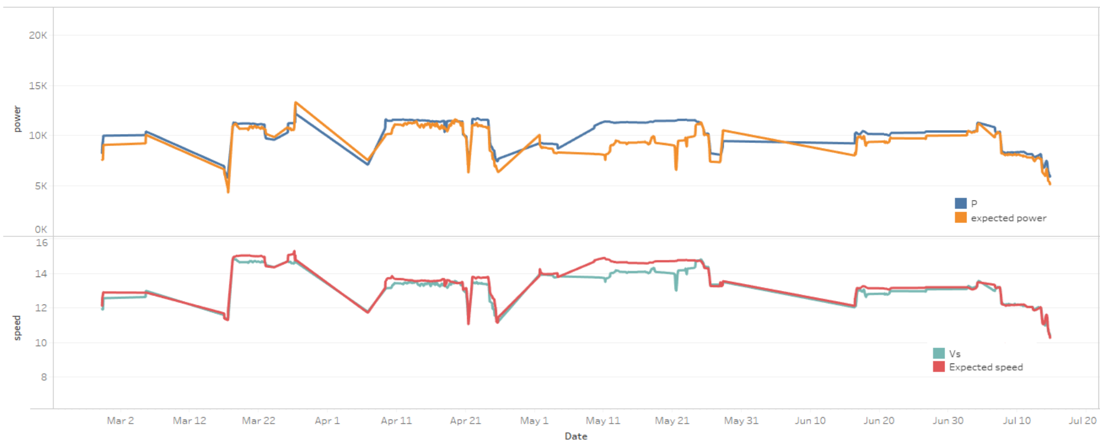

Fig.10: As Fig.9, but for denser mesh

- Missing Hull, Propeller and Appendages information
  Possibly the biggest pain in building the baseline model (unless extended sea trials are performed), is extracting detailed information on hull, propeller and appendages. When any of those is missing, the model builder will have to make assumptions with serious impact and possibly several trial and errors until a safe model is reached if at all.

- Interaction factors
  When energy-saving devices are used, either upstream or downstream of the propeller, their effects can vary with speed (primarily) and draft (secondarily) and simulation in all cases can be prohibitive, due to the level of detail needed and the sensitivity. Thus, an acceptable approach would be to incorporate their effects in the propeller interaction factors (w,t,n_R) produced by self-propulsion experiments (towing tank, virtual or full scale). Naturally, all methods mentioned have a potential problem that could affect the accuracy of calculations significantly and the only remedy is testing against real data of known (and diverse) conditions. As shown before, the most dangerous fallacy, is assuming good accuracy for the whole range, after verifying one point.

- Effects of swell missed by the existing model
  As already discussed in the past, the Standard fails to take into account the effects of swell, or even filter it. Filtering for weather using wind speed, does work in many cases and for winds below BF 4, the wind induced waves have quite a small effect on large vessels. However, if the wind speed is very small, there is no way of telling the actual sea state. Fig.11 shows such an example, combined with a propeller cleaning event. Vessel 2, after sailing in bad weather, got in better conditions for the last three days before reaching port, where the propeller was cleaned and almost after leaving got into the "tail" of a storm and a bad sea state, caused by the main storm that the ship never met. The first and second curve of the figure show the power change and speed loss not corrected by weather, while the third shows the power change after the correction. As it is clearly seen, the swell effect was not corrected, thus distorting the maintenance effect evaluation if taken into account when doing the average. Fig.12 shows an example of when the correction using wind worked fine. This figure will also be discussed later.

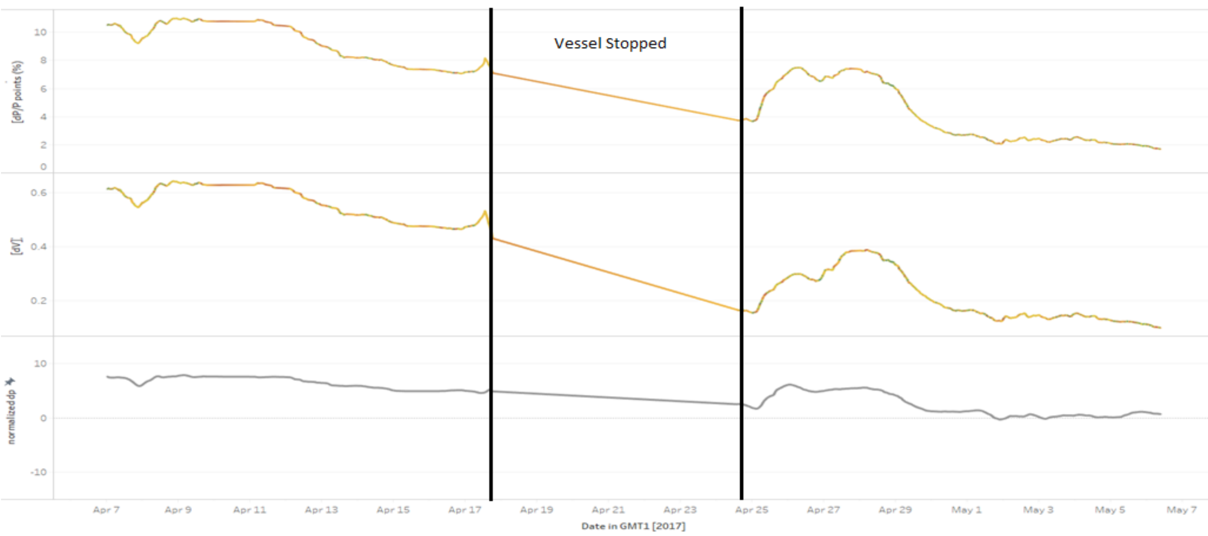

Fig.11: Power change, speed change and power change normalized for weather after filters (calculation based on wind), for Vessel 2

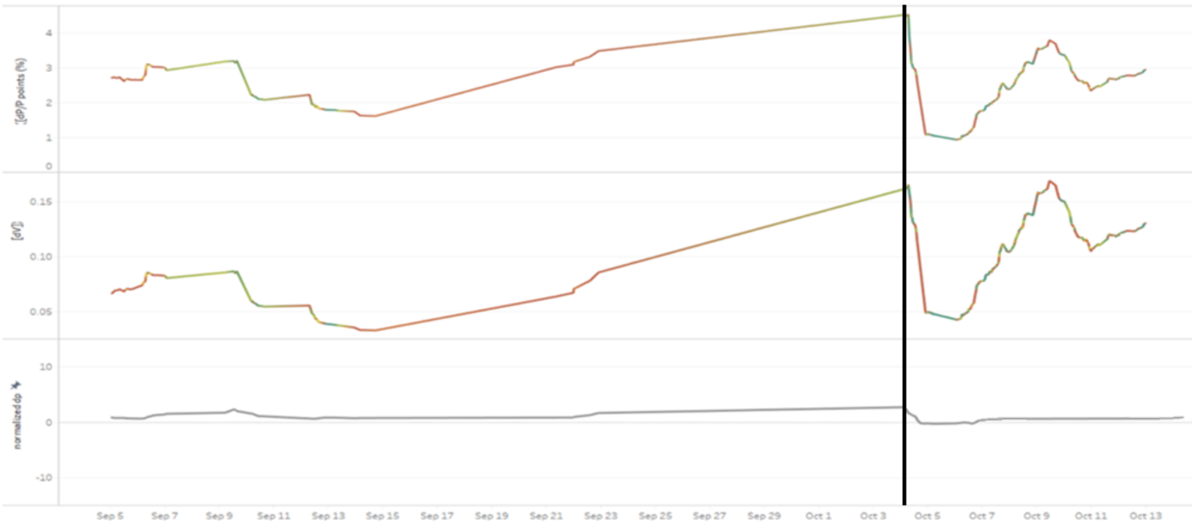

Fig.12: DP/P, Speed loss and weather corrected DP/P for Vessel 1. Planned propeller cleaning occurred at the end of September

5. Part 3 - The Ugly

With all the calculations hanging on the “Notorious” speed through water, *Antola et al. (2017)*, and knowing that the speed log could be faulty for a number of reasons, the reader can expect that there are many problems related to data quality. The solution of “proxy data”, is good for having an initial impression, but unless carefully filtered and validated, such solutions can increase the error significantly. On the other hand, knowledge of the risks and enumeration of the correlation between primitive and proxy data, can allow for filling gaps and cross-referencing the primitives.

- Missing Data
  Data necessary for the calculations, could be missing for various reasons. Salinity for example is rarely measured onboard vessels, though it is necessary along with temperature to define density and kinematic viscosity. Most dangerous, however, are data with small temporal gaps, due to connectivity or sensor problems, where the end user cannot easily know if points have been filtered out due to conditions or lost. Connectivity problems can be solved by having a larger local storage on board, but problems such as sensor lags, noise induced by other systems operating close to them (e.g. flow meters can be very sensitive to vibrations when real time feed rates are looked into closely). In addition, it has been observed that there are areas where GPS signals are lost or altered either due to problematic reception, or due to potential jamming/ spoofing attacks. In the case of the latter, obviously the concern is not the problematic data, but cross-referencing with log and current data and/or using multiple inputs can also act as a layer of defense.

- Too few data after filtering
  Though data density is expected to be very big and there is a general conception that the long averages will sort out everything, there is always a serious possibility of having too few data (or have to wait too long until a safe result is reached), when sensors are very noisy (due to sensitivity) or the vessel is going through many transient conditions (i.e. changing speed/ course). Still, sensitive high rate sensors are usually fitted with extra filters for noise and/or the high frequency signals can be filtered before taking the 15 s sample, and unless the speed changes every hour there should be at least a couple of valid points every hour.

- Conflicting Data
  A serious issue for any analyst (and analysis software developer) is deciding on which data to keep when various sources come into conflict (or lead to erratic results). Surely, the easy approach is to cut off such points (if they are few), or prioritize sources, but that does not

eradicate the possibility of losing important data or trusting a faulty sensor. The current version of the Standard, practically prioritizes, using primary and proxy parameters, but if the data is available it would seem a waste not using them, at least for producing system health diagnostics. Another set of data that is available to all, are the noon reports, which are definitely of lower fidelity and only one snapshot per day, but it could still provide (at least) a warning if discrepancies are serious.

6. Part 4 - "A Few More Dollars" or New Approaches to Old Problems

With the current standard, there are sources and solutions that fall under the category of ISO Part 3, which have the potential of producing more accurate and reliable results than the method of Part 2. A closer look into some of those is deemed important for future-proofing the standard and the methods of performance experts.

- External Weather, current and salinity sources

  The ISO standard filters and corrects for wind based on on-board wind measurements. Annex C in Part 1 explains how calculations of true wind speed and direction are done, but the primitive data are not always perfect. Also, salinity is rarely measured onboard vessels and temperature is not always taken from a representative point. Seawater temperature is used to filter out icy water conditions since the ISO standard cannot take into account the ice conditions directly (less than 2° C). For the time being, waves are not measured and not filtered out directly. However, wind generated waves will indirectly be filtered out by filtering for wind. Further revisions of the standard may take into account waves directly, but at the time of this version of the Standard, accuracy of wave measurements are not considered adequate. Nowadays, there are sources (i.e. NOAA maps, Metrocean etc.) that provide such information accurately, consistently and more importantly, without additional sensors to be installed on the vessel. Also, current data can be used to verify and/or improve speed log quality.

- "AI" solutions

  "AI" solutions have been rising in all sectors of all industries, but before rushing to over-optimistic ideas of one "remedy for all" which stumble on all the above problems, plus the diversity of operational profiles, there are some low hanging fruits that could be reaped (always after some careful consideration). Especially regression methods and signal filtering techniques show a great potential. More specifically, high-order regressions and predictive analytics could be used for baseline model construction, using the original database as a starting point and appending conditions and values when appropriate filters show that he vessel is operating in steady and well-defined state. Also, techniques that fall into the category of analytics, could be used as "smart filters" by recognizing patterns in noisy signals and giving values where there would be a total blank, or cleaning and verifying data when multiple sources are available. Still, caution is advised against using such solutions as black boxes.

- Solutions using ISO compatible data - Distinguishing propeller effects

  Probably the biggest challenge is distinguishing the effect of propeller from the hull, *Paereli et al. (2016)*, and due to the significant difference in the cost and consequences of cleaning propeller and hull, knowledge of the contribution of each part is of high importance for decision making. After having the data properly cleaned, the advance coefficient *J* and torque coefficient K_Q, as known from basics of ship resistance and propulsion, *Harvald (1983)*, are used:

$$J = V_S(1-w)/(ND) \qquad (1)$$

$$K_Q(J) = SHP\ \eta_R\ \eta_S\ /\ (2\pi\rho N^3 D^5) \qquad (2)$$

where:

where:	J	advance coefficient
	K_Q	torque coefficient
	V_S	ship speed through water

w	wake fraction coefficient
N	propeller revolutions in RPS
D	propeller diameter
SHP	shaft power
η_R	rotative efficiency
η_S	shaft efficiency
ρ	water density

For an isolated propeller, the change in efficiency due to varying propeller roughness was thoroughly investigated by *Mosaad (1986)* and it is commonly accepted that (within the obvious limitations of small changes) the curve of K_Q translates vertically as roughness increases, by a constant δK_Q. Had it not been for the change of wake fraction due to fouling, it would suffice to plot K_Q/J curves and check the difference from reference.

However, for the actual ship problem at an arbitrary time, there are two unknowns δK_Q and δw. As summarized by *Carlton (1994)* the wake fraction is considered to transpose with the increase of fouling, thus (always for small changes) δw can be considered a constant for a short period. Similar approaches have also been attempted by *Logan et al. (1980, 2012)*. Keeping the above in mind, an alteration of the method proposed by *Grigoropoulos and Theodosiou (2012)*, can be devised as follows:

For calm conditions and steady sailing, measurements of two different speeds are required to solve the problem:

$$\left.\begin{aligned} &K_Q(J_1)+\delta K_Q = SHP_1\ \eta_R\ \eta_S\ /\ (2\pi\rho N_1^3 D^5) \\ &K_Q(J_2)+\delta K_Q = SHP_2\ \eta_R\ \eta_S\ /\ (2\pi\rho N_2^3 D^5) \\ &J_1 = V_{S1}(1-w_1-\delta w)\ /\ (N_1 D) \\ &J_2 = V_{S2}(1-w_2-\delta w)\ /\ (N_2 D) \end{aligned}\right\rangle \quad (3)$$

Eq.(3) is a 2X2 system considering the baseline function $K_Q(J)$ has an analytical form (for small ranges of J a linear regression would suffice, but the system is solvable regardless of the order of the K_Q function) by simple substitution of J. All other parameters are obtained from baseline models.

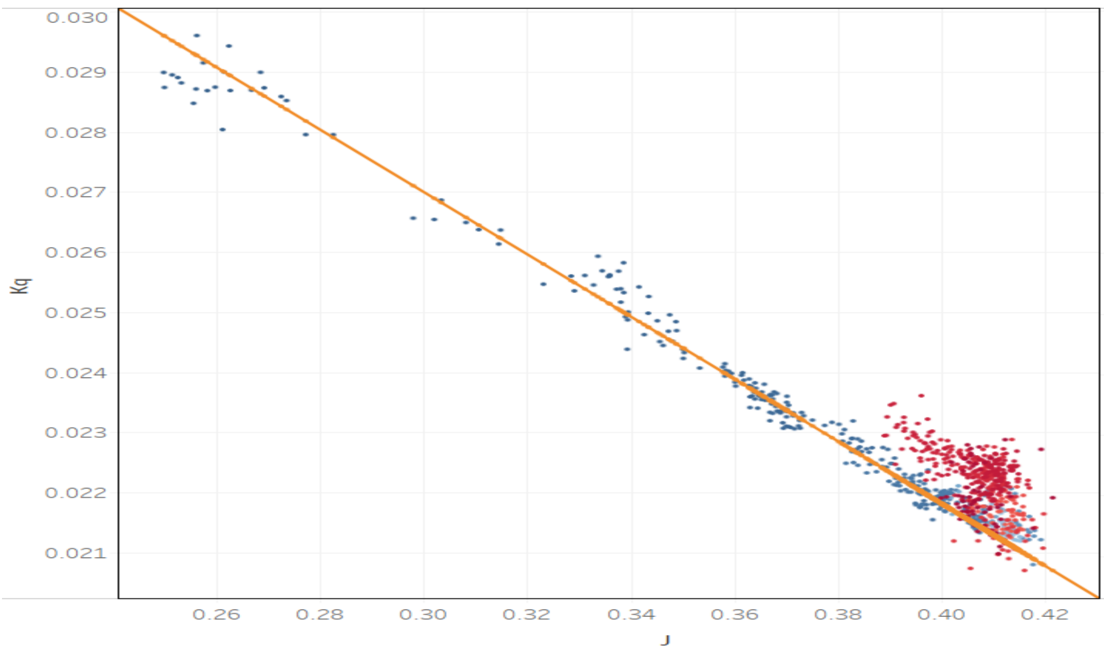

Fig.13: K_Q/J points of Vessel 2 for the same period as Fig.12, before (red) and after (blue) propeller cleaning/polishing (all data unfiltered). Orange line is for the nominal K_Q curve

Applying the above method, corrected K_Q, J points are obtained and Fig.13 displays the evaluation of the previously seen cleaning event of Vessel 1. Red points are before cleaning and Blue are after.

Given all the above, a different vessel with different operational profile which includes periodical propeller cleaning is observed in Fig.14. As also proposed by *Logan (2012)*, after propeller effects are isolated, the propeller could also be used as a dynamometer in order to measure the increase in resistance for same conditions.

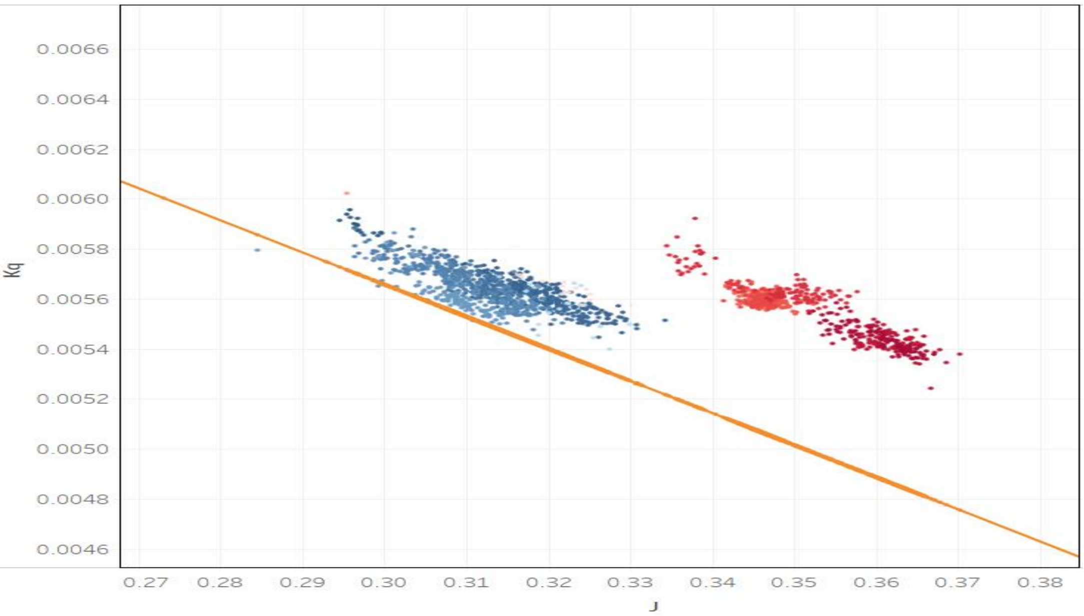

Fig.14: K_Q/J plot for Vessel 1 for the same period as Fig.3. Red points are for before the propeller cleaning and blue are for after. Orange line is for the nominal K_Q/J curve

7. Epilogue

ISO 19030 is definitely a good starting point in the effort to approach the problem of hydrodynamic performance and condition monitoring of a vessel and gives a solid foundation upon which further investigation systems can be built. However, despite the best efforts of its creators, there are some issues that have to be identified in order to be avoided.

Special care is needed in the construction of the baseline models, and the minimum requirements for quality of database should be stricter, if it is to protect the non-expert from misconceptions.

Also the weather effects should be taken into account more carefully. After applying the true wind speed filter, for the small winds, the added resistance due to swell, could quite safely be approached by using the methods of *Maruo (1960,1963)* or *Faltinsen (1980)*, but this also means that external source for weather data is needed.

Dependency on speed log accuracy and inability to capture sea state by using the anemometer are big liabilities, and can be tackled by user input (reported periods of bad or good conditions from crew), external sources (i.e. weather, currents, temperature, salinity etc. data from meteorological services), additional sensors (i.e. accelerometers, gyros and/or RTK GPS) or combinations of the above, along with ways to combine and cross reference.

For the system to allow for timely maintenance, early detection of problems (i.e. incomplete cleaning) or defense against claims, shorter period (if not real time) evaluations are needed to be made, which calls for extra care to avoid over filtering, or different type of filters (not cut-off type, or “AI”).

The problem of distinguishing propeller effects was touched with promising results, but is by no means solved. It remains an open challenge and all existing attempts are heavily dependent on speed log accuracy and propeller performance modelling.

The new era of predictive analytics in computing should definitely be taken into account and thoroughly tested, but it should be reminded that linearizations can only be considered acceptable for small differences and calm conditions (including omission of transient situations) and as said by many others before “Correlation does not imply Causation”.

Acknowledgements:

The authors would like to thank the Technical Department of Neda Maritime Agency Co Ltd, of Piraeus Greece for their constructive cooperation and for allowing to use their data, and Dmitriy Ponkratov, Senior Consultant of Technical Investigation Department of Lloyd’s Register for sharing data from the 2016 Workshop on Ship Scale Hydrodynamic Computer Simulation. Last but not least, the authors would like to thank Volker Bertram for the inspiring title of the present paper.

References

ANTOLA, M.; SOLONEN, A.; PYORRE, J. (2017), *Notorious speed through water*, 2nd HullPIC, Ulrichshusen

BAZARI, Z. (2006), *Ship energy performance benchmarking/rating: Methodology and application* World Maritime Technology Conf., London

BERLEKOM, W.B.v. (1981), *Wind forces on modern ship forms - Effect on performance,* Trans. NECIES 97, pp.123

BERTRAM, V. (2012), *Practical Ship Hydrodynamics,* Butterworth & Heinemann

BERTRAM, V. (2017), *Some heretic thoughts on ISO 19030,* 2nd HullPIC, Ulrichshusen

BOSE, N. (2008), *Marine Powering Prediction and Propulsors,* SNAME

CARLTON, J.S. (1994), *Marine Propellers and Propulsion,* Butterworth & Heinemann

FALTINSEN, O.M.; MINSAAS, K.J.; LIAPIS, N.; SKJØRDAL, S.O. (1980), *Prediction of resistance and propulsion of a ship in a seaway,* 13th Symp. Naval Hydrodynamics, Tokyo, pp.505-529

GRIGOROPOULOS, G.J.; THEODOSIOU, D.K.N. (2012), *Harmonising SEEMP with effective vessel operation,* SNAME 4th Int. Symp. SOME’12

HARVALD, S.A. (1983), *Resistance and Propulsion of Ships,* Wiley

ISO15016 (2002), *Ships and marine technology - Guidelines for the assessment of speed and power performance by analysis of speed trial data*, ISO, Geneva

ISO19030 (2016), *Measurement of changes in hull and propeller performance,* ISO, Geneva

ITTC (1999b), *Added resistance,* 22nd ITTC, Chapter 9 page 34, Seoul, Shanghai

ITTC (1999c), *The specialist committee on Trials and Monitoring,* 22nd ITTC, Seoul, Shanghai

ITTC (2002a), *Full Scale Measurements: Speed and Power Trials: Instrumentation, Installation and Calibration*, 23rd ITTC, Venice

ITTC (2002b), *The specialist Committee on Waves,* 23rd ITTC, Venice, pp. 497-543

ITTC (2002c), *The specialist Committee on Speed and Powering Trials,* 23rd ITTC, Vol. II, pp.341- 367

LOGAN, K.P. (2012), *Using a ship's propeller to detect hull fouling,* 4th Int. Symp. on Ship Operations Management and Economics SOME2012

MARUO, H. (1960), *The drift of a body floating on waves*, J. Ship Res. 4 (3), pp.1-10

MARUO, H. (1963), *Resistance in waves*, 60th Anniversary Series, The Soc. Naval Arch. of Japan 8, pp.67-102

PAERELI, S.; KRAPP, A.; BERTRAM, V. (2016) *Splitting propeller performance from hull performance – A challenge*, 1st HullPIC, Pavone

PONKRATOV, D. (2017), *2016 Workshop on Ship Scale Hydrodynamic Computer Simulation,* Lloyd's Register reference 8428

ISO 19030 in 2018 and Beyond –
Relevance of the Standard in this Period of Rapid Technological Change

Geir Axel Oftedahl, Jotun AS, Sandefjord/Norway, geir.axel.oftedahl@jotun.no

Abstract

Some are arguing ISO 19030, barely two years after initial publication, is already past its expiration date. Others argue that the standard is holding back the development and uptake of new and even better methods for measuring hull and propeller performance. This paper looks at the relevance of the ISO 19030 standard today and considers whether the standard is indeed holding back the development of new and even better methods. It finds the standard to be as relevant as ever and that, used in the right way, the standard does not hold back the development and uptake of new methods but rather serve to accelerate same.

1. Introduction

ISO 19030 is a measurement standard. It prescribes practical methods for measuring changes in ship specific hull and propeller performance and defines a set of performance indicators for hull and propeller maintenance, repair and retrofit activities, *ISO (2016)*. The standard includes specifications of what measurement technologies and procedures to use.

Measurement technologies and procedures are evolving. In the work leading up to the publication of the first revision of ISO 19030 in November 2016 two guiding questions for the Working Group when deciding on what should be included were:

- Is the measurement technology or procedure in question state of the art?
- Is it mature and generally available?

If state of the art, mature and generally available the technology or procedure was included. If state of the art but not mature or generally available, it was left for future revisions. In line with ISO's general revision process, the idea was to periodically revisit what measurement technologies and procedures are "state of the art, mature and generally available"- minimum every 3 years.

What measurement technologies and procedures are "state of the art, mature and generally available" is changing ever faster. Some are arguing ISO 19030, barely two years after initial publication, is already past its expiration date. Others argue that the standard is holding back the development of new and even better methods for measuring hull and propeller performance.

This paper looks at the relevance of the ISO 19030 standard in this period of rapid technological change and considers whether the standard is indeed holding back the development of new and even better methods.

2. Is ISO 19030 still relevant?

An implied purpose of any measurement standard is to provide a generally agreed upon method for measuring something. In the case of the ISO 19030 standard, a generally agreed upon method for measuring hull and propeller performance was expected to make it easier for decision makers to properly compare results from the past and thereby make better informed decisions for tomorrow. Also, to provide much needed transparency for buyers and sellers of technologies and services intended to improve hull and propeller performance. And finally, to make it easier for the same buyers and sellers to enter into performance based-contracts and thereby better align incentives, *Oftedahl and Soyland (2016).*

A generally agreed upon method for measuring hull and propeller performance appears equally relevant today.

In the absence of such a generally agreed upon method, there will be alternative methods in use and therefore difficult to compare measurement output across vessels and fleets. While it in theory always will be possible to implement and use the same alternative measurement method on all vessels of interest, in practice this will often prove complex and costly. Different methods will require implementation and use of different technologies and procedures and since most ships will change hands several times over its lifetime. This means measurement technologies and procedures will often have to be changed as well. Comparisons across fleets with different decision makers will be even more difficult.

Greater difficulties in making comparisons across ships and fleets will also result in less transparency for buyers and sellers of technologies and services intended to improve hull and propeller performance. Given availability of alternative methods, it will be possible for both buyers and sellers to "shop for" the method that best supports their argument. Focus will easily turn to discussions on method rather than what can be done to further improve performance.

Finally, absence of a generally agreed upon method for measuring hull and propeller performance will still make it more difficult for buyers and sellers of technologies intended to improve hull and propeller performance to enter into performance-based contracts. The parties to the contract then have to spend time and resources reaching agreement on how to measure on a case by case basis. Once such agreement has been reached, they may even need to invest additional time and resources in making changes to measurement technologies or procedures. Agreement on contracts involving more than 2 interested parties, not unusual in shipping, will be even more challenging.

3. Is the standard holding back the development of new and even better methods?

Even though the ISO 19030 is updated every 3 years or so, it is unlikely to remain on the cutting edge. Indeed, two criteria for inclusion of a measurement technology or procedure in the standard have been that the technology or procedure must be both mature and generally available.

This intentional inertia does not have to result in the ISO 19030 having to hold back the development and uptake of new and even better methods for measuring hull and propeller performance, however. ISO 19030 and new methods can coexist quite comfortably.

There are multiple purposes for measuring hull and propeller performance where comparability across ships and fleets and contractibility, both key drivers of the need for the standard, are not very important factors. An example is measuring hull and propeller performance for the purpose of triggering hull inspections and hull cleanings. In such a case, it will likely to be more important to get an earlier indication than to be able to compare or contract on measurement output. One way to deliver on such additional purposes without compromising on comparability and contractibility would be to develop measurement systems and solutions that have a ISO 19030 compliant core with the possibility of also adding methods as needed to deliver on other purposes. Another way would be to have an alternative method as the core but then add the ISO compliant method as an alternative.

Either way, if new methods for measuring hull and propeller performance are developed in such a way that they relate to whatever is the standard method at that time, both new methods and the standard method would stand to benefit.

Firstly, making sure the two methods do relate would provide quality assurance for both. If the methods cannot be made to relate this would be an indication that there is a problem somewhere. The problem could be with the new method, the standard method or both. If it turns out that the problem is with the standard method, it will of course be the standard method that will have to be updated.

The mutual quality assurance would likely serve to accelerate uptake of new methods. It would also make it easier to qualify and thereby adopt new measurement technologies and procedures into the standard. This would in turn make ISO 19030 even more relevant.

4. Summary

This paper has looked at the relevance of the ISO 19030 standard today and considered whether the standard is holding back the development of new and even better methods. It finds the standard to be as relevant as ever and that, used the right way, the standard does not hold back the development and uptake of new methods but rather can serve as a catalyst for same.

References

ISO (2016), *Measurement of changes in hull and propeller performance — Part 1: General principles,* ISO 19030-1, ISO, Geneva

OFTEDAHL, G.A.; SØYLAND, S. (2016), *ISO 19030 – Motivation, scope and development,* 1st HullPIC, Pavone

The Advantages of Proactive In-Water Hull Grooming from a Biologist's Perspective

Kelli Z. Hunsucker, **Cierra Braga**, **Caglar Ergodan, Harrison Gardner**, **John Hearin**, **Emily Ralston**, **Geoffrey Swain**, **Melissa Tribou**, **Ann Wassick,**
Florida Institute of Technology, Melbourne/USA, khunsucker@fit.edu, swain@fit.edu

Abstract

Ships will foul regardless of duty cycle. Most in-service ships develop biofilms and if they remain idle for long periods of time they will typically accumulate significant amounts of hard fouling. Grooming has been defined as the proactive gentle, habitual and frequent mechanical maintenance of a ship hull to keep it in a fouling free condition. Over the past decade, the U.S Office of Naval Research, has provided funding for the development of "grooming" as a method to control fouling. This paper will focus on understanding the ecology of the fouling community to guide the development of grooming technology.

1. Introduction

Ship-hull biofouling has significant impact on performance, fuel consumption, exhaust emissions, costs, invasive species transport and the environment, *Swain et al. (2007), Schultz et al. (2011), Hewitt and Campbell (2010)*. The process of biofouling is generally thought to occur in several steps, but can also occur in parallel or simultaneously. First, a clean surface will adsorb an organic layer within seconds of submersion, called a conditioning film. This is followed by the adhesion of microbes such as bacteria and algal cells, developing a slimy layer (also known as a biofilm). Following biofilm formation is the settlement of the juvenile phases of algae and macrofouling. This is called incipient fouling. These will then grow into their adult forms known as macrofouling (e.g. barnacles, seaweed, tunicates, tubeworms, mussels).

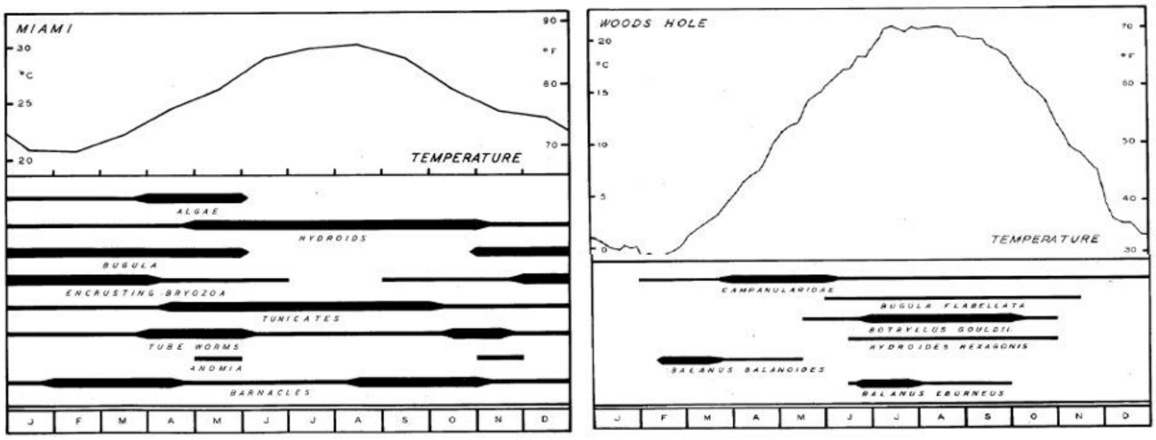

Fig.1: Annual fouling on panels exposed at Miami, Florida, USA (left) and Woods Hole, Massachusetts, USA (right). Graphs show the difference in fouling related to temperature and geographical location, *WHOI (1952)*.

The type and intensity of biofouling depends on the geographical location, time of year, environmental conditions (e.g. salinity, temperature, nutrient levels), substrate, and if present, the biofouling control system. An understanding of when and where fouling is likely to occur is fairly well understood, Fig.1. In this example, taken from the 1952 Woods Hole publication "Marine Fouling and Its Prevention", a comparison is made between the typical fouling organisms present at different times of the year and seasonal temperatures. In Miami temperatures range between 20-30ºC. Fouling is year-round, however, there is seasonality in the dominance by certain organisms. For example, encrusting bryozoan are most abundant in the winter months, hydrozoans in the summer and tubeworms and barnacles in the spring and fall. In Woods Hole the temperatures range from 0 -20ºC and seasonality is found for all fouling types. Here, the barnacle *Balanus balnoides* dominates in the spring with the barnacle *Balanus eburneus* in the summer. There is very little fouling between the months of November to February.

The fouling pressure that is present at any location will determine the grooming frequency required for fouling prevention. This includes selecting the appropriate fouling control coating to be used in synergy with grooming, the frequency of grooming, and the forces need to groom the surface.

2. Fouling Control Coatings

The most common method of preventing biofouling is through the application of fouling control coatings. Today's commercially available coatings may be divided into two main categories: coatings that use active ingredients to kill or deter the fouling organisms (antifouling systems), or coatings that create a surface to which the organisms find it difficult to attach (silicone-based fouling release systems), *Swain (2010)*.

Antifouling coatings are broadly separated into copper and copper-free systems. Many fouling organisms are copper tolerant, and as a result, booster biocides such as zinc pyrithione, econea and skeletope are incorporated within the paint to enhance the performance of the coatings. Copper and copper-free antifouling coatings are effective as long as they consistently release the active ingredient at a rate sufficient to prevent recruitment. There are, however, environmental concerns with the use of copper due to its persistence in sediments, bioaccumulation, and other environmental impacts, *Chambers et al. (2006), Thomas and Brooks (2010)*. Regulations are in place that limit the copper output from coatings and the release of copper during hull cleaning.

Fouling release systems have a low surface energy, low modulus, low micro roughness and may contain additives, which prevent a fouling organism from generating a strong bond to the surface. This weak bond reduces the ability of organisms to develop a strong attachment which limits recruitment and may cause removal due to the hydrodynamic stresses that are created as a ship moves through water, *Swain (1999), Omae (2003)*. These coatings are considered to be environmentally friendly, offer a smooth surface when correctly applied, reduce skin friction drag, and are easy to clean, *Swain (2010)*. However, they are costly, not easy to apply, are not as durable as their biocidal counterparts and the environmental impacts of many of the additives are unknown. Recently coatings are being designed that integrate a biocide into a fouling release matrix. These coatings demonstrate effectiveness in static environments for longer-term immersion.

3. Hull Husbandry

While fouling-control coatings provide an effective method to slow down the development of bio-fouling, most ships will require some sort of in-water husbandry during their operational cycles. In recent years, there has been increasing interest to develop in-water methods to remove or control fouling, *Curran et al. (2016)*. These may be divided into hull cleaning, which is a reactive process triggered once marine growth has reached unacceptable levels, or hull grooming, which is a proactive approach that removes biofilms and incipient fouling before they can become established.

3.1. Hull Cleaning

Mechanical removal of fouling through in-water hull cleaning is a reactive approach. Properly done hull cleanings may extend the life of a coating system, and return the performance of the ship to a condition similar to a clean hull, *Schultz (2011)*. However, if the fouling is well established, then more powerful brushes are required and these will damage the coating and release large amounts of debris into the water. Many ports and harbors now require this effluent be captured and treated which adds to the costs and logistics of the cleaning process. Cleaning cycles will be determined by the biofouling coverage. Slow operating speeds and long durations in port and between scheduled maintenance greatly increase the risk of accumulating biofouling. One such example is US Navy ships, which sit pier side for long periods of time, putting them at a high risk for biofouling. Routine underwater hull inspections are performed to determine the extent of fouling and coating damage, as set forth in the US Navy's Naval Ships' Technical Manual (NSTM), *US Navy (2006)*. Divers will record the Fouling Rating (FR) at several locations along the ship hull, struts, rudders, propellers, and sea chests. Fouling density and composition will vary depending on ship class, port of call, coating type, and coating condition. Because of this, the Navy does not specify routine hull cleaning. Instead the decision to clean is based on the regular in-water hull inspections, *US Navy (2006)*. The NSTM calls for a full hull cleaning when a ship has FR 40 over 20% of the hull (antifouling coatings) or a FR 50 over 10 % of the hull (fouling release coatings), *US Navy (2006)*. FR 40 refers to the growth of small calcareous fouling (or weed) less than 6 mm in diameter or height. FR 50 refers to calcareous fouling in the form of barnacles less than 6.4 mm in diameter or height. In addition to regular inspections, the NSTM also outlines several performance indicators for the presence of biofouling accumulation which call for an underwater hull inspection.

1) The loss of 1 knot of speed with shaft rpm set to standard speed
2) An increase in excess of 5% fuel required to maintain a given speed
3) An increase in shaft RPM of 5% to maintain a given speed

In-water hull cleaning on both Navy and commercial ships is usually conducted by divers using large underwater hydraulically driven brushes, Fig.2. The brushes are stiff and typically made of poly-propylene or wire, to be able to dislodge attached fouling organisms from the hull. Divers must try to delicately balance the forces imparted by the cleaning vehicle to remove the maximum amount of fouling while minimizing damage to the ship hull coating.

Fig.2: A SCAMP vehicle (left) is commonly used to clean ship hulls. Brushes are often stiff (larger red brush, right).

3.2 Hull Grooming

Grooming has been defined as the gentle, habitual, and mechanical maintenance of a ship hull. It provides a proactive method to control biofouling on ship hulls and maintain the coating surface in a smooth and intact condition without damaging the surface, *Tribou and Swain (2010, 2015,2017)*.

The grooming tool must provide sufficient force to remove the biofilms and incipient fouling without causing any damage to the coating. Initial testing of the grooming concept found that it works best in conjunction with active fouling control coatings and that it was ineffective on the hard inert coating types. Several different grooming tools have been evaluated and the vertically rotating brushes have been identified as providing the best results.

Fig.3: Hull grooming is conducted using a ROV (left) with several brushes mounted to the front (right). These brushes are smaller than traditional cleaning brushes and do not damage the coating.

Grooming is presently accomplished by a remotely operated underwater vehicle equipped with nine vertically rotating brushes that gently remove biofilms and incipient fouling before they have the time to become fully established, Fig.3. The majority of the cost associated with fouling is the increased frictional drag and the resultant fuel consumption, *Schultz et al. (2011)*. Research has shown that a well-managed grooming program can maintain fouling control coatings in a smooth and fouling free condition and it is recommended that routine grooming be applied to all ships whilst at anchor or pierside. It has been estimated that active grooming of a US DDG to prevent all but a light biofilm layer, has the potential to save 12M USD per ship over a fifteen-year period, *Schultz et al. (2011)*. In addition, grooming will eliminate the potential of invasive species transport.

3.3. Large-Scale Test Facility for the Development of In-Water Hull Maintenance

A large-scale seawater testing facility (LSTF), funded by the Office of Naval Research, was built at Port Canaveral, Florida for the testing and development of grooming technology and understanding the interaction with biofouling, *Hearin et al. (2015,2016)*. The LSTF has four large steel test assemblies which are coated with Navy qualified coatings (antifouling and fouling release) to represent a ship hull near the water line, Fig.4. The large test assemblies are fabricated from a 2.4 x 4.6 m, 6 mm thick steel plate welded to a 0.76 m diameter pipe for floatation. Two assemblies are bolted end to end to provide a large surface area, 9.2 m long by 2.4 m deep. The facility also includes a 11 m support vessel which serves as a floating laboratory, and allows for topside inspections of the test assemblies, Fig.5. The LSTF is located in an area of high fouling activity, and thus provides intensive year-round conditions to develop the grooming technology.

Fig.4: The large-scale seawater test facility (LSTF) consists of several large steel test assemblies coated with US Navy qualified antifouling coatings (left) and fouling release coatings (right). The test assemblies include a 2.4 x 4.6 m, 6 mm thick steel plate welded to a 0.76 m diameter pipe for floatation.

Fig.5: The large-scale seawater test facility (LSTF) also includes an 11 m support vessel which houses control and dive systems, aids in top-side inspections of the test assemblies (left), and allows deployment and retrieval of grooming vehicles (right).

4. Grooming and Biology

Grooming is not effective on inert surfaces, *Tribou and Swain (2010)*, but when used in synergy with antifouling and fouling release coatings has proven to prevent fouling in numerous long-term studies, *Hearin et al. (2015,2016)*. The mechanism by which grooming works differs between antifouling and fouling release coatings.

Grooming an antifouling coating prevents the buildup of a leached layer, silts and biofilms which reduce the effectiveness of the active ingredient. In essence grooming maintains an active surface that prevents organism attachment. There is no precise value for the amount of an active ingredient required to prevent fouling, as ambient conditions such as water chemistry and fouling will influence the effectiveness. However, estimates have been made. *LaQue (1975)* states that copper must be released in corrosion products at a minimum value of 50 $\mu g/cm^2/day$ and *Swain (1999)* suggests a minimum copper release of approximately 20 $\mu g/cm^2/day$ is required to prevent fouling. Average copper release rates (assuming 55% copper by volume) for groomed surfaces were measured to be 28.1 $\mu g/cm^2/day$ (weekly grooming) versus 17.5 $\mu g/cm^2/day$ ungroomed, *Tribou and Swain (2017)*. The ungroomed surface fouled demonstrating that grooming can maintain copper output at levels sufficient to prevent marine growth. Measurements of dry film thickness for an ablative copper coating showed that there was no significant increase in ablation rates due to routine grooming. In order for grooming to be effective with biocide based coatings, grooming brushes should be designed to keep a surface active without accelerating coating loss.

Grooming controls recruitment on a fouling release coatings by imparting a force which is greater than the organism's attachment to the surface. This is particularly important for biofilms. The adhesion strength of biofilms will differ not only with the coating type but by the species composition of the biofilm, *Hunsucker and Swain (2015)*. Several studies have identified the composition of groomed biofilms to be dominated by single-celled algae, known as diatoms, *Hearin et al. (2015, 2016)*, *Hunsucker et al. (2018)*. The diatom community present on groomed surfaces is similar to those reported on in-service ship hulls coated with fouling release coatings, *Hunsucker et al. (2014)*. It has been found that grooming will increase biofilm adhesion strength, *Fig.6*. Fouling release surfaces groomed once or twice a week developed a stronger biofilm than those groomed every other week or not at all. As a result of grooming, the biofilms which developed had a lower thickness than biofilms which were not groomed, *Fig.6*. The presence of this low profile adherent biofilms has prompted the development of more effective grooming brushes which impart higher forces.

Similarly, it was found that encrusting bryozoans and tubeworms can become established if the grooming force or frequency is not sufficient to remove them at an early stage. Both encrusting bryozoans and tubeworms have low profiles and therefore only receive limited forces from the brush.

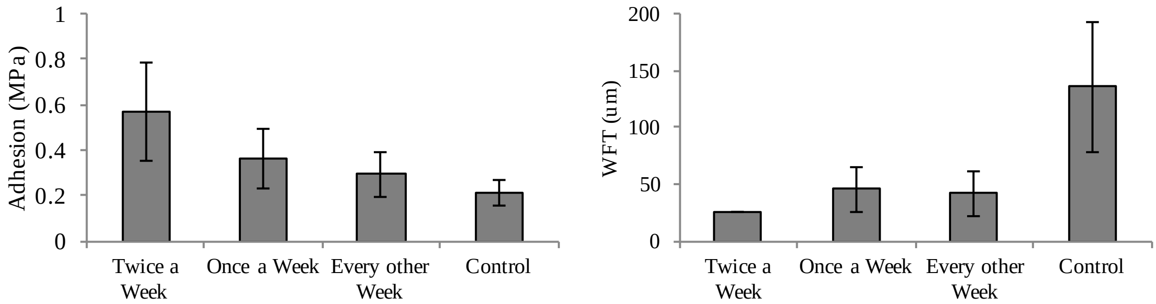

Fig.6: Average biofilm adhesion on different grooming treatments (left) and average biofilm thickness as measured by a wet film thickness gauge (right). All measurements were collected from a fouling release surface, which had been groomed for over a year.

Tubeworms can be particularly challenging, as the adhesion strength to fouling release coatings is typically higher than many of the other macrofouling types, Fig.7. Barnacles offer a higher profile than either the encrusting bryozoans and tubeworms and are thus easier to remove with grooming brushes. It is therefore important with fouling release coatings to use grooming brushes which impart sufficient force to remove tenacious biofilms and macrofouling organisms that have higher adhesion strengths and lower profiles.

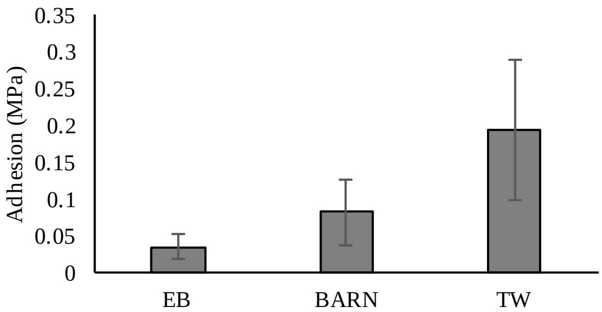

Fig.7: Average adhesion measurements for hard fouling organisms attached to a fouling release coating: encrusting bryozoans (EB), barnacles (BARN), and tubeworms (TW).

4.1. Long-term Grooming on Commercial Fouling Control Coatings

In 2015, a long-term grooming study was undertaken to assess the performance of several commercially available fouling control coatings, Fig.8. Three replicates of one ablative copper anti-fouling coating (AF) and one fouling release coating (FR) were applied to 15.2 x 30.5 cm panels, which were then attached to one of the large test assemblies located at the LSTF. Grooming was conducted using a nine-brush grooming tool mounted to a ROV, which allowed for a groomed swath of 55.9 cm, Fig.3. The polypropylene brushes rotated at approximately 500 RPM and were used to groom the surfaces once per week, a regime that was chosen based on previous testing at the LSTF, *Hearin et al. (2015,2016)*. The same coatings were applied to an additional panel set, which were immersed and remained ungroomed throughout the course of the experiment.

At the end of two years, grooming had successfully prevented biofouling accumulation on both the antifouling and fouling release coatings, Fig.8. The results demonstrated that grooming was effective at maintaining the copper ablative coating free of both biofilms and macrofouling, Fig.9. Grooming maintains the active ingredients within the paint to provide antifouling action and there was no indication that grooming significantly increased the rate of ablation.

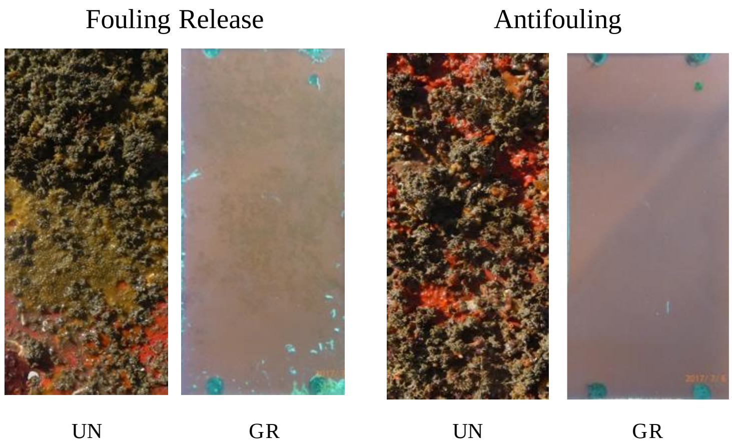

Fig.8: Representative photographs of fouling release and antifouling test coatings after two years of immersion. Coatings were either ungroomed (UN) or groomed (GR).

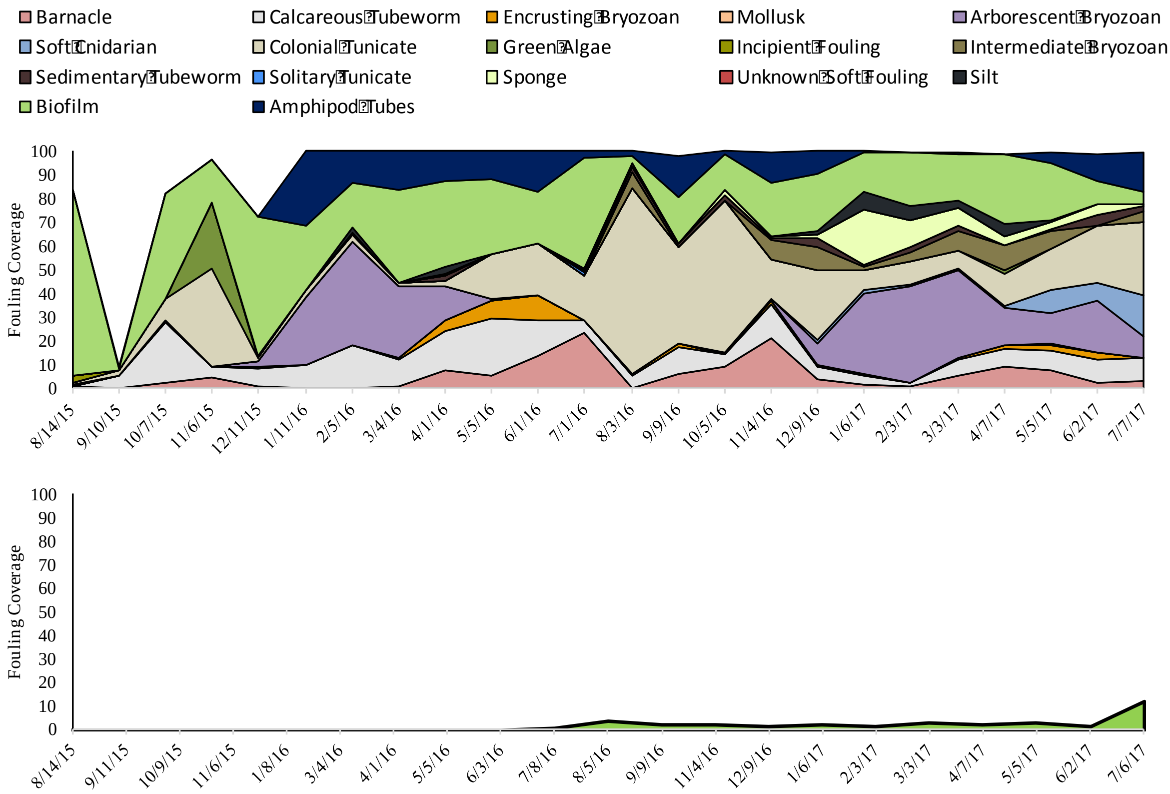

Fig.9: Monthly fouling of a copper ablative coating over a two-year period on ungroomed (top) and groomed (bottom)

On the fouling release coatings, grooming resulted in significantly lower fouling cover than on ungroomed surfaces, Fig.10. After two years, all ungroomed panels had a significantly greater coverage of macrofouling organisms. The groomed fouling release coating developed small numbers of tubeworms and encrusting bryozoans for short periods throughout the study. These are low profile organisms and they are able to develop when their adhesion strength is greater than the forces imparted by the grooming tool. Their presence was seasonal and they were removed over time. Based on these results, grooming forces have been increased and this has been found to effectively prevent fouling settlement, especially from low profile organisms such as tubeworms and encrusting bryozoans.

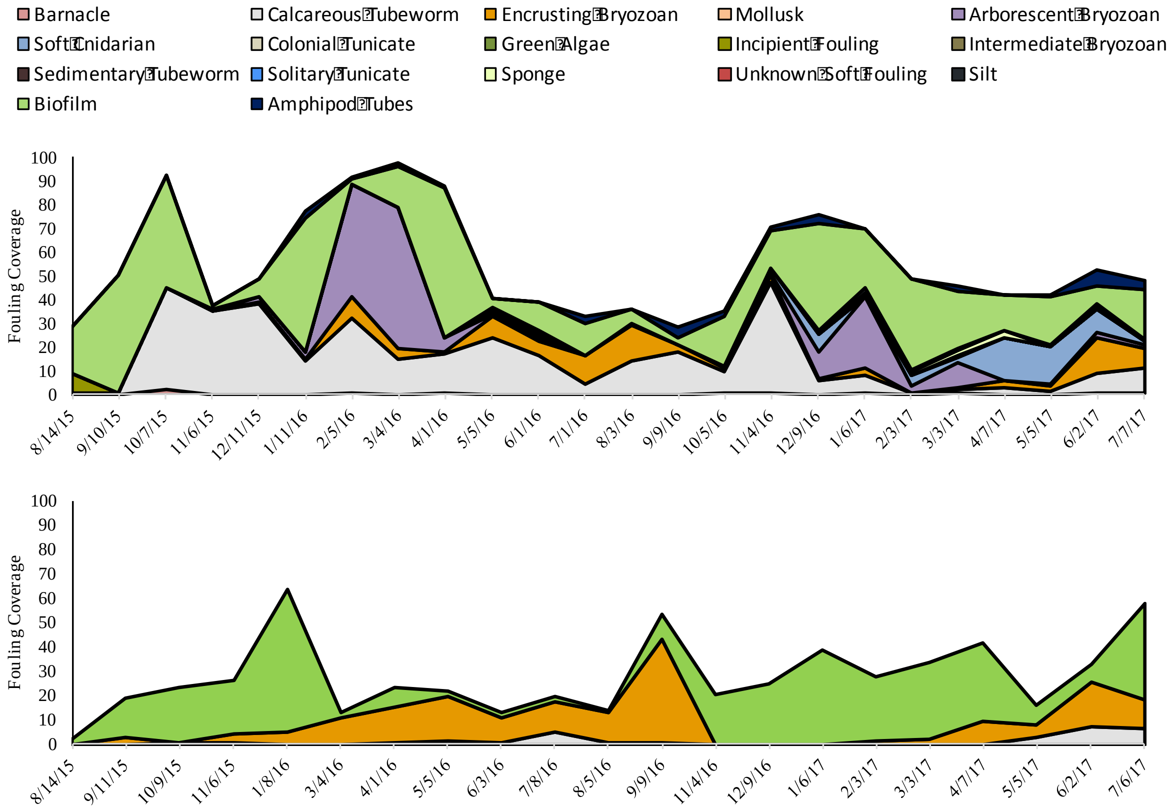

Fig.10: Monthly fouling on a fouling release coating over a two-year period on ungroomed (top) and groomed (bottom)

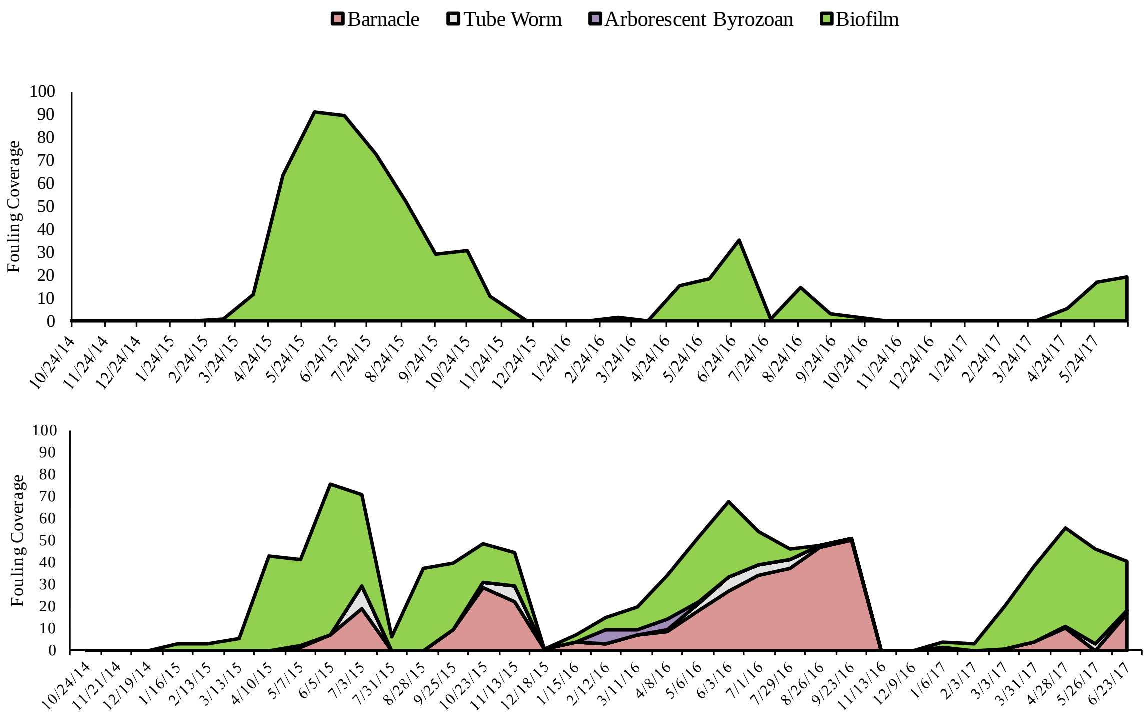

Fig.11: Monthly fouling on an ablative copper antifouling coating applied to the LSTF test assemblies and groomed over a 2.5 year period once a week (top) and every other week (bottom)

4.2. Grooming Frequency

Several long-term studies have demonstrated that grooming is effective at controlling the biofouling on both antifouling and fouling release coatings, *Hearin et al. (2015,2016).* The frequency at which grooming is required will depend on the coating type, coating age and condition, the geographical location and the forces imparted by the grooming tool. Grooming data generated over a two-and-a-half-year period at the LSTF demonstrated that a grooming regime of once per week controlled bio-fouling whereas grooming every two weeks resulted in the accumulation of barnacles, calcareous tubeworms, and arborescent bryozoans, Fig.11, requiring cleanings following the NSTM protocol for a full hull cleaning.

In areas of high productivity (such as Port Canaveral), grooming can prevent macrofouling settlement but a low-profile biofilm may develop (Fig.11, top). The occurrence of this biofilm has been related to changes in water temperature, and the overall abundance exhibited seasonal fluctuations (Fig.12). While the biofilm may develop as a result of grooming, the resultant frictional drag is significantly less than a surface that is ungroomed (Hunsucker et al. 2018).

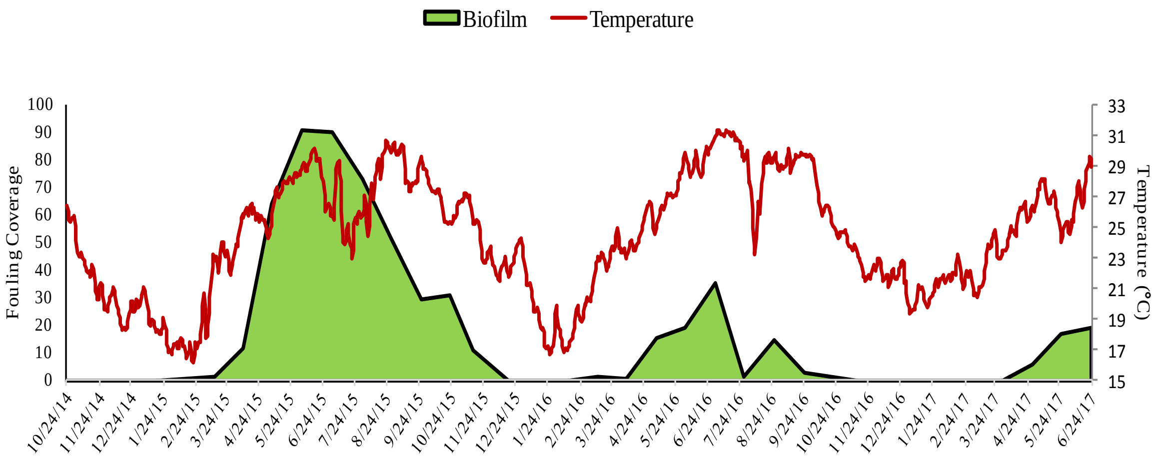

Fig.12: Monthly fouling on an antifouling coating groomed once a week with corresponding water temperatures to demonstrate the relationship between fouling and environmental parameters

4.3. Grooming and Invasive Species

One of the benefits of grooming, is the ability to prevent biofouling recruitment and thus the spread of invasive species. Biofouling via transport on ship hulls is one of the primary vectors of invasive species, Hewitt and Campbell (2010). Table I lists invasive species found at the LSTF (Port Canaveral, Florida) that have a potential to foul ship hulls. Using the coatings associated with the long-term grooming study, Fig.8, the abundance of the invasive organisms on the groomed versus ungroomed coatings was recorded, Table I. The presence of the ship hull coatings alone was able to deter the settlement of certain organisms, such as the Asian green mussel (*Perna viridis).* The ungroomed antifouling coating had the presence of several invaders: the striped acorn barnacle *(Balanus amphitrite),* arborescent bryozoan *(Bugula neritina),* calcareous tubeworm *(Hydroides elegans),* encrusting bryozoan (*Watersipora subtorquata complex),* and a filamentous bryozoan *(Zoobotryon verticillatum).* Whereas the panels exposed to weekly grooming did not have any of the above, and remained free of macrofouling species altogether. The ungroomed fouling release coatings also accumulated several invasive species: *B. amphitrite*, *B. neritina, H. elegans,* and *W.subtorquata.* Grooming was able to eliminate the *B.amphitrite*, *B.neritina*, and reduce *H.elegans.* Overall grooming was able to decrease the overall abundance of the invasive species on the coatings.

Table I: Invasive species present at the LSTF (Port Canaveral, Florida) on a fouling release and antifouling coating, with abundance on the ungroomed and groomed treatments

Species Name	Common Name	Fouling Release		Antifouling	
		Ungroomed	Groomed	Ungroomed	Groomed
Amphibalanus reticulatus	Reticulated Barnacle				
Balanus amphitrite	Striped Acorn Barnacle	0.33 ± 0.82		0.5 ± 0.84	
Balanus trigonus	Triangle Barnacle				
Botryllus schlosseri	Star Tunicate				
Bugula neritina	Arborescent bryozoan	0.50 ± 1.2		0.17 ± 0.41	
Diadumene lineata	Striped Sea Anemone				
Diplosoma listerianum	Colonial tunicate				
Hydroides elegans	Serpulid Worm	4.8 ± 1.6	1.7 ± 1.5	35.0 ± 13.4	
Lyrodus medilobatus	Shipworm				
*Lyrodus pedicellatus***	Blacktip Shipworm				
Megabalanus coccopoma	Titan Acorn Barnacle				
Mytella charruana	Charru Mussel				
*Paradella dianae***	Shipworm				
Perna viridis	Asian Green Mussel				
Styela plicata	Pleated Sea Squirt				
Teredo bartschi **	Shipworm				
*Teredo furcifera***	Shipworm				
Teredo navalis	Naval Shipworm				
*Victorella pavida***	Bryozoan				
*Watersipora subtorquata complex***	Encrusting Bryozoan	9.0 ± 3.5	15.3 ± 17.6	1.00 ± 1.3	
*Zoobotryon verticillatum***	Bryozoan			0.8 ± 2.0	

4.4. Grooming vs Cleaning

The advantages of a proactive grooming program compared to cleaning was demonstrated by comparing one of the test sections coated with an ablative copper antifouling coating that was not groomed for 23 months to one that was groomed on a weekly basis, Fig.8. The ungroomed section became heavily fouled with barnacles and the groomed section remained free of fouling. The ungroomed section was cleaned using a hand-held polypropylene brush, Fig.13. Fouling before cleaning was severe, consisting of calcareous organisms (barnacles and tube worms) on over 90% of the coating, Fig.13, left. When the diver applied sufficient force with the brush to remove all fouling organisms, the antifouling coating became damaged and was removed to expose the epoxy barrier coat, Fig.13, middle. When divers applied just enough force with the brush to remove fouling while preserving the coating, some calcareous growth (barnacles and barnacle baseplates) remained, Fig.13, right.

Fig.13: Cleaning Results. Fouling before cleaning FR 100 100% (left), anti-fouling coating damage (middle), fouling remaining after cleaning (right)

The coating roughness of the groomed and cleaned coatings was measured using a TQC hull roughness analyser. It was found that grooming decreased coating roughness whereas the removal of barnacles via cleaning not only damaged the coating but caused the roughness to increase over three times, Fig.14.

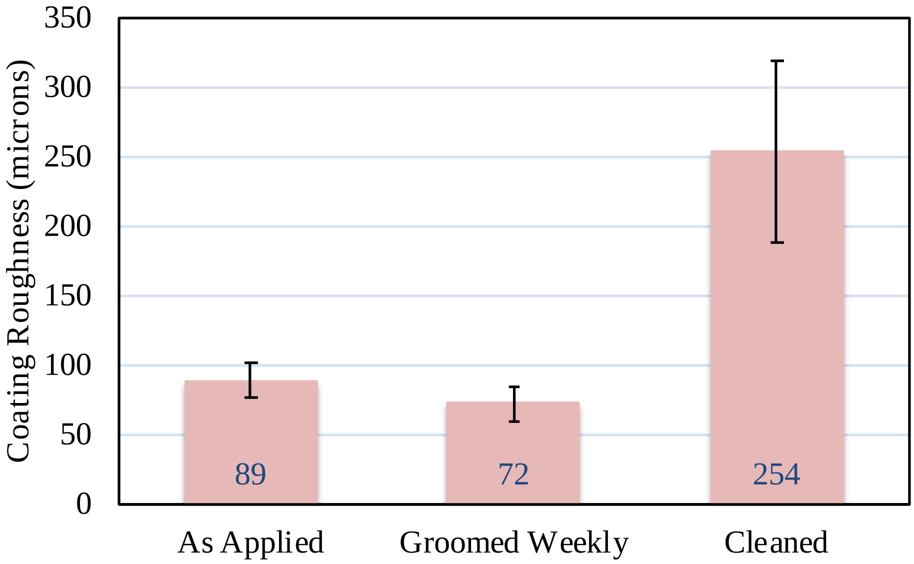

Fig.14: Ablative copper roughness data: as applied, two-year grooming and ungroomed after mechanical cleaning

5. Summary

Grooming has been shown to be an effective method to prevent fouling on fouling control coatings. With antifouling coatings, grooming maintains an active biocide layer which prevents fouling settlement. With fouling release coatings, grooming supplies sufficient force to remove biofilms and incipient foulers before they can become fully established and are difficult to remove. An effective grooming tool should provide sufficient force to maintain a surface free of fouling without causing damage to the coating. The frequency and forces required for grooming are determined by the coating type, coating condition, ambient seawater properties and the intensity of fouling.

The studies presented in this paper were conducted at Port Canaveral (FL, USA), an area of high fouling intensity. At this site, during most months, a grooming frequency of once per week was required to prevent biofouling on antifouling and fouling release coatings. It is anticipated that the required grooming frequency may be less in geographical locations with lower fouling intensity. The incorporation of a grooming program with a fouling control coatings is able to eliminate fouling and thus prevent the associated functional, financial and environmental penalties.

Acknowledgments

This work was funded by the Office of Naval Research (Grants # N00014-16-1-3123 and N00014-16-1-3050.

References

CANNING-CLODE, J.; FOFONOFF, P.; RIEDEL, G.; TORCHIN, M.; RUIZ, G. (2011), *The effects of copper pollution on fouling assemblage diversity: a tropical-temperate comparison*, PLoS ONE 6: e18026. doi: 10.1371/journalpone.0018026

CHAMBERS, L.D.; STOKES, K.R.; WALSH, F.C.; WOOD, R.J.K. (2006), *Modern approaches to marine antifouling coatings*, Surf. Coat. Tech. 201, pp.3642-3652

COUTTS, A.D.M.; PIOLA, R.F.; HEWITT, C.L.; CONNELL, S.D.; GARDNER, J.P.A. (2010), *Effect of vessel speed on survival of biofouling organisms: Implications for translocation of non-indigenous marine species*, Biofouling 26(1), pp.1-13

CROOKS, J.; CHANG, A.; RUIZ, G. (2011), *Aquatic pollution increases the relative success of invasive species*, Biol. Invas. 13, pp.165-176

CURRAN, A.; O'CONNOR, B.; LOWE, C.; KING, E. (2016), Analyzing the *Current Market of Hull Cleaning Robots*, U.S. Coast Guard, https://web.wpi.edu/Pubs/E-project/Available/E-project-121416-161958/unrestricted/USCG_Final_2016.pdf

DAFFORN, K.; GLASBY, T.; JOHNSTON, E. (2008), *Differential effects of tributyltin and copper antifoulants on recruitment of non-indigenous species*, Biofouling 24, pp.23-33

DAVIDSON, I.; McCANN, L.; SYTSMA, M.; RUIZ G. (2008), *Interrupting a multi-species bioinvasion vector: The efficacy of in-water cleaning for removing biofouling on obsolete vessels*, Mar. Poll. Bull. 56, pp.1538-1544

FLOERL, O.; INGLIS, G. (2005), *Starting the invasion pathway: the interaction between source populations and human transport vectors*, Biol. Invas. 7, pp.589-606

FLOERL, O.; POOL, T.; INGLIS, G. (2004), *Positive interactions between nonindigenous species facilitate transport by human vectors*, Ecol. Appl. 14, pp.1724-1736

HEARIN, J.; HUNSUCKER, K.Z.; SWAIN, G.; STEPHENS, A.; GARDNER, H.; LIEBERMAN, K.; HARPER, M (2015), *Analysis of long-term mechanical grooming on large-scale test panels coated with an antifouling and a fouling release coating*, Biofouling 31(8), pp.625-638

HEARIN, J.; HUNSUCKER, K.Z.; SWAIN, G.; GARDNER, H.; STEPHENS, A.; LIEBERMAN, L. (2016), *Analysis of mechanical grooming at various frequencies on a large scale test panel coated with a fouling-release coating*, Biofouling 32(5), pp.561-569

HEWITT, C.; CAMPBELL, M. (2010), *The relative contribution of vectors to the introduction and translocation of marine invasive species*, Report commissioned by The Australian Department of Agriculture, Fisheries and Forestry, p.42

HOPKINS, G.; FORREST, B. (2008), *Management options for vessel hull fouling: An overview of risks posed by in-water cleaning*, ICES J. Mar. Sci. 65, pp.811-815

HOPKINS, G.; FORREST, B.; COUTTS, A. (2010), *The effectiveness of rotating brush devices for management of hull fouling*, Biofouling 26, pp.555-566

HUNSUCKER, K.Z.; KOKA, A.; LUND, G.; SWAIN, G. (2014), *Diatom community structure on in-service ship hulls*, Biofouling 30(9), pp.1133-1140

HUNSUCKER, K.Z.; SWAIN, G. (2015), *In situ measurements of diatom adhesion to silicone-based ship hull coatings*, J. Appl. Phycol. 28(1), pp.269-277

HUNSUCKER, K.Z.; GARDNER, H.; SWAIN, G (2017), *Using Hydrodynamic Testing to Assess the Performance of Five Fouling Control Coatings Immersed at Two Field Sites along the East Coast of Florida*, American Towing Tank Conf., Bethesda

HUNSUCKER, K.Z.; VORA, G.J.; HUNSUCKER, J.T.; GARDNER, H.; LEARY, D.H.; KIM, S.; LIN, B.; SWAIN, G. (2018), *Biofilm community structure and associated drag penalties of a groomed fouling release ship hull coating*, Biofouling 34(2), pp.162-172

LAQUE, F. (1975), *Marine Corrosion: Causes and Prevention*, John Wiley & Sons

OMAE, I. (2003), *General aspects of tin-free antifouling paints*, Chem. Rev. 103, pp.3431-3448

PIOLA, R.; JOHNSTON, E. (2008), *The potential for translocation of marine species via small-scale disruptions to antifouling surfaces*, Biofouling 24, pp.145-155

PIOLA, R.; JOHNSTON, E. (2009), *Comparing differential tolerance of native and non-indigenous marine species to metal pollution using novel assay techniques*, Environ. Poll. 157, pp.2853-2864

PIOLA, R.; DAFFORN, K.; JOHNSTON, E. (2009), *The influence of antifouling practices on marine invasions*, Biofouling 25, pp.633-644

SCHIMANSKI KB, PIOLA RF, GOLDSTEIN SJ, FLOERL O, GRANDISON C, ATALAH J, HOPKINS GA (2016) Factors influencing the en route survivorship and post-voyage growth of a common ship biofouling organism, Bugula neritina. Biofouling 32(8): 969-978

SCHULTZ, M.P.; BENDICK, J.A.; HOLM, E.R.; HERTEL, W.M. (2011), *Economic impact of biofouling on a naval surface ship*, Biofouling 27(1), pp.87-98

SWAIN, G. (1999), *Redefining antifouling coatings*, J. Prot. Coat. Lin. 16(9), pp.26-35

SWAIN, G. (2010), *The importance of ship hull coatings and maintenance as drivers for environmental sustainability*, Ship Design Operation Environmental Sustainability Conf., London

SWAIN, G.; KOVACH, B.; TOUZOT, A.; CASSE, F.; KAVANAGH, C.J. (2007), *Measuring the performance of today's antifouling coatings*, J. Ship Production 23(3), pp.164-170

THOMAS, K.V.; BROOKS, S. (2010), *The environmental fate and effects of antifouling paint biocides*, Biofouling 26(1), pp.73-88

TRIBOU, M.; SWAIN, G. (2010), *The use of proactive in-water grooming to improve the performance of antifouling coatings*, Biofouling 26(1), pp.47-56

TRIBOU, M.; SWAIN, G. (2015), *Grooming using rotating brushes as a proactive method to control ship hull*, Biofouling 31(4), pp.309-319

TRIBOU, M.; SWAIN, G. (2017), *The effects of grooming on a coper ablative coating: A six year study*, Biofouling 33 (6), pp.494-504

US NAVY (2006), *Naval ships' technical manual chapter 081: Waterborne underwater hull cleaning of Navy ships*, 5th rev, US Naval Sea Systems Command, Washington (DC), Pub#S9086-CQ-STM-010/CH-081

WEISS, C. (1947), *The comparative tolerances of some fouling organisms to copper and mercury*, Biol. Bull. 93, pp.56-63

On-Board Real-Time Wave & Current Measurements for Decision Support

Rune Gangeskar, Miros, Asker/Norway, rg@miros-group.com
Gunnar Prytz, Miros, Asker/Norway, gp@miros-group.com
Vemund Svanes Bertelsen, Miros, Asker/Norway, vsb@miros-group.com

Abstract

Accurate information about ocean waves, surface currents, and the Speed Through Water is of great interest in many applications. These include fuel optimization, hull stress monitoring, as well as systems improving cargo safety and passenger comfort. During the recent decades, sensors and systems based on radar remote sensing principles have become increasingly more widespread, due to considerably improved accuracy and reliability. In addition, challenges and costs related to installing and maintaining in-situ or underwater equipment are avoided. This paper presents some of the principal radar-based sensors for wave and current monitoring.

1. Introduction

Digitalization is currently transforming many aspects of the modern society. This also holds true for shipping where easy access to data from a multitude of sources is fueling a wave of innovation that is changing the way vessels are designed, operated and maintained. The ship operation process used to be largely based on manual observations and retrospective analysis based on incomplete data sets. This is now rapidly shifting towards having access to detailed, accurate information in real-time. The information can be made available both on the vessels and at onshore operational centers and enables a wide range of improvements.

Situational awareness is key to unlocking the potential of digitalization. One area that has seen significant improvements recently is within real-time sea state measurements. Recent developments within radar-based technologies have given access to accurate sea state data that can be used to optimize ship operations. Radar-based sea state measurements can now provide both ocean wave and current data accurately under widely varying conditions. Both waves and currents can have a significant effect on ship performance. One example is ocean current measurements which can be used to accurately calculate the Speed Through Water (STW) of seagoing vessels.

A vessel has an optimal speed which in simple terms depends on the speed vs. fuel relationship of the vessel and the efficiency of the propulsion configuration (propellers etc.). Ocean currents of up to several knots can exist on the oceans which means STW might be quite different from Speed Over Ground (SOG). It is therefore STW and not SOG that should be used as the basis for speed optimization. Thus, STW is a very relevant parameter in ship performance optimization.

A number of applications are relevant in the light of accurate STW measurements. The most obvious is speed optimization taking STW as an input parameter which has the potential to lead to significant savings in fuel. However, there are also other foreseeable applications. Hull performance is one such example. With accurate STW measurements it is possible to benchmark the current performance of a vessel with respect to hull resistance and particularly the influence from hull fouling. With such information it is possible to have more accurate information about the state of the hull. This can be used to improve planning of hull cleaning or to investigate the effectiveness of hull cleaning procedures or hull coatings. Further use cases might also be possible such as studies of the performance degradation of parts of the drivetrain.

Ocean surface current measurements from moving vessels by traditional underwater (in-situ) instrumentation are associated with challenges and data heavily influenced by noise. Systems measuring the STW are equally influenced by similar disturbances affecting the vessel speed log, *Antola et al.*

(2017), Baur (2016), Bos (2016), Fritz (2016). Wave measurements from underwater instrumentation are only available on rare occasions. The following items are relevant for both acoustic Doppler current profilers (ADCPs), *Flagg et al. (1998), King et al. (1993), New (1992)*, and other instruments based on traditional in-situ measurement principles.

- Underwater equipment generally involves installation and maintenance procedures being both time-consuming and expensive.
- Underwater equipment is exposed to fouling, *Carchen et al. (2017), Goler et al. (2017), Kelling (2017)*.
- Measurements are disturbed by air bubbles, turbulence, and inhomogeneous hydrodynamics caused by the vessel motion and propellers, *Bos (2016), Carchen et al. (2017), Brown et al. (2001)*.
- Measurements are disturbed by other instruments, for instance acoustic echo sounders and vessel speed logs.
- The surface current itself is considerably affected by the vessel motion.
- Sensors are frequently inadequately calibrated, *Antola et al. (2017), Bos (2016)*, giving systematic errors in certain speed ranges, *Antola et al. (2017)*.

Thanks to considerable work and progress within the field of radar remote sensing during the recent decades, reliable ocean surface measurements can now be obtained using radar sensors. There are radars based on various technologies available on the market, and some of them are more suited than others for measuring from moving vessels. Systems based on imaging radar, Fig.1, using the on-board X-band radar, is probably the radar-based technology which is most suited for moving vessels, *Miros AS (2017c), Gangeskar (2014,2017)*. Microwave Doppler radars, Fig.2, can provide very accurate wave and current measurements from fixed installations and slowly moving vessels, but they are typically not recommended for vessels in transit, *Miros AS (2017a), Grønlie (2004,2006)*. Various sorts of vertical microwave radars, Fig.3, can provide very exact air gap time series that can be used to estimate the non-directional wave spectrum and parameters like the significant wave height, *Miros AS (2017b), Martín et al. (2001), Bushnell et al. (2005)*. By compensating the air gap measurements using data from a co-located motion reference unit (MRU), wave information can also be derived from moving installations. Such sensors can, however, neither provide directional wave information nor surface current measurements when used as single sensors, and they are typically not recommended for wave measurements during transit.

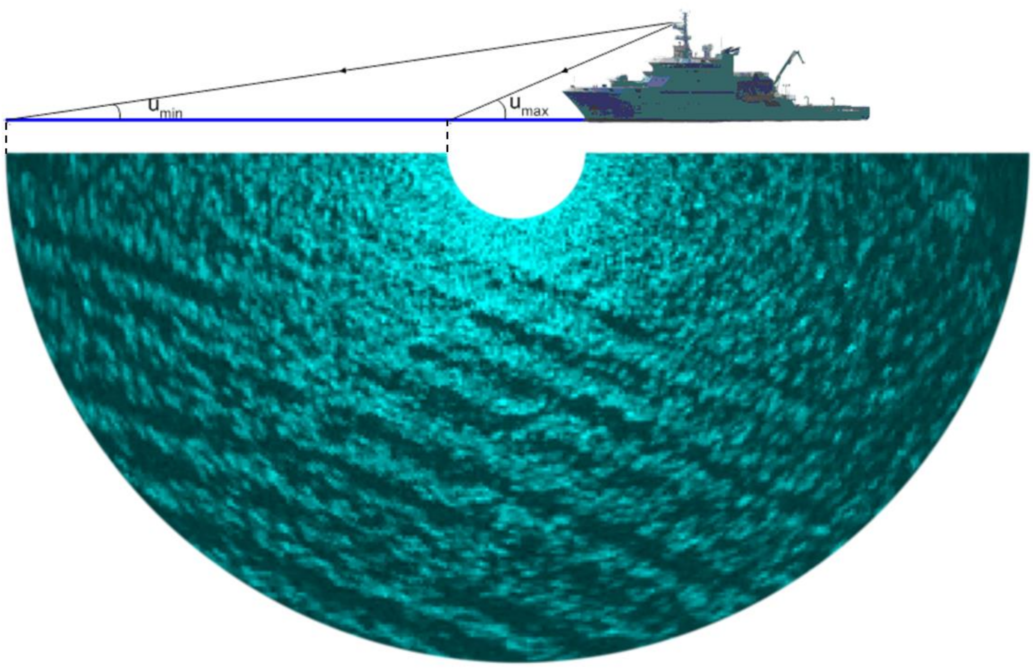

Fig.1: Imaging radar

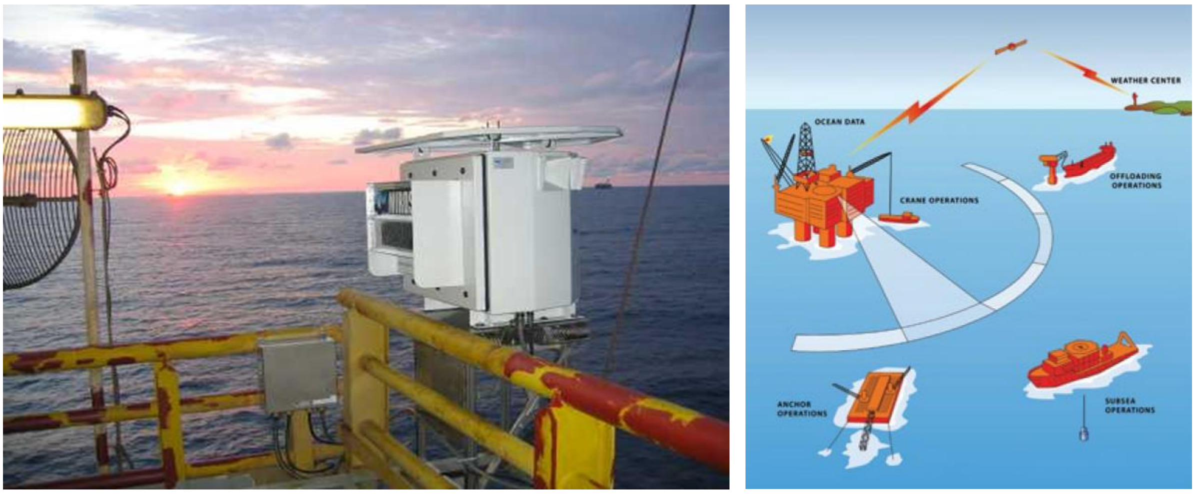

Fig.2: Microwave Doppler radar providing wave and surface current data

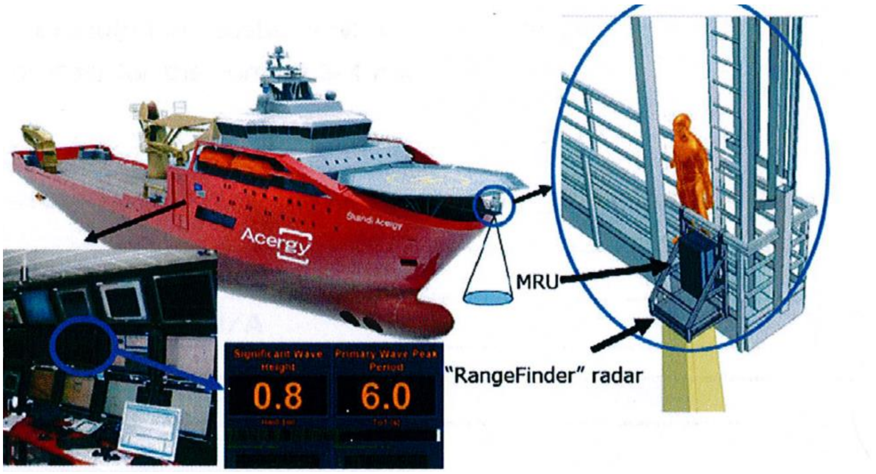

Fig.3: Example of vertical microwave radar in combination with an MRU

In the rest of this paper, we shall focus on a system based on imaging X-band radar that can provide reliable wave and current measurements from moving vessels during transit, as well as the STW. The system is type approved by DNV GL.

2. Measurement principle for system based on imaging X-band radar

Raw radar images are acquired from a marine navigation X-band radar and digitized by DNV GL type approved hardware especially developed for this application, Fig.4. Digitized images can also be acquired directly from radars with digital data feed, commonly known as IP (Internet Protocol) radars, eliminating the need for additional digitalization hardware.

In the context of wave and current measurement by radar, signals refer to gravity wave patterns visible to the radar, given the radar's spatial resolution in range and azimuth. To obtain optimum performance, an unfiltered signal from a radar operating in short pulse mode is required. In addition, a wind speed of at least 2-3 m/s is required to get sufficient electromagnetic backscatter from the ocean surface, *Skolnik (1980)*.

Measurement areas called Cartesian image sections, Fig.5, defined through system software configuration, are extracted from the digitized radar images and processed by dedicated algorithms. This provides the user with real-time wave spectra, as well as integrated wave parameters and surface current vectors. The measurement area can be changed by software reconfiguration at any time.

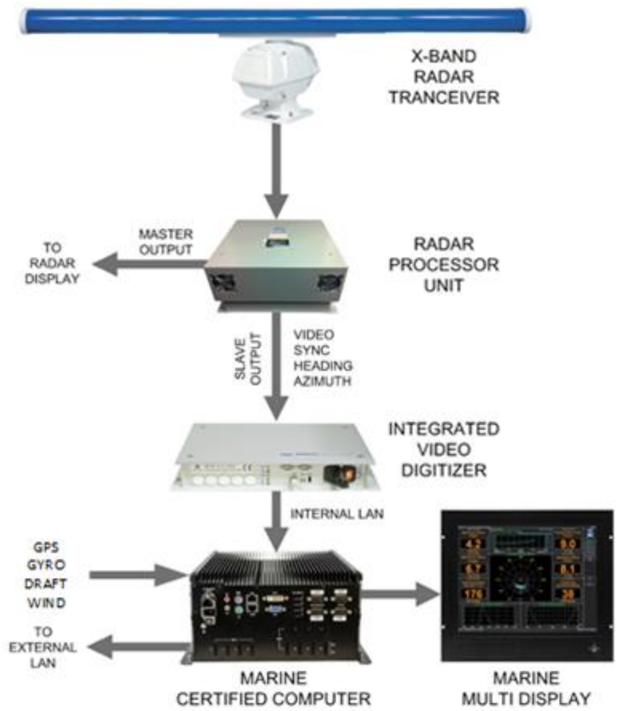

Fig.4: Schematic diagram of system based on imaging X-band radar

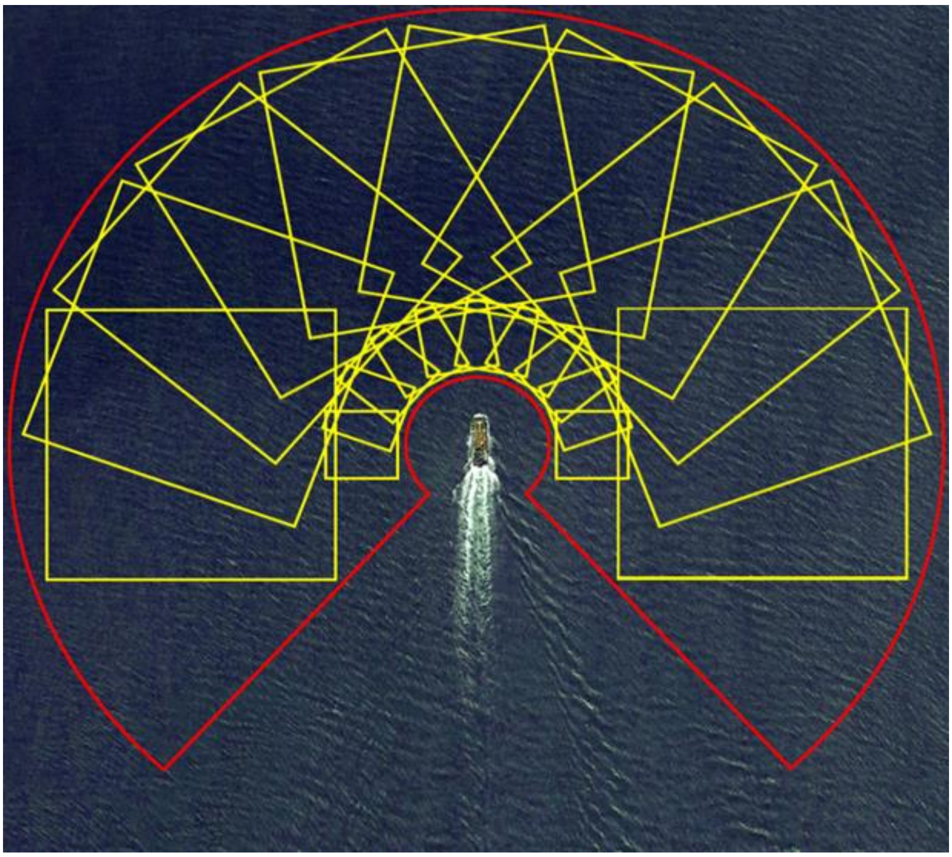

Fig.5: Illustration of how Cartesian image sections are extracted from polar radar image

3-D fast Fourier transforms (FFTs) are applied to time series of Cartesian images, giving 3-D spectra with information about the power present at various wavenumbers and frequencies, *Young et al. (1985)*. Ocean image spectra are obtained from these wavenumber-frequency spectra by integrating over frequency. Various sorts of noise filtering are also applied. The dispersion filtering, for instance, is based on knowledge about the relation between wavenumbers and frequencies, as explained below.

A transfer function is applied to the image spectrum to obtain a calibrated directional wave height spectrum. The transfer function is relatively complex, relying on several fundamental sub-methods, ensuring that the final wave height spectrum correctly describes the actual ocean surface, both with respect to shape and scaling. Integrated wave parameters are calculated from the calibrated wave height spectrum.

Ocean surface currents are estimated from the wavenumber-frequency spectra obtained by 3-D FFTs using a novel method recently developed by Miros. The method is, as previously known methods, based on our already existing knowledge about the relation between wavenumbers and frequencies of ocean gravity waves for zero current, i.e. the dispersion relation, *Pond et al. (1983)*:

$$\omega_0^2 = g\left|\vec{k}\right|\tanh\left(\left|\vec{k}\right|d\right)$$

where ω_0 is the wave frequency, $\vec{k}$ is the wavenumber vector, d is the water depth, and g is the gravity of Earth. If there is a surface current $\vec{U}$ relative to the radar, a Doppler frequency shift is introduced in the wave frequency:

$$\omega = \omega_0 + \vec{k} \cdot \vec{U}$$

This Doppler shift causes the energy in the 3-D spectra frequency planes to be located on ellipses, rather than circles. Based on the power distribution in the wavenumber-frequency spectra, the current vector can be estimated.

Miros has recently developed further improvements to the method used for estimating ocean surface currents from X-band radar images. This includes an improved method utilizing the full power distribution properties, improved motion compensation, as well as several improvements increasing performance under conditions with high current speeds and low signal-to-noise ratios. The method also includes various functionalities to automatically detect and tag data with respect to quality.

Based on kinematic data and the measured surface current, the STW can be calculated, Alternatively, the STW can be directly estimated from the radar images because they already contain sufficient information to directly determine the relative motion between the vessel and the water.

3. Data examples

Calibrated directional wave spectra and integrated wave parameters can be presented in many ways. Fig.6 shows one possibility, with the directional wave spectrum, integrated wave spectra with respect to direction and frequency, and some of the corresponding parameters for wave height, period and direction.

During the recent years, large amounts of data from the system have been acquired from various sites and geometries, using various radar types. For wave measurements, four principal test sites have made the basis for testing and verifying the system reliability and accuracy, *Gangeskar (2017)*. Data have been acquired for months at each of these sites, both from imaging X-band radar systems and reliable reference sensors. For convenience, some previous results are also provided here.

The four principal test sites, Fig.7, span a wide range of properties relevant for the measurements, Table I. Time series and scatter plots of the significant wave height look reasonable, Fig.8, Fig.9, and the statistics show that RMS deviations are well within 0.5 m and correlations close to unity for all sites, also without performing any sort of site-specific calibration, Table II. All available data are used in the studies, apart from data automatically tagged by built-in data quality controls relying on the signal-to-noise ratio and other parameters deduced from the data.

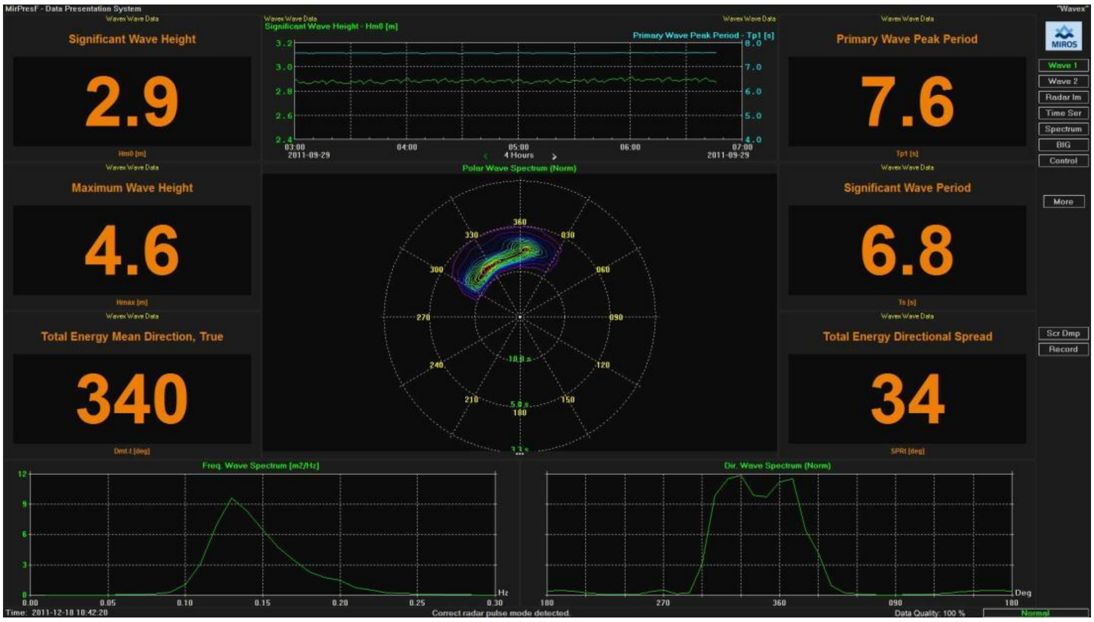

Fig.6: Presentation of calibrated directional wave spectra and integrated wave parameters

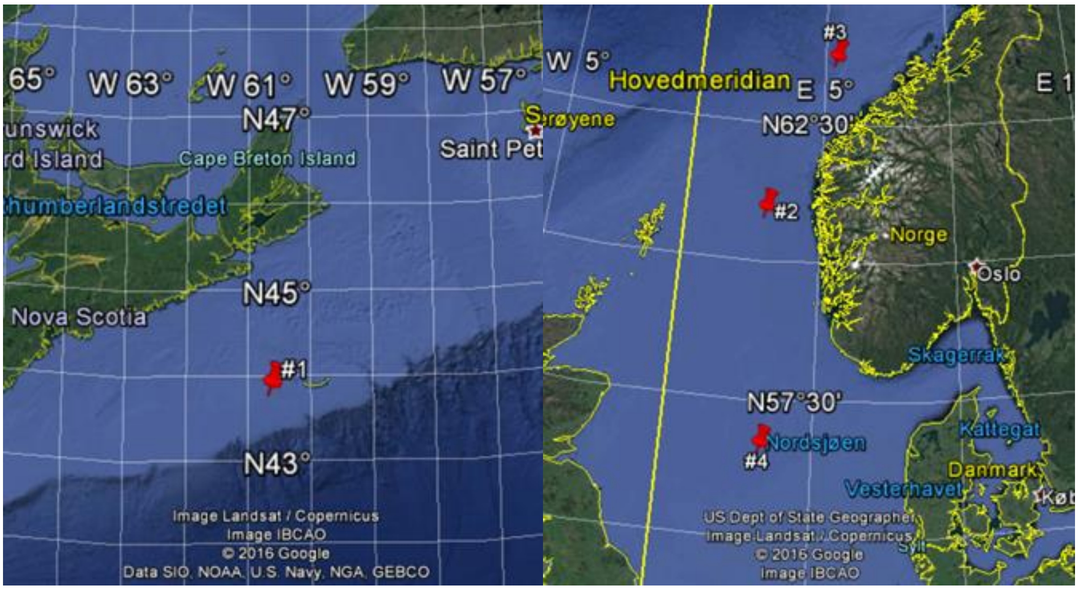

Fig.7: Four principal test sites indicated in Google Earth

Table I: Essential parameters related to four principal test sites

	#1 Deep Panuke (fixed)	#2 North Sea (fixed)	#3 West Navigator (moving)	#4 Ekofisk (fixed)
Radar brand	Furuno FAR 2117	Sperry Bridge-master II	Sperry Bridge-master II	Terma Scanter 5202
Antenna height	26.0 m	43.5 m	23.0 m	92.0 m
Antenna length	6.5 ft	4 ft	6 ft	12 ft
Antenna rotation speed	42 rpm	29 rpm	29 rpm	18 rpm
Range resolution in short pulse mode	10.5 m	7.5 m	7.5 m	3.0 m
Water depth	45 m	185 m	850-1100 m	70 m
Reference, at distance	Buoy, < 5 km	RangeFinder, < 1 km	Buoy, < 1 km	RangeFinder, 7 km

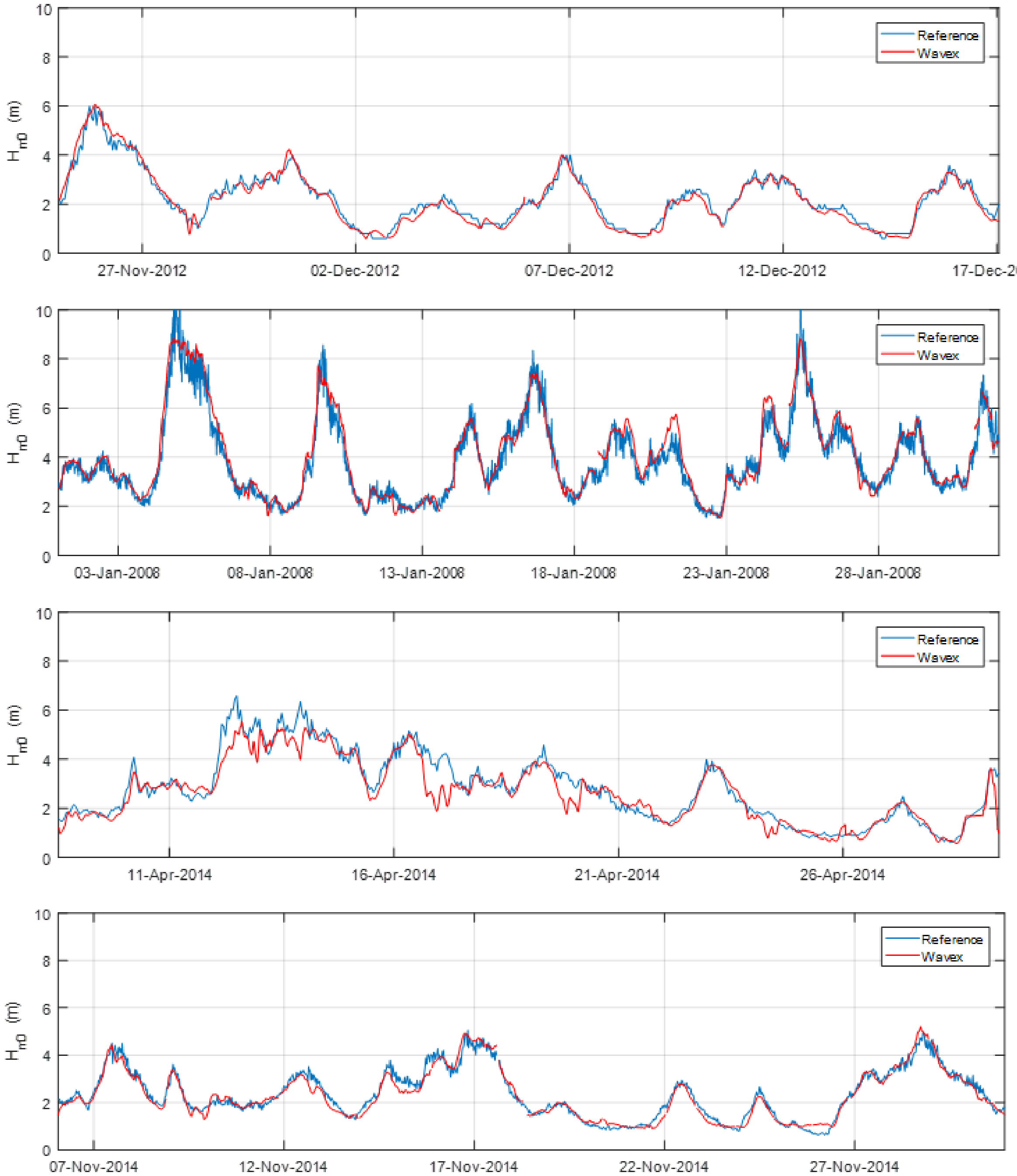

Fig.8: Time series from sites #1 - #4 (#1 on top), comparing significant wave height H_{m0} from imaging radar system and references

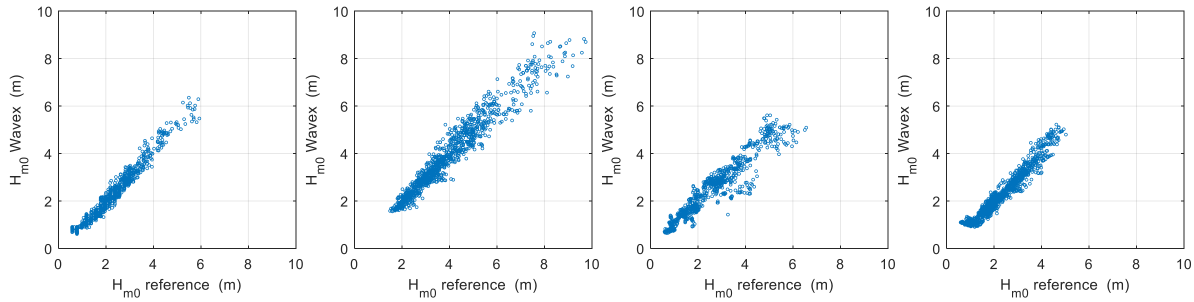

Fig.9: Scatter plots from sites #1 - #4 (#1 to the left), comparing Hm0 from imaging radar system and references. Data are decimated to improve the readability

Table II: Statistics of performance: Correlation, mean deviation, and RMS deviation between significant wave height H_{m0} from imaging radar system and references. Numbers in parenthesis represent statistics after performing site-specific calibration.

	#1 Deep Panuke	#2 North Sea	#3 West Navigator	#4 Ekofisk
Correlation	0.98 (0.98)	0.97 (0.97)	0.94 (0.94)	0.97 (0.97)
Mean deviation (m)	0.04 (0.00)	0.15 (0.00)	0.19 (0.00)	0.13 (0.00)
RMS deviation (m)	0.22 (0.19)	0.42 (0.38)	0.50 (0.46)	0.26 (0.22)

The reference sensors are based on measurement principles very different from the imaging radar system. This also includes spatial and temporal averaging strategies used in the sensors, implying that some differences must be expected due to the statistical properties of the ocean surface itself. Furthermore, the exact accuracy of the reference sensors is not known.

Imaging radar systems can also provide reliable surface current measurements. Recent field trials have shown that a high accuracy can be obtained from both fixed sites and moving installations, *Gangeskar (2018)*. Fig.10 shows a period of data acquired at the Ekofisk platform in the southern part of the North Sea. RMS measurement errors of 0.032 m/s and 9.1° for magnitude and direction, respectively, were estimated based on the entire trial during November and December 2015, as well as correlation coefficients of 0.93 and 0.94 for East-West and North-South current components, respectively, *Gangeskar (2018)*.

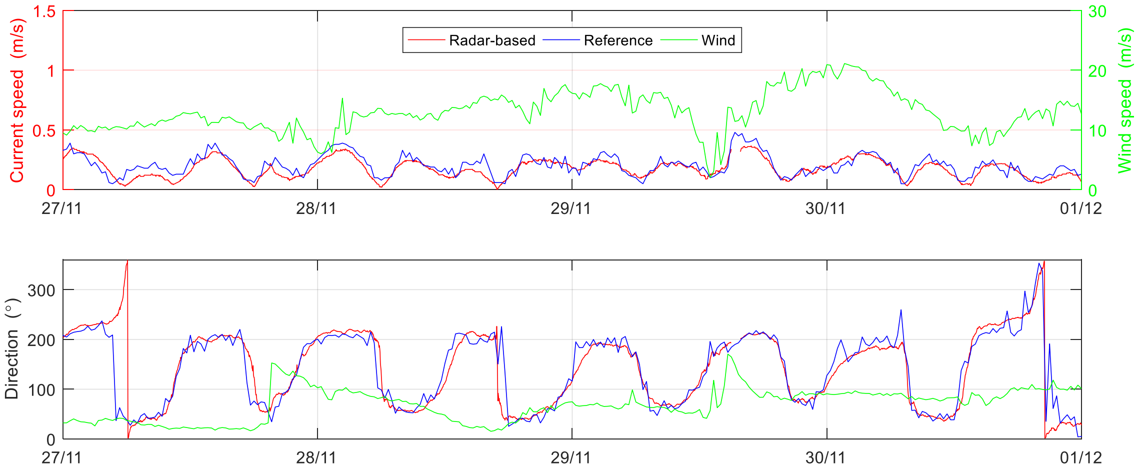

Fig.10: Time series of surface current and wind data from Ekofisk, comparing imaging radar system and reference Aquadopp

Convincing surface current measurements have also been obtained from moving vessels, and this also makes the basis for accurate STW measurements by imaging radar systems, avoiding challenges and noise associated with traditional underwater instrumentation, as discussed above. Fig.11 - Fig.13 show examples of STW data from an imaging X-band radar system installed at the Norwegian research vessel G.O. Sars. Data were acquired during a sea trial in the Norwegian Sea and the Barents Sea in November 2016, in close cooperation with the Institute of Marine Research (IMR) in Norway. In Fig.11, the vessel is moving back and forth, as can be seen from the direction (red). Data are rather smooth and in accordance with our expectations based on how the vessel was maneuvered. In Fig.12, the vessel is alternately moving and at rest to perform various experiments. Data still look reasonable and smooth. Direction estimates are less stable only when the magnitude is close to zero, which is, of course, as expected. The oscillatory changes in direction during the first period with magnitude close to zero are, however, related to actual small movements as the vessel was kept on an approximate constant position. Fig.13 shows another period in which the vessel is in transit along the Norwegian coast, occasionally changing the course.

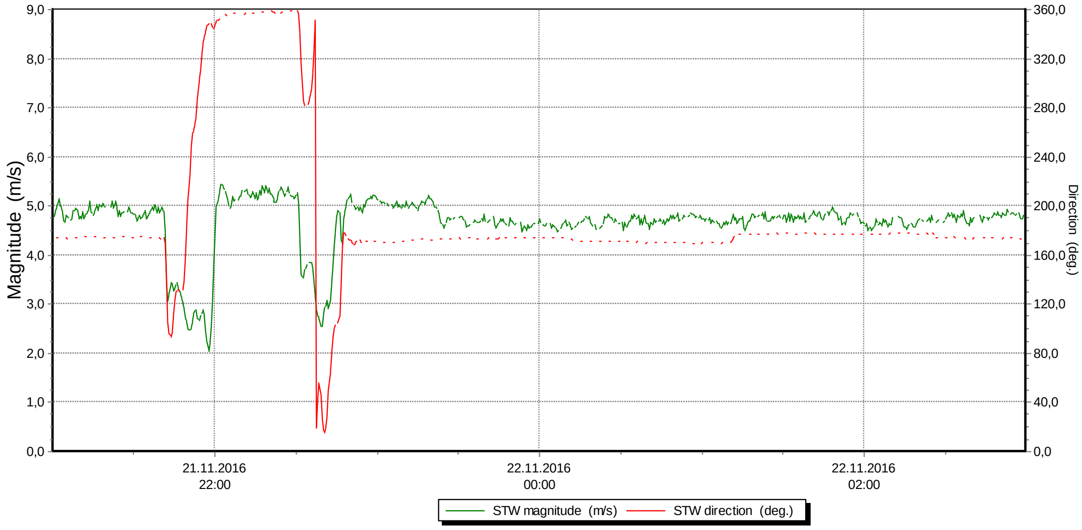

Fig.11: STW data from imaging radar system. Vessel is travelling back and forth during a sea trial

Fig.12: STW data from imaging radar system. Vessel is alternately moving and at rest to perform various experiments during a sea trial

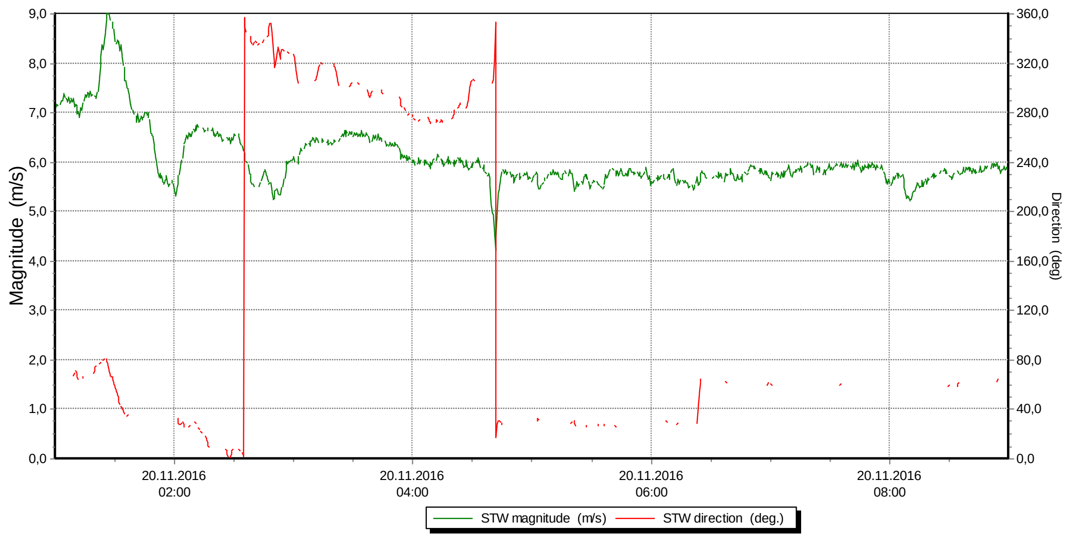

Fig.13: STW data from imaging radar system. Vessel is in transit along the Norwegian coast, changing the course from time to time

4. Conclusion

Information about ocean waves, surface currents, and the Speed Through Water can be of great value to applications such as fuel optimization, hull stress monitoring, and systems improving cargo safety and passenger comfort. Thanks to considerable work and progress within the field of radar remote sensing during the recent decades, such ocean surface measurements can now be performed with a high reliability and accuracy using radar sensors. Hence, challenges like data heavily influenced by noise and costs related to installing and maintaining traditional underwater equipment can be avoided. By means of radar remote sensing techniques, the user can measure the current in the water of interest, sufficiently far away from structures and the chaotic conditions close to a vessel hull that would otherwise disturb the measurements.

References

ANTOLA, M.; SOLONEN, A.; PYÖRRE, J. (2017), *Notorious speed through water,* 2nd HullPIC, Ulrichshusen, Germany, pp.156-165

BAUR, M. (2016), *Acquisition and integration of meaningful performance data on board - challenges and experiences,* 1st HullPIC, Pavone, pp.230-238

BOS, M. (2016), *How MetOcean data can improve accuracy and reliability of vessel performance estimates*, 1st HullPIC, Pavone, pp.106-114

BROWN, J.; COLLING, A.; PARK, D.; PHILIPS, J.; ROTHERY, D.; WRIGHT, J. (2001), *Ocean Circulation,* 2nd ed., The Open University, pp.130

BUSHNELL, M.; BOSLEY, K.; MERO, T. (2005), *Microwave air gap-bridge clearance sensor – Test, evaluation, and implementation report*, NOAA Technical Report NOS CO-OPS 042, Silver Spring

CARCHEN, A.; PAZOUKI, K.; ATLAR, M. (2017), *Development of an online ship performance monitoring system dedicated for biofouling and anti-fouling coating analysis,* 2nd HullPIC, Ulrichshusen, pp.90-101

FLAGG, C.N.; SCHWARTZE, G.; GOTTLIEB, E.; ROSSBY, T. (1998), *Operating an acoustic Doppler current profiler aboard a container vessel*, J. Atmospheric and Oceanic Techn. 15, pp.257-271

FRITZ, F. (2016), *Practical experiences with vessel performance management and hull condition monitoring,* 1st HullPIC, Pavone, pp.128-136

GANGESKAR, R. (2014), *An algorithm for estimation of wave height from shadowing in X-band radar sea surface images,* IEEE Trans. Geosci. Remote Sens. 52/6, pp.3373-3381

GANGESKAR, R. (2017), *Automatically calibrated wave spectra by the Miros Wavex system – Accuracy verified,* Miros AS, Asker

GANGESKAR, R. (2018), *Verifying high-accuracy ocean surface current measurements by X-band radar for fixed and moving installations,* submitted for publication

GOLER, H.; BOSKURT, K. (2017), *Speed loss analysis of high-speed ro-ro vessels coated with new antifouling technologies,* 2nd HullPIC, Ulrichshusen, pp.173-193

GRØNLIE, Ø. (2004), *Wave radars – A comparison of concepts and techniques,* Hydro Int. 8/5

GRØNLIE, Ø. (2006), *Wave radars: techniques and technologies – Advantages and disadvantages of different ground-based radar remote sensors,* Sea Technology, October

KELLING, J. (2017), *Ultrasound-based antifouling solutions,* 2nd HullPIC, Ulrichshusen, pp.43-49

KING, B.A.; COOPER, E.B. (1993), *Comparison of ship's heading determined from an array of GPS antennas with heading from conventional gyrocompass measurements,* Deep Sea Research Part I: Oceanographic Research Papers 40/11-12, pp.2207-2216

MARTÍN, B.; PÉREZ, B. (2001), *Assessment of accuracy and operational properties of different tide gauge sensors*, European Sea Level Service Research & Infrastructure, ESEAS-RI WP4, Deliverable D4.1

MIROS AS (2017a), *SM-050 Wave and Current Radar Mk III*
https://www.miros-group.com/wp-content/uploads/2017/11/SM-050-Wave-and-Current-Radar-MkIII-DB-101-Rev.03.pdf

MIROS AS (2017b), *SM-140 Range Finder,*
https://www.miros-group.com/wp-content/uploads/2017/11/SM-140-datasheet.pdf

MIROS AS (2017c), *Wavex v5.7*
https://www.miros-group.com/wp-content/uploads/2017/11/Wavex-v5.7-Datasheet.pdf

NEW, A.L. (1992), *Factors affecting the quality of shipboard acoustic Doppler current profiler data,* Deep Sea Research Part A: Oceanographic Research Papers 39/11-12, pp.1985-1996

POND, S.; PICKARD, G.L. (1983), *Introductory Dynamical Oceanography,* 2nd ed., Butterworth-Heinemann, pp.207-219

SKOLNIK, M.I. (1980), *Introduction to radar systems*, 2nd ed., McGraw-Hill, pp.474-482

YOUNG, I.R.; ROSENTHAL, W.; ZIEMER, F. (1985), *A three-dimensional analysis of marine radar images for the determination of ocean wave directionality and surface currents,* J. Geophys. Res. 90, no. C1, pp.1049-1059

Effective Data Handling for Practical Vessel Performance Analysis

Dafni Sofiadi, American Bureau of Shipping, Athens/Greece, dsofiadi@eagle.org
Soren Hansen, American Bureau of Shipping, Copenhagen/Denmark, shansen@eagle.org

Abstract

Identifying and analyzing key data in combination with recognizing the potential sources of error are critical to cost effective technical & operational management. Logging of data can be manual (by vessel's crew), semi-automated or fully automated. The paper describes how the integration of data collection with the vessel's control and monitoring systems can reduce crew burden and improve the process of qualifying and analyzing condition and performance data. The objective is to develop a standardized process for maintenance planning and practical decision making related to vessel operations on issues such as hull and propeller cleaning and main engine maintenance that affect fuel consumption. To ensure that data analyses are built on valid data, data validation procedures have to be initiated and executed before starting the data analysis process, leveraging a ship specific model. The paper will describe a typical set of data validation routines, used in performance evaluation, including the following aspects: outlier detection, faulty sensors and drift. Case studies are provided to exemplify the importance of logged parameters quality in the performance evaluation. Results illustrate the difference in accuracy between using noon data and auto logged data when it comes to assessing key performance indicators such as hull/propeller fouling and SFOC of the main engine.

1. Introduction

A Vessel Performance Management System (VPMS) should include features for data validation, collection and analysis, reporting and dissemination to the relevant stakeholders. This will provide the information required to understand energy efficiency and environmental performance and to make improvements. The data analysis and reporting should be done for each ship, for each class of vessels owned and across the entire fleet. The fleet-wide analysis provides useful comparative performance indicators and will give the owner/operator the necessary data to identify potential problems and determine if the ships have been deployed in the most efficient manner. The data collection is not just about fuel consumption figures. The data collection should also include voyage information, machinery operating parameters, hull and propeller inspection reports, maintenance and cleaning events. By linking issues related to machinery, propulsion and operation, together with operational measures applied, it is possible to obtain a holistic view of energy efficiency and the fully integrated nature of performance in terms of fuel consumption.

2. Data Logging

The data to be provided as input to a VPMS consist of vessel's data recorded on board either in the form of daily and voyage reports or continuously (automatically) logged performance data. A consistent and meaningful analysis offers valuable decision support to shore-based managers and on-board personnel to closely monitor and execute fuel efficient operations.

To ensure that logged data are valid before analysis is started, a series of data validation procedures should be applied. Data validation rules are applied at the data entry stage. The validation rules are based on a baseline model for the vessel and will capture invalid output and data outside the valid ranges of the model. Data can also be validated by external sources e.g. hindcast data for weather and AIS data for position and speed.

When an onboard autologging systems is installed, data are continuously collected from the source (sensor) or through logging devices such as the Voyage Data Recorder (VDR) and the Engine Automation System. Data recorded by the autolog system are stored onboard and/or transferred to shore through specific data transfer protocols that ensure safe transfer at minimum cost. An Autologger box is a shipboard installation that can interface with all primary and secondary machinery systems connected to available sensors. An integrated installation enables shore based operators to obtain insight from draft and tank level measurements to navigation systems and equipment, main engine performance metrics, automation and controls, cargo loading computer, fuel flow meters, ballast water management, etc. Data are imported to the system at specific, pre-defined time intervals to achieve higher accuracy performance analysis results.

3. The vessel model

The base line or the reference model for the vessel performance analysis comprises a hydrodynamic resistance and propulsion model of the vessel. The hydrodynamic model is based on design data and model tests and/or sea trials. The model can be enhanced with data from CFD computations, if available, to cover a wider range of speeds, draft and trim combinations.

The base line also includes a representative model of the ship's main engine and auxiliary systems. The model is developed from design information, OEM datasets, shop test results and a detailed electric load analysis describing the behavior of the equipment for different operational modes. The overall reference model is compared and validated towards the logged data for different operational conditions; where relevant, the model is tuned to reflect actual performance and specific characteristics of the vessel and its equipment. By using a validated reference model, the characteristics for different operating modes are known and guidance for efficient operations can be issued to operators and crews.

4. The vessel performance analyses

A VPMS should include a detailed analysis of the ship's most important performance parameters. Results of the analysis can be used to set-up KPIs to demonstrate and assess the efficiency of established operational activities and tactics. Customizable dashboards provide visualizations and charts to communicate insights from the KPIs and performance data. A meaningful analysis compares current KPIs to the vessel's baseline model and to stakeholder's expectations. Data from industry peers can also be included for comparison and decision support.

Fouling of the hull and propeller will create added resistance for the vessel. To overcome the additional drag and maintain a certain speed, more horse power is required and therefore, a fuel consumption increase is expected. Propulsive performance losses due to fouling can be monitored through the progressive change of the 'Added Hull and Propeller Resistance' KPI which is periodically evaluated towards the vessel's reference baseline. The baseline is established at sea trial/delivery event (see above vessel model section) or within a pre-determined period to capture the effect of key events such as hull surface treatments and coating application at dry-dock, hull cleaning and propeller polishing. Regular maintenance schemes can restore the vessel's propulsive performance to a certain extent. The reduction in the added resistance should be noticeable, as fuel savings are generated immediately. The added resistance will then start increasing gradually again with a rate that depends on the scheme selected but also the way this was applied. The effect of this KPI's progress on the daily fuel oil consumption is captured in the VPMS and clearly demonstrated in speed/draught – fuel tables covering the whole operational range.

The Main Engine is the vessel's prime consumer and represents the greater portion of the ship's direct operational expenses in the form of fuel consumption and maintenance as well as the indirect 'penalty' costs related to equipment downtime. Thus, Main Engine Performance monitoring and analysis can result in important financial and efficiency gains. Operational goals can be achieved by leveraging indices and trends to optimize maintenance and inspection intervals. To address performance from a holistic perspective, the VPMS should combine main engine performance with the hull and propeller condition. The ship is modeled as one integrated system rather than a collection of individual components, enabling a detailed understanding of the main causes of added fuel oil consumption over time. This is a tool for decision making but also a way to avoid excess consumption and huge costs related to incompliance with charter party terms.

Other than the Main Engine, energy is consumed by auxiliary engines and machinery. In vessels with a high electrical load, a base load reference model is established and performance of the base load is continuously monitored and analyzed to optimize performance. As an example, this can be achieved by optimal load and optimal number of auxiliary engines used, in order to minimize costs related to consumption but also to maintenance.

5. Case Study

A 35,000 DWT bulk carrier sailing in worldwide trade is used as a case study vessel. The vessel has been equipped with the ABS Autologger and Nautical Systems (NS) Voyage Manager to capture performance data. The Autologger installation is connected to the VDR, the Automation System and has in addition external weather and motion sensors connected. The Autologger framework is as described in Fig.1.

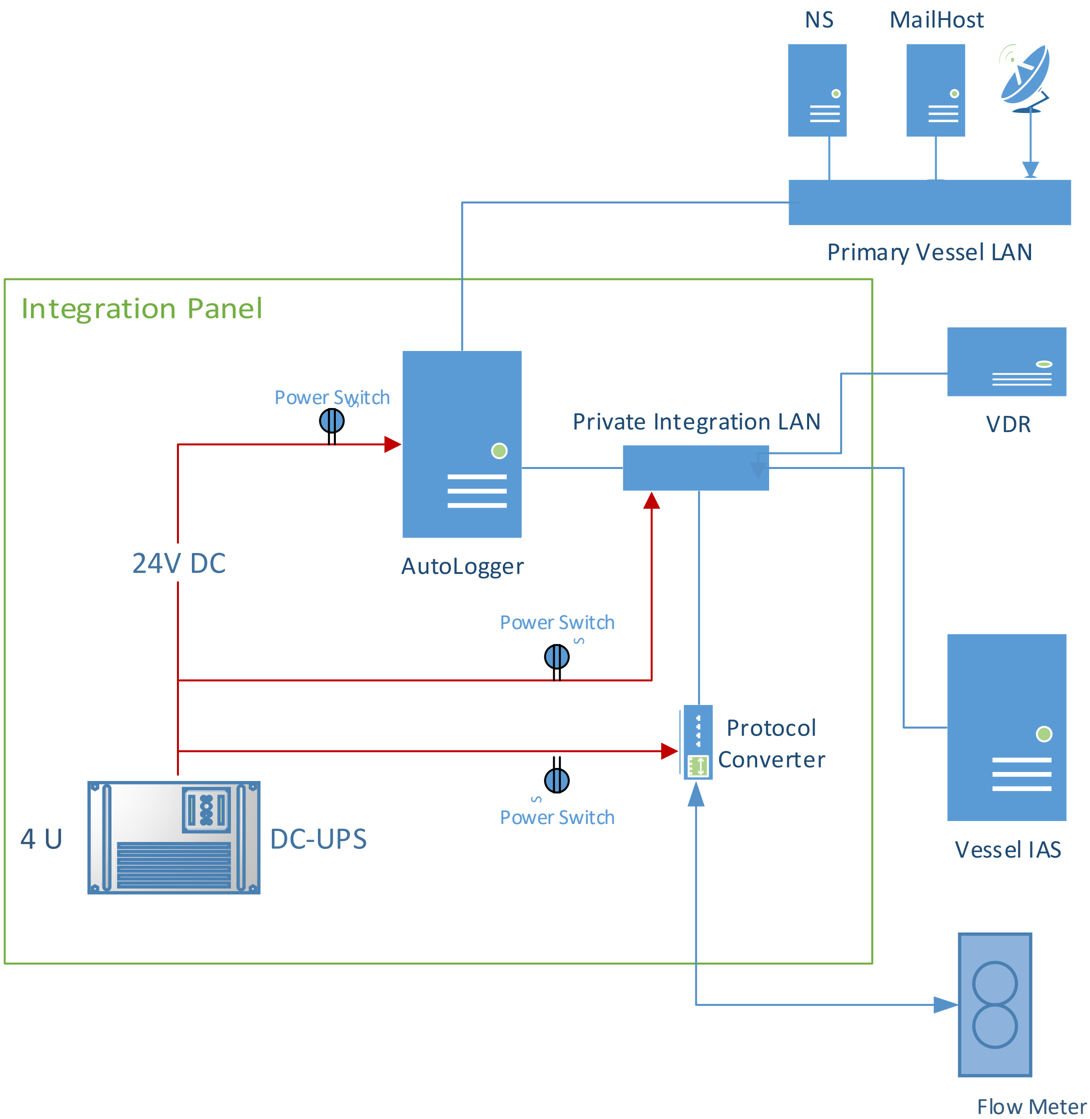

Fig.1: Automatic data logging set-up

The connection to the different systems has been made in agreement with the different equipment vendors and through established firewalls to avoid any risks of corrupting data in the system. The Autologger is equipped with a health monitor where sensor and equipment status are updated continuously. The monitor can be accessed on board and remotely from shore.

5.1. Data logging, storage & transfer

The various sensors capture data at different frequencies and the ABS Autolog system is used to convert all sensor outputs to a selected "master" frequency. The default frequency is set for 15 s to match the ISO 19030 method for hull/propeller performance. The data are stored in a database on board and data transfer to shore is configured according to the requirements from the ship owner. With consideration to transfer costs, the data can be transferred in packages with set intervals, transferred real time to shore, or stored on board and transferred by on-demand queries. It should also be considered if only selected parameters are to be transferred, or transferring data at a lower frequency such as e.g. 4 h or 24 h interval, pending on how data are to be used. Fig.2 shows a set of data logged with 15 s values and with a 1 h average as overlay (before validation and filtering).

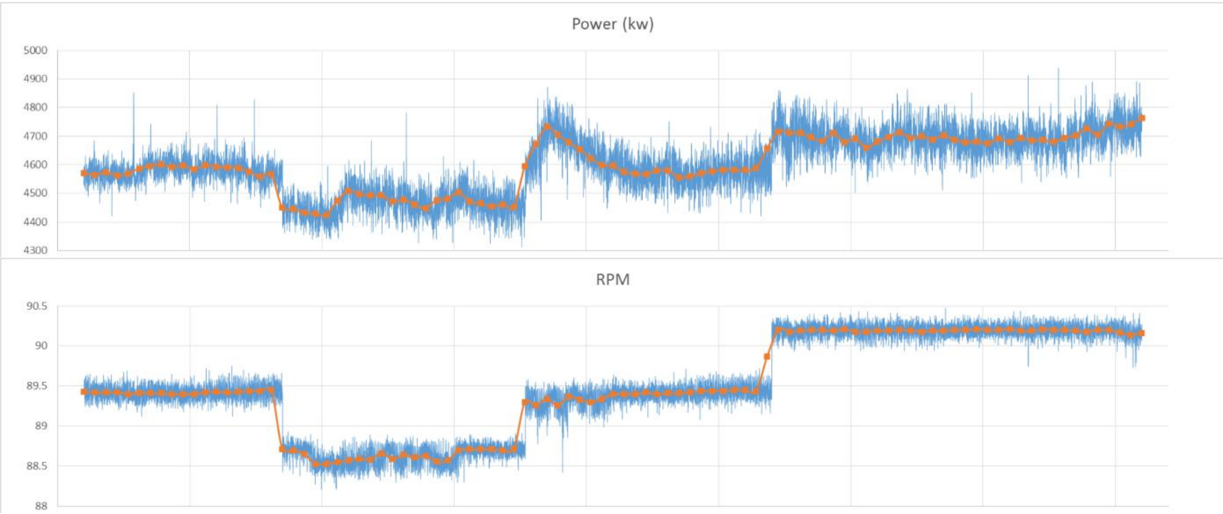

Fig.2: Logged Shaft Power and RPMs with 15 s interval. Overlay of 1 h averaged data. Logging period equals 4 days

The analysis of data shown in Sections 5.5 and 5.6 is based on 1-hour averaged data. The analysis has further been done with 4 and 24 hour averages and with manually logged noon data. An example of speed/consumption data for a selected period with the different data sets is shown in Fig.3. The figure shows a general offset between autologged and noon data, in this example the vessel's speed is reported 7% higher by the crew and ME FOC is reported 3% lower. In general, there is an offset of the logged data through the whole period, which also has an effect on the analyses.

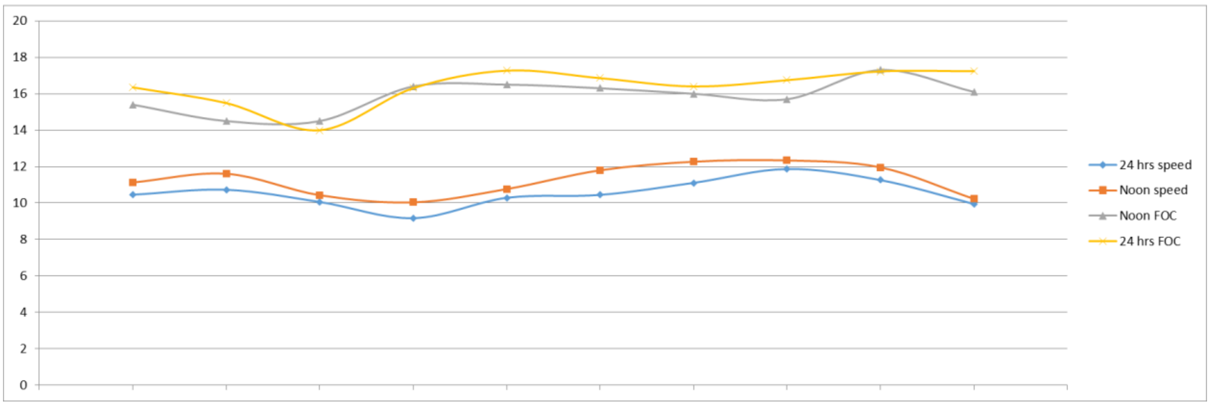

Fig.3: Averaged autologged data vs. noon data (speed and consumption) over a 10-day period

5.2. Logged parameters

The parameters that are related to and affects the propulsion of the vessel are monitored and analysed in the VPMS, the basic parameters can be seen in Table I.

Table I: Logged performance parameters

Parameters (Propulsion)	Source
Ship speed through water and GPS speed	Speed Log and GPS
Ship draft and trim	Draft sensors
ME fuel consumption	Fuel flow meters
ME power	Torque meter
ME RPM	Torque meter
Water depth	Echosounder
Wind speed and direction	Anemometer / Weather sensor
Vessel Motions	Accelerometer
Rudder angle / Rate of Turn	VDR

The basic parameters to establish a performance analysis are the net fuel inflow to the engine, the power to the propeller and the vessel's speed. In addition, there are performance influencing factors as the water depth, wind speed and direction (to identify weather effect on performance) and vessel motions/ rudder angle (to identify steady state periods).

The logging frequency has been varied in the case study, and in addition a set of manual logged data (noon data) for the same period has been analysed.

5.3. Data validation & filtering

The data are validated towards a model of the vessel. Outliers are found by setting boundaries based on the model and relations between key parameters involved in the analysis. The data validation can be set up in a dashboard as in Fig.4.

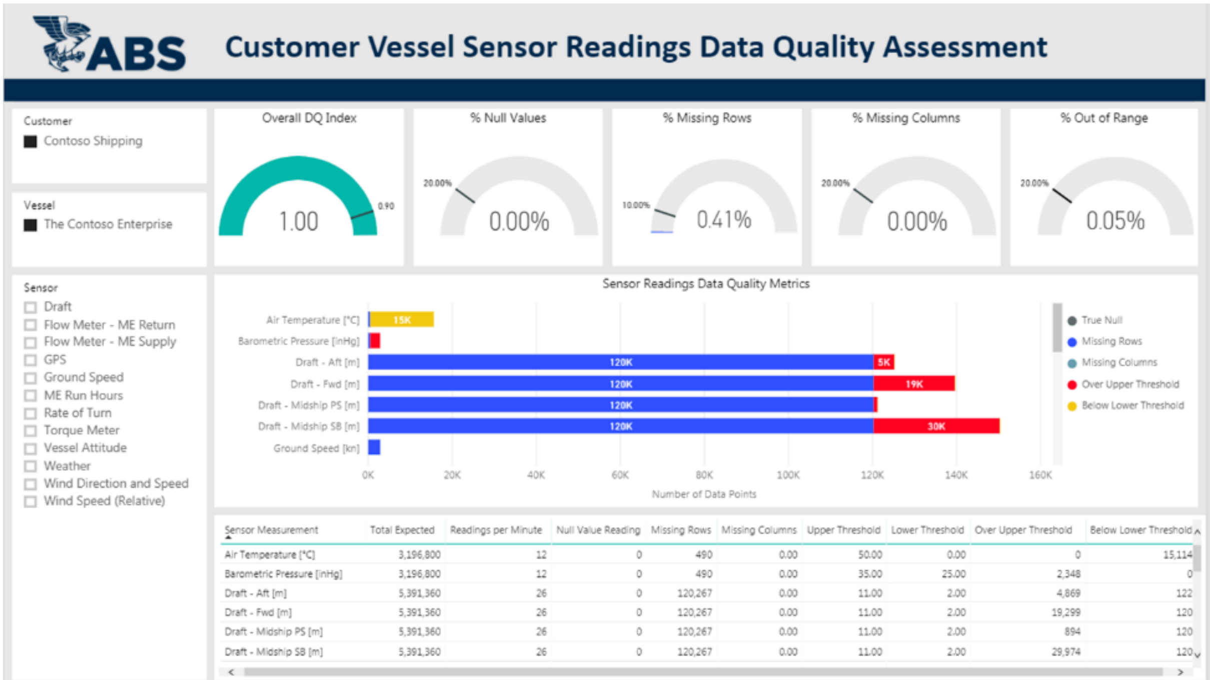

Fig.4: Data Quality Assessment dashboard

The mentioned boundary settings are illustrated in Fig.5 where the left-hand side shows the SFOC values towards the baseline. Dotted lines are -5% and +20% below and above the baseline. The right-hand side shows the engine load diagram with the measured values plotted. Once the data have been validated, they are filtered with respect to limitations and boundaries within the baseline model and hereafter processed for further analysis.

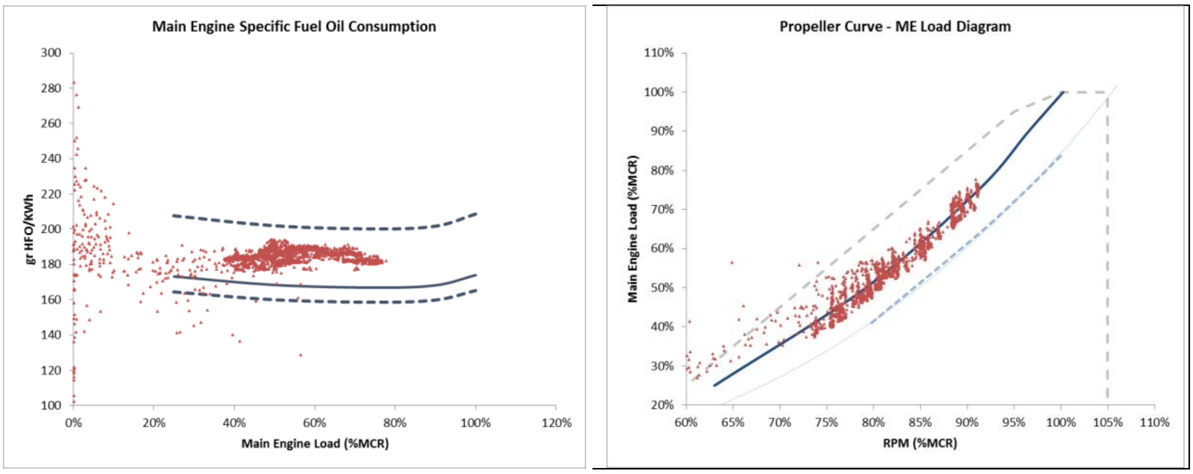

Fig.5: Data validation dashboards; SFOC values plotted with baseline (left) and main engine loads plotted in baseline load diagram (right)

5.4. Operational Profile

The analysis period is from January to December 2017. The vessel's operational profile with respect to speed/draft is as given in Fig.6. The vessel has been sailing mainly in laden condition and mostly with economical speed. The vessel sailed in worldwide trade, Fig.7. There is a data gap in the Indian Ocean from the autologging system. The data gap is covered by the parallel manual logging application installed on board.

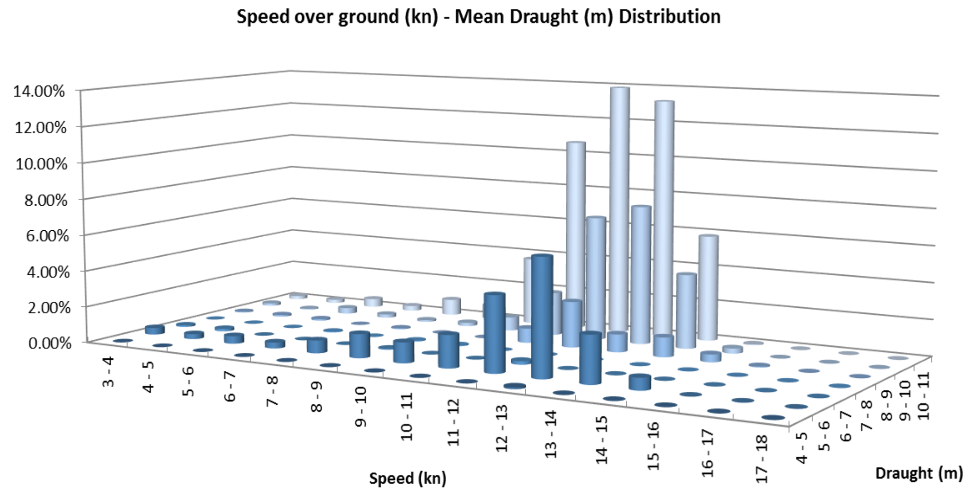

Fig.6: Speed/Draft distribution in the analysis period

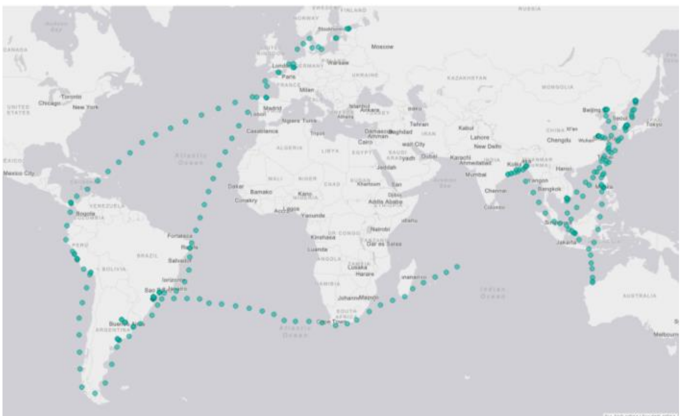
Fig.6: Operating area in the analysis period

5.5. Hull/Propeller

The hull/propeller performance analysis is based on calculations of added resistance over time (ΔCf). The added resistance is trended over time by a linear regression line and the slope of the line is considered to be the evolution of added resistance on the hull and the propeller. The analysis results in this paper are based on delivered power to the propeller and the vessel's speed. When direct power measurements are not available, alternative methods have been developed to estimate delivered power. The vessel's speed is given by either the GPS (speed over ground) or the SpeedLog (speed through water) and there are a few considerations to take into account for both methods.

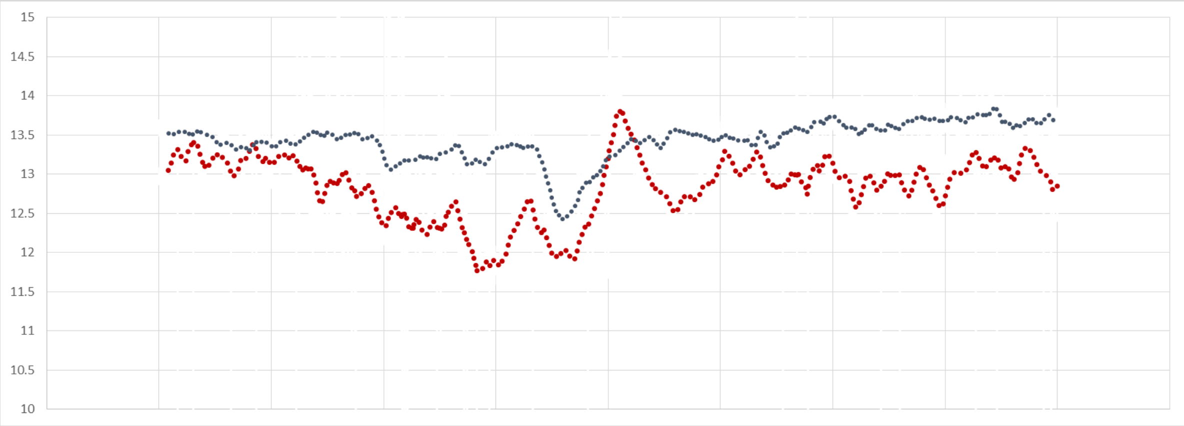

Fig.7: Speed through water, STW (blue line) versus speed over ground, SOG (red line) over 4 days. There is an offset between STW and SOG, if both sensors are showing correct measurements, the vessel is experiencing counter current where SOG is lower than STW.

The GPS speed is subject to effects of the current, i.e. speed is varying with current effect on the vessel, which will have an effect on the analysis result. The SpeedLog speed is by many considered to be unreliable, since it is sensitive to vessel's trim variation, weather, ship motions and water depth. This may also affect the analysis result. The effect in both cases will add to larger scatter in the results and can affect the trend line slope.

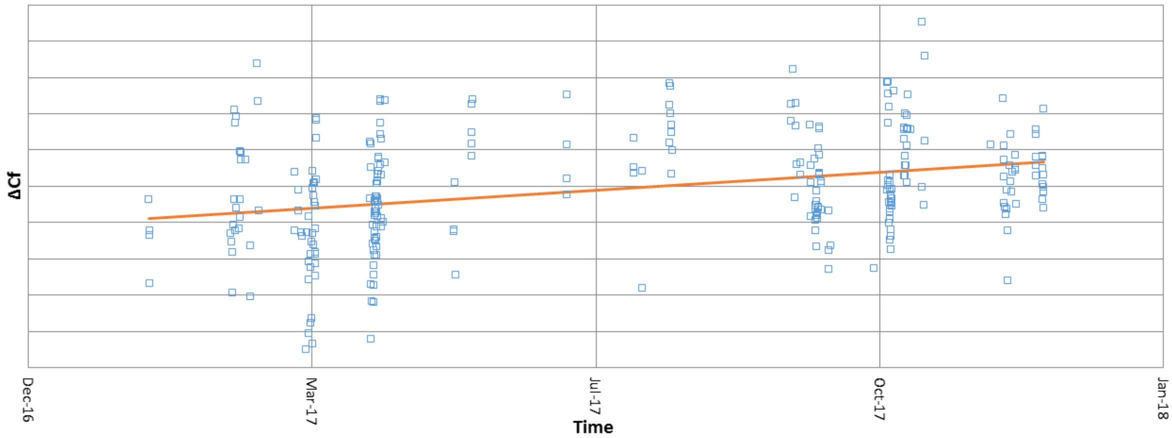

Fig.8: Added resistance (ΔCf) over the analysis period

After validating data and applying filters for the selected data logging period, the analysis suggests that over the year there is an increase in ΔCf, which relates to an increase in added power of 8%. This added power is considered to be due to fouling of the hull and propeller.

5.6. Main Engine

During a main engine's lifetime, the condition of its various components is expected to deteriorate compared to a new engine due to normal wear, off-design and/or incorrect operation. This deterioration can result in a fuel consumption increase over time. Relevant KPIs can be set for monitoring this process. Some of the typical engine component problems may include improper injection timing, reduced turbocharger efficiency, air compressor wear and air cooler malfunctions that lead to high scavenge air temperatures.

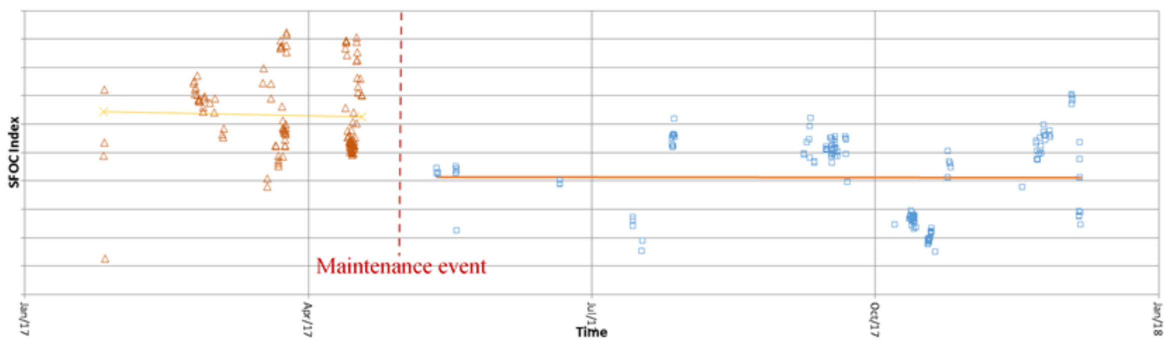

Fig.9: SFOC Index with a split in the analysis period

In this case study the focus has been on the Main Engine SFOC. The SFOC analysis is part of a complete main engine performance analysis and it can give answers to some of the issues mentioned above. In a VPMS, a model of the main engine is included and the actual measured SFOC is compared to the baseline SFOC. The derived KPI, the SFOC Index is used to identify if any added fuel oil consumption is related to engine issues. In the ΔCf analysis above it was found that during operation in 2017 the increase in power was 8%. To give a figure that an operator can relate to, the power increase can be converted to a fuel oil consumption value by using the actual SFOC value. The SFOC Index is plotted over the same timeline and the result is as given in Fig.9.

Since there is a maintenance event on the Main Engine after the first four months of the analysed period, the linear trending of the Index over the whole period is not correct. A closer look at the SFOC values before and after the maintenance event shows that the SFOC values were improved by an average of 3%. SFOC values before and after the event are shown in Fig.10.

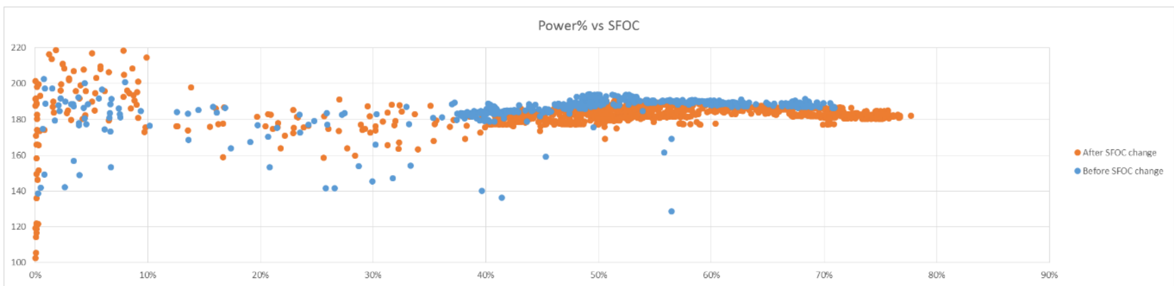

Fig.10: ME Load versus SFOC values, before and after the maintenance event (before filtering)

By monitoring and trending the SFOC Index over time, it is possible to detect if any engine maintenance is needed to lower fuel oil consumption and restore main engine performance. By having a full main engine performance monitoring system in place, it will in addition be possible to detect specific maintenance issues. Typical maintenance areas that affect the SFOC are worn injection pump elements, worn injection nozzles, fouled turbochargers and air coolers. Furthermore, fuel oil quality items such as fuel water content, sulphur content, ash content and fuel heat value can affect engine performance.

5.7. Combining hull/propeller and main engine performance analysis

The hull and propeller analysis is combined with main engine SFOC, from which the fuel consumption increase over time is assessed. A fuel table gives an overview of the fuel oil consumption at any given draft and speed. As an example, the fuel oil consumption figures at speed 13 knots and draft 10.65 m at the beginning and the end of the analysis are shown in Table II. The maintenance event referred to above has been taken into account.

Table II: FOC development over time (1 h average)

FOC at start (t/24 h)	FOC at end (t/24 h)	increase
20.5	21.3	4%

The analysis is focused on using the 1 hour average data points and a similar analysis can be done using various data averages.

The resulting KPIs from this analysis are related to fouling of hull and propeller, main engine condition and actual increase of fuel oil consumption. These KPIs are related to the fuel efficiency of the vessel and will add to the decision support in the daily vessel operations.

6. Conclusion and discussion

The analysis in this document is based on auto logged data averaged over 1 hour intervals. By choosing a logging interval with a significantly higher frequency than normal noon report data, it is possible to select shorter periods with steady state conditions and to identify the variations in the operations over a day.

In general, when choosing parameters and logging intervals, the purpose of the analysis should be considered. For a main engine performance analysis, the relevant parameters and intervals should be selected among the data available e.g. periods with steady state conditions and the relevant engine load. The same applies for a hull and propeller performance analysis. Also, it is the authors' experience that high-frequency sampling (with 15 s interval) of data does not add significant value to the analysis compared to using data e.g. at a frequency of 1 hour, while it adds significant more computation time. For environmental reporting like the Monitoring and Reporting Verification (MRV) CO_2 emissions report, high frequency data are not important and daily averages can be used, since voyage totals are considered sufficient to comply with regulations.

When working with auto logged data, data transfer costs are important and should be taken into consideration. Real time monitoring is relevant near coasts where broadband signals can be used in case of on-demand data requests, e.g. for offshore operations. When evaluating the different options, one should consider for which purpose the data will be used; in general it should be considered if the raw data should be kept on board and if only the data used in the different analyses should be transferred, e.g. snapshots in steady state periods or low frequency averages for reporting. Many of the analysis tools can be executed using on-board software, removing the need for raw data transfer but only transfer of analysis results to shore.

To conclude, the most important factor to obtain good analysis results is the data quality. It is important to have validation procedures in place both for auto-logged data and for manually logged data. The procedures can be model related (as shown in this paper) and can be combined with validation towards a data driven model.

References

BOOM, H.J.J.V.D.; HASSELAAR, T.W.F. (2014), *Ship speed-power performance assessment,* SNAME Annual Meeting, Houston

HANSEN, S.V. (2012), *Performance Monitoring of Ships,* Ph.D. Thesis, Technical University of Denmark (DTU), Lyngby

PERERA, L. (2017), *Handling Big Data in ship performance and navigation monitoring*, Smart Ship Technology Conf., London

SIMONSEN, B.C.; DE KAT, J.O.; JAKOBSEN, O.G.; PEDERSEN, L.R.; PETERSEN, J.B.; POSBORG, T. (2009), *An integrated approach towards cost-effective operation of ships with reduced GHG emissions*, Trans. SNAME 117, pp.1-18

Underwater Drones as Efficient Tool for Hull and Propeller Inspections

Knut Jarle Lysklett, Blueye Robotics, Trondheim/Norway, knut.lysklett@blueye.no

Abstract

Today, underwater hull and propeller inspections are carried out either by divers, by using external ROV companies, or in dry docks. While divers are expensive and represent HSE risks, the use of ROV's have traditionally been very costly and required extensive training to operate. Can underwater hull and propeller inspections be conducted both easier and at a lower cost? This paper discusses today's normal practice and presents a disruptive new technology that can be a vital tool for underwater hull and propeller inspections in the future – The Blueye Pioneer underwater drone.

1. Introduction – The case of underwater inspection

There are many different situations in which the conditions of a ship's underwater body need to be inspected. Some underwater inspections are planned and scheduled, while other inspections need to be done on short notice:

- Incidents
  In the case of a ship incident and there is suspicion that something may have happened to the ship's hull or propeller, it is valuable to get a clear picture of the situation before any decisions are made. With the Blueye Pioneer underwater drone, Fig.1, Annex 1, you can quickly and easily have your own eyes below the surface and conduct your own emergency hull and propeller inspections. You deploy it directly in the water yourself and within minutes you are given the opportunity for making good decisions, planning of activities and to reduce cost for unnecessary repairs or other expensive means of inspection.

- Hull surface and propeller conditions
  The hull surface and propeller conditions substantially impact a ship´s energy efficiency. It is the responsibility of the ship operator to keep the vessel´s hull and other underwater parts free from fouling. With your own Blueye Pioneer, you can perform your own hull surface inspections and do this more frequently than before. This gives you the opportunity to optimize your cleaning intervals and reduce the cost of underwater inspections, as well as performing anti fouling actions at optimized intervals.

- Class underwater inspections requirements
  In some situations, you may have to document the technical condition of the ship below the surface to a third party like class societies. By using the full HD underwater camera, you can provide documentation in form of high quality video files. In some cases, this may even be required for you to continue your operations. Having the possibility to do such inspections on your own and at your own convenience will dramatically reduce cost and time spent in this matter.

- Underwater surveys in connection with change of ownership
  Normally a ship is cleaned before a new owner overtake the asset. But how can you be sure that the hull and propeller actually is clean? And what are the additional cost both in terms of extra fuel cost and extra cleaning if you find out later that the ship was not clean? You may read a report that states that the ship has been cleaned on a specific date, but wouldn´t it be better if you could use the Blueye Pioneer to inspect the ship by yourself during the takeover? Clarifying this during the take-over will save both time and money for both parties.

- Investigations in connection with insurance settlement
  Insurance settlement is all about evidence and documentation. When did the incident happen? And what is the damage? Having the possibility to perform underwater inspections on your own at any time could both safe time, money and make the insurance settlement easier.

- Determine if explosives or contraband are attached to the ship hull
  In some parts of the world it is necessary to inspect the ship hulls to determine if explosives or contraband (usually narcotics) are attached unknowingly. Parasitic containers for smuggling narcotics may be secured to bow thrusters, bilge keels or rudder structures. Magnetic mines may be attached anywhere to a steel hull below the waterline.

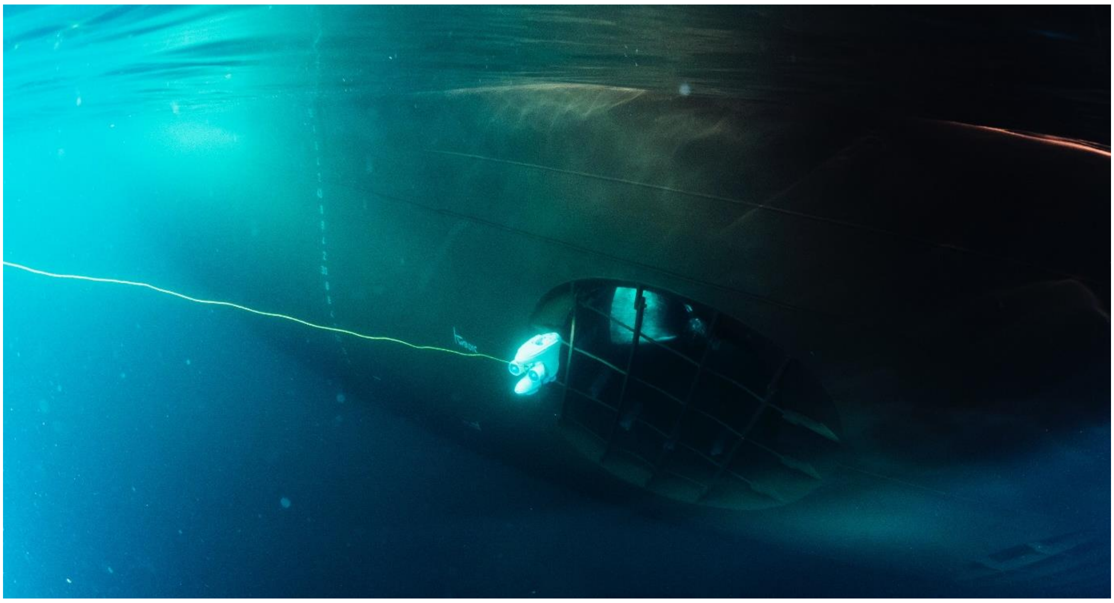

Fig.1: Blueye Pioneer drone during underwater hull inspection

2. Today's solutions for hull and propeller inspections

Hull and propeller can be inspected using various ways:

- Dry Docking
  The traditional and most expensive way of inspecting the underwater structure of a ship is by Dry Docking. New regulations are on the way to allow for lower frequencies of such inspections, as other means have become more available and utilized.

- Use of Divers
  The use of divers is today the most common way to perform underwater inspections of ships. A big advantage with divers is that not only can they perform the inspections; they can also carry out the work that needs to be done. Whether it is propeller cleaning or repairing, inspection of the hull, more advanced inspections with sensors, or the removal of marine growth. Many of the diving companies have stand-by dive teams who are ready to assist the vessels on short notice. The use of divers is expensive, time consuming, and they can be hard to find on short notice in certain areas of the world, resulting in expensive waiting time in port. In some ports, the visibility in the water is so poor that underwater inspections cannot be carried out due to both safety regulations and to the quality of the inspection. Human divers are susceptible to physical exhaustion, oxygen depletion, or other risks associated with extended dives. In confined spaces a diver will have difficulty getting access. The use of divers requires that the ship has to shut down all engines as a safety precaution for manned inspections. Sometimes this takes a lot of much time.

- Use of external ROV companies
  A more sophisticated way to conduct hull inspections under water is to use remotely operated vehicles (ROV). There are numbers of challenges to conducting hull inspections underwater. Underwater inspections may be carried out under conditions of limited or near zero visibility, limiting the range of underwater cameras. Hull shapes can be complex and make orientation and navigation difficult for both divers and underwater vehicles. A ROV often combines the use of underwater cameras and sonar. In this way, vessel inspections can be completed in far less time than possible with divers and with little or no risk. Using external ROV companies are costly, however, and the work has to be planned thoroughly. Tide current makes them in some areas of the world hard to operate.

- Use of mini ROVs
  A mini ROV is like the name says, a small version of the remotely operated vehicle (ROV). The use of mini ROVs offers a safe, efficient, and cost-effective alternative to the use of divers and ROV companies. Most of the existing mini ROVs is powered through the umbilical and require high voltage power supply topside. They typically have their own dedicated screen and controller system, which is developed to fit the purpose. Many of the mini ROVs also offers a wide range of applicable accessories such as sonar, positioning systems or a manipulator arm.

  Using a mini ROV can dramatically shorten inspection time, eliminate the need for vessel downtime, and mitigate nearly all the risks involved with diver deployment. A mini ROV inspection can continue uninterrupted for as long as the operator is willing, and makes it possible to access confined spaces, and prevent potential damages caused by accidental contact with the vessel's hull or propellers. Rather than completely shutting down the engine or taking the vessel out of service, which is a necessary safety precaution for diver inspections, mini ROV inspections usually only require shutting down a single thruster at a time. Through repeated field testing, mini ROV inspections have proven to be equally or even more thorough than diver inspection. However, the cost of the existing mini ROVs in the market is rather high. Of this reason, very few ships are equipped with their own mini ROV. So, ships wanting to use mini ROVs need to acquire external service providers. Some of the existing mini ROVs are also quite difficult to operate and requires extensive training.

3. Blueye Pioneer underwater drone

The Blueye Pioneer underwater drone has been developed by the Trondheim-based company Blueye Robotics, which has sprung out from the Norwegian University of Science and Technology’s centre for autonomous marine operations and systems (NTNU AMOS). Highly acclaimed ocean robotics experts with life-long experience with the harsh Norwegian offshore conditions are behind the core technology. The Blueye Pioneer is designed to satisfy industrial performance and reliability demands for underwater operations, and with a user-friendliness you normally would associate with consumer technology product:

- Easy to operate and can be handled by the crew on board
  Usually intensive training is required before one can operate ROVs or mini ROVs efficiently. After more than 50 demonstrations of our Blueye Pioneer prototype to a wide range of different professional customers, we have experienced that the first-time users are ready to conduct proper underwater inspections after less than 20 minutes’ practice. The main reason for this is the unique hull design of the Blueye Pioneer which is very different from all existing mini ROV and other underwater drones. The way the Blueye Pioneer is designed makes it very stable underwater, which in turn enhances manoeuvrability. The stability also gives stable video footage. Hence, it is possible for the crew on board to conduct proper hull and propeller inspection whenever and wherever they want it.

- Hull inspections can be conducted more regularly and on locations with better water conditions
  The quality of underwater hull and propeller inspections is highly dependent on the visibility in the water. If a vessel is equipped with a Blueye Pioneer underwater drone, the crew can conduct underwater hull and propeller inspections in clear waters. In many occasions, the visibility in the water in ports are rather poor, but while at anchor out at sea, the visibility in the water may be much better. Having the possibility to conduct your own underwater hull and propeller inspections while anchoring, can increase your vessel performance by getting the full picture of the hull and propeller conditions whenever you want.

- The Blueye Pioneer can handle relatively strong current
  In many Ports, there are tide current and rivers which makes underwater hull and propeller inspections difficult to carry out with ROV´s and the use of human divers. The Blueye Pioneer is powered by the battery inside the underwater drone which allows for having a thin low-drag tether. The combination of a powerful small self-stabilized underwater drone and thin tether, makes it possible to manoeuvre the drone even in in conditions with current.

- Portable and suitable for handling
  The weight of the Blueye Pioneer is less than 10 kg and is easy to carry. The underwater drone can be operated by a single person, which safes both time and money for the ship operator. You deploy the Blueye Pioneer directly into the water pulling it out with the tether which can stand more than 100 kg. This way you can easily deploy it from any location on the vessel or from shore. A practical tip is to deploy it as close to the place you want to inspect to safe both time and efforts with the tether management.

- Low maintenance cost
  The Blueye Pioneer is designed for optimal performance and easy operation. After use, you need only to rinse it in fresh water, charge the batteries, and it is ready for the next dive. In case you need to do several within a short time span or longer surveys, the battery inside the Blueye Pioneer can be easily replaced. If anything brakes, the Blueye Pioneer is designed in a way that makes it possible to carry out easy repair by your own. For example, you can easily replace the tether and thrusters by just undoing a few screws. If you brake the controller or the dedicated screen, you may buy these in any electronics store at a fairly low cost.

- Confidence in result of inspection made by yourself
  A wise man once said: do not expect – inspect! Conducting your own hull and propeller underwater inspection whenever and wherever you want it provides you, the one responsible for the technical condition, with the full picture of your assets below the water.

- The Blueye Pioneer is affordable and has a very high return of investment.
  The total cost of the Blueye Pioneer is 6000 USD ex shipping and tax. This equals less than 2 days of work with a dive team. Included in the package is:
  - Blueye Pioneer underwater drone
  - WiFi Surface Unit (WSU)
  - 75m cable (upgradeable for deeper or farther dives)
  - Wireless controller
  - Battery charger
  - Blueye MovieMask
  - Blueye App for iOS and Android, through which all drone and WSU software is updated as software development progresses with more features and refinements.

Fig.2: The Blueye Pioneer is easy to carry and to handle (Weight 8.5 kg). The operation can be carried out by 1 person.

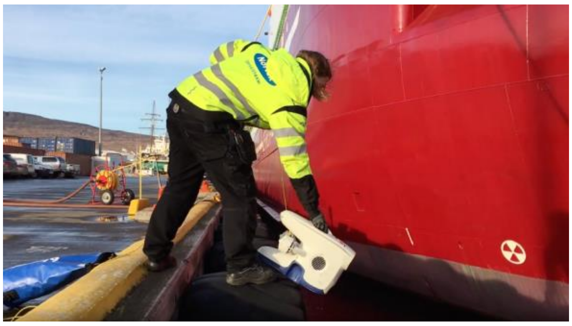

Fig.3: Quick and easy deployment. The underwater drone can be lowered into the water by the tether. Brake strength of tether is more than 100 kg.

Fig.4: The most efficient and safe way is to drive the drone on the surface until target object is reached and then dive down. The auto depth function is of good use!

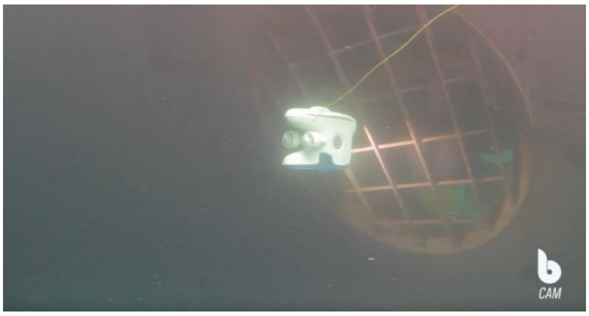

Fig.5: The Blueye Pioneer is very stable positioned in the water. Note that the tether is slightly positively buoyant in the water!

Fig.6: The drone camera provides full HD live video recording and is optimized for the underwater light and color conditions.

Fig.7: The controller is an ordinary game controller, with standard gaming configuration.

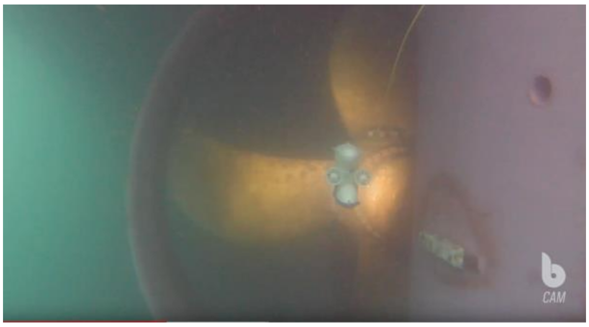

Fig.8: The onboard light (3000 lumen) is highly useful to inspect shaded areas.

Fig.9: The drone is easy to operate. There is no risk of breaking the drone on collision with propeller or hull.

Fig.10: Picture of zinc anode - The lateral thruster is highly useful for inspections alongside objects.

4. Blueye Pioneer Technical update - from prototype to serial production

During 2017 we made six major mechanical prototype iterations in addition to smaller changes in between. We have had two focus areas: Internals (sealed structures) and exteriors. The internals were optimized for structural strength (for depth rating), robustness and ease of production. To ensure that the drone can handle many dives in years to come, we have successfully conducted rapid age testing with high load factors. One of the greater achievements has been the development of the replaceable battery pack, enabling the users to replace batteries in the field in a fast, safe and easy way. We have also developed an in-field solution for changing thrusters and tether in the case of a thruster suffering under harsh conditions or the tether gets damaged somehow.

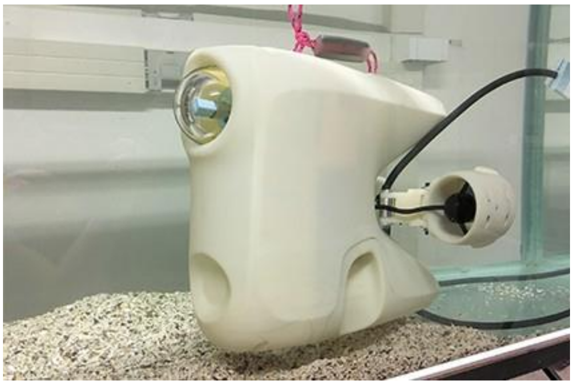

Fig.11: Prototype A - first with slim line design. Flexible prototype for testing a wide range of parameters.

Fig.12: Prototype B - with stabilizing fins and first complete internal assembly

Fig.13: Prototype B2 - refined thruster nozzles, new mounts for add-on equipment. Internal improvements.

Fig.14: Protoype B4 - added lateral thruster, easy accessible charging and rubber protection. Represents the final design.

On the external parts, the focus has been to create an agile, fast and stable drone. We have performed multiple hydrodynamic tests and design changes to optimize the performance in various conditions. One example of this is the thruster nozzles; we increased the pull force by 40% from the earlier prototypes to the current design by doing the testing and design right! On top of this we decided to add the lateral thruster (sideways motion) for maximum controllability and maneuverability. The rubberized bottom and the impact resistant hull makes the Blueye Pioneer a robust and elegant wrapping for the high-tech internals!

The Blueye Pioneer underwater drone is equipped with a built-in full HD 1080p camera, Fig.15. The ultimate underwater experience requires the ultimate visual image. The camera provides the full HD videostream to the user in the Blueye App on your phone, tablet or other chosen device, and is basically your eyes below the surface.

Fig.15: Camera of Blueye Pioneer

The main focus areas during the camera development has been white balance, light sensitivity and low latency streaming. Even though there exist a lot of cameras out there, very few tend to work well for underwater conditions. It is especially the automatic white balance function that typically performs poorly in most cameras. Fig.16 shows a screenshot from a video test we performed last July, where we compared the GoPro Session 5 and the built-in camera of the drone. Low latency is crucial for precise control of the drone. Our camera stream has approximately 150 ms latency, which gives the user a very responsive feel. The video stream is based on standard streaming protocols making it easy for 3rd party media players to playback the videostream as well. One of the advantages of having a full HD sensor is that it increases the pixel size which makes the camera more light sensitive than higher definition cameras.

Fig.16: Images from GoPro Session 5 (left) and Blueye Pioneer built-in camera (right)

In addition, we are working on manual camera controls as well as functions for live streaming to social media and third parties.

Fig.17: High-resolution images can be streamed live

Software is what breathes life into a hardware product. You would be surprised how many software components go into making a product like the Blueye Pioneer. On the drone, we run a customized version of Embedded Linux, hosting the video streaming server, the control system, and additional support systems for downloading files form the drone. In addition, low-level firmware on micro controllers read sensors and control power, lights and motors. The drone itself is controlled from a mobile application on your Android or iOS device, connected to a Wireless Surface Unit acting as the link between your device and the drone. These components require customized software to function in an optimal way.

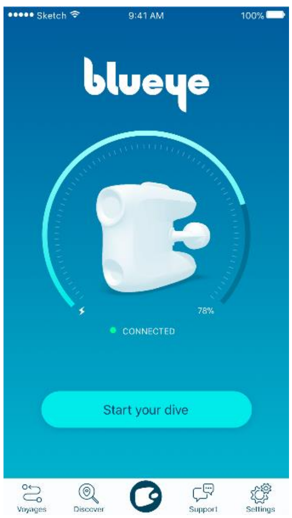

Fig.18: Blueye App

One of the main focuses of 2017 has been to establish a robust yet flexible core platform for the operating system running on the drone. A key feature for any modern hardware product is user upgradable firmware. This will enable us to release software upgrades adding new features and improvements to our customers after the drone has left the factory line. Allot of effort has been made to ensure we have a robust system for flashing the drones with new software. On the app side, we use the Xamarin framework to make native apps for iOS and Android, but at the same time enable a large degree of code reuse across each platform. This will enable us to release fully functioning Android and iOS apps for both tablets and phones when the drones ship, unlike some other products where one mobile platform is prioritized over the other.

The key features for a good control system are that it should be responsive, reliable and robust against external disturbances. The system must also behave like the user expects at all times. One of the biggest challenges this year, has been how to fulfil these requirements in very different environments. When the drone is diving in a shallow pool with still water, the motions are very different from diving in the river with lots of current, or at 150 m depth in the fjord. This made it difficult to find a good sensitivity setting for the joysticks that would work well in all conditions. Our solution was to implement the step less throttle buttons on the back side of the gamepad controller to boost (right trigger) or slow down (left trigger) the joystick inputs. After hours of testing we have found good parameters lets the user continuously regulate the sensitivity of the joysticks. The slow down feature has been great during inspections, because you typically want very small adjustments to get the video framing just right. Boost mode is also important in the surface if there are waves or strong currents you want to overcome. And off course, the boost button is extremely fun to play with in the surface, doing acrobatics and racing.

Designing a good control system always begins with designing a good hardware. The more stable the vehicle is in itself, the easier it will be to control with automatic functions. The main principle of our drone design is to make the drone as stable as possible in the water. The standing configuration gives us great righting stability, and the rudder shape of the entire body gives good forward speed stability. Even fins have been added to reduce roll motions of the drone when going up or down. With good hydrodynamics in place it was easier to design a stable control system for the auto-depth and auto-heading modes.

We have developed a custom fit battery package optimized for a combination of form factor for perfect mechanical fit, high discharge required to power the four 350W thrusters, and flight approved capacity of 99Wh, Fig.19.

Fig.19: Battery package for Blueye Pioneer

Annex 1 - Blueye Pioneer technical specifications

TECHNICAL SPECIFICATIONS

DRONE

Hull design	Hydrodynamic and hydrobalanced hull for stability and performance in ocean conditions. Engineering plastic and rubber protections that withstand impact.
Pressure rating	150 m.
Weight	Less than 8 kg.
Speed	At least 2 m/s (4 knop).
Run-time	2 hrs normal operation.
Thrusters	4 powerful thrusters, 4 x 350 W. 2 rear, 1 vertical center, 1 latheral.
Automation	Auto heading. Auto depth.
Camera	Full HD 1080p/30fps, wide angle lens.
Search light	Powerful LED below camera. Fittings for extra lights as payload.
Sensor	Inertial Measurement Unit (IMU) with 3-axis gyro and 3-axis accelerometer. Depth sensor. Magnetometer (compass). Temperature (inside and outside).
Payload	Standard fittings for payload on both top and bottom side of drone.
Software	Remote update of drone software.

DRONE CONTROLLER

Controller	Wireless drone controller for iOS and Android smartphones and tablets.

WIRELESS SURFACE UNIT (WSU)

Wireless transmitter	Wifi router for wireless connection to smartphones or tablets. Multiple smartphones may connect for a shared live experience.
Wireless rage	At least 30 m.
Cable	Thin and strong cable optimized for use with ocean drones. Cable is replaceable for easy handling and upgrade.
Cable length	75 m. Possible to upgrade to longer cable.

BLUEYE APP

App	App for android/iOS smartphone/tablet. Setup & control drone, manage and share dive data and recordings.

OTHER

Charger	Quick charger for charging drone, WSU and drone controller.

Blueye, Transittgata 10, Trondheim, 7042, Norway +47 40 00 46 43 contact@blueye.no www.blueye.no

Performance Measurements on Propeller and Hull Coatings

Job Klijnstra, Mark Bakker, Endures BV, Den Helder/The Netherlands, Job.Klijnstra@Endures.nl
Adrien Greff, Naval Group, Bougenais/France
Frans Kremer, Marin, Wageningen/The Netherlands

Abstract

Marine fouling on ship propellers can significantly contribute to increased roughness of propeller blades and thereby result in reduced propeller efficiency and ship performance. Providing a propeller with a suitable antifouling coating can help avoid propeller fouling. For navy ships a far more important driver for using propeller coatings is the potential to reduce the electric signature of the vessel. Past practical experience has shown that propeller coatings often get damaged during usage, especially on areas on or near the blade leading edge. To get more insight in the causative factor for this coating damage dedicated tests were carried out at the LEGI laboratory in Grenoble to investigate the vulnerability of propeller coatings to friction and cavitation erosion. The test protocol used and preliminary results of tests with commercially available coating systems are presented.

1. Introduction

To safe fuel ships are provided with hull coatings that control attachment and growth of marine fouling on a ship hull. This way increase in hull roughness can be diminished and lower hull roughness immediately results in lower fuel consumption and cost savings. Purpose of using a coating on a commercial ship propeller is protection against corrosion and prevention of marine fouling. These processes as well as cavitation erosion cause surface deterioration of propeller blades and as such result in increased roughness of the propeller surface. This on its turn has a negative influence on propeller efficiency and performance.

For navy ships the most important driver to make use of propeller coatings is signature reduction, especially electric signature, by decreasing the area of blank metal surface exposed to seawater, *Hubert and Wang (2012)*. So from navy perspective there is increasing attention for exploring pros and cons of propeller coatings. In the past, several attempts have been made to develop specific protective coatings for rudders and propellers that can resist the extreme hydrodynamic conditions these parts are exposed to. From mechanical point of view some coating types (such as epoxy or glass fiber reinforced vinyl-ester resins) may indeed resist such conditions quite well. Major disadvantage of these coatings is their poor resistance to marine fouling.

At this moment, the main focus for propeller coatings is on so-called fouling release coatings (FRCs) based on silicone binders. This type of coating is non-toxic and due to the low surface energy of the topcoat, fouling organisms have difficulty to adhere and settle on the surface. And in case organisms do settle, they are easily removed from the surface by water flow at a certain speed. FRCs do not erode or polish; if not damaged they have a long lifetime up to 10 years or longer.

FRCs for propeller application were first investigated by *Matsushita and Ogawa (1993)* who tested an FRC system on the propeller of a training vessel. Their experiments showed that such coating can protect the propeller against marine fouling for at least one year and what they also observed was a reduction in fuel consumption of about 6% when sailing with a coated propeller in comparison to a non-coated and fouled propeller. *Atlar et al.* (2002) and *Anderson et al.* (2003) reported a similar gain in efficiency of a coated propeller in comparison to the same propeller uncoated.

Korkut and Atlar (2009) carried out model tests with a coated propeller to investigate propeller efficiency, noise generation and cavitation aspects and found that coating the blades did not change cavitation inception characteristics of the model propeller. As the propeller loading increased, the uncoated blades displayed slightly more cavitation extent than the coated blades, so the coating might reduce cavitation development. Regarding noise aspects, their model study revealed that the coating reduced noise under non-cavitating conditions but slightly increased noise in developed cavitation condition. It is noted that these results should be taken with care, the coating was applied on the model propeller without scaling its thickness.

Coating damage is regarded a critical issue when talking to ship operators and ship builders on their willingness to explore or investigate the use of propeller coatings. Anecdotic stories go around that damage of the coating on a propeller would give rise to much more rapid and severe cavitation erosion of the propeller on the damaged spot but so far this has never been reported in literature. At the moment, it is unclear how coatings affect the cavitation behaviour, either in freshly painted or damaged condition.

To get more insight how propeller coatings may get damaged in practice the Royal Netherlands Navy, in collaboration with DRDC in Canada, has set up a research program in which field data from full scale ship tests will be collected and in parallel to this, laboratory tests are carried out for investigation of the vulnerability of propeller coatings to possible cavitation erosion damage. Main purpose of these laboratory tests is to compare different commercially available products and results of these tests can be the basis for selection of most suitable products for application on navy ships. This paper describes the results of preliminary cavitation erosion tests.

2. Methodology

2.1. Test samples for cavitation erosion tests

Test samples were made of bronze propeller material and machined to a diameter of 10 cm to fit in the test section of the PREVERO test set up, Fig.2. The top side of the disk was provided with a full coating system of a commercially available product suitable for propeller application. In total five coating products from five different suppliers were involved in the test: four products were silicone based fouling release coatings (samples C1, C4, C7 and M2; each system consisting of 3 layers: primer, tiecoat and topcoat) and one product was a hard coating with glass flakes (sample M5; consisting of 2 layers: primer and topcoat). This paper will show pictures of three coating products; in the presentation results of all coating systems will be shown.

Coatings were applied by the coating manufacturers according to the requirements in the technical data sheets. Layer thickness on each disk was determined using a Fischer SMP100 device with eddy current probe, specifically for soft coatings. After coating application, the thicknesses of the coated disks had to be fine machined to a size of 19.5 mm to compensate for the layer thickness and make it fit precisely in the test section of the set up. Figure 1 shows a picture of 3 coating systems applied onto 3 replicate disks.

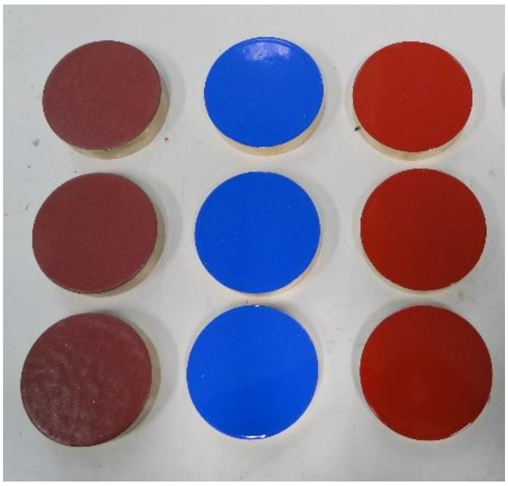

Fig.1: Three different propeller coatings applied onto 3 replicate bronze disks

2.2. Test set up and test protocol

The cavitation erosion tests were carried out in the PREVERO test setup at Laboratoire des Ecoulements Géophysiques et Industriels (LEGI) in Grenoble, *Chahine et al. (2014)*. The PREVERO test loop is designed for a maximum operating pressure of 40 bar. This high pressure provides high velocities and consequently, high erosive potential for cavitating flow. The liquid in the test loop is tap water, during operation the temperature is kept constant by means of a heat exchanger and the loop is equipped with transducers such as a flow meter, pressure transducer and temperature probe. Fig.2 shows the components of the PREVERO test setup.

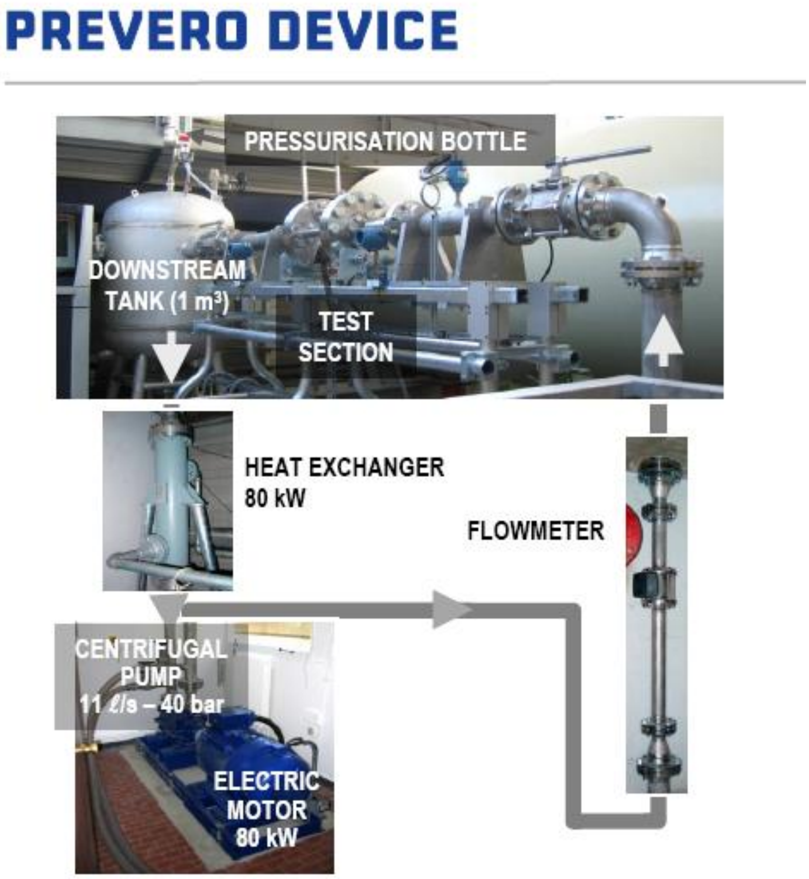

Fig.2: Overview of the PREVERO test setup at LEGI, Grenoble

The test section in this setup is axisymmetric and made of a nozzle of 16 mm diameter followed by a radial divergent of 2.5 mm thick. Under cavitating conditions a cavity is attached to the nozzle exit; the length of this cavity is depending on the cavitation number which in practice is obtained by changing the downstream pressure. The disk sample that is investigated is facing the nozzle exit at a distance of 2.5 mm of the nozzle exit, Fig.3. Due to the axial symmetry in the test section erosion of sample material appears in the form of a ring centred on cavity closure where erosive potential is maximum. At the pressure of 40 bar and a flow rate of 89.4 m/s the cavitation number was 0.9 and this results in an erosion ring with average diameter of ~45 mm.

One disk of each coating system was tested under the cavitation conditions as specified above. Procedure for testing basically consisted of a series of 10 minutes exposure phases to cavitation conditions. After each phase the coating surface was visually inspected and profile measurements were done at 4 pre-determined radial lines, Fig.4.

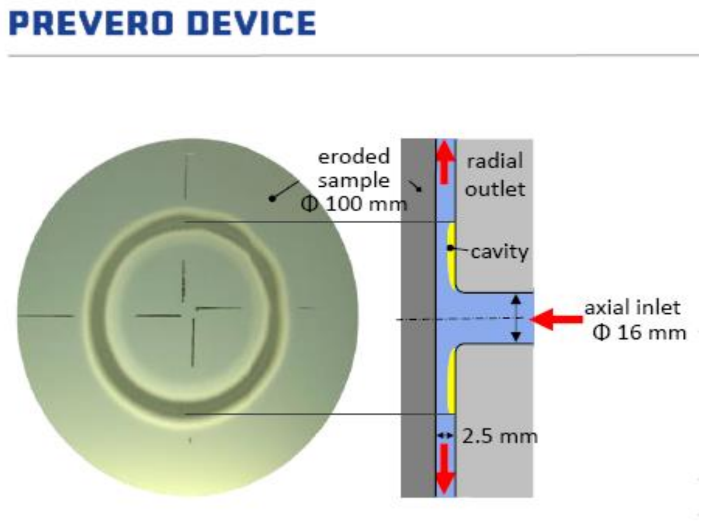

Fig.3: Left: expanded side view of test section in PREVERO test setup with position of coated disk.

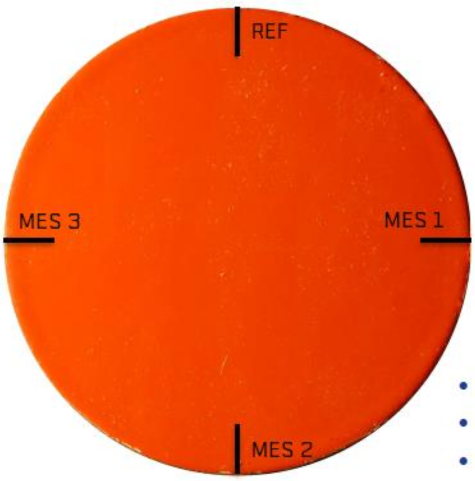

Fig.4: Coated disk with four measurement lines for profilometry

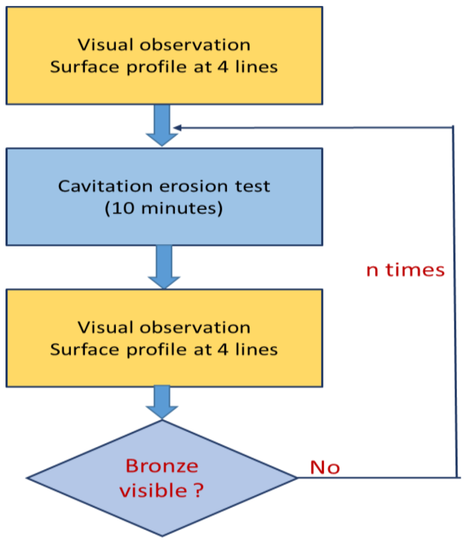

Fig.5: Schematic overview of test protocol

This was repeated [n] times until the bronze substrate underneath the coating became clearly visible and significant erosion of the entire coating system had taken place. Fig.5 gives a schematic overview of the test protocol.

The number of exposure phases and thus the total exposure time differed between the coatings: samples M5 (hard coating) and C1 (FRC) have been exposed for 260 minutes whereas for the fouling release coatings C7 and M2 the maximum exposure time was only 40 and 50 minutes, respectively. Sample C4, also an FRC, was tested for 180 minutes in total. Beyond phase 12 (so after 2 hrs cumulated exposure) successive exposure steps lasted longer than 10 minutes. After each exposure phase data on damage patterns and surface profiles were collected but in this paper only pictures of 3 coatings systems after phase 1 (10 minutes), phase 2 (20 minutes) and the final phase are shown.

After the final exposure phase, all samples were investigated under a 3D-microscope in order to obtain more detailed pictures of the damage pattern of the coatings. Some representative pictures of these damage patterns are shown.

3. Results

3.1. Phase 1

Already after the first 10 minutes of exposure the three coating systems illustrated here showed different responses. Fig.6 shows the three coating samples after the first phase. The hard coating, sample M5, shows superficial erosion starting at 10 mm from the centre and maximum depth at the expected location for cavitation erosion, 22 mm from the centre of the nozzle exit. The profilometry measurements suggest a slight indentation on all four measurement points but considering the large layer thickness of the entire coating system, the depth of the eroded layer may measure around 100 µm.

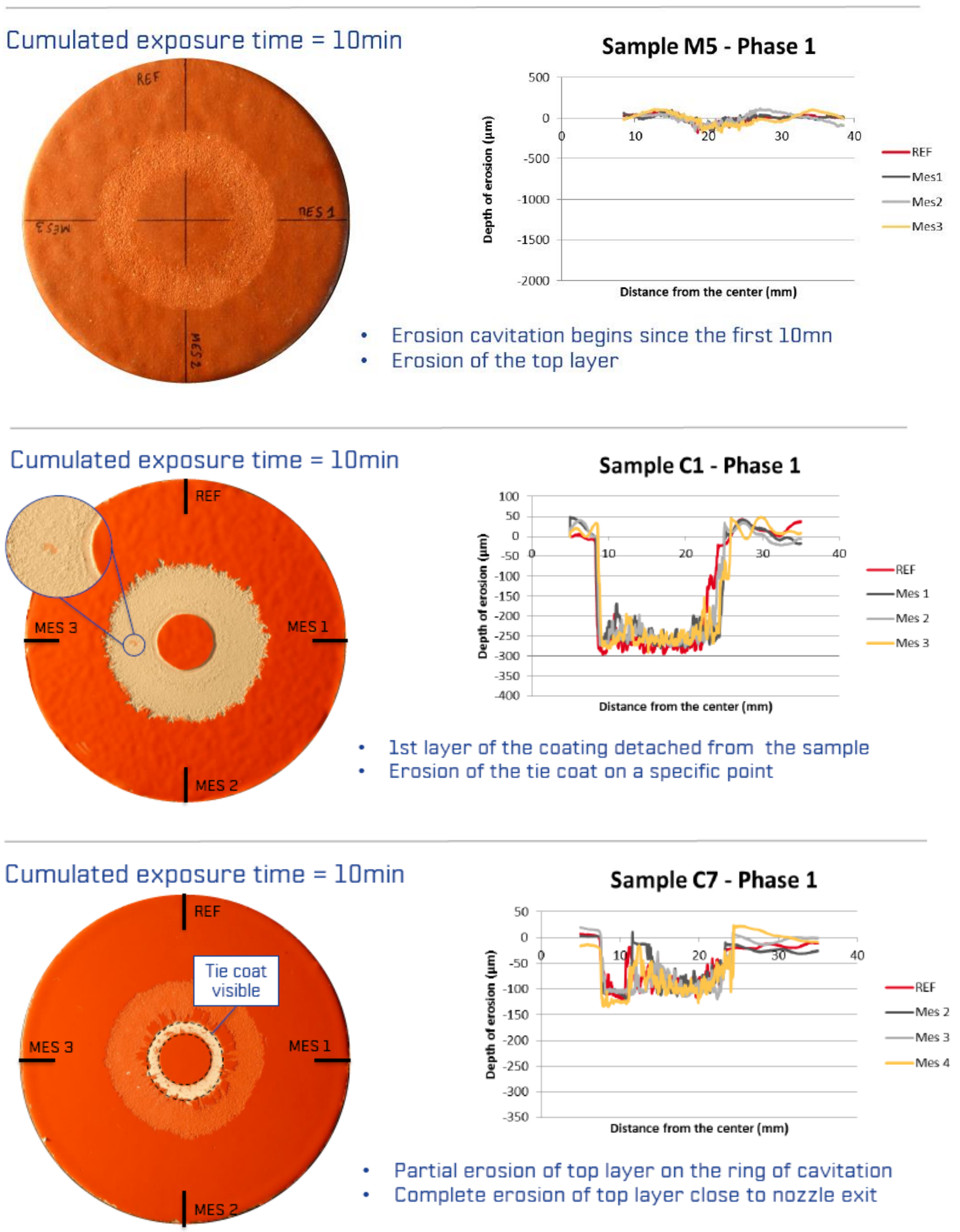

Fig.6: Damage pattern on surface of coating systems after first 10 min. exposure to cavitation conditions. Graph on the right gives profilometry measurements on the four spots indicated.

The silicone based fouling release coatings (samples C1 and C7) show very different behaviour. Both coatings remain intact on a central area of 16 mm diameter (exactly the size of the nozzle exit), so erosion of the topcoat starts already at 8 mm from the centre. Sample C1 shows erosion of the topcoat to a depth of ~250 µm over a wide area between 8 and 24 mm from the centre. On one specific small spot, Fig.6, the tiecoat was eroded as well. On sample C7 most erosion was found in a small ring between 8 and 10 mm from the centre. In this ring the tiecoat was clearly visible. At a distance of 10 to 13 mm from the centre the topcoat of this system was still present. In a wider area around this (between 13 and 22 mm) erosion of the topcoat until a depth of ~100 µm was found. The other two FRCs (samples C4 and M2) are not shown in this paper but they gave similar response as coating C7. The damage observed at this ring between 8 and 10 mm is not caused by cavitation but is due to shear stress. Compared to coating C7, the product C1 gives much deeper erosion at a wider area.

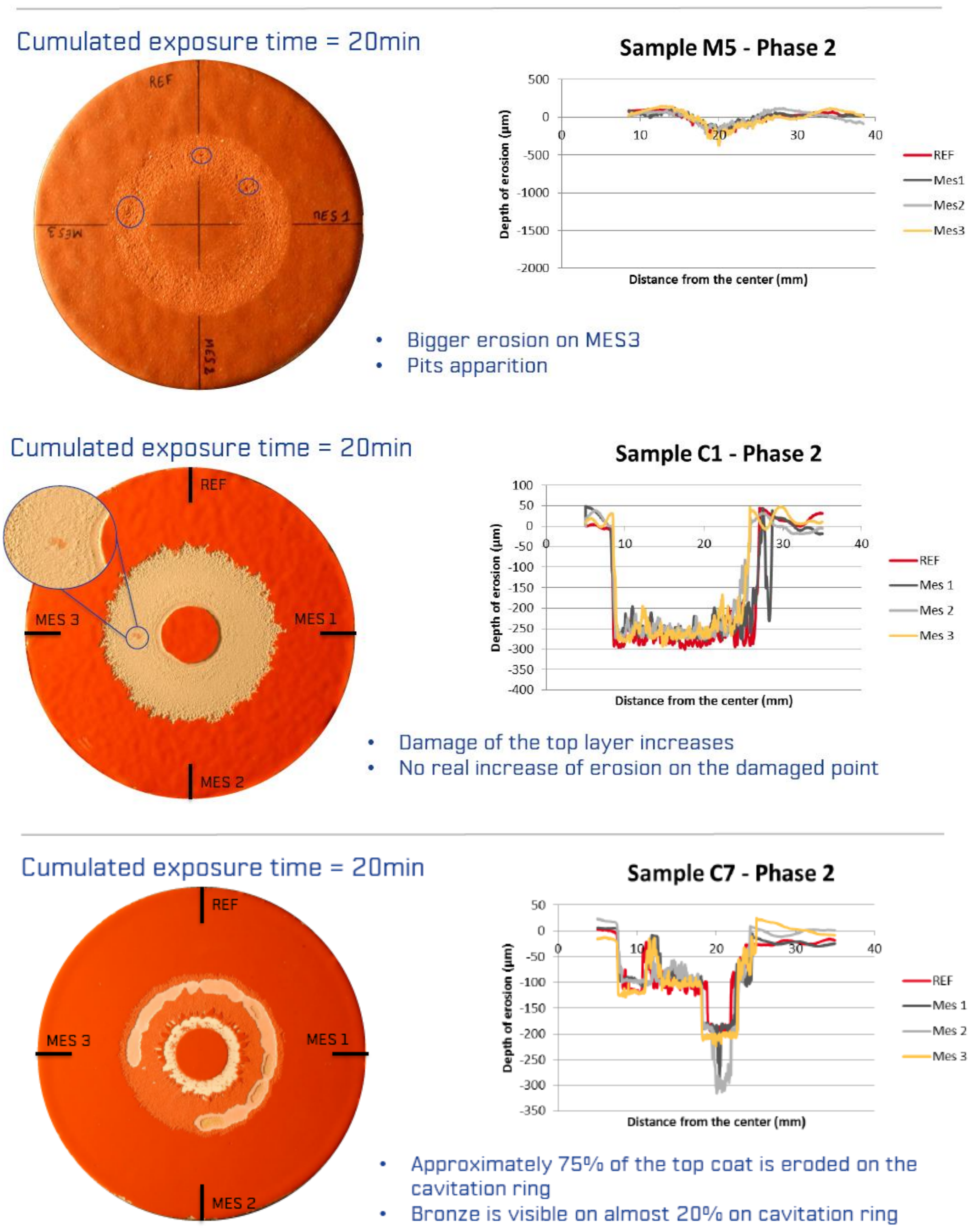

Fig.7: Damage pattern on surface of coating systems after second 10 min. of exposure to cavitation conditions. Graph on the right gives profilometry measurements on the four spots indicated.

3.2. Phase 2

Results obtained after another 10 minutes exposure period are shown in Fig.7. On sample M5 erosion is progressing mainly at the ring located at 22 mm from the centre that has deepened to ~250 µm. Next to this a few pits are found in which erosion has gone faster. On sample C1 not so much has changed: erosion of the topcoat over a wide area between 8 and 25 mm from the centre and on one location even up to around 28 mm. The tiecoat is still intact except for one tiny spot at the radial measurement line 3, Fig.7. Similar phenomenon was found on sample C4.

On sample C7 the surface looks quite different after phase 2. Here two rings of eroded material are found: of course, the first one at 8 mm distance that was already there after phase 1, and a second one at 22 mm distance from the centre. These two erosion rings are separated by a ring of topcoat that remained. In the cavitation ring the topcoat had eroded completely at 75% of the surface and on almost 20% bronze material was visible which means that here also the tiecoat and primer layer were worn off. On sample M2 (not shown in this paper) a similar phenomenon was found.

3.3. Final phase

As described above the final exposure phase and thus the total cumulated exposure time, differed between the various coatings. Samples M5 and C1 have been investigated up to a cumulated exposure time of 260 minutes (phase 15) whereas sample C7 could only be tested up to 40 minutes (phase 4) in total. Pictures of damage patterns of the three coating samples are shown in Fig.8.

With increasing exposure time the hard coating M5 showed more and more erosion especially at the cavitation ring around 20 mm. After phase 5 (50 minutes) the primer layer became visible on some spots and after phase 11 (110 minutes) the topcoat (~800 µm thick) had disappeared completely. After 260 minutes the bronze substrate was visible on one spot, Fig.8, so there the entire coating system (average layer thickness 1660 µm) had gone.

On coating C1 erosion of the topcoat is slowly progressing between phase 2 and phase 8 (80 minutes) but erosion does not go deeper than 275 µm and (part of) the tiecoat is still present on almost the entire eroded area. Only after 180 minutes (phase 14) the tiecoat seems to wear off deeper and wider. After another 80 minutes (phase 15) bronze material becomes visible at multiple spots, Fig.8.

For coating C7 the entire test lasted only 40 minutes. The erosion pattern as observed after phase 2 developed further with bronze being visible in the cavitation ring now on almost 70%. The profilometry measurements in Fig.8 clearly show the increased erosion as well. In the inner ring of erosion (at 8-10 mm) material wear off did not go deeper than ~100 µm. In between the two erosion rings part of the topcoat is still present. Another thing that can be observed on sample C7 is that erosion of the coating does not go wider than 25 mm from the centre, this is different from sample C1.

With a Keyence VHX5000 3D-microscope detailed pictures were made of the profiles of damage patterns observed on the coated disks. Representative pictures of the three samples discussed here are shown in Fig.9. The erosion pattern of sample M5 is clearly restricted to the so-called cavitation ring at ~22 mm from the centre of the disk. Erosion goes very deep, the decrease in layer thickness measured at this spot is around 1850 µm. Outside the cavitation ring with a width of ~ 9.5 mm, the coating surface is largely intact.

The two silicone coatings show quite another picture here. On sample C1 erosion of the coating took place over a wide area of ~23 mm. Until the first 7 mm from the centre the topcoat remained intact. Then on an area between 7 and 16 mm from the centre the entire topcoat was worn off but the tiecoat remained (partly) present. Adjacent to this in a ring of 6 mm wide, the entire coating system had gone and blank bronze material was visible. Beyond the distance of 23 mm from the centre of the disk, part of the tiecoat was still present and at larger distance also the topcoat remained intact.

The damage pattern of sample C7 in Fig.9 clearly shows the two erosion rings separated by an area of ~7 mm wide where the topcoat was fully or partly intact. At a distance of 16.2 mm from the centre an area began where the tiecoat was still visible whereas at a distance of 18.3 mm from the centre of the disk the damage due to cavitation erosion began. Here erosion went down onto the bronze substrate. At larger distance, starting from ~24 mm, the topcoat was largely or fully intact.

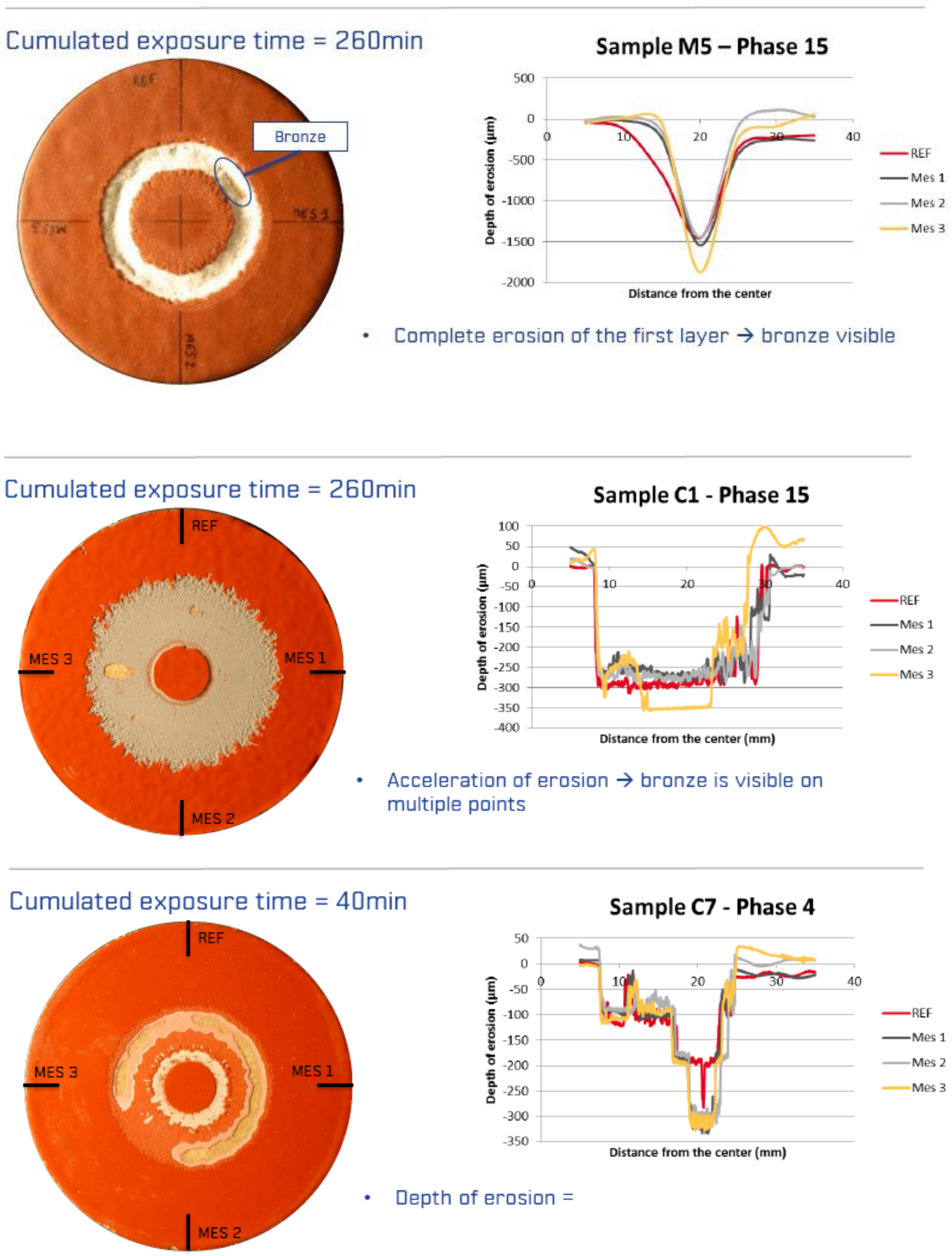

Fig.8: Damage pattern on surface of coating systems after final exposure phase to cavitation conditions. Graph on the right side gives profilometry measurements on the four spots indicated.

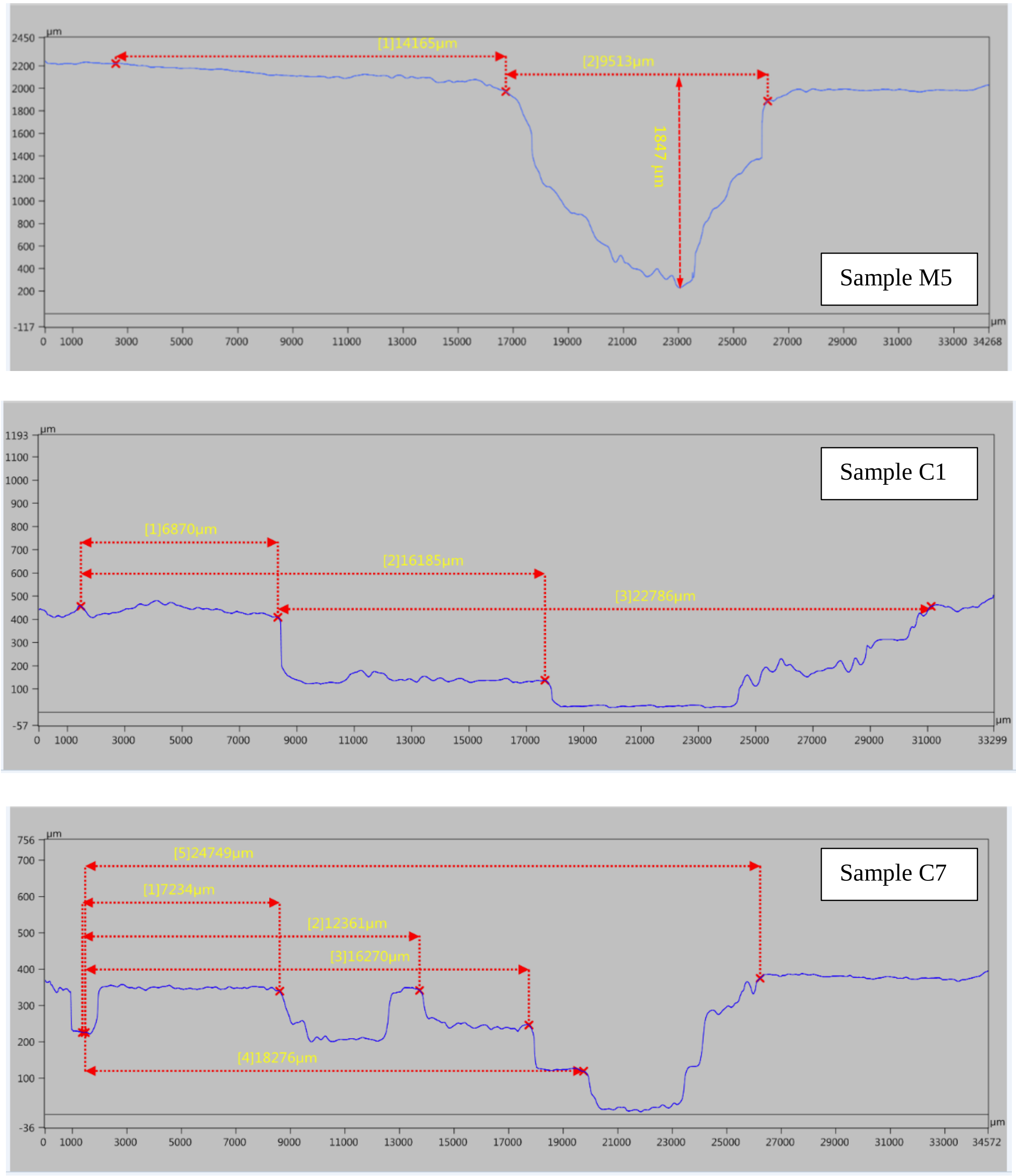

Fig.9: Profiles of damage patterns of coating surfaces after final exposure phase to cavitation conditions

3.4. Summary of results

The detailed damage patterns shown in Fig.9 clearly indicate differential response to cavitation conditions between the three coating systems. An overview of damage characteristics on all five products tested is given in Table I. The numbers shown here are average and standard deviation of the four measurement lines on each disk.

The silicone based fouling release coatings generally show more widespread erosion whereas the hard coating erodes only at the expected cavitation ring. At the first four coatings (all FRCs) in Table I erosion damage starts at a distance around 8 mm from the centre whereas at sample M5 (the hard coating) the erosion damage starts at around 14 mm. The width of the area with erosion damage is smallest on the hard coating and substantially larger on the fouling release coatings. Along the 4 measurement lines for profilometry the largest pit depths were determined. These numbers have limited value because the protocol of the erosion tests was such that we continued until the bronze substrate became clearly visible. Moreover, erosion pits that occurred on other locations and could be deeper, are not taken into account in Table I.

The time until the bronze substrate appeared is given in the far right column of Table I. Within the group of FRC's samples C7 and M2 were most susceptible to the exposure conditions, both coatings failed in 20 minutes. Samples C1 and C4 were more resistant because here bronze was first visible after 90 minutes cumulated exposure, for both products along 2 out of the 4 measurement lines. For coating C1 failure to bronze at the other 2 measurement locations even happened only after 260 minutes exposure. Especially for coating C1 it seems to be that the tiecoat is quite well resistant to cavitation erosion. For the hard coating it also took at least 260 minutes to be worn off until the bronze substrate. But it should be noted that this coating, with its average layer thickness of 1660 µm, is at least 4 times thicker than the silicone coatings.

Table I: Overview of damage characteristics after the final phase of cavitation erosion testing

Sample	Damage distance from centre (mm)	Damage width (mm)	Largest pit depth (µm)	Time to Bronze (min)
C1				
381 ± 12 µm	**8,1 ± 0,8**	**21,6 ± 0,9**	**366 ± 45,5**	90 (260)
C4				
365 ± 19 µm	**7,7 ± 0,5**	**17,7 ± 0,6**	**415 ± 51,5**	90
C7				
316 ± 21 µm	**7,9 ± 0,6**	**17,6 ± 0,3**	**322 ± 59**	20
M2				
379 ± 15 µm	**8,3 ± 0,3**	**16,6 ± 0,5**	**433 ± 30,5**	20
M5				
1660 ± 152 µm	**13,7 ± 1,1**	**10,6 ± 0,3**	**1851 ± 134**	260

4. Preliminary conclusions

Results reported here are based on only one sample per coating system, so firm conclusions cannot be drawn yet. Nevertheless, the hard coating showed damage only at the expected location for cavitation erosion and the silicone based fouling release coatings showed not just cavitation damage at the ring located at 22 mm but next to this significant erosion was found on other spots on the coating surface where friction is causing the damage. So on these locations a different damage mechanism played a role. To further investigate this mechanism, erosion tests under different speed conditions can be done.

An important aspect that should be mentioned here is that the cavitation conditions to which the coatings were exposed, are the most severe that could be created in this test setup. How relevant these test conditions are in relation to what may happen in practice on a ship propeller, is yet to be determined. We have used it as a worst-case scenario for a comparative test. If conditions in practice are less severe, tests can be repeated at lower pressure and/or flow and reveal best performing products under more realistic flow conditions. This applies to both the friction and cavitation damage mechanism.

Final conclusion from these preliminary experiments is that (some of) the soft silicone based coatings have quite well resistance to extreme cavitation conditions. Besides other laboratory investigations this particular test is seen as milestone to characterise propeller coatings in an early stage at low cost.

Acknowledgements

This work was done in close collaboration with Dr. Jean-Pierre Franc from LEGI, Grenoble, Dr. Layton Gilroy from Defense Research and Development Canada (DRDC) and Ir. Piet van der Gaag from the Defense Materiel Organisation of the Ministry of Defense in The Netherlands. The coating manufacturers are acknowledged for their willingness to supply the coated samples for the tests.

References

ATLAR, M.; GLOVER, E.J.; CANDRIES, M.; MUTTON, R.J.; ANDERSON, C. (2002), *The effect of a foul release coating on propeller performance,* ENSUS 2002, Newcastle

ANDERSON, C.; ATLAR, M.: CALLOW, M.; CANDRIES, M.; MILNE, A; TOWNSIN, R.L. (2003), *The development of foul-release coatings for seagoing vessels,* J. Marine Design & Operations No. B4, pp.11-23

CHAHINE, G.L.; FRANC J-P.; KARIMI, A. (2014), *Laboratory testing methods of cavitation erosion,* in "Advanced experimental and Numerical Techniques for Cavitation Erosion Prediction", Springer S+B Media

HUBER, T.; WANG, Y. (2012), *Effect of propeller coating on cathodic protection current demand: sea trial and modeling studies,* Corrosion 68 (5), pp.441-448

KORKUT, E; ATLAR, M. (2009), *An experimental study into the effect of foul release coating on the efficiency, noise and cavitation characteristics of a propeller*, 1st Int. Symp. Marine Propulsors, Trondheim

MATSUSHITA, K.; OGAWA, K. (1993), *Ship hull and propeller coatings using non-polluting and antifouling paint,* ICMES 93 - Marine system design and operation, Paper 24

An Ensemble Prediction of Added Wave Resistance to Identify the Effect of Spread of Wave Conditions on Ship Performance

Mark Bos, BMT, Marknesse/The Netherlands, mark.bos@bmtsmart.com

Abstract

The wind and wave conditions in which a ship is operating have a significant effect on the performance of the vessel. These conditions are difficult to estimate on-board ships, either by the crew or instrumentation, for this reason it has become more common to use the outputs from numerical models. Significant research by Meteorologists and Oceanographers has resulted in sophisticated wind, wave and current models. The accuracy of the data from those models has a direct impact on the accuracy of the ship performance analysis. This research focuses on the accuracy and spread of the wave predictions and the effect it may have on the predicted impact on the vessel performance. Using ensemble forecasts which provide a set of forecasts indicating a range of possible conditions, the effect of each forecast on vessel performance can be calculated. The theoretical model is kept consistent, so that the impact of the effect of varying wave conditions can be assessed. This results in an ensemble of added wave resistance predictions which can be used to identify the effect of the spread of wave conditions when reviewing ship performance.

1. Introduction

Weather conditions have a large influence on the fuel efficiency of a vessel and make it difficult to isolate the influence of other factors that have a smaller contribution. It is however relevant to trend the influence that fouling on the hull has on the performance so that cleaning the hull or dry-docking can be scheduled at best times. Likewise, it is relevant to identify the effect that the installation of an energy saving device has on performance to justify the investment. In such and similar cases the influence of the weather on performance is a disturbance that can be much larger than the information we are looking for. In order to reduce the disturbances from the weather on any analysis measurements in adverse weather conditions are ignored and measurements in mild weather conditions are corrected for the effects. In either case, it is essential to have a clear understanding of the weather conditions and the influence of the weather conditions on the performance.

The level of success to correct for the weather conditions depends on the accuracy of the method applied as well as the information that describes the weather conditions. Numerical models are a very common source of information for the description of the weather conditions. The Global Wave Ensemble System (GWES) operationally run by NOAA is used as a data source for de characterization of the wave conditions. GWES is a set of wave models with global coverage at ½ degree spatial resolution and consists of a control run and 20 ensemble members where each of the ensemble members is forced with slightly different wind conditions. The spread in the resulting waves from the different ensemble members are an indication of the confidence of the prediction from the control run. The modelled waves from GWES are used to create an ensemble of added wave resistance predictions. Our focus is on the influence of the spread of wave data on the spread in added wave resistance. Therefore, the method to calculate the added wave resistance is identical for all ensemble members. It would justify a separate investigation to look into the effect that a variation in the methodology has on the results.

Results have been compared with observations from satellites. Two sources of satellite measurements are used. The first being altimetry sea wave height (SWH) measurements from Sentinel-3A satellite. Those observations allow for a comparison of the total wave height with predicted wave height. The second source of observations is Synthetic Aperture Radar (SAR) wave mode measurements from Sentinel-1A and Sentinel-1B satellites, where two-dimensional spectra of ocean surface waves are made available by the European Space Agency.

2. Observed and predicted wave heights

Observations from the European Space Agency's Sentinel-3A satellite are made available by the Copernicus Marine Environment Monitoring Service (CMEMS) after some quality control and processing. The data used comes from dataset-wav-alti-l3-rt-global-s3a from the CMEMS product SEALEVEL_GLO_WAV_L3_NRT_OBSERVATIONS_008_052. Observations are available at 7km intervals along the ground track of the satellite. All observations for December 2017 and January 2018 are considered. After some filtering the total number of observations included in the analysis is about 2,500,000.

Each observation is compared with the prediction from GWES that matches best in time and space. That means that the difference in longitude or latitude between observation and prediction is less than ¼ degree and the difference in time is less than 1½ hours. It was confirmed that the time difference has no noticeable effect on the results.

Observations near the poles where the water surface may be partly covered by ice are not considered. Information about the ice concentration included in GWES is used to identify such cases, and all observations where the predicted ice concentration is more than 1% are excluded from the analysis.

Some statistics were calculated that quantify the differences between the observations (O) and predictions (P) as defined by the following equations.

$$bias = \frac{\sum_{i=1}^{n}(O_i - P_i)}{n}$$

$$rmse = \sqrt{\frac{\sum_{i=1}^{n}(O_i - P_i)^2}{n}}$$

$$80\%\ relative\ range = median\left(\frac{P_{(0.9)i} - P_{(0.1)i}}{P_{(0.5)i}}\right)$$

$$correlation\ coefficient = \frac{\sum_{i=1}^{n}(O_i - \bar{O})(P_i - \bar{P})}{\sqrt{\sum_{i=1}^{n}(O_i - \bar{O})^2}\sqrt{\sum_{i=1}^{n}(P_i - \bar{P})^2}}$$

The 80% relative range is the range of predicted values from the ensemble members defined by the 10th and 90th percentiles of the predicted values relative to the median. Similarly, the 50% relative range is defined by the 25th and 75th percentiles.

The observed wave heights are compared to the median of the predicted wave heights from the ensemble. The small bias and root mean square error, and high correlation coefficient for short forecast lead times indicate that the predicted wave heights are close to the observed wave heights. There is only a small difference in the reliability of the predictions for 0-day and for 2-day forecast lead time. For longer forecast lead times the predictions gradually become less reliable. Predictions are available for a forecast lead time of up to 10 days, and the statistics are computed for different lead times. Results are given in Figs.1 and 2. In terms of correlation coefficient and bias the results are similar to those reported by *Bernier* (*2015*).

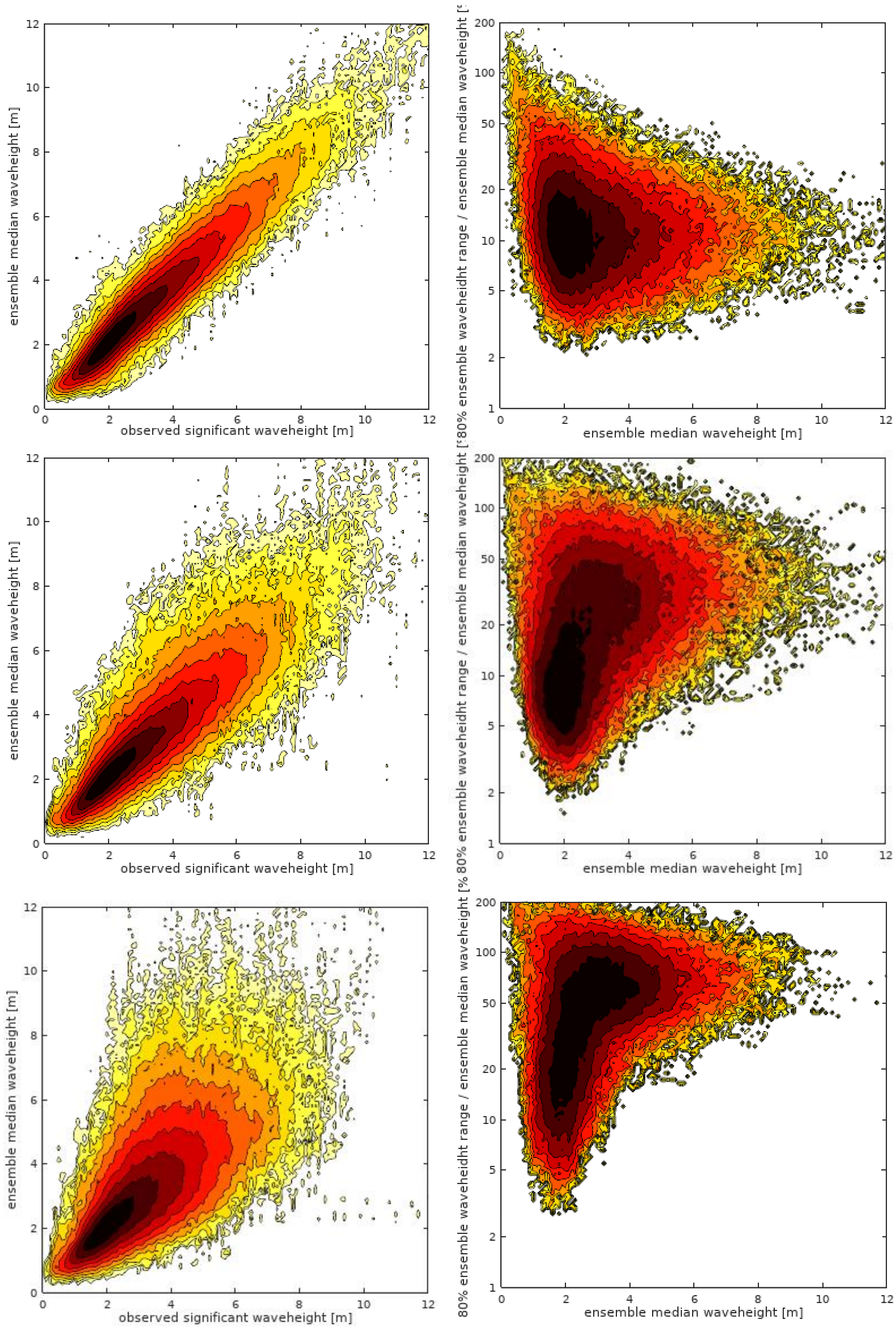

Fig.1: Scatter plots with the observed wave heights and median of the predicted wave heights (left) and relative range (right) for a 0-day forecast lead time (top), 4-day forecast lead time (middle) and 8-day forecast lead time (bottom).

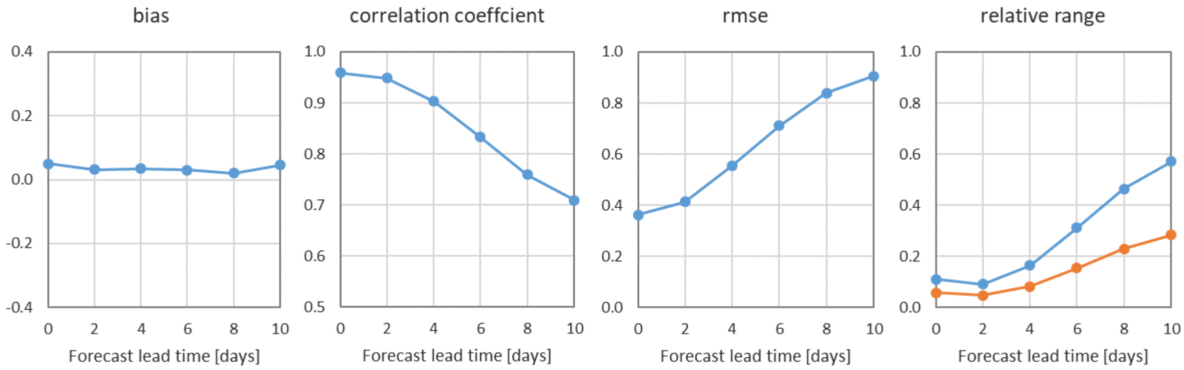

Fig.2: Bias, correlation coefficient, root mean square error and relative ranges for 80% and 50% for different forecast lead times for observations from Sentinel 3A

3. Spread in wave heights from ensemble predictions

Fig.11 (right) gives the 80% relative range as a function of ensemble median wave height. The ranges are about 11% for 0-day lead time irrespective of wave height and there is a large spread especially at lower wave heights. Although the average range for the 4-day forecast lead time is 16%, the range is closer to 40% for higher waves. As expected the spread is much larger than for the 0-day forecast lead time.

The spread in wave heights from the ensemble members is compared with the available observations. For each observation, the median wave height from the ensemble member predictions is calculated. The fraction of observation that does not exceed the median is counted. Whenever this fraction is off from 50% it indicates a bias between observations and predictions. The median of the predictions is the 50th percentile and the process is repeated for percentile levels of 10%, 25%, 75% and 90%. The results are plotted in Fig.4 (left). Ideally the colored lines that represent different percentile levels would coincide with the vertical grid lines of the graph. The median line is below 50% of the observations and indicates that – on average – the observations are somewhat higher than the predictions. This difference is reduced for larger forecast lead times. Although the bias between observations and predictions reduces slightly with longer lead times, most of the effect is a result of the larger range in the forecasts for longer lead times.

It is also observed that the percentile lines in Fig.4 are much closer to each other than the vertical grid lines. That indicates that the range in predicted wave heights is smaller than the spread in observed wave heights. This is more pronounced for shorter forecast lead times. The spread in wave heights from the ensemble predictions underestimates the spread in observed wave heights in this case.

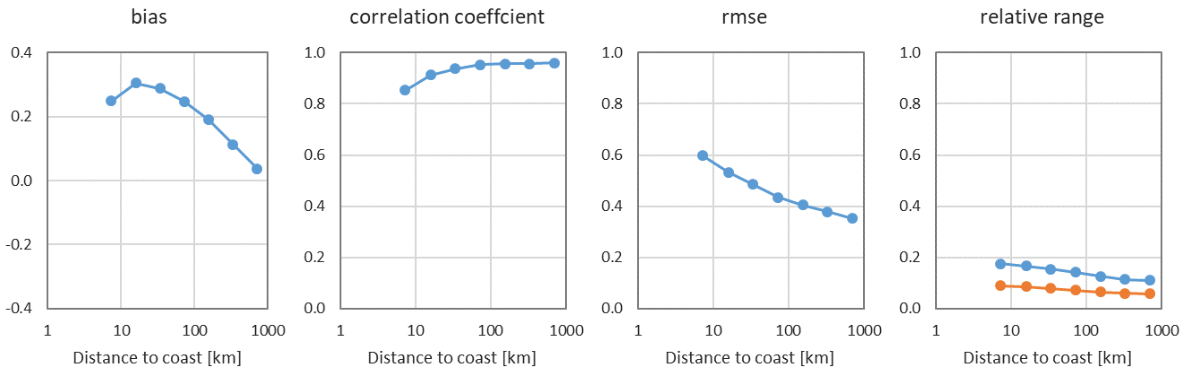

Fig.3: Bias, correlation coefficient, root mean square error and relative ranges for 80% and 50% for different distances to the nearest coast

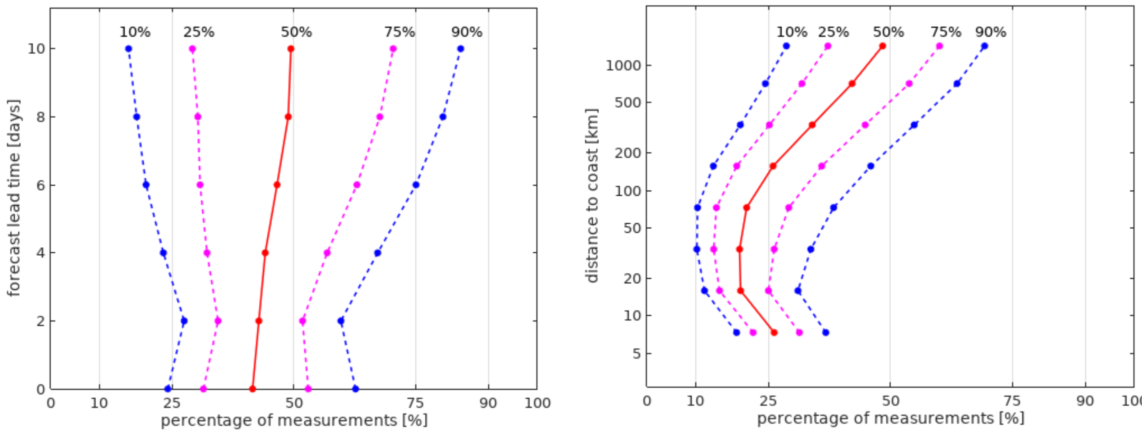

Fig.4: Number of observations not exceeding given percentile levels for different forecast lead times (left) and distance to coast (right)

The observations are grouped according to distance to the nearest coast and the same analysis was applied for 0-day forecast lead time. Results are given in Fig.4 (right) and Fig.3. The distance to the nearest coast has a remarkable effect on the results. At smaller distances, there are considerably more observations that exceed the given percentile levels. That means that predictions – on average – under-estimate the observations. In this case by more than 10% at small distances to the coast. This is also indicated by the positive bias. It has also been reported by others that wave predictions closer to the coast have larger scatter when compared to satellite altimetry observations. *Hoyer and Nielsen (2006)* concluded that altimeter wave observations are accurate at distances as close as 10 km to the coast. That suggests that the difference is due to the predictions. Not only very close to the coast, but also at distances of several hundreds of kilometers this has a noticeable effect. A minimum distance to the coast of 200 km was used in our analysis to limit the impact of distance to the coast.

4. Observations of wave spectra

The Sentinel-1 SAR wave mode observations are compared with predicted wave characteristics. All observed wave spectra from Sentinel-1A and Sentinel-1B for December 2017 and January 2018 are considered in the analysis. SAR wave spectra provide much more detail about the waves than wave height alone. Observed wave spectra however are limited in the wave frequency range and include only wave components with a length between 30 m and 1200 m. For certain wave directions, relative to the heading of the satellite this range is further restricted and only the longer waves are included. All waves with wave lengths outside this range are not included in the measurements. Two examples of measured wave spectra are illustrated in Fig.5.

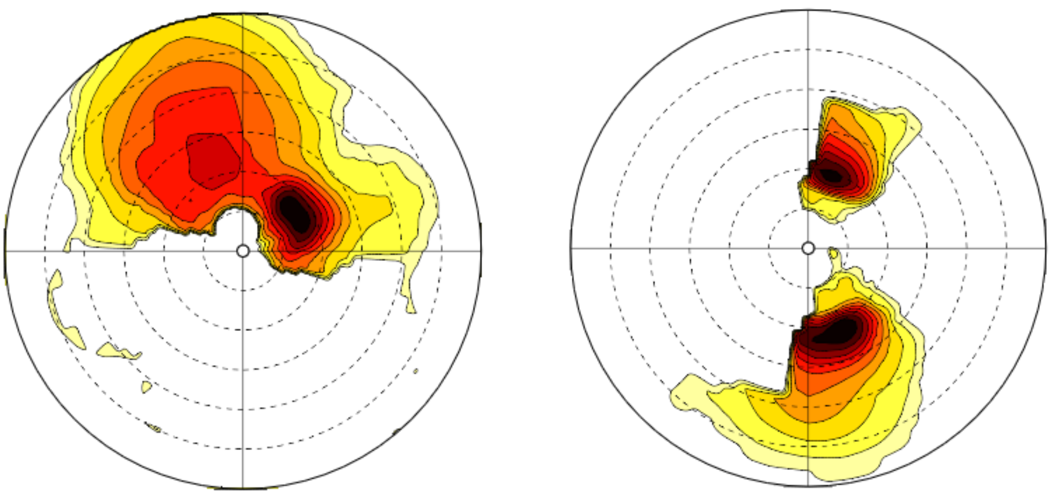
Fig.5: Observed wave spectra from Sentinel-1A on 1 December 2017 at different times and locations

One of the challenges when measuring waves by SAR is identifying the direction of the waves. Wave direction cannot always be identified with high level of confidence. In those cases, wave direction can be off by 180°. Measurements come with a flag that indicates if there is sufficient confidence in wave direction estimate. Occasionally wave spectra are a complex composition of several wave systems. That makes it difficult to identify the wave direction with high level of confidence. Both wave systems in the second wave spectrum in Fig.5 have sharp edges at their left-hand side that should be more smooth in reality. In order to reduce the impact this may have on the analysis a larger number of observations is eliminated based on the ambiguity values provided with the measurements. After filtering about 75,000 observed wave spectra are available for the analysis.

5. Modeling added resistance in waves

Our analysis follows the ITTC Recommended Procedures and Guidelines for the calculation of added resistance in waves. Wave resistance characteristics from model scale tests in regular waves for a 170,000 dwt bulk carrier with a length of 279 m, beam of 45 m and design draught of 16.5 m as published by *Matsumoto* (*2000*) are used. See Fig.6. The characteristics are valid for design draught at a vessel speed of 13 knots, and cover all wave directions. The current analysis is limited to these conditions.

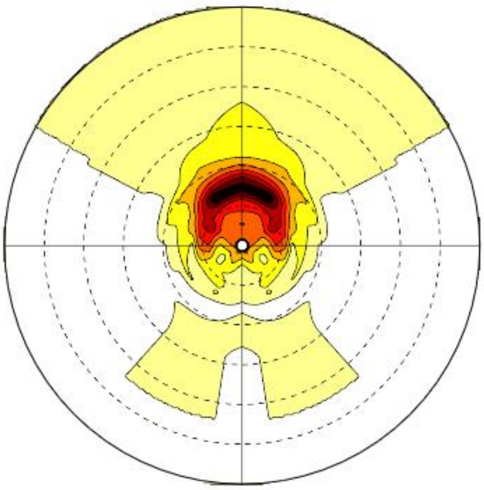

Fig.6: Non-dimensional added wave resistance in regular waves for a 170,000 dwt bulk carrier at 13 knots for wave lengths between 30 m (center) and 1200 m (outer circle)

Added wave resistance in irregular sea is calculated from the added wave resistance in regular waves, valid for a range of wave frequencies, wave directions and in this case only one vessel speed, together with the observed or predicted two-dimensional wave energy spectrum.

$$R_{AW} = 2\int_0^{2\pi}\int_0^{\infty}\frac{K_{AW}(\omega,\alpha,V_s)}{\zeta_A^2}E(\omega,\alpha)d\omega d\alpha$$

The heading of the vessel has been chosen to be perpendicular to the heading of the satellite. By doing so the full range of wave lengths available in the observations is for waves coming in on the bow and stern. For beam waves, the range of wave lengths is more restricted, but has limited impact because the added wave resistance is not so much affected by beam waves compared to head waves as can be seen in Fig.6.

Added wave resistance is calculated for the vessel with the observed wave spectrum and with wave spectra constructed from each of the ensemble members from the predictions. Added wave resistance calculated with the observed wave spectrum is compared with the median and spread in added wave resistance calculated from the 21 ensemble members.

Wave spectra are not available from the predictions. Therefore, wave spectra are constructed from the available wave height, mean wave direction and mean wave period. A separation into different wave partitions is included: wind sea and two swell components. A JONSWAP wave spectrum with a cos2s wave directional spreading has been assumed. A fixed directional spreading parameter (s) is used for wind seas and swells, where wind seas have larger spread than swells. No fine-tuning of the spreading parameter was applied to better fit the predicted wave spectrum to the observed wave spectrum. The wave spectra are limited to the same frequency range as the observations so that a direct comparison of the results is allowed. A consequence of the limited frequency range is that the added wave resistance as reported here will be lower than the actual added wave resistance in the actual sea state. All wave energy that is outside the frequency range does not contribute to the added wave resistance in our analysis. Especially the wind sea components will not be accurately modeled because the shorter wave lengths of the wind seas are outside the frequency range. On average the predicted wave heights are reduced by 17% due to the limited frequency range. We expect that the effect on added wave resistance will be lower than this due to the fact that the frequencies where the vessel is most sensitive to added wave resistance are included in the frequency range.

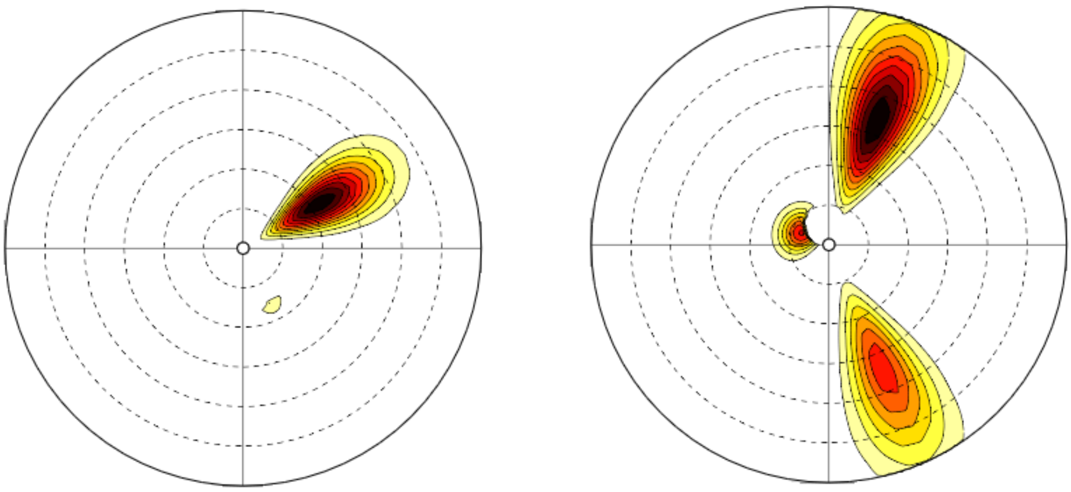

Fig.7: Predicted wave spectra from the ensemble control run for the conditions from Fig.5

Wave heights are calculated from the observed wave spectra and from the predicted wave spectra, accounting for the limited frequency range. Observed and predicted wave heights are compared by the same method as for the Sentinel 3A observations, Fig.8. Some noticeable differences in the results exist. Correlation between observations and predictions is less than for Sentinel 1A observations and a clear bias between observations and predictions exists. The root mean square error has increased for shorter lead times, but not for longer lead times. One possible reason for the larger differences between observation and prediction is a bias in the predicted period of the waves. The limiting frequency range would cut off a larger or smaller portion of the wave energy if the prediction of the wave period has a bias. The existence of a bias in the predicted wave period was not investigated.

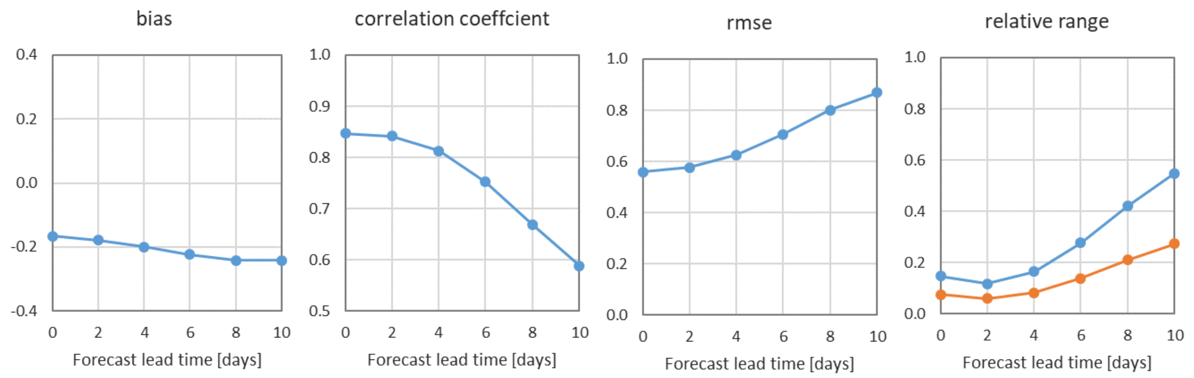

Fig.8: Bias, correlation coefficient, root mean square error and relative ranges for 80% and 50% for different forecast lead times for the combined observations from Sentinel 1A and Sentinel 1B

6. Added wave resistance from predicted waves and from observed waves

Added wave resistance calculated with observed waves is compared to the added wave resistance calculated with predicted waves. The results are presented in Figs.9 and 10. First the results for 0-days lead time are discussed, followed by the discussion for longer forecast lead times.

Fig.9 (left) shows the scatter between observation and median of the predictions. The average added wave resistance is about 90 kN, which is roughly 10% of the calm water resistance for such a vessel. It is also clear from the scatter plot that conditions with negligible added wave resistance are not so frequent. Roughly 98% of the time the effect of added wave resistance is more than 1% of the calm water resistance. Cases where the added wave resistance is negative, and the waves push the vessel forwards, do exist, but are rare.

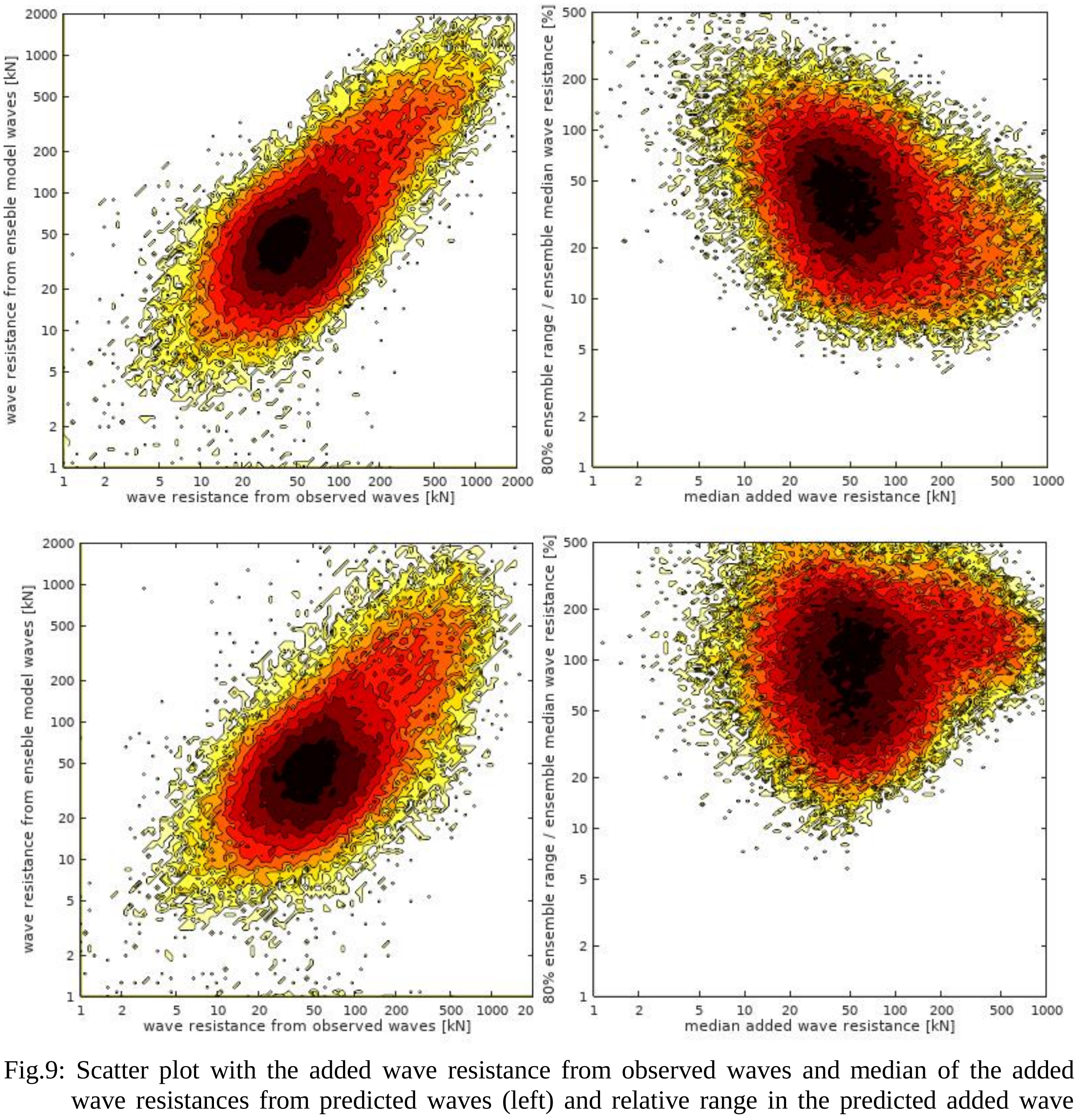

Fig.9: Scatter plot with the added wave resistance from observed waves and median of the added wave resistances from predicted waves (left) and relative range in the predicted added wave resistance (right) for 0-days forecast lead time (top) and 8-day forecast lead time (bottom).

The root mean square error for added wave resistance is close to 100 kN, which is rather large compared to a median of about 45 kN. Especially the lower estimates of added wave resistance are estimated with lower confidence. The average relative range is larger for lower predicted added wave resistance than for higher predicted added wave resistance and the extremes are predicted with higher confidence.

At 0-day lead time the correlation coefficient for added wave resistance is 0.77. The correlation coefficient for wave heights is 0.84, when the limiting frequency range is accounted. The difference with the correlation for the altimeter wave heights, where the frequency range is not limited, is much larger. The smaller correlation coefficient is because of the larger spread in added wave resistance.

The relative range in the predicted added wave resistance is 0.36 on average. This is 2.5 times higher than the relative range in wave heights. Added wave resistance depends on wave height squared in our analysis. Therefore, it is expected that the relative range for added wave resistance is twice as high as the relative range for wave height. The additional increase in relative range is because of approximations in wave spectra; idealised wave spectra, errors in the prediction for mean wave period and wave direction. Added wave resistance can be estimated with significantly lower accuracy than wave height.

For longer forecast lead times the reliability of the predicted added wave resistance gradually decreases, although the results for the first few days do not indicate that the predictions are affected much. The relative ranges for long forecast lead times are high and indicate that added wave resistance cannot be predicted reliably. Where a prediction for wave height a week ahead may still have some significance, a prediction of added wave resistance based on that wave height is not reliable.

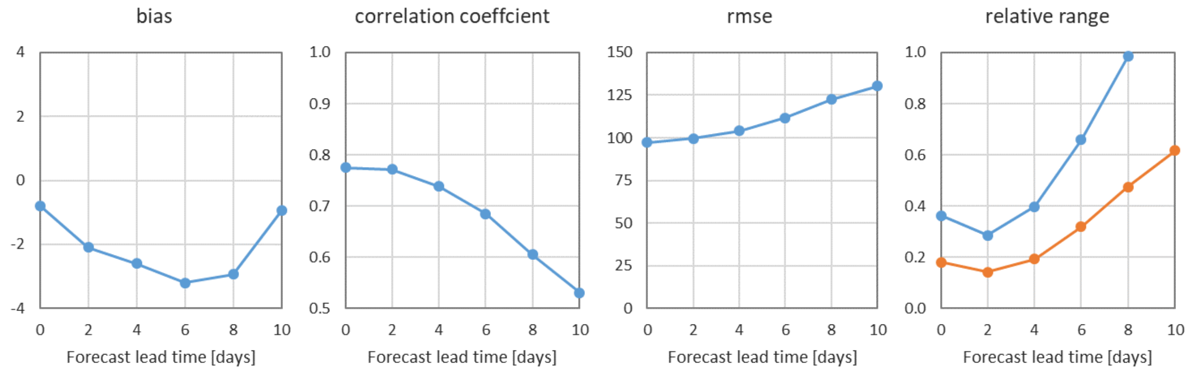

Fig.10: Bias, correlation coefficient, root mean square error and relative ranges for 80% and 50% for added wave resistance at different forecast lead times

7. Conclusions

An ensemble prediction for waves is extended to an ensemble prediction for added wave resistance to investigate the effect that a spread in wave predictions may have on accuracy of added wave resistance predictions. Only variations in wave input is included in the ensemble.

It was found that predicted wave heights are in good agreement with observations for short forecast lead times. Correlation coefficient is about 0.95 and root mean square error is 0.36 m and are similar to the numbers reported by others.

Based on the ensemble predictions for 0-day forecast lead time the range in predicted wave heights is about 11% on average, but the spread is large especially for lower wave heights. The number of observations that is outside the range of predicted wave heights from the ensemble is large and indicates that the ensemble under-estimates the range for wave heights. The spread in the ensemble results can be used to identify a level of confidence in the wave height predictions.

Added wave resistance has much larger bias and spread than wave height. Relative ranges in predicted added wave resistances from the ensemble is about 2.5 times higher than relative ranges in wave heights from the ensemble. This is more than can be explained by the assumption that added wave resistance depends on wave height squared. Other aspects such as the use of idealised wave spectra, errors in predicted wave direction and mean period also contribute to the larger relative ranges.

The accuracy of the added wave resistance characteristics of the vessel in regular waves and the accuracy of the theory applied to calculate the added wave resistance were not considered. Any such variations would lead to larger differences between added wave resistance calculated with observed waves and predicted waves.

References

BERNIER, N.B.; ALVES, J.H.; TOLMAN, H.; CHAWLA, A.; PEEL, S.; POULIOT, B.; BELANGER, J.M.; PELLERIN, P.; LENINE, M.; ROCH, M. (2015), *Operational wave prediction system at environment Canada: Going global to improve regional forecast skill*, J. Weather and Forecasting

MATSUMOTO, K.; HIROTA, K.; TAKAGISHI, K. (2000), *Development of energy saving bow shape at sea*, 4th Osaka Colloquium on Seakeeping Performance of Ships, Osaka
http://mararchief.tudelft.nl/file/22967/

HØYER, J.L.; NIELSEN, J.W. (2006), *satellite significant wave height observations in coastal and shelf seas*, 15 years in Satellite Altimetry" Symp., Venice
http://ocean.dmi.dk/staff/jlh/PAPERS/proceed_venice_2006.pdf

Improvement of Measuring Accuracy of Ship's Speed through Water by using MLDS (Multi-Layered Doppler Sonar)

Yasuhiro Sudo, MTI, Tokyo/Japan, yasuhiro_sudo@monohakobi.com
Norihide Igarashi, MTI, Tokyo/Japan, norihide_igarashi@monohakobi.com
Takashi Yonezawa, MTI, Tokyo/Japan, takashi_yonezawa@monohakobi.com
Masahiko Mushiake, Furuno Electric, Nishinomiya/Japan, masahiko.mushiake@furuno.co.jp
Satoshi Kawanami, Furuno Electric, Nishinomiya/Japan, satoshi.kawanami @furuno.co.jp
Takanori Hino, Yokohama National University, Yokohama/Japan**,** hino-takanori-nf@ynu.ac.jp

Abstract

A developed measuring system named "MLDS" (Multi-Layered Doppler Sonar) was introduced to measure distribution of relative flow velocity along water depth. The measuring systems were installed on a PCC and Product Tankers and the relative flow velocity at each layer was measured during voyages. The obtained data were evaluated by comparing with the result of CFD analysis and it is confirmed that the distribution measured on the PCC and Product Tankers had similar tendency with the results of CFD analysis of a blunt ship and a slender ship. Considering both the CFD analysis results and the onboard measured data, finally a new method to improve measurement accuracy of ship's speed through water is proposed.

1. Introduction to numerical fluid dynamics

No matter how correctly the devices are used to measure flow velocity of water, the area surrounding the ship is impacted by boundary layer, and flow is pushed away by the ship itself, so current at the original position cannot be measured as is. On the other hand, if measuring flow velocity at a deep position sufficiently away from the ship's bottom, there may be difference of velocity from the area surrounding the ship. From experience, ship's speed through water (STW) is usually measured by Doppler sonar at a position not too close and not too far away – 3 to 20 m from the bow bottom of the ship in the case of large vessels. However, there is still some possibility of influence of the ship itself although the area is out of boundary layer. So, the Doppler sonar is utilized by applying correction factor which is established at speed test of official sea trial by eliminating current and tide effect from GPS speed by making several round runs at same area. However, it is not assured that the correction factor can be used at any conditions because the correction factor determined in an official sea trial is a certain sea trial condition.

In order to improve accuracy of measuring ship's STW, Multi-Layered Doppler Sonar (MLDS) have been developed and following items have been researched: Study of measurement depth based on CFD flow distribution analysis results (Chapter 3); Verification test Phase 1: Measurement of flow velocity at deep zone under the actual ship (Chapter 4); and Verification test Phase 2: Measurement of flow velocity at close zone under the actual ship (Chapter 5)

2. Doppler Sonar

2.1. Conventional Doppler sonar

As shown in Fig.1, ultrasonic waves transmitted to downward direction from an ultrasonic transducer on the ship's bow bottom return to the transducer after reflected by suspended matter like plankton in the water. By frequency analysis of the transmitted and returned ultrasonic waves, relative flow velocity in the ultrasonic direction is calculated through Doppler shift. Conventional Doppler sonar, *Kihara (1978)*, obtains the relative flow velocity in ship's heading by transmitting the ultrasonic waves to three directions as shown in Fig.2 and combining and analyzing the three returned ultrasonic waves which reflected at 3 to 20 m from bow bottom of a ship.

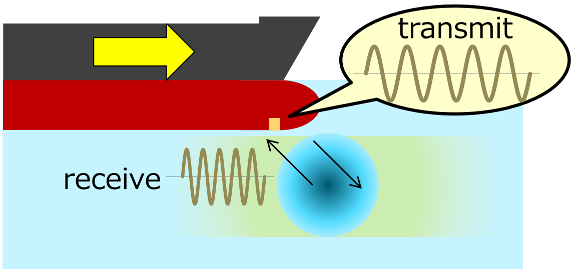

Fig.1: Principle of Doppler sonar

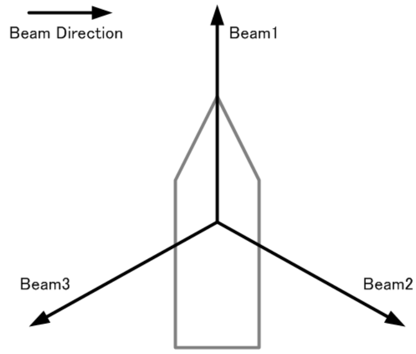

Fig.2: Example of ultrasonic beam direction of Doppler sonar

2.2. MLDS (Multi-Layered Doppler Sonar)

The latest Doppler sonar developed by Furuno Electric (Model:DS-60) transmits wideband ultrasonic waves which have multiple spectral peaks (= N) as shown in Fig.3, *Kawanami (2011)*. By doing so, about N times amount of data can be obtained by measuring Doppler shifts of each spectral peak at the same time independently. MLDS has been developed by using this function, which is continuously measuring the relative flow velocity at multi-layer of water as shown in Fig.4.

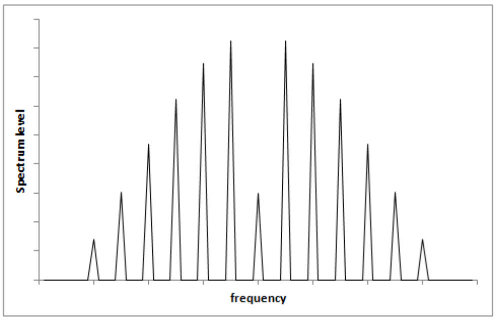

Fig.3: Example of spectrum using wideband signal

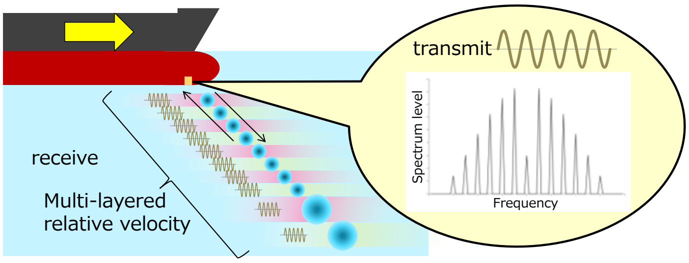

Fig.4: Multi-layered Doppler sonar

3. Study of measuring depth based on CFD flow distribution analysis

Flow fields of KRISO Container Ship (KCS), as an example of a slender ship, and Japan Bulk Carrier (JCB) as an example of a blunt ship, both of which are typical CFD benchmark hulls, *CFD (2015)*, were calculated by CFD solver SURF, *CFD (2015)*, developed at NMRI with the Spalart-Allmaras turbulence model. Calculations were made in a full scale, i.e., ship lengths are set 190 m (reduced from original 230 m) for KCS and 280 m for JBC. The flow velocity distributions are obtained along three beams shown in Fig.5, which run at 55° downward in three directions (ship's heading and 120° to port and starboard side) from the transducer mounting position. The distributions of relative flow velocity in heading direction and vertical direction under the ship's bow bottom were calculated as the average of three values on each beam.

The calculation results of KCS are shown in Figs.6 and 7, and those of JBC are shown in Figs.8 and 9. According to CFD calculation results, the relative flow velocity which is measured by conventional Doppler sonar at 3 to 20 m from bow bottom of ship is different from STW and varies depending on ship's speed and draft. If a single correction factor is used, it is necessary to use a relative flow velocity at below 30 m under ship's bow bottom.

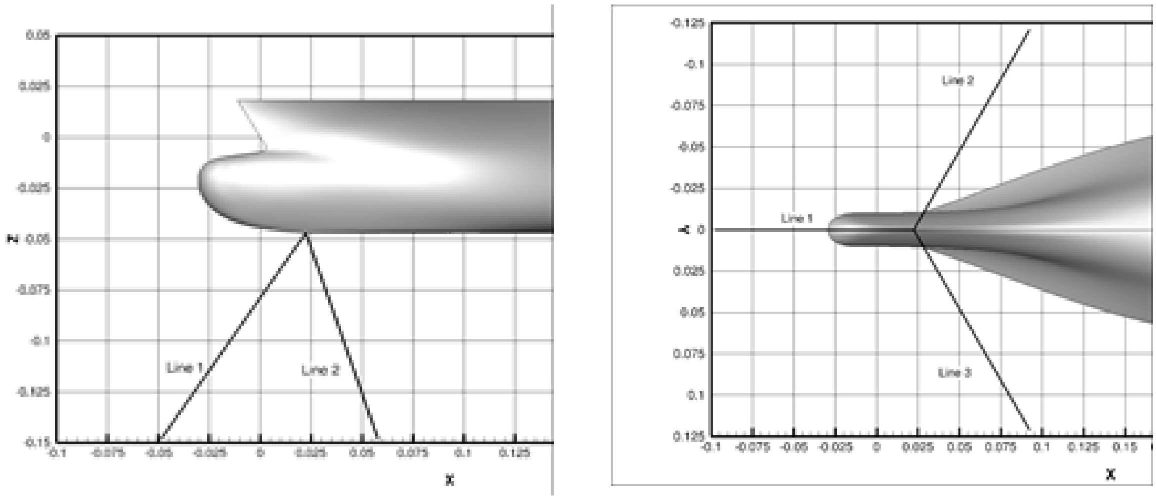

Fig.5: Velocity extraction lines

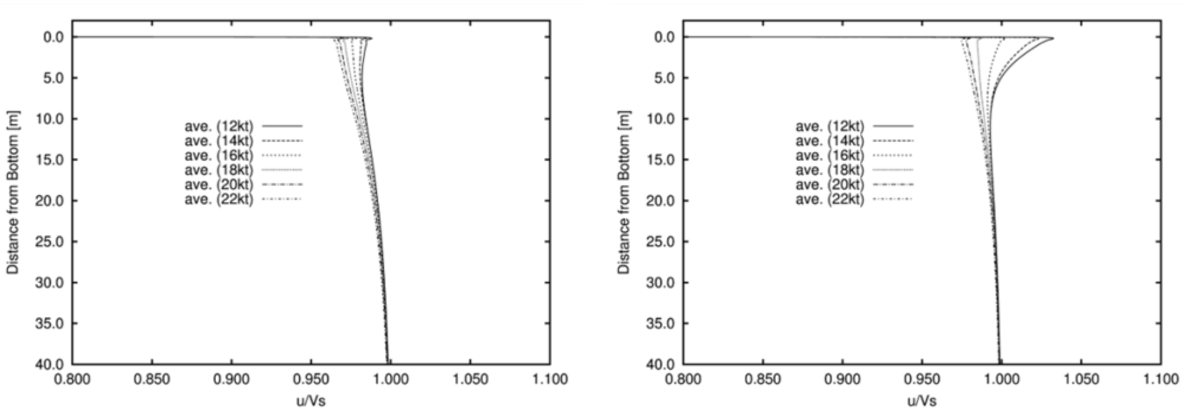

Fig.6: Averaged velocity distributions under bow bottom (KCS, Left: Laden, Right: Ballast)

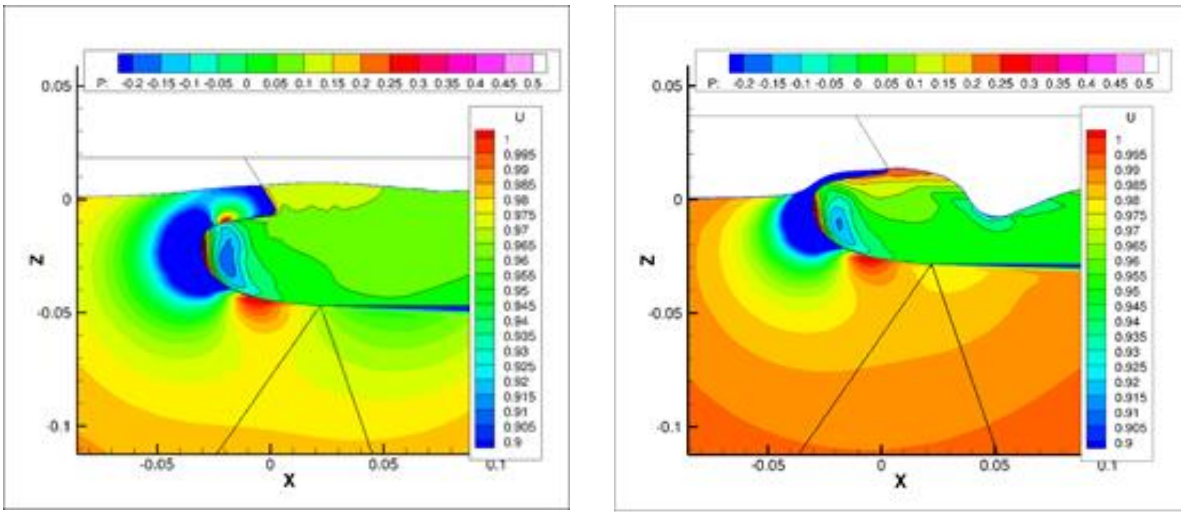

Fig.7: Hull pressure and velocity on center plane at 20kn (KCS, Left: Laden, Right: Ballast)

Fig.10 shows ratio of relative flow velocity to ship's speed at 3, 20, and 60 m under the bow bottom of KCS as ship's speed on the horizontal axis. The ratio is 100% for both laden and ballast conditions regardless of ship's speed at 60 m under the ship's bow bottom. However, the ratio varies from 98.9 to 99.5% at 20 m and from 96.8 to 100.8% at 3 m under the ship's bow bottom, which shows that there is variation of 0.6% and 4.0%, respectively.

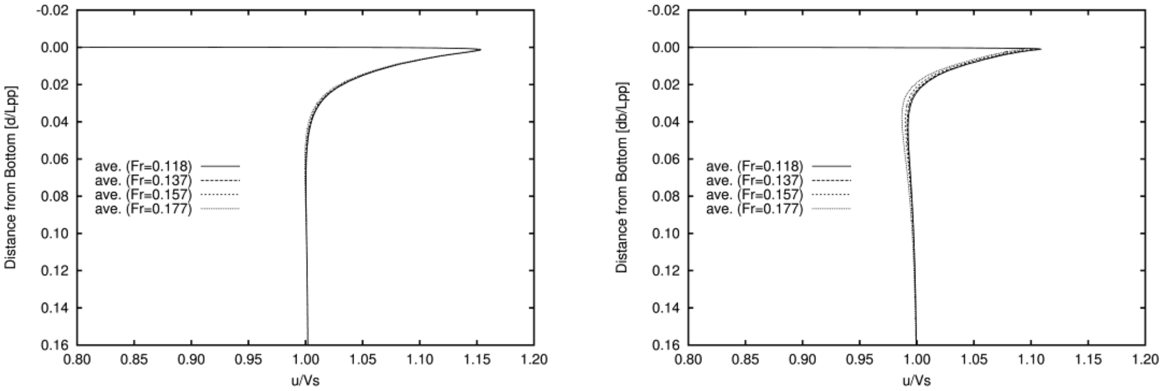

Fig.8: Averaged velocity distributions under bow bottom (JBC, Left: Laden, Right: Ballast)

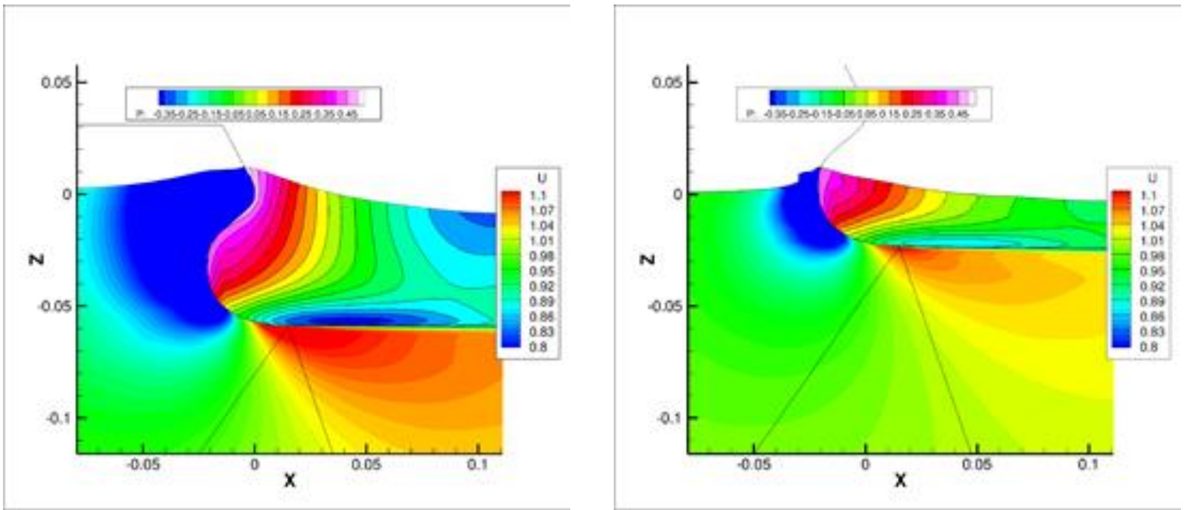

Fig.9: Hull pressure and velocity on center plane at 16kn (JBC, Left: Laden, Right: Ballast)

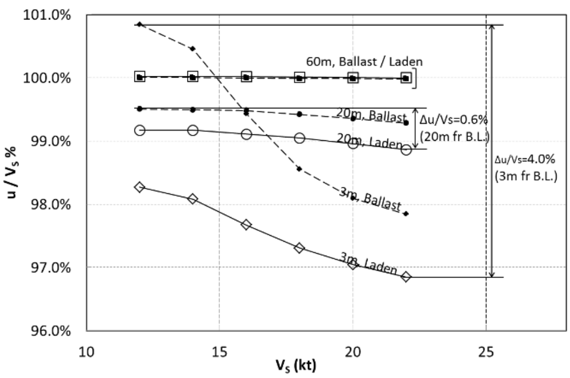

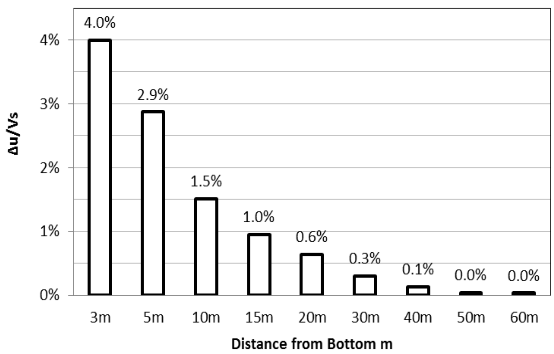

Fig.10: Variations of ratio of computed relative flow velocity under bow bottom to ship's speed against ship's speed (KCS)

Fig.11: Deviations of computed relative flow velocity under bow bottom from ship's speed against distance from bottom (KCS)

The fact that this ratio is not 100% is known empirically and correction factor has been used, which is established at speed test of official sea trial. However, the fact that the ratio of averaged relative flow velocity to ship's speed is changed by effect of ship's speed and draft has not been taking into consideration; the same correction factor has been used for all ship's speed and draft ranges. This means that the deviations indicated in Fig.10 could be the reason for error of ship's speed through water. The deviations of each depth are shown in Fig.11. This shows that the deeper the distance from ship's bow bottom, the smaller error factor for ship's speed through water.

4. Verification Test Phase 1: Measurement of flow velocity at deep zone under an actual ship

4.1 Measurement

According to CFD, the relative flow velocity under the ship's bow bottom could be significantly affected by the hull in a wide range. To confirm this hypothesis, the relative flow velocity at the range from 14 to 54 m under the bow of PCC was measured by MLDS. Table I shows principal particulars of the PCC, Table II shows measuring condition, and Fig.12 the position of Doppler sensor of MLDS on the PCC. Fig.13 shows time series variation of the ship's speed over ground during the time period. Table III shows data filter conditions so that the data during steady navigation speed in a certain direction in calm sea is extracted. 11628 sets of data satisfied these filter conditions. Fig.14 shows the initial one-second measurement results taken after each time zero during this period.

Table I: Principal particulars for PCC

L	190 m
B	32.2 m
Depth	34.8 m
Draft	10.3 m

Table II: Measuring condition

Item	Setting
Measuring depth	14, 19, 24, 29, 34, 39, 44, 49, 54 m
Distance resolution	7.8 m
Moving average time	10 s
One data period	1 s

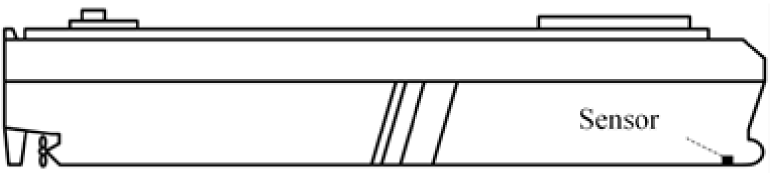

Fig.12: Position of sensor on PCC

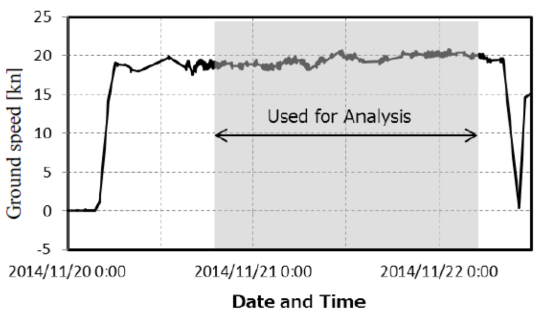

Fig.13: Time series of ground speed

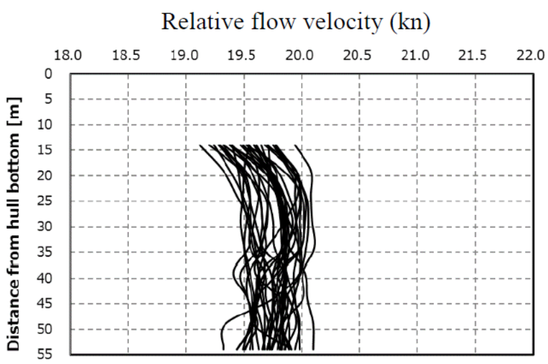

Fig.14: Distribution of 1-s of relative flow velocity

Table III: Filtering conditions

Sampling period	2014/11/20 19:00～2014/11/22 7:00
Ship speed	18.1 - 20.8 kn
Rolling	±5°
Pitching	±1.5°
Drifting	±3°
Acceleration of fore-aft direction through water	±0.01 kn/s

4.2 Analysis and considerations

Relative flow velocity in Fig.14 had variation at each time, depth and ship's speed. The data was filtered in specific conditions, so the causes of variation are assumed to be the following three factors.

(1) Speed through water was changed actually
(2) Current of each depth was changed as time and depth
(3) Hull itself made specific flow field

For analyzing ship's performance, (1) is necessary and (2), (3) should be removed. In Chapter 3, (3) was studied with CFD. To remove the influence of (3), measuring relative flow velocity in deep zone seems one answer, but effect of (2) should be considered.

Fig.15 shows distribution of dimensionless relative flow velocity ratio U_X/U_{14} (U_X: relative flow velocity of X m from ship's bow bottom, U_{14}: relative flow velocity at 14 m form ship's bow bottom), which draws the initial one second measurement results taken after each time zero. It is possible to consider that the effect of (1) has been removed at this Fig.15 because it can be considered the hull effect (3) is same during this measurement period thanks to limited draft and ship's speed if ship itself is considered in the same layer of current as 14 m depth which is shallowest depth of measurement at this time. This Fig.15 shows the depth is deeper, fluctuation of the ratio is bigger.

Fig.16 shows time variation of one-second, five-minute moving average and standard deviations of relative flow velocity of U_{54}/U_{14} from 00:00 to 01:30 on 22 November 2014, as an example. This shows that the fluctuation of relative flow velocity ratio comes from long time change of factor (2) which has 1.5% range, while the standard deviation of each time is limited, such as about 0.3%.

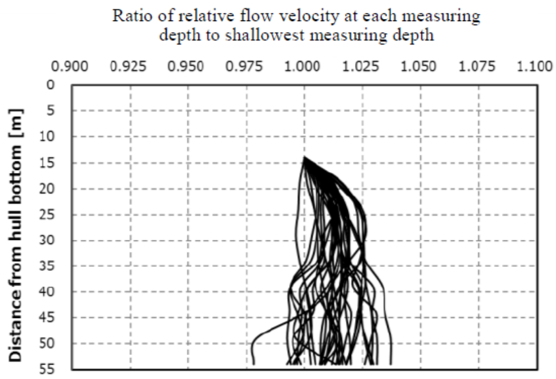

Fig.15: Distribution of one-second of relative flow velocity ratio U_X/U_{14}

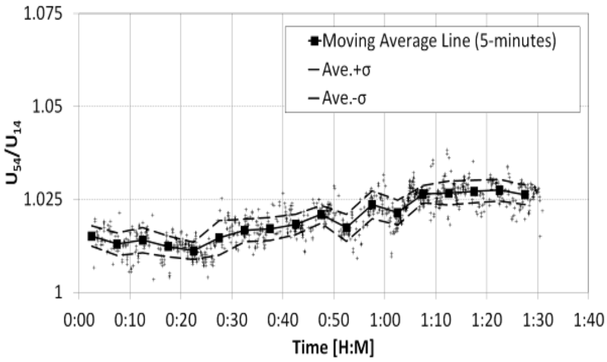

Fig.16: Five Distribution of one-second and five-minute average of relative flow velocity

Effect of this factor (2) is a movement that is independent from the ship, so it is difficult to predict and control for each time and location. However, it is possible to minimize the effect of (2) and obtain the characteristics of (3) by collecting sufficient amount of data and make average analysis. Fig.17 shows one method of learning the characteristics of (3), which means that the average analysis is useful method to lean the distribution of flow velocity under the ship's bow bottom. However, the data for making characteristics of (3) shown in Fig.17 should be carefully checked about its quality, i.e. number of data and bias, etc. As shown in Fig.18, the data obtained from this study looks like good results with general normal distributed.

Fig.19 shows standard deviation of overall average of relative flow velocity ratio at every layer to the shallowest layer. Considering standard deviation of U_{19}/U_{14} is 0.28%, if precision of 0.3% is demanded, the measuring target of shallowest depth should be within at least 5 m from the ship's bow bottom to obtain the characteristics of (3).

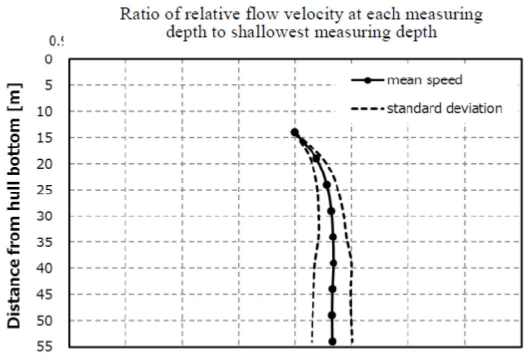

Fig.17: Overall average of relative flow velocity ratio at every layer to the shallowest layer

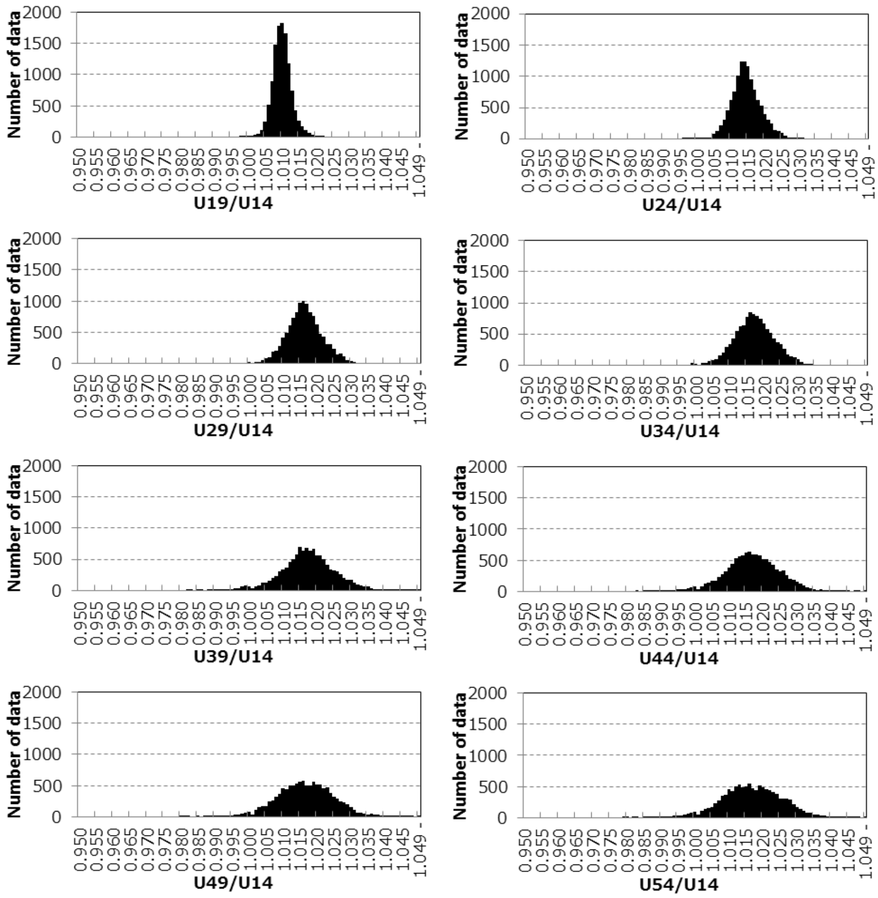

Fig.18: Distribution of relative flow velocity ratio at every layer to the shallowest layer

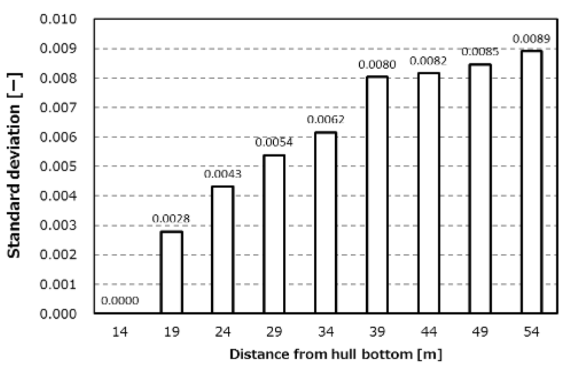

Fig.19: Standard deviation of overall average of relative flow velocity ratio at every layer to the shallowest layer

5. Verification test Phase 2: Measurement of flow velocity at close zone under the actual ship

5.1 Overview

It has been confirmed that measured relative flow velocity at too deep layer is NOT correct ship's STW through the measurement and analysis result in Chapter 4, while the tendency of CFD was confirmed from the actual data. Therefore, a new method is proposed in this chapter to obtain the distribution of relative flow velocity including hull effect by measuring between 2 m (nearer than before) to 40 m from ship's bow bottom.

The new proposal is as follows. Effectiveness of proposed new method was validated in this chapter. The results of Step-3 for PCC and tankers are introduced in this paper.

Preparation phase

(Step-1) Measure the relative flow velocity distribution of each layer bottom between 2 to 40 m under the ship's bow by MLDS and nondimensionalize by relative flow velocity nearest the hull.

(Step-2) Collect sufficient number of data and make average analysis for each group of draft and relative flow velocity to obtain flow velocity distribution around the hull with minimal current effect.

(Step-3) Determine convergence value by increasing depth and regard this value as ratio of relative flow velocity nearest the hull to true ship's STW (equivalent of 1.016 under 29 m in the case of Fig.17). Collect these values for each group of draft and relative flow velocity, and create a velocity ratio chart.

Usage phase

(Step-4) Measure relative flow velocity nearest the hull. Display the true ship's STW by selecting appropriate velocity ratio corresponding to measurement conditions (draft and relative flow velocity) from the velocity ratio chart and multiply it by measured value of relative flow velocity nearest the hull.

5.2 Measured Results

As measuring within 5 m from the ship's bow bottom is considered effective to restrain effect of hull itself through the analysis in Chapter 4, measurement and analysis of shallow-to-medium depth have carried out for PCC and tankers after modifying software and measurement resolution. Table IV shows principal particulars of PCC and tankers. Table V shows the measuring conditions.

Table IV: Principal particulars of PCC and Tankers

	Panamax PCC	Tankers
L	190.00 m	243.80 m
B	32.20 m	42.00 m
Depth	34.80 m	21.60 m
Draft	10.30 m	15.00 m

Table V: Measuring condition

Item	Setting
Measuring depth	2, 3, 4, 5, 6, 7, 8, 9, 10, 15, 20, 25, 30, 35, 40 m
Distance resolution	1.0 (2-10 m), 7.8 (15-40 m)
Moving average time	10 s
One data period	1 s

From the analysis result as shown in Figs.20 and 21, same as the calculation results of CFD, following items were revealed.

- Flow velocity distribution differs between PCC, i.e. slender ship and tankers, i.e. blunt ship, each has characteristic depends on hull form.
- Flow velocity distribution hardly changes by ship's speed under laden condition for both PCC and tankers.
- In tanker, flow velocity distribution varies according to draft.
- Flow velocity distribution changes by ship's speed under ballast condition for tankers.

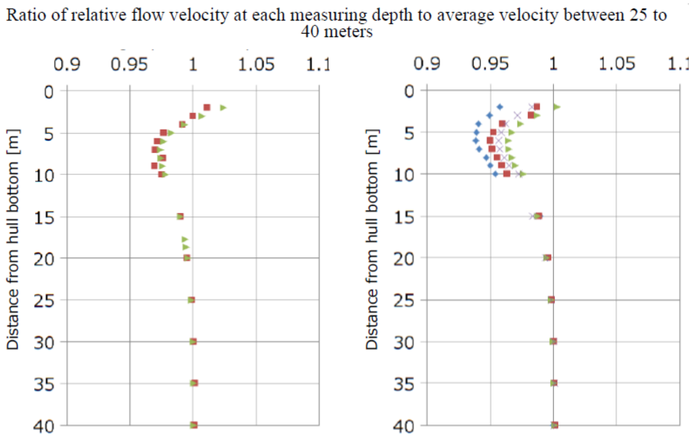

Fig.20: Overall average of relative flow velocity ratio at every layer to average velocity between 25 to 40 m of tankers (Left: Laden condition, Right: Ballast condition)

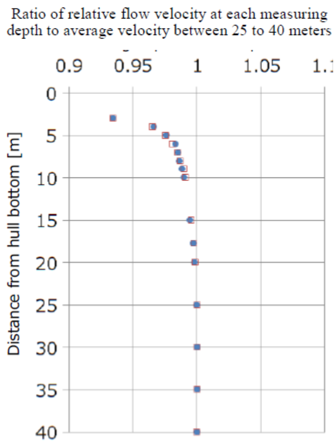

Fig.21: Overall average of relative flow velocity ratio at every layer to average velocity between 25 to 40 m of PCC

6. Conclusions

The conclusions of this paper are follows:

- With CFD analyses of KCS and JBC, relative flow velocity under ship's bow bottom is significantly affected by the hull in a wide range, and impact varies according to ship's speed and draft. The study showed that if a single correction factor is used, it is necessary to use a relative flow velocity at below 30 m under ship's bow.
- Medium-to-deep depth actual ship measurement and analysis show that the impact of current affects flow distribution under ship's bow bottom and that the depth deeper, the greater the impact is. To minimize this impact, the average analysis is useful by collecting sufficient number of data.
- Medium-to-deep depth actual ship measurement and analysis show that the measuring target of shallowest depth should be within at least 5 m from the ship's bow bottom to obtain the flow velocity surrounding the ship with 0.3% standard deviation.
- Shallow-to-medium depth actual ship measurement show that flow distribution under the bow bottom was affected by difference in ship type, draft and speed.

Based on this study, a new method to improve the measurement accuracy of ship's speed through water by using MLDS has been proposed. Establishing self-learning capabilities (automation of Step1~3 in chapter 5) for making flow velocity chart and function to display the true ship's speed through water (Step 4 in chapter 5) are themes for the future.

References

CFD (2015), *CFD Workshop Tokyo 2015*, http://www.t2015.nmri.go.jp

HINO, T. (1997), *A 3D unstructured grid method for incompressible viscous flows*, J. Soc. Naval Arch. Japan 182, pp.9-15

KAWANAMI, S. (2011), *Latest trends of Doppler sonar, navigation*, Japan Institute of Navigation 178, pp.35-39

KIHARA, K. (1978), *Doppler method tide gauge*, J. Japan Marine Engineering Soc. in Japan 16, pp.160-166

Quantification of Changes in Propeller Performance – Method Validation

Sergiu Paereli, Jotun, Sandefjord/Norway, sergiu.paereli@jotun.no
Manolis Levantis, Jotun, Sandefjord/Norway, manolis.levantis@jotun.com

Abstract

This paper is a continuation of the paper "Splitting Propeller Performance from Hull Performance" presented at the 1st HullPIC conference in 2016. Paper aims at validating the method proposed for identification of changes in propeller performance. For this purpose, in-service performance data from several vessels has been analysed and results discussed. Vessels have been chosen such that their propeller has been either confirmed not to be cleaned during a prolonged period, or propeller has been regularly cleaned, or propeller has been upgraded. Results obtained by implementing the proposed method are compared with computed deviation in modified propeller performance. The latter has been obtained by applying a machine learning approach. It has been concluded that having thrust data, it could be possible to observe changes in propeller performance and even quantify them. Nevertheless, it remains a fact that not all changes are captured. Furthermore, the practical use of this approach in splitting hull performance from propeller performance is discussed.

1. Introduction

For many years, maritime industry has been dealing with a challenging task – accurate evaluation of in-service performance of a vessel. As of today, the most common method is the one described in ISO 19030. The main idea behind the latter is to measure changes in the relationship between vessel speed (V_s) and delivered power (P_D) in time. Nevertheless, these changes are not related to changes in solely hull and propeller conditions but also to other factors that one should somehow deal with. As mentioned in the previous paper, there are two basic choices in this sense – either to estimate the contributions of the other factors influencing speed-power relationship or to filter performance data gathered from a vessel for comparable conditions.

The problem becomes more complex when it comes to splitting the in-service performance of a vessel into a hull component and a propeller component. The total propulsive efficiency of a vessel can be written as

$$\eta_D = \frac{P_E}{P_D} = \frac{P_E}{P_T} \cdot \frac{P_T}{P_D} = \eta_H \cdot \eta_B$$

P_E is effective propulsive power, P_T thrust power, η_H hull efficiency and η_B behind-hull propeller efficiency.

From the above equation, it might seem that splitting propeller efficiency from hull efficiency is quite straightforward. Nevertheless, as discussed in *Paereli et al. (2016)*, there are some challenges in this sense. In short, is it not possible to calculate hull performance for a vessel in operation because effective propulsive power is not measurable. Instead a pragmatic approach could be used in this sense if one considers that

$$P_E = R_T \cdot V_s$$

R_T is the total resistance, V_s ship speed.

By looking at changes in V_s/P_T in time and remembering that this ratio is speed dependent, one could eventually say something about changes in the surface character of the underwater hull area. However, at this point the calculation of hull performance or the efficiency of the propeller operating behind the hull resumes to the accurate calculation of thrust power.

$$P_T = T \cdot V_a \text{ ,}$$

T is thrust and V_a speed of advance.

Thrust power meters are often not available on-board. In cases when vessels are equipped with such a sensor, the accuracy of thrust measurements is still questionable. Assuming that thrust data is accurate enough though, one encounters another problem – speed of advance calculation. As such, the latter cannot be measured but only computed from wake (w) which is again normally not measured.

$$V_a = V_s \cdot (1 - w)$$

Considering the above, it becomes obvious that splitting propeller performance from hull performance is not that straightforward anymore. For evaluating changes in propeller performance for a vessel in-service, a method has been proposed by *Paereli et al. (2016)*. This paper aims at validating this method but also discussing its practical use.

2. Method validation and data analysis

The proposed method for evaluating changes in propeller performance for a vessel in operation has a similarity with propeller open water test. Propeller efficiency in open water η_0 is given by:

$$\eta_0 = \frac{T \cdot V_a}{Q \cdot n \cdot 2\pi} = \frac{K_T \cdot J}{K_Q \cdot 2\pi}$$

J	non-dimensional advance coefficient, $J = \frac{V_a}{n \cdot d}$
K_T	non-dimensional thrust coefficient, $K_T = \frac{T}{\rho n^2 d^4}$
K_Q	non-dimensional torque coefficient, $K_Q = \frac{Q}{\rho n^2 d^5}$
ρ	mass density of water
n	propeller speed
d	propeller diameter
T	propeller thrust
Q	propeller torque
V_a	speed of advance of the propeller through the water

One could make use of the above equation and plot η_0 as function of J and see how this relationship varies in time. As mentioned above, speed of advance cannot be directly measured and therefore, it has been suggested that modified advance coefficient is used instead.

$$J_{mod} = \frac{V_S}{n \cdot d}$$

Then modified propeller efficiency becomes

$$\eta_{mod} = \frac{J_{mod} \cdot T}{2\pi \cdot n \cdot Q}$$

Here, unlike in the previous paper, J_{mod} and η_{mod} are dimensionless numbers.

For validating the method proposed in 2016, three different vessels have been chosen and for each of them averages of η_{mod} were computed over 22 equally spaced intervals of J_{mod} in the range 0 – 0.44. Furthermore, changes in modified propeller performance have been compared with changes in η_{mod} deviation computed using machine learning approach (see chapter 3).

All vessels are equipped with a data logger configured to save data at a frequency of 1/15 seconds and all the necessary parameters needed for computing η_0 (speed through water, propeller rpm, torque, thrust) are available for analysis. Furthermore, a set of parameters has been used for data filtering, so that changes in modified propeller performance are being tracked in comparable conditions. For this purpose, vessel loading condition, wind speed and direction are used. Data has been filtered only for 1 loading condition for each of the vessels and for low true wind speeds (<10 knots). Further the results for each of the vessels are discussed separately.

3. Machine Learning approach

As an alternative approach to quantify propeller performance, machine learning algorithms together with a similar methodology in ISO-19030 was used. Machine learning algorithms were tested in order to develop a model for predicting η_{mod}. If modified propeller performance can be predicted with a high level of accuracy, the deviation in η_{mod} ($\eta_{mod,dev}$) in time can be computed and compared with changes in measured η_{mod} obtained using the above described method.

$$\eta_{mod,dev} = \frac{\eta_{mod,obs} - \eta_{mod,exp}}{\eta_{mod,exp}}$$

$\eta_{mod,obs}$ – computed modified propeller efficiency
$\eta_{mod,exp}$ - predicted modified propeller efficiency using machine learning approach.

Assuming that best efficiency of the propeller is achieved immediately after a dry-dock, the first six months were used as a training set to develop the machine learning model and "learn" the $\eta_{mod,exp}$. Modified propeller efficiency was calculated with the same formula as above.

As inputs (features) in the model draft, shaft power, wind speed and speed through water were used. Three different machine learnings algorithms were tested. Random Forest (RF), Gradient Boosting (GB) and Artificial Neural Networks (ANN) were selected and the one with the best metrics in terms of mean absolute error(MAE), root mean squared error (RMSE) and R square (R^2) was chosen. In addition, k-fold validation methodology was applied in order to avoid overfitting. In all three cases that were tested RF algorithm was producing overfitted models therefore disregarded. GB and ANN algorithms produced similar results. For simplicity reasons, no hyper-parameter adjustments were performed as achieved accuracy was good enough for the purpose of this paper.

Based on the findings, similar results were achieved with both GB and ANN. This could be explained by the fact that selected vessels do not have significant changes in their operational profile throughout the periods used in this analysis. Therefore, GB provides slightly better and faster results as vessel continues to have the same operational pattern.

3.1. Vessel 1

The first vessel exemplified in this paper is a 230,000 DWT ore carrier which has been in a fixed trade between China and Australia for about 20 months. After checking with the vessel operator, it was found that propeller has not been cleaned during the period with available data. At the same time, a visual inspection of the above-water hull area has been performed after 18 months in operation when vessel was in ballast. Inspection showed that there were no significant paint damages and that paint was in good condition with no signs of any type of marine fouling.

Fig.1 compares 1 modified propeller efficiency, thrust coefficient, torque coefficient and the ratio K_T/K_Q over four consecutive periods of 5 months. For a better view, the same modified propeller efficiency is represented in Fig.2. It can be observed that η_{mod} is steadily decreasing in time. The biggest gap in modified propeller efficiency over the whole range of J_{mod} is between period 1 and period 4. At the same time, no changes are observed in torque coefficient if comparing periods 1, 2 and 4 while thrust coefficient is visibly decreasing. This observation is in good agreement with what has been concluded in the previous paper for 319,000 DWT tanker but opposite of what was described by *Mosaad (1986)*.

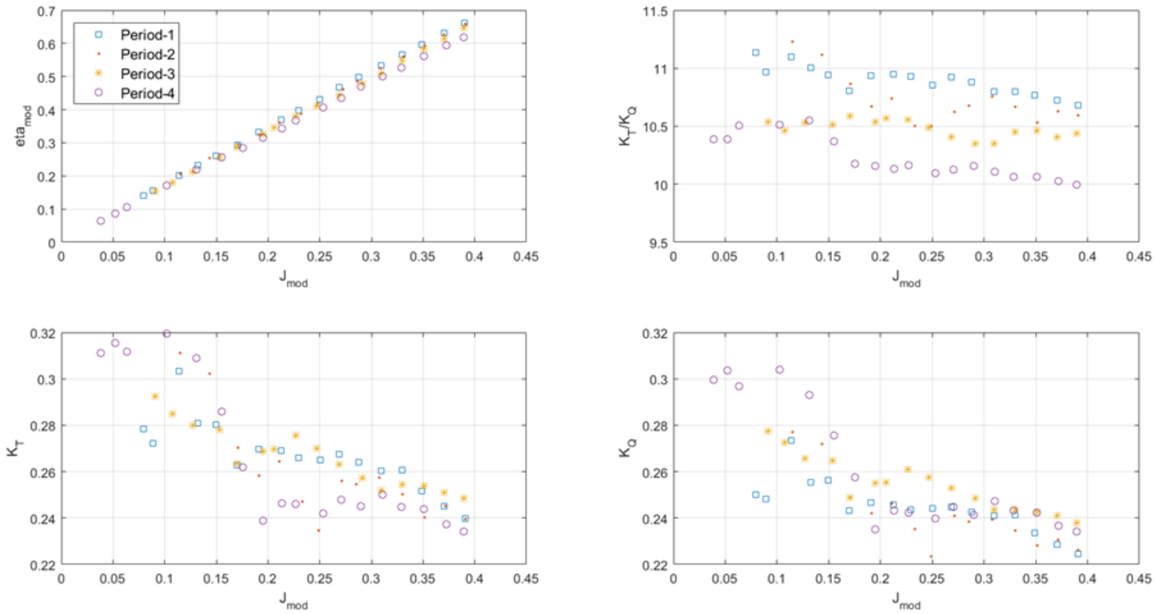

Fig.1: Modified propeller efficiency, thrust and torque coefficients, and the ratio K_T/K_Q as function of modified advance number over 4 consecutive periods (length of each period – 5 months)

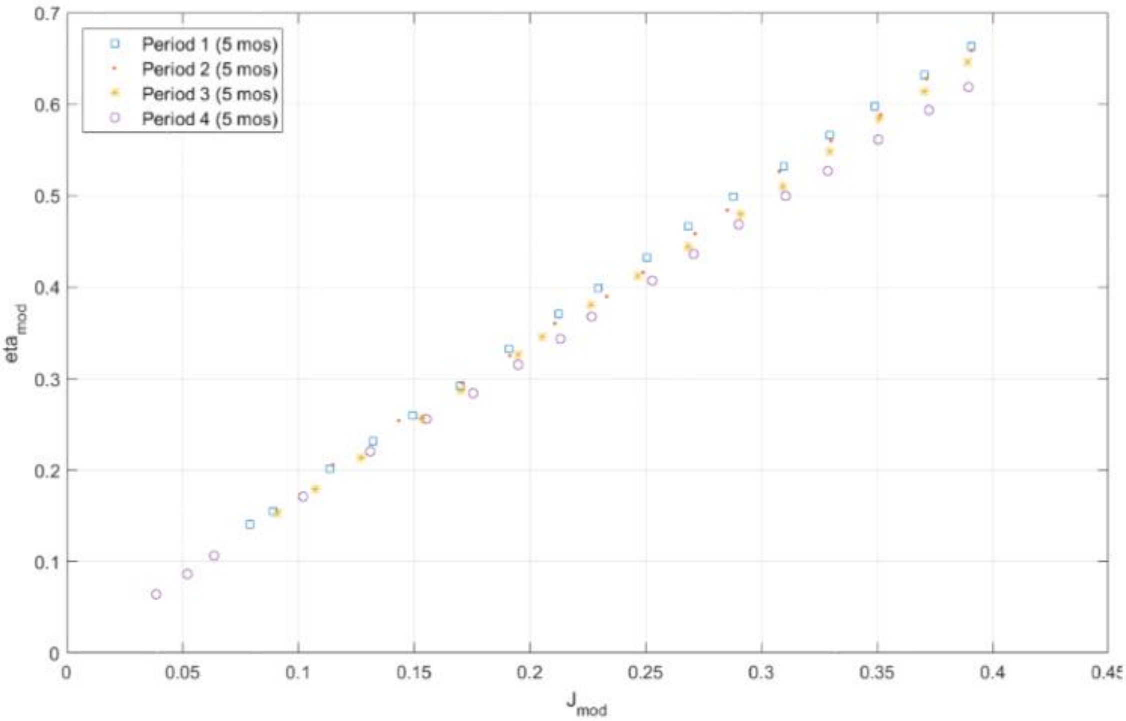

Fig.2: Modified propeller efficiency as function of modified advance number over 4 consecutive periods (length of each period – 5 months)

For quantifying the differences in η_{mod}, a 4th degree polynomial function has been fitted through the points of each dataset and the integral of that function has been calculated over the J_{mod} range 0.05-0.4. Table I shows the % difference between integrals, reference point being the value in period 1.

Table I: Difference between the areas under each of the fitted curves

Period	Difference in integral value [%]
1	0 (period 1 is taken as reference)
2	-1.1%
3	-3.6%
4	-6.4%

Similar trends have been obtained with machine learning approach where a GB algorithm was used to calculate propeller efficiency deviation. Time series of $\eta_{mod,dev}$ are shown in Fig.3. With this approach, a downward trend in $\eta_{mod,dev}$ is observed and this is as expected considering the fact that propeller is known not to be cleaned throughout the period with available data.

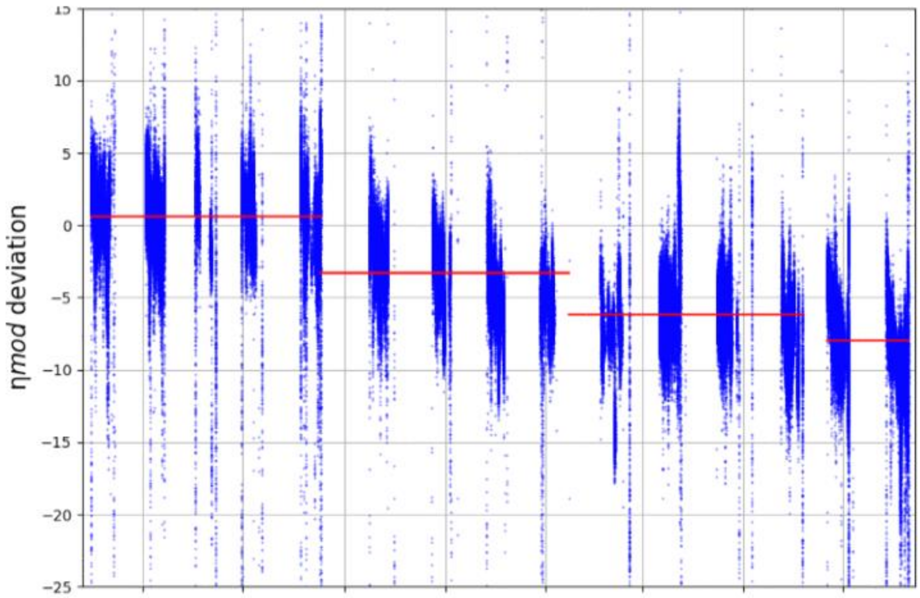

Fig.3: Time series of modified propeller efficiency deviation and its averages over 4 consecutive periods (length of each period – 5 months)

Table II: D Differences in the average of $\eta_{mod,dev}$ (1st period taken as reference)

Period	Difference in $\eta_{mod,dev}$ averages
1	0 (period 1 is taken as reference)
2	-3.9%
3	-6.8%
4	-8.6%

The changes in $\eta_{mod,dev}$ have been further quantified by calculating its averages over the same four consecutive periods. The differences in these averages are presented in Table II. If comparing results from Table I and II, one could see a similar trend in propeller degradation. Nevertheless, the differences in values are not similar and this could be explained by the fact that changes in propeller performance have been quantified in different terms, as a ratio of power values in the 1st approach and as deviation in this ratio in the 2nd approach.

Concluding what has been said above, the decrease in P_T/P_D and increase in $\eta_{mod,dev}$ throughout a 20-month period is mostly due to changes in propeller performance. Nevertheless, it should be mentioned that changes in η_{mod} and $\eta_{mod,dev}$ might not be related solely to changes in propeller performance but also minor changes in hull performance, such as for example changes in physical hull roughness. This is further discussed in chapter 4.

3.2. Vessel 2

Vessel 2 is a 290,000 DWT ore carrier from which all the necessary parameters have been collected over a period of 30 months. This was an interesting case for analysis since it was known that according to the operator policy, propeller has been cleaned every 3 months. For assessing changes in modified propeller performance, averages of P_T/P_D ratio have been calculated over consecutive 3-month periods. Results are represented in Fig.4. Note that in one of these periods only a few data points remained after filtering and therefore period was disregarded.

Fig.4 shows that modified propeller performance is quite stable in time. Some minor differences can be spotted, somewhat higher variations being at higher J_{mod}. These differences can be explained by the fact that data was not filtered for wind (no signal has been received from anemometer over the whole period) but also some minor changes in draft and trim. Nevertheless, differences in η_{mod} for this ore carrier over 27 months are negligible in comparison with changes in the same parameter for vessel 1 over 20 months. This could be concluded after fitting a 4th degree polynomial through each of the data sets and calculating the actual change in η_{mod} in time. Differences in modified propeller performance are represented in Table III, reference value being the average of η_{mod} over all the periods and over J_{mod} range 0.1-0.35.

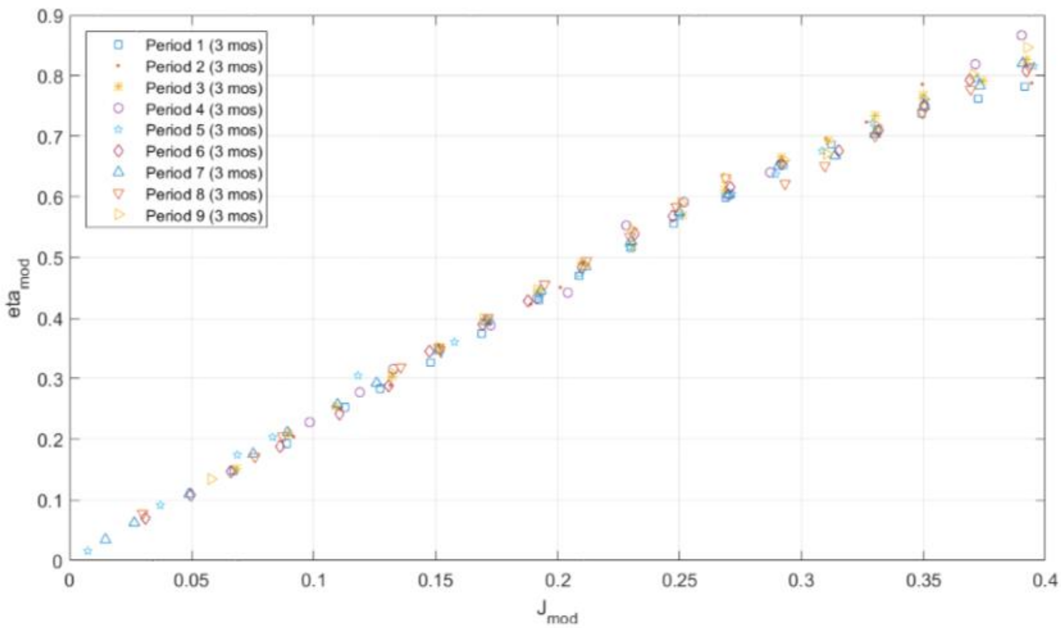

Fig.4: Modified propeller efficiency over consecutive 3-month periods

Table III: Variation in η_{mod} from the mean

Period	1	2	3	4	5	6	7	8	9
Diff. in integral value	-2.1%	0.1%	0.5%	1.2%	-0.1%	-0.3%	-0.4%	0.07%	1.4%

The obtained results have been further compared with differences in $\eta_{mod,dev}$ computed by using machine learning approach. As before, GB algorithm has been used to train the model over the first six months and thereafter predict the expected η_{mod} throughout the whole period. The deviation in modified propeller performance is then calculated and plotted in Fig.5. No significant changes in $\eta_{mod,dev}$ could be observed. The trend in both η_{mod} and $\eta_{mod,dev}$ is found to be similar and stable in time, and this is in good agreement with the propeller cleaning policy.

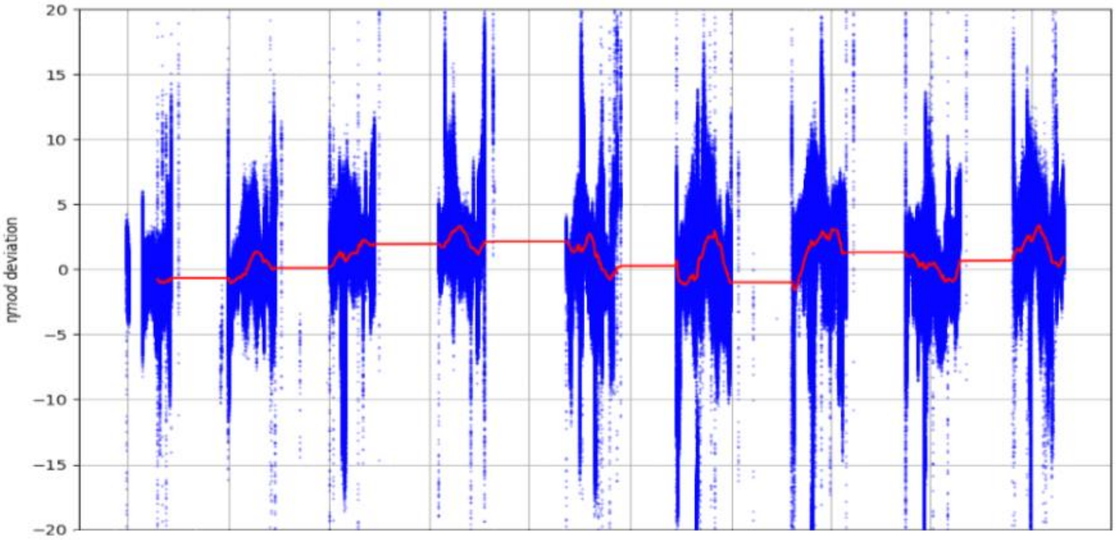

Fig.5: Time series of modified propeller efficiency deviation

3.3. Vessel 3

This is a 10,000 TEU container vessel which is sailing between China and Europe. During the period with available data vessel entered dry-dock when paint system was renewed but also propeller upgraded with a PBCF. It is to be noted that when vessel entered dry-dock the condition of the underwater hull area has been concluded to be very good. In Fig.6 the average modified propeller efficiency is shown for two periods – three months before dry-docking and 3 months after leaving dry-docking. A significant difference between these two periods in terms of average η_{mod} could be spotted.

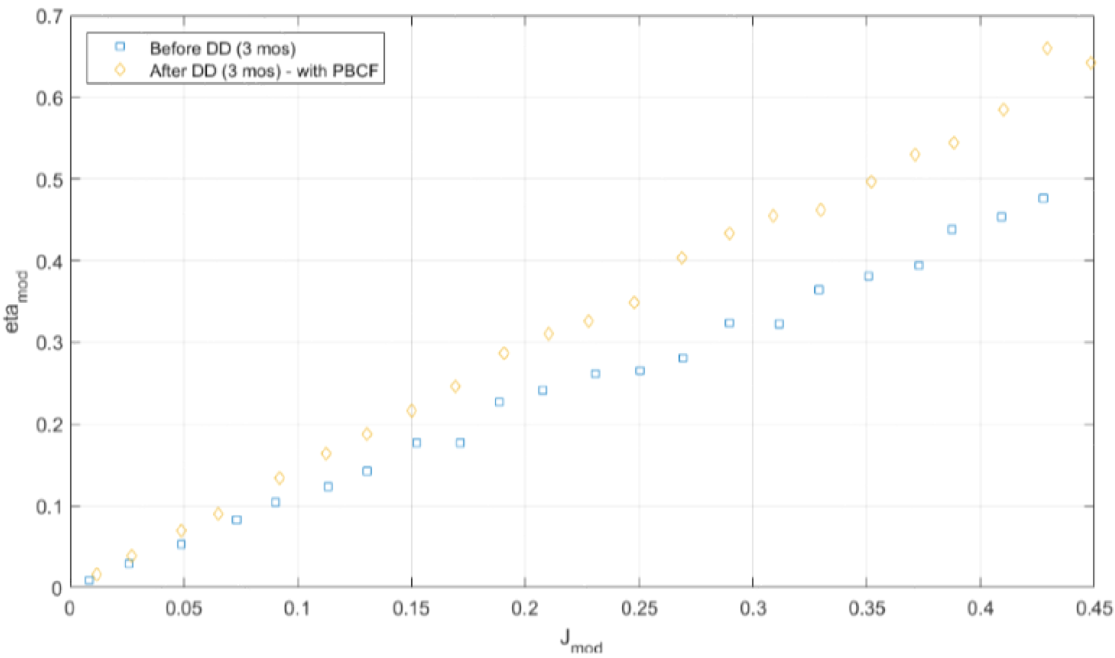

Fig.6: Modified propeller efficiency before and after DD (with upgraded propeller)

As mentioned before, the observed difference in computed modified propeller performance is most probably not attributed only to changes in propeller roughness but also some changes in hull roughness. For approximating the impact of the PBCF installation on the improvement in propeller efficiency, a similar approach as for vessel 1 and 2 has been used. A 4th degree polynomial function has been fitted through the points of each dataset and then the area under each curve calculated over the J_{mod} range

0.05-0.4. The difference in these areas is the average improvement in η_{mod} and the results are presented in Table IV.

Table IV: Difference between the areas under each of the fitted curves (vessel 3)

Period	Difference in integral value
Before dry-docking	0 (period 1 is taken as reference)
After dry-docking	+31.6%

The effect of PBCF installation has been quantified also using the machine learning approach. The deviation in η_{mod} is plotted in Fig.7. It could be observed that upon dry-docking there is a significant improvement in $\eta_{mod,dev}$. If taking the difference between average $\eta_{mod,dev}$ over three months before dry-docking and three months after dry-docking, a 34% increase in this performance indicator could be concluded. Just as before, the trend in both approaches is very similar and as expected. Nevertheless, one should consider that condition of the hull upon vessel dry-docking has also been improved and therefore some other references would be needed to understand what can the impact of hull improvement on the overall η_{mod} increase be.

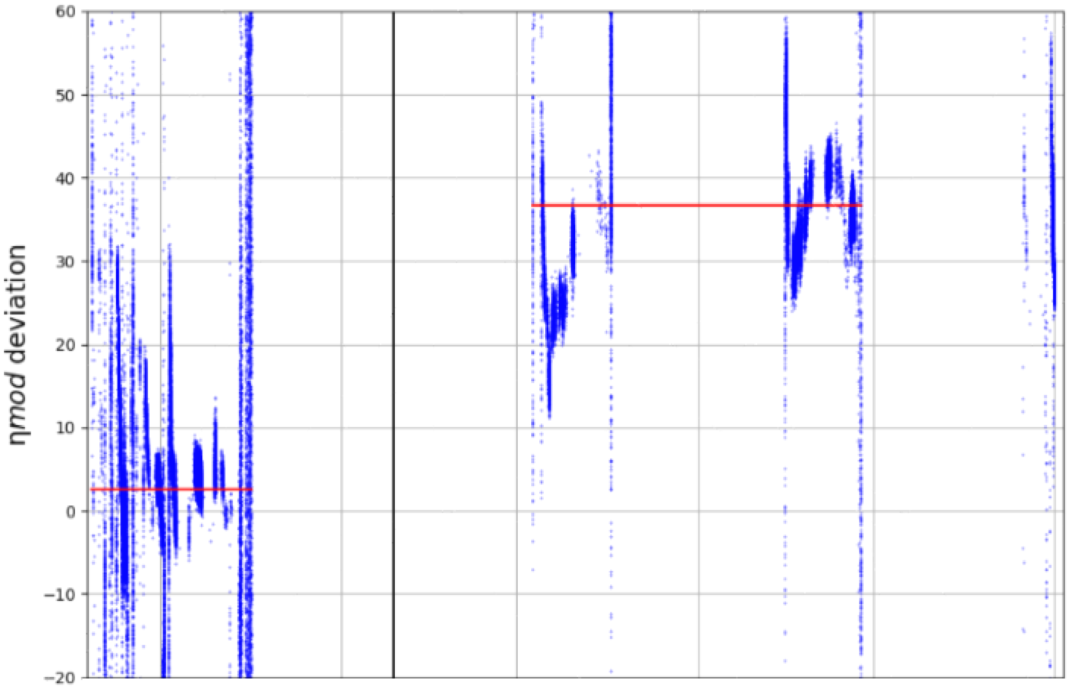

Fig.7: Time series of modified propeller efficiency deviation before and after dry-docking (black line). Red lines – average $\eta_{mod,dev}$ in each of the periods.

For this purpose, another two vessels (A and B) have been chosen. For both vessels data before and after dry-docking was available, in both cases hull condition has been concluded to be very good before high pressure filtered water (HPFW) washing and in none of these cases any propeller efficiency enhancement devices were installed.

Modified propeller efficiency for vessels A and B are plotted in Figs.8 and 9 and the difference between η_{mod} after dry-docking and before dry-docking are summarized in Table V.

Table V: Difference between the areas under each of the fitted curves (vessels A and B)

	Vessel A	Vessel B
Period	Difference in integral value [%]	
Before dry-docking	0 (period 1 is taken as reference)	
After dry-docking	+11.9%	9%

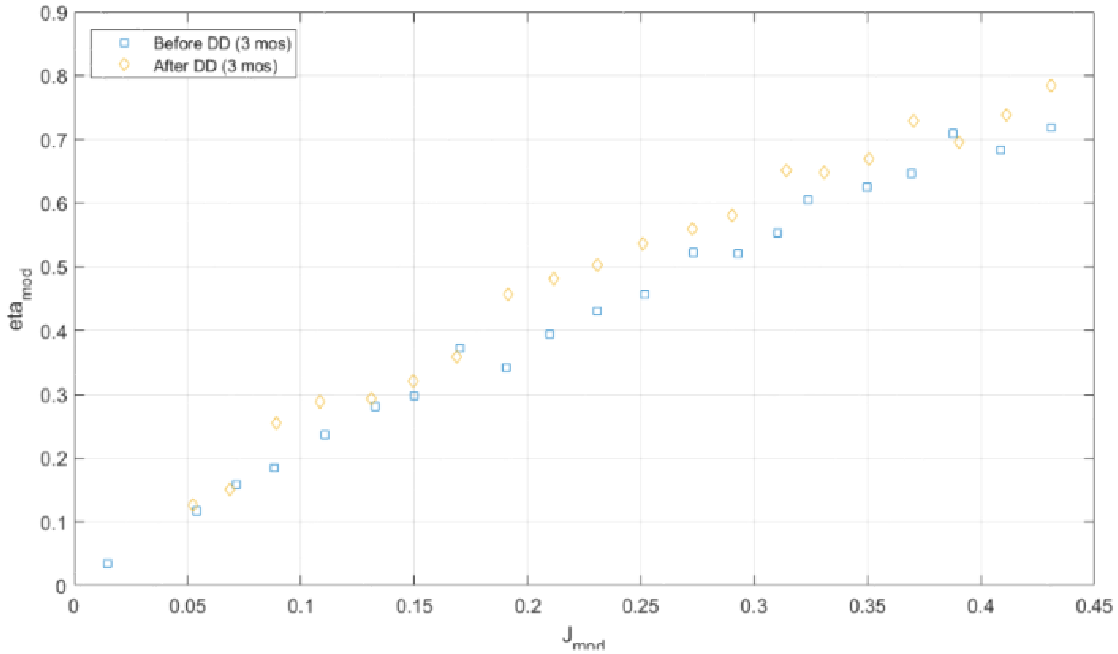

Fig.8. Modified propeller efficiency before and after DD for vessel A (without propeller upgrade)

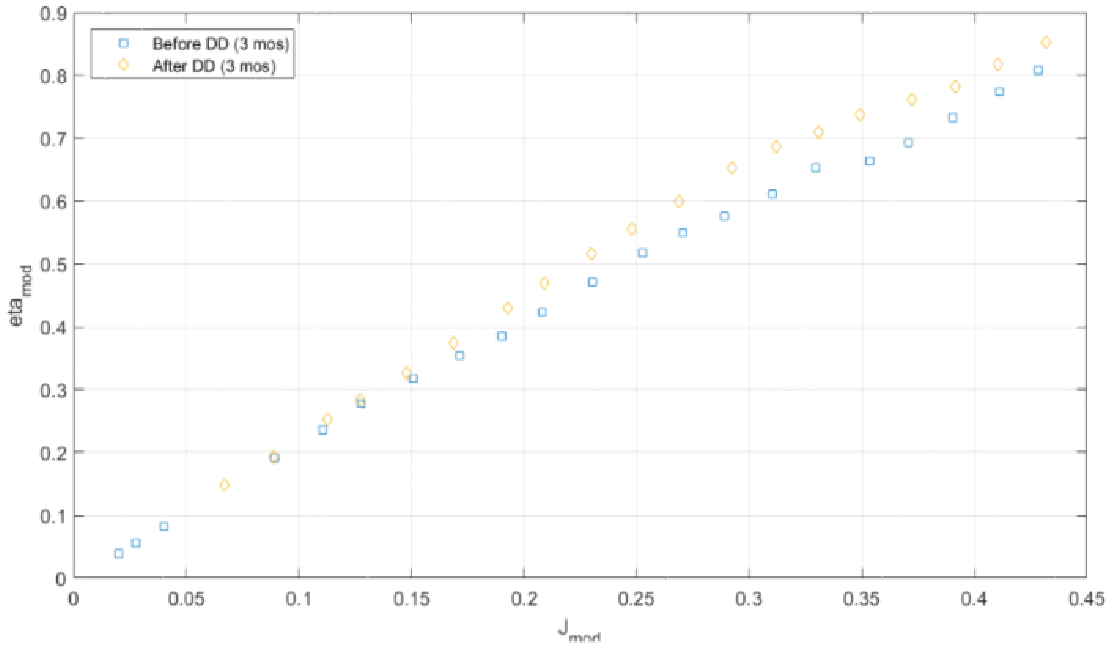

Fig.9. Modified propeller efficiency before and after DD for vessel B (without propeller upgrade)

One could easily spot that upon dry-dock η_{mod} of both vessel A and B increases. However, as mentioned in Table V, this average increase in modified propeller efficiency is ~10.5% – much smaller than for vessel 3. This brings to the idea that installation of PBCF on vessel 3 accounts for about 20%.

4. General discussion

The above analysis had as an initial assumption that speed of advance is equal to vessel speed through water. In other words, this would mean that wake was taken out of the equation which is the same as assuming that it does not change in time. Nevertheless, wake is an important component especially when there are changes in hull efficiency in time. This is because propeller is operating in a wake field behind the hull and its performance is influenced by the flow of water along the hull surface. If there are significant differences in hull roughness in time, wake field will undergo changes and as a result the velocity of water arriving to the propeller will be lower. This might lead to lower propeller efficiency. In all the exemplified cases in this paper, visual inspections of the either above-water hull area (vessels 1 and 2) or the under-water hull area (vessels 3, A and B) were done. It has been documented that hull condition was good in all the cases and neither significant mechanical damages nor any type of marine fouling was found. Assuming that this analysis is fairly accurate, it is now important to conclude whether there is any practical use of this approach.

When trying to split hull performance from propeller performance, it is obvious that one is after understanding what the influence of each of these components on the change in overall in-service performance is. It is therefore important that changes in propeller performance and changes in hull performance are computed in the same terms.

Since hull performance cannot be computed directly because of the unmeasurable effective propulsive power, one way of learning about changes in hull performance would be from changes in total hull and propeller performance and changes in propeller performance. However, the latter has been computed from a ratio of power values, while changes in total in-service performance are computed today either in terms of speed deviation or power deviation. One way to deal with this, would be to estimate changes in propeller performance also in terms of speed deviation.

For computing changes in hull and propeller performance, one would need first to know the ideal relationship between vessel speed and delivered power, Fig.11. Model test results or speed trial results can help in this sense. Alternatively, speed-power relationship could be found from collected performance data. Further, thrust-power relationship would be needed, so that it is possible to compute the expected delivered power ($P_{exp,T}$) for a certain measured thrust (T_m), Fig.10. When this is found and given that speed-power relationship is known, expected speed for a certain measured thrust ($S_{exp,T}$) can be computed. This expected speed could then be compared with measured speed (S_m) and the expected speed ($S_{exp,P}$) from measured delivered power (P_m).

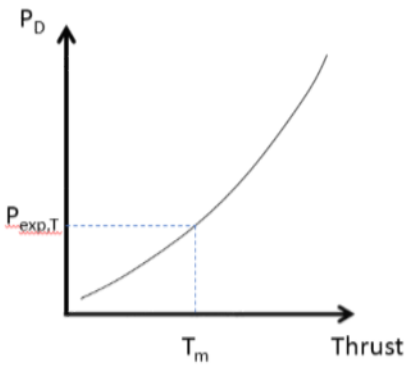

Fig.10: Thrust-power relationship

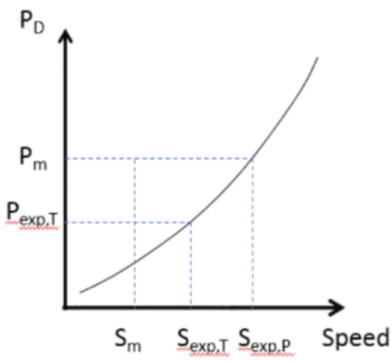

Fig.11: Speed-power relationship

If one would manage to isolate now the efficiency of the propeller in terms of speed deviation, it would be possible to subtract this from the combined hull and propeller efficiency and therefore compute hull efficiency. Nevertheless, the isolation of propeller efficiency is not as easy as one would think at first glance.

Assuming that speed, thrust and power are accurately measured and that accurate thrust-power and speed-power relationships are established, it is possible to compute the expected speed at a certain measured thrust. Three scenarios can be discussed further in terms of what happens to the expected speed from measured power and measured speed.

If neither hull roughness nor propeller roughness change in time then P_m=$P_{exp,T}$ and S_m=$S_{exp,T}$=$S_{exp,P}$.

If propeller roughness changes in time while hull roughness is stable, then power would need to be increased for reaching the same thrust level as before. This would also mean that $S_m = S_{exp,T}$ and that $S_{exp,P}$ is higher than $S_{exp,T.}$ One could also compute speed deviation due to changes in propeller performance (SD_p):

$$SD_p = \frac{S_{exp,T} - S_{exp,P}}{S_{exp,P}}$$

Things become more complex when hull roughness starts changing in time as well. When there are changes in the surface character of the hull, velocity of water arriving at the propeller becomes lower. Shaft power would need to be increased for the propeller to develop the same thrust level, and, at the same time, for the same thrust delivered by propeller vessel will reach a lower speed. This would mean that $S_m < S_{exp,T}$ and $S_{exp,T} < S_{exp,P}$ and the bigger the change in hull roughness is, the higher the difference between the three speeds will be. It becomes obvious now that one could not compute speed deviation due to changes in propeller efficiency with the same formula as before. It also seems to be impossible to measure changes in hull performance and changes in propeller performance separately in the same terms if wake is not known.

5. Summary

A method for tracking changes in propeller performance has been proposed and validated on several vessels. Vessels have been chosen such that their propeller has been either confirmed not to be cleaned during a prolonged period (vessel 1), or propeller has been regularly cleaned (vessel 2), or propeller has been upgraded (vessel 3). Analysis of each set of data has shown that it is indeed possible to capture differences in the surface character of the propeller but one should be very careful when doing this. The uncertainties of this method are strongly dependant on such factors as: accurate measurements of thrust, torque, speed, and also changes in the surface character of the hull.

Changes in propeller performance have also been quantified and results cross-checked with changes in propeller performance deviation computed using machine learning approach. Good consistency in results could be found. Nevertheless, the method validated in this paper appears not to have a big practical use in computing hull performance. This is because changes in propeller performance are not being measured in the same terms as changes in the combined hull and propeller performance. On the other hand, method provides a good overview on how propeller efficiency in terms of ratio of powers (P_T/P_D) can change in time if propeller is not being cleaned systematically or if propeller is being upgraded. It has been shown that P_T/P_D ratio can be increase by about 20% if upgrading the propeller with a PBCF. Analysis of two datasets have also indicated that the apparent propeller efficiency can be improved by about 10% if performance of hull increases (e.g. after a dry-dock).

References

MOSAAD, M.A. (1986), *Marine propeller roughness penalties*, PhD Thesis, University of Newcastle

PAERELI S.; KRAPP A.; BERTRAM V., (2016), *Splitting propeller performance from hull performance – A challenge*, 1st HullPIC, Pavone

From Measurement to Understanding, Insight and Decision

Anders H. Møller, Insatech A/S, Præstø/Denmark, anmo@insatech.com

Abstract

The paper describes our perception of how to turn measurements into a suitable base for a business decision. The example could be a flow measurement, on its own a meaningless value, but combined with information about the particulars of the pump, circulating the fuel that goes through the flow meter, we could at least say if it is a plausible value. Then we would compare the inlet flow with the outlet flow to get a consumed amount of fuel, which could again be compared to threshold values to see if it makes sense. That consumption would then be compared to the power production of the engine and the specific consumption compared to the engine particulars and so on. The fundamental idea is to identify issues with measurements, determine the source of the error and take action to rectify the error or mitigate the effect of the error until it can be rectified so that the data can be used in performance calculations.

1. Introduction

There are many ways to measure any given parameter, some are more robust and reliable, others are cheaper and simpler. In each case a compromise is made, and an instrument is chosen and installed. Regardless of the chosen measurement principle, the quality of the instrument and the precision of the installation, the measurement is often a near meaningless value on its own. For the measurement to add any value it must be put into context, compared to a baseline, validated and analyzed.

In the following it is assumed that the flow meter measurements are within negligible margins of the true flow (0.1 % of full scale, http://www.rotamass.com/files/Rotamass%20TI%20Brochure.pdf) but rendered inaccurate or even useless due to external factors. The data is analyzed to determine what the external factor(s) may be and how validations may be set up to identify recurrence of the same external factor and to trigger a warning.

2. Flow meter setup

In a common three flow meter setup, there is one common flow meter for the main propulsion engine and all generator engines, combined with a common inlet flow meter for all generator engines and a common outlet flow meter for all generator engines.

There are several ways that the calculated consumption based on these accurate measurements may be negatively impacted by defects and behavior.

2.1. Three flow meter setup

Fig.1 shows a simplified schematic of a common three flow meter setup. There are several important components missing from the schema compared to an actual installation, but these not relevant for the cases and have therefore been intentionally omitted.

2.1.1. Normal operation

Fuel flows from the service tank to the supply pump. The supply pump pumps the fuel through the common flow meter for main engine and generator engines. The fuel is now in the circulation loop and the only way that it leaves from here is through consumption by the main engine or the generator engines. The flow through the common flow meter is equal to the consumption of the main engine plus the consumption of the generator engines.

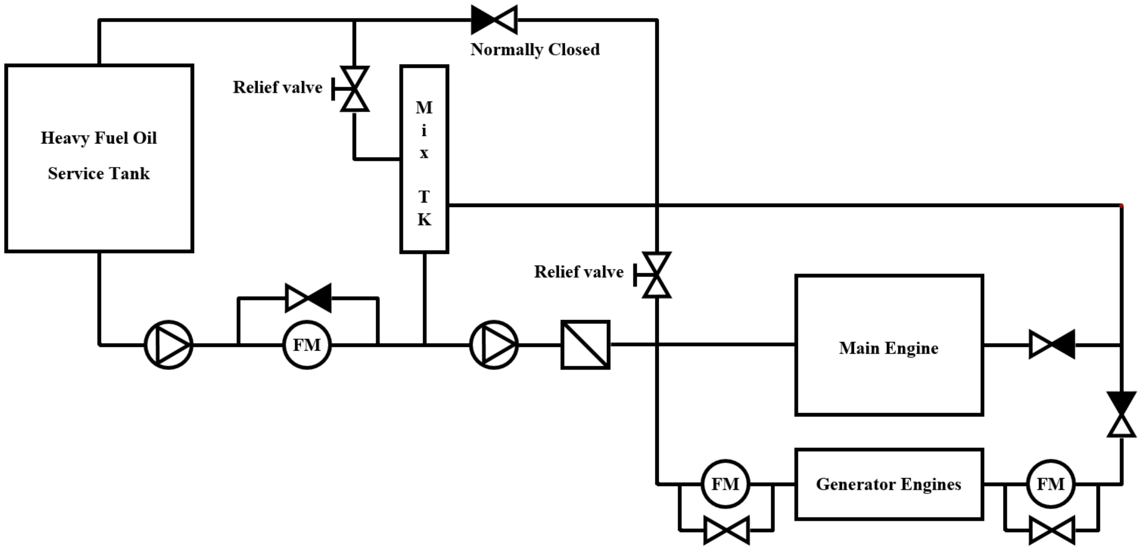

Fig.1: Common three flow meter setup

To separate the two consumers, two additional flow meters are fitted, one measures the inlet to the generator engines and the other the outlet. Subtracting the outlet flow from the inlet flow gives the generator engines consumption. The inlet and outlet flow meters are placed in the circulation loop and therefore measures a much higher flow than the consumption of the generator engines.

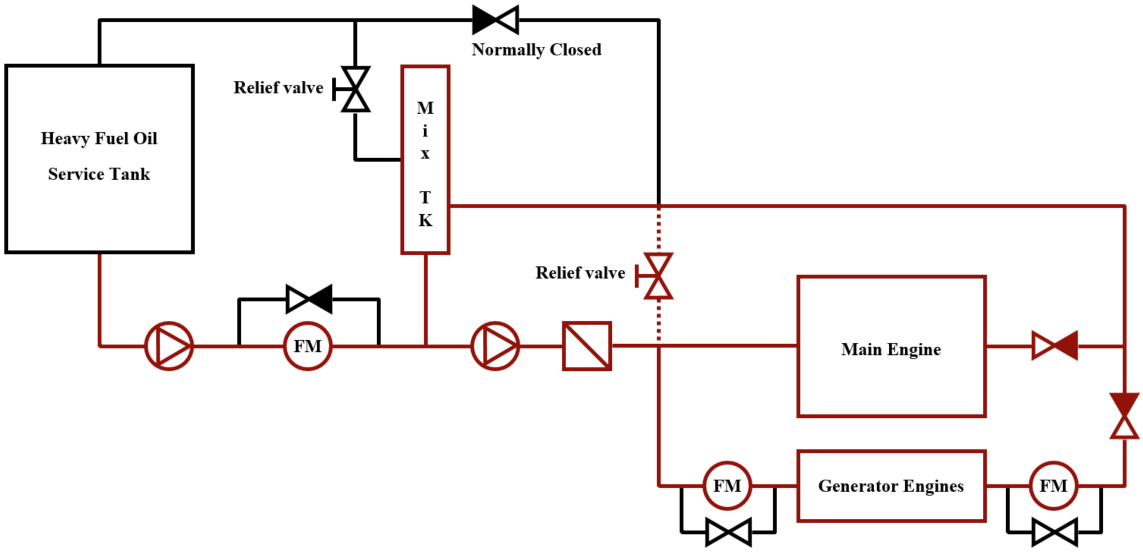

Fig.2: Flow measurements; Generator engines inlet flow: Stable throughout the period; Generator engines outlet flow: Drops for about half an hour; Common main engine and generator engines flow: Increases for about half an hour

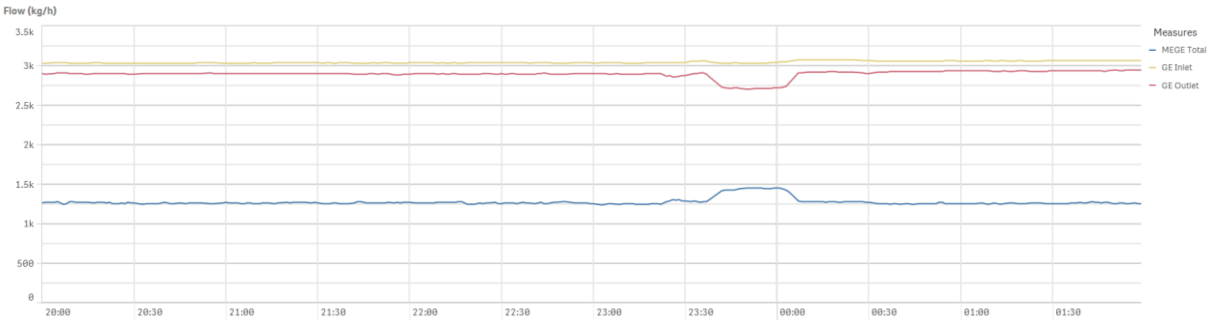

Fig.3: Main engine consumption; expect stable main engine consumption throughout the period.

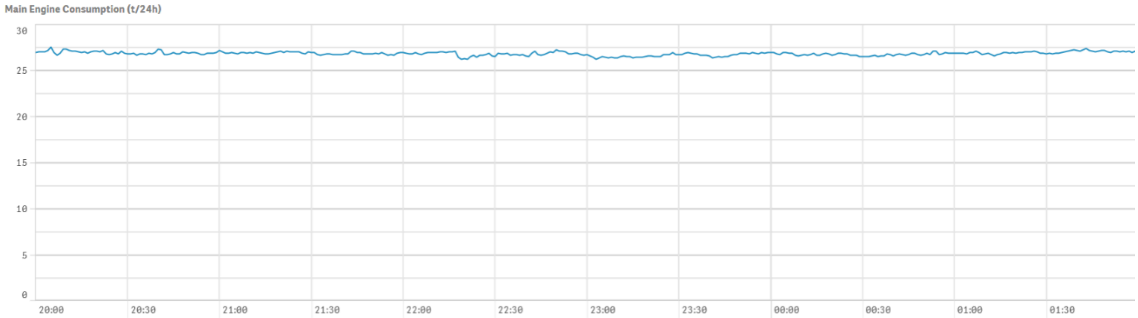

Fig.4: Generator engine consumption; expect that generator engines consumption increases for ~½ h.

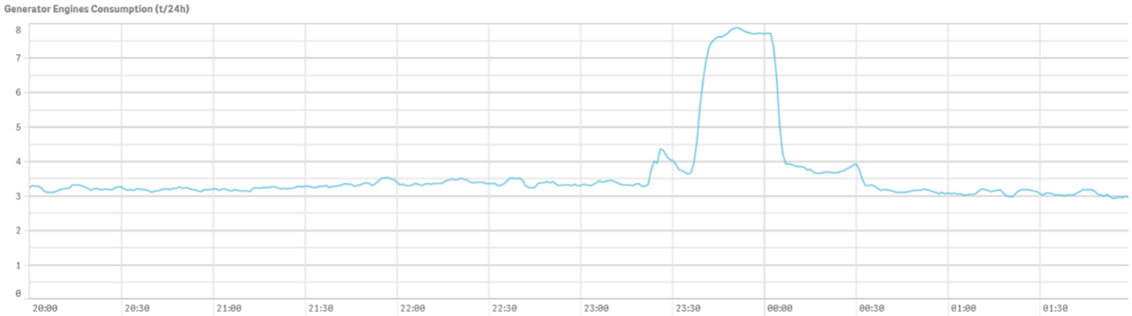

Fig.5: Generator engines load; expect increased load on generator engines for ~½ h.

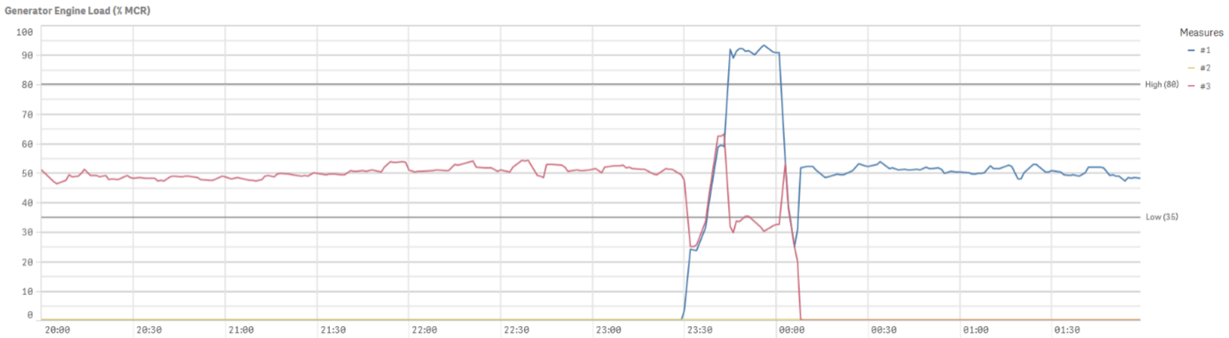

Fig.6: Generator engines specific fuel oil consumption (SFOC [g/kWh])

Fig.7: Generator engines specific fuel oil consumption (SFOC [g/kWh])

Fig.6 shows the generator engines SFOC. We expect to see the following:

- Increase prior to generator engine (GE) #1 taking load (during idle running)
- Increase while GE's #1 and #3 are running at low load in parallel
- Decrease while GE's #1 and #3 are running at load near design point (70% MCR)
- Increase while GE #1 is running high load and GE #3 is running low load

- Increase while GE #1 is off loading to GE #3 and subsequently shut down
- Stable at same level as when GE #1 was running at a comparable load

Fig.7 shows a recording that deviates from this expectation. There appears to be a 15 g/kWh difference between GE #1 (235 g/kWh) and GE #3 (220 g/kWh) when running at comparable load.

In conclusion, the system appears to be running well and there is a good cause and effect correlation throughout. There is however the limitation that no pump particulars have been considered and there is a risk that e.g. the circulation flow is not what it is supposed to be. The flow is measured accurately, but if the circulation flow is designed to be 4.000 kg/h then there may be a performance issue on the circulation pump.

Similarly, it would have been tempting to conclude that the generator engines were running efficiently, if #1 and #3 had been measured at the same SFOC. As it were #3 was about 6% more efficient than #1, but that still did not mean that #3 was running efficiently, it could just as well mean that #3 was just running less inefficiently than #1. To determine whether the engine was running effectively, particulars from the engine testbed is needed and the consumption would have to be normalized for the lower calorific value of the fuel and the air pressure and temperature conditions.

2.1.2. Common flow meter bypass:

A flow meter is often installed with a bypass to allow continued operation in case a mechanical flow meter is blocked and to allow replacement of the flow meter without disrupting operation, Fig.8. Should this valve start leaking or be partially or fully opened unintentionally or intentionally, then the fuel that goes through the bypass will not be measured and the consumption that is calculated for the main engine will be lower than actual, giving the impression of better performance. It will of course also result in a ROB (remaining on board) discrepancy over time.

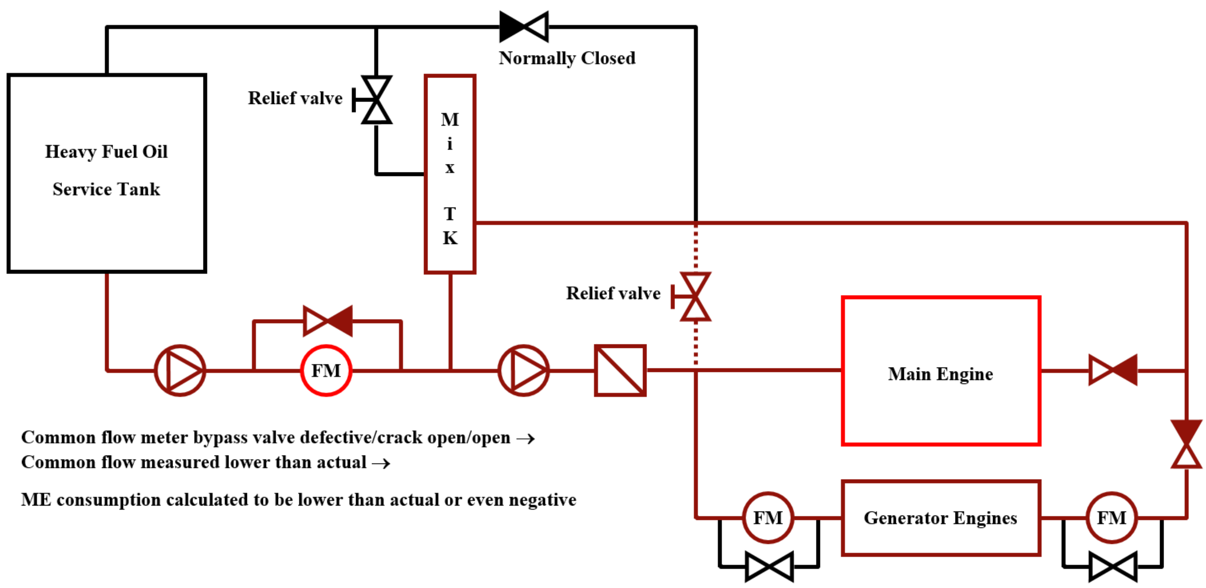

Fig.8: Set-up for situation in Ch.2.1.2

2.1.3. Generator engines inlet flow meter bypass

The generator engines inlet flow meter is similarly installed with a bypass, but fuel flow through this valve impacts the consumption calculation much differently. Firstly, it is placed in the circulation loop and is therefore measuring a much higher flow than the consumption of the generator engines. This means that a leak of a given quantity will have a much greater impact on the calculated consumption.

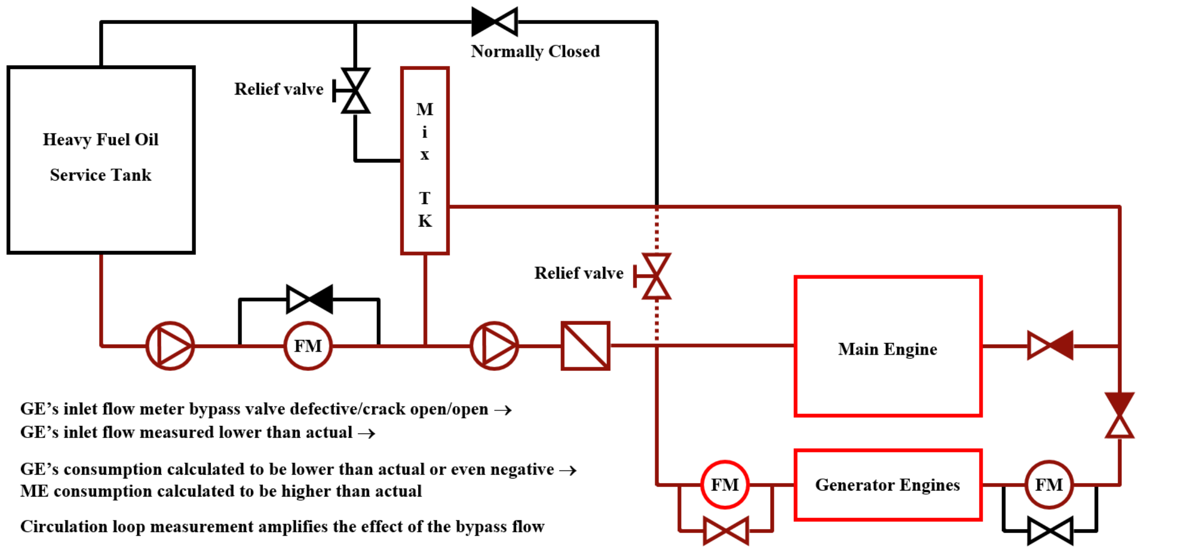

Fig.9: Set-up for situation in Ch.2.1.3

Flow measurements, Fig.10:

- The generator engines inlet flow meter measures a reasonably steady flow of 950 kg/h but drops to a steady 880 kg/h at some point.
- The generator engines outlet flow meter measures a steady 2550 kg/h but gradually drops to a steady 2150 kg/h around the same time that the inlet flow meter drops.
- The common flow meter measures a steady 160 kg/h throughout the period.

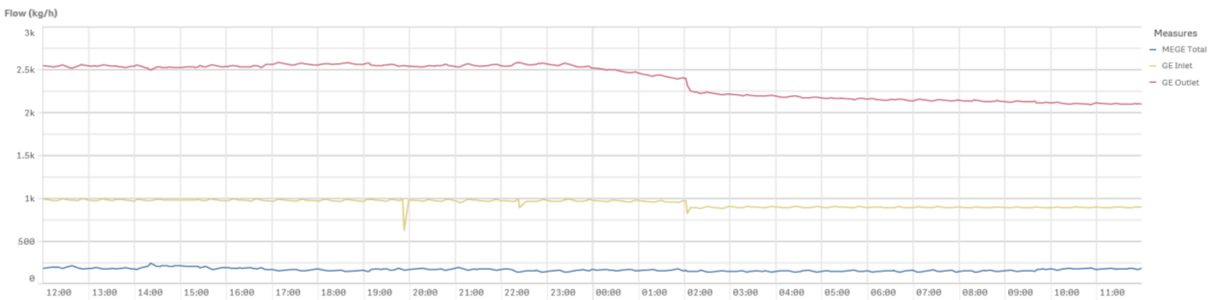

Fig.10: Flow measurements for inlet, outlet and common flow meter

As the main engine is not running the consumption can be assumed to be 0 kg/h and therefore it seems likely that the about 160 kg/h is consumed by the generator engines, but the inlet/outlet flowmeter indicate that the generator engines are producing 1300-1500 kg/h.

Assuming that the common flow meter measurement corresponds to the generator engines consumption when the main engine is not running, the Generator engines consumption in Fig.11 is calculated. The variations in consumption appears to be conspicuously cyclic.

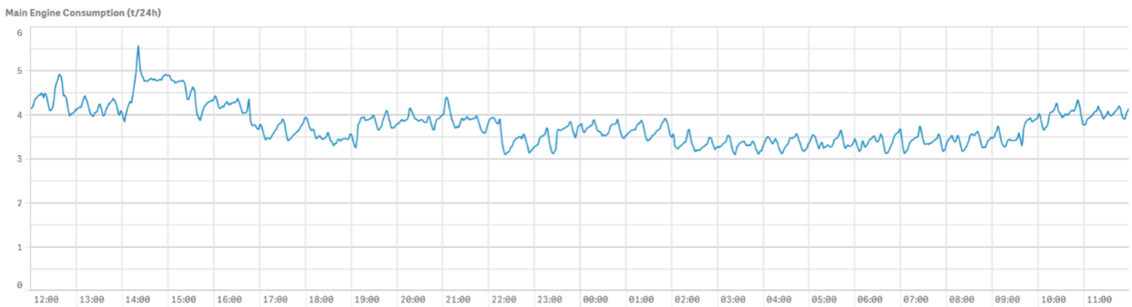

Fig.11: Generator engines consumption

Generator engines #1 and #3 are running in parallel at low load to begin with, but then #1 is stopped and #3 is running alone for the rest of the period, Fig.12. It turns out that the load is varying cyclically as well which appears to explain the variations in consumption.

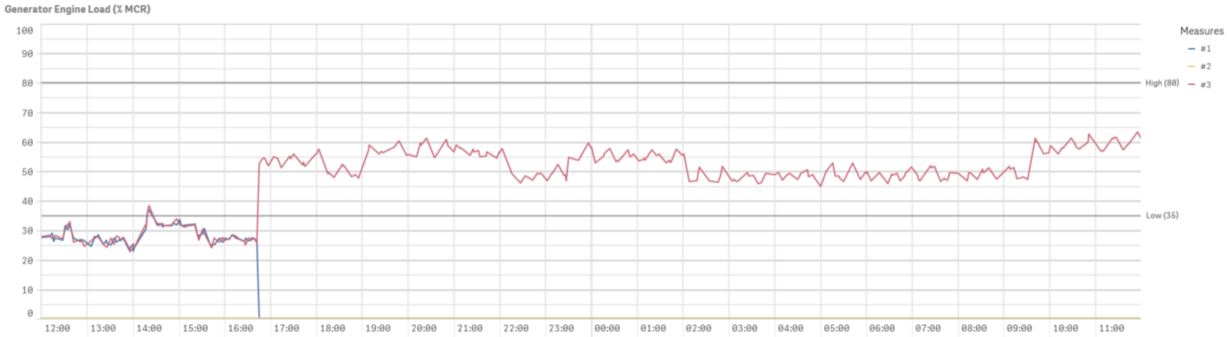

Fig.12: Generator engines load

We expect the generator engines SFOC to decrease when GE #1 is stopped and #3 loaded closer to its design point, Fig.13.

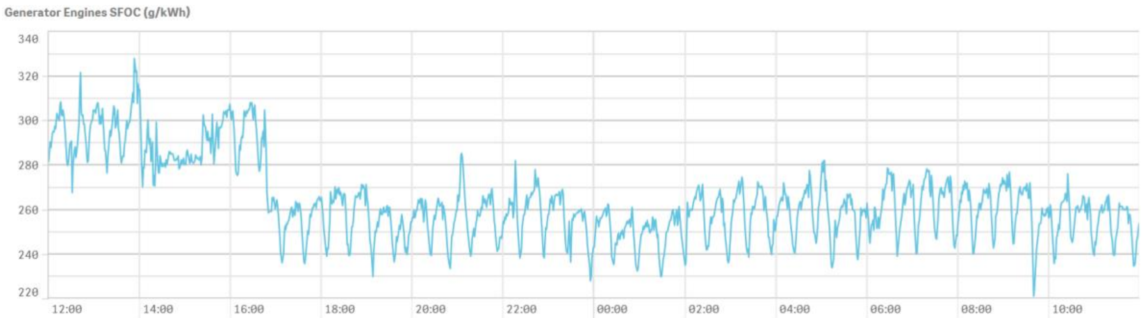

Fig.13: Generator engines SFOC

The load % MCR appears to have a significant impact on the SFOC, being about 290 g/kWh when running two generator engines at low load in parallel and dropping to about 255 g/kWh when stopping one generator engine and running one at higher load, Fig.14. Setting up a KPI for when an engine can be considered as running unnecessarily enables ranking of the vessels. The operational profile of the vessel will of course influence how much time the vessel is maneuvering in port where an additional generator engine may be kept running for safety reasons.

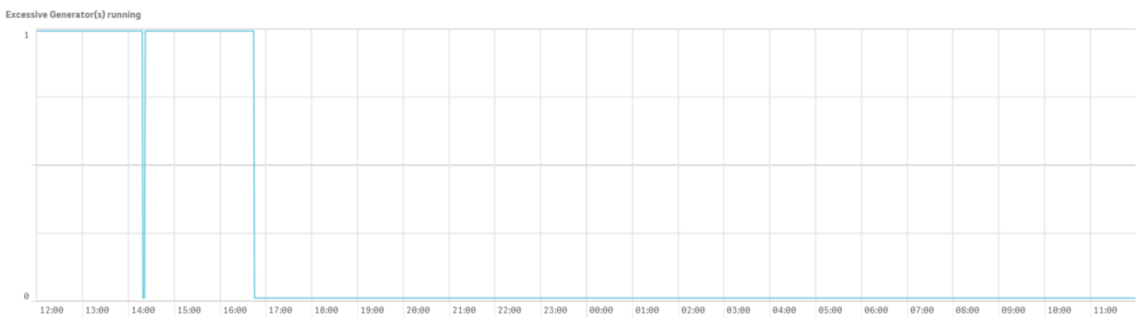

Fig.14: Effect of number of generators running

Both flow meters are isolated, and zero calibration carried out to ensure that they are measuring correctly. Following successful zero calibration, confirming that the flow meters were measuring accurately, both bypass valves were fully closed, Fig.15. In conclusion, the flow meters were measuring accurately throughout the period, but as the data was not being monitored, the open bypass valve remained undetected for an extended period. The crew was used to reporting consumption based on tank soundings and therefore did not report the zero consumption being calculated by the system.

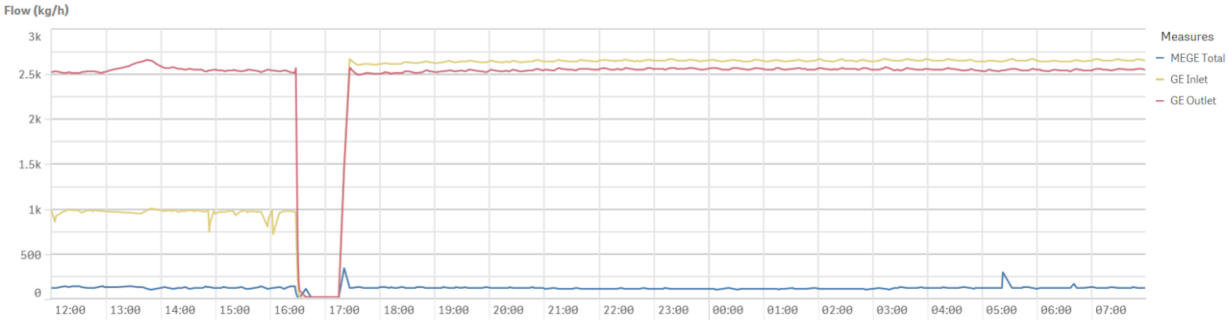

Fig.15: Effect of closing the bypass valve

2.1.4. Circulation loop pressure relief valve

When the pressure relief valve in the circulation loop fails, the fuel pressure becomes dependent on the combined consumption of the main engine and generator engines. The lower the consumption becomes the greater the pressure will be and eventually the high-pressure alarm will be triggered. One way to bring down the pressure is to open the normally closed valve between the circulation loop and the service tank. Throttling this valve, depending on consumption, allows the crew to maintain pressure in the circulation loop between the low and high alarm limits. The tradeoff of this workaround is of course that the common flow meter now accurately measure the amount of fuel consumed and circulated through the service tank.

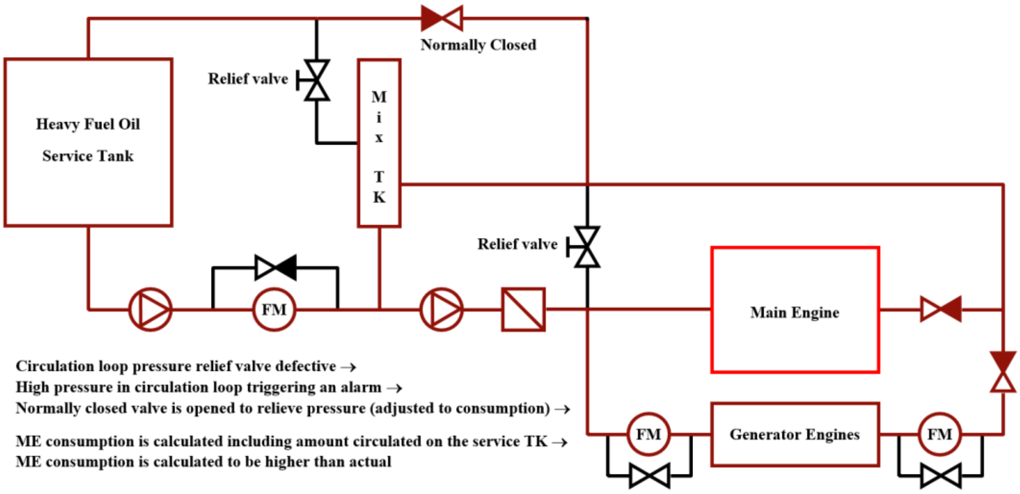

Fig.16: Set-up for situation in Ch.2.1.4

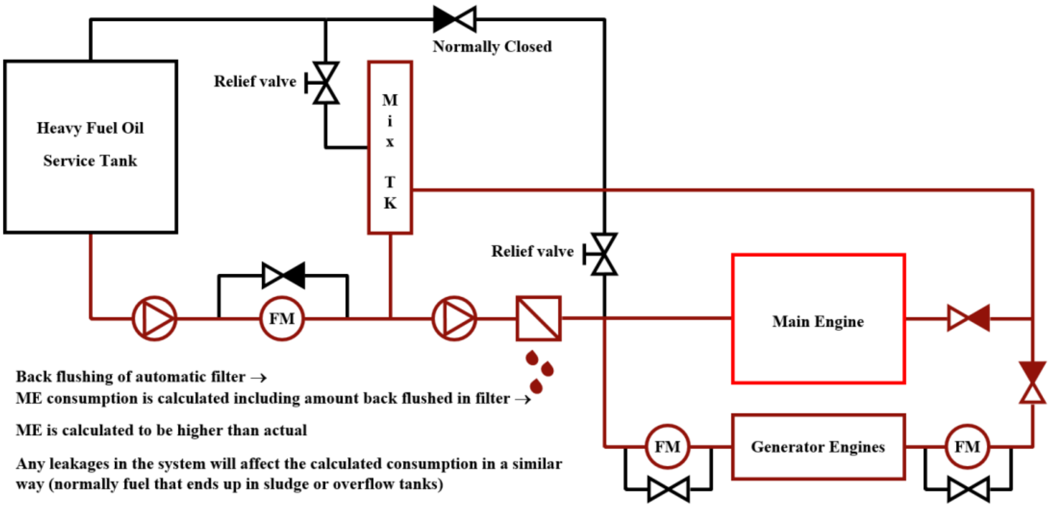

Fig.17: Filters and leakages

Automatic back flushing filters, drains and leakages have a similar impact, Fig.17, except that depending on where the fuel leaves the system, it will impact the consumption measurement in different ways. Any leakage between the generator engines inlet and outlet flow meters will make the consumption appear higher than actual and any leakages anywhere else in the circulation look will make the main engine consumption appear higher than actual.

3. Satellite positioning system and distance over ground

A satellite positioning systems that uses a given set of satellites, e.g. GPS, will generally, depending on the quality of the antenna, produce position fixes of equal accuracy. The way that these position fixes are processed may however vary significantly and the results calculated may vary significantly in quality.

There are usually several settings that the user may manipulate to improve the quality of the data derived from the position fixes, such as the length of time that is used when averaging data to calculate course over ground. If this averaging period is relatively short and the vessels is rolling significantly, then the calculated course over ground will become erratic. When the vessel is not rolling a relatively long averaging time will result in a delay in displaying the effect of maneuvers carried out.

The unit will also have some core calculations that the user has no control over, such as the way that distance over ground is calculated.

The distance over ground may be calculated in two ways:

1. Sum of distance between positions
   When the unit has two position fixes it calculates either the great circle distance or rhumb line distance between the two and adds these up over time. The time between positions is not considered

2. Sum of speed over ground
   Speed over ground is calculated when two consecutive timestamps have a position fix. If either the previous timestamp or the current timestamp does not have a position fix, no speed over ground is calculated.

When the dataset is complete, the distance over ground (DOG) is calculated as in Table I. When the dataset is incomplete the DOG is calculated as in Table II.

Table I: DOG for complete dataset

Timestamp	Position fix	Distance between positions	Speed over ground
00:00:00	Yes	0.03 nm	21.6 kn
00:00:05	Yes	0.03 nm	21.6 kn
00:00:10	Yes	0.03 nm	21.6 kn
00:00:15	Yes	0.03 nm	21.6 kn
00:00:20	Yes	0.03 nm	21.6 kn
00:00:25	Yes	0.03 nm	21.6 kn
DOG =		0.18 nm	0.8

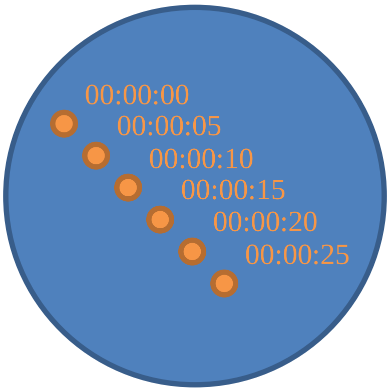

Table II: DOG for complete dataset

Timestamp	Position fix	Distance between positions	Speed over ground
00:00:00	Yes	0.03 nm	21.6 kn
00:00:05	Yes	0.03 nm	21.6 kn
00:00:10	No	-	-
00:00:15	Yes	0.06 nm	-
00:00:20	Yes	0.03 nm	21.6 kn
00:00:25	Yes	0.03 nm	21.6 kn
DOG =		0.18 nm	0.12

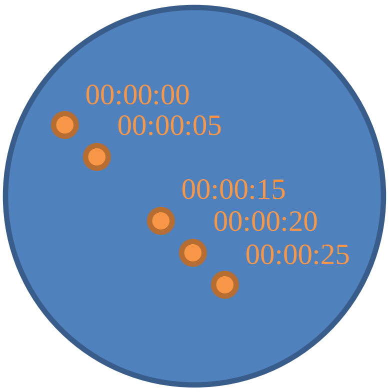

Skin Friction Database

Michael Leer-Andersen, Sofia Werner, Keunjae Kim, SSPA Sweden, Gothenburg/Sweden, mla@sspa.se

Abstract

Skin friction from vessels is responsible for 50-85% of the total resistance the ship must overcome to keep its speed. There is a theoretical lowest limit for how small this resistance can be on a very smooth surface, but the roughness is always larger than that on a vessel, even for newly build ship. It is therefore important from economical and environmental viewpoint to have an as smooth surface as possible. Today there are several databases linking coating and fouling to skin friction but none which covers all (or most) of possible surfaces seen on vessels. It is therefore difficult for shipowners and shipyards to decide which coating to use or how often the surfaces should be recoated or cleaned. The goal of the project is to increase the knowledge of rough surfaces efftect on skin friction and and create an accesible database.

1. Introduction

This paper will describe a method of estimating increased fuel consumption due to roughness on the wetted surface of the hull. The paper will not focus on details on measurements on rough surfaces or detailed predictions for full-scale ships. Instead it will discuss in some detail the different methods used. This will include measurement techniques used, description of measured surfaces (and the possibility to include measurements from other labs), model scale to full scale extrapolation methods, fuel consumption increase tool and additional investigation of skin friction on vessels and flat plate using CFD.

All these methods and tools are necessary to present the data in the homepage of the skin friction database. Skin friction due to rough surfaces is a difficult problem on vessels. In reality, laboratory measurements are necessary to obtain the skin friction, but from a hydrodynamical viewpoint the variation of surface roughness on vessel are immense, not to mention that only rarely can the entire vessel be considered be covered with the same roughness. This proposed method does not claim that the difficult nature of marine roughness can be solved with a very high degree of accuracy, but hopefully that better estimates becomes available for the ship owners to increase the confidence in decisions made for the treatment of a vessels surface.

The CFD approach offers the possibility solving the non-uniform roughness distribution, but is a time consuming and non-automated method. Still, in connection with this project an investigation of the use of CFD for skin friction on the plate and the full-scale ship have been included.

2. Skin friction database

The goal of the database is to collect SSPA's skin friction results along with several other laboratories results to present an easily navigable and interactive homepage. This homepage will be accessible publicly. Fig.3: shows the contents of the database. The graph shows the measured data in model scale in terms of C_F as a function of the Reynolds number. It is possible to change to a view where full scale (corresponding to the vessels full scale length) is shown as a function of increasing velocity calculated based on the model test results and the method described in section 0. This requires that the ship length is entered as a parameter.

Several other labs measurements will be adjusted to fit SSPA's measurements to make the database more complete which in the end will result in play 50 measurements. It is therefore possible to sort by laboratory, test equipment type and surface type. All selected measurements by the filters will show up as a list where the measurements can be deselected and a short description of any given measurement can be shown. A more comprehensive description with picture, roughness, k_s and other parameters can be selected as a pop-up window.

The bottom of the picture is dedicated to the fuel estimation as described in section 0. The parameters on the left must be filled in before the data can be presented.

The method assumes that the surface of the hull has the same surface condition on the entire wetted surface. This is often not the case. A reasonable estimate can still be achieved by finding a weighted average of the different surface conditions present on the hull. Of course, a more accurate estimate could be computed using the CFD application also explained briefly in this paper, even with different roughness at different areas. However, this approach is not automated but can be offered by SSPA.

3. Model tests

The flat plate is designed to be rigid and to generate as little residual resistance as possible at the highest possible Reynolds. These goals opposing as high Reynolds number requires long plate, low residual resistance requires very thin plate and long and thin are not particularly stiff. The compromise therefore is as follows:

The plate is 6921 mm long, 1002 mm high and 47 mm thick flat plate. The plate is made of a framework of 80x40 mm aluminium square tube covered with aluminium sheets. The leading and trailing edge has a NACA 0007 from 30% of the length of the cord from front to back. The suspension device allows movement in axial joints, rotation around a vertical axis to allow the plate to adjust in the direction of flow, and vertical wire turbulence stimulators were fitted 500mm aft of the leading edge, Figs.2-4. The plate is suspended at the trailing edge with a wire (free to sway) and the forward suspension is fixed and measures longitudinal and lateral forces. The plate is surface piercing with 100mm above the surface.

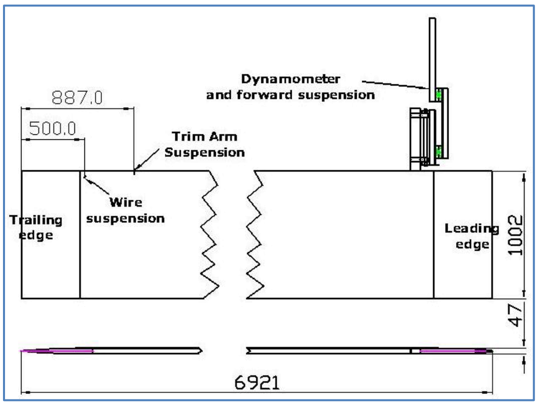

Fig.1: Skin friction plate

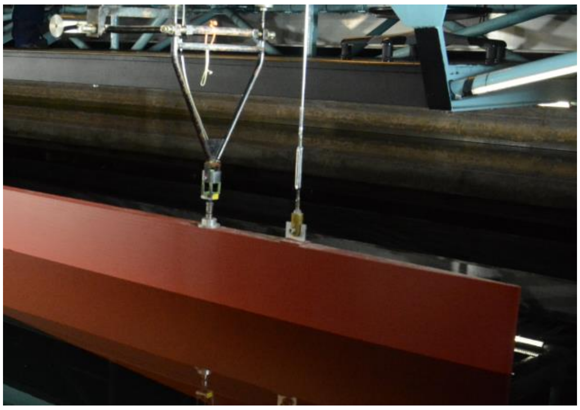
Fig.2: Skin friction plate in the towing tank, trailing edge

Before measurements are recorded the plate is aligned in the streamwise direction, by adjusting the suspension laterally at different towing speeds until the lateral force recorded is close to zero.

Hydraulically smooth surface was tested for both plates as a reference. At the maximum speed of 5 m/s, a C_f value of approximately 0.0025 can be used for y^+=5 (the theoretical value for a hydraulically smooth surface)

$$y = \frac{\upsilon y^+}{u_\tau} = \frac{\upsilon y^+}{U\sqrt{1/2C_f}} = \frac{1.1 \cdot 10^{-6} \cdot 5}{5\sqrt{0.5 \cdot 0.0025}} \approx \ 31\mu m$$

which is the maximum roughness height for hydraulically smooth surface.

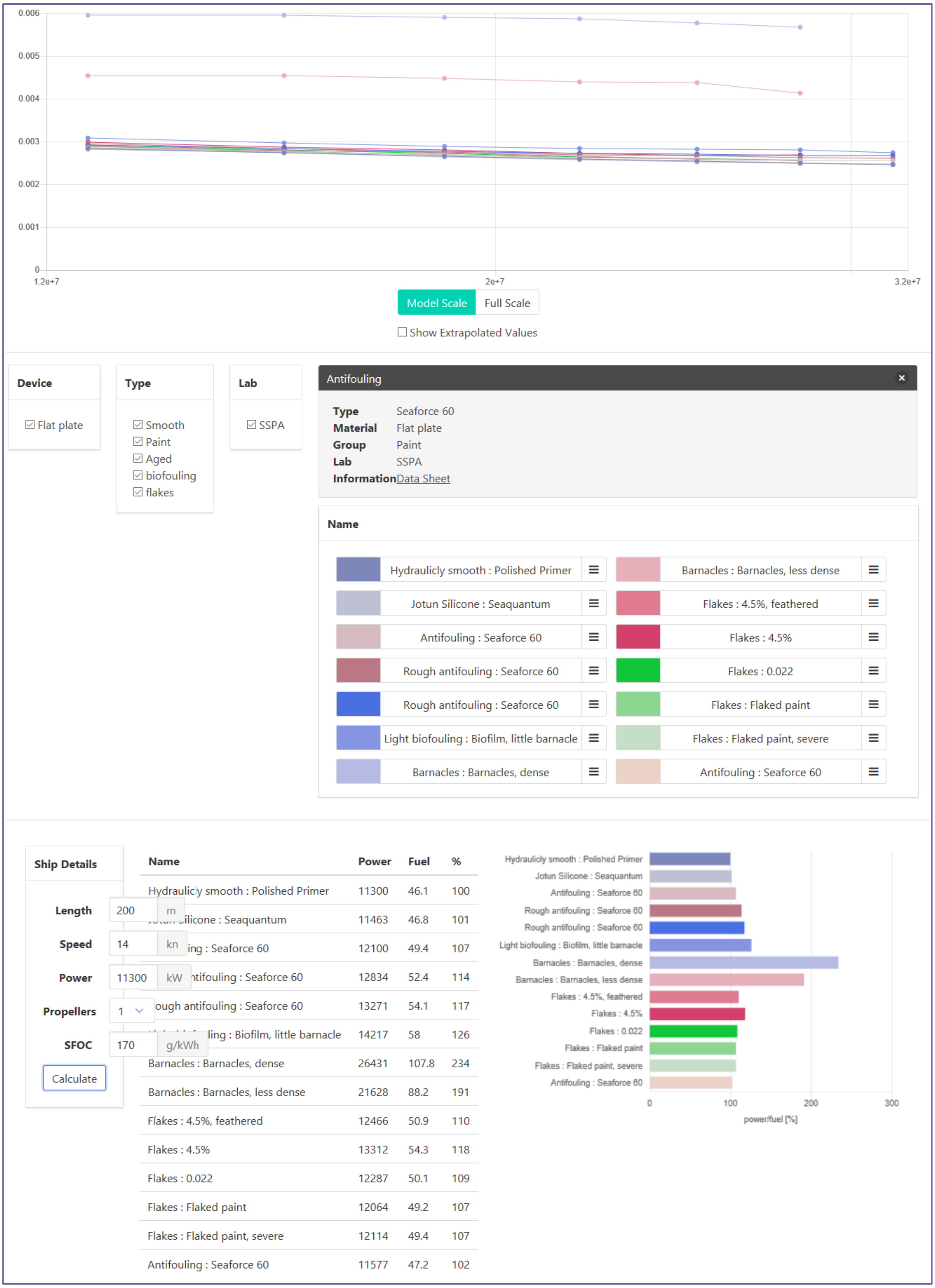

Fig.3: Interactive online database

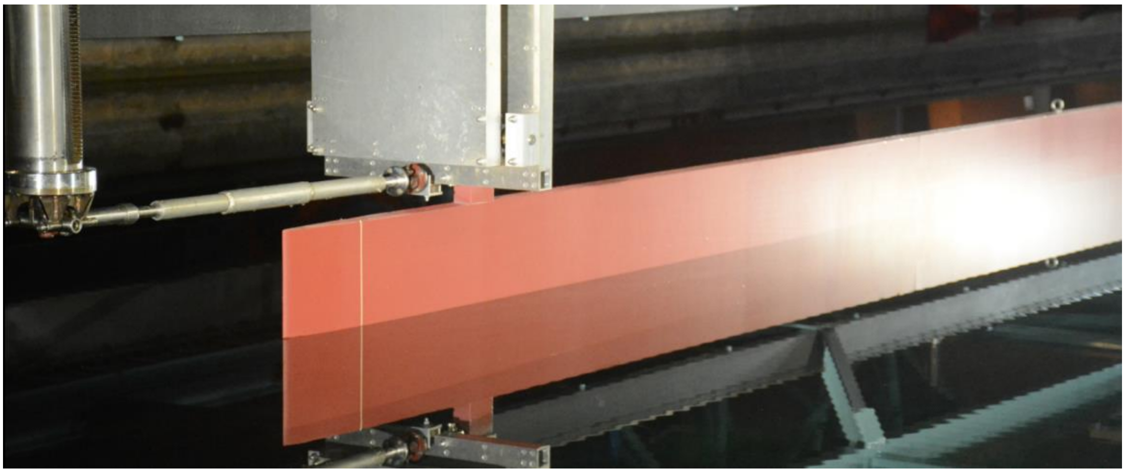

Fig.4: Skin friction plate in the towing tank, leading edge

The plates were coated with a primer and polished attaining a roughness height R_a of less than $5\mu m$. The resistance was measured for these plates, and the theoretical hydraulically smooth skin friction line (in this case the Schoenherr line) was used to obtain the residual resistance for each plate as

$$C_R(U) = C_{T,measured} - C_{F,Schoenherr}$$

This residual resistance (in this case wave, spray and form resistance) is considered constant and independent of the surface roughness. As shown in Fig.5 the resistance measurements for the both plates with hydraulically smooth surface are almost identical, for which reason only one correction have been used for all subsequent measurements on rough surfaces.

The test program for each surface consist of at least 8 runs in the towing tank. In each run, the speed is kept constant and the resistance is measured. The speed ranged from 1.5-5m/s. Some speeds are repeated twice in order to assess the repeatability.

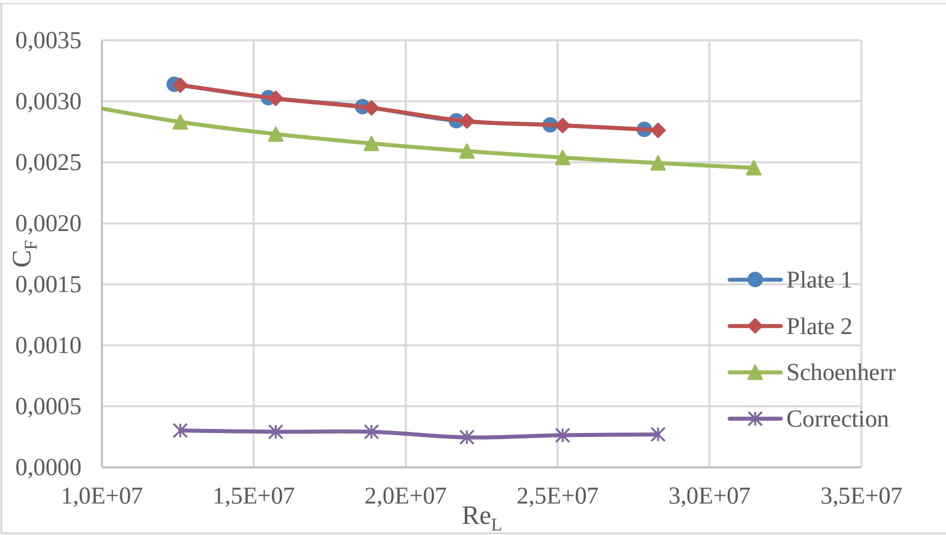

Fig.5: Correction for residual resistance

4. Rough surfaces

Three types of surfaces were tested. Newly coated (good and poorly applied), simulated aged or damaged coatings and biofouling. The surface roughness was measured for all cases when possible with a Hull Roughness Gauge (DC9000) using Mean Hull Roughness (MHR).

4.1. Coatings

Coating of the plates was subcontracted to a firm that usually apply marine coatings. I.e. the coatings were applied using the same conditions as for a real vessel both by technique and coating equipment, Fig.6. Coatings was applied to a high and low standard ranging from 65-130μm, with the roughest coatings applied by not following usual procedures and applying several layers (at some protest from the professional coaters), Figs.7-8. Seaforce 60 (antifouling) and SeaQuantum (silicon) both from Jotun were applied and tested.

Fig.6: Painting of the test plate in SSPA's work shop using spry tool

Fig.7: Dry-spray, 110 µm

Fig.8: Dry-spray, 130 µm

Fig.9: Test plate in sea water at Löven center

Fig.10: Test plate launching

4.2. Biofouling

Biofouling was grown on the plates by exposing the plates to sea water at the Löven center, Fig.9. The plate was hanging vertically 0.5-1.5 m below the water surface at a location of 8 m water depth between 2-6 weeks depending on the season and the desired level of growth. All plates where coated with an antifouling coating to simulate real roughness behind the fouling, however a less strong formulation in terms of antifouling was used to allow speedier fouling growth.

4.3. Aged or damaged coatings

Aged and damaged coatings as often seen on real vessels were simulated by two methods. The above described poorly applied coatings have a surface similar to hulls with several layers of coatings and the second method investigated flaking, also typically seen on vessels after a few years of operation. The reason can be mechanical damage from anchors, key side and tug boats, or it can be due to aged paint and several layers of paint. The height of the flake edge can well be several mm, even if the paint layer itself is thin. Water intrude under the damaged paint and lifts the paint edges. Therefore, several test cases were created to represent flakes of various kinds. One set of cases illustrate flakes with large edge-height, 3 mm. These were constructed by gluing a plastic foam sheet to the test plate and cut holes in it. The surface was painted with normal anti-fouling paint, Fig.11. The flakes covered 2% and 4% of the surface. An example of feathered edges was created by smoothing the edges of holes on the plate with 4% flakes, Fig.12. Included in the aged and damaged coatings is also cleaning of the bio-fouled surfaces, either mechanical cleaning or cleaning by high pressure water.

Fig.11: Test case flakes 3 mm edges

Fig.12: Test case flakes with feathered edges

Fig.13: Test case flakes 0.5 mm edges

Another set of cases illustrate flakes with edges still attached to the surface, i.e. the flake edges have the same size as old paint layers which has been painted over. These were created by covering patches of the test plate and paint the rest with many paint layers, Fig.13. In summary, the rough surfaces tested was:

Poorly applied paint • Anti-fouling dryspray (~110 µm) • Anti-fouling dryspray (~130 µm) Paint damages and repair • Paint damage sharp edges (3mm, 2% cover) • Paint damage sharp edges (3mm, 4% cover) • Feathered edges of flakes • Paint damage and repainted (0.5 mm) • Paint damage and repainted (0.6 mm edges)	Reference • Smooth (< 5µm) New paint • Self-polishing Silicon paint (~65 µm) • Anti-fouling paint (~65 µm) Biofouling • Light biofouling (slime) • Small barnacles, dens • Small barnacles, spars Cleaning • Mechanically cleaned, remaining's of barnacles (~140 µm) • High pressure cleaned (~110 µm)

5. CFD prediction on Roughness Effects of Flat Plate

CFD prediction on roughness effects have been performed with RANSE simulations assuming the effects of a uniformly distributed sand grain roughness on the flat plate. The roughness simulations have been performed with SHIPFLOW. In SHIPFLOW, the roughness modelling has been implemented in the wall boundary condition for ω by applying the no slip condition directly at the wall. The computations have been performed with the selected computation set-up (y+=0.0001; grid set L:394, M:169 and N:85) for all tested speed ranges, from 2.0 m/s to 5.0 m/s with 0.5 m/s interval, and varying roughness height k_s from 0 (hydrodynamically smooth surface) up to 3000 µm.

The predicted roughness effects on resistance coefficients are plotted in Fig.14. The figure clearly show that frictional resistance coefficients C_F, viscous pressure resistance coefficients C_{PV}, viscous resistance coefficients C_V increase with the growth of k_s for all speed ranges computed. In the figure, a drastic increase can be seen when roughness scale is growing from hydrodynamically smooth surface k_s =0 to the roughness height k_s =300 µm while the increase of Cv reached almost maximum level 55% at very high roughness height k_s =3000 µm.

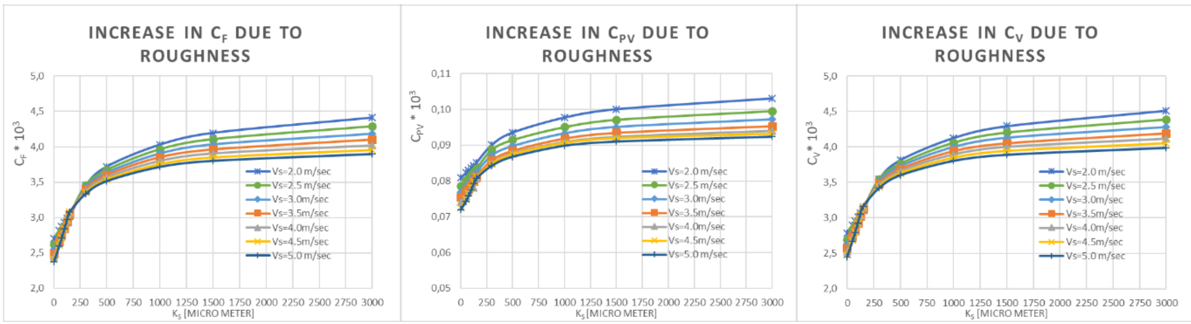

Fig.14: Increase of frictional resistance coefficients C_F, viscous pressure resistance coefficients C_{PV}, viscous resistance coefficients C_V due to roughness growth at various speeds.

The predicted skin friction lines with different sand grain height are compared the measured skin friction for the flat plate with different paint coating in Fig.15. It is promising that the predicted and measured skin friction lines compare well. Furthermore, C_F from computations will be fitted to the measured data by adjusting k_s. This will match the measured data to an appropriate computational k_s value, which is not necessarily the same as the measured roughness.

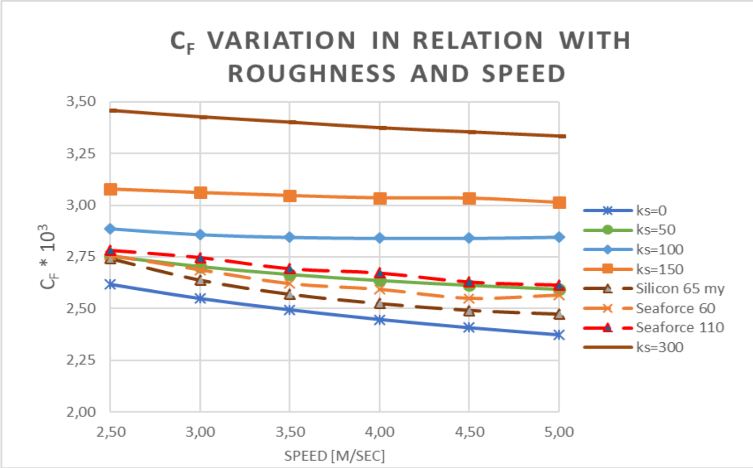

Fig.15: Predicted skin friction line against measured one for flat plate with different paint coating

6. Extrapolation to full scale

For extrapolation to full scale Reynolds number the Granville similarity laws are used. The reason for choosing this particular extrapolation have several reasons. First of all, it is based on the velocity shift of the boundary seen when fluid traverses a rough surface. It is therefore possible to derive specific equations for several different types of flows (flat plate, pipe flow or coquette cell for instance), which makes it more valid to compare lab measurements from different types of measurement devices for rough measurements. It is also very suitable for indirect methods (not measuring the local skin friction by for example shear stress measurement of boundary layer profile measurements) using only a towing force for flat plate or torque for couette cell. Effects of displacement thickness for a developing boundary is also included in the equations. Finally, it is the recommended method from, *ITTC (2017)*. For the full explanation of the Granville similarity see *Granville (1987)* or *Demirel (2014)*. Expressed as

$$k^+ = \left(\frac{k}{L}\right)\left(\frac{Re_L C_F}{2}\right)\left(\sqrt{\frac{2}{C_F}}\right)_R \left[1 - \frac{1}{\kappa}\left(\sqrt{\frac{2}{C_F}}\right)_R + \frac{1}{\kappa}\left(\frac{3}{2\kappa} - \Delta U^{+\prime}\right)\left(\frac{C_F}{2}\right)_R\right] \tag{1}$$

$$\Delta U^+ = \left(\sqrt{\frac{2}{C_F}}\right)_S - \left(\sqrt{\frac{2}{C_F}}\right)_R - 19.7\left[\left(\sqrt{\frac{C_F}{2}}\right)_S - \left(\sqrt{\frac{C_F}{2}}\right)_R\right] - \frac{1}{\kappa}\Delta U^{+\prime}\left(\sqrt{\frac{C_F}{2}}\right)_R \tag{2}$$

where k is the roughness height, L is the plate length, ΔU^+ is the roughness function and ‘ is the slope of the roughness function and finally R and S subscripts refers to rough and smooth surface respectively. The above equations are solved iteratively based on the measured data for the plate until the slope of ΔU^+ as a function of $\ln(k^+)$ calculated numerically based on the measurement points satisfies Eq.(2) (by least squares interpolation). For the smooth surface the Schoenherr smooth skin friction line is used (which is also solved iteratively)

$$\frac{0.242}{\sqrt{C_F}} = \log(Re_L C_F) \tag{3}$$

The same value of $(Re_L C_F)_S = (Re_L C_F)_R$ must be used in Eq.(1). Therefore, the smooth C_F value is not the value of Eq.(3) for the same Re_L as the measured rough point, but is the value of C_F using $(Re_L C_F)_R$ on the right-hand side of Eq.(3).

Second step in the method is to plot $(C_F)_S$ as a function of $\log(Re_L)$ and based on the value of ΔU^+ from equation 2 at one measured point for a rough surface to shift the smooth skin friction curve a distance of $\Delta U^+ \kappa / \ln(10)$ in the $\log(Re_L)$ direction, Fig.16. This line corresponds to C_F derived from the measurement point to a plate with varying length, but same speed as the measurement.

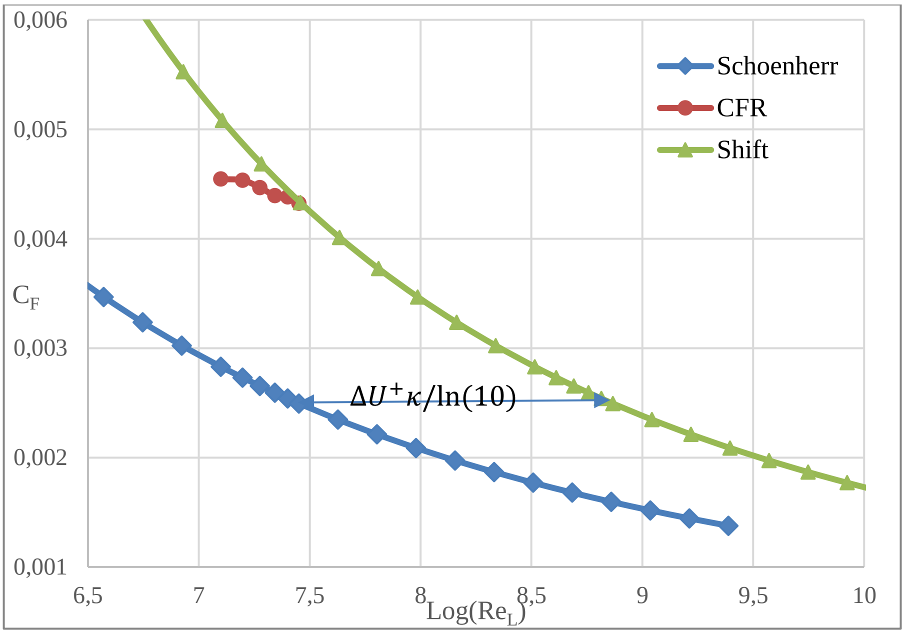

Fig.16: Schoenherr smooth skin friction and shift. C_{FR} is the measured data

The next step is to calculate the curve of constant L^+_{plate} using equation 4, where the constant value of L^+_{plate} is defined by a point from the measurements

$$Re_L = \frac{L^+_{plate}}{\sqrt{\frac{C_F}{2}}\left(1-\frac{1}{\kappa}\sqrt{\frac{C_F}{2}}\right)} \tag{4}$$

Thus, using the constant value of L^+_{plate} for the measurement point the curve of constant L^+_{plate} can be added by solving for Re_L as a function of C_F. The final step is to shift the curve a distance of $\log(\frac{L_{ship}}{L_{plate}})$, as can be seen in Fig.17. The intersection between the shifted Schoenherr and constant L^+_{plate} is the skin friction at a plate corresponding to a length of L_{ship} at a velocity corresponding to the velocity for the measurement point.

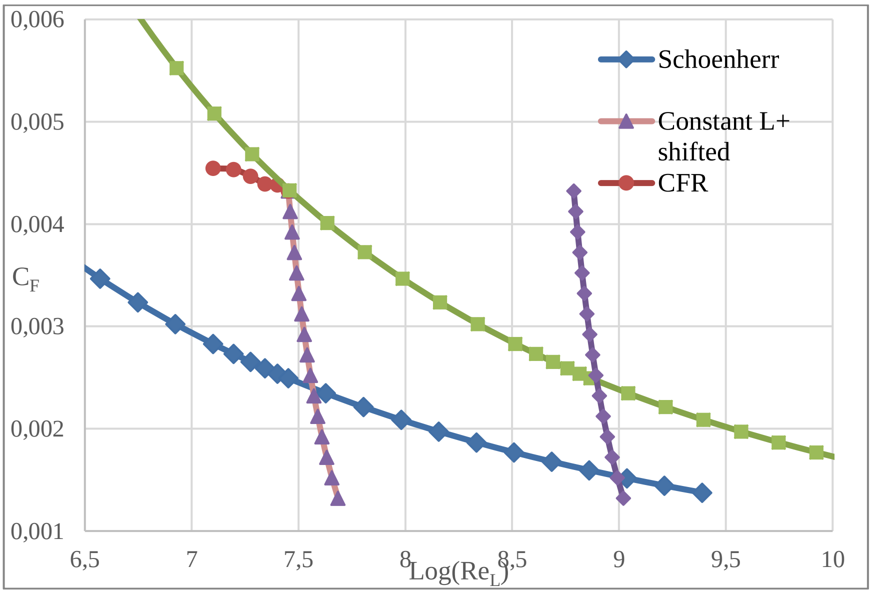

Fig.17: Constant L^+ and shift

This extrapolation in the plate length direction usually carries the estimation of C_F almost to full scale value in terms of Re_L for a vessel. To extrapolate in the velocity direction this method cannot be used directly, instead roughness functions must be used if the measured velocities does not match that of the full-scale ship. In the present study, the Grigson formulation is used, *Grigson (1992)*.

$$\Delta U^+ = \frac{1}{\kappa}\ln(1+k^+)$$

Whereas the extrapolation to full scale length scale is independent of the choice of roughness height k, the extrapolation along the velocity direction is not. Therefore, the choice of k must be fitted to the measured data, which will be done by introducing an efficiency parameter C reformulating the above equation to

$$\Delta U^+ = \frac{1}{\kappa}\ln(1+k^+) \Rightarrow \Delta U^+ = \frac{1}{\kappa}\ln\left(1+\frac{k^+}{C}\right) = \frac{1}{\kappa}\ln\left(1+\frac{ku_\tau}{\upsilon C}\right)$$

which will also allow for some scaling of topologically similar surfaces (surfaces with different roughness but same efficiency parameter for instance barnacle surface with different size of barnacles). This work is still ongoing and will not be presented in this paper.

7. Roughness effects on hydrodynamic performances of ships

The roughness effects on flow characteristics and hydrodynamic performances of ships were investigated by CFD simulations at full scale for sand grain roughness heights ranging from k_s =0 (hydrodynamically smooth surface) to 3000 µm. The ships selected have been tested at SSPA, built and have been in operation for some times now so the speed trial and actual operation performance data are available. Therefore, the ship considered suitable for investigating the roughness effect on ship powering performance.

Full-scale resistance coefficients were predicted and the roughness effects on friction, pressure and viscous resistance coefficients, C_F, C_P and C_V are presented in Fig.18. As expected skin friction resistance coefficient C_F is naturally sensitive to hull roughness and thus increases quite significantly with the growth of Ks, but the viscous pressure resistance coefficient C_P also increases.

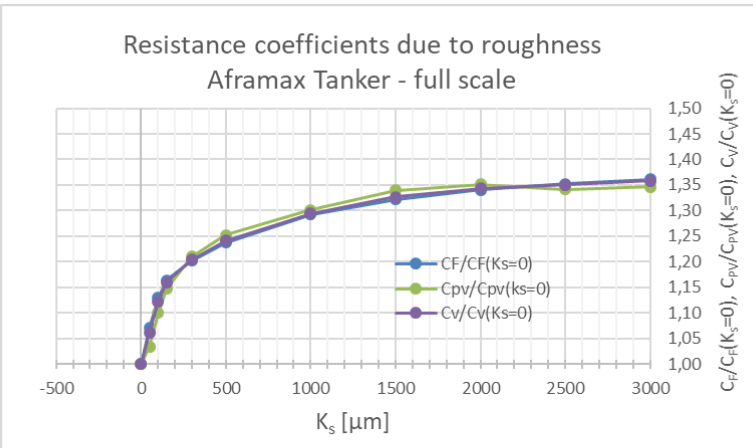

Fig.18: Increase of resistance coefficients C_F, C_P and C_V with the growth of hull roughness height k_s

The hull roughness does not affect only the near wall flow resulting in increase of resistance coefficients, but also wake field at the propeller plane. Fig.19 illustrates a gradual change of wake characteristics at the propeller plane with hull roughness growth. In the predicted full scale wake in case of hydrodynamically smooth hull (k_s=0), the longitudinal bilge vortex is already visible. The strengthening of bilge vortex with the increase of k_s can clearly be seen. This is a direct consequence of the thickening of boundary layer overall but especially in the region where the bilge vortex is formed.

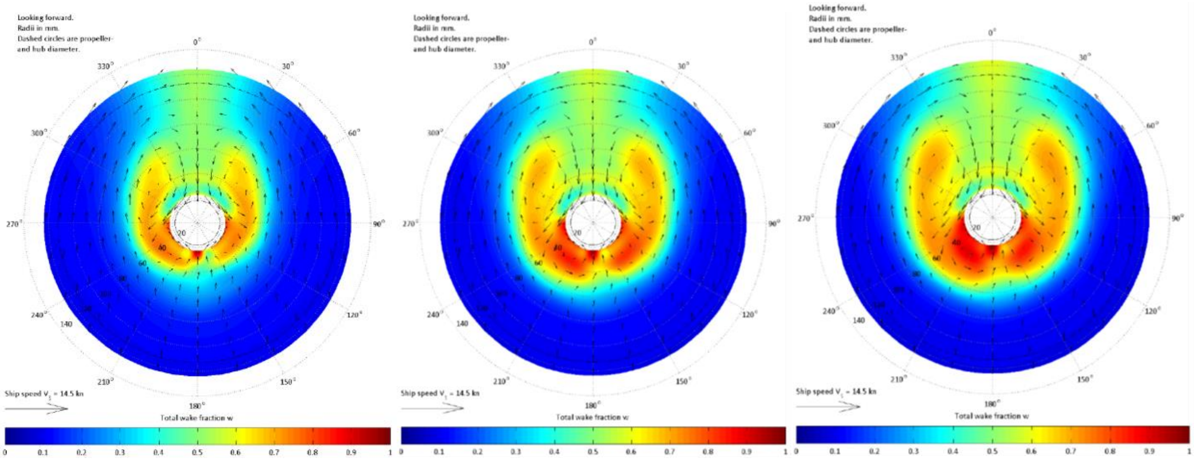

(a) Ks=0 *(b) Ks=300* *(c) Ks=3000*

Fig.19: Full-scale total wake fraction and transversal velocities at propeller plan due to roughness growth

The thicknening of boundary layer and strengthnening of bilge vortex with the growth of hull roughness height directly resulted in the increase of EHP and this is shown in Fig.20. A sharp increase of EHP is obtained when the roughness get started to grow from smooth surface within the first level (0 = Ks < 150 µm), and thereafter a gradual increase upto Ks=1500 in the second level and then minor increase in the third level (1500 µm < Ks < 3000 µm). It is interesting to note from the Fig.20 that the EHP predicted at Ks=100 µm is corresponding to the EHP predicted from model tests based on Bowden-Davison formula Ks=150 µm used in ITTC78 method.

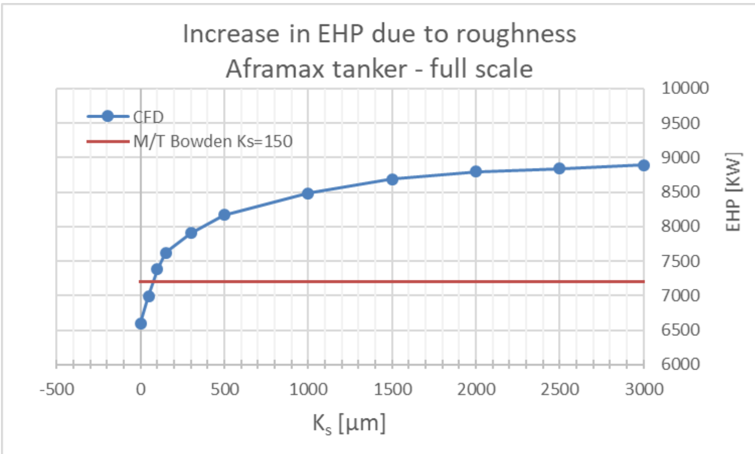

Fig.20: Increase of EHP with the growth of hull roughness of Aframax tanker in full scale

Similar trends can be observed for propeller thrust T, propeller torque Q and propeller revolution RPS from Fig.21.

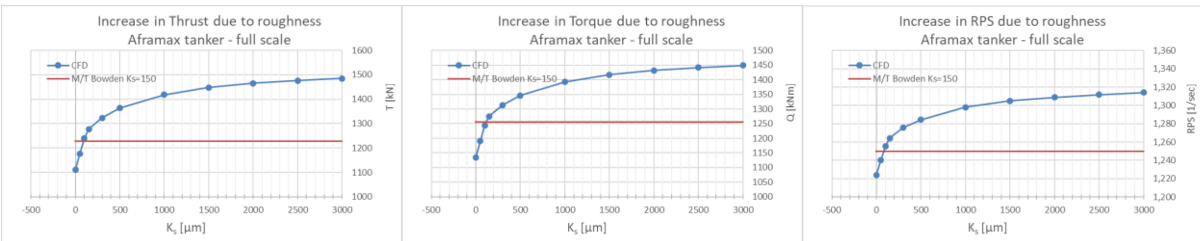

Fig.21: Increase of propeller thrust T, torque Q and RPS with the growth of hull roughness of Aframax tanker in full scale

This can be expected from the fact that the propeller should produce larger thrust and torque with rotating faster in order to overcome the resistance increase. The trends in the resistance, thrust, torque and rps due to hull roughness directlty result in increasing of DHP as can be seen in Fig.21.

8. Fuel Consumption

The purpose of the Fuel Consumption Tool is to make it possible for ship operators to estimate the fuel consumption of a given ship with a selected hull surface condition. The fuel consumption is always expressed relatively, i.e. the difference in fuel consumption between two surfaces from the database. The tool will be executed from the Skin Friction Database webpage after that the user has entered data for a specific ship. Therefore, the tool has to be rather simple, quick, and require only input data that is easily available to the ship operator. The following input is required: Length of ship (m), operational speed (knots), operational power (kw), number of propellers and specific fuel oil consumption (g/kWh)

The output is given as: change in power in kW, change in power in % and change in fuel oil consumption in t/day.

9. Power difference

The target is to extract a $\Delta P=P_1-P_2$ corresponding to two different hull surface roughness. The power difference should be valid roughly around a given operational power, which we call P_0. We use the ITTC method for sea trial evaluation (ITTC 7.5-04-01-01.1) to derive the change in power due to a change in resistance:

$$P_1 = P_1 - \frac{\Delta R \cdot V}{\eta_D}\left(1 - \frac{P_2}{P_1}\right)\xi_p$$

V ship's speed through water
η_D propulsion efficiency coefficient in ideal condition
ξ_P: overload factor derived from load variation model test
ΔR: resistance increase

In a sea-trial evaluation, P_1 is the ideal power and P_2 is the power affected by an added resistance. In the roughness evaluation tool, we assume instead that P_1 and P_2 are the powers corresponding to two different hull roughness. The first equation can be rewritten as:

$$P_2 = \frac{\frac{\Delta R \cdot V}{\eta_D} P_1 + {P_1}^2}{P_1 + \frac{\Delta R \cdot V}{\eta_D} \cdot \xi_p} = \frac{B \cdot P_1 + {P_1}^2}{P_1 + B \cdot \xi_p}$$

with

$$B = \frac{\Delta R \cdot V}{\eta_D}$$

The added resistance ΔR is the difference in resistance between the two hull surfaces:

$$\Delta R = \frac{1}{2}\rho V^2 S\left[C_{T_2} - C_{T_1}\right] = \frac{1}{2}\rho V^2 S\left[(1+k)\left(\Delta C_{F_2} - \Delta C_{F_1}\right)\right]$$

Hence, B is

$$B = \frac{\frac{1}{2}\rho V^2 S}{\eta_D} \cdot V\left[(1+k)\left(\Delta C_{F_2} - \Delta C_{F_1}\right)\right] = A \cdot V\left[(1+k)\left(\Delta C_{F_2} - \Delta C_{F_1}\right)\right]$$

with

$$A = \frac{\frac{1}{2}\rho V^2 S}{\eta_D}$$

A can be extracted from:

$$\frac{P_0}{V_0} = \frac{R_0}{\eta_D} = \frac{\frac{1}{2}\rho V^2 S}{\eta_D}[C_R + (1+k)C_{F0}] = A[C_R + (1+k)C_{F0}]$$

which gives

$$A = \frac{P_0}{V_0} \cdot \frac{1}{[C_R + (1+k)C_{F0}]}$$

ξ η_D, C_R and C_{FO} should be valid for the same condition, and P_0 should be equal to P_1. However, sensitivity analyses have shown that deviating from this is not at all important for derived value of ΔP. The sensitivity analysis is too lengthy to present here but showed that for 95% of the ships the expected error is smaller than ~1 percent-unit. This means that if the power increase ΔP is predicted to be 10% with the computation tool, it means ΔP is between 9%-11%.

10. Difference in fuel oil consumption

The change in fuel consumption can be computed from the power difference ΔP, in the following way:

$\Delta FOC = \Delta P * SFOC * 24/10^6$,

ΔFOC is the difference in fuel oil consumption in t/day
ΔP is the difference in fuel oil consumption in kw
SFOC is the specific fuel oil consumption in g/kWh

It is common that the ship operator knows the SFOC from performance logging or engine control panel onboard. If the user does not enter SFOC, a standard value of 170 g/kWh will be used.

11. Future work

In the short term, the extrapolation in the velocity dimension needs to be implemented in the calculation tool. Data from other labs measurements must be included to make the database more complete for every feasible surface seen on vessels. Finally, alongside the online database, the homepage will include instructions, BPG and descriptions of other labs methods. In the future, it is conceivable that an automated CFD tool will be included to investigate the influence of non-uniform distribution of roughness.

Acknowledgements

We would like to thank the contributors to this project being Jotun and the Löven Center as partners, and the funding organizations the Swedish Energy Agency and Region Västra Götaland for funding the project "Skin Friction database for the Maritime Industry"

References

DEMIREL, Y.K.; KHORASANCHI, M.; TURAN, O.; INCECIK, I.; SCHULTZ, M.P. (2014), *A CFD model for the frictional resistance prediction of antifouling coatings*, Ocean Eng. 89, pp.21-31

GRANVILLE, P.S. (1987), *Three indirect methods for drag characterization of arbitrarily rough surfaces on flat plates*, J. Ship Research 31/1, pp.70-77

GRIGSON, C. (1992), *Drag losses of new ships caused by hull finish*, J. Ship Res. 36, pp.182-196

ITTC (2017), *Recommended procedures and guidelines: Resistance and propulsion test and performance prediction with skin frictional drag reduction techniques*, Int. Towing Tank Conf.

Quantitative Comparison of Different Key Performance Indicators

Søren Hattel, FORCE Technology, Kgs. Lyngby/Denmark, shl@force.dk
Giannis P. S. Papageorgiou, FORCE Technology, Kgs. Lyngby/Denmark, gpp@force.dk
Vivien Rieu, FORCE Technology, Kgs. Lyngby/Denmark, vr@force.dk

Abstract

Based on data from a simple low-cost plug and play device for automatic logging of performance data we analyse the statistical properties of different performance indicators. Data originate from several ships from time periods of between one and twelve months of recorded data. We study correlations between the performance indicators and autologged signals in attempt to reveal shortcomings in the underlying model used for normalisation of the performance indicators. Furthermore, auto correlations of the performance indicators are studied in attempt to characterise completeness of the underlying model for normalisation of performance indicators.

1. Introduction

In this work we study the quality of different vessel performance indicators and their objective ability to describe the performance parameter they were designed for. The purpose of performance indicators is to as clearly as possible characterize a certain performance parameter. For instance, a performance indicator may be designed for studying the roughness of the hull and propeller surfaces and particularly the time evolution of the roughness. By monitoring the performance indicator over time, ideally it can be used for making decisions regarding hull and propeller treatments in order to optimize the performance in order keep the fuel consumption and emissions to a minimum. Since hull and propeller treatments are expensive and may require withdrawing the ship from service the reliability of the performance indicator is imperative. If the performance indicator is not reliable, the risk of making bad decisions is high and the potential for loss is correspondingly high.

The ship dynamics and propulsion system is influenced by many parameters for instance speed through water, draught and trim, wind and waves, water depth, water temperature, water salinity, rudder movements, ships motions and ship loading. These parameters influence the power demand to the propulsion system and to study only the effect of hull and propeller roughness the performance indicator has to deal with the influence of these parameters. Otherwise, the change in the performance indicator may simply be due to a change in one of these parameters. For instance, the increase in power demand may equally well be caused by an increase in speed through water as from an increased hull and propeller roughness, and if the performance indicator is not able to separate the effect of speed through water from the effect of hull and propeller roughness then we may not be able to make decisions about hull and propeller treatments.

In statistical terms the inability to differentiate two different effects on the conclusion is known as "confounding". One way of studying confounding for a performance indicator is to study the statistical correlations between different parameters and the performance indicator. A good performance indicator should exhibit strong correlation to the effect we wish to observe – say the hull and propeller roughness – while the correlation between other parameters and the performance indicator should be low.

Due to the complexity and nonlinearity of ship dynamics and ship propulsion systems it is not trivial to avoid confounding. Hence, different approaches to defining performance indicators have been proposed, *Pedersen (2014)* and references therein. Performance indicators are based on some underlying model of the ship dynamics and ship propulsion system. In some approaches, the performance indicator has been defined without explicit reference to an underlying model, but implicitly the performance indicator is always based on a model even if the creators of the performance indicator were not aware of the model. In these approaches the performance indicator may accidentally be confounded with other parameters leading to a poor performance indicator.

In other cases, the performance indicator is defined with a clear and explicit reference to a model explicitly including the effect that the performance indicator is designed to monitor. In the following section, we will discuss three different performance indicators. Two are based on implicit models and one is based on an explicit model. In the following sections, we study the correlations and auto-correlations of these performance indicators calculated from real world data collected by a simple and affordable autologging device, *Hattel et al. (2017),* onboard several ships.

We think the quest for defining the best performance indicators for ship performance as the holy grail in ship performance monitoring. This study is but a small contribution to our quest for the holy grail.

2. Definition of performance indicators

In this section, we introduce three performance indicators designed for monitoring hull and propeller fouling, and discuss their characteristics and properties. In the following sections, we will report our experience with the performance indicators from real world data.

2.1 Speed loss

A common performance indicator is known as "speed loss" in marine lingo. In this study, we apply the definition from the ISO19030 standard:

$$V_{loss} = \frac{V_m - V_e}{V_e}\ 100\% \tag{1}$$

where V_m is the measured speed through water and V_e is the calculated expected speed through water. The procedure for calculating V_e from the measured parameters – shaft power, wind, draught, trim etc – are described in the ISO19030 and were applied in this study. (Note that the expected speed is not corrected for wave effects. Also, the v_g(speed over ground) appearing in formula G.2 of the ISO19030 standard was replaced with v_{tw} (speed through water) as we believe the presence of v_g in G.2 is a typo.)

Note that $V_{loss} < 0$ when the measured speed is below expectations which suggest that the proper name is a speed gain. In any case, V_{loss} should be very close to zero for a well performing ship and negative values indicate poor performance.

The speed loss concept is widespread and very easy to understand: If the ship sails slower than expected, then it is evidently not performing optimally. However, the speed loss definition is not derived from an explicit model attempting to address the nature of the performance loss. Hence, the underlying model must be inferred from the definition (Eq.(1)).

The first assumption is that V_{loss} is indeed a good performance indicator which is independent of the actual speed V_m . Then the speed loss measured at one speed will represent the speed loss at all speeds. From the definition of V_e we got a reference speed-power curve $P_{cond}(v_{tw})$ for each relevant condition – draught, trim, wind and waves. (Wind corrections are included in $P_{cond}(v_{tw})$ instead of correcting the measured power for wind effects. The two approaches are completely equivalent.) Assuming V_{loss} is small we can derive the approximate speed power curve for the implicit performance model at each set of conditions:

$$P_{speedloss}(V_m) = P_{cond}(V_e) = P_{cond}\left(\frac{V_m}{1 + \frac{V_{loss}}{100\%}}\right)$$

$$\approx\ P_{cond}\left(V_m(1 - \frac{V_{loss}}{100\%})\right)$$

$$\approx P_{cond}(V_m) - \frac{\partial P_{cond}}{\partial V_e}(V_m)\frac{V_m\, V_{loss}}{100\%} \tag{2}$$

where the first power identity is based on the definition of V_e and the approximation is to first order in V_{loss}.

Eq.(2) is the implicit model description of the ship dynamics and propulsion at varying speeds for a certain condition assuming that Eq.(1) defines a speed independent performance indicator, V_{loss}. By inspection of Eq.(2) we observe this model predicts that the speed power curve is shifted upwards at reduced performances ($V_{loss} < 0$). The shift is proportional to both V_{loss}, V_m and the slope of the reference shaft power curve, $\frac{\partial P_{cond}}{\partial V_e}(V_m)$. Roughly estimating the speed power curve as $P_{cond}(V) \sim k\, V^{\epsilon}$ (with the exponent $\epsilon \gtrsim 3$) the model roughly estimates the shift to be proportional to V_{loss} and V^{ϵ}:

$$\Delta P_{speedloss}(V_m) \propto -V_{loss}\, V_m^{\epsilon}$$

Hence, this model roughly predicts that the upward speed power curve shift at 12 knots is $2^{\epsilon} \gtrsim 8$ times higher than the shift at 6 knots.

2.2 Excess resistance

A common performance indicator is defined in terms of an extra resistance that is observed when comparing the nominal provided thrust from the propeller compared to a reference hull resistance at the specified speed and conditions. The extra resistance is sometimes referred to as "added resistance due to fouling" but to avoid confusion with the often used phrases "added resistance due to waves/wind/shallow water" we will refer to this as the "excess resistance" indicating that the origin of the resistance is not addressed.

We define excess resistance as:

$$R_x = \frac{T - R_{cond}(V_m)}{½\big(T + R_{cond}(V_m)\big)} 100\% \tag{3}$$

T is the effective thrust $T = (1 - t)T_{prop}$. T_{prop} is the thrust provided by the propeller and t is the thrust deduction due to increased suction on the hull. $R_{cond}(v_{tw})$ is the reference speed-resistance curve at specified condition – draught, trim, wind and waves.

The definition of R_x is not derived from an explicit model and we wish to derive the model equivalent to the procedure for the speed loss. Assuming that R_x is a robust performance indicator then it should be independent of the actual speed V_m. In static conditions T will balance the actual hull resistance, $R_{actual}(V_m)$. Using this identity and assuming that R_x is small we can perform a derivation equivalent to the derivation for speed loss:

$$R_{actual}(V_m) \approx \left(1 + \frac{R_x}{100\%}\right) R_{cond}(V_m) = R_{cond}(V_m) + \frac{R_x R_{cond}(V_m)}{100\%} \tag{4}$$

This model predicts a shift of the speed-resistance curve proportional to excess resistance, R_x, and the reference speed-resistance curve. In order to compare with Eq.(2) we convert to the power domain by multiplying Eq.(4) with V_m/η_T:

$$P_{actual}(V_m) \approx P_{cond}(V_m) + \frac{R_x P_{cond}(V_m)}{100\%} \tag{5}$$

Comparing to Eq.(4) we observe that this model predicts the shift of the speed-power curve to be proportional to R_x and $P_{cond}(V_m)$ rather than $\frac{\partial P_{cond}}{\partial V_e}(V_m)V_m$ in Eq.(4). Again, using the rough estimate

$P_{cond}(V) \sim k\, V^{\epsilon}$ we observe that this model predicts the same shift:

$$\Delta P_{actual}(V_m) \propto R_x\, V_m^{\epsilon}$$

Hence, except for a scaling factor and a sign convention the speed loss and the excess resistance are essentially based upon the same implicit model. Consequently, a priori we may expect the two performance indicators to show similar correlations and autocorrelations. However, $R_{cond}(V_m)$ includes added resistance due to waves whereas the speed loss calculation does not correct for waves. Hence, we may expect some differences between the two performance indicators.

2.3 Speed index

The third performance indicator is the speed index. The definition of the speed index is based on a complete explicit steady state model of the hydro- and aerodynamics and propulsion system of the ship, *ITTC (2011)*, including hull surface roughness and propeller roughness. The influence of hull surface roughness is modeled by an increase, ΔC_F of the viscous coefficient and the influence of propeller roughness is modeled by an increase, ΔK_Q, of the propeller torque coefficient and a decrease, ΔK_T, of the propeller thrust coefficient. The model includes an effect of the hull fouling on the wake fraction and consequently on the hull efficiency.

For an observed speed, draught, propeller speed, propeller torque, wind, waves, water depth, etc., the three parameters ΔC_F, ΔK_Q and ΔK_T are estimated as the values providing the best consistency between the measured data and the model. The speed index is defined as:

$$V_{idx} = \frac{V_{norm}}{V_{ref}} 100\%$$

Here V_{norm} is the speed which the model predicts from the calculated values of ΔC_F, ΔK_Q and ΔK_T at a certain reference torque in calm sea and deep water. V_{ref} is the speed which the model predicts if ΔC_F, ΔK_Q and ΔK_T are zero.

In this model, the estimated parameters are required to calculate the shift of the speed power curves. The estimation of the three parameters depends differently for the three parameters. Since the speed index is the consequence of this shift it is not possible to quantify the shift only in terms of the speed index. This contrasts with the previous performance indicators where we could write the speed dependency in terms of the performance indicators themselves.

Essentially, the three parameters are the proper performance indicators in this model, and the speed index describes an aggregate of the three.

2.4 Discussion

The three performance indicators defined here reflect different approaches. Speed loss and excess resistance have very simple definitions. Our calculations show that the simple definitions implicitly assume models where the speed power curves are shifted upwards with a shift described directly by the performance indicator.

The speed index on the other hand attempts to model the actual effect of hull and propeller roughness from established hydrodynamic principles including the effect of speed according to the physical laws of the system. The observation that the model for the speed index cannot be formulated as a simple shift of the speed power curves suggests that the two simpler performance indicators may be incomplete for the description of the performance. For instance, it may turn out that their prediction of the speed dependency of the speed power curve shift is not properly describing underlying physics. Hence, we may expect the three performance indicators to show different correlations to the measured speed.

In the ISO19030 standard the key performance indicators are formulated as averages of the speed loss over substantial time spans. One may argue that this will compensate for the possible speed dependency of the speed loss provided the distribution of speeds over the different timespans are the same. However, in many cases the distribution of speeds will not be the same for two different timespans and even if the average speed for two timespans are the same then the distribution of speeds may be very different. Due to nonlinearities of the system the average speed loss may not be equal even if the average speeds are the same, *Hattel et al. (2017)*.

Apart from the understanding of the different models response to varying speeds it is also interesting to understand the models response to variations in draught and trim. We may explore this question in a future project.

3. Procedure

In the following sections, we present statistical observations of the behavior of the three performance indicators when applied to data recorded from ships in operation. We emphasize that all three performance indicators are calculated based on the same reference curves established from the same external data. Hence, the differences are not due to differences in the quality of the external data.

We have used data from fifteen tankers and bulk carriers in operation. All vessels have recorded the same complete set of signals – shaft power, propeller RPM, speed through water, rudder angle, wind angle and direction, water depth – and reported the draught and trim via noon reports. The vessels have recorded in varying time spans ranging from a few weeks to more than a year. The quality of the reference data for the fifteen ships varies.

All data were batched into datasets of one hour periods. Datasets were filtered for invalid data and outliers. Datasets were decimated by removing the least stable datasets as described in *Hattel et al. (2017)*. A total of 9874 datasets representing 9874 hours of collected data remained for use in the final analysis.

For the remaining datasets, the three performance indicators for speed loss, excess resistance and speed index were calculated. Datasets were grouped into laden condition and ballast condition. For ships with data series spanning more than three months' data were separated into groups spanning less than three months. The separation was made between two voyages. For each dataset for each vessel the correlations between the performance indicators and the different measured parameters were calculated. For each vessel, the autocorrelations of each performance indicator were calculated for one hour of lag. I.e. the correlation between a performance indicator value at one time and the performance indicator one hour later (if it exists and is not excluded by filtering):

$$\hat{\rho}_{1hour} = \frac{E[(y_{t+1} - \bar{y})(y_t - \bar{y})]}{E[(y_t - \bar{y})^2]}$$

where y_t is one of the performance indicators at time t.

4. Results

Fig.1 shows the calculated correlation coefficients between speed through water and the three performance indicators. Correlation between speed through water and speed index is plotted along x-axis. Correlations between speed through water and excess resistance (triangles) and speed loss (circles) are plotted on y-axis. Correlations for speed index ranges from -0.83 to 0.85 with the average at 0.18. Excess resistance ranges from -0.7 to 0.73 with the average at -0.16. Speed loss ranges from -0,48 to 0.82 with the average at 0.37. The general picture is that there are substantial correlations between speed through water and all the performance indicators. Hence, none of the performance indicators are clearly superior or inferior to the others.

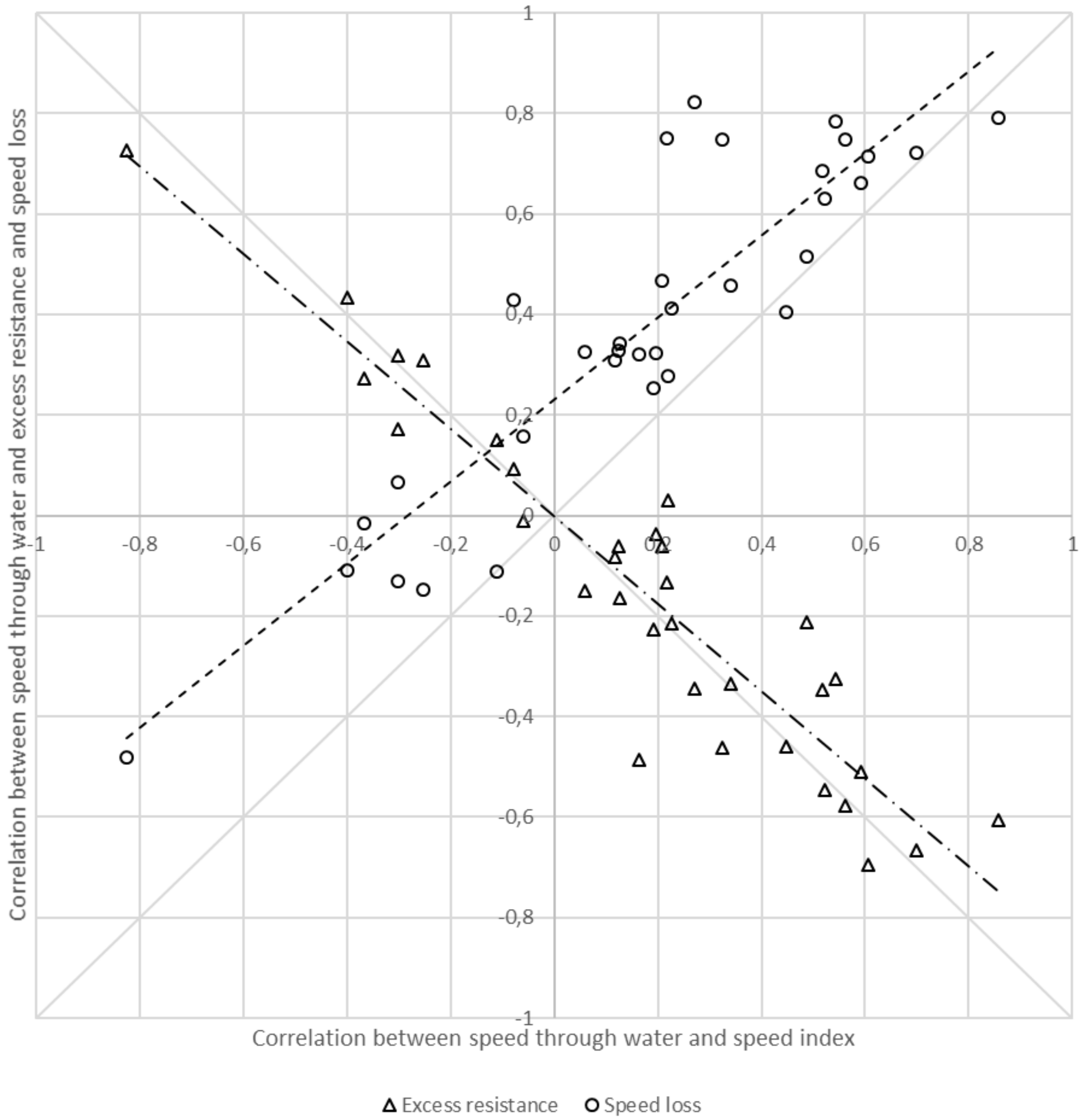

Fig.1: Correlation coefficients between speed through water and the three performance indicators: Speed index (x-axis), excess resistance (triangles, y-axis) and speed loss (circles, y-axis)

We observe a clear tendency that the speed index correlations and the speed loss correlations have the same sign whereas the speed index correlations and the excess resistance correlations have opposite signs. This reflects the fact that good performance corresponds both to higher speed index and higher speed loss (due to the confusing sign convention in Eq.(1)) whereas it corresponds to lower excess resistance.

The correlations for speed index and excess resistance are quite similar except for the opposite signs with points falling almost equally on each side of $y = -x$ line. In contrast, we observe that correlation coefficients for speed loss are generally falling on the high side of the $y = x$ line indicating generally higher correlations for speed loss than for speed index. Thus, the correlation coefficients for speed loss are between 0 and 0.55 higher than the correlation coefficients for speed index.

The observation of correlations generally does not proof a causality. Hence, the correlations we observe in Fig.1 do not suffice to say that the performance indicators depend on speed. In our dataset, we observed that most ships were sailing in a "fixed propeller RPM" mode. Hence, whenever wind and waves build up then the speed through water tend to fall. In other words, we observe some correlation between the wind and the speed through water. To at least to some extend the variations in speed are due to variations in wind and waves. This causality between weather conditions and speed through water may suggest that the observed correlations are describing a correlation between weather and performance indicators.

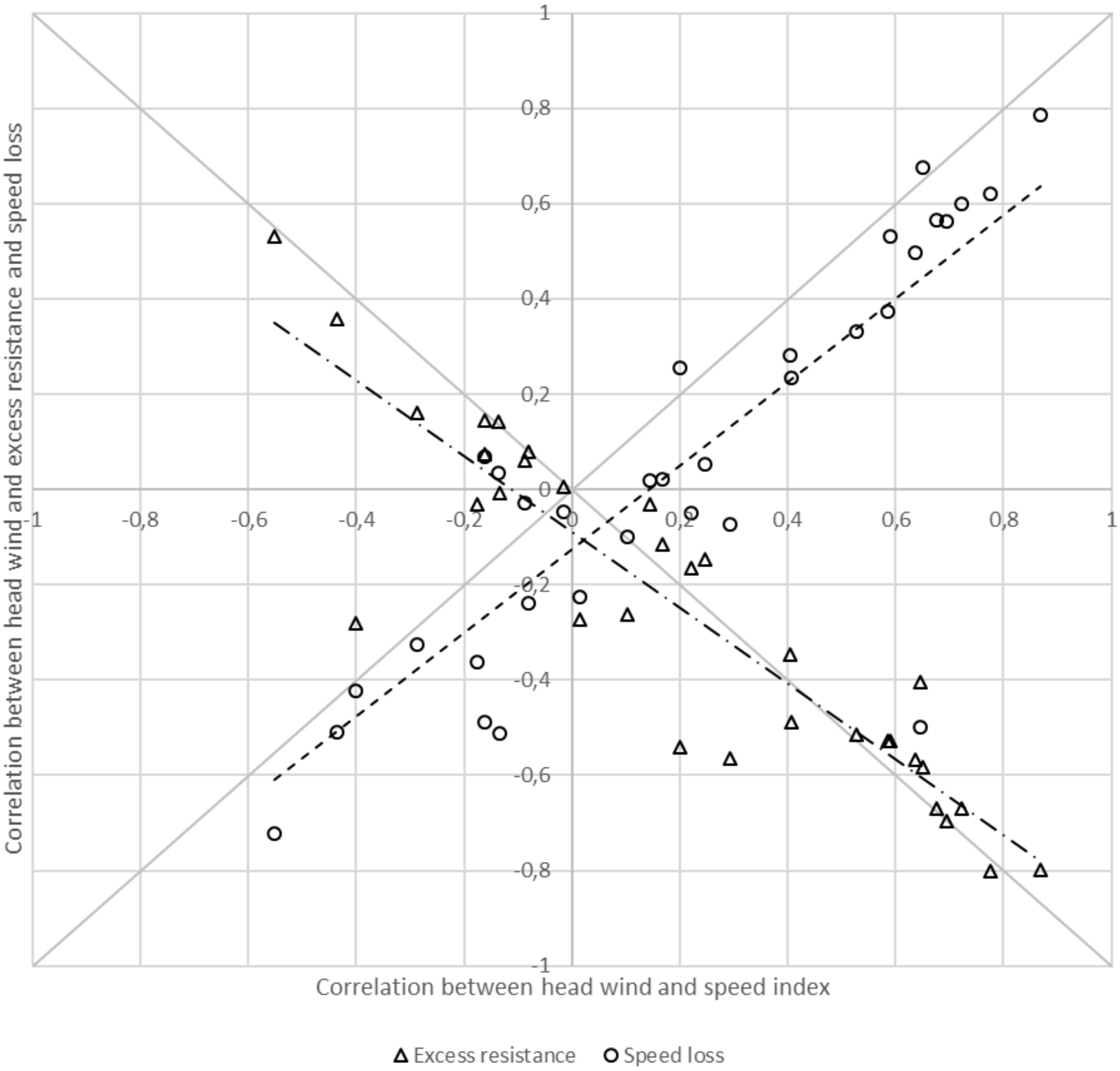

Fig.2: Correlation coefficients between head wind component and the three performance indicators: Speed index (x-axis), excess resistance (triangles, y-axis) and speed loss (circles, y-axis)

Fig.2 shows the correlation coefficients between the head wind component (relative wind vector projected onto ships heading) and the performance indicators. The general picture resembles that of Fig.1 except that the speed loss correlations are generally below the $y = x$ line and not above. This is probably the consequence of the speed loss not accounting for waves which are highly correlated to wind making the speed loss less dependent on weather conditions.

Fig.3 presents calculated autocorrelation coefficients for each performance indicator. All performance indicators show strong autocorrelations and there is no noticeable trends or differences between them.

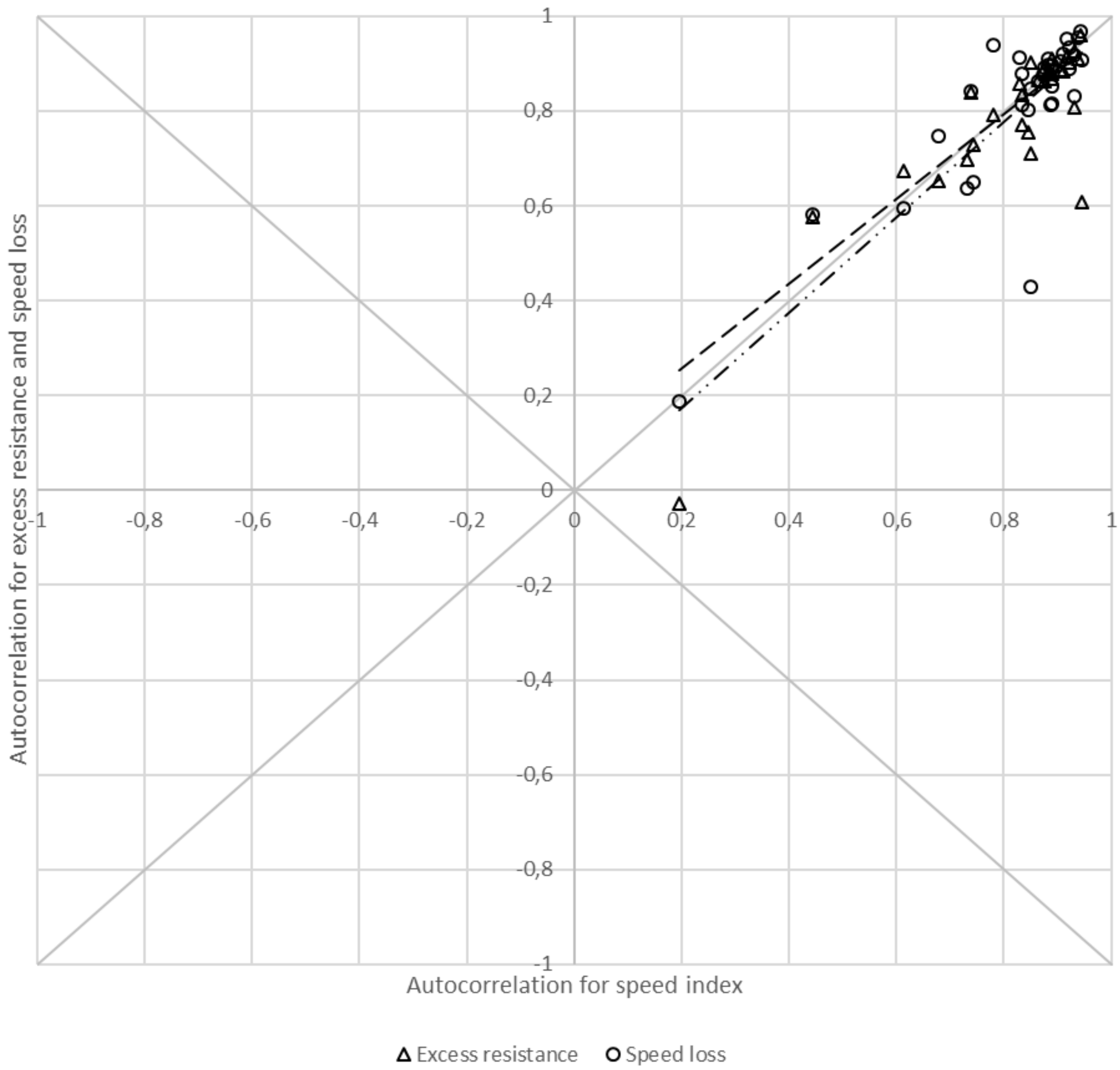

Fig.3: Autocorrelations for one hour lag for each performance indicator. Autocorrelation for speed index on the x-axis. Autocorrelation for excess resistance (triangles, y-axis) and autocorrelation coefficients for speed loss (circles, y-axis).

5. Discussion

The three performance indicators studied aim to characterize the state of the hull and propeller surfaces. Hence, ideally – if the underlying models adequately describe the physics of the ships - the performance indicators should not show any significant correlations to the input parameters and only show strong correlation to the hull and propeller surface states.

However, we observe substantial correlations between speed through water and the performance indicators as well as between the head wind and the performance indicators. In this study the variation in speed is linked to the variation in weather conditions due to the "fixed propeller RPM" mode used by the ships, and speed through water is partially a proxy for measuring the weather conditions. Hence, the effect of weather and speed through water are more or less confounded in our datasets.

All the performance indicators are defined in a way that should account for and subtract the effect of weather, but the correlations suggest that this effort fails to some extent. Our hypothesis is that the models for wind resistance and wave resistance are inadequate.

This hypothesis may be supported by the observed substantial autocorrelations. Strong autocorrelations are a sign that the underlying model is inadequately describing the actual system, since an adequate model would only leave uncorrelated random noise. Autocorrelations originate from some underlying mechanisms that are in themselves autocorrelated. In this system, the weather conditions are the most likely causes for the autocorrelation, as it is well known that the odds for the weather to be the same as the present within the next hour are quite high. The weather conditions are not to be considered a stochastic uncorrelated parameter.

With a more detailed view, we observe that the speed index and the excess resistance performance indicators behave very much the same with regards to the correlations except for the trivial sign convention. On the other hand, the speed loss correlations behave slightly but noticeably different.

The derivations in section 2 of the models that represent the performance indicators we expected that speed loss and excess resistance would be very similar whereas it was suspected that the speed index would behave differently. This contrasts with the observations.

Recall however, that the speed loss does not correct for waves whereas both speed index and excess resistance corrects for waves. This may explain why speed loss is behaving slightly differently from the two others. If all three performance indicators applied the same procedure to correct for weather conditions, we may observe higher agreement between all three performance indicators.

6. Conclusion

We have formulated a framework for studying the underlying models for different performance indicators. We derived the implicit models for speed loss and excess resistance and they turn out to be equivalent except for a sign convention and for a difference in the procedure for correction for weather conditions.

We calculated selected correlations and autocorrelations for the performance indicators from observed autologged data from fifteen ships. For all three performance indicators, substantial correlations and autocorrelations were observed and they showed remarkable agreement between them despite their different formulations especially considering the differences in the procedure for weather corrections.

The three performance indicators are equally poor as performance indicators. This is good news if you prefer one performance indicator for another as it really does not make any difference. The bad news is, of course, that the observed correlations to weather and speed may lead to false conclusions regarding the actual performance of hull and propeller. The correlations may hide or even reverse the effect of the hull and propeller performance on the performance indicators.

Acknowledgements

This project is partly funded by the the Danish government through the performance contract program managed by “Styrelsen for Forskning og Innovation”.

References

HATTEL, S.; BECKERLEE, J.S.; PAPAGEORGIOU, G.P.S. (2017), *Experience with and achieved benefits of a low-budget plug-and-play logging device,* 2nd HullPIC, Ulrichshusen

ISO19030 (2016), *Measurement of changes in hull and propeller performance,* ISO, Geneva

ITTC (2011), *Recommended Procedure. 1978 ITTC Performance Prediction Method* 7.5-02-03-01.4,

PEDERSEN, B.J. (2014), *Data-driven Vessel Performance Monitoring*, PhD Thesis, Technical University of Denmark, DCAMM Special Report No. S180

Tanker Operators' Perspective, Vessel Performance Monitoring

Francesco Bellusci, Scorpio Ship Management, Monaco, fbellusci@scorpiogroup.net
Gilyong Han, INTERTANKO, London/UK, gilyong.han@intertanko.com

Abstract

Tanker operators are committed to full compliance with environmental regulations while remaining competitive irrespective the market conditions. A couple of major challenges are (a) increase of tankers' operational performance combined with a significant reduction of GHG emissions and (b) how to assess and evaluate tankers' performance to assist them to take timely actions meeting Charterers' expectations. IMO's efficiency index and indicator (EEDI and EEOI respectively) are based on the fuel consumption per (cargo) ton mile. Is the EEOI the right indicator to demonstrate operational performance? Does any ship operator really understands how good his ship's performance is at any time? A constant increase of fuel consumption may prompt tanker operators to take actions such as hull cleaning and propeller polishing. But what else can be measured? In their dialogue with Charterers, tanker operators discussed the need to find more appropriate and workable means to measure and demonstrate the ship's operational performance. These measures should be commonly acceptable and understood by both tanker operators and Charters. This led INTERTANKO to establish a Working Group (WG) on Vessel Performance Monitoring. The WG is to investigate whether there could be a model for performance monitoring which is acceptable to both tanker operators and charterers. ISO 19030 inspires the WG to make such a search. The idea is to discuss whether it is possible to expand the concept of ISO 19030 beyond hull and propeller efficiency. The model must be an easy-to-understand, easy-to-implement, tool.

1. Introduction

In tanker industry, "performance or efficiency monitoring" is already an integral part of a tanker company's organizational structure. In new buildings, the EEDI is a governing index. However, once in operation under a Charter Party agreement, the level of efficiency that was assumed through EEDI needs to be monitored. The INTERTANKO Working Group (WG) on Performance Monitoring is tasked to study whether it is possible to develop such a tool or at least to provide a set of guidance in support of a tool that is most commonly accepted in the industry.

2. Aspects to be considered for tanker operators

The origin of ISO 19030 is the paint manufacturers' initiative to develop a standard based on which to measure how different marine coating systems impact on the performance and efficiency of a ship, say, over the 5 year period between two dockings. The ship's operator would then be able to make a sound judgement on the need to take action at the right time to improve the ship's efficiency whilst maintaining the ship's safety and environmental competitiveness in the eyes of the Charterer. The INTERTANKO WG finds that both ISO 19030 and the WG seek to achieve the same goal. Here are some thoughts behind the establishment of the WG.

2.1. New building

The INTERTANKO WG views the energy efficiency measurements at the stage of new building and the development of ISO 19030 as follows. ISO 15016 (sea trial standards) was put in place to assist owners/yards for their sea trial. However, there are a number of areas where different interpretation of the requirements is possible leading to lack of transparency, e.g. how a correction factor was devised and used, the usage of SOG and the lack of clarity on the normalization of current effect.

There are cases where the sea trial results were good but actual performance after delivery was not as good as sea trial data. Fuel consumption and power per each speed are two important quantities for the shop operator. However, the speed-power curve do not always reflect the full spectrum of operating conditions of a ship in her life time. Measurement methodologies are certainly different or, better to say, measurements in operation are not standardized. As the ship ages, the operator needs a more accurate power-speed curve.

According to the IMO 2014 Guidelines on Survey and Certification of EEDI (MEPC.1/Circ.855/Rev.1, Oct 2015), the verifier should use ISO 15016 as a verification tool when the attained EEDI is verified. ISO 15016:2015 applies to sea trials conducted on or after 1 Sept 2015.

The ship operator can predict speed power relation in fully or partially loaded condition and for example M/E fuel consumption at 85% and 100% MCR. However, a question still remains as to how a ship would perform in real sea states and realistic operating conditions. Hence, ISO 19030 comes into play. Instead of speculating speed/power relations, ship operators need to measure ship performance at any time of operation.

- What is the ship's Speed-Power curve at any time in different loading conditions?
- What is the ship's current fuel consumption as a function of speed and draft (and possibly trim)?

Fuel consumption is dependent, among many others, on how efficient the ship's M/E is and how good her antifouling is.

One way of examining it was to look at "speed loss" which is considered to be a core objective of ISO 19030. When fouling occurs, ships will move slower as time elapses. A question is how the speed loss could be measured and quantified. Two viewpoints in the case of fouling:

- If the ship wants to maintain a speed at a specific loading (draft/trim) condition, she needs more power and more fuel consumption.
- For a given power level generated by the M/E at a specific loading condition, the ship will travel at a lower speed.

After some period of operation, the ship can achieve approximately the same speed at the same power setting by means of hull cleaning and propeller polishing. To make an assessment on what is the power required to propel a ship, a number of parameters need to be measured, including as a minimum:

- Torque
- RPM
- Fuel consumption
- Speed through water

ISO 19030 considers that the M/E is assumed to be as efficient as when the ship is new and it has four KPIs on speed and power:

- Measurement of ship performance before and after a Dry Dock;
- Measurement of in service hull and propeller performance;
- A point at which maintenance is required, i.e. hull cleaning and propeller polishing, and
- Monitor the impact of such maintenance.

A disadvantage of ISO 19030 is the assumption that the M/E efficiency is not considered. SFOC of the M/E in operation is never the same as the one obtained at the shop test when the M/E is new. Depending on the M/E and maintenance, the SFOC curve may change over time (it may go up). ISO corrected the M/E SFOC measurement and calculation is however a simpler task.

ISO 19030 does not clearly address all factors influencing fuel consumption changes over a certain period of time. The ship operator wants to look at how the ship performs over a given time, i.e. a reference period such as:

- Measure before dry-dock
- Measure when the ship leaves dry-dock

Several alternatives are left for building up a reference line (sea trial, a reference period and CFD analysis).

2.2. Charterer's needs

A standard Charter Party agreement would have the following clause:

"Unless otherwise ordered by Charterers, the Vessel shall perform all voyages at the service speed stated in the Questionnaire."

Would the EEOI satisfy the need of the Charterer? In theory, the Charterer wants to know how efficient the ship is at the time of chartering the ship. In practice, they cover the transportation cost with due regard to the ship's draft (cargo loaded), weather factors (wind direction, waves and swell), the current, the ship traffic, the quality and specific energy of fuel and using the Speed Over Ground.

Therefore, there is a need to find a most appropriate and workable means to measure and demonstrate the ship's efficiency, bearing in mind that:

- ISO 19030's default method is the assumption that one can do very high frequency measurements. Ships equipped with such automated measurements systems are not many.
- ISO 19030 Part 3 provides alternative method for those who have not sophisticated data collection system. A frequency of 1-2 manual snapshot events is sufficient though it takes longer to build up a baseline than sensors.

The Charterer's need and the tanker operators' responses to such needs are one of main drivers of the establishment of the WG.

2.3. Existing ships

Under the mandatory SEEMP, tanker operators are implementing energy efficiency monitoring and interventions one way or another. To provide assistance to the membership, INTERTANKO commissioned a study to UCL Energy Institute with the data collected over 5 years from 11 sister ships all operated under the same management. The study investigated the impact of using various indicators in assessing the performance of ships in operation. The study was submitted to MEPC 72 (April 2018) and will be discussed in the context of IMO's (additional) technical and operational energy efficiency measures for both new and existing ships. It shows that the use of indicators (e.g. EEOI, EETI, SECT and AER) provided some surprising results and revealed a large degree of incompatibility between the efficiency as defined through an indicator and the actual CO_2 emissions. All these indicators are intended to represent "in-service" efficiency based on the actual activity and operation of a ship.

In a previous study commissioned by INTERTANKO, EETI was proposed as an alternative to EEOI. EETI is estimated by deducting the effects of speed and transport work (allocative and payload utilization) from the EEOI, a full derivation can be found in (MEPC 69/INF.26 and "Understanding the Energy Efficiency Operational Index: data analysis on ships tanker ships for INTERTANKO", UCL Energy Institute). In a nutshell, EEOI is an operational efficiency indicator whereas EETI is a technical efficiency indicator in a reference condition. Both are expressed as gCO_2/Nm.

A given ship's EEOI or total emissions in 1 year provided little indication of its EEOI or total emissions in the following year. The main cause was attributable to parameters that are predominantly outside of the shipowner/manager's control and are more commonly determined by the commercial conditions (e.g. type and transportation requirements for the cargo) and contractual conditions (speed, payload, etc.) as well as environmental conditions with the former being the predominant element.

The usability of EEOI thus has limited relevance in the context of energy performance monitoring. If one measures and averages the EEOI over a long period, the EEOI would become less sensitive to voyage related fluctuations that are beyond the control of the ship's operator. Even in this case, the EEOI would not be capable of capturing small energy efficiency improvements that the ship has taken.

EETI, a metric that corrects for the dominant sources of efficiency variability that are outside of the owner/manager's influence (speed and utilization), was shown to produce a more narrow-banded distribution than EEOI (consistent for a fleet of technically similar ships), and trends consistent over time with low average rates of performance deterioration (consistent for a fleet of aging ships). One issue which complicates EETI is its calculation, as the EETI must be determined for a reference condition, and requires a conversion relating speed and fuel consumption that if incorrect can misrepresent performance/efficiency at high or low speeds. As has been highlighted in many other publications, depending on the ship type and its machinery, the relationship between fuel consumption and speed is not always well captured by a simple cubic relationship. In such instances the speed factor may be calculated using a more sophisticated mapping of the relationship between speed and fuel consumption – if the data is available.

INTERTANKO may try to further investigate EETI as a meaningful indicator. However, there are challenges since it is an indicator related to performance in a standard condition and it is directly linked to the "reference speed" which needs a better definition.

2.4. INTERTANKO WG's first meeting, November 2017

The WG discussed the experience gained from applying ISO 19030 and possible improvements with a view to developing recommendations. Due to the complexities involved in the scope of work, the WG undertook a scoping exercise to identify achievable tasks with the limited resources available to them.

The WG identified the following fundamental questions:

- What kind of information the makers and the yards shall provide the shipowner at the time of new building?
- Whether and how the shipowners can ensure the quality of data so provided?
- How the shipowners are expected to use their own tools and optimize efficiency?
- How the ship owners are expected to communicate with Charterers about the ship's performance efficiency when the former has limited information? Both the shipoperators and Charterers need information transparency.
- There are concerns that the information on the ship's performance efficiency, if placed in public domain, could be misused.

The above questions led the WG to address data accuracy and measurement uncertainties and to propose improvements of ISO 19030 in this regard. Even each sensor has its accuracy and uncertainty limits. It is important to highlight that contrary to the expectations from Charterers, ISO 19030 measures individual ships but not compares different ships with the same model.

A possible outcome of this deliberation will be a guidance explaining the meaning of accuracy, data quality, uncertainty and their limitations. The tanker operator and the Charterer would then be able to communicate each other with the same understanding of performance data accuracy and uncertainty.

In addition, the WG noted that the ISO 19030 applicability range is the speed range taken from sea trial (13-17 knots). This range is rather limited compared to actual sailing conditions. The WG is unaware of how more detailed service conditions are extrapolated. This is one of areas where the WG finds worth more studies with the ISO 19030 developers.

The WG's next step will be an experience building and gathering exercise, i.e. how many INTERTANO Members are applying ISO 19030, what their experiences are in terms of accuracy data filtering, data normalization and transmission and why there are outliers in the gathered data. Based on this exercise, the WG will identify a next step.

2.5. Regulatory landscape for CO2 reductions from ships

In 2016, IMO developed a Roadmap for developing a comprehensive IMO strategy on reduction of GHG emissions from ships. An initial GHG reduction strategy will be adopted in April 2018 (MEPC 72). This is in response to the 2015 Paris Agreement that global efforts be made to keep the world's average temperature rise well below 2°C above pre-industrial levels within this century and given the grave risks, to strive for 1.5°C. IMO's mandatory requirement for ocean-going vessels to collect and report their annual CO2 emissions under MARPOL Annex VI/Regulation 23A will take effect from 2018 and the required first reporting will cover the period of Jan 2019 to December 2019. The collected data will be taken into account by IMO's future GHG studies which aim to estimate the GHG emissions from international shipping. This will enable IMO to identify what additional measures should be introduced to contribute to the wider global efforts meeting the 2.0/1.5 degrees Celsius targets. Generally speaking, it is the ambition of IMO that the international shipping should move towards zero CO2 emissions as quickly as the delivery of economically viable alternative fuels and new propulsion technology will allow, while in the interim taking advantage of other efficiency-enhancing technologies as and when they become available and economically viable.

Fig.1 shows estimated effects of 40% energy efficiency improvement with 40% emissions reduction relative to 2008 in 2040 and 50% in 2060 based on the data used in IMO's third GHG Study 2014. Note that the 2014 IMO GHG study estimated that GHG emissions from international shipping could grow by between 50% and 250% by 2050. Hence, the IMO's proposed alternatives for a vision statement indicates a commitment to reducing GHG emissions from international shipping "towards zero as soon as possible within this century" with a more specific option "by 2050".

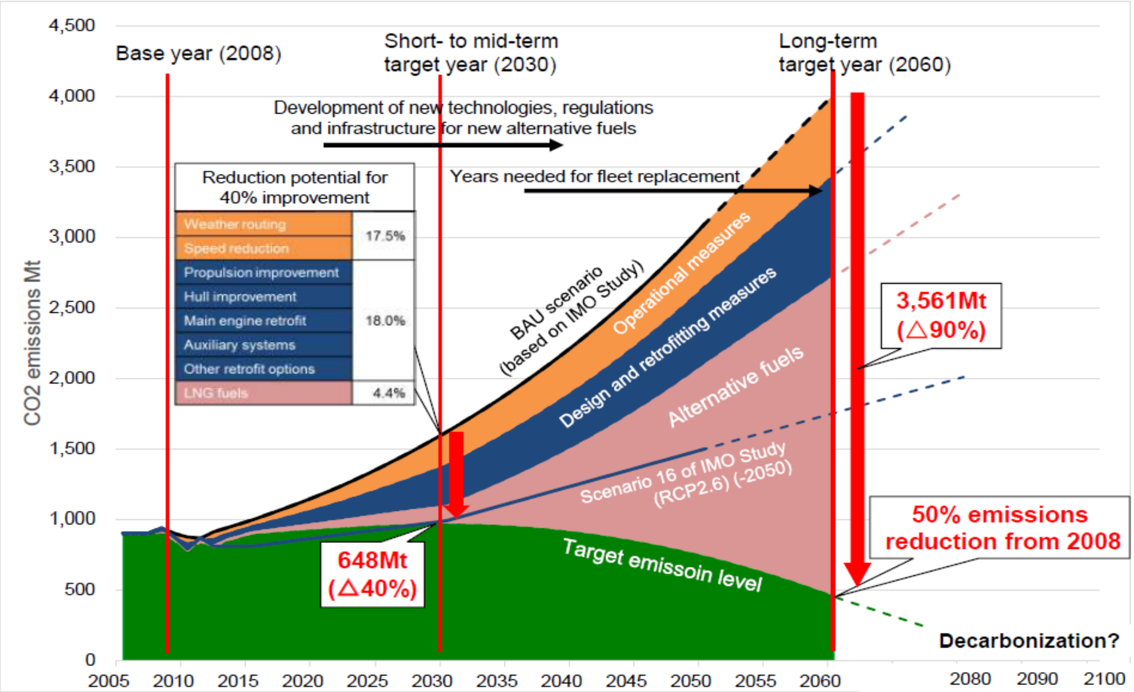

Fig.1: Estimated emission pathways in accordance with the proposed goals, *IMO (2017a)*

It is expected that IMO's new Strategy will build upon the annual CO2 emissions data collection, EEDI and SEEMP. The EEDI and its 3-phase scheme are designed such that after the initial phase zero in 2015, new ships being built today are required to meet the reference line 10% higher than the previous phase. This level will be strengthened incrementally every 5 years. On top of this, IMO is now conducting an investigative study of whether to advance the remaining phase 3 a few years in order to boost innovative technical design and alternative fuels.

Putting all this regulatory landscape into context, and examining at the regulators' thinking ahead of time in a schematic view as shown in Fig.1, a tanker operator would find it even more challenging to face such a strong commitment that regulates incremental improvement of the existing energy efficiency framework with EEDI and SEEMP.

2.6. Maritime Autonomous Surface Ships (MASS) – IMO work output

IMO (2017b) considered undertaking a regulatory scoping exercise to determine how the safe, secure and environmentally sound operation of Maritime Autonomous Surface Ships (MASS) shall be.

Ship automation is an emerging technology that is drawing upon the shipping industry. Reportedly, the new technology has the potential of a reduction of 5 or 6 crew within the next 10 years. IMO will find it inevitable to lay down future regulations for autonomous vessels focusing on the remotely controlled and autonomous navigation and propulsion systems. In this context, the scope of monitoring will be much larger than that of energy performance. To achieve the level of high frequency data gathering required in ISO 19030, the ship needs to install a data logger and torque meter, to name just a few.

ISO 19030 and MASS evoke the notion of a continuum, on which the energy efficiency monitoring occupies an important segment while autonomous vessel monitoring is located in its entire length. Though the effect of MASS may come to tankers in a slower speed than to other ship types, this new trend emerging on the horizon, no matter how distant it looks, bears close watch. For tanker operators, if they want to demonstrate full compliance with ISO 19030 with the ultimate goal of monitoring and controlling their fleet energy performance, a future demand of monitoring tools for automation will add another layer of variables to the immediate need for energy performance monitoring.

3. Summary

This paper indicates challenges facing the tanker operators and explains how these may be addressed through the tanker industry's self-driven initiative towards greener seaborne transportation, charterers' need, and regulatory landscapes reshaping the future industry. The work ahead of the INTERTANKO WG's task is more challenging. When the WG freely shares their experiences in their own energy efficiency monitoring based on ISO 19030, it will be able to achieve the objectives. The 2nd HullPIC Conference was brought to their attention only recently. The WG is well placed with the developers of ISO 19030 as well as tanker operators whose day to day job is to monitor their tanker fleet energy efficiency performance. It is hoped that the areas of improvement listed in item 2.3 above will be taken into consideration in the course of revision of ISO 19030.

References

IMO (2016*), Understanding the Energy Efficiency Operational Index: data analysis on ships tanker ships for INTERTANKO*, UCL Energy Institute, MEPC 69/INF.26

IMO (2017a), *Comments on the draft structure and suggested draft text for possible inclusion in the initial Strategy*, INTERTANKO et al, ISWG-GHG 2/2/1

IMO (2017b), *Maritime Autonomous Surface Ships, Proposal for a regulatory scoping exercise*, Denmark et al, MSC 98/20/2

IMO (2018a), *Finalization of the draft initial IMO Strategy on reduction of GHG emissions from ships,* ISWG-GHG 3/2

IMO (2018b*), Understanding CO2 emissions and challengers in assessing the operational efficiency for ships,* INTERTANKO, MEPC 72/7/1

Is Wave Height Necessary to Determine Ship Performance in Calm Water from Measurements?

P. Arun Lakshmynarayanana, University of Southampton, Southampton/UK, pl6g12@soton.ac.uk
Dominic A. Hudson, University of Southampton, Southampton/UK dominic@soton.ac.uk

Abstract

In order to monitor the performance of a vessel in calm seas it is important to ensure that the operational parameters are not biased by weather conditions. This paper makes a comparison between the relationship of true wind speeds obtained from on-board anemometer measurements and hindcast MetOcean data with the wave heights obtained from the MetOcean data. The insights obtained from the correlations between wind and waves is used to make a comparison calm water model derived from 'wind-wave' filtering and data filtered using only the wind speed. Finally, the increase in shaft power with respect to wind speed and wave heights for discrete intervals is presented. The results presented indicate that an average decrease of 4-5% in shaft power is seen when including an additional wave filter in the calm water model. However, this discrepancy improves when a stricter wind speed filtering is used.

1. Introduction

The powering performance of a ship is influenced by several factors, amongst which the operational conditions and the environment are of key importance. A ship in service predominately operates in stochastic weather conditions which can have a significant effect on the power requirements and the fuel consumption. However, the performance of a ship in calm water is vital to understanding performance against guarantees, monitoring coating and propeller performance as well as benchmarking energy-saving technologies. Sea trials to achieve the guarantee speed as per the contract specification are carried out in, or more usually corrected to, a calm water condition.

In order to monitor the performance of a vessel in calm seas it is important to ensure that the operational parameters are not biased by weather conditions. This is usually achieved by either filtering or normalising measured data, or a combination of both, to derive a calm water model, *Dinham-Peren and Dand (2010), Webb and Hudson (2015)*. Weather, or MetOcean, data (wind speed, wave height and their directions) may be obtained using hindcast models, measured at the site (shipboard instruments and/or wave buoys) or remote sensing by satellites. MetOcean data from hindcast modelling typically not only include the combined wave height but also primary and secondary swell and the wind-generated wave data. Automatic high-frequency data acquisition systems installed on-board ships now enable ship operators to obtain operational data of high quality, which not only facilitates monitoring performance more precisely but also in identifying changes in performance in smaller time periods, *Aldous et al. (2015)*. The performance prediction can be improved significantly by combining automatic data acquisition with MetOcean datasets to model the weather effects more accurately, *Bos (2016)*. However, more often than not the MetOcean data comes at considerable cost, which might not be affordable to the ship owners and operators.

Onboard a vessel the wind speed is either estimated visually by the Master or determined using an anemometer, but presently, wave measurements are practically impossible to obtain routinely from the available onboard instruments. Anemometer measurements are considered more reliable than visual estimations, although uncertainties do exist in readings from the anemometer, *Taylor et al. (1995)*. The errors in wind speeds measured by an on-board anemometer due to flow caused by the ship's superstructure can be as high as 30% for a tanker in a head wind condition, *Yelland et al. (2001)*. When comparing measured data to forecast (or hindcast) data, a higher wind speed will usually be recorded because the location of the ship's anemometer is generally much higher than the reference height of 10m used as a MetOcean standard. However, there are established relationships which can be applied to correct the anemometer measurements to a required reference height. Ocean waves are generated primarily due to the transfer of energy from the wind blowing on the ocean surface. The combined wave height or significant wave height of all the component sea states measured at a site exhibits a strong correlation with the wind speeds measured, *Khristoforov et al. (1994)*, and consequently it is likely to be possible to derive a correlation between the true wind speed from anemometer measurements and significant wave heights.

This paper attempts to find a relationship between the true wind speeds derived from onboard anemometer measurements and wave heights obtained from hindcast MetOcean data, including both the combined and the component sea-states. The hindcast datasets also incorporate the true wind speed and direction which is also used to deduce correlations with the wave heights. The correlations thus obtained between wind and waves are used to filter the high frequency data obtained from a merchant vessel to calculate the calm water powering. A comparison will be made between the accuracy of the calm water model derived from the deduced 'wind-wave' relationships and the MetOcean wave data directly. The analysis presented in this paper will provide insights into the accuracy and differences in calm water power models when the MetOcean data are not available. The independent effect of wind and wave on the power vs speed curves is also investigated.

2. Methodology

This section provides a brief description of the methodologies used to derive the relationship between wind and wave using on-board anemometer measurements and MetOcean data, respectively, together with the data filtering applied to derive the calm water model. Firstly, the nature of data acquired from the automatic data acquisition system on the vessel and MetOcean data from hindcast modelling are reported.

2.1 Ship Data Acquisition

High-frequency continuously monitored data was obtained for three sister merchant ships along with the weather data from a MetOcean hindcast model. The data logger installed on board recorded the shaft parameters at a sampling frequency of 1 Hz and averaged over 5 min intervals. The wind speed and direction were measured using an on-board anemometer. The total period of the measured data for the three ships was different with the maximum being two years and one month and the minimum being six months. The ship with maximum data was only considered for this study due to the quantity of data. The raw data for this ship yielded a total of 155814 data points. Fig.1 shows the operational profile of the vessel with reference to the ship speed, draft, trim and the significant wave height from the MetOcean dataset. The encountered significant wave heights mainly fall in the range of 1 to 3 m and the number of data points for a wave height $\leq$2.0 m is 63385 which comprises 41% of the total dataset.

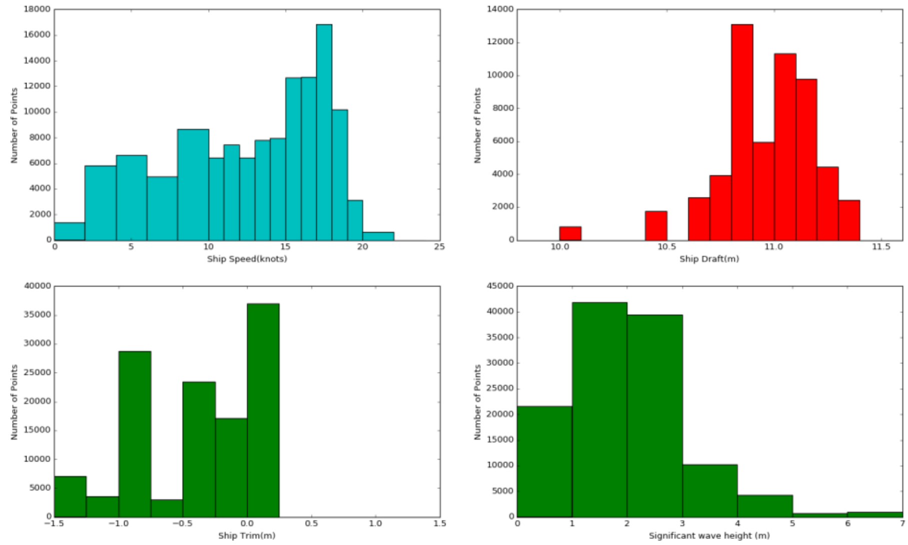

Fig.1: Histograms of ship speed, draft, trim and significant wave height during the analysis period

The apparent wind angle and the wind speed recorded using the anemometer are presented in Fig.2. The apparent wind is a relative effect which arises due to the combined effects of the true wind and the vessel speed. In section 2.2 the method to translate the apparent wind to true wind using the ship's speed and heading are described.

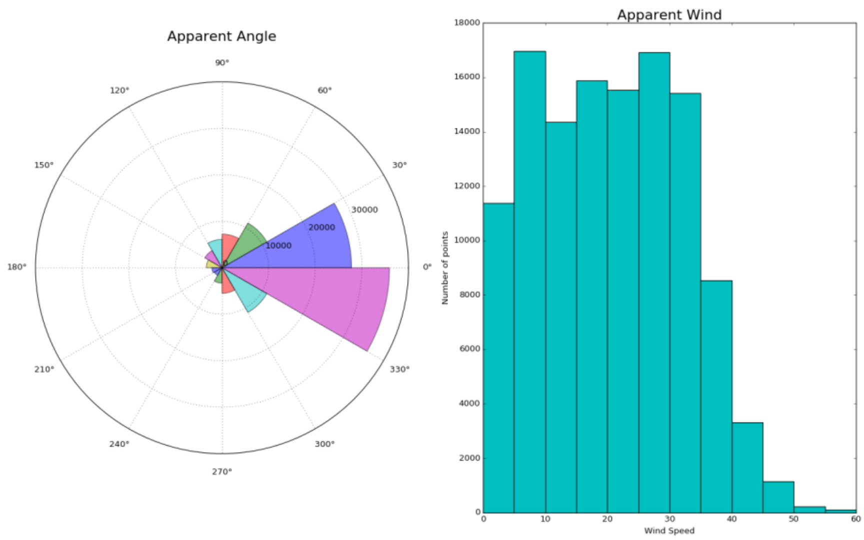

Fig.2: Apparent wind direction and wind speed experience by the vessel

2.2 MetOcean data and True Wind Speed

The MetOcean data obtained include primary swell, secondary swell, wind wave, combined wave, and true wind, which are shown as a block diagram in Fig.3. The primary and secondary swell are the components of the sea state in which the waves are not generated by local winds but rather remote from the location of interest and then travel towards it, whereas the wind wave consists of locally generated wave systems.

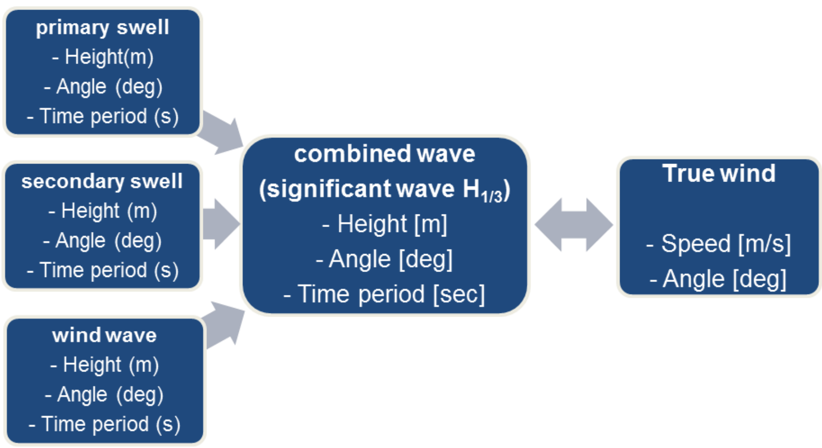

Fig.3: Schematic diagram of the hindcast weather dataset

In general, the primary, secondary and the local wind wave are related to the combined or significant wave height by the formula given below, *Barth and Eecen (2006)*. This relationship was verified, shown in Fig.4, for the data set obtained and the results are in good agreement. The comparison between the significant wave height from the MetOcean data and calculated using the formula are almost linear, as illustrated in Fig.4.

$$H_{1/3} = \sqrt{((1^o)^2 + (2^o)^2 + (wind)^2)}$$

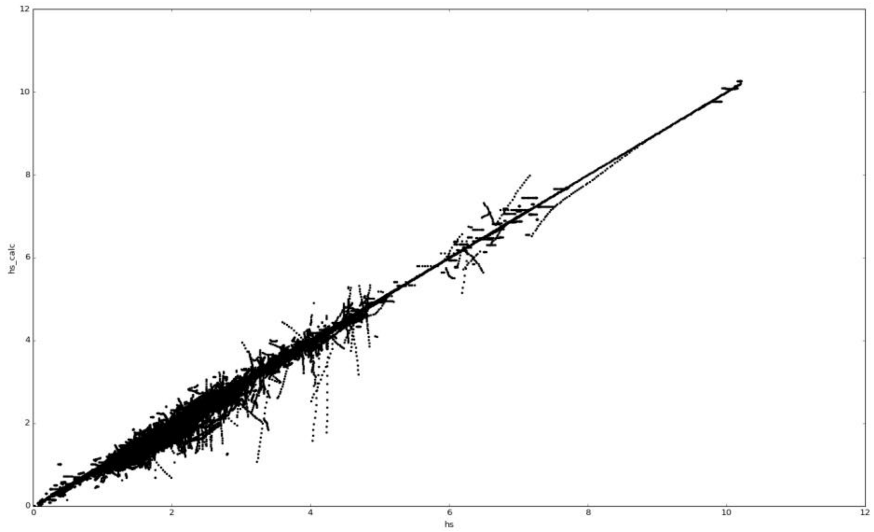

Fig.4: Significant wave height from MetOcean data vs that calculated using the component sea states

True wind speed and direction were determined by eliminating the influence of the ship speed from the apparent wind measurements using the relationship given below. The true wind angle and speed is also obtained from the hindcast weather data, where the angle of zero degrees indicates true north. For comparison, the true wind angle from the anemometer was corrected using the ship heading angle (ship data) and compared to the true wind angle from the MetOcean data.

The true wind speed and angle determined using the relationship are shown in Fig.5. The true wind speed histogram resembles a normal distribution curve, with most wind speeds recorded below 20 m/s.

$$V_{true} = \sqrt{V_{apparent}{}^2 + V_{Ship}{}^2 - 2V_{apparent}V_{Ship}}$$

$$\alpha = \text{accros}\left(\frac{V_{apparent}\cos(\beta) - V_{ship}}{\sqrt{V_{apparent}{}^2 + V_{Ship}{}^2 - 2V_{apparent}V_{Ship}}}\right)$$

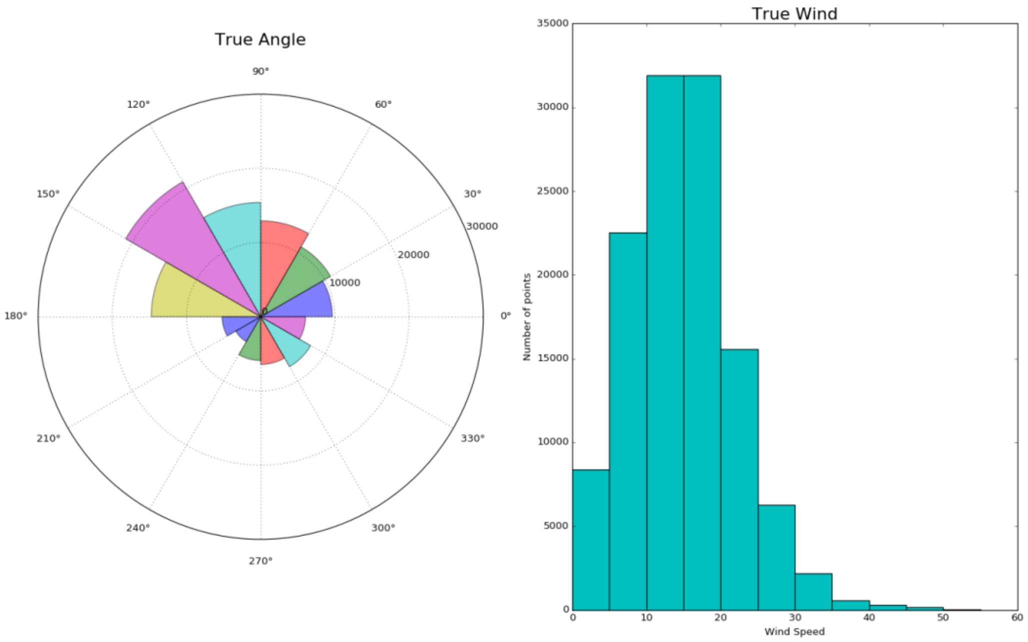

Fig.5: True wind speed and direction obtained by accounting for vessel speed and heading

2.3 Calm-water filtering

The in-service data are used to estimate the calm water power by appropriately filtering for weather effects. *ITTC (2014),* 'Recommended Procedures and Guidelines' provide procedures and sea states for speed/power trials that defines a suitable calm water condition to conduct the trials. These may be used as an initial means to define a calm water condition, although it should be noted that when conducting trials in these conditions, corrections for wind and wave effects would be applied to measured power/speed data.

According to the ITTC, wind and wave limits for conduct of sea trials are as follows:

- Wind speeds shall not be greater than Beaufort number 6 (L_{pp}> 100 m) or Beaufort number 5 (L_{pp} < 100 m)
- Significant wave height shall not be higher than $2.25\sqrt{L_{pp}/100}$
  (where L_{pp} is the length between perpendiculars [m]).

The wind and wave limits to define calm water based on the above conditions are 10 m/s and 3.74 m, respectively. When establishing calm water conditions, it is also necessary to examine how much the sea state influences the ship speed and shaft power. Fig.6 shows the power vs speed curves with different filtering criteria for true wind speeds. The trends look similar, but the regression curves for true wind speeds greater than 6 and 7 m/s require higher shaft power than at 5 m/s or less, albeit, the difference is not very substantial. In the case of significant wave height, the effect of waves can be discerned more clearly. The gradient of the fitted curve begins to be considerably higher for a significant wave height greater than 2 m. Thus, it is considered reasonable for these vessels to limit the true wind speed and significant wave height to 10 m/s and 1.5 m, respectively.

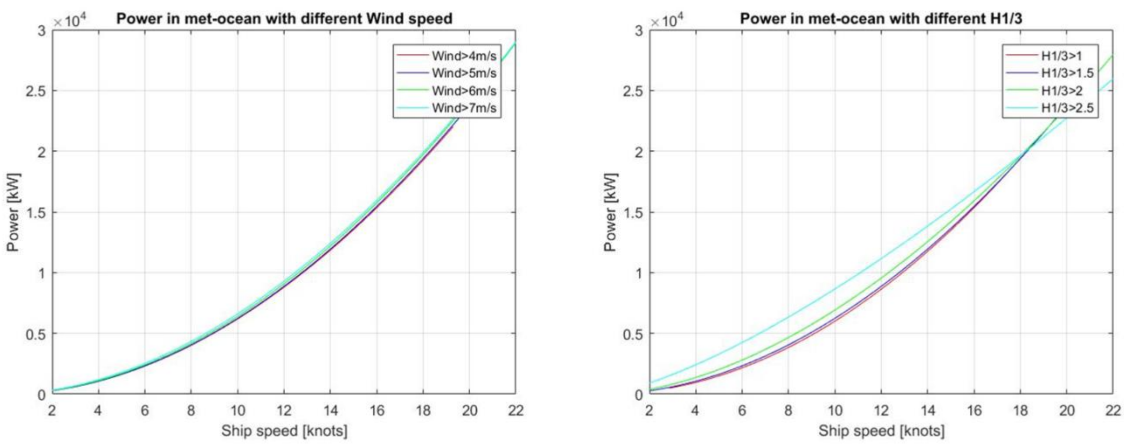

Fig.6: Power vs Speed curves for different wind speeds and wave heights.

To calculate the calm water powering characteristics for these vessels the raw data were filtered by applying the following constraints:

- True wind speed less than 10 m/s
- Significant wave height less than 1.5 m
- The difference between the speed over ground and the speed through water less than 1 knot. This constraint is to ensure that the effect of 'current' is small in the calm water model.
- Engine RPM is greater than zero, hence astern running is not included.
- Change in speed over ground between successive samples does not exceed 0.5 knots. In this case, only data points that represent the ship moving at a reasonably steady speed will be considered.

3. Results and Discussion

3.1. Wind and Wave correlation

According to the National Oceanic and Atmospheric Administration (NOAA), swell travels outside of the generated area and does not necessarily correlate well with the wind, whereas the wind wave is formed due to local winds, *Ainsworth (2006)*. Before trying to derive a correlation between the true wind recorded using the anemometer and the significant wave height, some insights are provided on the realtionship between the directions of the combined and the component sea-states.

Fig.7 illustrates the relationships between the true wind angle with the wind wave angle and the combined wave angle obtained from the hindcast data. It is to be noted that the angles are converted to 0-180° for convenience. As expected, the wind wave angle exhibits good correlation with the true wind angle, while a large degree of scatter apparently exists in the comparison with the combined wave. However, a density map of the data points, shown in Fig.8, unveils a possible trend between the combined wave angle and the true wind angle. High-probability points are depicted with bright yellow and red colours and a linear behaviour can be infered between the variables. Hence, it would not be erroneous to speculate that typically the combined wave direction is dominated by the wind wave, unless otherwise affected by a strong swell.

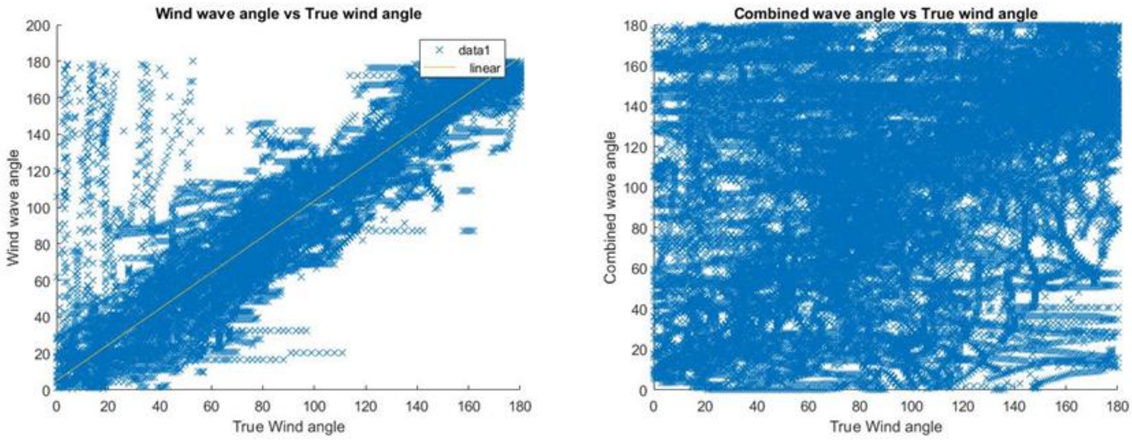

Fig.7: True wind angle (MetOcean) compared with wind wave and combined wave angle

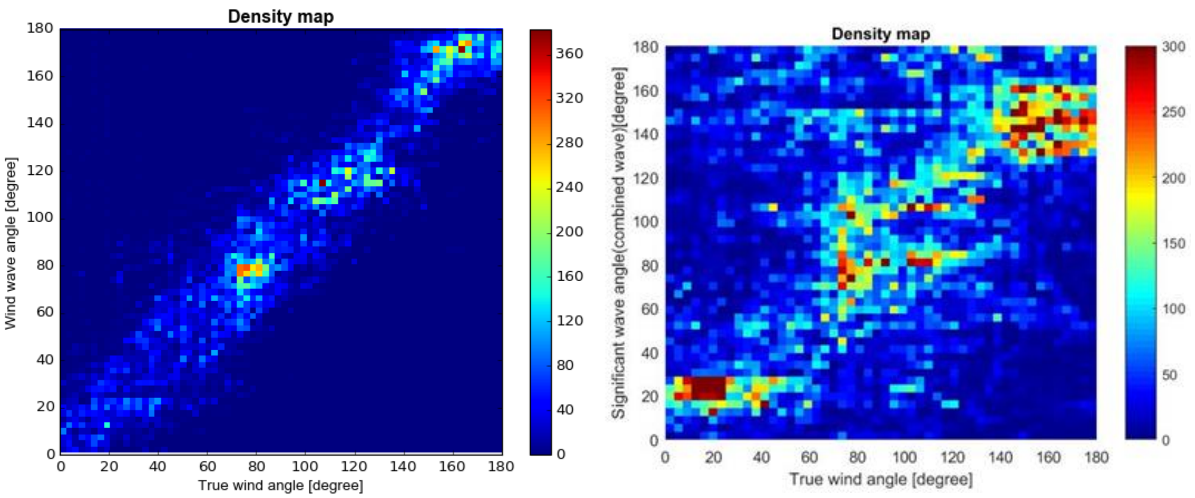

Fig.8: Density map for true wind angle (MetOcean) compared with wind wave and combined wave angle

Fig.9 is a scatter plot between the true wind speeds measured onboard and those from the hindcast MetOcean data. The scale of the true wind speed taken directly from these onboard measurements is approximately 50 % higher than the corresponding speed in the hindcast data. In the majority of cases, wind speed should be measured or corrected to a reference height of 10m above the surface. Since virtually all merchant ship anemometers are higher than 10m, the wind speeds measured onboard should be corrected before making such comparisons *Moat et al. (2005*). In the present study, without precise details of the anemometer mounting position, an assumption is made that the ship anemometer is mounted at a height of 20 m above the sea level. When considering light winds, under stable atmospheric conditions, the surface air layer exhibits strong shear effects and the wind at 10m can be as low as 40% of the wind speed at 20 m, *Isemer and Hasse (1991)*. Fig.10 shows the comparison between the measured true wind speed corrected using a factor of 0.4 and the true wind from the hindcast data. The scales of both the axes are now identical and the density plot understandably reveals a linear correlation between them, if the data points with lower probability are omitted.

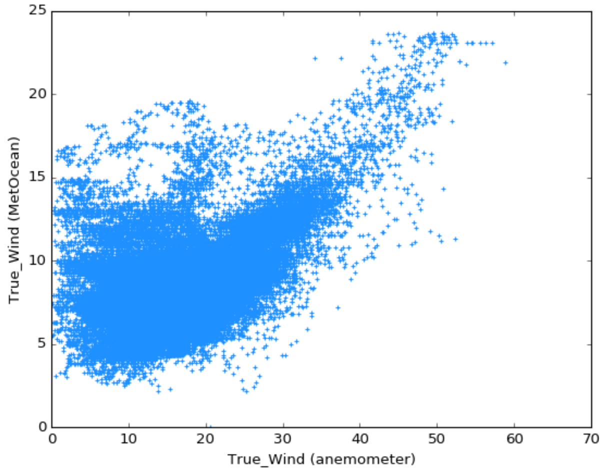

Fig.9: True wind speed (MetOcean) vs True wind speed (anemometer)

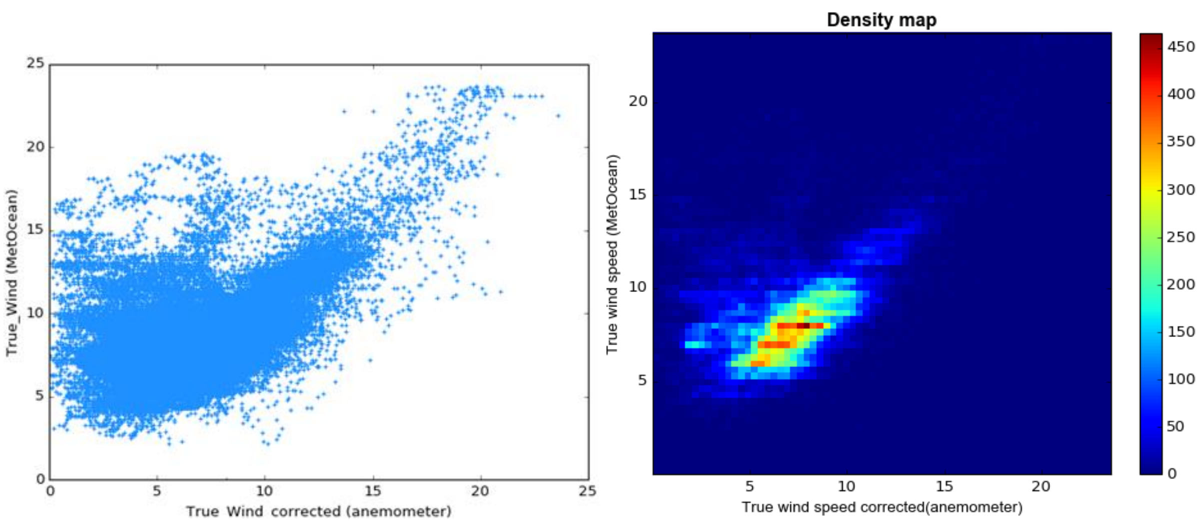

Fig.10: Scatter plot and density map for true wind speed (MetOcean) vs true wind speed (anemometer corrected using a factor of 0.4)

The relationship between the true wind speed and the significant wave height is approximated in the form of $H_{1/3} = kV^{n}_{truewind}$ to obtain a best fit relationship for these data, where the coefficients k and n are obtained through curve-fitting. Fig.11 presents the scatter plot and the best fit lines for the true wind speeds from both the hindcast MetOcean data and the ship's anemometer with the significant wave height. There is a considerable difference in the correlations obtained from the best fit when using the two different true wind speeds, which is also confimed from the coefficients shown in Table I. The true wind speed obtained from the hindcast data exhibits a linear trend with the significant wave height, which is not surprising since the combined wave parameters are dominated by the wave generated by the local winds rather than the swell, as seen in Fig.7. Although the coefficients in Table I are appreciably different from each other it is encouraging to note that using either true wind speed results in a the significant wave height of less than 2 m for wind speeds less than 5 m/s and 10 m/s. This is particulary important in trying to understand whether the ship's anemometer readings may be used to filter data and predict vessel performance with minimum uncertainty due to the influence of waves. Almost all standards found in the literature (e.g. (ISO19030)) use a filtering criteria of significant wave height less than 1.5 m or 2.0 m to define the calm water performance of a vessel. Comparing the plots and the coefficients obtained in Fig.11 and Table I it can be presumed that using a criteria of true wind (anemometer) less than 5.0 m/s or 10.0 m/s would not be inaccurate in this regard, since it would filter out most of the wave influence in establishing a calm water model. Additionally, the density maps shown in Fig.12 also suggests this possibility, displaying a good comparison in the probability distribution between the wind speed from the hindcast model or the anemometer measurements with the significant wave height. However, difficulty may arise in calculating ship added power due to a larger uncertainity in the predicted significant wave heights using the two alternative means of obtaining the true wind speed.

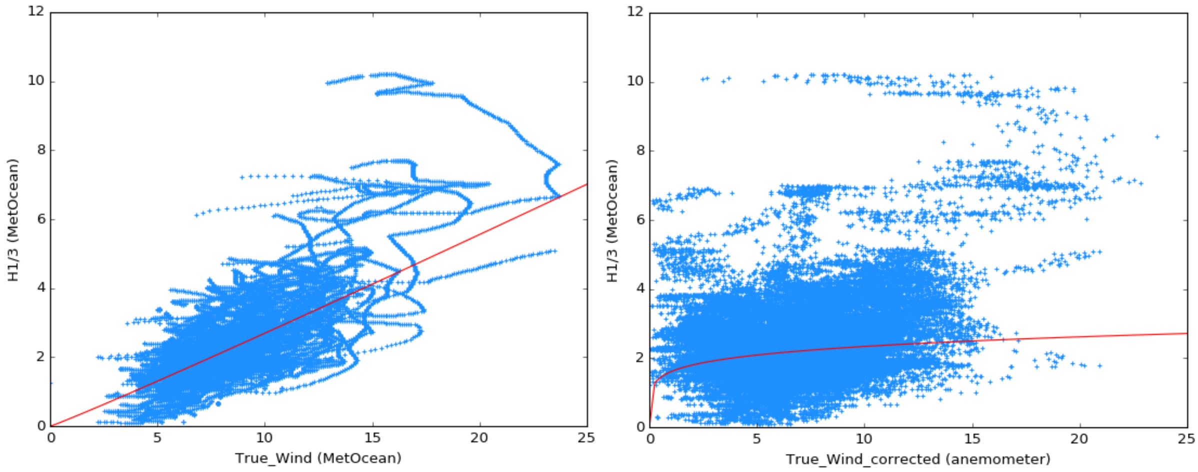

Fig.11: True Wind speed (Met Ocean and anemometer) data compared with the significant wave height. The redline shows the fit obtained using a regression analysis

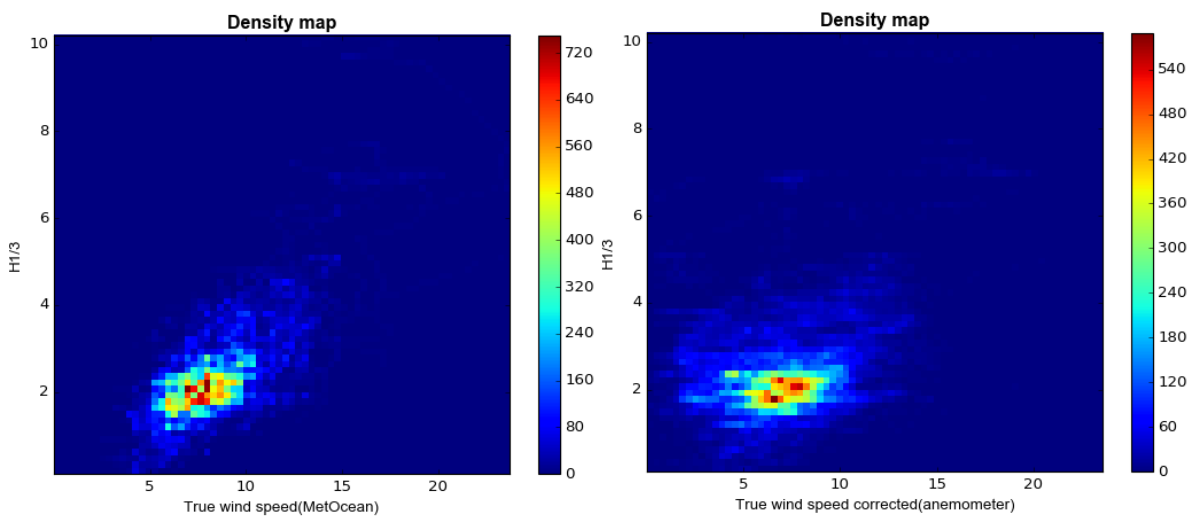

Fig.12: Density plot for true wind speeds (Met Ocean and anemometer) data compared with the significant wave height showing close similarity in the high probability data points

There are a number of data points in Fig.11 for the onboard true wind measurements vs wave height plot that lie in the wave height region greater than 2.0 m for a wind speed less than 10 m/s. Even though the concentration of points in the density plot for this wind speed range is shown to be less (Fig.12) than 2.0 m, it is advised to investigate the effect of wind and wind-wave filtering separately on the power vs speed curves to quantify the difference for a given data set.

Table I: Coefficients k and n for relationship between true wind speed and significant wave height

	k	N
True wind (Met) vs $H_{1/3}$	0.25	1.04
True wind (onboard) vs $H_{1/3}$	1.45	0.21

3.2. Power vs speed analysis

This section presents the results of the power vs speed in calm water, using different wind and wave filtering criteria and the findings from the wind-wave correlation presented in section 3.1.

Firstly, the comparison between the calm water performance in laden condition (>10.0 m draft) of the vessel with the filtering criteria listed in section 2.3 and that obtained by omitting the wave height filtering criteria is shown in Fig.13. In the laden condition, the vessel primarily operates with a speed over ground above 16.0 knots, which aggregates to 76% of the total number of data points. The shaft power predicted with wind and wave filtering is lower for the higher operating speeds and the difference in predicted power varies from 2% to 8% for a speed range of 16-19 knots. When a stricter wind speed filtering criteria is used – true wind speed less than 5.0 m/s – the percentage differences in predicted power improves to about 1-4% for the operating speed ranges, as shown in Fig.14. Nevertheless, the Figs.13 and 14 do demonstrate an apparent improvement in the calm water predictions when using the significant wave height as an additional filtering criteria, as opposed to using only the true wind speed from the anemometer measurements. Figs.13 and 14 show that it is most likely that the calm water power predicted, especially for operating speed ranges, may exhibit an average difference of 2-3% when hindcast weather data are unavailable, provided a strict filtering of true wind speed is used.

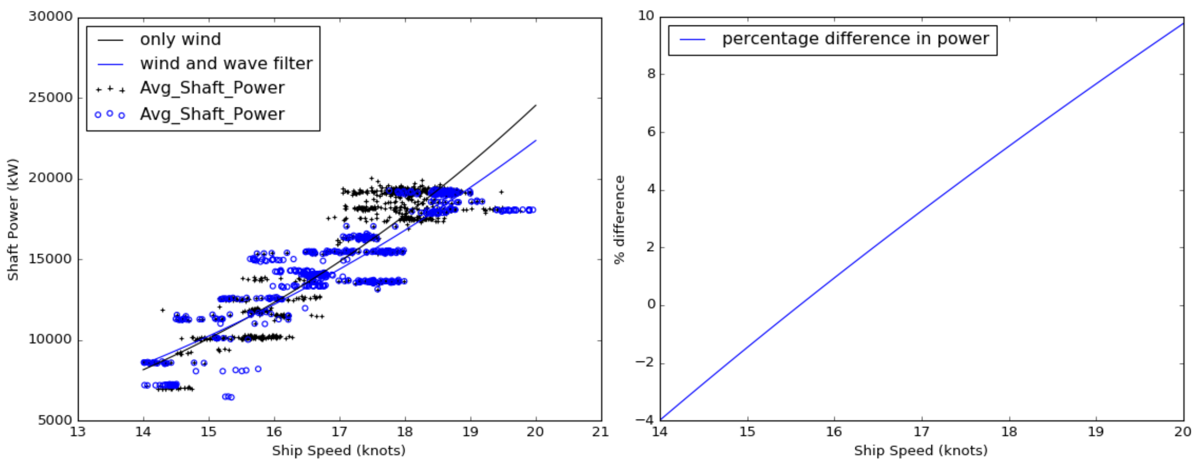

Fig.13: Power vs speed curves comparison between 'wind-wave' filtering and only wind filtering

To further explore the sensitivity of power vs speed curve fitting to the inclusion of wind and waves, data analysis is performed by 'binning' the wind speed and wave heights into regular intervals. The true wind speed is divided into 2.5 m/s intervals. Additionally, the direction of the wind is also considered in this analysis in the sense that only head winds, categorized as a true wind direction of 0 to 30° are considered. The air resistance caused due to the vessel sailing into head winds causes an increase in shaft power when compared to winds from other directions, *Molland et al. (2017).*

Fig.15 represents shaft power against ship speed in the laden condition for various wind intervals. In this case the calm water power is calculated using a wind and wave filtering of 5 m/s and 1.5 m, respectively. The increase in shaft power is obvious in the curves with respect to the increase of wind strength. The results obtained by calculating shaft power by binning the wave heights shows a trend similar to that with the strength of head winds. The fewer number of data points for significant wave heights greater than 3.5 m skews the regression curves, making these unreliable for comparison.

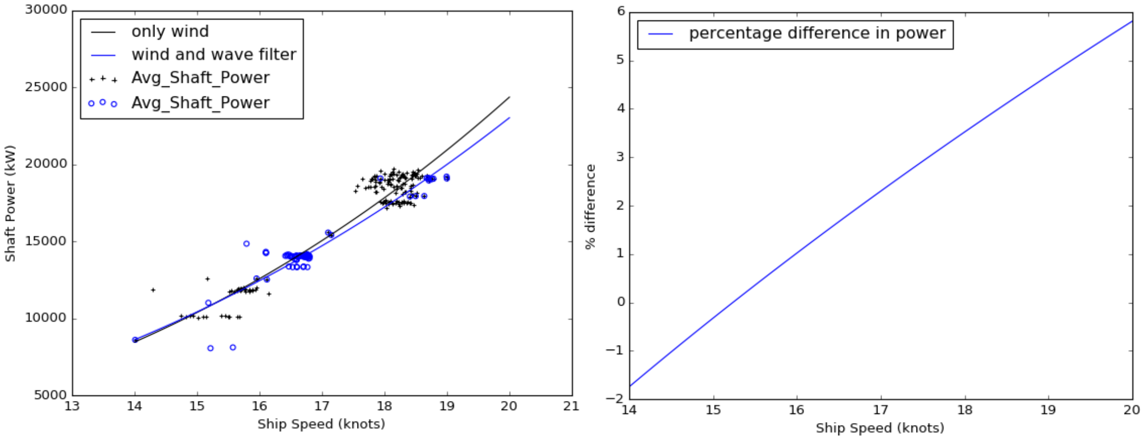

Fig.14: Power vs speed curves comparison between 'wind-wave' filtering and only wind filtering. The wind speed filtering criteria is decreased from 10 m/s to 5 m/s.

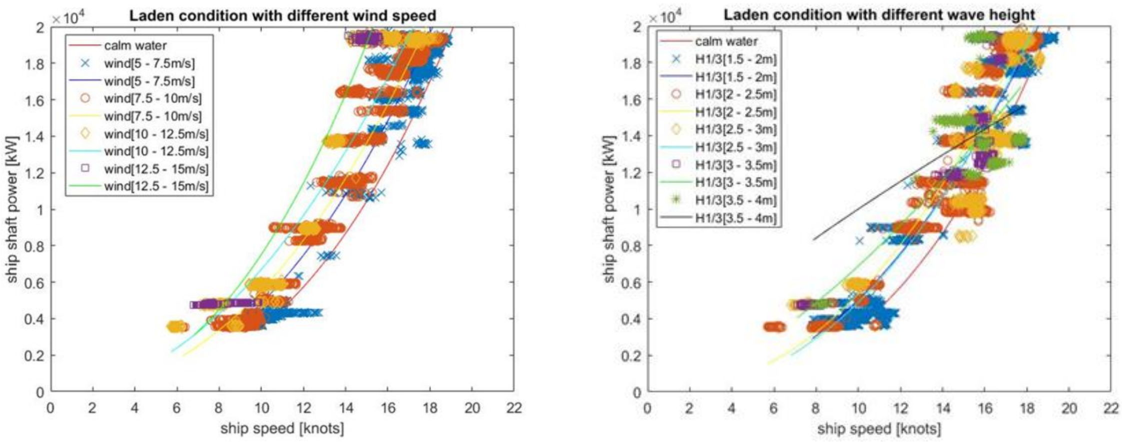

Fig.15: Power vs Speed curves with various wind speed bins (head wind) and wave height bins in laden condition

4. Conclusions

The correlation between the true wind speeds measured using the ship's anemometer and the significant wave height from MetOcean hindcast data are presented in this paper. By comparing the combined significant wave height direction with the true wind direction from hindcast models, it is shown that, whilst there is considerable scatter in the total ranges of data, the majority of points demonstrate a good correlation. This indicates that true wind angle may be used as a reasonable indicator of combined wave angle. The study also uses the true wind speeds obtained from the hindcast MetOcean data and the two are compared. It is shown that the true wind speed from the anemometer should be corrected to a reference level of 10m to correspond with the true wind speed obtained from the hindcast (or other) MetOcean models. Although the true wind speeds obtained from the two sources does not show an exact correlation with the significant wave height, it is demonstrated that for true wind speeds less than 10 m/s (anemometer and MetOcean) the predicted significant wave height is under 2 m. The calm water power is overestimated by a maximum of 8% for the vessel used in this study when using a true wind under 10 m/s as the only filtering criteria for weather, when compared to using both wind and wave filtering. This overestimate in power reduces to 4% when a stricter criterion of 5 m/s true wind speed is used. When MetOcean datasets are not available it is imperative to investigate the sensitivity of true wind speed (anemometer) filtering on the calm water performance for both laden and ballast condition to deduce an appropriate filtering criterion. The above investigations illustrate that by using only true wind speed as a filtering criterion for the weather will, on average, produce a difference of about 2-3% in calm water predictions for the operating speed range as compared to when MetOcean data sets are available to complement the analysis.

References

AINSWORTH, T. (2006), *When do ocean waves become 'significant': A closer look at wave forecasts*, Mariners Weather Log 50(1)

ALDOUS, L.; SMITH, T.; BUCKNALL, R. (2015), *Uncertainty analysis in ship performance modelling*, Ocean Engineering 110, pp.29-38

BARTH, S.; EECEN, P.J. (2006), *Description of the relation of wind, wave and current characteristics at the offshore wind farm Egmond aan Zee (OWEZ) location in 2006*, Muiden

BOS, M. (2016), *How MetOcean data can improve accuracy and reliability of vessel performance estimates*, 1st HullPIC Conf., Pavone, pp.106-114

DINHAM-PEREN, T.A.; DAND, I.W. (2010), *The need for full scale measurements*, William Froude Conference: Advances in Theoretical and Applied Hydrodynamics - Past and Future, Portsmouth, pp. 1-13

ISEMER, H.J.; HASSE, L. (1991), *The scientific Beaufort equivalent scale: Effects on wind statistics and climatological air-sea flux estimates in the North Atlantic Ocean*, J. Climate 4, pp.819-836

ITTC (2014), *Analysis of Speed/Power Trial Data*, ITTC-Recommended Procedures and Guidelines

KHRISTOFOROV, G.N.; ZAPEVALOV, A.S.; SMOLOV, P.E. (1994), *The relationship between the amplitudinal characteristics of the high-frequency spectral components of wind-generated waves and the wind velocity over the sea*, Phys. Oceanography 5(221)

MOAT, B.I.; YELLAND, M.J.; MOLLAND, A.F. (2005), *The effect of ship shape and anemometer location on wind speed measurements obtained from ships*, 4th Int. Conf. Marine Computational Fluid Dynamics, pp.133-139

MOLLAND, A.F.; TURNOCK, S.R.; HUDSON, D.A. (2017), *Ship Resistance and Propulsion: Practical Estimation of Ship Propulsive Power*, Cambridge University Press

WEBB, A.; HUDSON, D.A. (2015), *Identifying added shaft power in weather from voyage analysis of a RORO carrier*, 18th Int. Conf. Ships and Shipping Research, Milan

YELLAND, M.J.; MOAT, B.I.; TAYLOR, P.T. (2001), *Air Flow distortion over merchant ships*, Southampton Oceanography Centre, Southampton

Ultrasound – The Silent Revolution in Antifouling

Jan Kelling, HASYTEC Electronics, Schönkirchen/Germany, j.kelling@hasytec.com

Abstract

Hull fouling protection becomes more and more relevant every year due to its environmental impact as well as upcoming hull performance monitoring regulations. Innovative and sustainable solutions are required for the future. This paper describes different ultrasound working principles, examples of applications and results in general as well as latest development, progress and results of ultrasound based hull protection.

1. Different ultrasound working principles

1.1. Biofilm in general

The biofilms are formed when bacteria adhere to a solid surface and enclose themselves in a sticky polysaccharide. Once this polysaccharide is formed the bacteria can no longer leave the surface, and when new bacteria are produced they stay within the polysaccharide layer. This layer, which is the biofilm, is highly protective for the organisms within it. In fact, it is considered a fact that many bacteria could not survive in the environment outside of biofilms. Biofilms are ubiquitous in the environment. They form on our teeth, inside our bodies, in our streams and oceans, on natural surfaces continually wetted by dripping water. They also are formed inside of all of our water pipes, toilets, and drains, and, in fact, everywhere where there is persistent water.

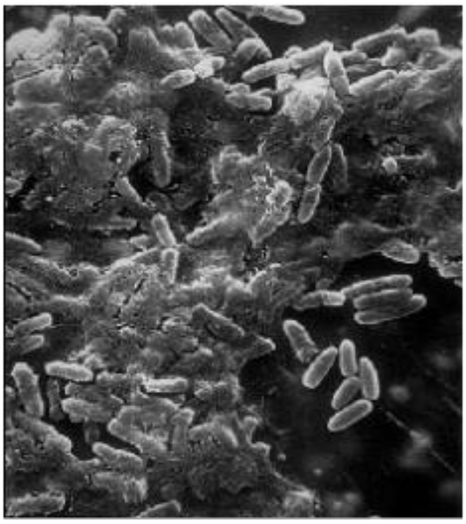

Fig.1 Biofilms under the microscope

While some fungi can form their own biofilms and a few inhabit bacterial biofilms, the so-called "moulds" generally do not grow in or even on the surface of biofilms. This is because there is generally too much water. Most fungi will not grow under water, while biofilms are always under water at least most of the time. Biofilms will not go away on their own, and considerable effort is required to eliminate them. Biofilms on teeth, components of which contribute to plaque formation and tooth decay, are removed by diligent scrubbing with abrasive materials. Unfortunately, the biofilms return within hours, and teeth cleaning is an endless process.

Biofilms on other surfaces can be scrubbed away, or can be disrupted using very hot water (or steam) and concentrated oxidizing agents. However, they will return quickly unless the water source is removed. Hence, there are always biofilms present where water is present (e.g., in the ocean, rivers, our mouths, and our water pipes).

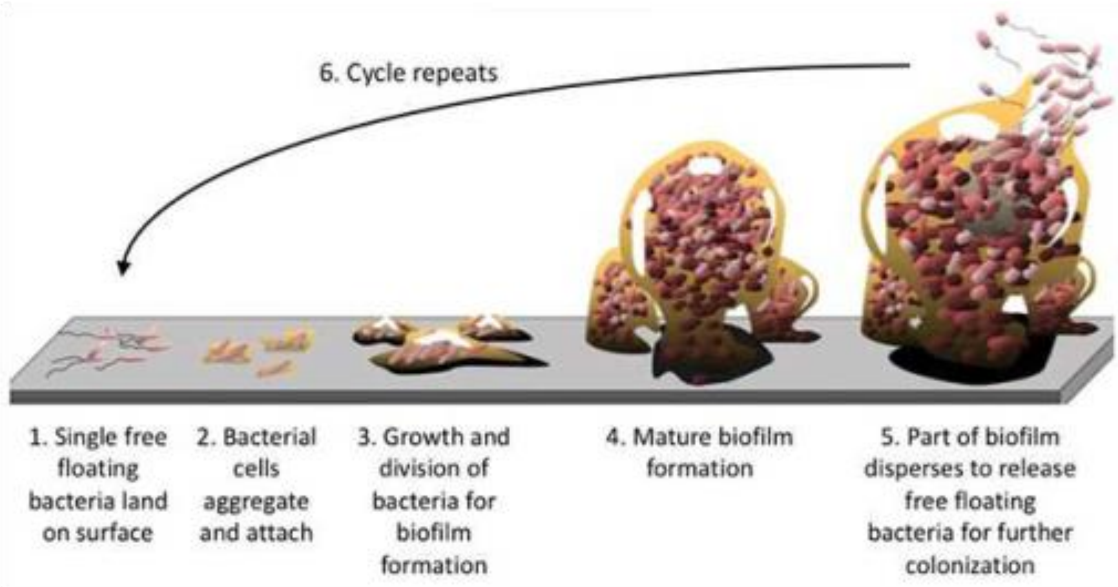

Fig.2: Biofilm growth cycle

1.2. High-powered ultrasound causing cavitation

Older ultrasound methods followed the idea of getting rid of hard growth which had already attached. Using hard cavitation, this working principle might work in certain situations but may also damage the vessel's steel itself. As a consequence, this approach was not accepted by the market.

1.3. Low-powered ultrasound not causing cavitation

Using low-powered ultrasound (which does not cause cavitation in a certain combination of frequencies, altitudes and power consumption) follows only one idea: avoiding biofilm on every liquid carrying surface. Avoiding biofilm means at the same time avoiding marine growth as barnacles, shells and algae. This working principle is relatively new and unknown on the market. But this new kind of antifouling system has a huge potential regarding protecting the environment, being sustainable and not harming humans or animals.

1.4 Response of fish to low-powered ultrasound

Fig.3 shows the startle response of fish to the low-powered ultrasound. The fish that responded to the stimuli increased their swimming speed and often made tight turns. No startle response was ever seen during test periods apart from during signal presentation. In almost all cases when a startle response was seen, the fish swam away from the sound source. The fish always resumed normal swimming behaviour within a few seconds of the end of the 900 ms acoustic stimulus presentation.

For sea bass, 50% reaction threshold ranges were reached for signals between 0.1 and 0.7 kHz, Fig.4A. The sea bass did not react to the maximum received levels that could be produced for the higher frequency signals. For thicklip mullet, 50% reaction thresholds were reached for signals between 0.4 and 0.7 kHz, Fig.4B. The fish did not react to the maximum received levels that could be produced for the other frequencies. However, the mullet reacted to one of the twelve 0.1 kHz signal trials and two of the 0.125 kHz signal trials, which suggests that the 50% reaction threshold level for those frequencies was only a few dB above the maximum level that could be produced with the available equipment. For pout, 50% reaction thresholds were reached for signals between 0.1 and 0.250 kHz, Fig.4C. The pout did not react to the maximum received levels that could be produced for the higher frequency signals. For Atlantic cod and common eel, no 50% reaction thresholds could be reached with the maximum levels for the frequencies that could be produced with the available equipment, Fig.4D and E.

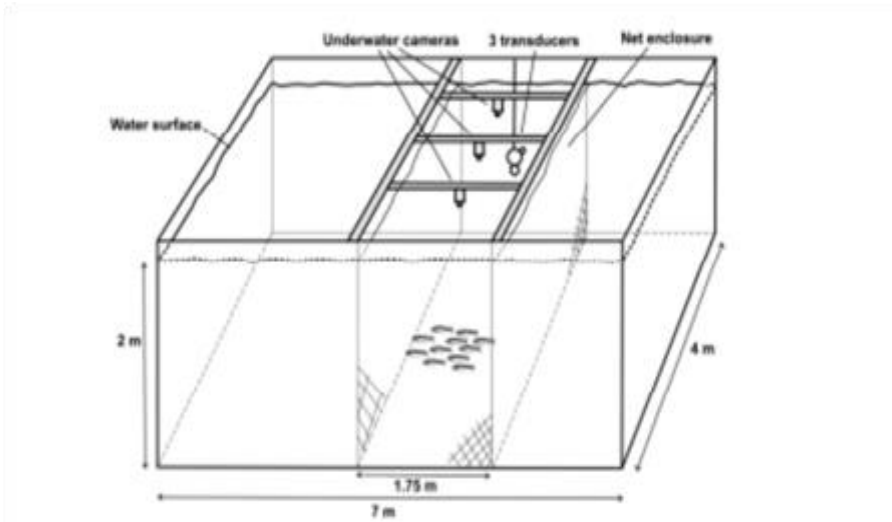

Fig.3: Startle response of captive North Sea fish species to underwater tones 0.1 to 64 kHz, source: Science Direct from 7.9.2008

For pollack, no 50% reaction thresholds could be reached with the maximum levels for the frequencies that could be produced with the available equipment, Fig.4F. However, there was some reaction to the maximum levels that could be produced for signals of 0.1 kHz (reaction in 4 of the 15 trials), 0.125 kHz (4 trials), 0.250 kHz (2 trials) and 0.4 kHz (3 trials). For horse mackerel, 50% reaction thresholds were reached for signals between 0.1 and 2 kHz, Fig.4G. The horse mackerel did not react to the maximum received levels that could be produced for the higher frequency signals. Atlantic herring reacted to two frequencies. The 50% reaction threshold was reached only for the 4 kHz signal, Fig.4H. There was also some reaction to the 0.4 kHz signal (in 2 of the 12 trials). The herring did not react to the maximum received levels that could be produced for the other frequencies.

We judged that the researchers used consistent criteria for classing a trial as a response trial or a non-response trial, because their classifications were always identical, and the startle response was very obvious (not a subtle increase in swimming speed or swimming depth as was observed in a previous study; *Kastelein et al. (2007)*.

The size of their tank influences the general swimming behaviour of many fish species. Before the fish were put in the test tank, they were kept in much smaller circular tanks, in which they swam very slowly or not at all. In the net enclosure in the large test tank, the fish were much more active; they behaved in the same way as fish in the previous study in this tank, which had the entire tank available to them, *Kastelein et al. (2007)*. So, although the test tank was far from a natural environment, it was a much better study area than the smaller tanks used in several previous studies on reactions of fish to sound.

The study fish had been housed, for at least part of their lives, in tanks at aquaria and fish farms. However, those facilities had water filtration systems that were relatively quiet, so the study animals had probably not been exposed to higher sound levels than wild conspecifics. As the location of the study site was selected because of its remote location and quiet environment, the tank was designed specifically for acoustic research, and the area around the tank was strictly controlled (nobody was present within 100 m of the tank, except the researchers who sat quietly), there was little background noise, and startle responses were not observed outside the signal presentations.

The reactions of the fish in the present study were probably dependent on the context in which the sounds were produced, and the fish probably responded differently than would wild fish. Even in the wild, animals behave differently depending on location, temperature, physiological state, age, body size, and school size. So, even if the present study had been conducted in the wild, the findings may not have been of universal value.

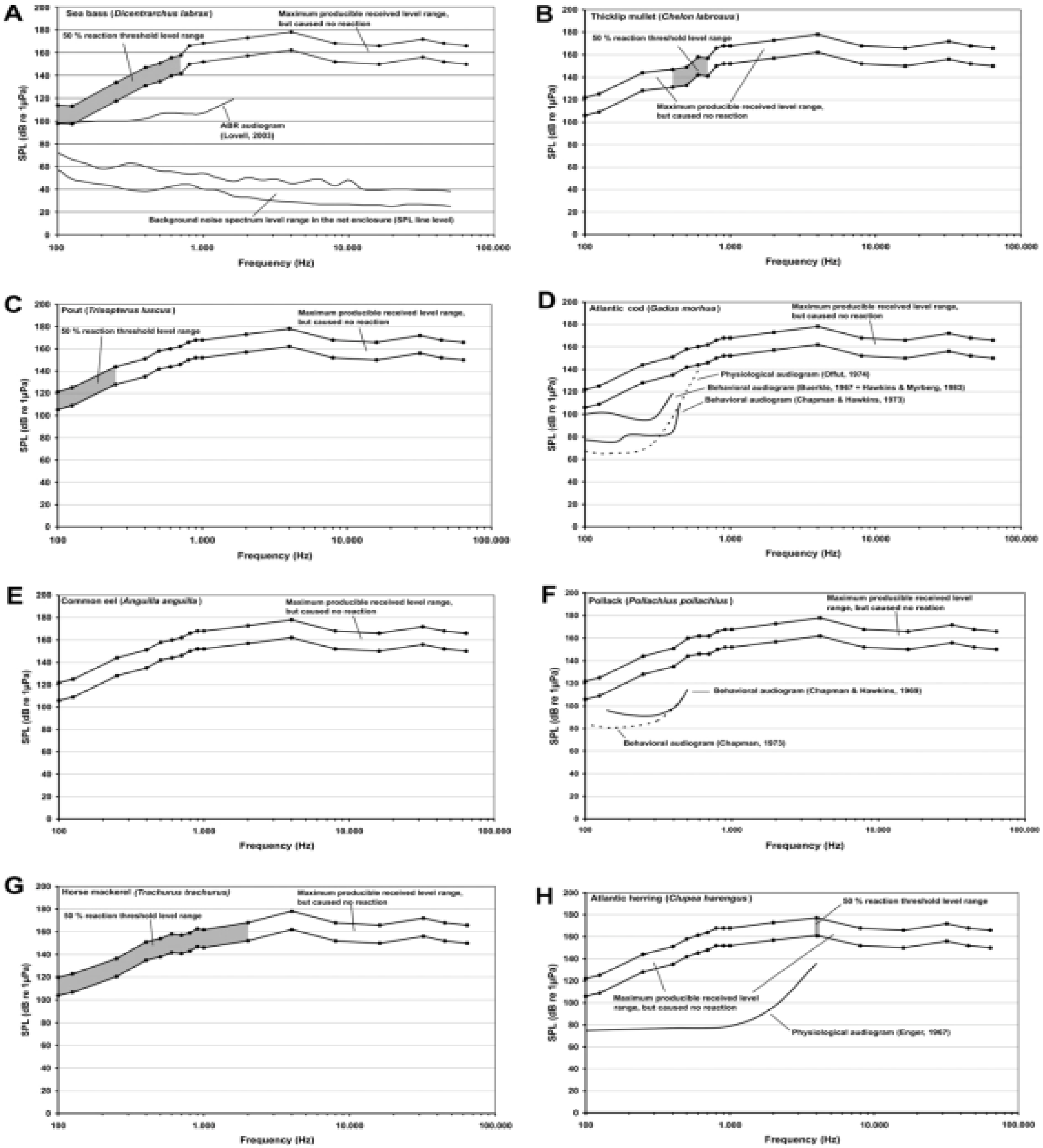

Fig.4: The maximum received level range that could be produced in the tank for the test frequencies causing no reactions, and, for some species, the 50% reaction SPL ranges (shaded areas represent ±8 dB of average received level).

(A) Sea bass (0.1-0.7 kHz; school size: 17 fish), and background noise range in net enclosure, which applies to all species. Also shown is the auditory brainstem response (ABR) audiogram of sea bass. (B) Thicklip mullet (0.4-0.7 kHz; school size: 11 fish). (C) Pout (0.1-0.250 kHz; school size: 9 fish). (D) Atlantic cod (school size: 5 fish). (E) Common eel (school size: 10 fish). (F) Pollack (school size: 4 fish). There was some reaction (<50%) to the maximum levels that could be produced for signals of 0.1 kHz, 0.125 kHz, 0.250 kHz and 0.4 kHz. (G) Horse mackerel (0.1-2 kHz, school size: 13 fish). (H) Atlantic herring (4 kHz, school size: 4 fish).

References

KASTELEIN, R.A.; HEUL, S.v.d.; VEEN, J.v.d.; VERBOOM, W.C.; JENNINGS, N.; REIJNDERS, P. (2007), *Effects of acoustic alarms, designed to reduce small cetacean bycatch, on the behaviour of North Sea fish species in a large tank*, Marine Environmental Research 64, pp.160-180

Appendix 1 - Examples of applications and results in general

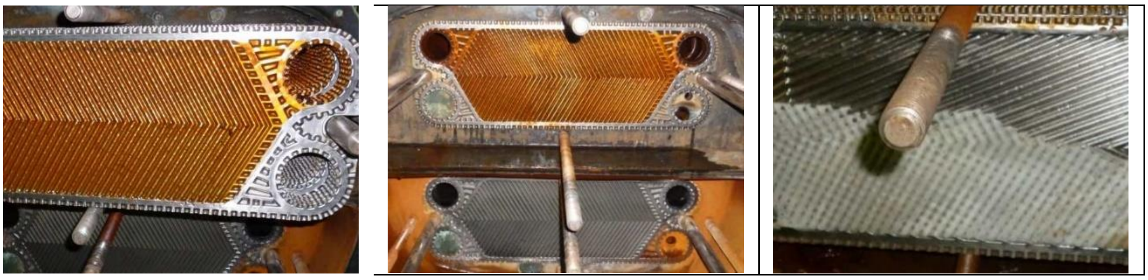

Fig.4: Fresh Water Generator usually after 6-8 weeks

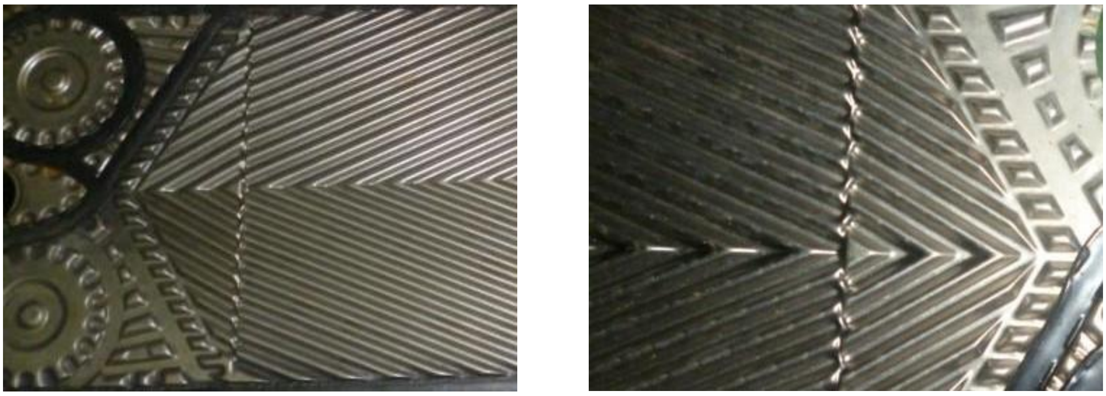

Fig.5: Fresh Water Generator protected with HASYTEC DBP after 6 months

Fig.6: Box coolers & Sea Chest Grids after 12 months (left) and after 18 months (right) protected with HASYTEC DBP

Fig.7: Sea Chest Grids after 15 months protected with HASYTEC DBP

Fig.8: Propeller after 8 months protected with HASYTEC DBP

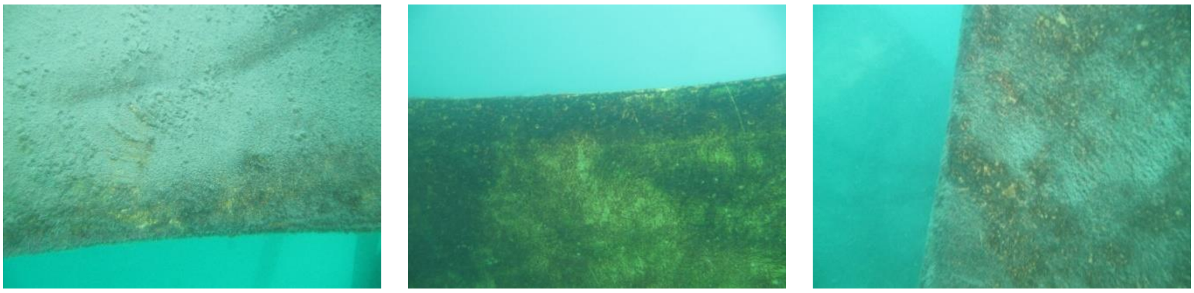

Fig.9: Propeller usually after 6 months

Fig.10: Propeller after 14 months protected with HASYTEC DBP

Appendix 2 - Latest development, progress and results of ultrasound based hull protection

Test vessel: bulk carrier trading North & Baltic Sea, coated with a biocide-free 2k epoxy coating

Fig.11: Vessel in dry dock 2017 after 12 months trading


Fig.12: Vessel in dry dock 2017 after 12 months trading


Fig.13: Portside after 10 months trading North & Baltic Sea, intermediate pictures in 2018

Fig.14: Portside after 10 months trading North & Baltic Sea, intermediate pictures in 2018

Fig.15: Portside after 10 months trading North & Baltic Sea protected with HASYTEC DBP, intermediate pictures in 2018

Fig.16: Portside after 10 months trading North & Baltic Sea protected with HASYTEC DBP, intermediate pictures in 2018

Index by Authors

4th Hull Performance & Insight Conference (HullPIC)

Gubbio / Italy, 6-8 May 2019

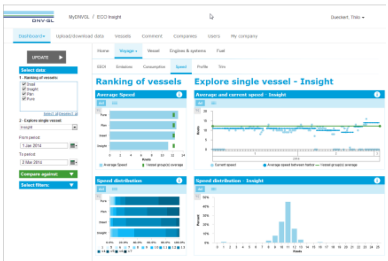

Topics: ISO 19030 and beyond / sensor technology / information fusion / big data / uncertainty analysis / hydrodynamic models / business models / cleaning technology / coating technology / ESDs

Organiser: Volker Bertram (Tutech Innovation)
Geir Axel Oftedahl (Jotun)

Advisory Committee:

Torsten Büssow	DNV GL	**Liz Haslbeck**	NSWC-CD	**Tor Østerveld**	ECOsubsea
Johnny Eliasson	Chevron Shipping	**Tsuyoshi Ishiguro**	JMUC	**Hideaki Saito**	JSTRA
Erik Hagestuen	Kyma	**Jeppe S. Juhl**	BIMCO	**Geoff Swain**	FIT
Simon Hayes	BMT Smart	**Andreas Krapp**	Jotun	**Diego M. Yebra**	Hempel

Venue: The conference will be held at the Bosone Palace Hotel in Gubbio/Italy

Format: Papers to the above topics are invited and will be selected by a selection committee. Papers may have up to 15 pages. The proceedings will be made freely available to the general public.

Deadlines:

anytime	Optional “early warning” of interest to submit paper
20.12.2018	First round of abstract selection (1/3 of available slots)
20.01.2019	Second round of abstract selection (remaining slots)
04.04.2019	Payment due for authors
04.04.2019	Final papers due

Fees:
700 € – early registration (by 04.04.2019)
800 € – late registration

Fees are subject to VAT (reverse charge mechanism in Europe)
Fees include proceedings, lunches, coffee breaks and conference dinner

Limited seating capacity

Sponsors: Jotun (further sponsors to be announced)

Information: www.HullPIC.info

volker.bertram@dnvgl.com